The role of the tumour microenvironment in the phenotype of pituitary adenomas

Thesis presented by:

Pedro Miguel Pereira de Sousa Marques, MD

Thesis submitted in partial fulfillment of the requirements of the Degree of:

Doctor of Philosophy (PhD)

Under the supervision of:

Prof. Márta Korbonits, MD, PhD

Prof. Frances Balkwill, PhD

Centre for Endocrinology,

William Harvey Research Institute,

Barts and the London School of Medicine and Dentistry,

Queen Mary University of London

London, UK, January 2020

Statement of originality

I, Pedro Miguel Pereira de Sousa Marques, confirm that the research included within this thesis is my own work or that where it has been carried out in collaboration with, or supported by others, that this is duly acknowledged below and my contribution indicated. Previously published material is also acknowledged below.

I attest that I have exercised reasonable care to ensure that the work is original, and does not to the best of my knowledge break any UK law, infringe any third party's copyright or other Intellectual Property Right, or contain any confidential material.

I accept that the College has the right to use plagiarism detection software to check the electronic version of the thesis.

I confirm that this thesis has not been previously submitted for the award of a degree by this or any other university.

Signature:

Date: 16/01/2020

Details of publication

Publications containing the data presented in this thesis:

Marques P, Barry S, Carlsen E, Collier D, Ronaldson A, Awad S, Dorward D, Grieve J, Mendoza N, Muquit S, Grossman A, Balkwill F, Korbonits M. Chemokines modulate the tumour microenvironment in pituitary neuroendocrine tumours. *Acta Neuropathol Commun* 2019 Nov 8; 7(1):172. doi: 10.1186/s40478-019-0830-3.

Marques P, Barry S, Carlsen E, Collier D, Ronaldson A, Awad S, Dorward N, Grieve J, Mendoza N, Muquit S, Grossman A, Balkwill F, Korbonits M. Pituitary tumour-fibroblast derived cytokines influence tumour aggressiveness. *Endocr Relat Cancer* 2019 Oct 1. doi: 10.1530/ERC-19-0327. [Epub ahead of print]

Marques P, Caimari F, Hernández-Ramírez LC, Collier D, Iacovazzo D, Ronaldson A, Magid K, Lim C, Stals K, Ellard S, Grossman A, Korbonits M. Significant benefits of *AIP* testing and clinical screening in familial isolated and young-onset pituitary tumors. *[In revision]*

Marques P, Magalhães D, Caimari F, Hernández-Ramírez LC, Collier D, Lim C, Stals K, Ellard S, Druce M, Akker S, Waterhouse, Drake W, Grossman A, Korbonits M. *MEN1* and *AIP* mutation-positive pituitary neuroendocrine tumours (PitNETs): remarkable phenotypic differences in patients with distinct forms of familial PitNETs. *[In preparation]*

Publications in the field of pituitary adenomas:

Marques P, Grossman A, Balkwill F, Korbonits M. The role of the tumour microenvironment in pituitary tumours. *[In preparation]*

Barry S, Carlsen E, Marques P, Stiles C, Gadaleta E, Berney D, Roncaroli F, Chelala C, Solomou A, Herincs M, Caimari F, Grossman A, Crnogorac-Jurcevic T, Haworth O, Gaston-Massuet C, Korbonits M. Tumor microenvironment defines the invasive phenotype of *AIP*-mutation-positive pituitary tumors. *Oncogene* 2019 Mar 12. doi: 10.1038/s41388-019-0779-5.

Marques P, Collier D, Barkan A, Korbonits M. Coexisting pituitary and non-pituitary gigantism in the same family. *Clin Endocrinol (Oxf).* 2018; 89(6):887-888. doi: 10.1111/cen.13852.

Marques P, Barry S, Ronaldson A, Ogilvie A, Storr H, Goadsby P, Powell M, Dang M, Chahal H, Evanson J, Kumar A, Grieve J, Korbonits K. Emergence of pituitary adenoma in a child during surveillance - Clinical challenges and the family members' view in an *AIP* mutation positive family. *Int J Endocrinol*. 2018. Apr 4; 2018: 8581626. doi: 10.1155/2018/8581626. eCollection 2018.

Marques P, Spencer R, Morrison P, Carr I, Dang M, Bonthron D, Hunter S, Korbonits M. Cantú syndrome with coexisting familial pituitary adenoma. *Endocrine*. 2018; 59(3): 677-684. doi: 10.1007/s12020-017-1497-9.

Marques P, Korbonits M. Genetic aspects of pituitary adenomas. *Endocrinol Metab Clin North Am* 2017; 46(2):335-374. doi:10.1016/j.ecl.2017.01.004.

Publications in other fields during the period of my PhD:

Marques P, Stelmachowska-Banas M, Collier D, Wernig F, Korbonits M. Pachydermoperiostosis mimicking the acral abnormalities of acromegaly. *Endocrine* 2020 Jan 8. doi: 10.1007/s12020-019-02168-5. [Epub ahead of print]

Marques P, Korbonits M. Pseudoacromegaly. *Front Neuroendocrinol.* 2019; 52:113-143. doi: 10.1016/j.yfrne.2018.11.001.

Marques P, Tufton N, Bhattacharya S, Caulfield M, Akker S. Hypertension due to a deoxycorticosterone-secreting adrenal tumour diagnosed during pregnancy. *Endocrinol Diabetes Metab Case Rep* 2019. pii: EDM180164. doi: 10.1530/EDM-18-0164.

Dahlqvist P, Spencer R, Marques P, Dang M, Glad C, Johannsson G, Korbonits M. Pseudoacromegaly - a differential diagnostic problem for acromegaly with a genetic solution. *J Endocr Soc* 2017;1(8):1104-1109. doi: 10.1210/js.2017-00164.

Abstract

Non-neoplastic cells in the tumour microenvironment (TME) influence tumoural aggressiveness and oncogenic mechanisms. Little is known about the TME in pituitary adenomas (PAs). This work aimed to characterise the TME of PAs and its effects in tumour aggressiveness and oncogenic mechanisms, focusing on the cytokine network, infiltrating immune cells and PA-associated fibroblasts (TAFs).

To study the cytokine secretion of tumour/non-tumoural cells, cytokine bead arrays were performed on culture supernatants. PA-infiltrating immune cells, angiogenesis, epithelial-to-mesenchymal transition (EMT) and matrix metalloproteinases were assessed by immunohistochemistry. *In vitro* pituitary tumour–macrophage/TAF interactions were assessed by conditioned medium (CM) of GH3 (pituitary tumour) and RAW264.7 (macrophage) cell lines, as well as primary TAFs, in terms of morphology, migration, invasion and EMT activation.

IL-8, CCL2, CCL3, CCL4, CXCL10, CCL22 and CXCL1 were the main PA-derived cytokines, which facilitate macrophage, neutrophil and T lymphocyte recruitment. More FOXP3+ T cells, lower CD8:CD4 or CD8:FOXP3 ratios and deleterious immune phenotype ($CD68^{hi}CD4^{hi}FOXP3^{hi}CD20^{hi}$) correlated with tumour proliferation, whereas M2:M1 ratio correlated with microvessel density and area. Invasive PAs had higher TAF-derived IL-6 levels, whereas TAFs from PA with more vessels and increased proliferation secreted more CCL2, both inhibited by pasireotide. GH3 cell-CM increased macrophage chemotaxis, while macrophage-CM/TAF-CM changed morphology, migration, invasion and EMT in GH3 cells. These data support that different TME elements affect PA tumourigenesis and aggressiveness.

Data from different *in vitro* cell models suggest that AIP deficiency may not lead to differential cytokine secretion, and thus unlike to play a crucial role in the cytokine secretory function. The clinical study revealed that *AIP*mut and *MEN1*mut PA phenotypes are variable, including highly aggressive but also indolent cases such as prospectively-diagnosed *AIP*mut PAs, which are less aggressive and associated with more favourable clinical outcomes comparing to clinically-presenting *AIP*mut PAs, highlighting the benefits of *AIP* genetic and clinical screenings.

Table of contents

List of figures

List of tables

List of abbreviations

ACTH	adrenocorticotropic hormone
ADAM	a disintegrin and metalloproteinase domain
AIP	aryl hydrocarbon receptor-interacting protein
*AIP*mut	*AIP* mutation-positive
*AIP*neg	*AIP* mutation-negative
AHR	aryl hydrocarbon receptor
α-MSH	α-melanocyte-stimulating hormone
ARG1	arginase 1
ARNT	AHR nuclear translator
α-SMA	α-smooth muscle actin
AVP	arginine-vasopressin
BMP-4	bone morphogenetic protein-4
CABLES1	cdk5 and ABL enzyme substrate 1
cAMP	cyclic adenosine 3´5´-monophosphate
CDK	cyclin-dependent kinase
CDKI	cyclin-dependent kinase inhibitor
cDNA	complementary DNA
CM	conditioned medium
CNC	Carney complex
CRH	corticotrophin-releasing hormone
CT	cycle threshold
DAB	3.3´-diaminobenzidine tetrahydrochloride
DAPI	4',6-diamidino-2-phenylindole
DES	diethylstilbestrol
DMEM	Dulbecco´s Modified Eagle´s Medium
DNMT1	DNA methyltransferase 1
ECM	extracellular matrix
EGF	epithelial growth factor
ELISA	enzyme-linked immunosorbent assay
EMT	epithelial-to-mesenchymal transition
EpCAM	epithelial cell adhesion molecule
ESRP	epithelial splicing regulatory protein
FAP	fibroblast activation protein
FBC	full blood count
FBS	foetal bovine serum
FGF	fibroblast growth factor
FIPA	familial isolated pituitary adenoma
FLI-1	Friend leukaemia virus integration 1
FOXP3	forkhead box P3
FSH	follicle-stimulating hormone
FT4	free thyroxine
GAPDH	glyceraldehyde-3-phosphate dehydrogenase
GFAP	glial fibrillary acidic protein
GH	growth hormone
GHRH	growth hormone-releasing hormone
GLUL	glutamate-ammonia ligase
GM-CSF	granulocyte macrophage-colony stimulating factor
GNAS	guanine nucleotide-activating α-subunit
GnRH	gonadotrophin-releasing hormone
HIF-1α	hypoxia-inducible factor-1α
HPF	high power field
HSP90	heat shock protein 90
IGF-1	insulin-like growth factor-1
IFNγ	interferon gamma
IL	interleukin
IL-1ra	interleukin-1 receptor antagonist
iNOS	inducible nitric oxide synthase
JAK	janus-activated kinase
LCA	leukocyte common antigen
LH	luteinising hormone
LIF	leukaemia inhibitory factor
LMR	lymphocyte-to-monocyte ratio
MAPK	mitogen-activated protein kinase
MEN1	multiple endocrine neoplasia type 1
*MEN1*mut	*MEN1* mutation-positive
MEN4	multiple endocrine neoplasia type 4
MET	mesenchymal-to-epithelial transition
MIF	migration inhibitory factor
MMP	matrix metalloproteinase

MRI	magnetic resonance imaging
MVD	microvessel density
NCAM	neural cell adhesion molecule
NET	neuroendocrine tumour
NF-kβ	nuclear factor-kβ
NFPA	non-functioning pituitary adenoma
NLR	neutrophil-to-lymphocyte ratio
NP	normal pituitary
NK	natural killer
PA	pituitary adenoma
PBS	phosphate buffered saline
PCR	polymerase chain reaction
PDE2A	phosphodiesterase subtype 2A
PDE4A5	phosphodiesterase subtype 4A5
PDGF	platelet-derived growth factor
PD-L1	programmed death ligand 1
PERP	TP53 apoptosis effector
PHPT	primary hyperparathyroidism
PI3K	phosphatidylinositol 3-kinase
PIK3CA	phosphatidylinositol 3-kinase subunit p110α
Pit-1	pituitary-specific transcription factor 1
PKC	protein kinase C
PKP2	plakophilin 2
PLR	platelet-to-lymphocyte ratio
PMA	phorbol 12-myristate 13-acetate
pNET	pancreatic neuroendocrine tumour
PPIase	peptidyl-prolyl cis-trans isomerase
PRKAR1A	protein kinase A type 1α regulatory subunit
PRL	prolactin
RET	rearranged during transfection tyrosine-kinase receptor
ROBO1	roundabout axon guidance receptor homolog 1
RT-qPCR	real-time quantitative polymerase chain reaction
SD	standard deviation
SDF-1	stromal cell-derived factor-1
SDH	succinate dehydrogenase
SEM	standard error of the mean
SF-1	steroidogenic factor-1
SOCS	suppressors of cytokine signalling
SSA	somatostatin analogue
SST	somatostatin receptor
STAT	signal transducer and activator of transcription
TAF	tumour-associated fibroblast
TCDD	2,3,7,8-tetrachloro-*p*-dioxin
TGF	transforming growth factor
TIL	tumour-infiltrating lymphocyte
TME	tumour microenvironment
TMVA	total microvessel area
TNF	tumour necrosis factor
T-Pit	T-box transcription factor TBX19
TPR	tetratricopeptide-repeat
Tregs	T regulatory cells
TRH	thyrotrophin-releasing hormone
TSH	thyroid-stimulating hormone
ULN	upper limit of the normal
USP8	ubiquitin-specific protease 8
VEGF	vascular endothelial growth factor
XLAG	X-linked acrogigantism
yr	year
ZEB1	zinc finger E-box binding homeobox 1

Acknowledgments

I would like to acknowledge Barts and The London Charity for generously funding two years of my research and the Centre for Endocrinology, William Harvey Research Institute for supporting my third PhD year awarding me with the Joan Adams Fellowship. I'm also grateful to the Society for Endocrinology and to the Portuguese Society of Endocrinology, Diabetes and Metabolism who funded my participation in national and international conferences over the last 3 years, allowing me to present my research, to network with other colleagues and to identify new research directions.

I am especially thankful to Professor Márta Korbonits for the opportunity to integrate her research group and for her guidance, encouragement, support and availability, but also for her friendship, throughout these 3 years of my PhD. Márta is definitely the best mentor I could ever wish for, contributing enormously for my academic and clinical careers. I also would like to thank all the other colleagues and friends from the Centre for Endocrinology for their technical assistance, cooperation and dedication, particularly Dr David Collier, Dr Sayka Barry and Dr Edwin Garcia who helped me the most in mastering the different lab techniques and completing my research projects.

I would like to thank my second supervisor, Professor Frances Balkwill, for her support and guidance in my research. I also would like to express my gratitude to Professor Ashely Grossman for his positive influence in my PhD and for proofreading this thesis.

A special thanks to my first two mentors Professor Valeriano Leite and Professor Maria João Bugalho, who were determinant for my clinical training in Endocrinology and Diabetes in Portugal, but also an inspiration to pursue a career in science.

I am infinitely grateful to my fabulous wife Patricia for her love, support and patience, as well as to all my family and friends which were essential in the different stages of this journey.

Details of collaboration

Collaborations:

This work was supported by the Barts and The London Charity [Clinical Research Training Fellowship] and by the Centre for Endocrinology, William Harvey Research Institute and the Medical College of Saint Bartholomew´s Hospital Trust [Joan Adams Fellowship].

Dr Giulia Marelli (Barts Cancer Institute, London, UK) – provided the RAW 264.7 macrophages for cell culture experiments

Dr Leo Guasti (William Harvey Research Institute, London, UK) - provided the normal skin fibroblasts for cell culture experiments

Dr Hilde van Esch and Dr Wim Huybrechts (UZ Leuven Belgium, UK) - provided the *AIP* mutation-positive skin fibroblasts for cell culture experiments

Dr Oliver Haworth (William Harvey Research Institute, London, UK) - provided assistance with flow cytometry, as well as some reagents and antibodies for this experiment

Dr George Elia (Pathology Services, Barts Cancer Institute, London, UK) – performed the Ventana immunostainings

Dr Eivind Carlsen (Telemark Hospital Pathology Department, Skien, Norway) – provided assistance with the quantification of immunoreactivities

Dr Federico Roncaroli (Division of Neuroscience and Experimental Pathology, Faculty of Biology, Medicine and Health, University of Manchester, Manchester, UK) – provided critical input regarding immunohistochemical studies

Dr Daniela Magalhães (Centro Hospitalar de São João, Porto, Portugal) – collected the clinico-pathological data from the MEN1 patients included in the clinical study

Dr Sherine Awad (William Harvey Research Institute, London, UK) – performed the data deconvolution using the webtool xCell from Affymetrix microarray data generated previously by Dr Sayka Barry (William Harvey Research Institute, London, UK) as part of another study

Eve Technologies (Calgary, Canada) – performed the multiplex cytokine arrays

General aims of the study

1) To characterise the tumour microenvironment in pituitary adenomas and its role in the clinical phenotype and tumour aggressiveness, focusing on the cytokine network and infiltrating immune cells and their complex interaction

2) To characterise the cytokine secretome of pituitary adenoma-associated fibroblasts and study its role in the clinical phenotype and pituitary tumour aggressiveness, as well as its responsiveness to somatostatin analogues

3) To study the role of the cytokine network and infiltrating immune cells or pituitary adenoma-associated fibroblasts within the microenvironment of pituitary adenomas in the modulation of different oncogenic mechanisms

4) To investigate the role of AIP deficiency in the pituitary tumour cell cytokine secretome

5) To study the benefits of genetic and clinical screening of *AIP* mutation carriers by characterising prospectively-diagnosed *AIP*mut pituitary adenomas and compare to those with a clinical presentation

6) To characterise *AIP*mut and *MEN1*mut pituitary adenoma patients in general and by subtype and to provide a comparative analysis between *AIP*mut and *MEN1*mut pituitary adenomas

Chapter 1: Introduction

1.1 The pituitary gland

The pituitary gland, or hypophysis, is one of the most important glands of the endocrine system as it is involved in the regulation of other endocrine glands, such as thyroid, adrenals or gonads. The pituitary gland secretes different hormones that regulate numerous physiological processes such as growth, sexual development, reproduction, metabolism, thermoregulation, sleep, water balance, stress responses and adaptation to the external environment, among others[1].

Anatomy

The pituitary is a small gland with a size in adults of approximately 13 mm across by 3-9 mm in height and 9 mm in the anteroposterior depth; its weight ranges from 0.5 to 1.0 g, but it can be larger in younger individuals, in female adolescence or in pregnancy[2,3].

The pituitary is located in the sella turcica, a depression in the sphenoid bone of the skull[4], and covered superiorly by dura mater (the diaphragma sellae) through which the pituitary stalk passes, a structure composed of axons of the hypothalamic neuronal cell bodies and blood vessels connecting the hypophysis to the hypothalamus[5].

The lateral walls of the sella turcica are formed by the cavernous sinuses[6], which contain the internal carotid artery and the cranial nerves III, IV, V_1,V_2 and VI, and superiorly lies the optic chiasm (Figure 1.1)[7].

These anatomical relationships of the pituitary are critical in processes causing enlargement of the gland, such as a pituitary tumour, which may lead to significant mass effects: a tumour extending superiorly impinging on the optic chiasm may lead to visual deficits, most frequently bitemporal hemianopia, whereas a pituitary tumour extending laterally may cause oculomotor paralysis[8].

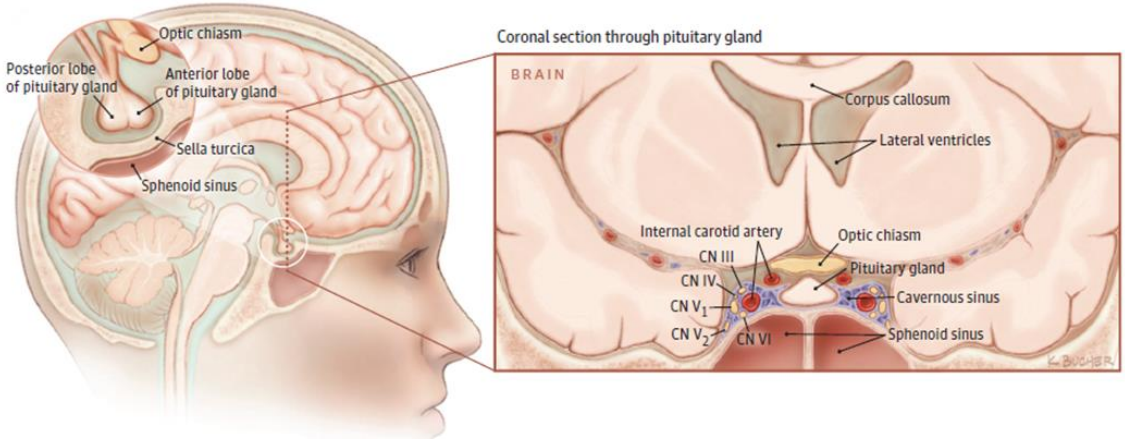

Figure 1.1: Anatomy surrounding the pituitary gland
CN, cranial nerve. Molitch (2017)[7].

Structure

The pituitary gland is divided into 2 main parts: the adenohypophysis (anterior pituitary) and the neurohypophysis (posterior pituitary). The adenohypophysis, originated from oral epithelia, is arranged in clumps or branching cords of cells separated by capillaries and sinusoids, and contains 5 main different hormone-secreting cell types: corticotrophs that produce adrenocorticotropic hormone (ACTH), gonadotrophs that produce luteinising hormone (LH) and follicle-stimulating hormone (FSH), thyrotrophs that produce thyroid-stimulating hormone (TSH), somatotrophs that produce growth hormone (GH), and lactotrophs that produce prolactin (PRL). A small subset of mammo-somatotrophs producing both GH and PRL is also recognised[9]. There are also non-hormone producing cells in the anterior pituitary, namely the agranular folliculo-stellate cells accounting for 5-10% of all adenohypophyseal cells which provide mainly mechanical support, but they also have other functions such as nurture of the secretory cells, phagocytosis of debris and apoptotic cells, regulation of ion balance and water transport[10,11]. The neurohypophysis, originating from the neural tissue of the forebrain, consists mainly of axons of hypothalamic neurons that secrete arginine-vasopressin (AVP) (or antidiuretic hormone) involved in the regulation of water balance, and oxytocin involved in social and biological behaviours as well as in uterine contractions during deliver and milk letdown[12]. A third pituitary lobe, termed the intermediate lobe, is recognised in other species, particularly in rodents, and it is regarded as a homogeneous area of melanotroph cells that synthesise peptide products of the proopiomelanocortin gene (α-melanotrophin or α-melanocyte-stimulating hormone (α-MSH)). However, in the human, only a vestigial fragment remains in adult life[12].

Function and regulation

The major role of the hypothalamus in the regulation of pituitary function was first recognised by Harris[13]. The pituitary hormones are secreted in a pulsatile manner, reflecting the fact that the pituitary is under the control of the nervous system through the hypothalamus. External stimuli, such as environment temperature, physical exercise, stress, nutrients, among others, lead to a secretion of specific hypothalamic releasing or inhibitory factors[5]. These hypothalamic factors are transported through the hypophyseal portal system and act on the surface receptors of adenohypophyseal cells. As a response, pituitary hormones are synthesised and secreted or inhibited[5,12]: corticotrophin-releasing hormone (CRH) and AVP induce ACTH secretion; thyrotrophin-releasing hormone (TRH) induces TSH secretion; GH secretion is stimulated by GH-releasing hormone (GHRH) and ghrelin and is inhibited by somatostatin; gonadotrophs have receptors for gonadotrophin-releasing hormone (GnRH) and when stimulated will produce variable amounts of LH and FSH, depending on the frequency and amplitude of GnRH pulses[14]; PRL is the only hormone that is not stimulated by a specific hypothalamic releasing factor (although in severe primary hypothyroidism TRH may lead to PRL secretion), but remains under the negative influence of dopamine[14,15].

The pituitary hormones are released by exocytosis of the storage granules and diffuse through the perivascular extracellular space to the blood vessels, and thereafter elicit specific responses in peripheral target tissues, mainly in endocrine glands: ACTH regulates cortisol and, in some extent, the androgen production by the adrenals; LH and FSH stimulate sex hormone production by the gonads, playing a key role in the regulation of the reproduction; TSH stimulates the production and release of thyroid hormones; GH targets different tissues directly or through the production of insulin-like growth factor-1 (IGF-1) in the liver, playing a crucial role in linear growth and in metabolic processes; PRL is the main regulator of lactation[5,12], but has also been involved in the maturation and regulation of the immune system[16-18].

The specific hormones produced by stimulated peripheral glands, in turn, will act via a feedback loop to control anterior pituitary function. There are mainly 2 mechanisms by which peripheral gland hormones regulate hypothalamus and pituitary functions: negative and positive feedback. The negative feedback, which is the main regulatory mechanism, is exerted by hormones released from the target glands: pituitary GH secretion is inhibited both by GH and by IGF-1; glucocorticoids secreted by the adrenals inhibit the secretion of both ACTH and CRH; TSH and TRH are negatively regulated by the thyroid hormones produced in the thyroid gland; FSH and LH are inhibited by a negative feedback of sex steroid hormones [5,12]. The positive feedback is less common, from which

the main example is the positive feedback exerted by oestrogens during the female menstrual cycle, resulting in the midcycle LH surge and ovulation[14].

1.2 Pituitary adenomas

Definition and epidemiology

Pituitary adenomas (PAs) are common tumours arising from adenohypophysis cells, accounting for 15% of all intracranial tumours, corresponding to the third most common intracranial neoplasm after meningiomas and gliomas[19]. The term pituitary neuroendocrine tumour has been suggested to replace the term PA, as it may reflect more accurately the complex biology and the clinico-pathological aspects of pituitary tumours[20], however this proposal is controversial and not supported by many authors[21]. The prevalence of PAs is high in autopsy and radiological studies, ranging from 14.4 up to 22.5%, but most have no clinical relevance[22]. In fact, up to 10% of PAs are discovered on imaging in asymptomatic or individuals previously unsuspected to have a pituitary lesion (pituitary incidentaloma)[23,24]. Clinically relevant PAs are less common, with a prevalence varying from 1:1064 up to 1:1470 in the general population[22].

The great majority of PAs are histologically benign; however, they can cause a significant burden to patients due to tumour mass effects on relevant surrounding structures and/or due to hypersecretion or hyposecretion of some or all (pan-hypopituitarism) pituitary hormones[7]. Pituitary carcinomas with distant metastasis or discontinuous intracranial extension are rare, accounting only for 0.1-0.2% of all pituitary tumours[25].

About two thirds of PAs may secrete pituitary hormones in excess[7,26], with the most common type being prolactinomas (prevalence ranges between 46.2-66.2%), followed by non-functioning PAs (NFPAs) (14.7-37%), somatotrophinomas (9-16.5%), corticotrophinomas (1.58-5.9%), and more rarely thyrotrophinomas (0-1.2%)[22,27-31].

Histopathological and clinical classifications

Following the 2017 WHO guidelines[32], PAs and their clinical syndromes are classified according to the type of endocrine cell they arise from and the hormone in excess: prolactinomas (PRL excess leading to galactorrhoea, amenorrhoea and other hypogonadal symptoms), TSH-secreting PA (secondary hyperthyroidism), ACTH-secreting PA (Cushing's disease), GH-secreting PA (acromegaly or gigantism), as well as LH/FSH-positive PAs, corresponding to most clinically NFPAs,

as these PAs, although histologically usually display immunoreactivity for LH and/or FSH, lack clinically relevant LH or FSH overproduction (occasionally measurable in the serum of NFPA patients), hence not leading to an sex hormone excess syndrome[33]; clinically active gonadotroph adenomas, leading to enlarged ovaries or testes, have been described but are rare[34]. Sometimes, however, clinically NFPAs do not stain for gonadotropins and demonstrate immunoreactivity for ACTH, TSH, GH or PRL (or for the corresponding transcription factors T-Pit (T-box transcription factor TBX19) and Pit-1 (pituitary-specific transcription factor 1) consistent with a well-differentiated lineage-specific adenoma[34] despite not oversecreting these hormones, thus referred to as "silent" corticotroph, thyrotroph, somatotroph or rarely lactotroph tumours, respectively[7,26]. Following this concept, the majority of clinically NFPAs are silent gonadotroph tumours expressing LH, FSH and/or their transcription factor SF-1 (steroidogenic factor-1). A very rare category that do not exhibit immunoreactivity for pituitary hormones or transcription factors is identified and termed as null-cell PAs[35].

PAs have been classified for years based on their histopathological features and hormone content assessed by immunohistochemistry and tumoural cells' ultrastructural features[36]. However, with the most recent 2017 WHO classification of pituitary tumours, the main principle guiding PA classification is the adoption of a pituitary adenohypophyseal cell lineage: acidophilic lineage (somatotroph, lactotroph and thyrotroph), corticotroph and gonadotroph lineages. The adenohypophyseal cell lineage differentiation is driven by transcription factors during the maturation of neuroendocrine cells from Rathke´s pouch, and shown to be expressed in PAs in a similar pattern to normal pituitary (NP). Thus, the classical immunohistochemistry for pituitary hormones, when appropriate, can be combined with immunostaining for pituitary transcription factors such as T-Pit, SF-1 and Pit-1 (Table 1.1)[32].

Pituitary adenoma type	**Morphological variants**	**Pituitary hormones**	**Transcription factors and other co-factors**
Somatotroph adenomas	Densely-granulated adenoma Sparsely-granulated adenoma Mammo-somatotroph adenoma Mixed somatotroph-lactotroph adenoma	GH ± PRL ± α-subunit GH ± PRL GH ± PRL (same cells) ± α-subunit GH ± PRL (different cells) ± α-subunit	Pit-1 Pit-1 Pit-1, ERα Pit-1, ERα
Lactotroph adenomas	Densely-granulated adenoma Sparsely-granulated adenoma Acidophilic stem cell adenoma	PRL PRL PRL, GH (focal and variable)	Pit-1, ERα Pit-1, ERα Pit-1, ERα
Thyrotroph adenomas		β-TSH, α-subunit	Pit-1
Corticotroph adenomas	Densely-granulated adenoma Sparsely-granulated adenoma Crooke´s cell adenoma	ACTH ACTH ACTH	T-Pit T-Pit T-Pit

Gonadotroph adenomas		β-FSH, β-LH, α-subunit (various combinations)	SF-1, GATA-2, ERα
Null-cell adenomas		None	None
Plurihormonal adenomas	Plurihormonal Pit-1 positive adenoma Adenomas with unusual immunostaining combinations	GH, PRL, β-TSH ± α-subunit Various combinations: ACTH+GH or PRL	Pit-1

Table 1.1: Classification of pituitary adenomas according to 2017 WHO classification
Adapted from Lloyd (2017)[32].

In the 2017 WHO classification of pituitary tumours, there are morphological variants recognised as potentially more aggressive due to their intrinsic histological features: sparsely-granulated somatotroph adenomas, silent corticotroph adenomas, Crooke´s cell adenomas (corticotroph adenomas composed mainly by cells with a ring-like deposition of cytokeratin) and plurihormonal Pit-1 positive adenomas[32].

Most of the PAs are monohormonal, but some may be plurihormonal (secreting 2 or more hormones, most commonly GH and PRL)[26]. Plurihormonal PAs may be monomorphous when there is one cell type producing more than one pituitary hormone, or plurimorphous consisting of 2 (or more) distinct cell populations each secreting different pituitary hormones[34].

PAs are classified according to their diameter into microadenomas (<10 mm), macroadenomas (≥10 mm) or giant adenomas (≥40 mm). Macroadenomas account for around 50% of all PAs[7].

Aggressiveness of pituitary adenomas

The definition of an aggressive PA varies in the literature, from that of a large invasive rapidly growing PA to a tumour with early recurrence despite optimal surgical or medical treatment[34,37]. In general, the concept of an aggressive PA entails an adenoma that deviates from the typical benign clinical behaviour[34]. Raverot *et al.* defined aggressive PAs as a "subset of non-metastatic invasive tumours displaying aggressive behaviour leading to multiple recurrences and resistant to conventional treatment including radiation therapy"[25]. Furthermore, the terms "aggressive" and "invasive" are often used interchangeably and synonymously to describe such cases[37].

To aid clinicians identifying such cases, in the 2004 WHO classification of pituitary tumours, apart from the benign "typical" adenomas and the aggressive pituitary carcinomas, identified a third category of clinically aggressive adenomas – termed "atypical adenomas" - as these tumours had

"atypical" morphological features, high mitotic index, Ki-67>3% as well as extensive p53 nuclear staining[36]. However, several studies demonstrated that not all atypical PAs were associated to aggressive clinical behaviour[38,39]. Hence, in the revised 2017 WHO classification of pituitary tumours, the term "atypical adenoma" has been abandoned: emphasis is still given to the evaluation of Ki-67 and mitotic count (but no specific cut-offs recommended) and in tumoural invasion of soft tissue or bone as determined radiologically or histopathologically[32].

Some radiological markers, as cavernous/sphenoid sinus invasion or bone erosion (Knosp[40] and Hardy[41] classifications), as well as histological markers (Ki-67, mitotic count, p53 staining, certain histiotypes such as Crooke´s adenoma, sparsely-granulated somatotroph adenomas or null-cell PAs) are regarded as indicators of aggressiveness[37]. Extensive research has identified different biological markers for PA aggressiveness, including chromosomal alterations, DNA aneuploidy, altered microRNAs, overexpression of growth factors and their receptors, alteration of factors related to angiogenesis (such as vascular endothelial growth factor (VEGF)) or to cell adhesion (matrix metalloproteinases, neural cell adhesion molecule (NCAM) or galectin-3), but no single biomarker independently predicts aggressiveness, and thus none is routinely used in clinical practice[37].

Aiming to determine the PA aggressiveness and predict the probability of post-operative complete remission, as well as to identify patients with high risk of early recurrence or progression, a new prognostic clinicopathological classification has been proposed[42,43]. This classification (Trouillas classification) is based on 3 main characteristics: tumour diameter given by MRI scanning, tumour type determined by immunocytochemistry (GH, PRL, ACTH, LH/FSH and TSH), and tumour grade determined by invasion defined as histological or radiological signs of cavernous or sphenoid sinus invasion and proliferation determined by p53 staining, Ki-67 and mitoses. Of these, evidence of invasion and the Ki-67 index are most important. Five grades are established: 1a: non-proliferative and non-invasive, 1b: proliferative but non-invasive, 2a: invasive but non-proliferative, 2b: invasive and proliferative, and 3: metastatic[43].

Pituitary tumourigenesis

PAs are believed to be monoclonal in origin, expanding from intrinsic molecular genetic abnormalities in a single somatic anterior pituitary cell (except folliculo-stellate cells)[44]. In early tumour clonality studies, through X-chromosomal inactivation analysis, the monoclonal origin of GH, PRL and ACTH-secreting PAs as well as in NFPAs was seen in female patients heterozygous for variant alleles of X-linked genes. PAs have only one X-inactivation type, paternal or maternal, and

never both[44-49]. PA monoclonality is supported by other findings: the tissue surrounding the PA normally has no hyperplasia features; complete resection may result in long-term remission; activating or inactivating mutations in hypothalamic hormone receptors are not common[26].

But why are the vast majority of pituitary tumours benign[50]? Cellular senescence has been suggested to explain the benign nature of PAs. Cellular senescence is an anti-proliferative response, induced by DNA damage, oxidative stress, age-linked telomere shortening, chromosomal instability and aneuploidy, loss of tumour suppressor genes or, paradoxically, by oncogene activation, which leads to irreversible cell cycle arrest. Senescent pituitary cells are growth-constrained by cell cycle inhibitors, and thus protected from deleterious consequences of oncogenes or transforming factors preventing malignant transformation[26,51,52], but the senescence pathway may not be universal for all PAs[53].

The majority of PAs occur sporadically (95%). Factors most commonly involved in the pituitary tumourigenesis are cell cycle deregulation, altered signaling pathways, epigenetically silenced tumour suppressor genes or overexpressed oncogenes, growth factors and hormonal overstimulation[26,45,54,55]. The role of environmental factors has also been suggested[56-58]. Acquired genetic or epigenetic changes confer an advantage to modified cells in terms of abnormal cell cycle activation, growth and proliferation, allowing monoclonal expansion. PAs have lower levels of somatic mutations compared to other tumours, but they frequently have cell cycle proteins and altered expression of growth factors, often due to epigenetic mechanisms[19].

Cell cycle protein expression abnormalities may be present in up to 80% of PAs[59]. The main cell cycle regulators are cyclin-dependent kinases (CDKs) and their inhibitors (CDKIs). CDKs are activated by cyclins promoting initiation and progression of the cell cycle[60-62]. In sporadic PAs, CDKIs are often downregulated as consequence of epigenetic alterations such as promoter hypermethylation or histone modification[63-66]. On the other hand, overexpression of cyclins has been documented in PAs[60,67-69]. Altered expression of other genes have been reported in PAs (Appendix 1). Growth factors, signal transduction mediators, such as protein kinase C (*PKC*) and phosphatidylinositol 3-kinase (PI3K) subunit p110α (*PIK3CA*)[70-72], and transcription factors, are commonly overexpressed in PAs (Appendix 1)[22,73-75]. The expression of microRNAs, small noncoding RNA involved in post-translational gene expression regulation[76], is often altered in PAs and may contribute to the pituitary tumourigenesis[51,76-78].

Genetic alterations in sporadic PAs include also somatic mutations typically in oncogenes, such as in the guanine nucleotide-activating α-subunit (*GNAS*) gene responsible for up to 40% of somatotrophinomas, or in ubiquitin-specific protease 8 (*USP8*) gene in corticotrophinomas

causing about 1 to 2 thirds of Cushing´s disease cases[26,79-81], or gene amplifications as in the *PIK3CA* found in up to 1 third of all PAs[71,82]. Mutations in tumour suppressor genes such as *TP53* and *RB1*, or in oncogenes such as *HRAS* and *MYC*, are rarely seen and exclusively found in aggressive PAs or carcinomas[51,71,83,84]. In particular, *HRAS* mutations were found mostly in carcinomas, which suggests that this must be important in malignant transformation rather than PA initiation[22,83].

PAs can also occur in the context of mosaic mutations, such as McCune-Albright syndrome and some patients with X-linked acrogigantism (XLAG). McCune-Albright syndrome is caused by *GNAS1* gene mutations occurring at a post-zygotic level (i.e. somatic) and characterised by the triad polyostotic fibrous dysplasia, café-au-lait skin pigmentation and precocious puberty, but also other endocrinopathies can be found, including acromegaly or gigantism[85] due to pituitary hyperplasia or GH-secreting PAs[86-88].

1.3 Familial pituitary adenomas (due to germline alterations)

Although most PAs occur sporadically, 5% of PAs occur in a familial setting, due to a germline genetic defect that predisposes to PAs, either isolated or as part of a syndrome (Figure 1.2)[19]. Despite their rarity, inherited PAs are important entities because they often present in younger patients, have a more aggressive course and are more refractory to therapy[51].

Syndromic presentation occurs in multiple endocrine neoplasia type 1 (MEN1), MEN4, Carney complex (CNC) and, more rarely, in *DICER1* syndrome and in familial phaeochromocytoma/ paraganglioma syndrome due to germline genetic abnormalities in the genes *SDH* (succinate dehydrogenase)[19] or *MAX*[89,90].

Familial isolated PAs (FIPA) can be observed in aryl hydrocarbon receptor-interacting protein (*AIP*) mutation-positive cases[91] and in XLAG syndrome due to *GPR101* duplications[92,93]. More recently, 4 patients with ACTH-secreting macroadenomas were identified with germline mutations in the Cdk5 and ABL enzyme substrate 1 (*CABLES1*) gene[94]. Germline mutations in the gene *CDH23*, encoding the cadherin-related 23 protein, were found in both familial and sporadic PAs, raising the possibility for its involvement in pituitary tumourigenesis[95].

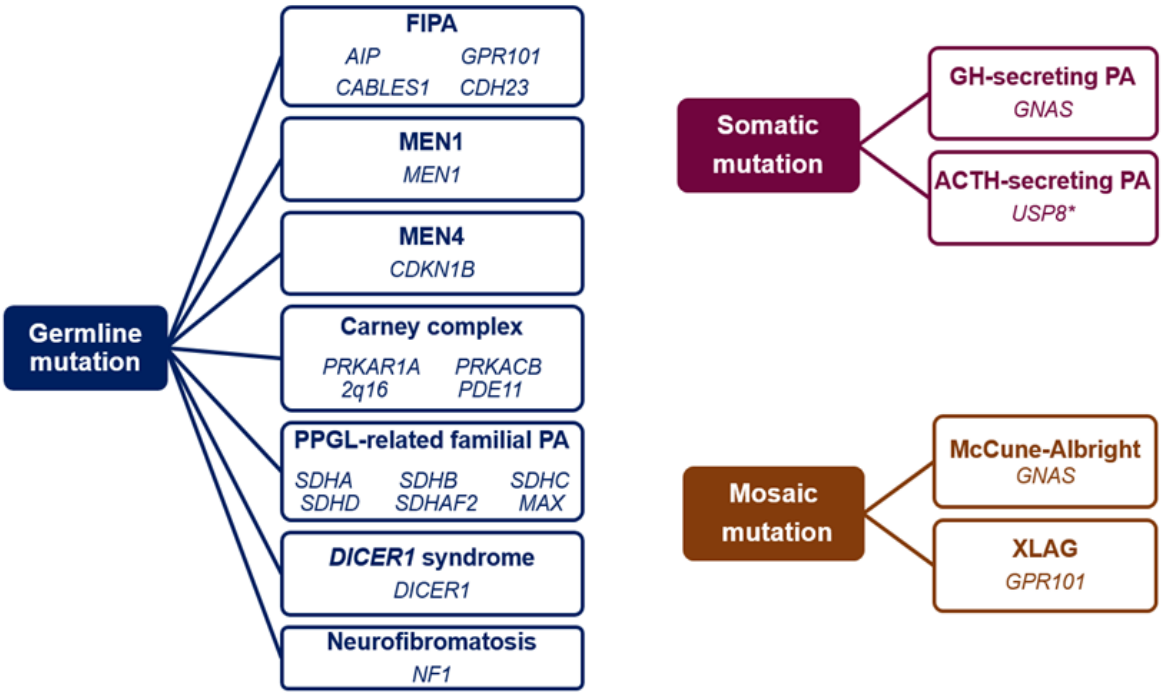

Figure 1.2: Pituitary adenomas due to a genetic origin
Adapted from Marques & Korbonits (2017)[19]. *There was a patient recently described with a *de novo* germline *USP8* mutation with recurrent Cushing´s disease and multiple other medical problems (developmental delay, dysmorphic features, ichthyosiform hyperkeratosis, chronic lung disease, chronic kidney disease, hyperglycaemia, dilated cardiomyopathy, hyperinsulinism and partial GH deficiency), suggesting that Cushing´s disease can also occur as part of an hereditary complex syndrome related to germline *USP8* mutations[96].

Syndromes predisposing to pituitary adenomas

Multiple Endocrine Neoplasia type 1 (MEN1)

MEN1 is an autosomal dominant disorder caused by mutations in the *MEN1* gene that predisposes mainly to primary hyperparathyroidism (PHPT), pancreatic neuroendocrine tumours (pNETs) and PAs, but other tumours can also occur such as adrenocortical tumours, thyroid tumours, lipomas, angiofibromas, meningiomas, gastric, thymic and bronchial neuroendocrine tumours (NETs)[97,98]. MEN1 diagnosis is established in a patient with 2 or more MEN1-associated tumours, in a patient with one MEN1-associated tumour and a first-degree relative with MEN1, or in a *MEN1* mutation (*MEN1*mut) carrier[97,98].

Clinical features

The prevalence of MEN1 is approximately 1:30,000 occurring in 1-18% of patients with PHPT, 16-38% of patients with gastrinomas and <3% of patients with PAs[97]. MEN1 penetrance is generally

high, with biochemical manifestations present by the 5th decade of life in 95% of cases. However, MEN1 penetrance depends on patient's age and gender and is organ-specific[98,99].

The penetrance of PAs in MEN1 is 30-40%, although can vary from 10 up to 76%[100-102]. The mean age at PA presentation is 38 years, but these can occur as early as the age of 5 or late in the 9th decade of life[98,103,104]. PAs are more common in females, which is as yet unexplained but it has been postulated that oestrogens may exert a proliferative stimulus leading to tumourigenesis[103,105] considering their stimulatory effects on pituitary lactotroph secretion and proliferation[106,107]. Prolactinomas are the most common PA subtype in MEN1, occurring in 60-70% of cases, followed by NFPAs (15-20%), somatotrophinomas (10%), corticotrophinomas (5%) and rarely thyrotrophinomas (<1%)[98,100-103,108]. *MEN1*mut PAs occur at younger age and are frequently more aggressive, bigger and refractory to treatment[97,103,109,110].

Genetic testing and clinical screening

MEN1 genetic analysis allow clinicians to confirm the diagnosis in a MEN1 patient and to identify other *MEN1* mutation-positive (*MEN1*mut) relatives who may benefit from appropriate screening and monitoring[98,111]. *MEN1* analysis should be undertaken in: i) index cases with 2 or more MEN1-asociated endocrine tumours; ii) asymptomatic first-degree relatives of a known *MEN1*mut carrier; iii) first-degree relatives of a *MEN1*mut carrier expressing familial MEN1; iv) individuals with suspicious or atypical MEN1 (PHPT before the age of 30 or multigland parathyroid disease, gastrinoma or multiple pNETs at any age, existence of two or more non-classical MEN1 tumours[98]). Patients with childhood-onset macroprolactinomas, especially if there is a positive family history of prolactinomas, should also be considered for genetic analysis[110,112]. *MEN1* analysis in asymptomatic individuals should be performed in the first decade of life, as there have been endocrine tumours reported by the age of 5 years[97,98,104].

MEN1 gene / menin protein

The *MEN1* gene encodes the menin protein and is regarded as tumour suppressor gene because heterozygous inactivating mutations predispose to neoplasia, and most MEN1-related tumours show loss of heterozygosity at 11q13[113,114]. Menin is ubiquitously expressed, predominantly located in the nucleus, and has several functions in transcription regulation, genome stability, cell division and cell cycle control, apoptosis and epigenetic regulation[97,108,115,116], as a result of its numerous interaction partners[97,117]. Menin interacts with activin in NP, negatively regulating cell

proliferation and secretion of PRL, GH and ACTH. Different proliferative factors in endocrine neoplasms are negatively modulated by menin, such as IGF binding protein-2, IGF-2 and parathyroid hormone-related protein[118,119]. Menin may also increase or decrease the expression of different genes[97,120]. Menin activates the transcription of *CDKN1B* and *CDKN1C*, genes predominantly expressed in endocrine organs, which can explain, at least in part, the selectivity of MEN1 tumourigenesis[121]. More recently, it was shown that MEN1 loss leads to activation of DNA (cytosine-5)-methyltransferase 1 (DNMT1) involved in DNA hypermethylation and driving MEN1-related tumourigenesis in endocrine tissues (but not in exocrine tissues)[117].

More than 1500 *MEN1* mutations are known, and they are distributed throughout the whole gene, involving coding regions and splice sites[115,122]. The majority of *MEN1* mutations are deletions or insertions resulting in frameshift or nonsense mutations, leading to truncation or absence of menin[115,123]. Most *MEN1* mutations are familial, but 10% of the cases occur due to *de novo MEN1* mutations[97,124]. The clinical phenotype of MEN1 patients, family members, even identical twins, or unrelated families, with the same *MEN1* mutation may differ[108,115,125]. A recent study involving 797 MEN1 patients from 265 kindreds reported significant intra-familial correlations for PAs, adrenal tumours and thymic NETs, estimating their heritability (proportion of the phenotypic expression that is attributable to gene effects) at 64%, 65% and 97%[126].

Multiple Endocrine Neoplasia type 4 (MEN4)

MEN4 is a rare autosomal dominant syndrome seen in patients with MEN1-like features but no mutations in the *MEN1* gene. Around 3% of patients with MEN1-associated tumours fulfilling the clinical diagnostic criteria for MEN1, but with no *MEN1* mutations, carry a germline mutation in the *CDKN1B* gene[97,116]. Mutations in other genes coding CDKIs have also been reported: p15 (*CDKN2B,* 1%), p18 (*CDKN2C*, 0.5%) and p21 (*CDKN1A,* 0.5%)[127]. A comprehensive MEN4 phenotype is not yet established due to the small number of cases identified thus far, but it seems to resemble the MEN1 phenotype which is likely explained by the known interactions between these CDKIs and the protein menin[97,116].

Carney complex (CNC)

CNC is a rare autosomal dominant multiple neoplasia syndrome caused mainly by an inactivating germline mutation in the protein kinase A type 1α regulatory subunit (*PRKAR1A*) gene, responsible for more than 70% of CNC cases[128]. A second genetic locus located at 2p16 has been also

associated with CNC, but the gene residing in this region remains unknown[129]. Moreover, duplications of the catalytic subunit gene *PRKACB* has been linked with CNC[130].

CNC manifestations include skin pigmentation alterations, blue nevus, myxomas (benign tumours of skin, breast, heart and other sites), non-endocrine (breast ductal adenomas, schwannomas, osteochondromyxomas) and endocrine tumours (thyroid, testis and adrenals), as well as somatotroph hyperplasia and PAs[131]. Cyclic adenosine 3´5´-monophosphate (cAMP) pathway upregulation affects somatotrophs and lactotrophs, with up to 75% of CNC patients displaying abnormal GH, IGF-1 or PRL levels, but PAs can be detected in only 10% of cases[132,133]. CNC-associated PAs are mostly GH or GH/PRL-secreting PAs, frequently multiple, small and surrounded by hyperplasia regarded as a putative precursor of PAs[131]. Acromegaly prevalence in CNC is estimated at 10-12%, and usually apparent by the third decade of life[128,131]. Pure prolactinomas[134,135] and Cushing´s disease[136,137] are very rare.

Phaeochromocytoma/Paraganglioma and Pituitary Adenoma syndrome

In 2006 a patient with PA and an *SDHB* mutation[138], and later in 2008 a patient with PA and a *SDHC* mutation-related paraganglioma were described[139]. The coexistence of these 2 diseases could be a coincidence, but loss of heterozygosity and immunohistochemistry studies confirmed the predisposition to phaeochromocytomas, paragangliomas and PAs in subjects carrying germline *SDHx* mutations[140-142]. *SDHx* mutation-positive PAs can be somatotrophinomas, prolactinomas or NFPAs, and are more commonly macroadenomas, aggressive and refractory to treatment[140,141,143].

Although the coexistence of PAs and phaeochromocytomas/paragangliomas is usually associated with *SDHx* mutations[144], pathogenic variants in the gene *MAX* (another predisposing gene for hereditary phaeochromocytomas/paragangliomas[145]) have recently been described in 4 patients with PAs (two with acromegaly and two with prolactinoma) and phaeochromocytomas/ paragangliomas[89,90].

DICER1 syndrome

DICER1 syndrome is a rare disorder caused by a heterozygous germline mutations in the *DICER1* gene that encodes a small RNA endoribonuclease that regulates RNA expression[146,147]. The main DICER1 syndrome manifestations are pleuropulmonary blastomas, cystic nephromas, Sertoli-Leydig cell tumours, goitre, and more rarely pituitary blastomas[148-150]. The first case of pituitary blastoma was described in a 13 month-old female who presented with Cushing´s disease and

diabetes insipidus. The "blastoma" designation was given to reflect the embryonic-primordial appearance and neonatal presentation[151], and is now recognised in the most recent 2017 WHO classification of pituitary tumours[32]. Pituitary blastoma is regarded as a pathognomonic feature of DICER1 syndrome and has low penetrance (<1%), but can behave aggressively, metastasising or being lethal in approximately 40% of the cases[146,147].

Familial Isolated Pituitary Adenomas (FIPA)

FIPA is a term used to describe the occurrence of a PA in 2 or more members of the same family in the absence of other syndromic clinical features, such as those characteristic of MEN1, MEN4 or CNC[152]. FIPA is a heterogeneous condition with significant differences in phenotype among the various subtypes. FIPA kindreds may have the same PA type among affected family members (homogeneous FIPA) or a mixture of different PA types (heterogeneous FIPA)[19]. Most of homogeneous FIPA kindreds consist of acromegaly (54% of homogeneous FIPA), followed by prolactinomas (27%) and NFPAs (17%), whereas heterogeneous FIPA kindreds have different PA types, with the acromegaly and prolactinoma combination being the most common phenotype[91].

Despite the numerous studies on PA pathogenesis in FIPA, the genetic aetiology for most of FIPA cases remains unknown. However, significant advances in this field have been made since 2006, when a linkage analysis study in 2 Finnish FIPA families identified a truncating germline mutation in the *AIP* gene (p.Q14*) as predisposing for PA - *AIP* mutation-positive (*AIP*mut) FIPA[19,153]. Isolated familial PAs can also be observed in XLAG due to *GPR101* duplications[93]. Whether *CABLES1*[94] and *CDH23*[95] gene can cause FIPA remains to be proven.

***AIP* mutation-positive FIPA**

Heterozygote loss-of-function germline *AIP* mutations are responsible for around 20% of all FIPA cases, with a prevalence up to 50% in families with only somatotrophinomas[19,152,154]. Up to 8% of apparently sporadic PA cases are due to an *AIP* mutation[91]. The *AIP* mutation prevalence is even higher in young patients (under the age of 30 years) with sporadic pituitary macroadenomas (12%) or in apparently sporadic pediatric PAs (20%)[155]. In fact, germline *AIP* mutations can be identified in seemingly sporadic cases due to the low penetrance of PAs, and therefore lacking a suggestive family history[19].

Clinical features

*AIP*mut FIPA patients present at a younger age and usually with large, invasive, functional PAs (mainly GH and/or PRL-secreting) and poorly responsive to therapy[19]. Clinical manifestations are related to hormone excess or mass effects, with gigantism being particularly frequent, representing over one third of *AIP*mut patients[91,92,152]. *AIP*mut patients are also at increased risk for pituitary apoplexy[91,156-158]. Most *AIP*mut PAs are macroadenomas (90%), commonly invasive and/or with extrasellar extension (>50%). Around 80% of these are GH- and/or PRL-secreting PAs, with some clinically NFPAs being found (although they often have GH and/or PRL immunoreactivity), while corticotrophinomas and thyrotrophinomas are rare[91,154]. *AIP*mut PAs are more aggressive than sporadic PAs[152]: they are more often sparsely-granulated[156] and have lower cellular AIP levels, a possible marker for PA invasiveness[159,160].

*AIP*mut PAs require a multimodal therapeutic approach often including more than one surgery. Prolactinomas often require surgery possibly due to reduced dopamine agonist responsiveness[161], and *AIP*mut somatotrophinomas are commonly resistant to somatostatin analogues (SSA), having lower GH/IGF-1 reductions and tumour shrinkage to SSA in comparison to *AIP* mutation-negative somatotrophinomas[155,156,161]. Interestingly, *AIP* is upregulated in sporadic somatotrophinomas treated with SSA prior to surgery, and the *AIP* expression may predict SSA responsiveness[162,163]. Sporadic PAs with low AIP were resistant to first-generation SSAs, while they had similar responsiveness to pasireotide in comparison to tumours with conserved AIP expression. Tumours with low AIP had reduced somatostatin receptor (SST) type 2 compared to normal AIP expressing PAs, but no differences regarding SST5 expression[164].

Genetic testing and clinical screening

Genetic screening is now available for selected patients with PAs (Figure 1.3). The detection of a germline mutation in the *AIP* or other PA-related genes will have major implications not only for the patient (namely in syndromic forms), but also for his/her relatives at risk of carrying the same genetic abnormalities and thus to develop the disease. The penetrance of PAs among *AIP*mut carriers is around 12-30%. Data from large families have shown an overall penetrance of 23%[91]. This relatively low penetrance of PAs among *AIP*mut carriers, together with their variable features, suggests the involvement of other disease-modifying genes or factors[165,166].

Genetic testing and clinical screening will allow the early detection of PAs in apparently unaffected subjects facilitating its management and avoiding some consequences of unrecognised PAs[19,167].

If a patient with a PA has a relative with a PA without associated syndromic features, the diagnosis of FIPA is made and genetic testing for *AIP* mutations could be offered[168]. Genetic testing for *AIP* is suggested in FIPA cases, childhood-onset PAs of any size, and young-onset (<30 years) macroadenomas even in the absence of family history of PA[167,168]. Recently, a risk categorisation system was proposed based on 4 independent predictors (age of onset, family history, GH excess and tumour size) aiming to aid clinicians identifying PA patients at higher risk for *AIP* mutation[169].

If an *AIP* mutation is identified in a kindred, genetic screening should be then offered to first degree family members, taking into account its autosomal dominant inheritance pattern. *AIP*mut carriers should undergo baseline assessments as approximately a quarter of subjects initially thought to be unaffected *AIP*mut carriers may have pituitary and/or biochemical abnormalities[91]. Clinical evaluation including monitoring of children growth, PRL and IGF-1 measurements, and a baseline pituitary MRI scan, is recommended[91]. If a PA is diagnosed prospectively in an apparently unaffected *AIP*mut carrier, its management should be similar as for sporadic PAs[23,170,171]. For unaffected *AIP*mut subjects, annual clinical assessment and pituitary function tests are recommended, as some PAs may emerge during follow-up[167].

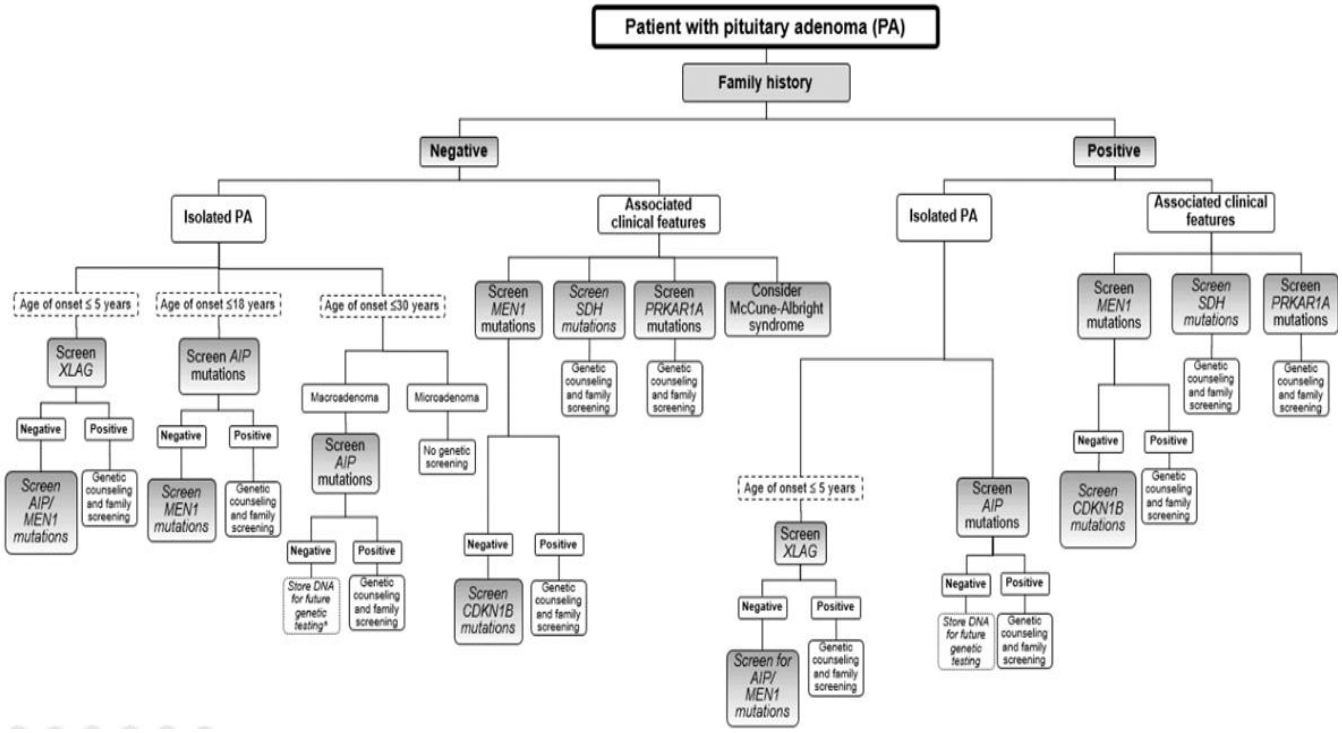

Figure 1.3: An approach to genetic testing in a patient with a pituitary adenoma
Marques & Korbonits (2017)[19].

AIP gene / protein

The *AIP* gene was first described in 1996 as an inhibitor of hepatitis B virus X protein-mediated transactivation[172]. Mapping the *AIP* gene in PA patients was a long process which started in 1993

when 4 non-MEN1 patients with acromegaly and loss of heterozygosity for chromosome 11q13 were reported[173]. This region was further narrowed in 1999[174], and later in 2005[175]. Interestingly, *MEN1* is located in this region, but as the phenotype is different and linkage analysis showed close by different location, the existence of a different gene was predicted. In 2006 Vierimaa *et al*. found linkage to chromosome 11q12-q13 by genotyping 2 large Finnish FIPA families[153], which turned out to be of the same genetic origin. *AIP* is located at chromosomal region 11q13.2, has 6 exons, and encodes the AIP protein with 330 amino-acids. The AIP protein is a co-chaperone that belongs to the group of proteins harbouring conserved C-terminal tetratricopeptide-repeat (TPR) domains of 34 amino-acids residues forming 2 palindrome α-helices. AIP contains 3 TPR domains and a final helix in the C-terminal region; the N-terminal has a peptidyl-prolyl cis-trans isomerase (PPIase)-like domain (Figure 1.4-A)[176-178].

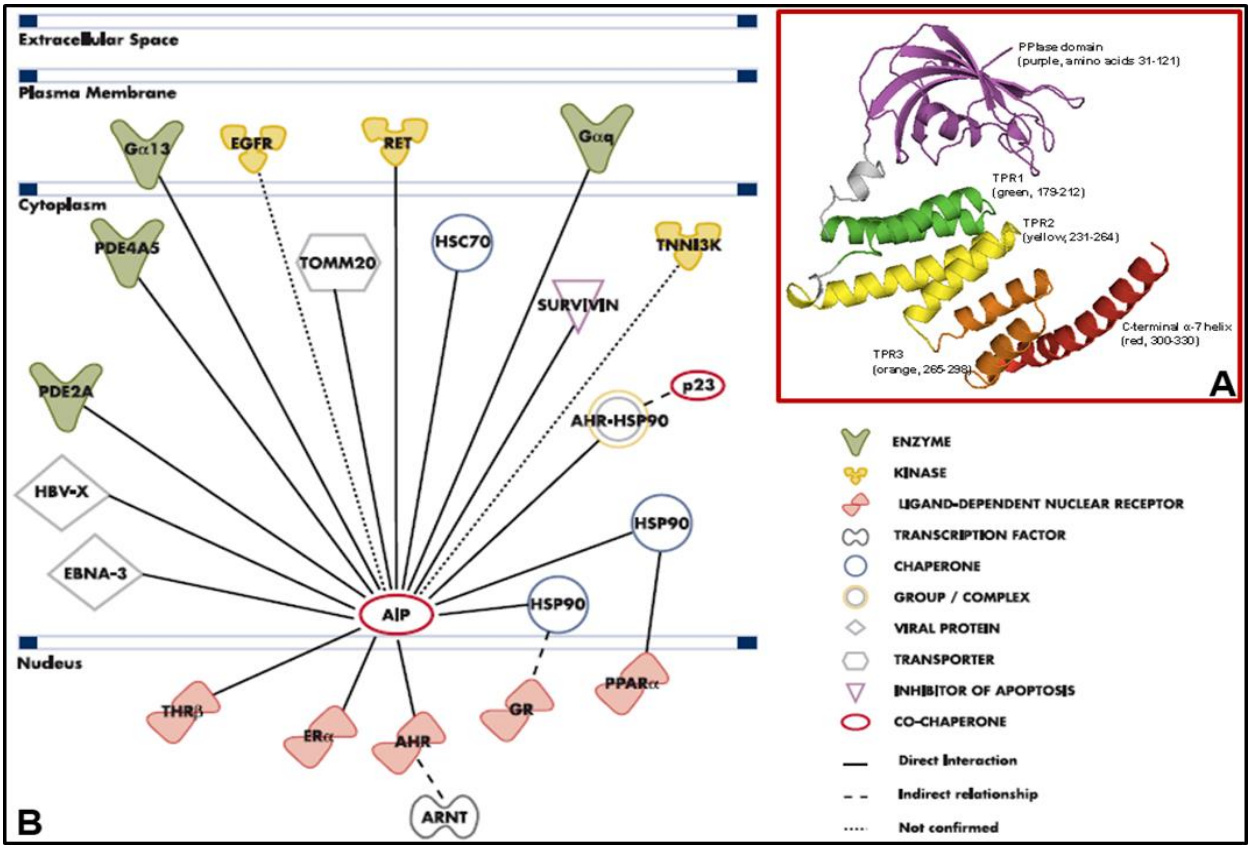

Figure 1.4: AIP protein structure (A) and interaction partners (B)
A) The most highly conserved residues are in the tetratricopeptide-repeat (TPR) domains, 3 antiparallel double helices and the final α-helix; the N-terminal has a peptidyl-prolyl cis-trans isomerases (PPIase)-like domain. B) AIP interaction partners and their functional class of protein. AIP, aryl hydrocarbon receptor interacting protein; AHR, aryl hydrocarbon receptor; ARNT, AHR nuclear translator; EBNA-3, Epstein Barr virus nuclear antigen 3; EGFR, epidermal growth factor receptor; ERα, estrogen receptor-α; Gα13, guanine nucleotide binding protein (G protein) α 13; Gαq, G protein α q peptide; GR, glucocorticoid receptor; HBV-X, hepatitis B virus X protein; HSC70, heat shock cognate 70; HSP90, heat shock protein 90; PDE, phosphodiesterase; PPARα, peroxisome proliferator-activated receptor-α; RET, rearranged during transfection tyrosine kinase receptor; THRβ, thyroid hormone receptor-β; TNNI3K, cardiac troponin-I interacting protein kinase; TOMM20, mitochondrial import receptor subunit TOM20 homolog. Adapted from Aflorei *et al.* (2018)[178], and Beckers *et al.* (2013)[152].

AIP is ubiquitously expressed in both developmental and adult stages, with some variation among different tissues, but is particularly concentrated in heart, brain, skeletal, liver, muscle, kidney, testis, ovary and pituitary[172,176]. At the cellular level AIP is predominantly located in the cytoplasm, but nuclear expression has been reported. In NP, *AIP* is expressed predominantly in somatotrophs and lactotrophs, normally within cytoplasmic secretory vesicles, but is absent in normal corticotrophs and gonadotrophs. In sporadic PAs, AIP is expressed in all types: in sporadic somatotrophinomas AIP co-localises with GH in secretory vesicles, but in sporadic prolactinomas, NFPAs and corticotrophinomas AIP resides in the cytoplasm[156].

AIP involvement in pituitary tumourigenesis

Several binding partners of the AIP protein have been identified: aryl hydrocarbon receptor (AHR), heat shock protein 90 (HSP90), phosphodiesterase subtype 4A5 (PDE4A5), PDE2A, heat shock cognate 70, survivin, peroxisome proliferator-activated receptor-α, thyroid hormone receptor β1, oestrogen receptor-α, Epstein-Barr virus-encoded nuclear protein-3, hepatitis B virus X protein, rearranged during transfection tyrosine-kinase receptor (RET), along with many other proteins (Figure 1.4-B)[152,176]. Thus, *AIP* inactivation may interfere with several cell and environmental signals.

The best known AIP binding partner is AHR, which is a ligand-activated transcription factor. It was originally described as the mediator of the toxic effects of the environmental toxin 2,3,7,8-tetrachloro-*p*-dioxin (TCDD), but endogenous ligands have been described since. Upon TCDD binding, the cytoplasmic AHR+AIP+HSP90 complex is translocated to the nucleus, where AHR is released from the complex and creates a dimer with AHR nuclear translator (ARNT) to bind to xenobiotic response element regions of DNA. The role of AHR may include regulation of the activity of other nuclear receptors, transcription factors and protein kinases, leading to changes in cell cycle, adhesion, migration and intracellular signaling[152,177]. However, AHR involvement in pituitary tumourigenesis is unclear. AHR knockout mice do not develop PAs[179-182]. AHR promotes the cell cycle in the absence of ligand binding[183] and interacts with cyclin D1 and CDK4 in breast cancer cells [184]. *AIP*mut PAs have decreased AHR and ARNT levels, whereas the AHR repressor is overexpressed in sporadic somatotrophinomas[185,186]. Genetic variants in AHR pathway might be associated with larger somatotrophinomas and SSA resistance in polluted areas[56], but further studies are needed to confirm these data.

cAMP-PKA pathway disruption is important for somatotroph tumourigenesis as seen in CNC and McCune-Albright syndrome[85]. AIP interacts with PDE4A5, an enzyme involved in the inactivation

of cAMP, and *AIP* mutations lead to the loss of this AIP-PDE4A5 interaction[156,187]. AIP deficiency causes a dysfunction in cAMP signalling, elevating cAMP concentrations through defective Gαi-2 and Gαi-3 proteins, which normally inhibit cAMP synthesis. Additionally, immunostaining of Gαi-2 showed that AIP deficiency is associated with decreased Gαi-2 protein expression in human and mouse GH-secreting PAs highlighting a defective Gαi signaling. Thus, failure to inhibit cAMP synthesis through dysfunctional Gαi signaling may explain the development of *AIP*mut somatotrophinomas[188]. There are other mechanisms potentially involved in *AIP*-related pituitary tumourigenesis (Figure 1.4-B), particularly those related to the *Survivin* and *RET* pathways[189].

It is postulated that in *AIP*mut PAs, AIP loses the ability to bind its partners, and thus loses its activity as tumour suppressor[152,154,176]. The role of *AIP* as tumour suppressor gene is supported by the association of several loss-of-function mutations with the development of PAs and the presence of loss of heterozygosity in 11q13 in *AIP*mut PAs[19]. Heterozygote *AIP* knockout mice develop GH-secreting PAs, with 100% penetrance by the age of 18 months, which differs from the wild-type mice where only around one third spontaneously developed prolactinomas but no somatotrophinomas[190]. Moreover, *AIP* overexpression decreases cell proliferation while *AIP* knockdown increases[156,162,185,186], with *AIP*mut PAs displaying low AIP expression[156,186]. Enhanced proteasomal degradation is one of the pathogenic mechanisms for most *AIP* missense mutations and the nonsense p.R304* mutation[191].

More than 100 *AIP* gene variants are described, including insertions, deletions, single nucleotide polymorphisms, nonsense and missense mutations, duplications, promoter and splice-site mutations and large genomic deletions. Truncating mutations account for most *AIP* mutations, and around 70% of all known *AIP* mutations cause a disruption in the C-terminus[91,152]. The most common mutation site is p.R304 locus (R304*)[91,152]. The R304* site is a mutational hotspot and has been identified independently in several countries. One of these represent a founder mutation in Ireland[192], as the same haplotype including the p.R304* mutation was found in several Irish families, including in a 'giant' from the 18th century[192,193]. Other hotspots are in codons R81 and R271[110,153,194,195].

GPR101 duplication in X-linked acrogigantism

X-linked acrogigantism (XLAG) syndrome was identified in patients with very young-onset gigantism and PA or hyperplasia[93], and is responsible for 10% of pituitary gigantism cases[92,196]. XLAG is caused by microduplications of the orphan G-protein coupled receptor *GPR101* located at the Xq26.3 locus[93]. Most patients with XLAG syndrome have been reported as having sporadic *de*

novo duplications with a few having familial germline Xq26.3 microduplications[196-198]. In addition, mosaic mutations have been described in males[92,198,199].

XLAG syndrome clinical features are striking, with the cardinal manifestation being rapid growth (gigantism) starting at a very early age, between the age of 1-24 months[92,196,197]. Other features include: acral enlargement, coarsen facies, increased appetite, and less frequently sleep apnea, hyperhidrosis, acanthosis nigricans and/or abdominal distension[196,197,200].

Patients with XLAG may develop pituitary macroadenomas, but some have isolated hyperplasia or hyperplasia combined with PA, together with marked GH and IGF-1 elevations. Hyperprolactinaemia accompanies GH elevations in 85% of cases[92]. Histologically, most XLAG-related PAs are mixed somatotroph and lactotroph adenomas containing both densely and sparsely granulated somatotrophs, and usually have a low Ki-67 and negligible mitotic counts[92].

CABLES1 mutation-positive FIPA

Four out of 181 (2.2%) patients with Cushing´s disease due ACTH-secreting PAs were identified with germline mutations in *CABLES1* gene[94]. Although further studies are needed to establish the role of *CABLES1* gene in corticotrophinomas, it has been postulated that *CABLES1* is a tumour suppressor gene that negatively regulates cell cycle by inactivating several CDKs and may also interfere with the signalling pathway of the epidermal growth factor (EGF)[94,201]. All 4 reported patients were affected with large corticotrophinomas with a high Ki-67 and difficult to manage[94].

CDH23 mutation-positive FIPA

Recently, germline mutations in the *CDH23* gene, encoding the protein cadherin-related 23 which display functions in cell-cell interactions and adhesion, were associated with familial and sporadic PAs, suggesting the involvement of *CDH23* in the PA pathogenesis. A kindred with 4 members with PAs and 17 asymptomatic members underwent whole-exome sequencing, which identified the co-segregation of PA phenotype with a heterozygous *CDH23* missense mutation, predicted to impair cell-cell adhesion. Genomic screening was then performed in 12 FIPA families, in 125 patients with sporadic PAs and in 260 healthy controls, with functional *CDH23* variants being identified in 33, 12 and 0.8% of the cases in each group, respectively[95]. However, *CDH23* is a large gene associated with the Usher syndrome leading to deafness and none of the patients reported had deafness[202]; there is no known association between deafness and PAs, thus further research focusing on this genetic defect is needed.

FIPA with undetermined genetic cause

AIP mutation-negative (*AIP*neg) FIPA display age of onset similar to sporadic PAs, while tumour behaviour is often more aggressive. The penetrance is incomplete, even lower than in *AIP*mut kindreds. The distribution of PAs types in *AIP*neg FIPA kindreds is heterogeneous (Figure 1.5)[19].

Genetic and clinical screening of *AIP*neg PA families is controversial. Several PAs have been prospectively-diagnosed in *AIP*neg FIPA families, thus education for PA symptoms should be given, and eventually baseline screening and follow-up can be considered in some cases. As PA are relatively common, there is a possibility that some *AIP*neg FIPAs might be coincidental[203] or due to unknown complex pituitary-related mutant gene(s)[19].

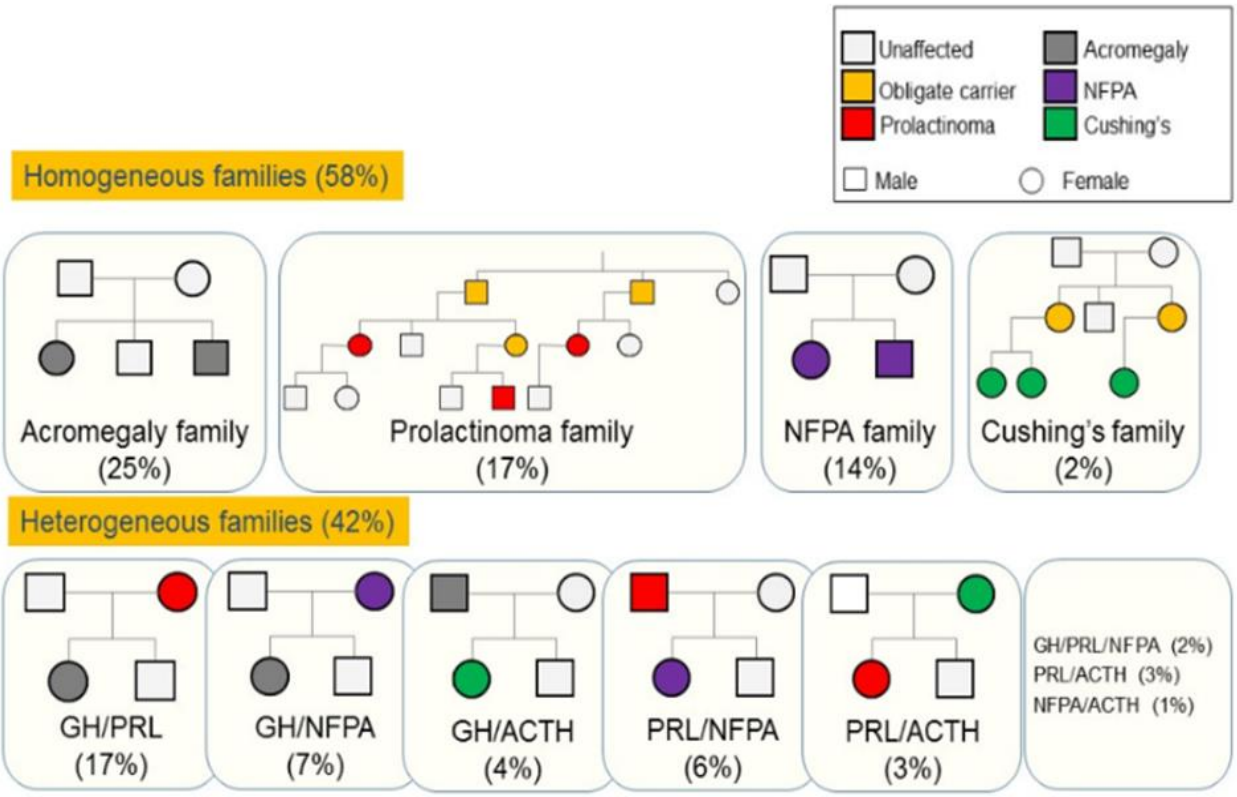

Figure 1.5: Distribution of PA types in *AIP*neg FIPA kindreds
Examples of the most commonly found *AIP* mutation-negative FIPA family trees, with representative percentage proportions in a cohort of 179 *AIP*neg kindreds. Adapted from Marques & Korbonits (2017)[19].

1.4 Tumour microenvironment (TME)

Tumours are more than just a mass of malignant cells, but rather they are a complex and heterogeneous conjunction of tumour and non-tumoural cells (such as immune and stromal cells), together with enzymes, growth factors and cytokines within the local extracellular matrix (ECM), which form the basis of the so-called tumour microenvironment (TME) (Figure 1.6)[204].

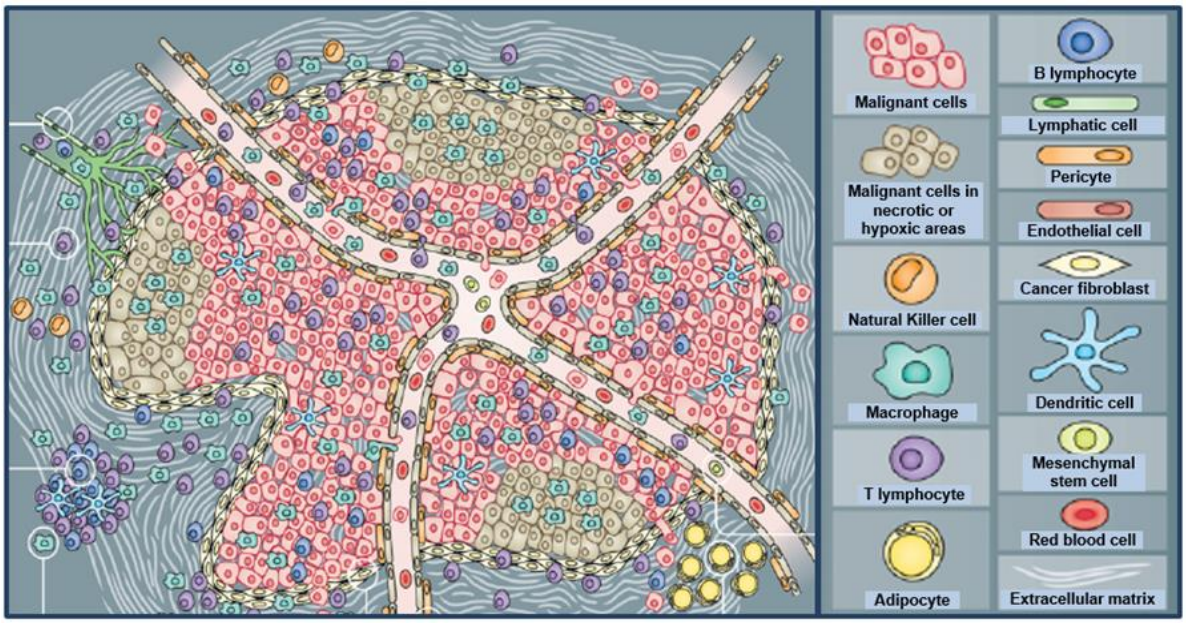

Figure 1.6: The tumour microenvironment
Adapted from Balkwill *et al.* (2012)[204].

The TME concept emerged in 1989, when Stephen Paget proposed the "seed and soil" theoretical hypothesis based on his observations, on an autopsy series of 735 breast tumours, in which 32.8% of patients had liver metastasis and only 2.3% had spleen metastasis[205]. This non-random pattern of metastasis suggested that some tumours have a specific affinity for certain organs. Paget described tumour cells (with metastatic ability) as the "seed" and the host microenvironment (organs providing advantage for "seeds to grow") as the "soil", and their interaction crucial for disseminated tumour cells to grow[205]. A current perspective of "seed and soil" hypothesis includes three principles: 1) neoplasms consist of both tumour and host cells, which are heterogeneous and contain populations of cells with different metastatic properties; 2) the metastatic process is selective, favouring growth and survival of a cell population from primary neoplasm; 3) metastases can only develop in specific organs, given that the TME from different organs ("soil") are biologically unique, and may influence behaviour of metastases[206].

TME has emerged as a key modulator of tumour initiation, progression, invasion and therapy responses[207,208]. The TME is determined by the surrounding cells including inflammatory (such as

macrophages or lymphocytes), stromal (such as fibroblasts), endothelial cells and pericytes (Figure 1.6), and is well-known that tumour cells and non-tumour cells influence each other[207]. The communication between different cells in the TME is driven by a complex network of cytokines, growth factors and matrix-remodelling enzymes[204,209-211]. In cancer, cytokines and chemokines and their receptors are essential TME elements, promoting cell trafficking and contributing to the phenotype of tumour-associated immune and stromal cells, angiogenesis, invasion and metastatisation processes[209].

1.5 The cytokine network in pituitary adenomas

Cytokines: structure, receptors, pathways, biological functions and role in cancer

Cytokines are soluble peptide mediators controlling autocrine or paracrine communications within and between individual cell types, playing important roles in immunity, inflammation, repair, cell growth and differentiation, as well as in tissue homeostasis[212]. Cytokines are small (around 150 amino-acids) but extremely potent peptides, pleiotropic in nature, meaning that they are produced by different cells and act on multiple cell types (Table 2). Another recognised cytokine property is redundancy, i.e. multiple cytokines can exert similar actions[213]. Cytokines may act, in paracrine or autocrine ways, on the same cells in which they are produced[214]. Cytokines are generally produced by haematopoietic or inflammatory cells, but other cell types can also produce them including cells of the endocrine system[215]. Cytokines are secreted or expressed directly in the cell membrane or accumulate in the ECM. Cytokine expression is usually induced by infectious agents, toxic stress, or other stress-induced molecules, and may occur both transcriptionally as well as by precursor processing[216]. However, cellular cytokine reservoirs cytoplasmic granules are available for rapid release in response to stimulation[216].

Cytokines are traditionally classified regarding their immune response nature, i.e. grouped by their pro-inflammatory or by their anti-inflammatory actions on adaptive immune system cells (Table 1.2)[213,217,218]. Cytokines can also be classified according to their main source, target cells or their specific roles (Table 1.2)[213,217]. T lymphocytes, namely those expressing CD4 (known as T helper cells), are a crucial source of cytokines during inflammatory processes. T-cell derived cytokines are often categorised as Th1 or Th2 cytokines depending on their effect in inflammatory responses: Th1 cytokines, such as interferon gamma (IFNγ) and interleukin (IL)-2, are pro-inflammatory, leading to neutrophil/macrophage activation, viral immunity by killing intracellular parasites and perpetuating inflammation; Th2 cytokines (IL-4, IL-5, IL-10, IL-13) are anti-inflammatory, counteracting Th1 responses, and they are also associated to humoral responses[213,217].

Classification of cytokines by immune response				
Immune response		**Members**		
Adaptive immunity		IL-2, IL-3, IL-4, IL-5, IL-7, IL-9, IL-13, IL-15, IL-21, GM-CSF, G-CSF, M-CSF, EPO, TSLP		
Pro-inflammatory signalling		IL-1 (IL-1α, IL-1β, IL-1ra), IL-6, IL-11, IL-17A, IL-18, IL-25, IL-31, IL-33, IL-36, IL-36ra, IL-37, IFNα, IFNβ, IFNγ, IFNλ, IFNκ, TNFα, TNFβ, CNTF, CT-1, LIF, OPN, OSM, Limitin		
Anti-inflammatory signalling		IL-10, IL-12, IL-19, IL-20, IL-21, IL-22, IL-24, IL-26, IL-27, IL-28, IL-29, IL-35		
Classification of cytokines by main source, target cell and primary function				
Family	**Cytokine**	**Main source**	**Target cell**	**Primary function**
Interleukins	IL-1	M, DC, B cells	B, NK and T cells	Pyrogenic, pro-inflammatory, proliferation, differentiation, angiogenic
	IL-2	T cells	B, NK and T cells	Proliferation, cell activation (Th1 cytokine)
	IL-3	T cells, NK cells	B and T cells, SC	Haematopoietic precursor proliferation and differentiation
	IL-4	Th cells	B cells, T cells, M	Proliferation of B and T cells, stimulation of IgG and IgE production, enhances MHC class II expression
	IL-6	Th cells, fibroblasts, M	Activated B cells, plasma cells	Differentiation into plasma cells, IgG production, pro-inflammatory, proliferation (Th1 cytokine), angiogenic
	IL-7	BM stromal cells, EC	SC	B and T cell growth factor, thymocyte growth, survival T cells, haematopoiesis
	IL-8	M	Neutrophils	Chemotaxis, pro-inflammatory
	IL-9	T cells	T cell	Cell growth and proliferation
	IL-10	T cells	M, B cells	Inhibits cytokine production and mononuclear cell function, anti-inflammatory (Th2 cytokine)
	IL-11	BM stromal cells	B cells	Differentiation, induction of acute phase proteins
	IL-12	T cells	NK cells	Activation of NK cells, pro-inflammatory (Th1 cytokine)
	IL-13	T cells	M, B cells	Inhibits cytokine production and mononuclear cell function, anti-inflammatory (Th2 cytokine)
	IL-15	Monocytes	T, NK and mast cells	Mast cell growth, NK cell development and activity, T cell proliferation
	IL-18	T cells	B, NK and T cells	Proliferation, cell activation (Th1 cytokine)
	IL-21	T cells	B cells	Inhibits B cell proliferation
Tumour necrosis factors	TNF-α	M, monocytes	M, tumour cells	Phagocyte cell activation, endotoxic shock, Tumour cytotoxicity
	TNF-β	T cells	Phagocytes, tumour cells	Chemotaxis, phagocytosis, oncostatic, induction of other cytokines
Interferons	IFN-α	Leukocytes	Various	Anti-viral, anti-angiogenic
	IFN-β	Fibroblasts	Various	Anti-viral, anti-proliferative, anti-angiogenic
	IFN-γ	T cells	Various	Anti-viral, macrophage activation, increase neutrophil function, increase expression of MHC
Colony stimulating factors	G-CSF	Fibroblasts, endothelial cells	SC in BM	Granulocyte production
	GM-CSF	T cells, M, fibroblasts	SC in BM	Granulocytes, monocytes and eosinophils production
	M-CSF	Fibroblasts, endothelial cells	SC in BM	Monocyte production and activation
	EPO	Endothelial cells	SC in BM	Red blood cell production

Others	TGF-β	T and B cells	Activated T and B cells	Inhibit T and B cell proliferation, inhibit haematopoiesis, promotes fibrosis and wound healing
	FGF	Various	Fibroblasts	Angiogenic, promotes fibrosis and wound healing, cell proliferation and differentiation, fibroblast proliferation
	VEGF	Various	Endothelium	Angiogenic, lymphangiogenesis, chemotaxis

Table 1.2: Classification of cytokines
BM, bone marrow; CNTF, ciliary neurotrophic factor; CT-1, cardiotrophin-1; DC, dendritic cells; EC, epithelial cells; EPO, erythropoietin; FGF, fibroblast growth factor; G-CSF, granulocyte-colony stimulating factor; GM-CSF, granulocyte macrophage-colony stimulating factor; IFN, interferon; Ig, immunoglobulin; IL, interleukin; LIF; leukaemia inhibitory factor; M, macrophage; M-CSF, macrophage-colony stimulating factor; MHC, major histocompatibility complex; NK, natural killer; OPN, osteopontin; OSM, oncostatin; SC, stem cells; TGF, transforming growth factor; TNF, tumour necrosis factor; TSLP, thymic stromal lymphopoietin; VEGF, vascular endothelial growth factor.

Cell surface cytokine receptors belong to the tyrosine kinase receptors family, usually grouped in 4 large families of receptors (types I-IV)[214], which are linked to intracellular pathways that impact on nuclear transcriptional events[213]. Several cytokine pathways are described[213,218], with janus-activated kinase (JAK)-signal transducer and activator of transcription (STAT), nuclear factor-kβ (NF-kβ) or hypoxia-inducible factor 1α (HIF-1α) pathways being particularly relevant in cancer and inflammation (Figure 1.7-A)[210,219]. In cancer, cytokines coordinate host responses against cancer, but also they can promote tumour growth, invasion, neovascularisation, ECM remodelling, host immunosuppression and survival of tumour cells (Figure 1.7-B)[212,220-222].

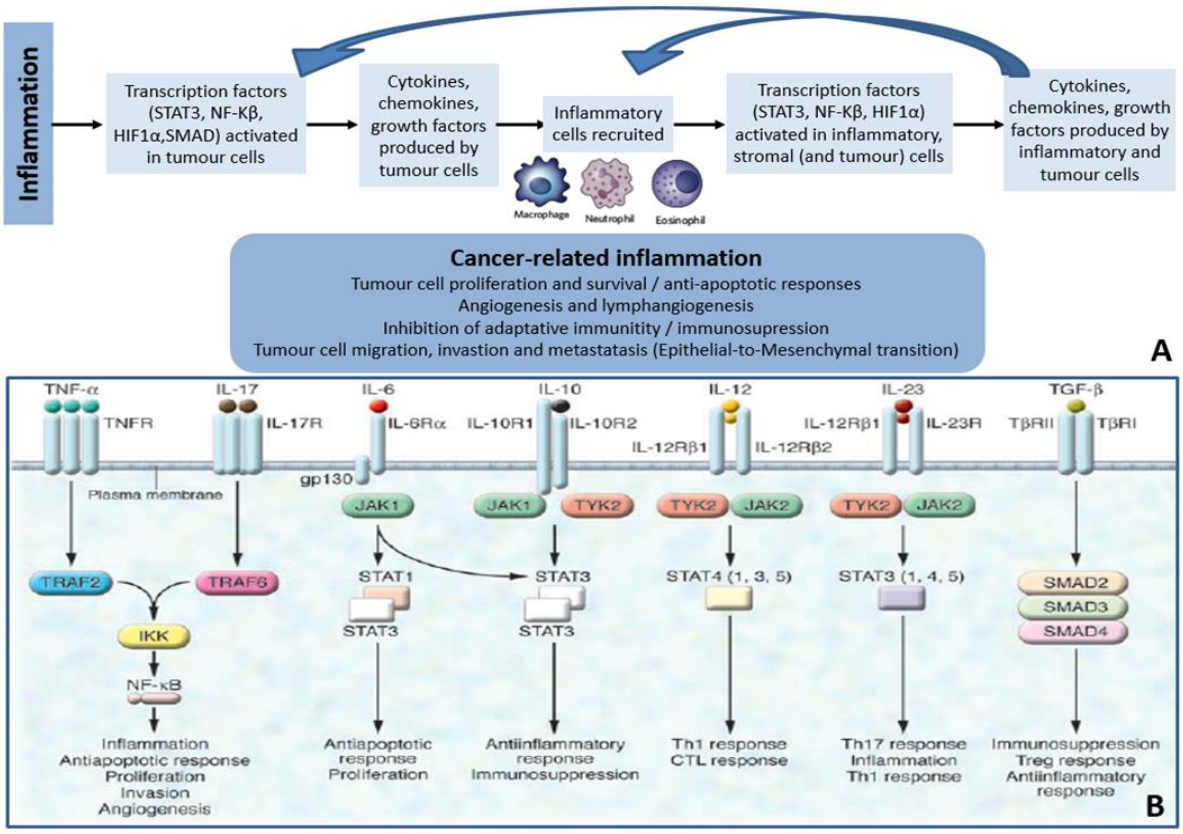

Figure 1.7: Relationship between cytokines, inflammation and cancer
A) Connections between inflammation and cancer. Chronic inflammation and/or inflammatory cells may induce a transformation in the epithelial cells, including leading to a genetic event that cause neoplasia (such as oncogene activation by mutation, chromosomal rearrangement or amplification, or also tumour suppression genes inactivation). Tumour cells acquire specific properties including the capacity to produce inflammatory mediators (cytokines, chemokines and growth factors), thereby generating/modulating the inflammatory surrounding tumour microenvironment (TME). Following activation of certain transcription factors, mainly the JAK-STAT, NF-kβ and hypoxia-inducible factor 1α, cytokines are produced and secreted in the TME, and in turn they can themselves stimulate transcription of such factors amplifying the cancer-related inflammatory and subsequently tumour cell behaviour and aggressiveness. B) Signal transduction pathways and major biological responses of inflammation-modulating cytokines in cancer. The pathways shown in the figure are some of the main cytokine-related cancer signalling pathways and demonstrate how cytokines can control tumour development, either directly in tumour cells or indirectly through immune or endothelial cells. gp130, glycoprotein 130; IKK, Ikβ kinase; JAK, Janus activated kinase; NF-kβ, nuclear factor-kβ; STAT, signal transducer and activator of transcription; TRAF, TNF receptor–associated factor 2; TYK2, tyrosine kinase 2. Adapted from Mantovani *et al.* (2008)[222] and Lin & Karin (2007)[219].

Chemokines: structure, receptors, pathways, biological functions and role in cancer

Chemokines are a group of small cytokines that act together with their cell surface receptors in normal physiology and immune responses, directing cells to specific locations in the body. Chemokines control the movement of immune and non-immune cells, immune system development, normal haematopoiesis, cell growth, neovascularisation, ECM remodelling and inflammatory responses, and they also regulate embryo implantation and organogenesis[209,212].

Chemokines are small peptides that possess conserved amino-acids important for their tertiary structure, such as the four cysteines that interact with each other in pairs to create their typical Greek key shape. Intramolecular disulphide bonds typically join the first to third, and the second to fourth cysteine residues, numbered as they appear in the chemokine protein sequence. Chemokines are divided into four families based on the number and spacing of the cysteine residues in the N-terminus as C, CXC, CC and CX3C (Figure 1.8)[209,212].

Chemokine receptors are G protein-coupled receptors usually found on the leucocyte surface, but not exclusively. In general, several chemokines can bind to one receptor, and conversely, a given chemokine may recognise more than one receptor, hence there is redundancy in the chemokine system[223]. Approximately 19 chemokine receptors have been characterised to date, which are divided into 4 families depending on binding chemokine type: CXCR binds CXC chemokines, CCR binds CC chemokines, CX3CR1 binds only CX3CL1, and XCR1 binds the two XC chemokines (XCL1 and XCL2) (Figure 1.8)[224,225]. Chemokine receptor activation leads to 2 main responses: 1) integrin activation, which causes adhesion of the cells, and 2) polarisation of the actin cytoskeleton by accumulation of small GTPases at the leading edge resulting in actin polymerisation and F-actin formation[209].

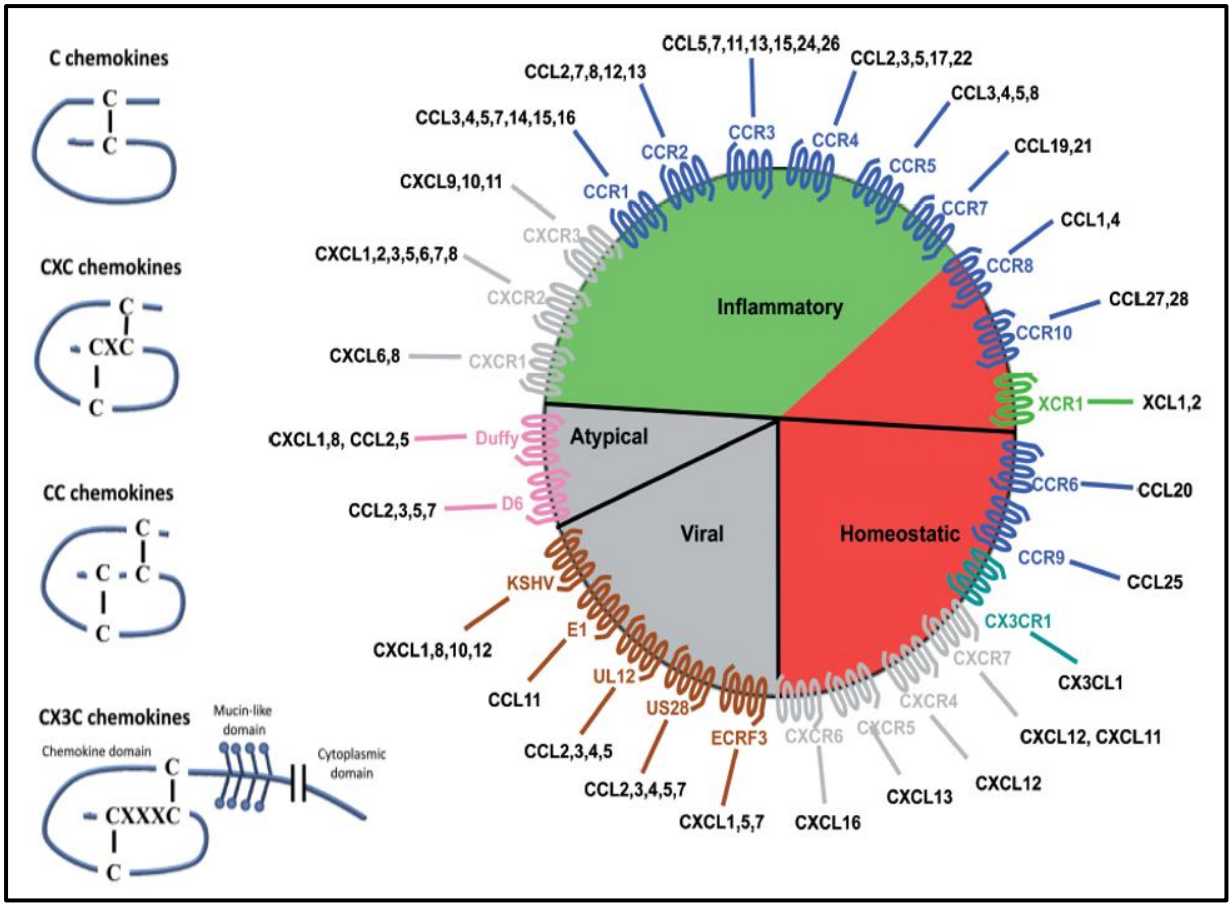

Figure 1.8: Chemokine general structures and classes
Chemokines possesses conserved amino-acids important for their tertiary structure, creating their typical Greek key shape. The chemokine wheel shows the major constituents of the chemokine system. "Inflammatory" chemokines are inducible and involved in all processes of immune response. "Homeostatic" chemokines are usually involved in the development and in normal physiological processes. "Atypical" chemokine receptors are generally silent and can act negatively in the regulation of different systems. "Viral" chemokine and their respective receptors allow pathogens to modulate immune responses following an infection. Inflammatory, homeostatic and atypical chemokines can be found in the tumour microenvironment. Adapted from Bestebroer *et al.* (2010)[225], and Balkwill (2012)[209].

Chemokine system dysfunction is involved in many diseases, including immunodeficiency, autoimmune or chronic inflammatory disorders, neurodegenerative diseases and cancer[211]. The role of chemokines and their receptors has been well demonstrated in many cancers, such as in breast, prostate, melanoma, oesophageal, lung, bladder and pancreas cancer[209,226], and also in some endocrine tumours such as thyroid cancer[227]; however, remains largely unexplored in PAs.

In cancer, chemokines are produced by malignant and stromal cells in the TME, contributing to cell trafficking, angiogenesis, modulation of immune cells and survival of malignant cells. Chemokines are highly soluble in the ECM or become immobilised on the cell surfaces, creating a concentration gradient essential for cell trafficking into and out of the TME[227]. Tumour cell or

stromal cell-derived chemokines lead to the recruitment of immune cells such leukocytes or monocytes/macrophages, which in turn influence the phenotype, proliferation, survival, migratory and invasive properties of tumour cells[209]. In general, CC chemokines attract cells of myeloid lineage, dendritic cells, natural killer (NK) cells, mast cells and basophils, whereas CXC chemokines attract mainly neutrophils and B or T lymphocytes. Thus, chemokines are important contributors to the inflammatory milieu, regulating the amount of inflammatory cells in the TME and their activity[209].

In tumour cells, certain oncogenic changes are known to modulate the chemokine system: in some cancers, there is an overexpression of certain chemokines, leading to increased inflammatory cell content and a deleterious TME, whereas in other tumours downregulation of certain chemokines impair immune cytotoxic responses against tumour cells[209,227]. Several oncogenes, such as the tyrosine kinase RET in papillary thyroid cancer or beta-catenin in breast cancer, activate a transcriptional profile which includes cytokines and chemokines[209,210,228]. Tumour cells often acquire chemokine receptors, not found in their normal counterparts, which contribute to their migratory and metastatic activity, as then malignant cells respond to chemokine gradients at metastasis sites[209].

Chemokine receptor activation in tumour cells may also lead to activation of signalling pathways, such as tyrosine kinase receptors and the JAK–STAT pathway, relevant for proliferation and survival of tumour cells[209]. Chemokines are also important for angiogenesis, regulating different mechanisms such as endothelial cell proliferation, the release of angiogenic factors, activation of metalloproteases involved in ECM degradation, and recruitment of angiogenic cells (such as macrophages, fibroblasts or endothelial cells) into the TME[209,222,226,228,229].

Cytokine-chemokine network in the normal pituitary

Cytokines and chemokines play important roles in pituitary function and physiology, affecting not only the hormone secretion but also cell proliferation. The effects of cytokines in the pituitary have been extensively investigated[214,216,230]. The pituitary gland is not only an important target of cytokines, but is itself a site of cytokine production[215]. A summary of the expression and effects of the most studied cytokines/chemokines and their receptors in the NP, as well as in human PAs and pituitary tumour cell lines is provided in the Table 1.3.

Cytokine	Expression and effects	Normal human pituitary	Normal rat (R) / mouse (M) pituitary	Human pituitary adenoma	Pituitary adenoma cell lines
IL-1	Expression	ND	IL-1β, IL-1ra (R,M), higher after LPS	Yes	ND
	Receptors	ND	IL-1β receptor (R,M)	ND	IL-1β receptor in AtT-20 cells
	Proliferation	ND	IL-1 inhibits, effect reverted by IL-1ra (R,M). IL-1β stimulates (R)	ND	Stimulates in AtT-20 cells No effect in GH3 cells
	Hormone secretion	ND	IL-1β stimulates ACTH, GH, LH and TSH, while inhibits PRL (R) IL-1α has no effect on ACTH (R)	Stimulates ACTH in corticotroph cell cultures	Stimulates GH in GH3 cells IL-1β increase CRH-stimulated ACTH in AtT-20 cells
IL-2	Expression/ Production	Yes	ND	In corticotrophinomas	Expressed by both AtT-20 and GH3 cells
	Receptors	IL-2 receptor present	IL-2 receptor (R)	IL-2 receptor present	IL-2 receptor present in AtT-20 and GH3 cells
	Proliferation	ND	Inhibits (R)	ND	Stimulates in both GH3 and AtT-20 cells
	Hormone secretion	ND	Stimulates ACTH, TSH, PRL (R) Inhibits GH, FSH, LH (R)	ND	Stimulates PRL in GH3 cells, and ACTH in AtT-20 cells
IL-6	Expression/ Production	Yes (ACTH and LH/FSH cells)	Yes, and expression stimulated by LPS, IFN, TNF-α, PACAP, VIP (R)	Expression in all PA types, mainly ACTH- and GH-PAs	ND
	Receptors	IL-6 receptor present	IL-6 receptor (R)	Mainly in ACTH- and GH-PAs	ND
	Proliferation	ND	Inhibits (R)	Stimulates	Stimulates in GH3 cells
	Hormone secretion	Stimulates GH, PRL Inhibits TSH	Stimulates ACTH, PRL, GH, LH, FSH (R)	Stimulates GH in GH-PAs, and ACTH in ACTH-PAs	Stimulates GH, PRL in GH3 cells, and ACTH in AtT-20 cells
TNF-α	Expression/ Production	ND	ND	Yes	Expressed by both AtT-20 and GH3 cells
	Receptors	ND	Binding sites detected (R,M)	ND	Binding sites in AtT-20 cells
	Proliferation	ND	Inhibits (R)	ND	ND
	Hormone secretion	Activates the PRL promoter	Stimulates ACTH, GH, TSH in hemipituitary cultures. Chronic exposure to TNF-α inhibits GH, PRL, TSH (R)	ND	ND
IFN-γ	Expression/ Production	ND	ND	ND	ND
	Receptors	IFNγ R1/2 in ACTH cells	ND	IFNγ R1/2 in corticotrophinomas	IFNγ R1/2 expressed in AtT-20 cells
	Proliferation	ND	ND	ND	Inhibits in AtT-20 cells
	Hormone secretion	ND	Inhibits ACTH and GH Stimulates PRL (via IL-6)	Inhibits ACTH in corticotrophinomas	Inhibits ACTH in AtT-20 cells
LIF	Expression/ Production	Yes	Yes, present in rat explants, and induced in mouse by LPS	Mainly in GH and ACTH-secreting PAs	ND
	Receptors	Yes	LIF receptor induced by LPS (M)	Yes	Receptor present in AtT-20 cells
	Proliferation	ND	Stimulates corticotrophs, inhibits somatotrophs in a transgenic mice overexpressing LIF	ND	Inhibits in AtT-20 cells
	Hormone secretion	ND	ND	ND	Stimulates ACTH in AtT-20 cells
MIF	Expression/ Production	Yes	ND	Yes, higher than in NP	ND
	Receptors	ND	ND	ND	ND
	Proliferation	ND	ND	ND	ND
	Hormone secretion	ND	ND	ND	ND

TGF-β	Expression/ Production	TGF-β1, β2 and β3 in lactotrophs	ND	Yes, TGF-β1, TGF-β2 and TGF-β3 present	ND
	Receptors	TGF-β-R-II	TGF-β-R-II (R)	TGF-β-R-II present in different PAs	TGF-β receptor described in GH3 cells
	Proliferation	ND	Inhibits in oestrogen-treated rats	Inhibits	Inhibits in GH3 and GH4 cells
	Hormone secretion	ND	Inhibits PRL (M)	TGF-β1 inhibits/ stimulates FSH at high/low concentrations	ND
BMP-4	Expression/ Production	Yes	Increased in oestrogen-treated rats; present in DA-R knockout mice	Higher in prolactinomas Lower in corticotrophinomas	ND
	Receptors	ND	ND	ND	ND
	Proliferation	ND	ND	ND	Stimulates in GH3 cells Inhibits in AtT-20 cells
	Hormone secretion	ND	ND	ND	Inhibits ACTH in AtT-20 cells
CXCL12	Expression/ Production	Yes, mostly in corticotrophs, also in FS cells	Yes (R)	Yes, higher than in NP	Expressed by AtT-20 cells, but not by GH3 and GH4 cells
	Receptors	CXCR4 in around 34% pituitary cells	CXCR4 present in normal rat pituitary, and also in embryonic mouse pituitary	CXCR4 present CXCR7 present	CXCR4 both present in AtT-20 and GH3 and GH4 cells CXCR7 present in AtT-20 cells
	Proliferation	ND	ND	Stimulates	Stimulates in GH3 and GH4 cells, and in AtT-20 cells
	Hormone secretion	ND	Stimulates GH (R)	ND	Stimulates GH in GH3 cells, and GH, PRL in GH4 cells
IL-8	Expression	Not expressed	ND	Yes, in different PA types	ND
	Receptors	CXCR2 present	CXCR2 present (R)	CXCR2 present	ND
	Proliferation	ND	ND	ND	ND
	Hormone secretion	ND	Inhibits FSH, LH (R)	ND	ND
CXCL1	Expression	ND	Yes (R)	Yes	ND
	Receptors	CXCR2 present	CXCR2 present (R)	CXCR2 present	ND
	Proliferation	ND	ND	ND	ND
	Hormone secretion	ND	Stimulates PRL, GH and ACTH (R) Inhibits FSH and LH (R)	ND	ND
CXCL10	Expression	ND	CXCL10 expressed in FS cells (R)	ND	ND
	Receptors	ND	CXCR3, TLR4 in ACTH cells (R)	ND	ND
	Proliferation	ND	ND	ND	ND
	Hormone secretion	ND	ND	ND	ND

Table 1.3: Cytokines and their receptors in normal and neoplastic pituitary

Expression and effects of cytokines and their receptors on human, rat and mouse normal pituitary, as well as in human pituitary adenomas and pituitary adenoma cell lines (mouse corticotrophinoma AtT-20 cells and rat somatomammotroph adenoma GH3/GH4 cells)[211,214,215,223,230,231]

BMP-4, bone morphogenetic protein-4; CRH, corticotropin-releasing hormone; DA-R, dopamine receptor; FS, folliculo-stellate; IFNγ, interferon-γ; IL, interleukin; IL-1ra, interleukin-1 receptor antagonist; LIF, leukemia inhibitory factor; LPS, lipopolysaccharide; MIF, macrophage migration inhibitory factor; ND, not determined; NP, normal pituitary; PA, pituitary adenoma; PACAP, pituitary adenylate cyclase-activating polypeptide; TGF-β, transforming growth factor-β; TLR4, toll-like receptor-4; TNF-α, tumour necrosis factor-α; VIP, vasoactive intestinal peptide.

Cytokine-chemokine network in the neoplastic pituitary

The cytokine network may play key roles in PAs, affecting not only their hormone secretion, but also different intrinsic tumourigenic mechanisms such as angiogenesis, invasion, proliferation and modulation of the TME and immune cell infiltrates (Figure 1.9).

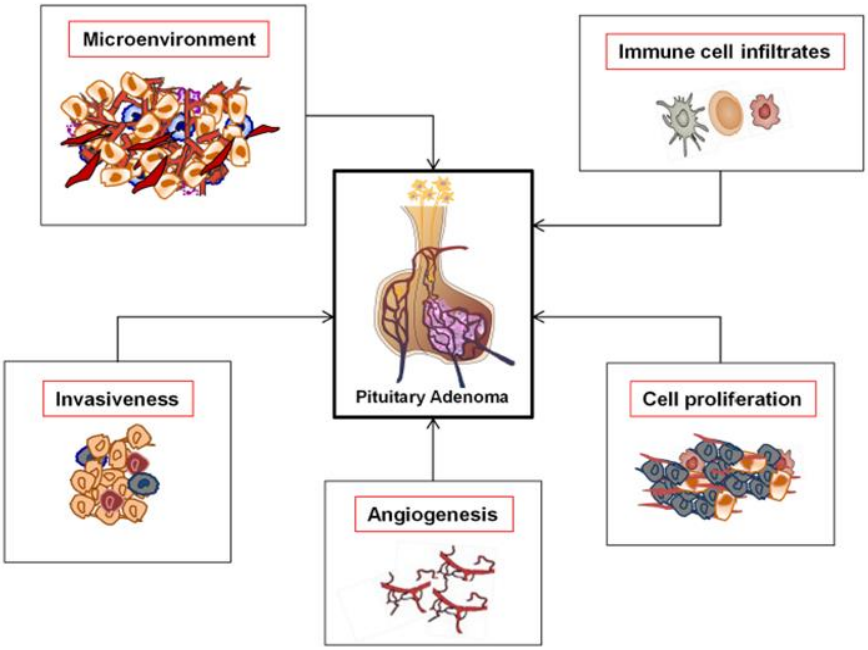

Figure 1.9: Cytokine network role in different tumourigenic mechanisms in PAs
Grizzi *et al.* (2015)[211].

However, in contrast to the extensive available data regarding cytokines in the NP, the amount of studies exploring the cytokine network in pituitary tumours is remarkably scarce. Nevertheless, some cytokines, chemokines and growth factors have been investigated in PAs, particularly IL-8, IL-6, IL-1, CXCL12, transforming growth factor-β (TGF-β), tumour necrosis factor-α (TNF-α), VEGF, as summarised in the Table 1.3 and described in detail below.

IL-8 (or CXCL8)

In 1996, Green *et al.* reported one of the first studies exploring the cytokine expression profile in 17 human PAs, using RT-PCR to identify the presence of mRNA of the following cytokines: IL-1α, IL-1β, IL-2, IL-4, IL-5, IL-6, IL-7, IL-8, TNF-α, TNF-β, TGF-β1, TGF-β2 and TGF-β3. All PAs expressed IL-8 and none expressed IL-2, IL-5 or IL-7, suggesting that IL-8 may be important for pituitary tumourigenesis. IL-6 was expressed in all 4 somatotrophinomas, 3/7 NFPAs, 2/4 prolactinomas and in the corticotrophinoma case. At least one TGF-β isoform was found in all but 2 PAs, while IL-1α, IL-β, IL-4, TNF-α and TNF-β were sporadically expressed[232].

In 1999, Suliman *et al.* studied IL-8 expression in 25 human PAs and 2 NPs using *in situ* hybridisation. IL-8 mRNA was not identified in 2 NP specimens, and only 12% of PAs (3/25) were positive for IL-8 mRNA. There was no difference in size, type or degree of vascularisation between IL-8 positive and IL-8 negative PAs[233]. These findings contrast with those earlier reported[232], likely due to different study methods or due to PA heterogeneity.

Later in 2011, Vindelov *et al.* shown that IL-8, and also IL-6, are secreted from primary human somatotroph adenoma cells in significant concentrations and in a constant manner; GHRH and somatostatin were shown to inhibit IL-8 and IL-6 secretion, while IL-1β stimulated the secretion of IL-8, IL-6 and also GH[234]. Such findings confirmed a physiological relation between endocrine cells and cytokines reflecting their possible involvement in pituitary tumourigenesis, as well as a potential therapeutical effect of drugs targeting the cytokine network in acromegaly.

Recently, Salomon *et al.* contrasted RNAseq data from 7 recurrent and 23 non-recurrent PAs identifying 68 genes that were significantly differentially expressed. Of these, genes involved in chemokine receptor binding were highly enriched in recurrent PAs particularly those integrating the IL-8 pathway (*IL8, CXCR1* and *CXCR2*)[235], suggesting the IL-8 involvement in PA aggressiveness and/or resistance to treatment, as well-known in other cancers[236].

IL-6

IL-6 is one of the most studied cytokines in PAs, displaying potential roles in the development, progression and biological behaviour of PAs. IL-6 production has been localised to folliculo-stellate cells in the NP, whereas in PAs is secreted by adenohypophyseal tumour cells[230]. IL-6 mRNA was detected in different PA subtypes[214]. Jones *et al.* cultured 100 human PAs and found that 53% expressed and secreted IL-6, synthesised by adenohypophyseal tumour cells as shown by *in situ* hybridization for IL-6 mRNA in 3 out of 4 PAs[237]. IL-6 and its receptor are expressed in human PAs[238,239] more prominently in somatotrophinomas and corticotrophinomas[239], as well as in a human pituitary cell line[240].

In rat GH3 cells, IL-6 stimulates GH and PRL release, as well as proliferation and DNA synthesis; however, at the same concentration IL-6 inhibited the growth of pituitary cells[241]. In AtT-20 cells and human corticotrophinoma cultures, IL-6 stimulates ACTH secretion[242,243]. In TtT/GF and MtT/E cells, IL-6 stimulated growth[244-246]. Moreover, IL-6 enhances VEGF release[230,247] and alter the production of matrix metalloproteinases (MMPs) by folliculo-stellate cells[244,248], contributing to angiogenesis and ECM remodelling, and thus favouring tumour progression and invasiveness.

An immunohistochemical study analysed IL-6 and TNF-α expression in 40 invasive and 40 non-invasive PAs, both expressed mainly in the tumour cell cytoplasm. Of the invasive PA, 67.5% had IL-6 expression, whereas only 22.5% of non-invasive PAs stained for IL-6. Similarly, higher number of invasive PAs had positive TNF-α expression (65%, comparing to 25% in non-invasive PAs)[249]. These data suggest that IL-6 and TNF-α may play a role in the invasiveness of PAs.

Paoletta *et al.* measured serum IL-6 and IL-1β levels in 11 Cushing´s disease patients undergoing bilateral inferior petrosal sinus sampling. ACTH and cytokine levels were higher in the ipsilateral petrosal sinus than in the contralateral one or in peripheral blood, and after CRH infusion these interleukins raised and correlated with stimulated ACTH levels, suggesting that central production of IL-6 and IL-1β can potentially be involved in autocrine-paracrine ACTH hypersecretion in Cushing´s disease[250]. However, in an earlier study including six Cushing´s disease patients, IL-6 (as well as IL-1α, IL-β, TNF-α and IL-2) were undetectable in most samples collected during bilateral inferior petrosal sinus sampling[251]. Shah *et al.* reported elevated serum IL-6 (and IL-1β) levels in patients with active Cushing´s disease in comparison to healthy controls: these remained raised despite surgical remission and decrease in body mass index, insulin-resistance, visceral, hepatic and inter-muscular adiposity, reflecting a chronic inflammatory state in Cushing´s disease despite cure that may contribute to the increased cardiovascular mortality associated to this condition[252].

IL-6 has also been involved in PA senescence. A dual role of IL-6 in both pituitary tumourigenesis and senescence seems to be demonstrable in PAs, as IL-6 paracrine effects seems to allow initial pituitary cell growth, whereas the IL-6 autocrine effects in the same tumour promote senescence and restrains aggressive growth and malignant transformation[253,254].

IL-1

IL-1 production has been demonstrated in human PAs[232], and its receptor was found in NP, as well as in the mouse AtT-20 and rat GH3 tumour cell lines[230,255]. IL-1 is associated with a stimulatory effect on hormone secretion[214,230,256], except for PRL which is inhibited by IL-1[230,231], but its effect in the tumourigenesis remains unknown. Some studies have also shown an inhibitory effect of IL-1 in TSH and ACTH secretion[216,257-259]. IL-1's stimulatory effect on ACTH and GH secretion was shown in AtT-20[260] and GH3 cells[261], respectively, as well as in human somatotrophinomas[234]. Patients with active acromegaly had also increased serum levels of IL-1, but not IL-6[262].

The role of IL-1 in pituitary cell proliferation and in the tumourigenesis remains controversial. IL-1 inhibited the growth of normal rat pituitary cells[215,230]. However, IL-1 has been reported to show

no effect on GH3 cell growth[263], and there is even a stimulatory effect of IL-1β on normal rat pituitary proliferation[264].

CXCL12 (and its receptors CXCR4 and CXCR7)

CXCR4 is a key receptor in the crosstalk between tumour cells and the surrounding TME in cancer, and one of its ligands is CXCL12 (also known as stromal cell-derived factor-1, SDF-1)[265].

The CXCL12/CXCR4 axis has been studied in normal and neoplastic pituitary[211]. CXCL12 binding sites were first described in adult rat pituitary by an autoradiographic assay using ^{125}I labelled CXCL12[266]. In contrast to rats, human pituitary CXCR4 expression is confined to a subset of cells, particularly GH, PRL and ACTH-producing cells, where its ligand CXCL12 is mostly, but not exclusively, found in ACTH-producing cells[223,267]. The expression levels of CXCR4 and CXCL12 are lower in NP than in human PAs[268], suggesting a possible role in tumourigenesis[223]. Moreover, pituitary cells do not co-express CXCL12 or CXCR4, contrarily to what happens in PAs, reinforcing the involvement of this axis in PAs[211,268]. Horiguchi *et al.* also showed that CXCL12 and CXCR4 are expressed in S100β-protein-positive cells of the anterior pituitary, and CXCL12/CXCR4 axis between its cells have a role in the extension of cytoplasmic processes and interconnections[269]. Barbieri *et al.* showed that CXCL12 is markedly overexpressed in PAs in comparison to NP[268]. In another study, CXCR4 was highly expressed in somatotrophinomas and NFPAs[270].

In vitro studies in rat and human pituitary tumour cells supported the stimulatory effect of CXCL12 in cell proliferation, DNA synthesis and GH secretion[271-273], corroborated by the findings that a CXCR4 antagonist inhibits GH production and cell proliferation, and also induced GH3 cell apoptosis[268,274]. Combined treatment with CXCR4 antagonist and octreotide was more effective in inhibiting somatolactotroph adenoma formation[274], and in another study a CXCR4 antagonist suppressed hypoxia-mediated GH production from GH3 cells[275]. These findings suggest that antagonising CXCR4, in isolation or in combination with SSAs, may have a role in the management of patients with acromegaly[274].

Xing *et al.* studied CXCR4 and CXCL12 expression levels in human PAs and their correlation with invasiveness. Flow cytometry studies showed that the percentage of CXCR4 and CXCL12-positive cells from invasive PAs was higher than from non-invasive counterparts, and CXCR4 and CXCL12 staining scores were higher in invasive PAs than from non-invasive PAs[276].

CXCL12 expression was correlated with microvasculature density in PAs, suggesting that hypoxia may regulate this chemokine[277]. CXCL12 behave as an angiogenic factor in PAs, mobilising

endothelial progenitor cells to the tumour parenchyma under hypoxic conditions[277]. *In vitro* CXCL12 secretion by mouse AtT-20 cells was inversely correlated to oxygen levels, with more severe hypoxia degrees leading to increased CXCL12 secretion[277].

The distribution and function of another CXCL12 receptor, CXCR7, was studied in human PAs and AtT-20 cells[278]. CXCR7 is expressed in human PAs, more prominently in macroadenomas and in GH and PRL-secreting PAs. CXCR7 was associated with upregulation of cell cycle genes and with downregulation of other genes related to amino-acid metabolism and ligase activity[278]. Immunohistochemical analysis of neuroendocrine cells and their neoplastic counterparts showed high expression of CXCR2 in both human PAs and NP[268,279].

Transforming growth factor-β (TGF-β)

TGF-β is expressed in most human PAs[232], as well as in normal and neoplastic rat pituitary[230,280]. TGF-β has been studied in prolactinomas, in which there is a reduced expression and activity of TGF-β1. TGF-β inhibits lactotroph proliferation and PRL secretion[280,281]. The anti-proliferative effect of TGF-β was demonstrated in rat GH3 and GH4 cells[230,282], and in the human pituitary tumour HP75 cell line[283]. Treatment of HP75 cells with TGF-β for 24 hours changed the RNA profiling, with a large number of genes becoming up or downregulated, some of them involved in cell proliferation[283].

TGF-β signalling was investigated in a study including 29 invasive NFPAs, 21 non-invasive NFPAs and 5 NPs. Smad3 and p-Smad3 protein levels decreased from NP, to non-invasive PAs and to invasive PAs. TGF-β1 mRNA level decreased while the Smad7 mRNA increased from NP to non-invasive PAs and to invasive PAs. Moreover, proliferating cell nuclear antigen mRNA was markedly increased in invasive NFPAs compared to non-invasive ones and its level correlated negatively with Smad3 mRNA. These data suggest that TGF-β pathway may be restrained in NFPAs and can be associated with tumour development and invasion[284].

Gu *et al.* studied the expression of TGF-β receptor I and II by RT-qPCR, western blot and immunohistochemistry in invasive and non-invasive NFPAs. mRNA and protein levels of TGF-β receptor II decreased progressively from NP to non-invasive NFPAs and then to invasive NFPAs, while TGF-β receptor I expression levels did not differ between NP and PAs. These data suggest that TGF-β receptor II (but not receptor I) may contribute to the tumourigenesis and invasiveness of NFPAs[285].

Tumour necrosis factor-α (TNF-α)

TNF-α expression has been demonstrated in AtT-20 and GH3 cells[286] and in human PAs[232,249]. TNF-α has effects on cultured pituitary cells, blunting ACTH release and other pituitary hormones in response to hypothalamic factors[287]. However, in ovine pituitary cells TNF-α enhanced GH expression[288], and increased ACTH, GH and TSH secretion from hemipituitaries[289]. TNF-α may play a role in PA intra-tumoural haemorrhage by upregulating VEGF and MMP-9. TNF-α administration caused haemorrhagic transformation and enhanced VEGF and MMP-9 expression in PA cell xenografts in mice[290]. Arita *et al.* found a positive relation between haemorrhage and VEGF in human PAs[291] but other studies showed no association[292,293], hence TNF-α role in PA haemorrhage remains unclear.

TNF-α expression has also been correlated with PA invasiveness. Wu *et al.* reported more often TNF-α expression in invasive (65%) than in non-invasive PAs (25%)[249], and later Zhu *et al.* observed higher TNF-α expression in bone-invasive than in non-invasive PAs, which together with *in vitro* data, suggested that TNF-α can induce osteoclast differentiation in bone-invasive PAs[294].

VEGF

The role of VEGF in proliferation and angiogenesis has been studied in PAs[295-297]. McCabe *et al.* showed an increase in VEGF expression in human PAs in comparison to NP, despite PAs being less vascular[298]. VEGF expression was also associated with suprasellar extension[299,300], and pituitary carcinomas showed stronger VEGF immunoreactivity than PAs[299]. VEGF expression was higher in dopamine agonist resistant prolactinomas than somatotrophinomas, NFPAs and corticotrophinomas[301]. However, Lloyd *et al.* reported decreased VEGF expression in PAs in comparison to NP, in keeping with the subnormal microvessel densities and PA benign behaviour[299,302,303]. Moreover, Takano *et al.* reported a limited role for VEGF in the development of vascular architecture and angiogenesis in PAs[304]. Lohrer *et al.* showed that most human PAs secrete VEGF, and PACAP-38, TGF-*α* and IGF-1 increase VEGF expression in NFPAs, somatotrophinomas and prolactinomas[305]. Patients with PAs had higher plasma VEGF levels than controls[306]. A high proportion of GH3 cells express VEGF, which may be altered by different growth factors[307]. GH3 cell conditioned medium have 13 times higher VEGF levels than control media, which might explain the stimulated growth of endothelial cells after treatment with GH3 conditioned medium[308]. VEGF is also produced by folliculo-stellate cells and by lactotrophs within the normal anterior pituitary, and its secretion can be influenced by the ECM[309].

Drugs targeting VEGF pathway have been used to treat aggressive or refractory PAs, namely bevacizumab, which can be effective as monotherapy or in combination with other treatments in some cases[310,311] (reviewed in detail in[312]). Other drugs targeting VEGF have also been used but with minimal success[312].

Other cytokines, chemokines or growth factors in pituitary adenomas

In 2011, Qiu *et al.* reported positivity for IL-17, IL-17R and MMP-9 expression in invasive PAs, and a positive correlation between IL-17 and IL-17R and MMP-9 expression levels. Moreover, higher serum IL-17 levels were found in patients with invasive PAs[313]. Qiu *et al.* collected blood samples from 75 patients with PAs, pre-operatively and at 1, 3, and 6 months after surgery, and measured serum IL-17, IL-4, IL-5, TNF-α, INF-γ. Serum IL-4, IL-5 and IL-17 were higher before surgery and decreased significantly after surgery. Pre-operative IL-17 levels were also higher in the subgroup with invasive PAs. Among the invasive subgroup, patients with PAs totally excised presented lower IL-17 than those with residual PA after surgery[301,302]. Glebauskiene *et al.* reported higher serum concentrations of IL-17A in 60 PA patients in comparison to 64 control subjects, but there was no association between IL-17A serum levels and PA invasiveness or recurrence[314]. These findings suggest that different interleukins, particularly IL-17, might be important for PA tumourigenesis or invasiveness[313,315].

IL-2 expression, as well as its receptor, were detected in human corticotrophinomas, in mouse AtT-20 and in rat GH3 cells[316]. They co-localize with PRL, GH and ACTH[230], and it was shown that IL-2 may influence the secretion of these hormones[317,318], as well as stimulate the growth of human somatotrophinoma and GH3 cells[241,319]. However, IL-2 expression was not shown in all studies, with some reporting absent IL-2 expression among all PAs studied[232].

Cannavo *et al.* reported higher serum IL-22 in subjects with PAs, and patients with prolactinomas had significantly higher IL-22 levels than NFPAs, but no correlation was noted with size or pituitary dysfunction. These authors found also strong IL-22 receptor immunoreactivity in 4/4 prolactinomas and 6/10 NFPAs[320].

IFNγ was associated with inhibition of hormonal secretion and cell proliferation[214,230], as shown in human corticotrophinomas and mice AtT-20 cells via JAK-STAT1/NF-kβ inhibitory pathway[321], or as also in folliculo-stellate cells[322].

Granulocyte macrophage-colony stimulating factor (GM-CSF) derived from NFPA cells has been recently involved in the polarisation of macrophages into the M1-subtype and in the impairment of monocyte recruitment[323].

Migration inhibitory factor (MIF) is expressed in the pituitary, and its expression is increased in the cell nuclei in PAs; however, it is unclear whether it plays a role in the tumourigenic process[324].

Leukaemia inhibitory factor (LIF) was detected in normal and neoplastic pituitary[230,325]. Specific LIF binding sites are found in AtT-20 cells, and LIF attenuates growth in this cells by blocking cell cycle progression. In terms of hormonal secretion, LIF stimulates ACTH secretion[326], and inhibits the secretion of PRL and GH from the rat MtT/SM pituitary cell line[327]. Kontogeorgos *et al.* studied LIF expression in 98 PAs, reporting LIF immunopositivity in the majority of cases (92%) and in all PA subtypes. Prolactinomas had the highest immunostaining grade, but overall NFPAs had a significantly higher immunohistoscore when compared to functioning PAs[328].

Bone morphogenetic protein-4 (BMP-4) overexpression was reported in PAs, particularly prolactinomas[329]. In contrast, BMP-4 is differently expressed in normal and adenomatous corticotrophs and has an inhibitory action in corticotrophinoma cell proliferation[330,331].

1.6 Non-tumoural cells in the TME of pituitary adenomas

Immune cells in pituitary adenomas

Macrophages

Macrophages are innate immune cells that play important roles in tissue homeostasis, responses to pathogens, presentation of foreign or self-antigens to immune cells, phagocytosis, inflammatory reactions, inflammation resolution and wound healing. Macrophages exist in almost all tissues, usually resulting from the differentiation of blood monocytes, but there are also tissue resident macrophage subpopulations, such as Langerhans cells in skin or microglia in brain[332].

Macrophages are recognised as a major component of the immune cell infiltrates in tumours and therefore playing a major role in the TME[229]. Macrophages are heterogeneous and can have distinct phenotypes depending on the surrounding TME. In general, two main macrophage phenotypes are recognised: M1 (or classically-activated) and M2 (or alternatively-activated) macrophages. This binominal macrophage polarisation correspond, in a simplistic way, to two phenotypic extremes of a continuum polarisation spectrum (Figure 1.10)[229,332,333].

M1 and M2 macrophage types are different in terms of their biological properties, membrane receptors, cytokine secretome and effector functions[229,332,334]. M1-macrophages arise following stimulation with Th1 cytokines, in particular IFNγ or TNF-α, or exposure to bacterial moieties such as lipopolysaccharide. M2-macrophages result from direct stimuli with Th2 cytokines, particularly IL-4, IL-10 and IL-13, but also from other factors such TGF-β or glucocorticoids[229,335].

In terms of membrane receptors, M2-macrophages express high levels of scavenger receptors A and B, Mannose receptors (CD206), CD163 and CD23 (Fcε-RII), whereas in M1-macrophages these markers are usually not found, but others such as TLR2, TLR4 CD16, CD32, CD64, CD80 and CD86 are normally expressed (Figure 1.10)[229,335]. M1-macrophages secrete high levels of proinflammatory cytokines such as IL-12, IL-23, IL-1, IL-6 and TNF-α, and have high concentrations of superoxide anions and oxygen/nitrogen radicals, agents with bactericidal and tumouricidal effects. In contrast, M2-macrophages produce high levels of IL-10 and IL-1 receptor antagonist (IL-1ra), and have a predominance of the effector arginase pathway with generation of ornithine and polyamines which are precursors necessary for collagen synthesis, ECM remodelling and cell proliferation, conferring to this type functions in tissue repair, immune modulation and tumour progression. Polarised macrophages also tend to express different chemokines: M1-macrophages express higher levels of CXCL9, CXCL10, CXCL11, CCL2, CCL3, CCL4, CCL5, whereas M2-macrophages have increased CCL16, CCL17, CCL18, CCL22 production (Figure 1.10)[229,332,333].

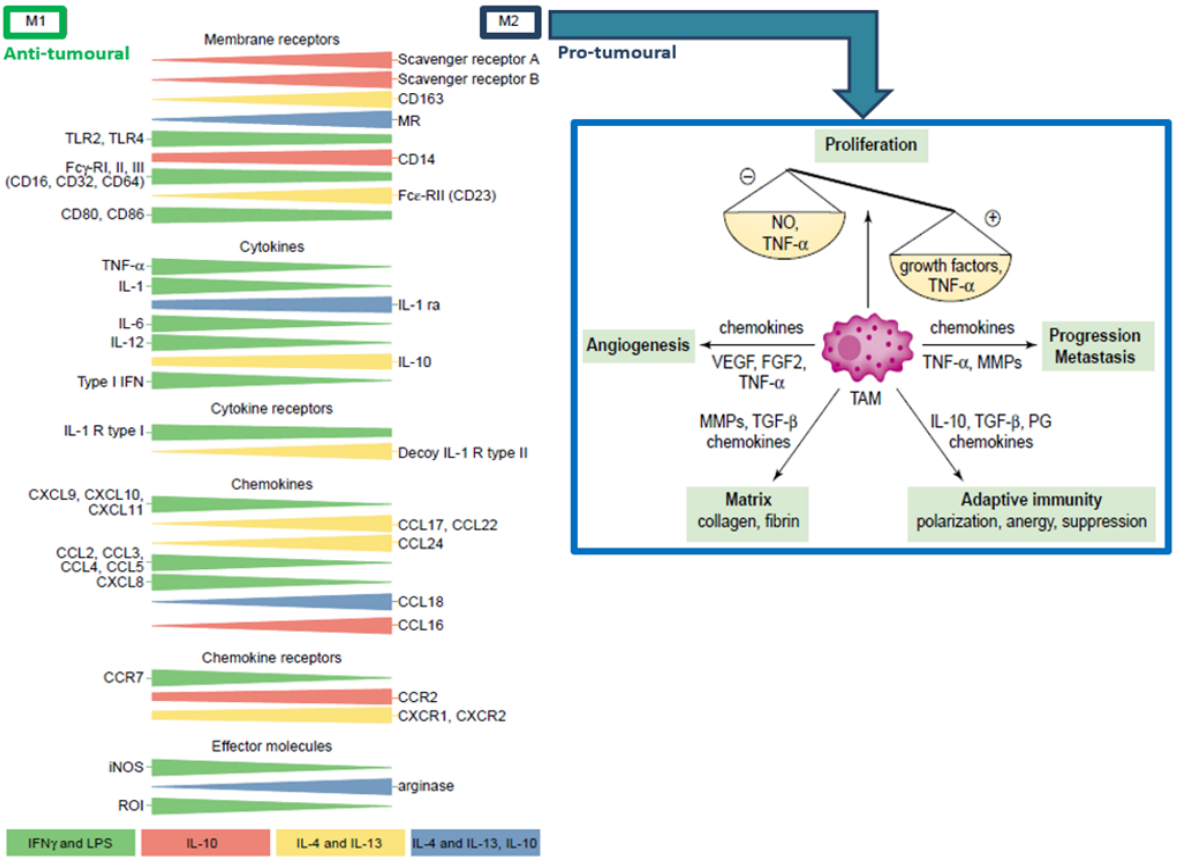

Figure 1.10: M1 and M2 macrophages
FGF, fibroblast growth factor; IFN, interferon; IL, interleukin; iNOS, inducible nitric oxide; LPS, lipopolysaccharide; MMP, matrix metalloproteinase; MR, mannose receptor; NO, nitric oxide; PG, prostaglandin; ra, receptor antagonist; ROI, reactive oxygen intermediates; TAM, tumour-associated macrophages; TGF, transforming growth factor; TLR, toll-like receptor; TNF, tumour necrosis factor; VEGF, vascular endothelial growth factor. Adapted from Mantovani *et al.* (2002)[229].

Both M1 and M2-macrophages have been identified in tumours. Polarised macrophages change their membrane markers and secretome according to the surrounding stimuli, i.e. macrophages can polarise in response to different stimuli present in the TME, which in turn allow them to modulate the inflammatory milieu of the local TME and influencing the behaviour of the tumour cells[229,336,337]. M1-macrophages usually demonstrate anti-tumour activity and are associated with good outcomes in cancer[332,338]. However, M2-macrophages are generally associated with tumour initiation, progression and invasiveness, angiogenesis, ECM remodelling and metastasis (Figure 1.10), and are thus associated with poorer outcomes in cancer[229,339-342]. M2-macrophages may also directly promote epithelial-to-mesenchymal transition (EMT) through the activation of different pathways, such as NF-kB, TGF-β, IL-10 or FoxQ1[334,335,343].

Macrophages are present in the pituitary gland. This was first demonstrated by Hume *et al.* who identified macrophages in the anterior pituitary of mice[344], and later by Mander *et al.* in the rat pituitary[345]. Fujiwara *et al*. using immunohistochemistry and electron microscopy reported M1 and M2-macrophages in the normal rat anterior pituitary and in prolactinomas induced by diethylstilbestrol (DES). Most macrophages were located near capillaries in the NP, and more than half of the macrophages were M2-macrophages. M1 and M2-macrophages were similar in their structural properties, although phagosomes were only seen in the cytoplasm of M2-macrophages, whereas the endoplasmic reticulum and Golgi apparatus were poorly developed in M2-macrophages. DES-induced prolactinomas had more M2-macrophages than NP, and interestingly, the number of M2-macrophages increased during the first 2-4 weeks of treatment with DES, before PA formation, supporting a potential role for M2-macrophages in the tumourigenesis[346].

Lu *et al.* reported CD68+ macrophage infiltration in all 35 PAs studied, with higher macrophage content in both sparsely-granulated somatotrophinomas and null-cell PAs in comparison to densely-granulated somatotrophinomas or corticotrophinomas. The number of macrophages was correlated with size and Knosp grades for invasiveness, i.e. macrophage-rich sparsely-granulated somatotrophinomas and null-cell PAs were larger and more invasive than densely-granulated somatotrophinomas or corticotrophinomas[347]. Sato *et al.* found more M2-macrophages in NFPAs with cavernous sinus invasion than in non-invasive NFPAs, but the number of infiltrating M2-macrophages did not correlate with tumour volume[348]. More recently, Yagnik *et al.* performed

flow cytometry analysis of CD11b-expressing myeloid cells (precursors of macrophages) in 16 NFPAs, and found that most CD11b-enriched NFPAs were larger and more proliferative. Interestingly, NFPAs with cavernous sinus invasion had a M2:M1 macrophage gene expression ratio>1, whereas 80% of non-invasive NFPAs showed a M2:M1 ratio<1[323]. M2-polarised THP-1 cells (monocyte cell line) conditioned medium led to increased proliferation, invasion and migration of primary NFPA cells compared to conditioned medium from M1-polarised THP-1 cells[323]. M2-macrophage conditioned medium also increased the expression of the genes *EZH2* (involved in cell proliferation) and *S100A9* (involved in cell invasion) in primary NFPA cells[323].

These findings support an association between macrophage infiltration and PA behaviour, thus suggesting that macrophages may influence pituitary tumourigenesis and determine increased aggressiveness, as seen in neuroblastoma[349], Hodgkin´s lymphoma[341], breast[332,350], ovarian[351,352] and prostate[353] cancer, as well as in endocrine cancers such as thyroid cancer[340,354] or neuroendocrine tumours[342].

Lymphocytes

Lymphocytes are detectable in the TME or in draining lymph nodes of individuals with cancer. There are different tumour-infiltrating lymphocytes (TILs)[204]. CD8+ T lymphocytes are usually beneficial to the host because they are capable to initiate a cytotoxic cascade killing tumour cells. CD4+ T helper 1 cells usually supports cytotoxic T cells through the secretion of Th1 cytokines being associated with a good cancer prognosis[355-357]. In contrast, CD4+ T helper 2 cells produce immunosuppressive cytokines, such IL-4, IL-5 and IL-13, which promote tissue inflammation and tumour growth. A third T cell type with immunosuppressive function, so-called T regulatory cells (Tregs) characterised by forkhead box P3 (FOXP3) and CD25 expression, are the main sources of Th17 cytokines (IL-17 and IL-22). Higher Tregs content in the TME is associated with poor prognosis in many cancers, although in some has been linked to good outcomes[204]. B lymphocytes can be found at the invasive margin of tumours, although are more frequent in draining lymph nodes and lymphoid structures adjacent to the TME. B cell infiltration in the TME is usually associated with a good prognosis in cancer, but there has been described an immunosuppressive IL-10-secreting B cell population that inhibits immune responses, thereby increasing tumour aggressiveness[358-361]. Innate NK cells also infiltrate tumours and exert their tumour-killing activity, thus predicting better cancer outcomes. However, malignant phenotypes may induce anergic NK cells, compromising their cytotoxic activity[204,362].

In contrast to autoimmune hypophysitis[363-365], little data are available regarding immune infiltrates in PAs. One of the first studies dates from 1990, in which Rossi *et al.* evaluated the immune cell infiltrate in 28 PAs, concluding that PAs have a low degree of cellular immune response. In this study, CD8+ and CD4+ lymphocytes were detected in 80% and 14% of the PAs, whereas B lymphocytes were present in only 1 case, and NK cells were seen in 1 out of 13 cases; moreover, a low number of macrophages was also reported[366]. Another study described reduced NK cell activity in hyperprolactinaemic patients in comparison to bromocriptine-treated prolactinoma patients and healthy controls[367]. In another older study was reported a higher percentage of B cells in prolactinoma patients than in healthy subjects; in contrast, there were no differences regarding total T or suppressor T cells between these groups[368]. Later in 1998, Heshmati *et al.* reported that lymphocytic infiltrates are rare in a large series of PAs. In this study, lymphocytic infiltrates were stained for LCA (leukocyte common antigen), CD45RO (T cell marker) and CD20 (B cell marker), which were present in only 40 out of 1400 PAs and were almost exclusively T cells[369].

More recently, in a study investigating lymphocyte infiltrates in different brain tumours, it was noted that PAs, as well as benign meningiomas, had no infiltration of Tregs, in contrast to malignant tumours which exhibited remarkable infiltrates as well as increased circulating levels of these cells[370]. Lupi *et al.* studied TILs in patients with PAs, and reported a higher prevalence of TILs in PAs (25%), mostly mild infiltrations. There was no difference among the PA types: 1/14 corticotrophinomas, 5/18 somatotrophinomas, 8/32 NFPAs, 2/4 prolactinomas and 2/4 thyrotrophinomas. The prevalence of TILs was higher in PAs than in NP, but lower than in autoimmune hypophysitis. A poor outcome, assessed in terms of hormonal hypersecretion and structural disease by MRI, was more frequent in patients with PAs with TILs than in those with no TILs; moreover, a multivariate regression analysis pointed out TILs as an independent factor for PA persistence/recurrence[371], establishing a correlation between cell-mediated autoimmunity and PA behaviour. Immunohistochemistry data from Qiu *et al.* revealed that PAs may have a higher number of inflammatory cells around neoplastic cells, more prominently in invasive PAs[315].

The PA infiltration of CD4+ and CD8+ T cells was relatively scant in the Lu *et al.* study, with somatotrophinomas having more CD4+ and CD8+ T lymphocytes than non-GH secreting PAs; no correlation was seen between the number of CD4+ cells and tumour size or invasiveness[347]. In Mei *et al.* study, TILs were observed in all studied PAs and correlated with the expression of programmed death ligand-1 (PD-L1)[372], often viewed as a potential biomarker for response to checkpoint inhibitors[373]. TILs subclasses CD3+ and CD4+ were increased in functioning PAs in comparison to NFPAs, and all lymphocytic markers (CD3, CD4, CD8 and CD45) were higher in PAs with increased Ki-67. PD-L1 expression was higher in somatotrophinomas and prolactinomas, and

primary PAs had increased PD-L1 levels than recurrent tumours[372]. More recently, in a large cohort of 191 patients with PAs, Wang *et al.* described CD8+ T lymphocytes in 87% of cases. CD8+ lymphocytes positively correlated with PD-L1 levels, as well as with GH levels, but not with Ki-67, gender, age or tumour size. This study showed that PD-L1 was frequently expressed in functioning PAs and associated with increased aggressiveness[374]. High expression of PD-L1 in all PA types was demonstrated on another series, and somatotrophinomas tend to display higher levels of PD-L1 than NFPAs and corticotrophinomas[235]. In this study, Salomon *et al.* observed in all PA subtypes that PD-L1 expression was heterogeneous throughout the tissue and coincided with presence of immune infiltrates[235]. Human corticotrophinomas are also infiltrated by T cells and express PD-L1[375]. In another study, PD-L1 expression was higher in NFPAs with cavernous sinus invasion, and the number of CD8+ T cells tended to be higher in the invasive NFPAs than in those without cavernous sinus invasion[348].

In general, increased PA aggressiveness may be associated with a shift towards a more immunosuppressive lymphocyte phenotype. These data also highlight that immune cells within the TME of PAs may influence their behaviour and lead to increased aggressiveness, suggesting a promising role for immunotherapy, including immune checkpoint inhibitors, in the management of aggressive and surgically non-curable PAs[348,372,374], including in Cushing´s disease[375,376].

Other immune cells

Other immune cells have been described in the TME of some cancers but not in PAs, such as myeloid-derived suppressor cells, dendritic cells and neutrophils[204].

Myeloid-derived suppressor cells are heterogeneous inhibitory immune cells that infiltrate a number of tumours leading to Tregs development and M2-macrophage polarisation[377-379].

Dendritic cells play an important role in presenting antigens to the surrounding immune cells triggering immune responses in the TME[377,380].

The role of neutrophils in cancer is controversial, with a dual function being described to these cells: they may have a pro-tumour effect in some cancers by promoting angiogenesis, degrading ECM and inducing immunosuppression; however, some studies showed that tumour-associated neutrophils can eliminate malignant cells, displaying an anti-tumoural action[204,381,382].

Stromal/mesenchymal cells in pituitary adenomas

Tumour-associated fibroblasts

Fibroblasts are the most abundant cell type in connective tissues, and play a key role in secreting ECM components forming a structural tissue framework. Fibroblasts are the main cells responsible for the production of ECM proteins (such as collagen, hyaluronan, fibronectin) as well as MMPs. Quiescent fibroblasts may undergo activation and become myofibroblasts in different processes, such as tissue remodelling, wound healing or fibrosis, but also in cancer. Fibroblasts are a major component of the tumour stroma, and in cancer they acquire morphological changes and an activated phenotype, often termed as tumour-associated fibroblasts (TAFs)[383,384].

TAFs are a heterogeneous cell population originating from resident fibroblasts, bone marrow-derived mesenchymal stem cells, hematopoietic stem cells, epithelial cells, endothelial cells or even adipocytes. The most widely used markers to detect activated fibroblasts are α-smooth muscle actin (αSMA), fibroblast activation protein and fibroblast-specific protein 1, but other markers (tenascin-C, desmin, vimentin) may provide additional information[384].

TAFs play a crucial role in tumour proliferation, invasiveness, angiogenesis and metastasis by secreting various growth factors, cytokines (such as IL-6) and chemokines (such as CXCL12). TAFs actively remodel the ECM in the TME by promoting the expression of ECM proteins (collagen, hyaluronan, fibronectin), MMPs and by inducing EMT[383,384]. TAFs have been also associated with resistance to anti-cancer drugs[384,385]. Hence, TAFs are often associated with poor outcomes in cancer, as reported in breast[386,387], prostate[388], lung[389], gastric[390] and pancreatic cancer[385,391].

The role of stromal cells in PAs has been poorly studied. A variety of human collagen-producing cells were described in PAs, including fibroblasts, myofibroblasts, myoepithelial cells, pericytes and chondrocytes, but their role remains unclear[392-395]. Tofrizal *et al.* studied the characteristics of stromal collagen-producing cells in human PAs and NP, relying on *in situ* hybridisation for collagen I and III and immunohistochemistry for α-SMA (marker for pericytes, but also activated fibroblasts) and cytokeratin (an epithelial marker)[395]. The only collagen-producing cells in NP were pericytes, whereas PAs had a variety of cells: pericytes, fibroblasts, myofibroblasts (activated fibroblasts) and myoepithelial cells. In PAs, fibroblasts and myofibroblasts were identified in the intra-tumoural fibrous matrix and in the PA capsule, whereas myoepithelial-like cells were located in the base of tumour cell clusters and had long cytoplasmic projections[395]. The number of collagen-producing cells and the number of different cell types correlated with the degree of fibrous deposition in PAs: PAs with no or few collagen-producing cells had less fibrous matrix deposition, whereas PAs with more collagen-producing cells had increased desmoplasia. Thyrotrophinomas

more collagen-producing cells and fibrous matrix, while most somatotrophinomas and null-cell PAs had little fibrosis[395].

Lv *et al.* cultured TAFs from 3 invasive and 3 non-invasive human PAs, and found that TAFs derived from invasive PAs had higher expression levels of α-SMA and VEGF than non-invasive TAFs or normal fibroblasts. TAFs from invasive PAs lead to higher proliferation in GH3 cells, as well as to significant tumour growth of GH3-derived xenografts in mice, effects not observed with normal fibroblasts or non-invasive PA-derived TAFs. Moreover, VEGF expression was higher in mouse GH3 xenografts co-injected with TAFs from invasive PAs than with TAFs extracted from non-invasive PAs or normal fibroblasts[396].

Pericytes

Pericytes are stromal cells located in the perivascular spaces, integrating the tissue vasculature. In cancer, pericytes not only provide support to the microvasculature within the tumour, but are also active elements in the TME, displaying an ability to recognise pro-inflammatory stimuli and mount a complex secretory response producing a variety of cytokines. Pericytes also express adhesion molecules that regulate transendothelial migration and recruitment of immune cells to the TME[397]. Moreover, pericytes can regulate other cancer-related mechanisms such as angiogenesis and EMT[397,398]. Several studies described an association between low amounts of pericytes and increased cancer invasiveness and metastasis, suggesting that a normal pericytes coverage of the tumour vasculature may negatively regulate metastases, leading to better cancer outcomes[399,400].

In the anterior pituitary gland, collagen-producing pericytes were first described in the rat. The expression of collagen I and III were located around the capillaries, corresponding to pericytes, which were the only collagen-producing cells described in the normal rat anterior pituitary[401] and also in the NP in humans[395]. Pericytes have also been described in human PAs, where they are mainly located in the perivascular spaces[395].

Folliculo-stellate cells

The major non-hormone secreting agranular pituitary cell type are folliculo-stellate cells, accounting for 5-10% of all the anterior pituitary cells. Folliculo-stellate cells have a star-shaped morphology, and are positive for S100 protein and glial fibrillary acidic protein (GFAP). They have several functions in pituitary homeostasis: scavenger activity with ability to perform phagocytosis removing cell debris of apoptotic endocrine pituitary cells; mechanical support to the surrounding

endocrine cells; and regulation of ion balance, water transport, and nurture of surrounding cells. In addition, folliculo-stellate cells produce a wide range of cytokines, chemokines, growth factors and enzymes that influence the surrounding endocrine cells[10,11,402].

Several studies have investigated folliculo-stellate cells in PAs. Höfler *et al.* analysed 7 NPs and 28 PAs for folliculo-stellate cell markers, and found that 5% of the normal anterior pituitary cells stained for S100, whereas S100 reactivity was not found in PAs except in one case[403]. Iwaki *et al.* reported few or no S100 or GFAP-positive cells in PAs, in comparison to NP adjacent to the neoplastic tissue; however, somatotrophinomas and prolactinomas had an appreciable number of folliculo-stellate cells[404]. In this study, no folliculo-stellate cells were seen in NFPAs, except in one case which was mainly composed by folliculo-stellate cells and immature glandular cells[404]. Other studies showed that folliculo-stellate cells are more representative of the PA cellular component, particularly in GH-producing PAs, in which they can be detectable in over two-thirds[405-408]. Voit *et al.* detected folliculo-stellate cells in 198 out of 286 somatotrophinomas; plurihormonal PAs had the highest folliculo-stellate cells density, but no correlation was found with gender, age, symptoms duration or PA size[408]. Another study also reported no correlation between folliculo-stellate cells content and PA aggressiveness[409].

The role of folliculo-stellate cells in pituitary tumourigenesis is not entirely clarified. These cells produce nitric oxide, activin, follistatin, VEGF, FGFs (fibroblast growth factors), PDGFs (platelet-derived growth factors), TGF-β, IL-6, IL-10, IL-11, CXCL10, CXCL12, LIF and MIF[10,269,402,410,411]. The folliculo-stellate cells' secretome is relevant for paracrine interactions with the surrounding cells, and may be involved in tumourigenesis. IL-6, a key cytokine in PA development, progression and biological behaviour[237,239], was localised to folliculo-stellate cells in the NP; however, in PAs IL-6 seems to derive from adenohypophyseal tumour cells[230,412]. Immunohistochemical data from PAs with limited T-cell mediated inflammatory reaction within the adenomatous tissue suggested that folliculo-stellate cells may be induced by inflammation within the TME and perform antigen presentation, thus being involved in tumour immunosurveillance[413].

Folliculo-stellate cells express different integrin subunits, which are cell surface receptors for ECM, and display marked changes in shape and proliferative activity in the presence of laminin, fibronectin and different types of collagen[410]. Folliculo-stellate cells produce metalloproteinase inhibitors, which protect the basement membrane from proteolysis[414]. On the other hand, folliculo-stellate cells were shown to be involved in basal lamina degradation[10,415]. These findings support the folliculo-stellate cells' ability to remodel the ECM in PAs.

Endothelial cells and angiogenesis in pituitary adenomas

Angiogenesis is the process by which new blood vessels are formed from pre-existing ones, and is of major importance for solid tumours growth which is depend on the vascular network for their nourishment and extension[303]. Endothelial cells are essential for angiogenesis, which determines the capacity for tumour dissemination. CD31 and CD34 are both endothelial cell antigens and sensitive microvessel markers[416]. Quiescent endothelial cells 'sense' the stimuli in the TME provided by neoplastic or inflammatory/stromal cells via angiogenic growth factors (such as VEGF, FGF and PDGF), cytokines and chemokines (such as IL-8), or owing to hypoxic conditions within the TME, which results in neovascularisation. However, the new tumour vessels are usually abnormal in terms of structure and function[417,418]. Lymphatic endothelial cells are also recruited to the TME under the influence of growth factors and cytokines within the TME, but these lymphatic vessels are abnormally formed allowing the dissemination of tumour cells[419,420].

PAs have a lower microvessel density than NP, while carcinomas appear to have the highest microvessel densities[302,303,415,421-424]. In general, there are no differences in vascularisation between different PA histiotypes[303,304,421]; however, microprolactinomas[421] and GH-secreting PAs[303] may be the least vascularised. Dopamine agonists or SSAs do not seem to affect microvessel density[303,422,425]. Some studies excluded association between vessel density and PA proliferation or invasiveness, indicating that other factors underlie the invasive potential of PAs[302,303,426,427]. Turner *et al.* did not find differences in microvessel density between invasive and non-invasive somatotrophinomas and corticotrophinomas, although invasive prolactinomas were significantly more vascular than the non-invasive ones[422].

The lack of significant vascularisation in PAs, and the lack of association between vascularisation and invasiveness in PAs, may explain the slow pace of PAs proliferation and their benign nature[297,303,416]. In contrast, increased microvessel density described in pituitary carcinomas is in line with the fact that distant metastasis occurrence depends on angiogenesis[303].

Exploring this further, within the context of the complex interactions within the TME in PAs, may provide invaluable insights in PA pathophysiology and therapeutic advances for aggressive PAs, as illustrated by the case of an aggressive silent corticotrophinoma which progressed to a carcinoma and was treated successfully with bevacizumab (anti-VEGF monoclonal antibody)[428].

1.7 Extracellular matrix and remodelling enzymes in pituitary adenomas

The ECM is composed of different molecules such as collagens, glycosaminoglycans and laminin, and its characteristics are different from tissue to tissue, which is a determinant in the tissue-specific features such as architecture, organisation, consistency and biological functions, influencing normal physiology of surrounding cells[429]. Besides its physiological role, the ECM plays a key role in several pathological conditions, including cancer. ECM's role in TME is not limited to mechanical protection against tumour invasion, but also acts as a reservoir for proteins, growth factors and enzymes that affects the surrounding cells. In turn, tumour and stromal cells may modify the composition and function of ECM mainly by secreting proteases and protease inhibitors[430-432], and thus interfere with cell-cell and cell-ECM interactions[429]. ECM remodelling proteases play a role in angiogenesis, where they can regulate endothelial cell proliferation and vascular morphogenesis. These proteases are needed to degrade the ECM and allow endothelial cells to penetrate the tumour stroma[433,434]. The crosstalk between ECM and neoplastic and non-neoplastic cells affects tumour cell behaviour, proliferation, invasion and metastasis[435-438].

MMPs are one of the most important ECM-degrading proteases. They belong to the family of zinc-binding endopeptidases, containing a signal peptide, a propeptide, a catalytic domain, and a hemopexin domain able to degrade ECM, basement membrane and connective tissues, essential for tissue remodelling, inflammatory response, and in cancer for invasion and angiogenesis[207,439]. Under inflammatory conditions, MMPs are upregulated and released in the TME either by neoplastic or non-neoplastic cells, such as fibroblasts or macrophages. An association between MMP activity and invasiveness has been shown in different cancers[440-443]. MMP activity is inhibited by tissue inhibitors of metalloproteinases[439].

In the anterior pituitary, ECM is composed mainly by collagen types I and III[395,401]. In PAs, ECM deposition is variable, and collagens are its main stromal component, although their expression differ from NP[395,444]. Jarzembowski *et al.* noted that PAs have less type IV collagen in their basement membranes[445]. Collagen type IV is the main component of the pituitary capsule and medial wall of cavernous sinus[446-448]. The collagen type may determine mechano-transduction pathways that regulate cell invasion/migration ability as seen in GH3 cells[449].PAs are mostly 'benign', but up 30-45% of them invade structures such as cavernous or sphenoid sinuses[448,450]. Several studies described an association between MMPs expression and invasive PAs, with a great focus on MMP-2 and MMP-9, considering that these are type IV collagenases, essentially degrading type IV collagen. Most studies indicate that MMP-2 and MMP-9 correlate with PA invasiveness[450-453], confirmed in a meta-analysis that included in total 24 studies (1320 patients)[448].

Patients with recurrent disease had higher MMP-9 levels providing evidence that MMP-9 overexpression is likely associated to worse outcomes[448]. One study showed that MMP-2 and MMP-9 may stimulate hormone secretion[454]. The regulation of MMP-2 and MMP-9 expression in PAs is not yet clarified, but some different proteins may be involved[455-459]. A recent study analysed the role of MMP-14 (cleaves collagen types I, II and III) in PAs, suggesting that MMP-14 plays a role in invasion and angiogenesis[460]. The protease kallikrein-like peptidase 10 was found overexpressed in PAs and correlated with aggressiveness[461,462]. Prolactinomas, thyrotrophinomas and carcinomas were strongly immunopositive for kallikrein-like peptidase 10; in gonadotroph adenomas and somatotrophinomas its immunoreactivity was mild to moderate and seen only in few cells. Another study showed higher kallikrein-like peptidase 10 expression in corticotrophinomas than in NFPAs or normal corticotrophs[461]. Expression of cathepsin B, a lysosomal protease with ability to degrade ECM, also correlated with the invasiveness of PAs[463].

Integrins are important transmembrane molecules that mediate cell-cell and cell-ECM adhesion. Farnoud *et al.* reported that some integrins were downregulated or abrogated in human PAs in comparison to NP, while the stromal cells expressed many more integrin subunits in comparison to normal connective pituitary tissue. However, these changes were not associated with invasiveness or with PA type[464]. Fibronectin, another ECM element, is expressed differently in the connective tissue of NP and PAs[465]. Taking these findings together, the ECM in NP differs from PAs which therefore may influence tumourigenic processes.

1.8 Epithelial-to-mesenchymal transition (EMT) in pituitary adenomas

EMT in cancer

EMT is a reversible complex process whereby tumour cells are reprogrammed to acquire a mesenchymal phenotype acquiring a migratory and invasive phenotype, by losing the epithelial polarity and adhesion molecules, in particular E-cadherin, and concomitantly gaining a spindle-shaped morphology and migratory phenotype (Figure 1.11). EMT is involved in physiological phenomena, such embryonic development, wound healing and fibrosis[466,467]. In cancer, EMT is determined by the complex interactions between different TME elements and EMT plays a key role in tumourigenesis, tumour invasion, progression and metastasis[466-468]. The surrounding non-neoplastic cells in the TME, such as lymphocytes, macrophages, or fibroblasts, are potent regulators of EMT[335,466,469-472]. Moreover, TME hosts cytokines, chemokines, growth factors and enzymes derived from tumour or non-neoplastic cells that can directly induce EMT[467,469,473-478].

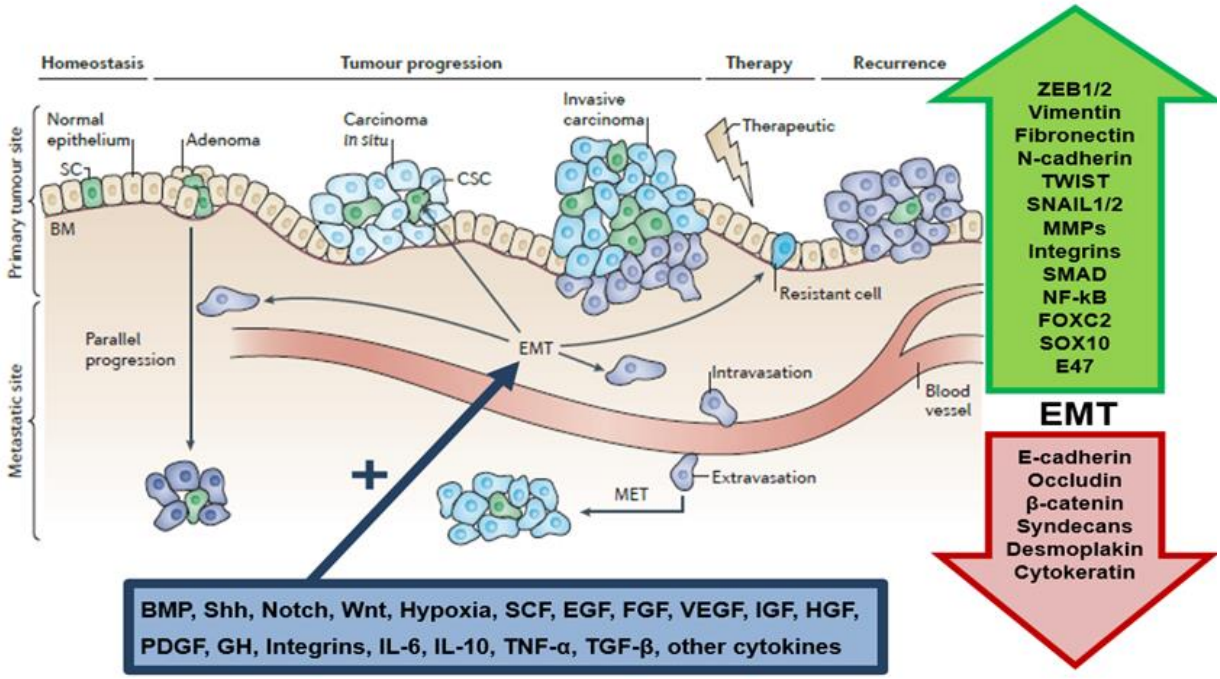

Figure 1.11: EMT in cancer and its signalling pathways.
In tumour cells, EMT-inducing transcription factors may redefine epithelial status of the cell, assigning stem cell (SC) characteristics to these dedifferentiated tumour cells. EMT can also redefine altered stem cells to be cancer stem cells (CSCs). Dissemination and subsequent migration of tumour cells after breakdown of the basement membrane (BM) can be achieved when all EMT component pathways are: if the tumour cell acquired the necessary genetic aberrations and receives the appropriate signals at the tumour–host interface, the cell moves towards metastasis. At this point, the contribution of the EMT-associated programme is to provide survival signals and to maintain the mesenchymal status of the metastasising cell. Moreover, it is likely that EMT also has a role in tumour progression. EMT features may further promote resistance during therapy, leading to recurrence and a poor cancer outcomes. The degree of EMT and mesenchymal-to-epithelial transition during the different steps in cancer probably depends on the imbalance of several regulatory networks with activated oncogenic pathways. Multiple signalling pathways

and agents, such as growth factors or cytokines, are able to induce EMT both during embryonic development and human diseases such as in cancer. BMP, bone morphogenetic protein; CSC, cancer stem cell; EGF, epidermal growth factor; EMT, epithelial-to-mesenchymal transition; FGF, fibroblast growth factor; FOXC2, fork-head box protein 2; GH, growth hormone; HGF, hepatocyte growth factor; IGF, insulin-like growth factor; IL, interleukin; MET, mesenchymal-to-epithelial transition; MMP, matrix metalloproteinase; NF-kβ, nuclear factor-kβ; PDGF, platelet-derived growth factor; SC, stem cell; SCF, stem cell factor; SOX10, SRY-box 10; TGF-β, transforming growth factor-β; TNF-α, tumour necrosis factor-α; VEGF, vascular endothelial growth factor; ZEB, zinc finger E-box-binding homeobox. Adapted from De Craene & Berx (2013)[466], and Thiery *et al.* (2009)[467].

Epithelial cells that undergo EMT loose epithelial markers, most notably E-cadherin, but also markers such β-catenin, claudins, cytokeratins and syndecans[467,479,480]; concomitantly, they adopt a mesenchymal morphology, overexpressing mesenchymal markers such as zinc finger E-box-binding homeobox-1 (ZEB1), N-cadherin or vimentin (Figure 1.11)[466,467,481].

EMT involves multiple regulatory pathways, which can be grouped into four main networks[466]: (i) the most extensively studied network is EMT transcription regulation by a number of transcription factors such as ZEB1, ZEB2, SNAIL, SLUG, TWIST, E47, KLF8, FOXC2, E2-2, homeobox protein SIX1 and goosecoid. SNAIL, ZEB and TWIST are regarded as the master EMT transcription factor regulators as they repress not only the promoter of *CDH1* (encoding E-cadherin), but also other epithelial adhesion molecules such claudins or desmossomes[466,467,481-487]; (ii) expression of small non-coding RNAs, in particular miR200, miR34, miR101, potent modifiers of gene expression which are able to influence cell phenotype by suppressing genes involved in epithelial or mesenchymal states[488-490]; (iii) EMT-related alternative splicing events, in which different splicing of mRNA precursors lead to distinct proteins from the same gene[466], with epithelial splicing regulatory proteins 1 and 2 (ESRP1 and ESRP2) being particularly relevant in cancer[491-494]; (iv) post-translational dysregulation of EMT-transcription factors, affecting their protein structure and function[466,495-498].

Recent studies have suggested that GH can induce EMT either indirectly via IGF-1 or through the activation of several signalling pathways (JAK-STAT or mitogen-activated protein kinase (MAPK) pathways) with subsequent influence in the transcription of EMT-related genes, in both non-cancerous or cancerous epithelial cells, as shown in melanoma, breast, colorectal, endometrial and pancreatic cancer[499].

EMT-related reversible plasticity, i.e. when mesenchymal cells revert to an epithelial phenotype, a phenomenon termed mesenchymal-to-epithelial transition (MET), has been shown in cancer, and seems crucial for the establishment of metastatic deposits[466,467]. Cancer behaviour is

intrinsically related to this EMT-MET balance. Advanced carcinomas may adopt some mesenchymal features, yet retaining well-differentiated epithelial features, and this tumour heterogeneity may be due to incomplete EMT or reversion to an epithelial phenotype (partial MET). Hence, EMT is part of the complex metastatic process[500,501].

EMT in pituitary adenomas

The relevance of EMT to the pituitary embryonic development is being increasingly revealed. Recent studies have shown that Sox2-expressing stem/progenitor pituitary cells undergo EMT under the control of specific EMT transcription factors, but also by some pituitary specific transcription factors. These progenitor cells change their properties by EMT under the influence of the local microenvironment, acquiring migratory ability during embryogenesis but also in the postnatal period, and develop ultimately into anterior pituitary specialised cells[55,502].

EMT in pituitary tumourigenesis is, however, largely unexplored. Qian *et al*. have shown that the expression of E-cadherin and β-catenin seem to be significantly lower in invasive prolactinomas in comparison to non-invasive ones: macroprolactinomas had lower E-cadherin expression, and decreased E-cadherin expression was associated with a higher Ki-67. These findings suggest that reduced expression of E-cadherin and β-catenin may lead to more aggressive prolactinomas[503].

Later in 2007, Qian *et al.* shown that downregulation and methylation of *CDH1* (E-cadherin) and *CDH13* (H-cadherin) genes correlate with more aggressive PAs. In this study, reduced expression of H-cadherin was noted in 54% of PAs and was associated with more aggressiveness; on the other hand, E-cadherin expression was reduced in 32% and completely lost in 30%, and its expression was lower in grade II, III, and IV than in grade I PAs. Promoter hypermethylation of *CDH13* and *CDH1* was detected in 30% and 36% of the 69 PAs, respectively, but not in 5 NPs, and was associated with PA invasiveness. *CDH1* and *CDH13* downregulation was correlated with the respective promoter hypermethylation suggesting that the tumour-specific methylation and downregulation of *CDH13* and *CDH1* is involved in the development of PAs[504].

In acromegaly, lower E-cadherin expression was associated to larger PAs, increased invasiveness and reduced response to SSA[449,460,461]. In contrast, E-cadherin was positively correlated with GH mRNA and GH serum levels, and also with serum IGF-1[505]. Lekva *et al.* performed a microarray analysis on 16 somatotrophinomas, 8 with low and 8 with high E-cadherin expression, and reported 29 known EMT-related genes differentially regulated. None of the classical EMT regulators (ZEB1, ZEB2, SNAIL, SLUG, TWIST, E47, Goosecoid) nor the classical mesenchymal

markers (vimentin, desmin, N-cadherin) were increased in GH-secreting PAs with low E-cadherin expression. This show that despite the E-cadherin decrease, these PAs do not have a true EMT phenotype. This is consistent with the fact that PAs are benign and rarely metastasise, which may explain this partial EMT signature[505]. Human microarray data was validated by RT-qPCR, which showed lower expression of *ESPR1*, plakophilin 2 (*PKP2*), TP53 apoptosis effector (*PERP*), interferon regulatory factor 6, roundabout axon guidance receptor homolog 1 (*ROBO1*), bicaudal C homolog 1 and serine peptidase Kunitz type I, and higher expression of clusterin and glutamate-ammonia ligase (*GLUL*) in PAs with low E-cadherin expression. Considering that ESPR1 is a key gene in EMT-alternative splicing, and was downregulated in somatotrophinomas expressing low E-cadherin[505], further studies silencing *Esrp1* in GH3 cells were performed, showing that *Esrp1* transiently regulates several EMT-related genes, whereas *Cdh1* silencing in GH3 cells changed expression of only 2 genes (*Glul* and *Pkp2*), indicating that E-cadherin is likely a marker but not a mediator of EMT in GH3 cells[505]. These findings suggest ESRP1 as an EMT regulator in somatotrophinomas[505].

Chen *et al.* investigated the expression of the transmembrane proteins involved in cell adhesion TROP1 (also known as epithelial cell adhesion molecule (EpCAM)) and TROP2 in PAs, with both being overexpressed in PAs and associated with tumour invasiveness and higher Ki-67[506].

Chapter 2: Materials and methods

Materials

Human pituitary adenoma samples

Fresh human PA tissues from 24 patients were obtained at the time of transsphenoidal surgery from the National Hospital for Neurology and Neurosurgery, UCLH, NHS Trust. A fragment was processed for the primary culture studies, whereas the other part was processed for the immunohistochemical studies as well as for the histopathological diagnosis. The clinico-pathological and biochemical data from each patient were collected from their medical records, clinical letters and imaging and/or pathology reports. This study was approved by the local Ethics Committee (MREC No. 06/Q0104/133) and written informed consent was obtained from all the patients. NP autopsy samples from my lab collection (specimens derived from healthy subjects deceased from road traffic accidents, who had no autoimmune, inflammatory or oncological disorders, neither were on medications that could potentially affect the immune system such as glucocorticoids or immunosuppressive drugs) were included in the immunohistochemical studies for comparison.

Human PA and skin fibroblasts

Human PA-associated fibroblasts were isolated from 16 out of the 24 PA samples obtained after surgery, as described below. Early passage human skin fibroblasts, isolated from skin biopsies on two healthy young individuals (one male and one female), were a kind gift from Dr. Leo Guasti (William Harvey Research Institute, Queen Mary University of London, UK). Early passage human skin fibroblasts from individuals with germline *AIP* mutations (in homozygosity and in heterozygosity), used in the cytokine array studies (Chapter 6), were a kind gift from Dr. Hilde van Esch and Dr. Wim Huybrechts (UZ Leuven, Belgium).

Cell lines

The rat pituitary somatomammotroph GH3 cell line was obtained from the European Collection of Authenticated Cell Cultures. A stably lentiviral-transduced shRNA knockdown of *Aip* in the GH3 cells (GH3-*Aip*-KD), as well as a non-targeting shRNA control (GH3-NT), were produced by Sirion

Biotech, Germany [507], and used in the cytokine array studies (Chapter 6). Early passage murine RAW 264.7 macrophages were a kind gift from Dr. Giulia Marelli (Barts Cancer Institute, Queen Mary University of London, UK).

Methods

Primary cell culture of pituitary adenomas

Fresh human PA tissue was obtained at transsphenoidal surgery and collected in complete medium - high glucose Dulbecco´s Modified Eagle´s Medium (DMEM, Sigma, Gillingham, UK, cat. no. D6429) supplemented with 10% heat-inactivated foetal bovine serum (FBS, Gibco, Loughborough, UK, cat. no. 16000044) and 0.5% gentamicin (Sigma, cat. no. G1397). The PA samples were carried to the laboratory and the primary cultures established on the same day of the operation. Representative images from PAs on pre-operative MRI scans, and the appearances of a tumour fragment before culturing and of a PA primary culture prior to supernatant collection, are shown in Figure 2.1.

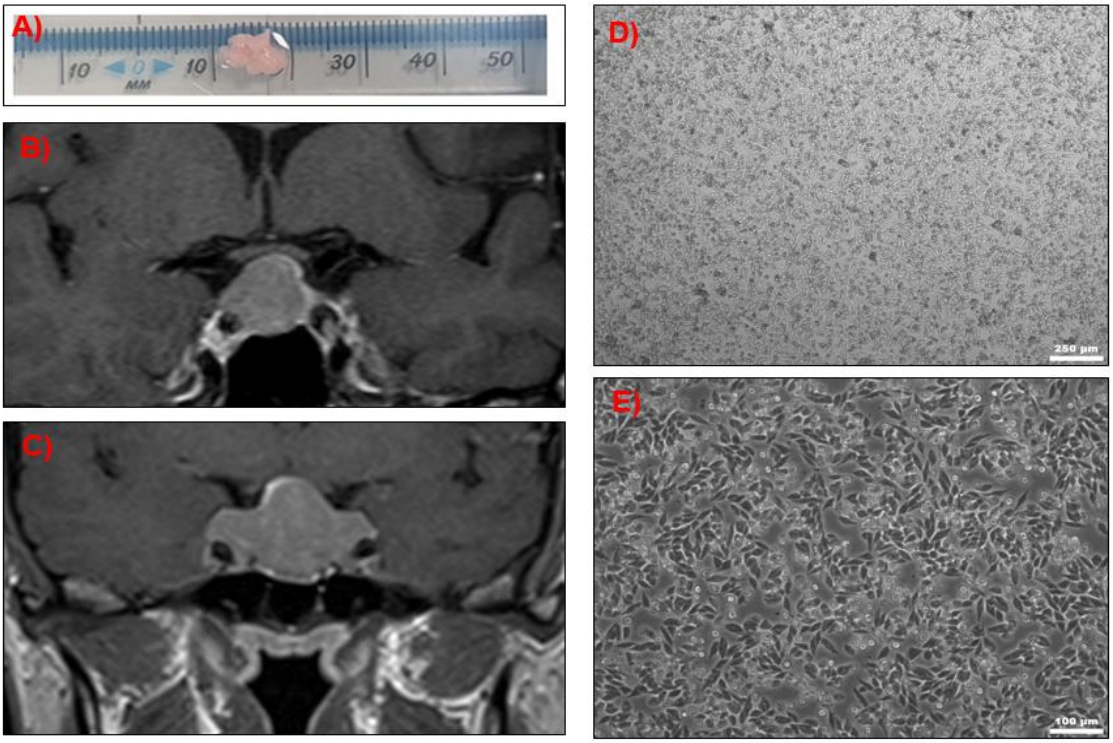

Figure 2.1: Appearances of a PA on MRI, a PA fragment before culturing and a PA primary culture
A) Macroscopic appearance of a fresh human pituitary adenoma (PA) fragment. This small piece of tissue (approximately 10 mm) was obtained via transsphenoidal surgery, collected on complete medium, and washed before mechanical and enzymatic dispersion. B-C) Pituitary MRI of a NFPA (B) and a somatotrophinoma (C). In both cases, the MRI scan at the time of diagnosis show a pituitary macroadenoma with suprasellar extension impinging the optic chiasma. D-E) Somatotrophinoma primary culture prior to supernatant collection after 24h on serum-free medium. Seeding concentration per well: $2x10^6$ cells (6-well plates). Picture magnifications: 4x (D) and 10x (E).

The excised PA tissue was placed in a Petri dish, washed at least 3 times with magnesium and calcium-free Phosphate Buffered Saline (PBS) (Sigma, cat. no. D8537), cut into small pieces and incubated for 45min at 37ºC in 10 times diluted Trypsin-EDTA 0.05% (1X) Phenol Red (Gibco, cat. no. 25300054) with frequent pipetting allowing effective cell dispersion. Trypsin digestion was stopped by adding complete medium, then cells were transferred to a tube and allowed to stand for 10min for sedimentation of undigested debris (used for isolation of PA-associated fibroblasts as explained below). Supernatants containing tumour cells were transferred to a separate tube, centrifuged at 800g for 5min, and gently re-suspended in 1mL complete medium. Viable cells were assessed with Tryptan Blue Solution (Sigma, cat. no. T8154) and manually counted using a haemocytometer. When cell viability was >90%, $2x10^6$ cells were seeded in complete medium in a well from a 6-well plate previously coated with Poly-L-lysine (Sigma, cat.no. P4707). The well coating was done by completely covering the well surface with a mixture containing Poly-L-lysine (10µL) and PBS (1mL) for at least 5min at room temperature, after which this solution was aspirated and the well washed with PBS in order to prevent toxicity to the cells. Cells were then incubated overnight at 5% CO_2 and 37ºC overnight. Next day the cells were examined under a bright field microscope, then old medium was aspirated and new medium was added.

Primary cell culture of fibroblasts

PA-associated fibroblasts (TAFs) were isolated through the so-called outgrowth method[391]: undigested debris pieces, obtained after mechanical and enzymatic dispersion of freshly collected human PA tissues (as explained above), were placed in a manually scratched uncoated 6-well plate and incubated at 5% CO_2 and 37ºC in complete medium. Plates were examined under the microscope daily, and complete medium was replaced 3 times a week. After 2-3 weeks, TAFs migrated out of the debris and, when confluent (about 4 weeks later), were transferred to uncoated culture flasks; no other cells, including pituitary tumour cells, were seen at this late stage. Healthy human skin fibroblasts, as well as human *AIP*mut skin fibroblasts, were grown in complete medium replaced 3 times a week. Trypsin-EDTA 0.05% (1X) Phenol Red was used for mobilising both TAFs and skin fibroblasts after incubation at 5% CO_2 at 37ºC for 5min.

Cell lines culture

Cell lines (GH3 cells and RAW 264.7 macrophages) were incubated at 5% CO_2 and 37ºC, and cultured in complete medium (high glucose DMEM supplemented with 10% FBS and 0.5%

gentamycin). 100 µL of puromycin (10mg/mL, Science Warehouse, cat. no. P9620) was added to GH3 cells medium allowing a positive selection for GH3-*Aip*-KD and GH3-NT cells. Once cells were 70-90% confluent, they were passaged after aspirating medium, 2 washes with magnesium- and calcium-free PBS and mobilisation with Trypsin-EDTA 0.05% (1X) phenol-red solution for GH3 cells, or with Accutase® solution (Sigma, cat. no. A6964) for RAW 264.7 macrophages. Once cells were detached (confirmed by light microscopy), the cell/trypsin solution was put into new flasks or spun (3min, 1200g), and re-suspended in DMEM to be further use in *in vitro* experiments.

Preparation of cell culture conditioned medium for *in vitro* experiments and supernatants for cytokine multiplex array

GH3 cell conditioned medium (CM) was generated by seeding $5x10^6$ GH3 cells in T75 culture flasks for 72h in 10mL complete medium. Macrophage-CM was generated from $5x10^6$ RAW 264.7 macrophages in T75 culture flasks for 24h in 10mL of complete medium (-PMA_Raw-CM) or stimulated with 5nM of Phorbol 12-Myristate 13-Acetate (PMA) (Sigma, cat. no. P8139) in 10mL of complete medium (+PMA_Raw-CM).

Cell culture supernatants for cytokine array were generated by seeding $5x10^5$ GH3 cells in 12-well plates for 24h in serum-free medium conditions at baseline and after treatment with RAW 264.7 macrophage-CM. Supernatants were collected by tilting the plate (avoiding direct contact with the cells) and transferred to clean 1.5mL-Eppendorf tubes and immediately placed on ice (to avoid cytokine degradation). The tubes were then centrifuged at 10,000rpm for 10min at 4ºC (to remove cellular debris), and supernatants containing the cytokines were collected in a new tube and stored in -80ºC (for a short time, 3-6 months) until assay.

Fibroblast supernatants for cytokine array were collected from $5x10^5$ early passage fibroblasts seeded in T75 culture flasks and grown in complete medium until 90% of confluence. Following washes, and culture in 6mL serum-free medium, supernatant was collected after 24h and stored at -80ºC until assay. After 48h in complete medium, cells were treated with 10^{-7}M pasireotide (Novartis Pharma, Basel, Switzerland) in 6mL serum-free medium for 24h. The supernatants were then carefully transferred to clean tubes, centrifuged at 10,000rpm for 10min at 4ºC, and then collected and stored in -80ºC for 3-6 months until assay. CM from TAFs or normal human skin fibroblasts were generated similarly, but in complete medium conditions.

Cytokine multiplex arrays

Cytokine arrays on human primary culture supernatants (PAs, TAFs and skin fibroblasts) were performed by Eve Technologies (Calgary, Alberta, Canada), according to their protocol (available at https://www.evetechnologies.com/discovery-assay/) by using the Bio-Plex™ 200 system (Bio-Rad Laboratories, Inc., Hercules, CA, USA) and the human cytokine/chemokine array with IL-18 (HD42) kit (Millipore, St. Charles, USA). This array measures 42 different cytokines, chemokines and growth factors in the same sample: G-CSF, GM-CSF, IFNα2, IFNγ, IL-1α, IL-1β, IL-1ra, IL-2, IL-3, IL-4, IL-5, IL-6, IL-7, IL-8, IL-9, IL-10, IL-12(p40), IL-12(p70), IL-13, IL-15, IL-17A, IL-18, CXCL1, CXCL10, CCL2, CCL3, CCL4, CCL5, CCL7, CCL11, CCL22, CX3CL1, sCD40L, Flt-3L, PDGF-AA, PDGF-BB, TGF-α, TNF-α, TNF-β, VEGF-A, EGF and FGF-2.

Cytokine array studies on supernatants from rat GH3 cells and mouse RAW 264.7 macrophages were also performed by Eve Technologies, using a different species-specific kit array. In GH3 cells supernatants 27 different cytokines were measured with the rat cytokine/ chemokine array 27-plex (RD27) kit (Millipore): G-CSF, GM-CSF, IFNγ, IL-1α, IL-1β, IL-2, IL-4, IL-5, IL-6, IL-10, IL-12(p70), IL-13, IL-17A, IL-18, CXCL1, CXCL2, CXCL5, CXCL10, CCL2, CCL3, CCL5, CCL11, CX3CL1, TNF-α, VEGF, EGF and Leptin.

Mouse RAW 264.7 macrophages supernatants were assessed with the mouse cytokine/ chemokine array 31-plex (MD31) kit (Millipore) measuring: G-CSF, GM-CSF, M-CSF, IFNγ, IL-1α, IL-1β, IL-2, IL-3, IL-4, IL-5, IL-6, IL-7, IL-9, IL-10, IL-12(p40), IL-12(p70), IL-13, IL-15, IL-17A, CXCL1, CXCL2, CXCL5, CXCL9, CXCL10, CCL2, CCL3, CCL4, CCL5, CCL11, TNF-α, VEGF and LIF.

The multiplexing Millipore MILLIPLEX cytokine arrays provided by Eve Technologies is based on colour-coded polysterene beads conferring unique colour/fluorophore signature that can be individually identified by the bead analyser Bio-Plex 200 system. Bio-Plex 200 includes a dual-laser system, one laser activating the fluorescent dye within the beads and the second laser exciting the fluorescent conjugate streptavidin-phycoerythrin, as well as a flow cytometry system. The amount of the conjugate detected by the analyser is directly proportional to the amount of the target analyte. The results are quantified according to a standard curve. With this assay, different analytes (i.e. cytokines, chemokines or growth factors) can be measured concomitantly in the same sample, and each one can be distinguished from the others because they are bound to different coloured/fluorescent beads (Figure 2.2)[508].

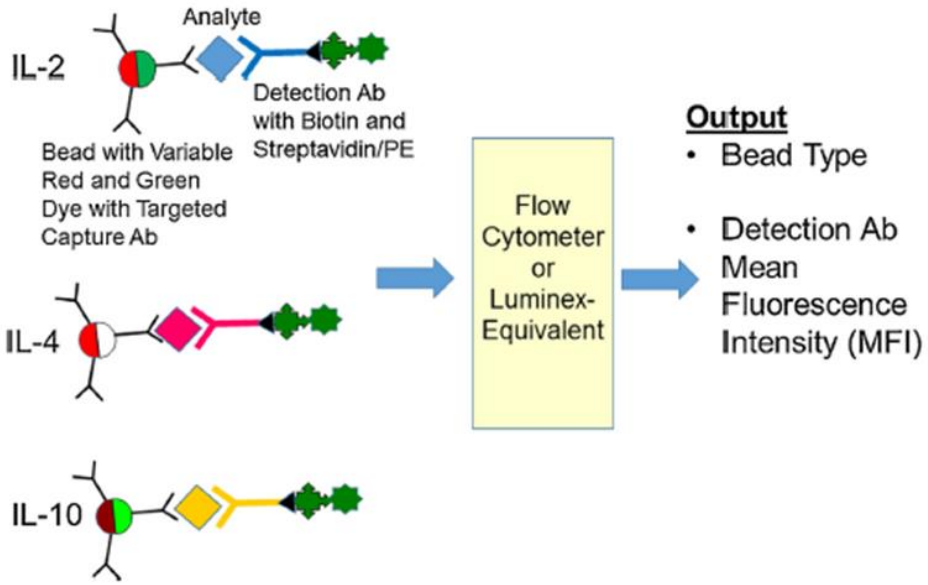

Figure 2.2: Overview of the multiplexing cytokine bead-based immunoassays
Adapted from Stenken & Poschenrieder (2015)[508].

Enzyme-linked immunosorbent assay (ELISA)

The CX3CL1 (fractalkine) rat ELISA Kit (Abcam, cat. no. ab100761) was used for the quantitative measurement of CX3CL1 in GH3 cell supernatants, following the manufacturer´s protocol. Briefly, this assay employs a specific antibody for rat CX3CL1 coated on the 96-well plate. A fresh set of standards were prepared through serial dilutions from the vial of CX3CL1 standard prior to use, and ELISA kit reagents were also prepared fresh before the experiment. The ELISA procedure was done at room temperature. Standards and samples were pipetted into the wells (100µL) and incubated for 2.5h (allowing the CX3CL1 present in the samples and in the standards to bind to the wells by the immobilised antibody). The wells were washed and 1X biotinylated anti-rat CX3CL1 detection antibody was added (100µL) and incubated for 1h. After washing away unbound biotinylated antibody, 1X HRP-conjugated streptavidin (100µL) was pipetted to the wells, following which the wells were washed and a TMB one-step substrate reagent was added (100µL) and incubated for 30min at room temperature in the dark on a plate shaker. The colour developed in proportion to the amount of CX3CL1 bound to the wells, and the Stop solution (50µL) changed the colour from blue to yellow, and its intensity measured at 450nm in a time-resolved fluorometer. The obtained optical density data for each sample were uploaded into an ELISA Analysis Website (http://www.elisaanalysis.com/app) which assisted with the calculation of each sample CX3CL1 concentration extrapolated from the standard curve.

Cell morphology analysis

Cell shape analysis and morphological changes were assessed by measuring 6 different shape parameters using the software ImageJ (National Institutes of Health, USA): area (area of selection in calibrated square units, μm^2); perimeter (μm); Feret's diameter (longest distance between any 2 points along selection boundary); roundness (representing shape, $4 \times [Area] / \pi \times [Major\ axis]^2$, with value of 1 for a circle and 0 for very elongated shape); circularity (representing perimeter smoothness, $4\pi \times [Area][Perimeter]^2$, with a value of 1 indicating a perfect circle and value close to 0 indicating elongated shape) and solidity (representing cell stiffness and deformability, [area] /[Convex area], with a value of 1 indicating more stiff and less deformable cell). Per treatment condition, 5 images at 40x were taken and 15 cells were measured per image, hence 75 cells were analysed per experiment (a minimum of 3 experiments were done).

Invasion assay

Invasion assays were carried out using the BioCoat Matrigel Invasion Chambers with 8μm pores (24-well insert; BD Biosciences, CA, USA, cat. no. 354480). Invasion chambers were hydrated for 2h with 500μl of serum-free medium at 5% CO_2 at 37°C. After matrigel rehydration, 750μL of macrophage-CM, TAF-CM, normal skin fibroblast-CM or complete medium was added to the lower chamber (acting as chemoattractant) and $2.5x10^4$ GH3 cells in 500μL serum-free medium were added to the upper chamber and incubated at 37ºC. After 72h, invading cells through matrigel were fixed in 100% methanol and stained with 2% Giemsa blue (Sigma-Aldrich, MO, USA, cat. no. G5637-5G). The total number of invading cells per chamber were counted, and normalised to invading cells towards complete medium. Invasion assays were run in duplicates and were repeated at least 3 times.

Transwell migration assay

GH3 cell migration and macrophage chemotaxis were evaluated by using transwell biocoat cell culture migration insert plates with 8μm pores (24-well insert; Corning Fisher Scientific, USA), following a similar protocol as described for the invasion assay. The total number of migrated cells per chamber were counted, and normalised to migrated cells towards complete medium. Transwell migration assays were run in duplicates and were repeated at least 3 times.

Wound healing migration assay

GH3 cell migration was also assessed by wound healing assay using Ibidi culture inserts (two reservoirs in μ-Dish 35 mm; Ibidi GmbH, Germany, cat. no. 81176) as follows: GH3 cells were seeded in complete medium to the inserts (70μl; 7×10^5 cells/mL), and incubated at 5% CO_2 at 37°C. After 24h, inserts were removed to generate a 500μm cell-free gap in a monolayer of cells. Detached cells were removed by replacing with the fresh complete medium or macrophage-CM. Photographs of the gap area were taken immediately and then at different times by an inverted microscope.

Immunocytochemistry

Fibroblasts or GH3 cells ($5x10^4$) were plated on 15mm coverslips in 12-well plates in complete medium. After overnight attachment, fibroblasts were fixed and stained, while GH3 cells were further treated for 24h under different conditions (-PMA_Raw-CM, +PMA_Raw-CM, TAF-CM or complete medium). Cells were fixed in 4% paraformaldehyde for 15min at room temperature, following washes with PBS cells were permeabilised with 0.1% Triton X-100 in PBS for 5min at 4°C. Cells were washed and blocked with 1% bovine serum albumin for 30min at room temperature, and then incubated with primary antibodies (listed in Appendix 2) followed by a 30min incubation with secondary conjugated antibodies (Alexa Fluor 568-conjugated goat anti-mouse IgG, Alexa Fluor 488-conjugated donkey anti-mouse IgG and Alexa Fluor 488-conjugated donkey anti-rabbit IgG; Molecular Probes, Invitrogen; dilution 1:1000). Actin staining was performed using Actin Stain (Molecular Probes, cat.no. R37110, 2 drops/ml, dilution 1:500). Coverslips with stained cells were mounted with Fluoroshield with 4',6-diamidino-2-phenylindole (DAPI) mounting medium (Sigma, cat. no. F6057). Stained slides were visualised on a confocal microscope LSM 880 Zeiss and images taken at 63x magnification. E-cadherin and ZEB1 fluorescent intensities were quantified using the software Carl Zeiss Zen Blue Edition v2.3.

Flow cytometry

Cells were harvested and spun down into a pellet (1200g/8min). The cell pellet was resuspended in PBS, and then transferred to a 96-well plate (100μL/well). The plate was spun at 2000g for 5min, and after plate was flicked to remove the supernatant. Fc receptors were blocked using 50μL of supernatant harvested from the 2.4G2 (CD16/32) hybridoma (kind gift from Dr. Oliver Haworth (1:5 dilution on PBS) and incubated on ice for 20min. The plate was again spun at 1200rpm for

5min, supernatants discarded, then the mix solution containing the antibodies (anti-CD86, eBioscience, cat. no. E20040-104; anti-CD206, BioLegend, cat. no. 141721; anti-MHCII, BioLegend, cat. no. 107621; anti-CCR2, R&D Systems, cat. no. FAB5538P; anti-CCR5, BioLegend, cat. no. 107055) diluted in PBS-20%FBS (1:200), as well as the respective isotype controls, were added to the corresponding well (50µL/well) and allowed to incubate for 20min on ice in the dark. Supernatants were discarded, cell resuspended in PBS-20%FBS (100µL/well) and then the plate was carried to the BD LSRFortessa 2 cell analyser (BD Biosciences). The data were analysed with the software FlowJo (FlowJo LLC, USA).

RNA extraction

RNA from GH3 cells, RAW 264.7 macrophages, TAFs and normal skin fibroblasts was extracted using Qiagen´s RNeasy mini kit (Qiagen, cat. no. 74004) following the manufacturer´s protocol. Cells were harvested and homogenised through repeated pipetting within a proprietary solution containing a high concentration of guanidine isothiocyanate which acts as an RNase enzyme inhibitor. Ethanol was added to aid the binding of RNA to the silic-based membrane found within the Qiagen spin columns. DNase digestion was performed with the Qiagen kit DNase I incubation mix, which was applied directly to the RNeasy MinElute spin column membrane (avoiding the walls or the O-ring of the spin column) in order to ensure complete DNAse digestion and to prevent DNA contamination in further RT-qPCR experiments. Centrifugation enables the contaminants to be isolated and washed away. RNA was eluted in distilled water, and its concentration and purity assessed with the NanoDrop ND-1000 spectrophotometer (A260/280 ratio should range between 1.8–2.1; values outside this interval indicate DNA or protein contamination, and in that case such samples were discarded and not used for further experiments).

Reverse transcription

Complementary DNA (cDNA) was synthesised from 1µg of RNA using the High-Capacity cDNA Reverse Transcription Kit (Thermofisher Scientific, cat. no. 4374966), following the manufacturer´s protocol. Briefly, 2X RT Master Mix was prepared on ice and with RNase-free reagents (to avoid RNase contamination), by adding per reaction 2.0µL 10X RT Buffer, 0.8µL 25X dNTP Mix (100mM), 2.0µL 10X RT Random Primers, 1.0µL MultiScribe™ Reverse Transcriptase, 1.0µL RNase inhibitor, 3.2µL Nuclease-free water. Then, 10µL of 2X RT Master Mix was added to 10µL of water in an individual tube (one per reaction), mixed well and shortly spun (to allow its content to settle down

and to eliminate any air bubbles). Negative RT control samples (–RT), where reverse transcriptase was omitted, were also prepared. The reverse transcription was performed in a thermal cycler according with the following 4-step programme: step 1) 25ºC for 10min; step 2) 37ºC for 120min; step3) 85ºC for 5min; Step4) 4ºC ∞. Synthesised cDNA was stored at -20ºC.

Real-time quantitative polymerase chain reaction (RT-qPCR)

RT-qPCR reactions were prepared using Brilliant III Ultra-Fast SYBR Green QPCR Master Mix (Agilent Technologies, Palo Alto, CA, USA, cat. no. 600882), as a fluorescent reported dye. The qPCR Master Mix was prepared on ice as follows (amount of reagent per reaction): MM Brilliant III SYBR Green PCR (10µL), Forward and Reverse Primer 10µM (0.3 µL of each), specific for the gene of interest and for the reference gene for normalisation of the data (*GAPDH,* glyceraldehyde-3-phosphate dehydrogenase), and nuclease-free water (7.4µL). After vortex, 18µL of the Master Mix was added per well to a PCR 96-well plate placed on ice, and then 2µL of the prepared –RT control and +RT cDNA samples was added (cDNA concentration at 5ng/µL, meaning adding a total of 10 ng of cDNA per well). After loading the PCR plate, the wells were covered with plastic strips, the plate was centrifuged for 3min at 2,000rpm (this corrects any adherent drop and bottom-bubbles), and then placed in the Thermal Cycler with MxPro software (Agilent) running on the channel "SYBR Green (with Dissociation Curve)", with the following 2-step thermal programme: pre-incubation 3min at 95ºC, then 40 cycles of 20s at 95ºC and 20s at 60ºC. Upon qPCR reaction completion, cycle threshold (CT) values were analysed by comparative relative quantification using the ΔΔCT quantification method for RT-qPCR in the cell lines, and the standard curve method for RT-qPCR in human samples from TAFs and skin fibroblasts. In RT-qPCR experiments involving human samples, the standard curve was generated from qPCR Human Reference cDNA Olido(dT)-primed (Clontech, cat. no. 639654), as well as a positive control template for validation of each gene primer design. Target gene expression was normalised to *GAPDH* expression used as internal control. In order to assess the reaction specificity, dissociation curves were obtained per gene, where a single peak (narrow and symmetric) were observed. The sequence of the primers (Sigma-Aldrich) used in the RT-qPCR experiments are listed in Appendix 3.

Ventana immunohistochemistry

Immunostains were performed on 4µm paraffin-embedded tissue sections using Ventana Discovery DAB Map System (Ventana, Illkirch, France). In this automated immunohistochemistry

system, streptavidin-horseradish peroxidase conjugate (OmniMap HRP) is used to catalyse the 3,3′-diaminobenzidine tetrahydrochloride (DAB) / H_2O_2 reaction to produce an insoluble dark brown precipitate that can be visualised targeting the antigen of interest. Briefly, the slides were deparaffinised and processed for antigen retrieval for 30min with cell conditioning solution CC1 (Ventana), which is a Tris base buffer (pH~9). After blocking with Blocker D solution (Ventana), slides were incubated with primary antibody for 60min (listed in Appendix 2) and then with the universal secondary antibody (Ventana) for 20min. Slides were counterstained with haematoxylin. A negative control, where primary antibody was omitted, was included per experiment, to exclude areas of endogenous peroxidase activity and/or non-specific antibody binding, ensuring the specificity of the staining reaction. A positive control, using a tissue with known high expression levels of the protein of interest (tissues where the dilution and immunohistochemical experiment conditions were first optimised for each one of the primary antibody), was also included per experiment serving as a baseline for evaluating run-to-run and/or day-to-day consistency.

Automated immunohistochemistry with Ventana is a powerful tool in showing antigens in tissues and cells with enhanced specificity and sensitivity, providing stainings with clean background and remarkable signal-to-noise ratios. Other advantages of immunohistochemistry with Ventana in comparison to manual immunohistochemistry procedures are: automation of antigen retrieval and staining protocols allow standardisation and reproducibility between experiments; performing the Ventana protocols on automated instruments are less time-consuming and less demanding; and the staining process is also less affected by the researcher's expertise, providing lower intra- and inter-individual methodology variabilities[509].

Immunohistochemical analysis

Stained slides were scanned and analysed with Pannoramic Scanner and Viewer Software (3DHISTECH, Budapest, Hungary). Immunohistochemical studies assessed macrophages using CD68, CD163 and HLA-DR, lymphocytes using CD8 for cytotoxic T cells, CD4 for T helper cells, FOXP3 for T regulatory cells, CD20 for B cells and neutrophil elastase for neutrophils. Endothelial cells were assessed with CD31 and fibroblasts with vimentin as well as by their location and morphology.

Immunopositive cells were counted in 5 different "hot spots" high power field (HPF) using the software ImageJ (National Institutes of Health, USA); counterstained nuclei identifying tumour cells were also counted, and the data were expressed as percentage of immunopositive immune cells relatively to the total number of tumour cells per HPF.

Vessels (stained for CD31) were manually counted in 3-5 different fields (20x magnification) allowing the estimation of microvessel density (number of vessels per HPF), and the vessels contour was manually traced using ImageJ to obtain an estimation of total microvessel area (μm^2).

E-cadherin and ZEB1 (markers used to study EMT), as well as, MMP-9, MMP-14 and NCAM immunoreactivities were measured semi-quantitatively by an experienced pathologist (Dr. Eivind Carlsen, Skien, Norway) blinded to the diagnosis or clinicopathological features of each case, on the basis of both the extent and intensity of the immunoreactivity. The extent of immunoreactivity was scored according to the percentage of stained cells in relation to the entire section as (0 points for no staining, 1 point for less than 20%, 2 points for 20-50% and 3 points for more than 50% of the cells). Staining intensity was graded on a 0-3 scale 0 (no staining), 1 (weak), 2 (moderate) and 3 (strong). Sum of extent and intensity scores was used as final staining score.

RNAscope

RNAscope is a novel *in situ* hybridization technique identifying mRNA transcripts in tissue sections at the single cell level within its morphological/spatial context and in a highly specific and sensitive manner through a probe design strategy (double Z) and effective hybridization-based signal amplification system (Figure 2.3)[510]. Thus, RNAscope offers significant advantages over conventional techniques to assess gene expression changes[511], being increasingly used in many research areas, and is particularly useful to investigate different elements of the TME[374,511,512].

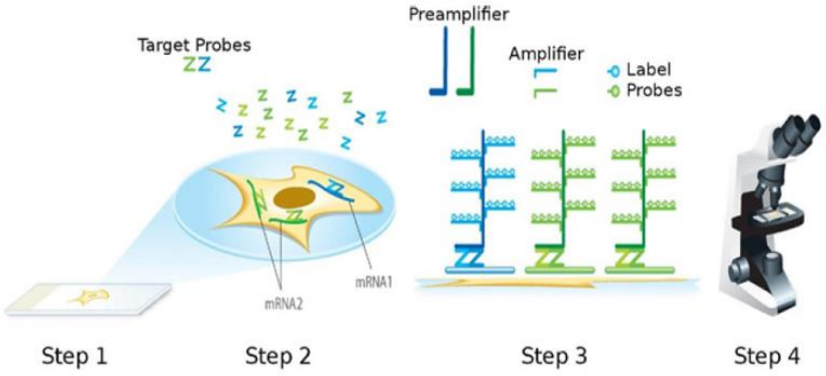

Figure 2.3: RNAscope assay procedure
In step 1, cells or tissues are fixed and permeabilised to allow target probe access. In step 2, target RNA-specific oligonucleotide probes (Z) are hybridized in pairs (ZZ) to multiple RNA targets. Each target probe contains an 18- to 25-base region complementary to the target RNA molecule, a spacer sequence, and a 14-base tail sequence (conceptualized as Z). A pair of target probes (double Z), each possessing a different type of tail sequence, hybridize contiguously to a target region (~50 bases). The two tail sequences together form a 28-base hybridization site for the preamplifier, which contains 20 binding sites for the amplifier, which in turn contains 20 binding sites for the label probe. In step 3, multiple signal amplification molecules are hybridized, each recognising a specific target probe, and each unique label probe is conjugated to a different enzyme or fluorophore. In step 4, signals are detected using a bright-field microscope (for enzyme label) or epifluorescent microscope (for fluorescent label). Wang *et al.* (2012)[510].

IL-8 and CCL2 and the chemokine receptors CXCR2 and CCR5 were detected using the RNAscope 2.5 HD Duplex Chromogenic Assay (Advanced Cell Diagnostics, ACD, USA), according to the manufacturer´s protocol (available at https://acdbio.com/rnascope%C2%AE-25-hd-duplex-assay). Briefly, 4µm paraffin-embedded PA tissue sections were baked at 60ºC for 90min and then deparaffinised in xylene and ethanol. To block endogenous peroxidases, 5-8 drops of H_2O_2 was added to cover each tissue section and incubated at room temperature for 10min, after which the H_2O_2 was removed by tapping the slide on absorbent paper and immediately submerged in distilled water. Afterwards, the slides were boiled with pre-treatment 1X Target Retrieval Reagent (ACD) for 15min and then washed in distilled water and 100% ethanol. Protease digestion was performed at 40ºC for 30min, followed by hybridization for 2h at 40ºC in the HybEZ II Oven (ACD) with Probe mix according to 1:50 ratio of C2 to C1 probes: mix IL-8 (ACD, cat. no. 310381-C2) and CXCR2 (ACD, cat. no. 468411), and mix CCR5 (ACD, cat. no. 601501-C2) and CCL2 (ACD, cat. no. 423811). Hybridization signals were amplified using the Amp 1-10 Reagents (ACD) and visualised with RNAscope 2.5 HD Duplex Chromogenic Assay reagents (Red and Green solutions, ACD). Cell nuclei were counterstained with haematoxylin, and slides were mounted with VectaMount mounting medium (Vector Laboratories, cat. no. H-5000). Probe-DapB (ACD) was used as negative control. Slides were scanned and analysed with Pannoramic Scanner and Viewer Software (3DHISTECH, Budapest, Hungary).

Affymetrix microarray analysis and xCell deconvolution

As part of Dr. Barry´s study[513], total RNA from a different set of human sporadic PA samples (3 somatotrophinomas and 4 NFPAs) and 5 NPs were isolated using the Qiagen´s RNeasy micro kit according to the manufacturer's protocol. RNA samples were assessed by NanoDrop ND-1000 spectrophotometer and Agilent Bioanalyzer (Agilent Technologies, Palo Alto, CA, USA). Target labelling and hybridization were performed using Affymetrix GeneChip 3' IVT Express Kit (Affymetrix, Santa Clara, CA, USA) according to the manufacturer's instructions. Briefly, 250ng of total RNA was reverse-transcribed using the T7-(T)24 primer and cDNA synthesis kit. Double stranded cDNA was used as a template for *in vitro* transcription and amplification reaction in the presence of biotin-labelled ribonucleotides; 15µg of labelled biotinylated cRNA was fragmented, mixed with hybridization solution and hybridized to Affymetrix Human Gene Chip HG-U133 Plus 2.0 arrays for 16h at 45°C. After hybridization and scanning, raw data were analysed using Bioconductor packages (www.bioconductor.org) within the open source 'R' statistical environment (www.r-project.org). Microarray data have been deposited with the National Center

for Biotechnology Information Gene Expression Omnibus (www.ncbi.nlm.nih.gov/geo, accession number GSE63357). For deconvolution, Dr. Sherine Awad used the webtool xCell[514,515], which infers different immune and stromal cells from microarray expression data (Figure 2.4) giving an xCell Fraction Score per cell type.

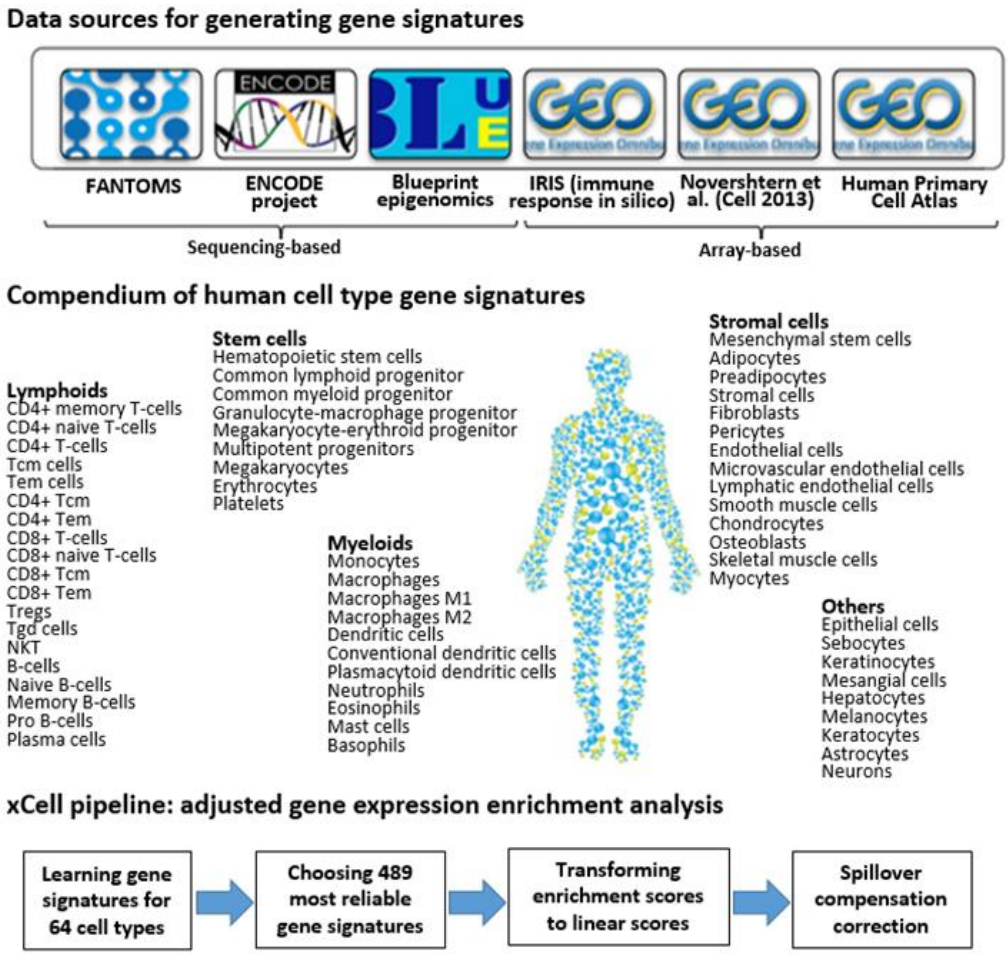

Figure 2.4: xCell study design
The data sources to generate xCell gene signatures, the compendium of the 64 human cell type gene signatures (based in 489 reliable cell type gene signatures) and the xCell pipeline are shown. The raw xCell score is given based on the average score of all signatures corresponding to the cell type, and then from simulations of gene expression for each cell type the non-linear scores are transformed to linear scores after which dependencies between cell type scores are adjusted by a spill over compensation correction method. Adapted from Aran *et al.* (2017)[514].

DNA extraction

In order to study loss of heterozygosity in TAFs derived from a patient with a proven germline *AIP*mut (c.910C>T; p.R304*), DNA from 2x10^6 TAFs isolated *in vitro* was extracted with the Qiagen´s QIAamp DNA Mini Kit (Qiagen, cat. no. 51304) according to manufacturer´s protocol ("Protocol: DNA Purification from Blood or Body Fluids (Spin Protocol)" and "Appendix B: Protocol for Cultured Cells" both available in the kit user's manual). QIAamp DNA purification procedure

was carried out using the QIAamp Mini-spin columns. The lysate buffering conditions are adjusted to allow optimal DNA binding to the QIAamp membrane before the sample is loaded onto the QIAamp spin column. DNA is adsorbed onto the QIAamp silica membrane during centrifugation, but proteins and other contaminants (that can inhibit the PCR and other downstream enzymatic reactions) are not retained in the membrane. Purified DNA was eluted from the QIAamp Mini spin column in Buffer AE.

Polymerase chain reaction and DNA sequencing

After extracting DNA from *AIP*mut PA-associated TAFs, I aimed to amplify the DNA region where the known germline *AIP* mutation c.910C>T is by PCR before sequencing this genomic region. Primers comprising an amplicon (size 244bp) in the *AIP* region of interest (exon 6) were designed: Forward primer sequence 5´-GTGTGGAATGCCCAGGAG-3´; Reverse primer sequence 5´-TGCTGCGTCATGCTTCTG-3´.

The PCR master mix was prepared on ice as follows: 9.9375µL of deionized water, 1.25µL of 10X Taq buffer, 0.25µL of 10mM dNTPs, 0.25µL of 10µM Forward Primer, 0.25µL of 10µM Reverse Primer, 0.0625µL of Taq polymerase – total volume per reaction 12µL. The PCR master mix was then vortexed and shortly spin. In separate PCR tubes, 3µL of DNA sample (at concentration of 33.3ng/µL, i.e. a total of 100ng) was added to 22µL of the master mix. A negative control using 3µL of deionized water (instead of DNA) was included. The PCR reaction was done in the thermal cycler G-Storm GT-12061 under the following conditions: initiation at 95ºC for 5min, then 40 cycles - denaturation step at 95ºC for 30s, annealing step for 30s at 60ºC and elongation step for 30s at 68ºC. The samples (5µL) were mixed with glycerol (5µL) and then loaded into a 2% Agarose gel (containing 10µL of Gel Red per 100mL allowing the DNA bands visualisation), after loading in the first gel well 5µL of the ladder mix (GeneRuler 1kb plus DNA Ladder, ThermoFisher Scientific, cat. no. SM1331) and in the last well water was loaded serving as negative control (to exclude contamination in the PCR reaction). Gel electrophoresis was performed in a BioRad PowerPac machine at 100V for approximately 40-50min, and the gel/bands then visualised in the LI-COR Odyssey machine (images acquired with the Image Studio software).

The amplified DNA was sent to GATC Biotech company (Germany) for Sanger DNA sequencing (together with 2µL of Forward and Reverse Primers required for the sequencing reaction). The DNA sequencing results were then analysed in the software FinchTV (Geospiza, Inc, USA).

Serum inflammation-based scores

Pre-operative full blood count (FBC) data from the included PA patients were collected from their medical records, including the overall white cell count, as well as the differential neutrophil, lymphocyte, monocyte, eosinophil and basophil count, and also the platelet and red blood cell counts. The immune inflammation score ratios were calculated per patient from these FBC data as follows: i) the neutrophil-to-lymphocyte ratio (NLR) was calculated by dividing the absolute neutrophil count by the absolute lymphocyte count; ii) lymphocyte-to-monocyte ratio (LMR) was calculated by dividing the absolute lymphocyte count by the absolute monocyte count iii) platelet-to-lymphocyte ratio (PLR) was calculated by dividing the absolute platelet count by the absolute lymphocyte count.

Clinical databases – International FIPA Consortium

Clinico-pathological data from each case were retrieved from hospital notes, clinical reports (blood test, imaging, histopathological) and from letters, fax or emails sent to us from the different referring clinicians integrating the International FIPA Consortium research group (http://www.fipapatients.org/fipaconsortium/). Informed consent was obtained from all patients before their inclusion in the study. The International FIPA Consortium database has been under constant updating since February 2007, when the study commenced, until April 2019. I have been updating this database since September 2016. I transferred the data stored in the Microsoft Office Excel® FIPA database into a database created with the software SPSS (version 20, IBM, USA) for the purpose of statistical analysis.

Statistical analysis

Quantitative (or continuous) variables, represented as mean and standard deviation (SD) or standard error of the mean (SEM), were tested for Gaussian distribution with the Shapiro-Wilk test, and non-parametric and parametric data were further analysed with the Mann-Whitney U test and Student´s T test, respectively, and one-way or two-way ANOVA tests with post-hoc comparison tests were also applied as appropriate. Chi-squared test and Exact Fisher´s test were applied to analyse qualitative (or categorical) variables. Correlation between continuous variables were determined by the Pearson correlation coefficient *r*. P values <0.05 were considered significant. All the statistical analyses were carried out using the SPSS version 20 (IBM, USA), and the graphs and figures designed in the GraphPad version 6 (Prism, USA).

Chapter 3: The cytokine network and immune cells in the tumour microenvironment of pituitary adenomas

Introduction

The TME consists of neoplastic, immune and stromal cells together with enzymes, growth factors and cytokines within the ECM and plays a crucial role in tumour initiation, progression, invasion, metastasis and angiogenesis[204,207,209-211]. Chemokines produced by neoplastic cells contribute to immune cell trafficking, as well as to invasion and survival of tumour cells[204,209,227]. Immune cells are recruited to the tumour by a chemokine gradient or recognition of tumour antigens[211,223,231]. Macrophages are a major component of the TME and determinant for tumour aggressiveness, particularly M2-macrophages[229,339-342]. CD8+ T cells are beneficial to the host as they are cytotoxic to tumour cells. CD4+ Th1 cells are associated with good outcomes, whereas CD4+ Th2 cells and FOXP3+ Tregs are immunosuppressive[204,516]; B cells are usually associated with good outcomes but an immunosuppressive B cell population has been described[358-361]. Neutrophils orchestrate responses against tumour cells, although their effects can be also detrimental[517,518].

The TME has been widely investigated[204,207,209-211], but little is known about it in PAs. However, there is some evidence that different TME elements may determine increased aggressiveness, rendering PAs larger[278,347], more proliferative[268,372,519] and more invasive[275,276,313,371]. Investigating the TME in PAs may provide novel insights into PA biology and identify markers for aggressiveness which can be useful for patient risk stratification and management. Moreover, it may lead to therapy advances, namely immunotherapy, which is a promising option for aggressive PAs[374], as recently shown in a patient with an ACTH-secreting pituitary carcinoma managed with ipilimumab and nivolumab[376], in a prolactinoma treated with immunotherapy[520] or in a murine model of Cushing´s disease[375]. Previous studies assessed CXCL12[268,271-273,276-278], IL-8[232-234] and immune cells[204,347,371,372,374] in PAs, but the interactions between the PA cytokine network and immune cells, and their role in determining PA aggressiveness, has not been comprehensively explored.

Serum inflammation-based scores, estimated from the pre-treatment differential FBC data, have been increasingly used in cancer[521,522]. Such scores are inexpensive and widely available, as virtually every patient will have a pre-treatment FBC, and several lines of evidence show these can predict cancer outcomes and prognosis[521,522]. Different scores have been used, with the most well-established being the neutrophil-to-lymphocyte ratio (NLR)[522-524]. Platelet-to-lymphocyte ratio

(PLR) and lymphocyte-to-monocyte ratio (LMR) were also shown to have a prognostic value in some cancers[522,525,526]. In general, increased NLR, increased PLR and low LMR are indicative of poor cancer outcomes[41,44,45]. There are no data on serum inflammation-based scores in PAs.

Aims

Overall aim

To characterise the TME in PAs and its role in the clinical phenotype and tumour aggressiveness, focusing on the cytokine network and infiltrating immune cells and their complex interactions.

Specific aims

1. To study the main human PA-derived cytokines and their role in recruiting immune cells into the TME and in determining the clinical phenotype and aggressiveness of PAs
2. To characterise different immune cell types within the TME of PAs and their role in determining the clinical phenotype and aggressiveness of PAs
3. To assess the functional effect of pituitary tumour-derived factors in macrophage chemotaxis and in its biological behaviour
4. To assess the functional effect of macrophage-derived factors in pituitary tumour biological behaviour, migration, invasiveness and EMT pathway activation
5. To characterise the circulating immune cells and inflammation-based scores in patients with PAs and study their relationship with PA phenotype and aggressiveness, aiming to determine whether these have any value predicting outcomes and prognosis of patients with PAs

Results

The cytokine network in human pituitary adenomas

Pituitary tumour cells are an active source of cytokines particularly chemokines

In order to identify the most relevant cytokines derived from human PAs, we established primary cultures from 24 PAs. The baseline clinicopathological features of these 24 patients are shown in

the Table 3.1. We studied 16 NFPAs and 8 somatotrophinomas: all cases were macroadenomas, 10 had cavernous sinus invasion and 5 had a Ki-67≥3%. We had more PAs deriving from males (66.7%) and the patients' mean age at diagnosis was 48.8±15.5 years. The mean number of treatments and operations were relatively low, respectively 1.6±0.9 and 1.2±0.5, taking into account the short follow-up duration of this cohort (2.5±9.1 years).

Clinicopathological features	**Total of PAs (n=24)**
Gender *[n (%)]* Male Female	 16 (66.7%) 8 (33.3%)
Current age (years) *[mean±standard deviation (SD)]*	51.9 ± 15.1
Age at diagnosis (years) *[mean±SD]*	48.8 ± 15.5
Clinical diagnosis *[n (%)]* Acromegaly NFPA	 8 (33.3%) 16 (66.7%)
Hyperprolactinaemia at diagnosis *[n (%)]*	8 (33.3%)
Headache *[n (%)]*	8 (33.3%)
Visual Impairment *[n (%)]*	13 (54.2%)
Hypopituitarism at diagnosis *[n (%)]*	11 (45.8%)
Macroadenoma *[n (%)]*	24 (100%)
Suprasellar extension *[n (%)]*	24 (100%)
Cavernous sinus invasion *[n (%)]*	10 (41.7%)
Ki-67 ≥ 3% *[n (%)]*	5 (20.8%)
Mean number of treatments *[mean±SD]*	1.6 ± 0.9
Mean number of surgeries *[mean±SD]*	1.2 ± 0.5
Re-operation *[n (%)]*	5 (20.8%)
Radiotherapy *[n (%)]*	3 (12.5%)
Hypopituitarism at last follow-up *[n (%)]*	14 (58.3%)
Active disease at last follow-up *[n (%)]*	4 (16.7%)
Follow-up duration (years) *[mean±SD]*	2.5 ± 9.1

Table 3.1: Baseline features of the 24 studied patients with PAs

I assessed 42 different cytokines in fresh culture supernatants from these 24 PAs (Table 3.2). The cytokine array identified IL-8, CCL2, CCL3, CCL4, CXCL10, CCL22, CXCL1 and CX3CL1 as the main PA-derived cytokines, all chemokines specialised in immune cell recruitment[209], followed by FGF-2, IL-6, PDGF-AA and VEGF-A. In general, interleukins were undetectable or in low concentrations. IL-1ra, IL-2, IL-3, IL-5, IL-7, IL-9, IL-13, CCL7, sCD40L, TNF-β and TGF-α were undetectable in PA-derived supernatants (Table 3.2).

Cytokine/ Chemokine/ Growth factor	Overall PAs (n=24) Mean concentration (pg/mL) ± SEM	Serum-free medium Concentration (pg/mL)	NFPAs (n=16) Mean concentration (pg/mL) ± SEM	Somatotrophinomas (n=8) Mean concentration (pg/mL) ± SEM
IL-8	854.18 ± 445.79	7.06	1250.95 ± 652.15	60.65 ± 36.68
CCL2	578.03 ± 222.66	4.00	839.92 ± 316.52	54.27 ± 23.69
CCL3	150.55 ± 88.22	0	224.04 ± 129.69	3.57 ± 0.86
CCL4	94.25 ± 47.20	3.09	139.32 ± 68.67	4.11 ± 1.86
CXCL10	76.67 ± 47.58	0	112.04 ± 70.39	5.94 ± 2.80
CCL22	67.25 ± 16.74	20.78	68.36 ± 22.62	65.03 ± 19.25
CXCL1	60.30 ± 26.14	20.78	80.62 ± 38.46	19.65 ± 6.39
CX3CL1	35.14 ± 17.12	6.73	46.09 ± 25.42	13.23 ± 4.12
FGF-2	26.65 ± 4.11	0	21.40 ± 4.91	37.15 ± 6.33
IL-6	24.90 ± 19.27	0	37.21 ± 28.70	0.28 ± 0.11
PDGF-AA	22.36 ± 6.78	0.12	30.09 ± 9.50	6.89 ± 3.83
VEGF-A	15.85 ± 4.06	0	16.01 ± 5.15	15.51 ± 7.01
PDGF-BB	13.37 ± 6.09	0	18.35 ± 8.94	3.41 ± 1.34
IFNα2	4.90 ± 1.00	1.79	4.61 ± 1.27	5.48 ± 1.68
IL-4	4.75 ± 1.47	0	4.26 ± 1.83	5.74 ± 2.62
G-CSF	3.97 ± 1.25	0	4.14 ± 1.85	3.61 ± 0.88
GM-CSF	3.89 ± 1.71	0	4.93 ± 2.53	1.79 ± 0.62
CCL5	3.83 ± 0.97	0.66	4.33 ± 1.39	2.84 ± 0.81
IL-12p40	3.66 ± 0.96	0	3.49 ± 1.24	3.98 ± 1.58
TNF-α	3.01 ± 2.24	0.19	4.33 ± 3.35	0.37 ± 0.09
IL-18	2.87 ± 0.66	1.91	2.78 ± 0.84	3.06 ± 1.14
Flt3L	2.79 ± 0.34	1.72	2.82 ± 0.47	2.74 ± 0.44
CCL11	2.77 ± 0.66	0	2.83 ± 0.87	2.66 ± 1.02
IL-1α	1.75 ± 0.70	0	2.61 ± 0.99	0.04 ± 0.04
EGF	1.69 ± 0.43	0	1.37 ± 0.52	2.33 ± 0.75
IFNγ	1.23 ± 0.24	0.34	1.33 ± 0.35	1.03 ± 0.22
IL-10	1.16 ± 0.39	0.55	1.02 ± 0.49	1.43 ± 0.68
IL-1β	0.90 ± 0.24	0.06	1.05 ± 0.36	0.61 ± 0.13
IL-12p70	0.86 ± 0.22	0.11	0.75 ± 0.27	1.06 ± 0.41
IL-15	0.76 ± 0.20	0.55	0.69 ± 0.27	0.88 ± 0.30
IL-17A	0.68 ± 0.12	0.01	0.73 ± 0.18	0.59 ± 0.14

Table 3.2: Cytokine secretome from the 24 human PA-derived supernatants
PA-derived cell culture supernatants were collected at 24h on serum-free medium and the cytokine secretome determined with the human Millipore MILLIPLEX cytokine 42-plex array. Data are shown as concentration (pg/mL), mean±SEM for all detectable cytokines, chemokines and growth factors for the overall cohort of PAs (n=24), and for the NFPA (n=16) and somatotrophinoma (n=8) subgroups. IL-1ra, IL-2, IL-3, IL-5, IL-7, IL-9, IL-13, CCL7, sCD40L, TNF-β and TGF-α were undetectable (i.e. below the lowest standard curve point and serum-free medium).

In Table 3.3 is shown the proportion of PA cases with detectable level of cytokines (i.e. concentrations below the lowest standard curve point and the serum-free medium). Ninety percent of the PAs secreted IL-8, CCL2 and CCL3, while CXCL1 and CXCL10 were secreted by half of the PAs; CCL4, CX3CL1, FGF-2 and VEGF-A were secreted by three-quarters of the PAs, whereas IL-6 was found in 50% of the cases. TNF-α, IL-1 α, EGF, IL-10, IL12p70, IL-15 and IL-17A were present in less than 50% of cases (Table 3.3).

Cytokine/ Chemokine/ Growth factor	n (%) of PAs with detectable cytokine (n=24)	n (%) of NFPAs with detectable cytokine (n=16)	n (%) of somatotrophinomas with detectable cytokine (n=8)	*p* value (NFPAs vs somato-tropinomas)
IL-8	22 (91.7%)	16 (100%)	8 (75.0%)	**0.037**
CCL2	21 (87.5%)	16 (100%)	5 (62.5%)	**0.009**
CCL3	22 (91.7%)	15 (93.8%)	7 (87.5%)	0.602
CCL4	18 (75.0%)	14 (87.5%)	4 (50.0%)	**0.046**
CXCL10	14 (58.3%)	10 (62.5%)	4 (50.0%)	0.558
CCL22	15 (62.5%)	10 (62.5%)	5 (62.5%)	1.000
CXCL1	12 (50.0%)	8 (50.0%)	4 (50.0%)	1.000
CX3CL1	19 (79.2%)	14 (87.5%)	5 (62.5%)	0.155
FGF-2	19 (79.2%)	11 (68.8%)	8 (100%)	0.076
IL-6	12 (50.0%)	11 (68.8%)	1 (12.5%)	**0.009**
PDGF-AA	20 (83.3%)	16 (100%)	4 (50.0%)	**0.002**
VEGF-A	18 (75.0%)	13 (81.2%)	5 (62.5%)	0.317
PDGF-BB	15 (62.5%)	10 (62.5%)	5 (62.5%)	1.000
IFNα2	13 (54.2%)	8 (50.0%)	5 (62.5%)	0.562
IL-4	11 (45.8%)	7 (43.8%)	4 (50.0%)	0.772
G-CSF	19 (79.2%)	12 (75.0%)	7 (87.5%)	0.477
GM-CSF	15 (62.5%)	11 (68.8%)	4 (50.0%)	0.371
CCL5	16 (66.7%)	11 (68.8%)	5 (62.5%)	0.759
IL-12p40	12 (50.0%)	8 (50.0%)	4 (50.0%)	1.000
TNF-α	6 (25.0%)	5 (31.2%)	1 (12.5%)	0.317
IL-18	12 (50.0%)	8 (50.0%)	4 (50.0%)	1.000
Flt3L	17 (70.8%)	11 (68.8%)	6 (75.0%)	0.751

CCL11	12 (50.0%)	8 (50.0%)	4 (50.0%)	1.000
IL-1α	8 (33.3%)	8 (50.0%)	0 (0%)	**0.014**
EGF	11 (45.8%)	6 (37.5%)	5 (62.5%)	0.247
IFNγ	15 (62.5%)	10 (62.5%)	5 (62.5%)	1.000
IL-10	10 (41.7%)	5 (31.2%)	5 (62.5%)	0.143
IL-1β	12 (50.0%)	8 (50.0%)	4 (50.0%)	1.000
IL-12p70	10 (41.7%)	6 (37.5%)	4 (50.0%)	0.558
IL-15	8 (33.3%)	4 (25.0%)	4 (50.0%)	0.221
IL-17A	10 (41.7%)	7 (43.8%)	3 (37.5%)	0.770

Table 3.3: Detectable cytokine levels in the supernatant of 24 human PA primary cultures
PA-derived cell culture supernatants were collected at 24h on serum-free medium and the cytokine secretome determined with the human Millipore MILLIPLEX cytokine 42-plex array. Data are shown as the n(%) of PAs with detectable cytokine levels (i.e. cytokine concentration above the lowest standard curve point and serum-free medium quantification). Data are shown for the overall cohort of PAs (n=24), and for the NFPA (n=16) and somatotrophinoma (n=8) subgroups. Chi-squared test was used to calculate *p* value for the comparative analysis between NFPAs and somatotrophinomas.

NFPAs release higher amounts of cytokines and are more often secretory than somatotrophinomas

NFPAs secreted higher amounts of cytokines/chemokines than somatotrophinomas, especially CCL2 (16x more), IL-8 (25x more) and CCL4 (27x more), except for FGF-2 which was found in higher concentrations in somatotrophinoma supernatants than in NFPAs (p=0.076) (Table 3.2 and Figure 3.1-A).

NFPAs were more often secretory in comparison to somatotrophinomas, particularly regarding IL-8 (100 vs 75%, p=0.037), CCL2 (100 vs 62.5%, p=0.009), CCL4 (87.5 vs 50%, p=0.046), IL-6 (68.8 vs 12.5%, p=0.009), PDGF-AA (100 vs 50%, p=0.002) and IL-1α (50 vs 0%, p=0.014) (Table 3.3 and Figure 3.1-B).

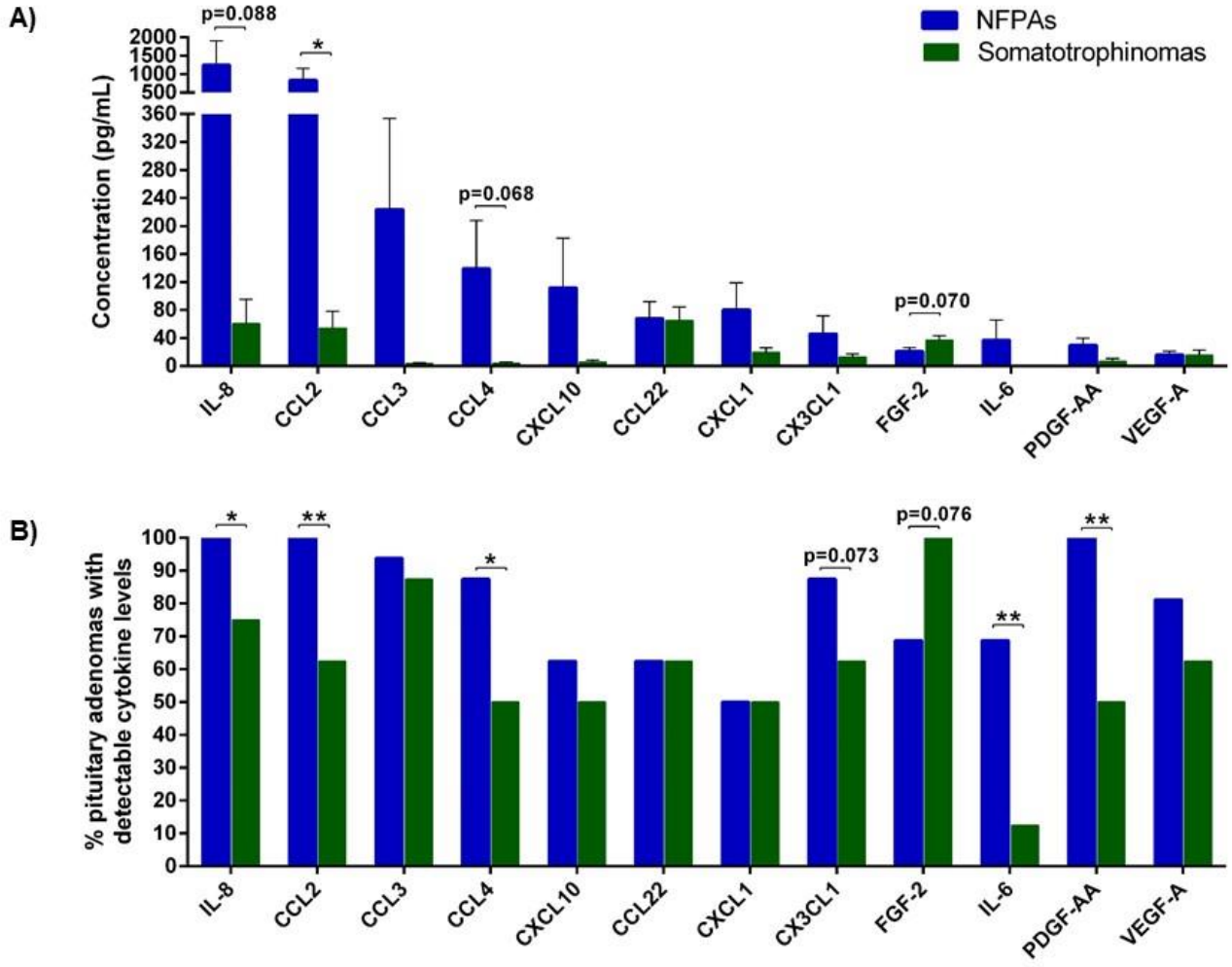

Figure 3.1: Cytokine secretome differences between NFPAs and somatotrophinomas
A) Cytokine secretome from NFPAs (n=16) and somatotrophinomas (n=8). Data are shown for the top 12 secreted proteins as concentration (pg/mL), mean±SEM. *, <0.05, **, <0.01, ***, <0.001 (Mann Whitney U test). B) Percentage of NFPAs and somatotrophinomas with detectable cytokine levels (i.e. concentration above the lowest standard curve and serum-free medium quantification). Data are shown as percentage and for the top 12 secreted proteins as identified by the Millipore MILLIPLEX assay in primary cell culture supernatants. *, <0.05, **, <0.01, ***, <0.001 (Chi-squared test).

Secretome differences between NFPAs and somatotrophinomas were not explained by pre-operative SSA treatment, as there were no secretome differences between pre-treated and non-pre-treated somatotrophinomas (Figure 3.2-A), nor by the cytokeratin granulation pattern in somatotrophinomas as there were no secretome differences between sparsely-granulated and densely-granulated somatotrophinomas (Figure 3.2-B).

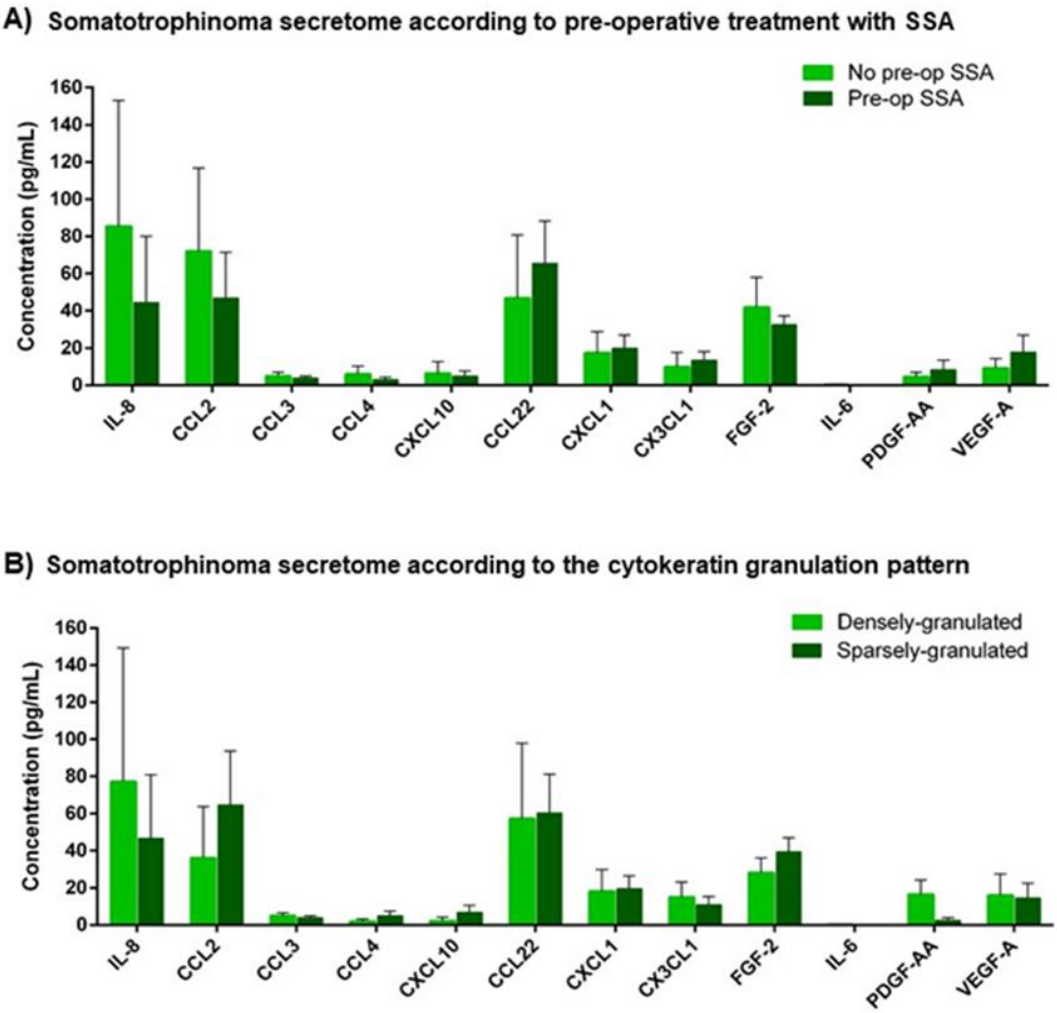

Figure 3.2: Somatotrophinoma secretome according to pre-operative SSA or granulation pattern
A) Cytokine secretome from somatotrophinomas treated pre-operatively with somatostatin analogues (Pre-op SSA, n=5) vs not treated (No pre-op SSA, n=3). B) Cytokine secretome from densely-granulated (n=3) vs sparsely-granulated (n=5) somatotrophinomas. Data are shown for the top 12 secreted proteins as concentration (pg/mL), mean±SEM. *p* values were non-significant (Mann Whitney U test).

Cytokine secretome of PAs and clinico-pathological features

The PA-derived cytokine secretome was not significantly associated *per se* with an elevated Ki-67 or cavernous sinus invasion (Table 3.4), recognised markers of PA aggressiveness[7,37,43,527]. Less proliferative PAs showed a tendency to have higher absolute concentrations for most of the top 12 highly secreted cytokines. Regarding cavernous sinus invasion, there were no significant differences (or trends) among invasive and non-invasive PAs for each one of the top 12 highly secreted cytokines (Table 3.4). There were also no cytokine secretome differences among the different PA grades (Table 3.5) according to the prognostic grade classification proposed by Trouillas *et al.*[43].

Cytokine/ Chemokine/ Growth factor	Ki-67 Mean concentration (pg/mL) ± SEM			Cavernous sinus invasion Mean concentration (pg/mL) ± SEM		
	<3% (n=19)	≥3% (n=5)	*p* value	No (n=14)	Yes (n=10)	*p* value
IL-8	1058.49 ± 556.36	77.80 ± 36.54	0.383	821.71 ± 620.08	899.64 ± 664.01	0.934
CCL2	674.97 ± 227.06	209.67 ± 113.38	0.135	593.55 ± 322.21	556.30 ± 306.65	0.936
CCL3	185.26 ± 110.61	18.66 ± 9.97	0.455	70.81 ± 36.77	262.20 ± 206.46	0.295
CCL4	114.41 ± 59.03	17.66 ± 6.48	0.417	84.23 ± 63.50	108.29 ± 73.96	0.808
CXCL10	92.76 ± 59.83	15.55 ± 9.24	0.522	91.91 ± 75.42	55.34 ± 47.92	0.714
CCL22	65.30 ± 20.95	74.66 ± 14.47	0.826	78.82 ± 27.21	51.06 ± 13.11	0.426
CXCL1	69.62 ± 32.76	24.89 ± 10.52	0.499	49.45 ± 28.33	75.49 ± 50.22	0.634
CX3CL1	40.54 ± 21.56	14.60 ± 2.73	0.550	45.21 ± 28.93	21.03 ± 8.21	0.498
FGF-2	25.75 ± 3.95	30.06 ± 14.01	0.681	27.46 ± 4.88	25.52 ± 7.44	0.822
IL-6	31.24 ± 24.26	0.82 ± 0.26	0.534	34.44 ± 32.68	11.54 ± 9.18	0.570
PDGF-AA	25.09 ± 8.21	12.00 ± 9.06	0.445	30.15 ± 10.65	11.54 ± 9.18	0.179
VEGF-A	15.79 ± 4.83	16.04 ± 7.54	0.981	18.71 ± 5.98	11.84 ± 5.10	0.417

Table 3.4: Cytokine secretome of PAs according to Ki-67 and cavernous sinus invasion
Data are shown as concentration (pg/mL), mean±SEM for the top 12 secreted cytokines/chemokines as identified by the Millipore MILLIPLEX assay in the primary cell culture supernatants of the 24 PAs. *p* values were non-significant for the comparative analysis between less vs more proliferative PAs, as well as for PAs without or with cavernous sinus invasion (Mann Whitney U test).

Cytokine/ Chemokine/ Growth factor	Grade 1a (non-invasive and non-proliferative) n=11	Grade 1b (non-invasive and proliferative) n= 3	Grade 2a (invasive) n=8	Grade 2b (invasive and proliferative) n=2	*p* value
IL-8	1032.91 ± 784.43	47.31 ± 21.31	1093.67 ± 825.47	123.53 ± 92.23	0.867
CCL2	676.41 ± 408.35	289.75 ± 182.92	672.99 ± 375.84	89.56 ± 64.15	0.876
CCL3	82.66 ± 46.46	27.35 ± 15.37	326.34 ± 256.07	5.62 ± 1.49	0.588
CCL4	100.99 ± 80.84	22.73 ± 10.04	132.84 ± 91.44	10.07 ± 4.60	0.871
CXCL10	111.92 ± 95.97	18.52 ± 15.91	66.41 ± 60.01	11.08 ± 7.74	0.907
CCL22	82.43 ± 34.62	65.58 ± 33.15	41.76 ± 13.78	88.27 ± 26.21	0.759
CXCL1	55.12 ± 36.07	28.64 ± 15.09	89.54 ± 62.45	19.26 ± 19.26	0.862
CX3CL1	54.31 ± 36.69	11.86 ± 1.10	21.62 ± 10.32	18.70 ± 6.54	0.802
FGF-2	28.02 ± 5.48	25.41 ± 13.03	22.64 ± 5.83	37.04 ± 37.04	0.843
IL-6	43.60 ± 41.57	0.87 ± 0.48	14.24 ± 11.41	0.76 ± 0.08	0.854
PDGF-AA	33.73 ± 12.97	17.01 ± 15.57	13.20 ± 6.76	4.49 ± 0.60	0.491
VEGF-A	18.75 ± 7.05	18.54 ± 13.14	11.73 ± 6.39	12.29 ± 5.20	0.890

Table 3.5: Cytokine secretome of PAs according to Trouillas grade classification system
Data are shown as concentration (pg/mL), mean±SEM for the top 12 secreted cytokines/chemokines as identified by the Millipore MILLIPLEX assay in primary cell culture supernatants of the 24 PAs. *p* values were not significant for the comparison for each cytokine among different grades (one-way ANOVA test).

There were also no differences between cytokine-secreting vs non-secreting PAs and high Ki-67 or presence of cavernous sinus invasion (Table 3.6) or tumour grade (Table 3.7). However, there was a tendency for more proliferative PAs being more often secretory, particularly for CCL4 (p=0.147), CCL22 (p=0.052), IL-6 (p=0.132) and VEGF-A (p=0.147), and more invasive PAs tended to be more often secretory for CCL4 (p=0.151).

Cytokine-secreting PAs	Ki-67			Cavernous sinus invasion		
	<3% (n=19)	≥3% (n=5)	*p* value	No (n=14)	Yes (n=10)	*p* value
IL-8	17 (89.5%)	5 (100%)	0.449	13 (92.9%)	9 (90.0%)	0.803
CCL2	16 (84.2%)	5 (100%)	0.342	12 (85.7%)	9 (90.0%)	0.754
CCL3	18 (94.7%)	4 (80.0%)	0.289	12 (85.7%)	10 (100%)	0.212
CCL4	13 (68.4%)	5 (100%)	0.147	9 (64.3%)	9 (90.0%)	0.151
CXCL10	10 (52.6%)	4 (80.0%)	0.269	7 (50.0%)	7 (70.0%)	0.327
CCL22	10 (52.6%)	5 (100%)	0.052	8 (57.1%)	7 (70.0%)	0.521
CXCL1	9 (47.4%)	3 (60.0%)	0.615	6 (42.9%)	6 (60.0%)	0.408
CX3CL1	14 (73.7%)	5 (100%)	0.197	11 (78.6%)	8 (80.0%)	0.932
FGF-2	16 (84.2%)	3 (60.0%)	0.236	12 (85.7%)	7 (70.0%)	0.350
IL-6	8 (42.1%)	4 (80.0%)	0.132	7 (50.0%)	5 (50.0%)	1.000
PDGF-AA	15 (78.9%)	5 (100%)	0.261	13 (92.9%)	7 (70.0%)	0.139
VEGF-A	13 (68.4%)	5 (100%)	0.147	11 (78.6%)	7 (70.0%)	0.633

Table 3.6: Ki-67 and cavernous sinus invasion among cytokine-secreting PAs
Data are shown as n(%) representing the proportion of PAs with detectable cytokine levels (i.e. cytokine secreting PAs) regarding the top 12 secreted proteins as identified by the Millipore MILLIPLEX assay in the primary cell culture supernatants of the 24 PAs. *p* values were non-significant for the comparison between less vs more proliferative PAs, and PAs without vs with cavernous sinus invasion (Chi-squared test).

Cytokine-secreting PAs	Grade 1a (non-invasive and non-proliferative) n=11	Grade 1b (non-invasive and proliferative) n= 3	Grade 2a (invasive) n=8	Grade 2b (invasive and proliferative) n=2	*p* value
IL-8	10 (90.9%)	3 (100%)	7 (87.5%)	2 (100%)	0.886
CCL2	9 (81.8%)	3 (100%)	7 (87.5%)	2 (100%)	0.792
CCL3	10 (90.9%)	2 (66.7%)	8 (100%)	2 (100%)	0.338
CCL4	6 (54.5%)	3 (100%)	7 (87.5%)	2 (100%)	0.188
CXCL10	5 (45.5%)	2 (66.7%)	5 (62.5%)	2 (100%)	0.508
CCL22	5 (45.5%)	3 (100%)	5 (62.5%)	2 (100%)	0.225
CXCL1	4 (36.4%)	2 (66.7%)	5 (62.5%)	1 (50.0%)	0.648
CX3CL1	8 (72.7%)	3 (100%)	6 (75.0%)	2 (100%)	0.642
FGF-2	10 (90.9%)	2 (66.7%)	6 (75.0%)	1 (50.0%)	0.509
IL-6	5 (45.5%)	2 (66.7%)	3 (37.5%)	2 (100%)	0.403
PDGF-AA	10 (90.9%)	3 (100%)	5 (62.5%)	2 (100%)	0.266
VEGF-A	8 (72.7%)	3 (100%)	5 (62.5%)	2 (100%)	0.500

Table 3.7: Trouillas grade classification among cytokine-secreting PAs
Data are shown as n(%) representing the proportion of PAs with detectable cytokine levels (i.e. cytokine secreting PAs) regarding the top 12 secreted proteins as identified by the Millipore MILLIPLEX assay in the primary cell culture supernatants of the 24 PAs. *p* values were non-significant for the comparative analysis between the different PA grades (Chi-squared test).

The supernatants of cultured PA cells from male patients had in general higher absolute levels of cytokines than those from females, nearly significant for IL-8 (p=0.088), CCL2 (p=0.092) and CCL4 (p=0.097) (Figure 3.3). It is unclear, however, if there is a gender difference in the PA cytokine secretome, or whether this finding is only due to the higher proportion of males in the NFPA group (75%), the more active PA subtype in terms of cytokine secretion (Table 3.2 and Figure 3.1).

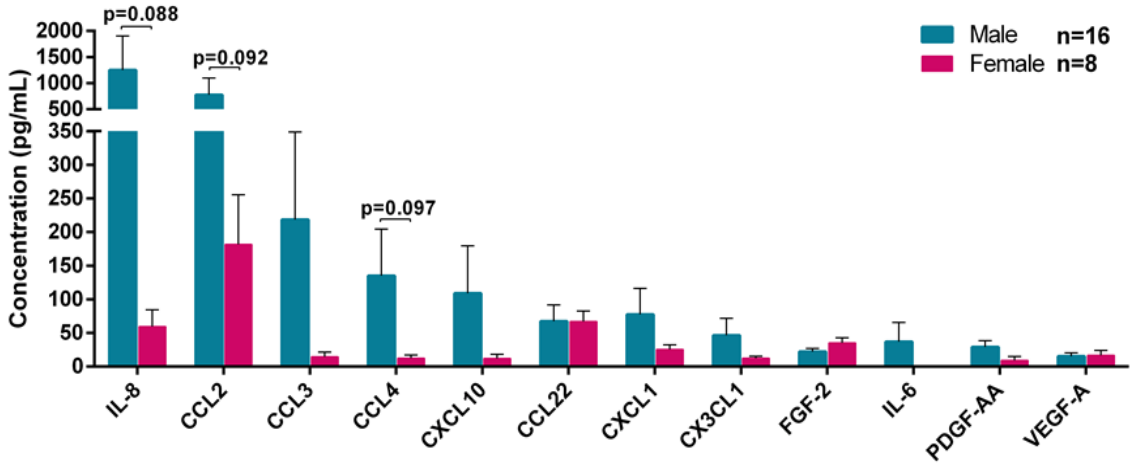

Figure 3.3: Cytokine secretome of PAs according to gender
Data are shown as concentration (pg/mL), mean±SEM for the top 12 secreted cytokines as identified by the Millipore MILLIPLEX assay in primary culture supernatants of 24 PAs. *p* values were non-significant (Mann Whitney U test).

In general, except for FGF-2, CX3CL1 and VEGF-A, the age at diagnosis positively correlated with the concentration of cytokines, significant for IL-8 and CCL4 and borderline for IL-6 (p=0.051) (Table 3.8), suggesting that older patients may have PAs secreting more actively cytokines.

		age at diagnosis (years)	n pituitary deficiencies at diagnosis
IL-8	Pearson correlation *r*	0.435	0.047
	p value	**0.034**	0.831
CCL2	Pearson correlation *r*	0.264	0.177
	p value	0.213	0.419
CCL3	Pearson correlation *r*	0.319	0.247
	p value	0.128	0.255
CCL4	Pearson correlation *r*	0.419	0.107
	p value	**0.041**	0.628
CXCL10	Pearson correlation *r*	-0.057	0.188
	p value	0.828	0.390
CCL22	Pearson correlation *r*	0.053	-0.270
	p value	0.807	0.213
CXCL1	Pearson correlation *r*	0.342	0.098
	p value	0.101	0.658
CX3CL1	Pearson correlation *r*	-0.038	0.072
	p value	0.860	0.743
FGF-2	Pearson correlation *r*	-0.385	-0.430
	p value	0.063	**0.041**
IL-6	Pearson correlation *r*	0.403	-0.115
	p value	0.051	0.601
PDGF-AA	Pearson correlation *r*	0.298	-0.128
	p value	0.158	0.562
VEGF-A	Pearson correlation *r*	-0.117	-0.162
	p value	0.585	0.461

Table 3.8: Cytokine secretome of PAs and age or number of pituitary deficiencies at diagnosis
p value was determined by the Pearson correlation coefficient *r*.

Headache, visual impairment and hypopituitarism at diagnosis are clinical features suggestive of more aggressive behaviour of PAs, as they usually are more common in patients with large and invasive PAs[7]. There were no secretome differences between PAs presented with headache vs no headache (Figure 3.4-A), or those who presented with visual impairment vs normal vision (Figure 3.4-B). Similarly, there were also no differences between PAs associated with hypopituitarism at diagnosis vs those diagnosed in eupituitarism (Figure 3.4-C), as well as no correlation between the number of pituitary deficiencies at diagnosis and the different PA-derived cytokines, excepting the significant negative correlation with FGF-2 (Table 3.6).

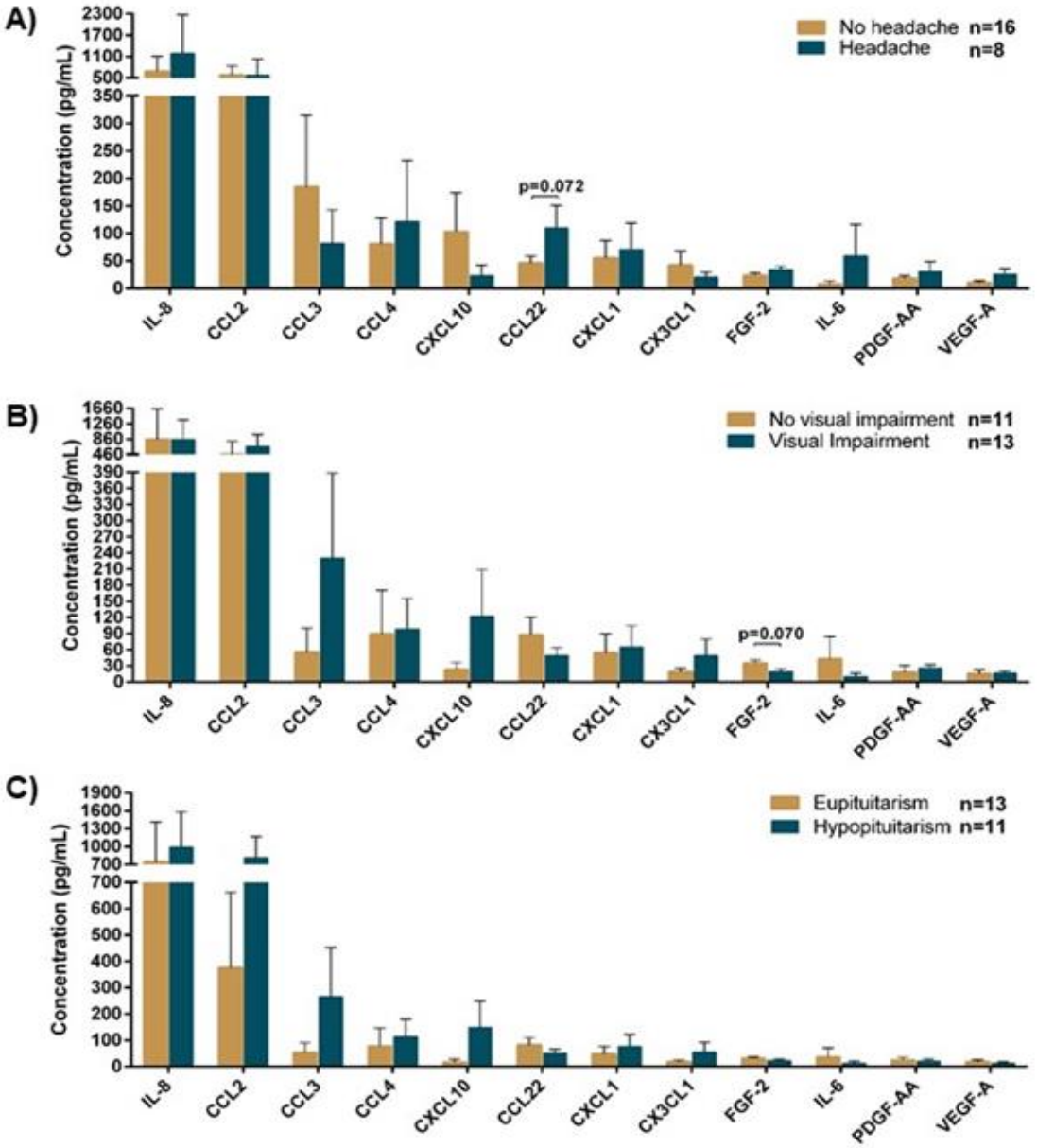

Figure 3.4: Cytokine secretome of PAs according to headache, visual impairment or hypopituitarism at diagnosis

Data are shown as concentration (pg/mL), mean±SEM for the top 12 secreted cytokines/chemokines as identified by the Millipore MILLIPLEX assay in primary culture supernatants of 24 PAs. P values were non-significant for the different comparative analysis (Mann Whitney U test).

Patients with no headache at diagnosis had less often IL-8-secreting PAs (p=0.037), while visual impairment at diagnosis was more frequent in CCL2 (p=0.044) and PDGF-AA (p=0.017) secreting PAs, but there were no other significant associations between cytokine-secreting vs non-secreting PAs and headache, visual impairment or hypopituitarism at diagnosis (Table 3.9).

Cytokine-secreting PAs	Headache			Visual impairment			Hypopituitarism at diagnosis		
	No (n=16)	Yes (n=8)	*p* value	No (n=11)	Yes (n=13)	*p* value	No (n=13)	Yes (n=11)	*p* value
IL-8	16 (100%)	6 (75.0%)	**0.037**	9 (81.8%)	13 (100%)	0.108	12 (92.3%)	10 (90.9%)	0.902
CCL2	14 (87.5%)	7 (87.5%)	1.000	8 (72.7%)	13 (100%)	**0.044**	11 (84.6%)	10 (90.9%)	0.642
CCL3	15 (93.8%)	7 (87.5%)	0.602	10 (90.9%)	12 (92.3%)	0.902	13 (100%)	9 (81.8%)	0.108
CCL4	11 (68.8%)	7 (87.5%)	0.317	8 (72.7%)	10 (76.9%)	0.813	10 (76.9%)	8 (72.7%)	0.813
CXCL10	8 (50.0%)	6 (75.0%)	0.242	7 (63.6%)	7 (53.8%)	0.628	8 (61.5%)	6 (54.5%)	0.729
CCL22	9 (56.2%)	6 (75.0%)	0.371	7 (63.6%)	8 (61.5%)	0.916	7 (53.8%)	8 (72.7%)	0.341
CXCL1	7 (43.8%)	5 (62.5%)	0.386	6 (54.5%)	6 (46.2%)	0.682	6 (46.2%)	6 (54.5%)	0.682
CX3CL1	12 (75.0%)	7 (87.5%)	0.477	7 (63.6%)	12 (92.3%)	0.085	10 (76.9%)	9 (81.8%)	0.769
FGF-2	12 (75.0%)	7 (87.5%)	0.477	10 (90.9%)	9 (69.2%)	0.193	11 (84.6%)	8 (72.7%)	0.475
IL-6	8 (50.0%)	4 (50.0%)	1.000	4 (36.4%)	8 (61.5%)	0.219	5 (38.5%)	7 (63.6%)	0.219
PDGF-AA	15 (93.8%)	5 (62.5%)	0.053	7 (63.6%)	13 (100%)	**0.017**	10 (76.9%)	10 (90.9%)	0.360
VEGF-A	12 (75.0%)	6 (75.0%)	1.000	7 (63.6%)	11 (84.6%)	0.237	11 (84.6%)	7 (63.6%)	0.237

Table 3.9: Headache, visual damage and hypopituitarism at diagnosis among cytokine-secreting PAs
Data are shown as n(%) representing the proportion of PAs with detectable cytokine levels (i.e. cytokine secreting PAs) regarding the top 12 secreted proteins as identified by the Millipore MILLIPLEX assay in the primary culture supernatants from 24 PAs. *p* values were non-significant for the comparison between PAs with vs without headache, visual impairment or hypopituitarism at diagnosis (Chi-squared test).

Association between cytokine secretome and clinico-pathological features

Taking into account that the cytokine secretome between NFPAs and somatotrophinomas was significantly different (Table 3.2 and Figure 3.1-A), clinical features were analysed in each subgroup aiming to dissect potential associations between secreted cytokines and clinico-pathological features within NFPAs or somatotrophinomas.

In general, less proliferative NFPAs tended to have higher absolute concentrations of cytokines than those with a Ki-67≥3%, although lacking statistical significance (trend for CCL2, p=0.079) (Figure 3.5-A). The opposite was observed for somatotrophinomas, although we had only one case with Ki-67≥3% which secreted significantly more CCL4 and FGF-2 than less proliferative somatotrophinomas (Figure 3.5-B). No secretome differences were seen between non-invasive PAs and PAs invading the cavernous sinus, either in NFPAs (Figure 3.5-C) or somatotrophinomas (Figure 3.5-D).

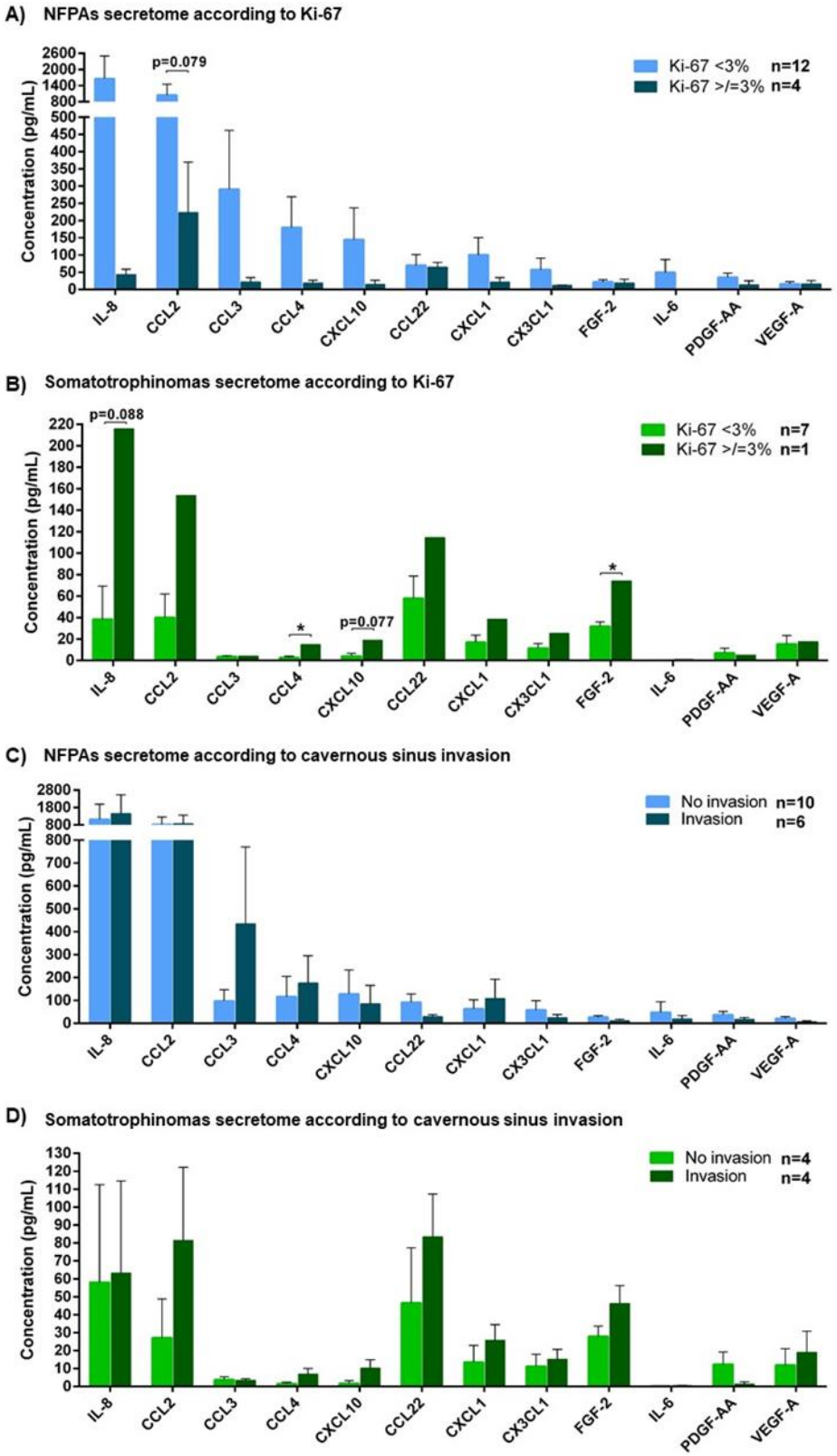

Figure 3.5: NFPAs and somatotrophinomas secretome according to Ki-67 and cavernous sinus invasion
A) NFPA cytokine secretome according to Ki-67; B) Somatotrophinoma cytokine secretome according to Ki-67; C) NFPA cytokine secretome according to cavernous sinus invasion; D) Somatotrophinoma cytokine secretome according to cavernous sinus invasion. Data are shown as concentration (pg/mL), mean±SEM and for the top 12 secreted proteins as identified by the Millipore MILLIPLEX assay in the primary culture supernatants of the 24 PAs. *, <0.05, **, <0.01, ***, <0.001 (Mann Whitney U test).

In general, there were no differences regarding low/high Ki-67 and absence/presence of cavernous sinus invasion between cytokine-secreting vs NFPAs or somatotrophinomas not secreting cytokines (Table 3.10).

		Ki-67			Cavernous sinus invasion		
		<3%	**≥3%**	***p* value**	**No**	**Yes**	***p* value**
Cytokine-secreting NFPAs (n=16)	**IL-8**	12/12 (100%)	4/4 (100%)	1.000	10/10 (100%)	6/6 (100%)	1.000
	CCL2	12/12 (100%)	4/4 (100%)	1.000	10/10 (100%)	6/6 (100%)	1.000
	CCL3	12/12 (100%)	3/4 (75.0%)	0.074	9/10 (90.0%)	6/6 (100%)	0.424
	CCL4	10/12 (83.3%)	4/4 (100%)	0.383	8/10 (80.0%)	6/6 (100%)	0.242
	CXCL10	7/12 (58.3%)	3/4 (75.0%)	0.551	6/10 (60.0%)	4/6 (66.7%)	0.790
	CCL22	6/12 (50.0%)	4/4 (100%)	0.074	6/10 (60.0%)	4/6 (66.7%)	0.790
	CXCL1	6/12 (50.0%)	2/4 (50.0%)	1.000	5/10 (50.0%)	3/6 (50.0%)	1.000
	CX3CL1	10/12 (83.3%)	4/4 (100%)	0.383	9/10 (90.0%)	5/6 (83.3%)	0.696
	FGF-2	9/12 (75.0%)	2/4 (50.0%)	0.350	8/10 (80.0%)	3/6 (50.0%)	0.210
	IL-6	8/12 (66.7%)	3/4 (75.0%)	0.755	7/10 (70.0%)	4/6 (66.7%)	0.889
	PDGF-AA	12/12 (100%)	4/4 (100%)	1.000	10/10 (100%)	6/6 (100%)	1.000
	VEGF-A	9/12 (75.0%)	4/4 (100%)	0.267	9/10 (90.0%)	4/6 (66.7%)	0.247
Cytokine-secreting somatotrophinomas (n=8)	**IL-8**	5/7 (71.4%)	1/1 (100%)	0.537	3/4 (75.0%)	3/4 (75.0%)	1.000
	CCL2	4/7 (57.1%)	1/1 (100%)	0.408	2/4 (50.0%)	3/4 (75.0%)	0.465
	CCL3	6/7 (85.7%)	1/1 (100%)	0.686	3/4 (75.0%)	4/4 (100%)	0.285
	CCL4	3/7 (42.9%)	1/1 (100%)	0.285	1/4 (25.0%)	3/4 (75.0%)	0.157
	CXCL10	3/7 (42.9%)	1/1 (100%)	0.285	1/4 (25.0%)	3/4 (75.0%)	0.157
	CCL22	4/7 (57.1%)	1/1 (100%)	0.408	2/4 (50.0%)	3/4 (75.0%)	0.465
	CXCL1	3/7 (42.9%)	1/1 (100%)	0.285	1/4 (25.0%)	3/4 (75.0%)	0.157
	CX3CL1	4/7 (57.1%)	1/1 (100%)	0.408	2/4 (50.0%)	3/4 (75.0%)	0.465
	FGF-2	7/7 (100%)	1/1 (100%)	1.000	4/4 (100%)	4/4 (100%)	1.000
	IL-6	0/7 (100%)	1/1 (100%)	**0.005**	0/4 (0%)	1/4 (25.0%)	0.285
	PDGF-AA	3/7 (42.9%)	1/1 (100%)	0.285	3/4 (75.0%)	1/4 (25.0%)	0.157
	VEGF-A	4/7 (57.1%)	1/1 (100%)	0.408	2/4 (50.0%)	3/4 (75.0%)	0.465

Table 3.10: Ki-67 and cavernous sinus invasion in cytokine-secreting NFPAs and somatotrophinomas
Data are shown as n cases/total cases (% of the total) representing the proportion of PAs with detectable cytokine levels (i.e. cytokine secreting PAs) regarding the top 12 secreted proteins as identified by the Millipore MILLIPLEX assay in the primary culture supernatants of the 24 PAs. *p* values were non-significant for the comparative analysis between less vs more proliferative PAs, as well as for PAs without or with cavernous sinus invasion (Chi-squared test).

There were no differences between the cytokine secretome of NFPAs or somatotrophinomas that presented with headache vs no headache (Figure 3.6-A). There were also no differences within NFPAs presenting with visual impairment vs normal vision, or hypopituitarism vs eupituitarism at diagnosis (Figure 3.6-B). Within somatotrophinomas, of the 8 cases only 1 presented with visual impairment at diagnosis and only 2 had hypopituitarism at diagnosis, and their secretomes did not seem to differ from cases with normal vision or eupituitarism at diagnosis (statistical analysis not shown in Figure 3.6 due to low sample sizes for this subgroup analysis).

Supernatants of cultured NFPAs from male patients had in general higher absolute levels of cytokines than those from females except for FGF-2 (non-significant *p* value), whereas somatotrophinoma females had higher absolute concentrations of almost all cytokines, although statistical significance was lacking (Figure 3.6-C). Hence, the gender effect in the NFPA or somatotrophinoma cytokine secretion is unclear.

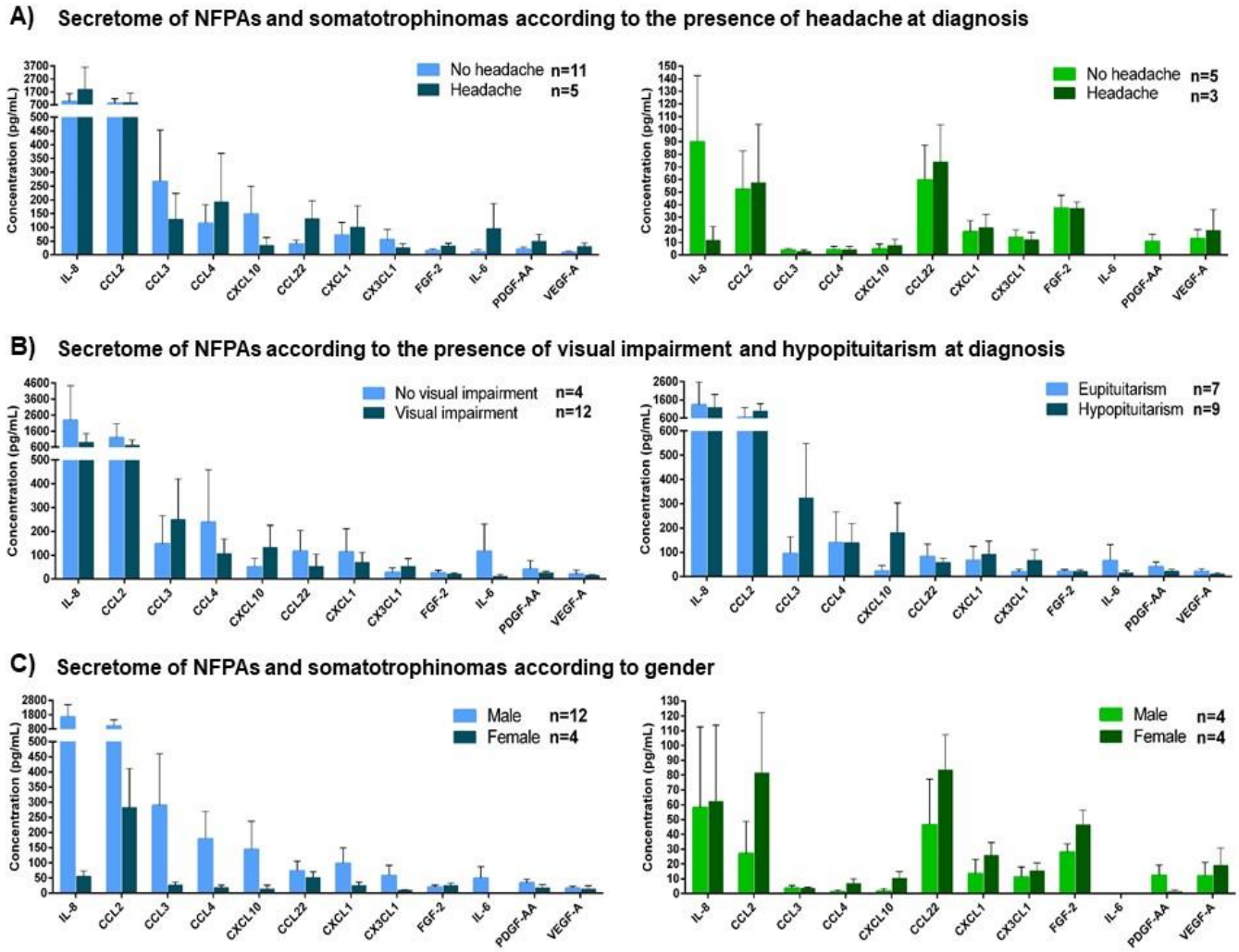

Figure 3.6: Cytokine secretome NFPAs and somatotrophinomas according to different clinical features
A) Headache at diagnosis shown for both NFPAs and somatotrophinomas; B) Visual impairment and hypopituitarism at diagnosis for NFPAs; C) Gender distribution for both NFPAs and somatotrophinomas. Data are shown as concentration (pg/mL), mean±SEM for the top 12 secreted proteins as identified by the Millipore MILLIPLEX assay in primary culture supernatants of the 24 PAs. *p* values were non-significant (Mann Whitney U test).

Patients with acromegaly often have increased PRL[7,170]. Somatotrophinomas from patients with concomitant hyperprolactinaemia at diagnosis had increased levels of IL-8 in their supernatants comparing to those with a normal serum PRL (Figure 3.7). CCL4 and FGF-2 levels in somatotrophinoma supernatants were positively correlated with serum PRL, while PDGF-AA and VEGF-A were positively associated with basal GH and IGF-1 levels (Figure 3.8).

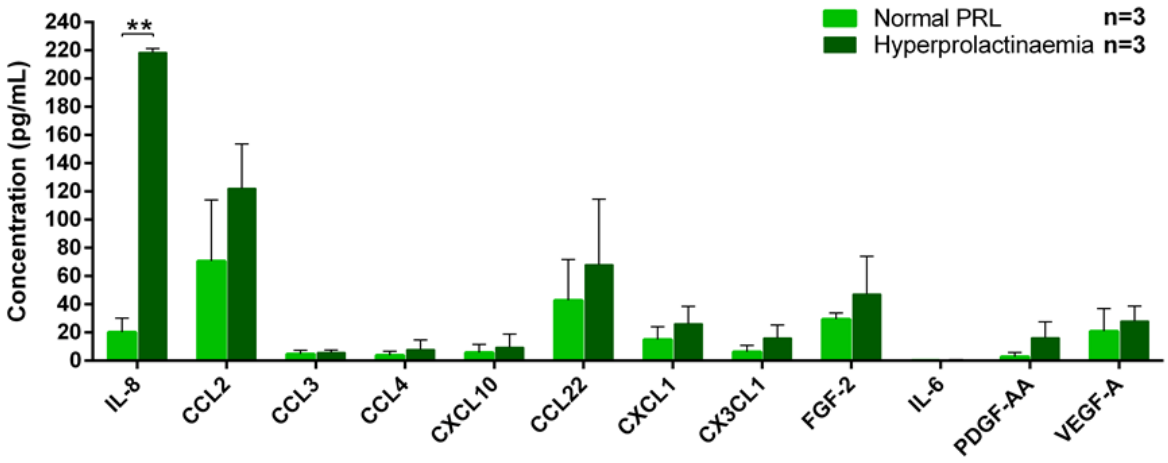

Figure 3.7: Cytokine secretome of somatotrophinomas with normal PRL or hyperprolactinaemia
Data are shown as concentration (pg/mL), mean±SEM for the top 12 secreted cytokines/ chemokines as identified by the Millipore MILLIPLEX assay in primary culture supernatants of the 6 somatotrophinoma cases with available PRL biochemical data. *, <0.05, **, <0.01, ***, <0.001 (Mann Whitney U test).

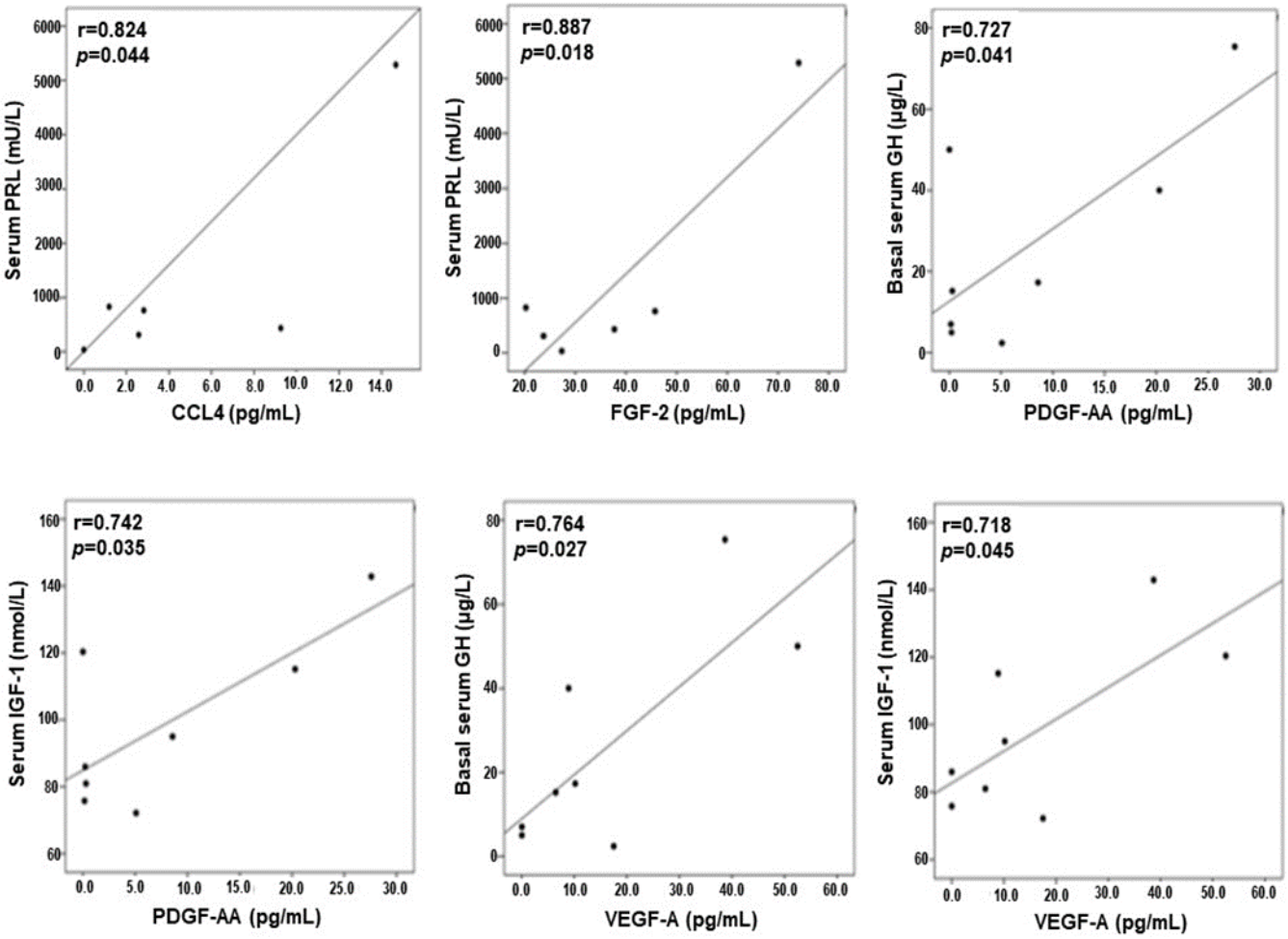

Figure 3.8: Correlation between cytokine secretome from somatotrophinomas and serum hormones
p value was determined by the Pearson correlation coefficient *r*.

There were no significant correlations between the cytokine secretome from NFPAs and serum pituitary hormone levels, but this needs to be interpreted cautiously as most NFPA patients had hypopituitarism at diagnosis related to the tumour mass effect, thus limiting the conclusions regarding a possible effect of cytokines on hormone secretion among NFPAs (Table 3.11).

Cytokine/ Chemokine/ Growth factor		GH (mcg/L)	IGF-1 (nmol/L)	PRL (mU/L)	TSH (µU/mL)	FT4 (pmol/L)	LH (U/L)	FSH (U/L)	Cortisol (nmol/L)
IL-8	Pearson *r*	-0.197	-0.050	-0.281	0.118	-0.179	-0.188	-0.191	-0.132
	p value	0.539	0.866	0.330	0.688	0.541	0.520	0.512	0.667
	n	12	14	14	14	14	14	14	13
CCL2	Pearson *r*	-0.259	-0.159	-0.353	0.135	-0.265	-0.253	-0.177	-0.253
	p value	0.417	0.588	0.216	0.646	0.361	0.383	0.546	0.405
	n	12	14	14	14	14	14	14	13
CCL3	Pearson *r*	-0.117	0.133	-0.222	0.009	-0.282	-0.177	-0.169	-0.099
	p value	0.718	0.649	0.445	0.976	0.329	0.546	0.564	0.747
	n	12	14	14	14	14	14	14	13
CCL4	Pearson *r*	-0.220	-0.087	-0.307	0.117	-0.224	-0.207	-0.188	-0.128
	p value	0.491	0.767	0.286	0.691	0.442	0.479	0.521	0.677
	n	12	14	14	14	14	14	14	13
CXCL10	Pearson *r*	-0.226	-0.106	-0.245	0.073	-0.225	-0.220	-0.126	-0.316
	p value	0.481	0.718	0.398	0.803	0.439	0.449	0.668	0.293
	n	12	14	14	14	14	14	14	13
CXCL1	Pearson *r*	-0.139	0.058	-0.268	0.093	-0.212	-0.177	-0.167	-0.060
	p value	0.666	0.844	0.354	0.753	0.467	0.545	0.568	0.844
	n	12	14	14	14	14	14	14	13
CCL22	Pearson *r*	-0.025	-0.031	-0.137	0.174	-0.022	-0.173	-0.180	0.195
	p value	0.938	0.917	0.641	0.553	0.939	0.555	0.538	0.523
	n	12	14	14	14	14	14	14	13
CX3CL1	Pearson *r*	-0.204	-0.004	-0.229	0.091	-0.165	-0.204	-0.145	-0.283
	p value	0.525	0.989	0.430	0.757	0.572	0.484	0.621	0.350
	n	12	14	14	14	14	14	14	13
FGF-2	Pearson *r*	0.264	0.264	-0.134	0.137	0.143	0.058	0.047	0.158
	p value	0.407	0.362	0.649	0.641	0.626	0.845	0.873	0.606
	n	12	14	14	14	14	14	14	13
PDGF-AA	Pearson *r*	-0.253	-0.099	-0.482	0.118	-0.002	-0.023	-0.041	-0.070
	p value	.427	0.736	0.081	0.689	0.995	0.938	0.889	0.819
	n	12	14	14	14	14	14	14	13
VEGF-A	Pearson *r*	-0.220	-0.074	-0.362	0.204	-0.083	-0.003	-0.080	0.043
	p value	.493	0.801	0.203	0.484	0.778	0.993	0.786	0.890
	n	12	14	14	14	14	14	14	13

Table 3.11: Correlation between cytokine secretome of NFPAs and serum hormonal levels
p value was determined by the Pearson correlation coefficient *r*.

Infiltrating immune cells in human pituitary adenomas

In the same cohort of PAs used for primary culture and cytokine secretome assessment, I analysed macrophages, CD4+ T helper cells, cytotoxic CD8+ T cells, FOXP3+ Tregs, B cells and neutrophils by immunohistochemistry; 5 NP sections were also included for comparison (Figure 3.9).

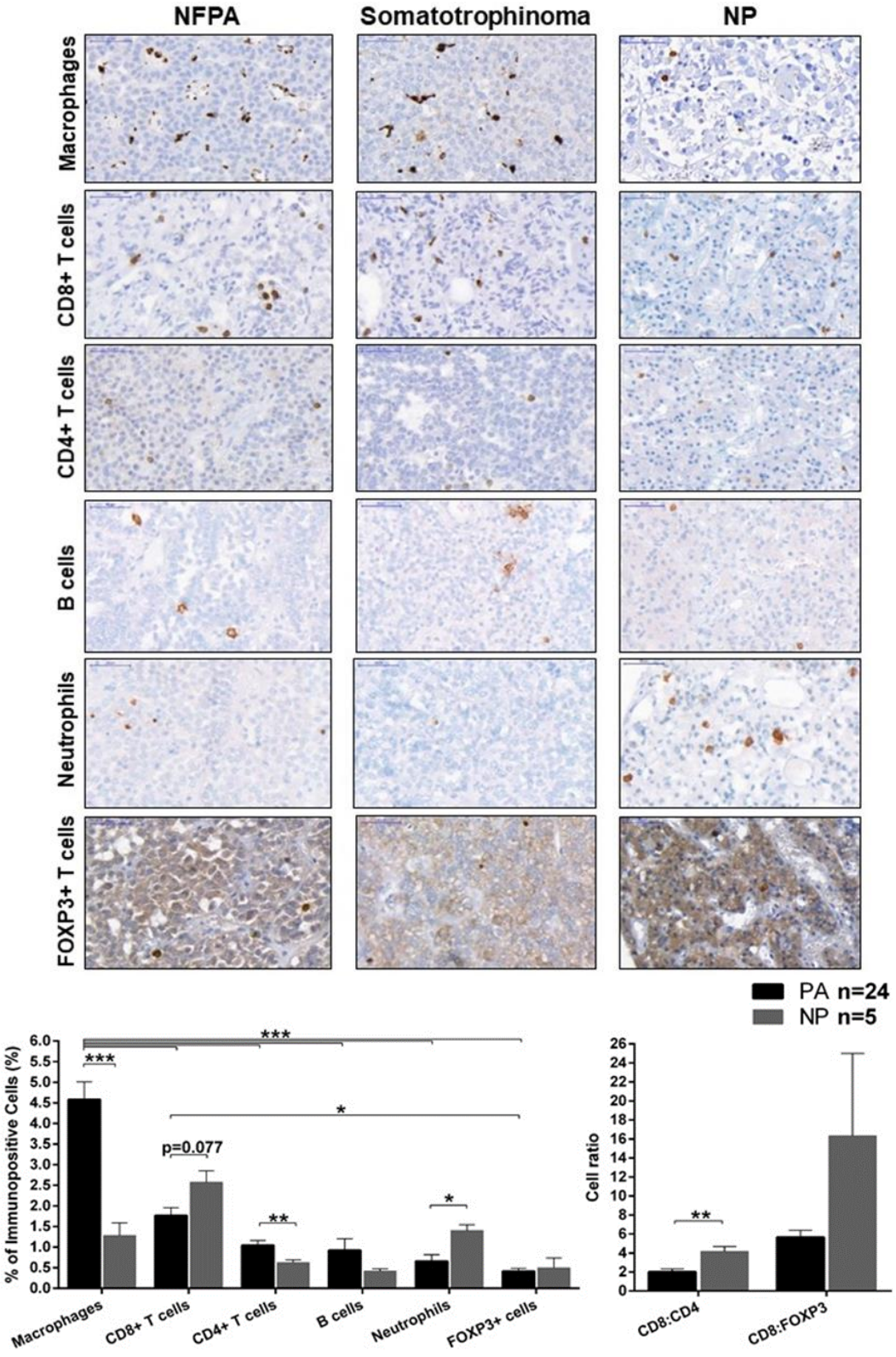

Figure 3.9: Immunohistochemical analysis of immune cells in PAs and NPs
Immune cells analysed: macrophages (CD68+), cytotoxic T lymphocytes (CD8+), T helper lymphocytes (CD4+), T regulatory cells (FOXP3+), B cells (CD20+) and neutrophils (neutrophil elastase+). Data are shown as mean±SEM for percentage of immune cells compared to the total number of tumour cells, and for CD8:CD4 or CD8:FOXP3 cell ratios. Representative images are shown for a NFPA, somatotrophinoma and NP (normal pituitary). Scale bar 50µm. PAs, n=24; NPs, n=5. *,<0.05, **,<0.01, ***,<0.001 (two-way ANOVA with Bonferroni test for immunopositive cell analysis; Mann Whitney U test for ratios analysis).

Compared to NPs, PAs contained more CD68+ macrophages (4.6±0.4 vs 1.2±0.2%, p<0.001) and CD4+ T cells (1.0±0.1 vs 0.6±0.1%, p=0.005), but fewer neutrophils (0.7±0.2 vs 1.4±0.1%, p=0.047) and a trend for fewer CD8+ T cells (1.8±0.2 vs 2.6±0.3%, p=0.077), with a significant 2-fold decrease in the CD8:CD4 cell ratio. There were no significant differences in B cell or FOXP3+ T cell contents between PAs and NPs, or the CD8:FOXP3 cell ratio (Figure 3.9). Macrophages were the most abundant immune cell type in PAs, while other immune cells were present in lower amounts (Figure 3.9). Macrophages in PAs are predominantly M2-macrophages (CD163+), while M1-macrophages (HLA-DR+) predominate in NPs, resulting in a 3-fold increased M2:M1 macrophage ratio in PAs (Figure 3.10-A). This predominant M2-macrophage phenotype in PAs may be due, at least in part, to higher concentrations of PA-derived M2-polarising cytokines, as IL-4 levels were almost 5x higher than IFNγ, a classical M1-polarising cytokine (Figure 3.10-B).

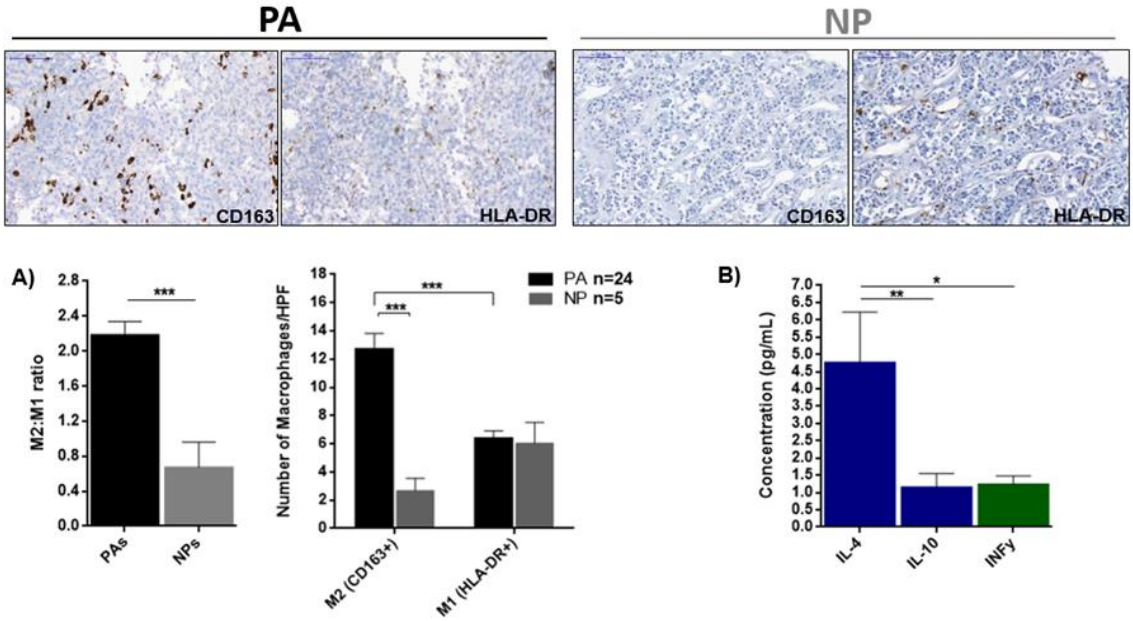

Figure 3.10: M2- and M1-like macrophages and macrophage-polarising cytokines in PAs
A) Immunohistochemical analysis of M2 (CD163+) and M1 (HLA-DR+) macrophages in PAs and normal pituitary (NP). Data are shown as mean±SEM for M2:M1 macrophage ratio and for the number of CD163+ and HLA-DR+ cells per high power field (HPF). Representative images are shown for a PA and NP. Scale bar 50µm. ***, <0.001 (Mann Whitney U test and two-way ANOVA with Bonferroni multiple comparison test). B) Macrophage-polarising cytokines in PA culture supernatants. Supernatants were collected at 24h in serum-free medium conditions and cytokine secretome determined with the human Millipore MILLIPLEX cytokine 42-plex array. Results are shown as concentration (pg/mL), mean±SEM for IL-4 and IL-10 (M2-polarising cytokines, blue bars) and IFNγ (M1-polarising cytokine, green bar). *,<0.05, **,<0.01, ***,<0.001 (one-way ANOVA with Bonferroni multiple comparison test).

These immunohistochemical findings were confirmed on a different set of samples (7 PAs, including 4 NFPAs and 3 somatotrophinomas, as well as 5 NPs) using available gene expression data analysed with xCell. PAs had a higher xCell score than NPs for macrophages (0.090±0.016 vs 0.031±0.013; *p*=0.025) and for M2 macrophages (0.042±0.007 vs 0; *p*=0.001) (Figure 3.11). Although significant differences were only observed for macrophages, I noted a tendency for a higher absolute xCell score regarding CD4+ T and B cells, and lower scores for CD8+ T cells and neutrophils, in PAs than in NPs in line with my immunohistochemical data. Moreover, the mean M2:M1 and CD8:CD4 ratios estimated from xCell, were respectively higher and lower in PAs than those observed in NPs (Figure 3.11), consistent with my immunohistochemical data.

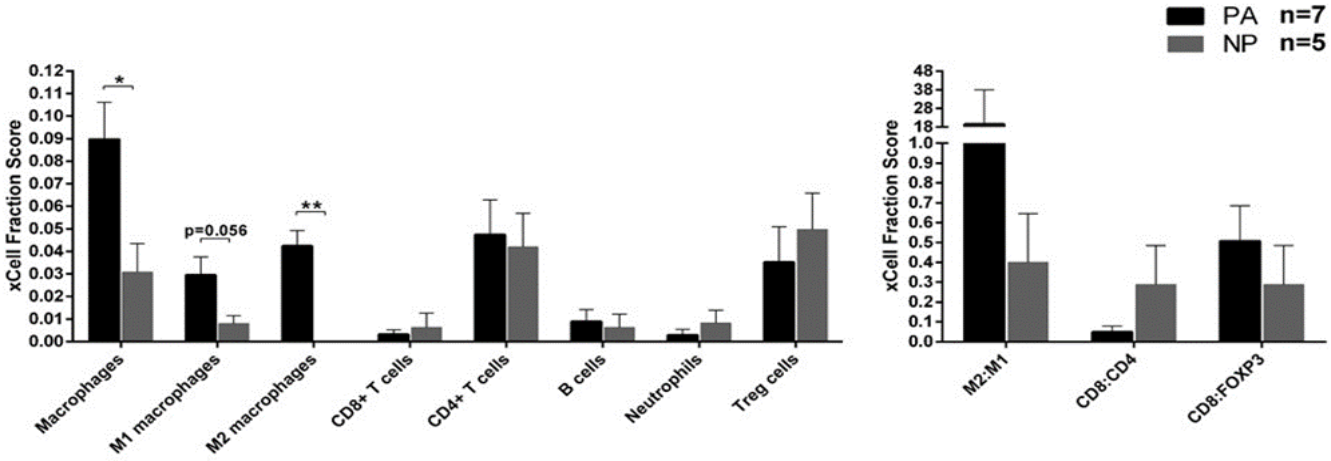

Figure 3.11: xCell scores in PAs and NPs
xCell Fraction Scores were obtained from microarray expression data from a different set of samples (7 PAs, 4 NFPAs and 3 somatotrophinomas; and 5 NPs). Data are shown as xCell Score, mean±SEM for the immune cell types and cell ratios previously analysed by immunohistochemistry in our cohort of 24 PAs. *, <0.05, **, <0.01, ***, <0.001 (Mann Whitney U test).

Significant correlations were observed between PA-infiltrating immune populations, namely CD8+ and CD4+ T cells, CD8+ and FOXP3+ T cells, CD4+ T cells and neutrophils (Table 3.12).

n PAs = 24		**% of macrophages**	**% of CD8+ T cells**	**% of CD4+ T cells**	**% of B cells**	**% of neutrophils**	**% of FOXP3 Tregs**
% of macrophages	Pearson correlation *r*	1	.349	.198	-.351	.035	.354
	p value		.095	.354	.093	.872	.089
% of CD8+ T cells	Pearson correlation *r*	.349	1	.534**	-.128	.360	.504*
	p value	.095		**.007**	.553	.084	**.012**
% of CD4+ T cells	Pearson correlation *r*	.198	.534**	1	.187	.490*	.389
	p value	.354	**.007**		.381	**.015**	.060
% of B cells	Pearson correlation *r*	-.351	-.128	.187	1	-.092	-.060
	p value	.093	.553	.381		.670	.780
% of neutrophils	Pearson correlation *r*	.035	.360	.490*	-.092	1	.050
	p value	.872	.084	**.015**	.670		.817
% of FOXP3+ Tregs	Pearson correlation *r*	.354	.504*	.389	-.060	.050	1
	p value	.089	**.012**	.060	.780	.817	

Table 3.12: Correlation between infiltrating immune cells in PAs
P value was determined by the Pearson correlation coefficient *r*.

NFPAs had more neutrophils than somatotrophinomas (0.9±0.1 vs 0.1±0.1%, p=0.002), but there were no differences regarding other immune cells, neither M2:M1, CD8:CD4 nor CD8:FOXP3 cell ratios (Table 3.13). There were no significant differences in infiltrating immune cells among the different NFPA subtypes (Table 3.13).

	Gonadotroph adenoma (n=13)	Silent corticotroph adenoma (n=1)	Null cell adenoma (n=2)	*p* value (GA vs SCA vs NCA)	NFPAs (n=16)	Som (n=8)	*p* value (NFPA vs Som)
% of macrophages	4.23 ± 0.60	4.97	6.37 ± 1.79	0.456	4.54 ± 0.54	4.66 ± 0.70	0.897
% of CD8+ T cells	1.62 ± 0.29	1.17	1.76 ± 0.61	0.891	1.61 ± 0.24	2.09 ± 0.29	0.245
% of CD4+ T cells	1.10 ± 0.17	0.81	1.12 ± 0.20	0.897	1.09 ± 0.14	0.96 ± 0.20	0.629
% of B cells	1.03 ± 0.48	0.66	0.68 ± 0.18	0.946	0.97 ± 0.39	0.84 ± 0.33	0.836
% of neutrophils	1.05 ± 0.24	0.09	0.50 ± 0.13	0.420	0.92 ± 0.21	0.14 ± 0.06	**0.002**
% of FOXP3+ Tregs	0.34 ± 0.10	0.85	0.28 ± 0.34	0.372	0.37 ± 0.09	0.52 ± 0.11	0.310
M2:M1 ratio	2.36 ± 0.22	1.98	1.96 ± 0.77	0.752	2.29 ± 0.19	1.98 ± 0.25	0.351
CD8:CD4 ratio	1.79 ± 0.38	1.33	1.50 ± 0.23	0.391	1.73 ± 0.31	2.62 ± 0.60	0.154
CD8: FOXP3 ratio	6.12 ± 1.12	1.33	5.08 ± 0.42	0.678	5.69 ± 0.95	5.56 ± 1.25	0.932

Table 3.13: Immune cells and cell ratios among NFPA types, and between NFPAs vs somatotrophinomas
Immune cells analysed: macrophages (CD68+), CD163+ macrophages, HLA-DR macrophages, cytotoxic T lymphocytes (CD8+), T helper lymphocytes (CD4+), T regulatory lymphocytes (FOXP3+), B cells (CD20+) and neutrophils (neutrophil elastase+). Data are shown as mean±SEM for percentage of immune cells compared to the total number of tumour cells and for cell ratios. One way-ANOVA test was used to calculate *p* value among the NFPA types: gonadotroph adenoma, silent corticotroph adenoma and null cell adenoma (GA vs SCA vs NCA). Mann Whitney U test was used to calculate *p* value for the comparison NFPAs vs somatotrophinomas (NFPA vs Som).

Recruitment of immune cells into the TME of pituitary adenomas

PAs with a higher macrophage content were associated with higher levels of IL-8 (p=0.023), CCL2 (p=0.216), CCL3 (p=0.065), CCL4 (p=0.036) and CXCL1 (p=0.024) (Figure 3.12-A), chemokines known to promote macrophage chemotaxis[209,226,333,528].

Higher CCL2 (p=0.036), CCL4 (p=0.086), CXCL10 (p=0.134) and VEGF-A (p=0.025) levels were found in supernatants from PAs with higher CD8+ T cell contents (Figure 3.12-B).

PAs with more neutrophils released higher levels of CCL2 (p=0.033) and CCL4 (p=0.044), chemokines classically involved in macrophage recruitment[209,226,333,528] but that also attract neutrophils[517,529,530]. PA with higher contents of neutrophils also showed a trend to secrete higher levels of chemokines involved in neutrophil chemotaxis, namely IL-8 (p=0.073), CXCL1 (p=0.097) and CXCL10 (p=0.098) (Figure 3.12-C).

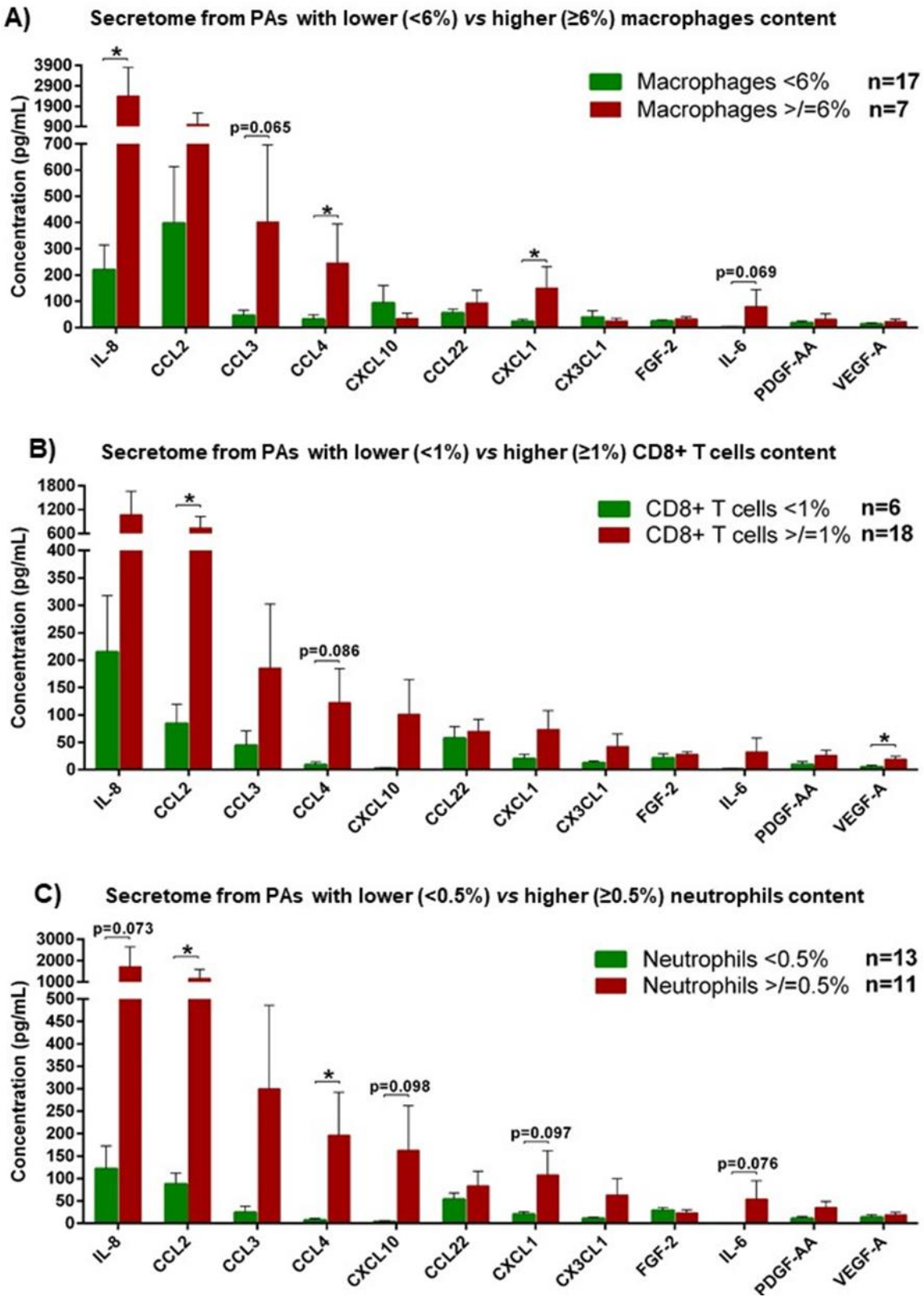

Figure 3.12: Cytokine secretome of PAs and infiltrating immune cells

A) Cytokine secretome from primary cell culture supernatants of PAs with lower *vs* higher content of macrophages (A), CD8+ T cells (B) and neutrophils (C). The cut-offs used to define low and high immune cell contents were: 6% for macrophages, 1% for CD8+ T cells and 0.5% for neutrophils. Data are shown as concentration (pg/mL), mean±SEM for the top 12 secreted proteins. *, <0.05, **, <0.01, ***, <0.001 (Mann Whitney U test).

There were no significant associations between PA-derived cytokine secretome and infiltrating CD4+ T, FOXP3+ T and B cells (Figure 3.13).

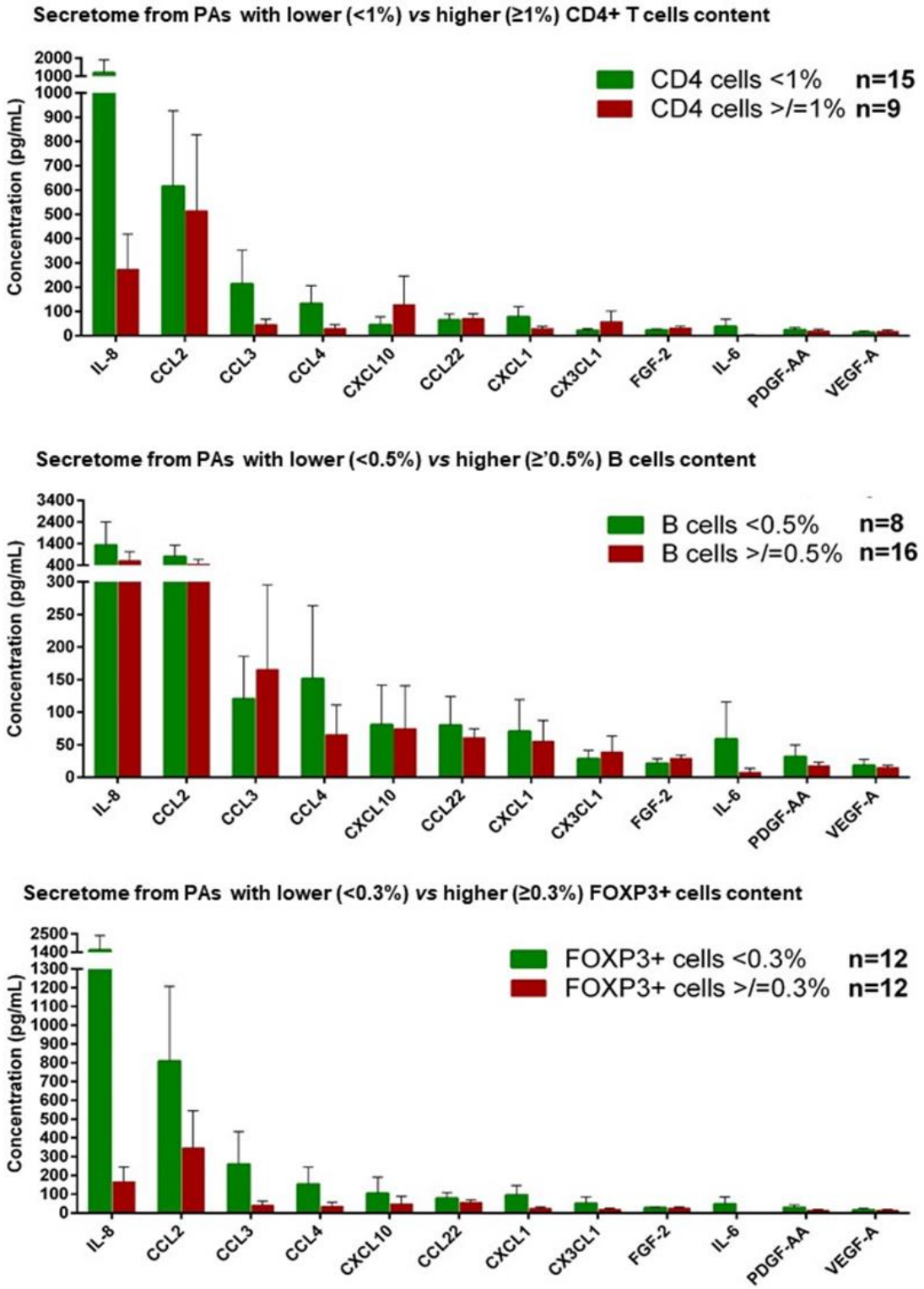

Figure 3.13: Cytokine secretome of PAs and infiltrating CD4+ T cells, Tregs and B cells
The cutoffs used to define low and high immune cell contents were: 1% for CD4+ T cells, 0.5% for B cells and 0.3% for FOXP3+ T cells. Data are shown as concentration (pg/mL), mean±SEM for the top 12 secreted proteins. *p* values were non-significant (Mann Whitney U test).

RNAscope data showed that CCL2 and IL-8, the two highly secreted chemokines released by the great majority of PAs, are mainly synthesised by pituitary tumour cells where most mRNA transcripts for these chemokines are detectable in the PA tissue section. However, pituitary tumour cells have low expression of the respective chemokine receptors CXCR2 and CCR5, which were in turn are strongly expressed in scattered perivascular cells morphologically distinct from tumour cells, likely corresponding to immune cells potentially transmigrating from the blood vessels into the TME of PAs (Figure 3.14).

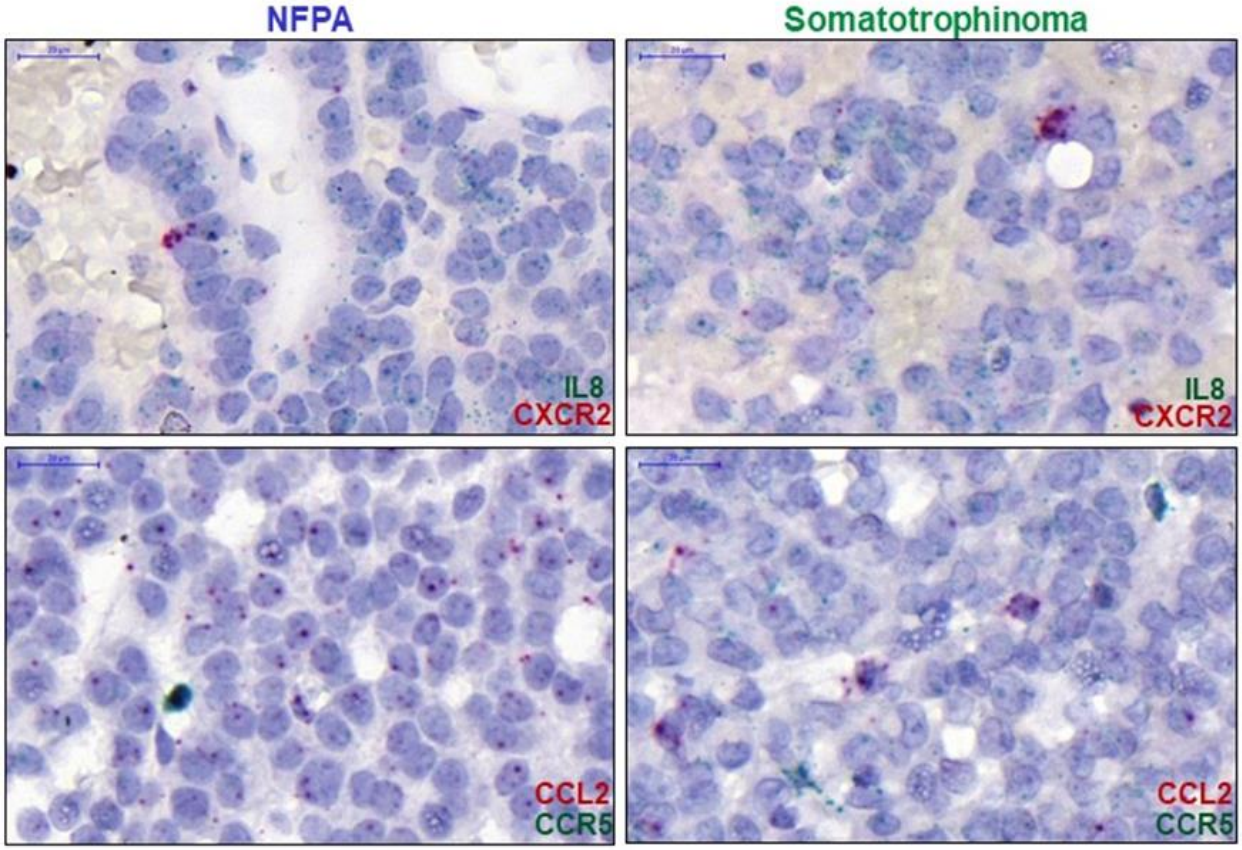

Figure 3.14: IL8-CXCR2 and CCL2-CCR5 mRNA expression in PAs
RNAscope staining of IL8 (green)-CXCR2 (red) and CCL2 (red)-CCR5 (green) mRNA in a NFPA and in a somatotrophinoma. CCL2 and IL-8 are mainly expressed in pituitary tumour cells, while the chemokine receptors are strongly expressed in scattered perivascular cells morphologically distinct from tumour cells, likely corresponding to immune cells. Scale bar 20µm.

PA-infiltrating immune cells did not correlate with circulating immune cell types, suggesting that immune infiltrates are subject to differential recruitment into the PA rather than altered bone marrow production (Figure 3.15). There was only one significant correlation between serum lymphocyte count and PA-infiltrating CD8+ T cells, but this seems to be due to an outlier case.

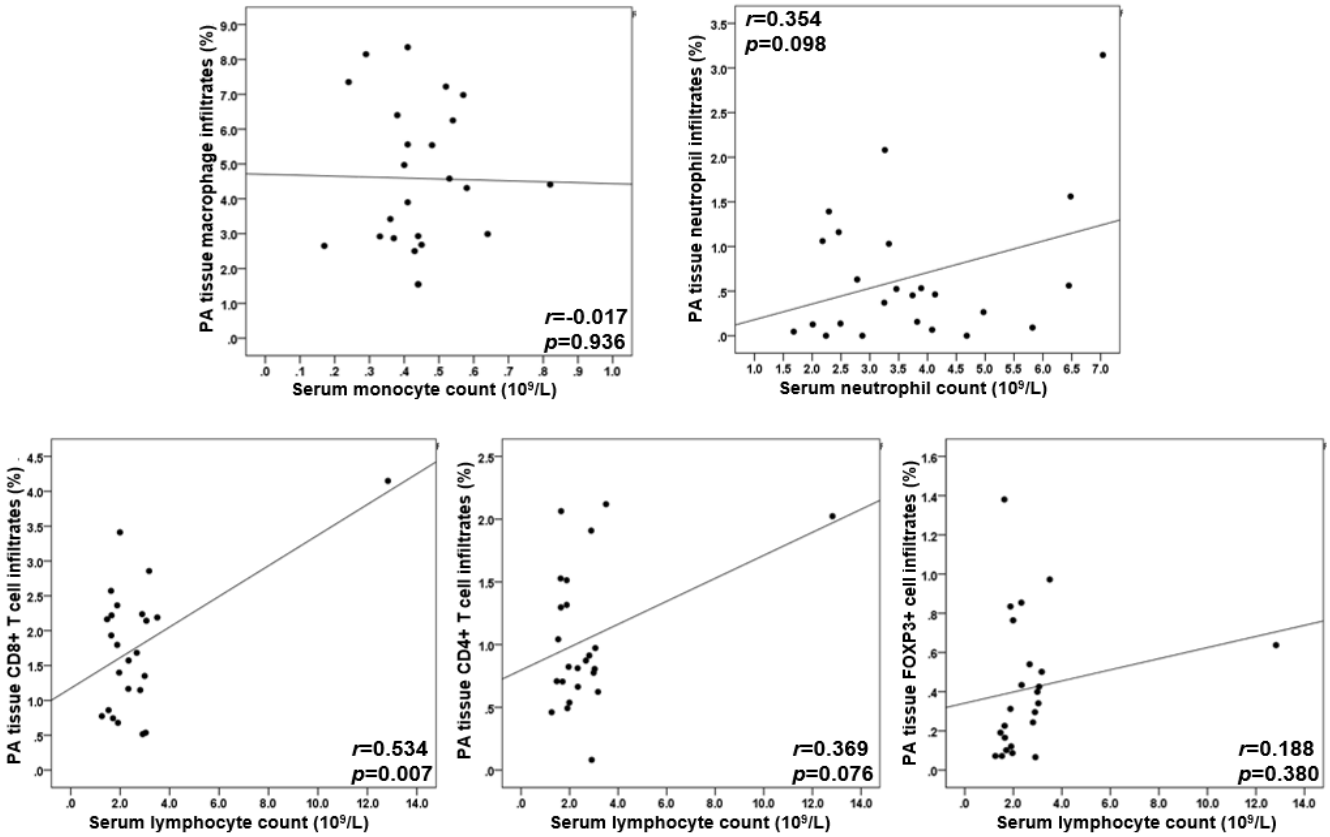

Figure 3.15: Correlation between PA tissue infiltrating and circulating immune cell subpopulations
p values were determined by the Pearson correlation coefficient *r*.

The role of infiltrating immune cells in the PA phenotype and aggressiveness

PAs with a higher Ki-67 (≥3%) had a lower CD8:CD4 ratio, as well as lower CD8:FOXP3 and CD68:FOXP3 ratios as a result of an increased infiltration of FOXP3+ T cells (0.7±0.2 vs 0.3±0.6%; p=0.013) (Figures 3.16-A and B). Macrophages and CD4+ T helper lymphocytes were found in significantly higher amounts in PAs comparing to NP, the B cell content tended to be higher in PAs in immunohistochemical (Figure 3.9) and xCell (Figure 3.11) data, and FOXP3+ T cells were associated to a higher Ki-67 (Figure 3.16-A), suggesting the involvement of these immune cell types in the pituitary tumourigenic process and a "deleterious effect" in PA phenotype, as shown in other cancers[332,359,360,531,532]. In fact, all PAs with a "deleterious immune infiltrate phenotype", i.e. higher content of macrophages, CD4+ T, FOXP3+ and B cells ($CD68^{hi}CD4^{hi}FOXP3^{hi}CD20^{hi}$) had a Ki-67≥3% (Figure 3.16-C and D). There were no differences between PAs with or without cavernous sinus invasion regarding immune cell contents or ratios (Figure 3.16-E). These data suggest that, at least in part, immune cells in the TME of PAs may determine increased aggressiveness, namely tumour proliferation.

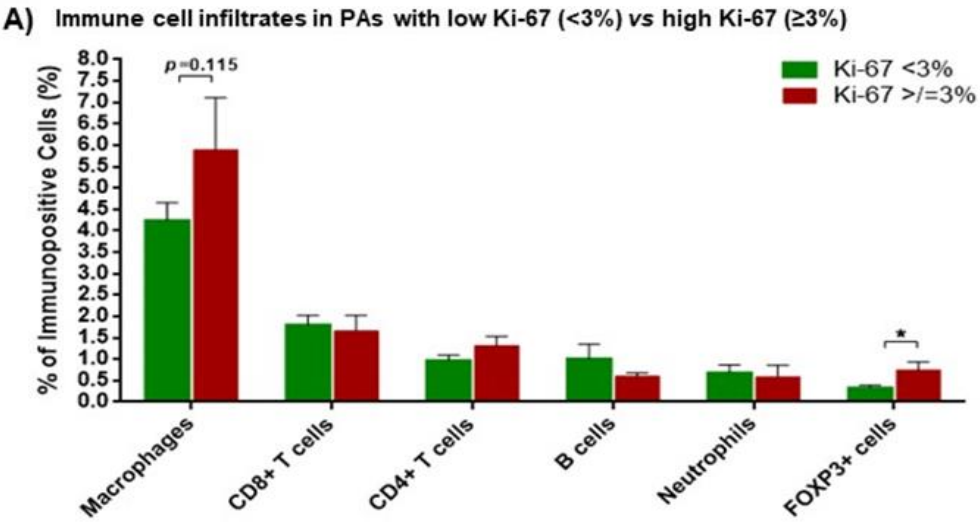
A) Immune cell infiltrates in PAs with low Ki-67 (<3%) vs high Ki-67 (≥3%)
% of Immunopositive Cells (%)
p=0.115
Ki-67 <3%
Ki-67 >/=3%
*
Macrophages
CD8+ T cells
CD4+ T cells
B cells
Neutrophils
FOXP3+ cells

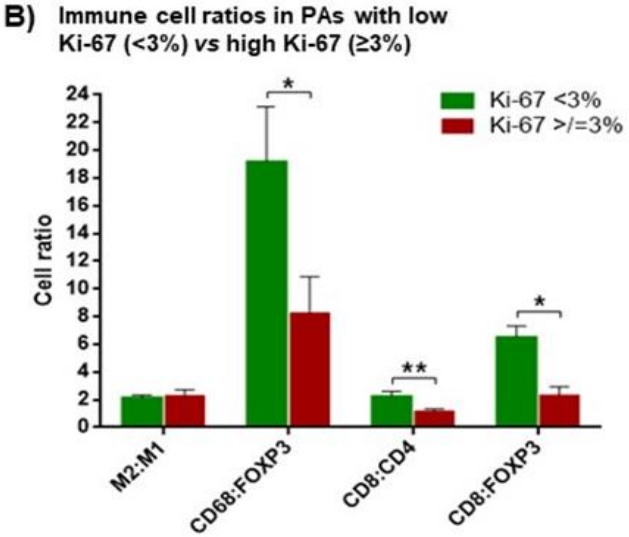
B) Immune cell ratios in PAs with low Ki-67 (<3%) vs high Ki-67 (≥3%)
Cell ratio
Ki-67 <3%
Ki-67 >/=3%
*
**
*
M2:M1
CD68:FOXP3
CD8:CD4
CD8:FOXP3

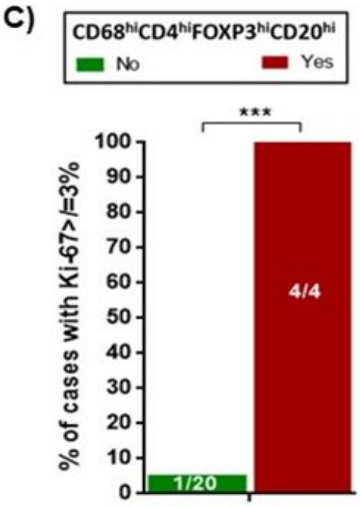
C)
CD68hiCD4hiFOXP3hiCD20hi
No
Yes
***
% of cases with Ki-67>/=3%
4/4
1/20

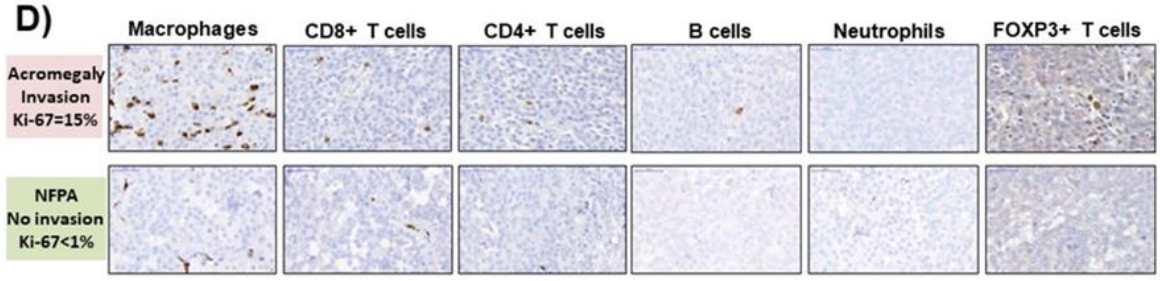
D)
Macrophages
CD8+ T cells
CD4+ T cells
B cells
Neutrophils
FOXP3+ T cells
Acromegaly
Invasion
Ki-67=15%
NFPA
No invasion
Ki-67<1%

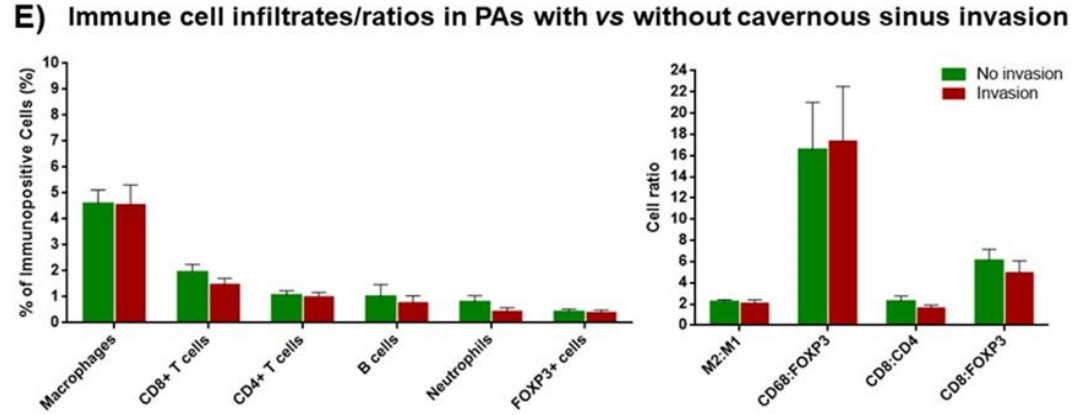
E) Immune cell infiltrates/ratios in PAs with vs without cavernous sinus invasion
% of Immunopositive Cells (%)
Macrophages
CD8+ T cells
CD4+ T cells
B cells
Neutrophils
FOXP3+ cells
Cell ratio
No invasion
Invasion
M2:M1
CD68:FOXP3
CD8:CD4
CD8:FOXP3

Figure 3.16: Immune cell infiltrates in PAs and Ki-67 and cavernous sinus invasion
Immune cell infiltrates (A) and cell ratios (B) in PAs with lower (<3%) *vs* higher (≥3%) Ki-67. PAs with lower Ki-67, n=19; PAs with higher Ki-67, n=5. *, <0.05, **, <0.01, ***, <0.001 (Mann Whitney U test). C) Percentage of PAs with Ki-67≥3% according to presence of a "deleterious immune infiltrate phenotype", i.e. higher content of macrophages, CD4+ T cells, FOXP3+ T cells and B cells ($CD68^{hi}CD4^{hi}FOXP3^{hi}CD20^{hi}$). PAs with "deleterious immune infiltrate phenotype", n=4; PAs without "deleterious immune infiltrate phenotype", n=20. *, <0.05, **, <0.01, ***, <0.001 (Exact Fisher´s test). D) Representative images are shown from a somatotrophinoma with high Ki-67 and cavernous sinus invasion which had a "deleterious immune infiltrate phenotype", and from a NFPA with low Ki-67 and no cavernous sinus invasion which did not display a "deleterious immune infiltrate phenotype". Scale bar 50µm. E) Immune cell infiltrates and cell ratios in PAs with (n=10) *vs* without (n=14) cavernous sinus invasion. *, <0.05, **, <0.01, ***, <0.001 (Mann Whitney U test).

M2:M1 macrophage ratio (CD163+:HLA-DR+ cells) was positively correlated with microvessel density (p=0.015) and total microvessel area (p<0.001) (Figure 3.17), suggesting that immune cells, particularly M2-macrophages, may influence PA angiogenesis (details in Chapter 5).

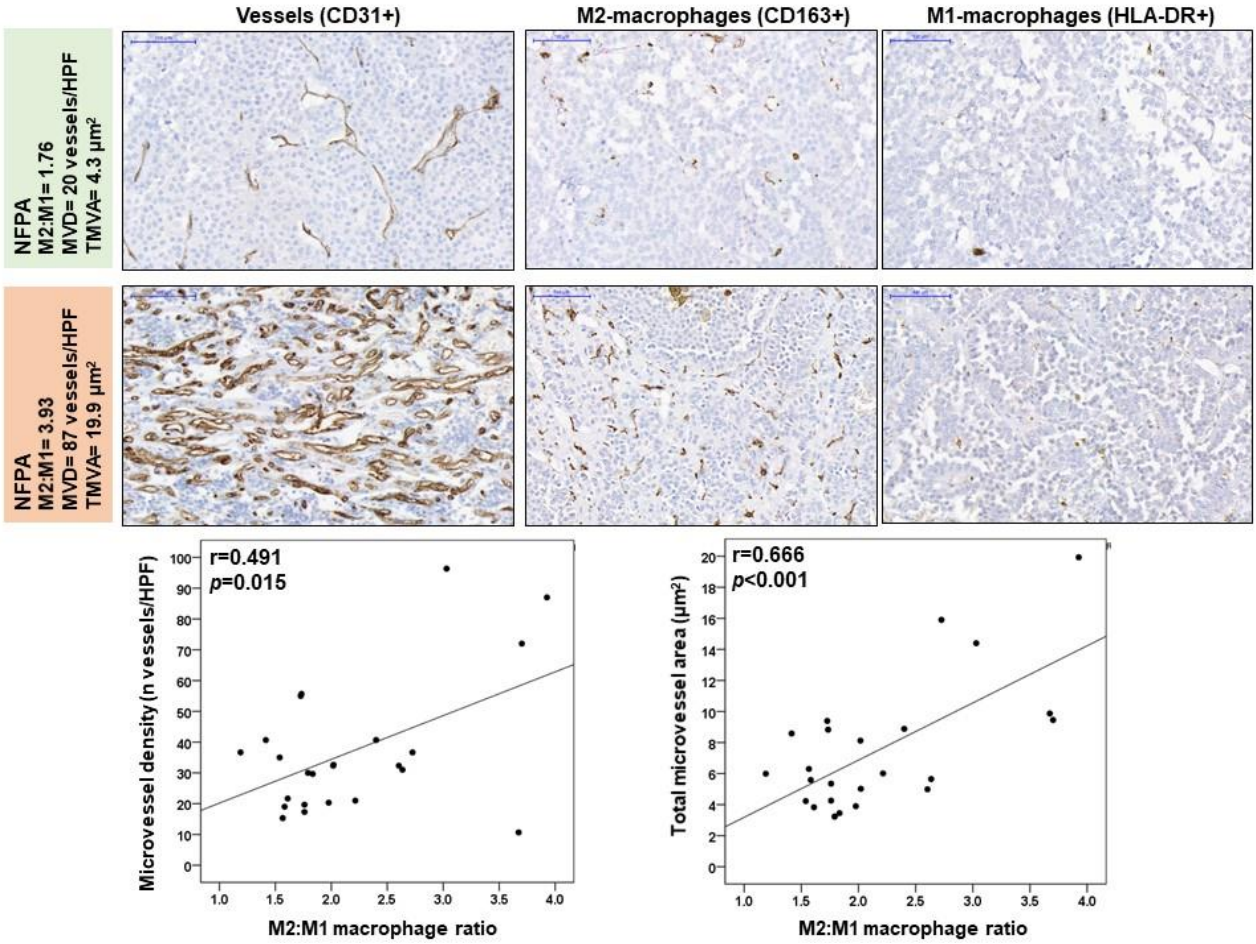

Figure 3.17: M2 and M1 macrophages and angiogenesis in PAs
Microvessel density (MVD) or total microvessel area (TMVA) correlation with M2:M1 macrophage ratio. Representative images are shown from samples with low and high M2:M1 macrophage ratio. Scale bar 100µm, n=24. *P* values were determined by the Pearson correlation coefficient *r*.

The effect of immune cell infiltrates on the phenotype of PAs

The immune cell infiltrates did not differ between NFPAs and somatotrophinomas, except for neutrophil content which was lower in somatotrophinomas (Table 3.13). Nevertheless, the effect of infiltrating immune cells on the phenotype of NFPAs and somatotrophinomas can be different considering the distinct histiotypes and the fact that gonadotrophs or somatotrophs may respond or interact differently with the surrounding immune cells. This could theoretically influence different clinico-pathological features including pituitary hormone secretion. Hence, a comprehensive subanalysis was performed in the subgroup of NFPAs and somatotrophinomas, and the results shown in the supplemental tables in Appendix 4.

Overall, infiltrating immune cells do not seem to impact significantly on the different clinico-pathological features among NFPAs. There were also no correlations between serum pituitary hormone levels and NFPA-infiltrating immune cells, except for the negative correlation noted between infiltrating neutrophils and IGF-1 index (r=-0.582 p=0.029). However, there was a trend for female patients to have higher content of macrophages and FOXP3+ T cells than males (6.0±0.7 vs 4.1±0.6%, p=0.118 and 0.7±0.3 vs 0.3±0.1%, p=0.174, respectively), as well as a higher M2:M1 ratio (2.8±0.4 vs 2.1±0.2, p=0.173) and lower CD8:FOXP3 (3.3±1.0 vs 6.5±1.1, p=0.154). There were almost significant correlations between age at diagnosis and FOXP3+ T cell amount (r=-0.480; p=0.060), CD8:CD4 ratio (r=0.424; p=0.102) and CD8:FOXP3 ratio (r=0.447; p=0.109). PAs with cavernous sinus invasion tended to be associated with a higher content of CD4+ T cells than non-invasive ones (1.2±0.2 vs 0.9±0.1%, p=0.187). PAs with Ki-67≥3% tended to have more FOXP3+ T cells (0.7±0.3 vs 0.3±0.1%, p=0.163) and a significantly lower CD8:FOXP3 ratio (2.4±0.7 vs 6.8±1.1, p=0.037) than less proliferative PAs. The M2:M1 ratio correlated positively with microvessel area (r=0.676, p=0.004) (Appendix 4).

Regarding somatotrophinomas, there were significant correlations between age at diagnosis and both FOXP3+ cell amount (r=-0.746; p=0.034) and M2:M1 ratio (p=0.856, p=0.007). A significantly higher CD8:CD4 ratio was noted in the somatotrophinoma case with visual impairment (p=0.036) and for the 2 cases with hypopituitarism at diagnosis (p=0.005). There were no correlations between infiltrating immune cells or cell ratios and GH or IGF-1 levels. There was one highly proliferative somatotrophinoma (Ki-67=15%) which had twice more macrophages than all others (8.4 vs 4.1±0.5%). M2:M1 and CD8:CD4 ratios correlated positively with microvessel density and area (p=0.017 and p=0.045) (Appendix 4).

***In vitro* studies investigating interactions between macrophages and pituitary tumour cells**

To study the interactions between pituitary tumour cells, modelled here by GH3 mammosomatotroph tumour cell line, and macrophages (RAW 264.7 cell line), I established an *in vitro* model using conditioned medium (CM) from each of the cell lines as a chemoattractant agent for the other. My *in vitro* studies focused on macrophages, as these were the predominant immune cell type in PAs (Figure 3.9).

I selected the murine RAW 264.7 macrophage cell line for a number of reasons: i) lack of a reliable rat macrophage cell line; ii) high homology between mouse and rat cytokines; iii) is an appropriate cell line to study cell interactions and cytokine effects, including CX3CL1, the main GH3 cell-derived chemokine according to my cytokine array data (Appendix 5), which express high levels of its receptor CX3CR1[533]; and iv) to validate some of Dr. Sayka Barry's previous observations on a different cell model employing primary bone-marrow derived rat macrophages and GH3 cells[513].

Figure 3.18 illustrates the *in vitro* cell model and the functional studies to investigate the interaction between pituitary tumour cells and macrophages. Briefly, RAW 264.7 macrophages were cultured with GH3-CM. Following washes and medium change, supernatants were collected at 24h and secretome changes assessed by cytokine bead array and RT-qPCR. I performed also morphology studies and chemotaxis assay to study how GH3 tumour cells influence macrophages. Flow cytometry and RT-qPCR experiments were conducted to assess whether GH3-CM induce macrophage polarisation assessing different M1-like (CD86, IFNy^{high}, IL-12^{high}) and M2-like (CD163, CD206, IL-10^{high}, IL-12^{low}) macrophage markers before and after treatment with GH3-CM. On the other hand, GH3 cells were cultured with macrophage-CM. Secretome profile using cytokine array, morphological studies, RT-qPCR and immunocytochemistry for EMT markers (E-cadherin, ZEB1) were performed. I also performed transwell and wound healing migration assays and matrigel invasion assays to evaluate how macrophages influence GH3 cells migratory behaviour.

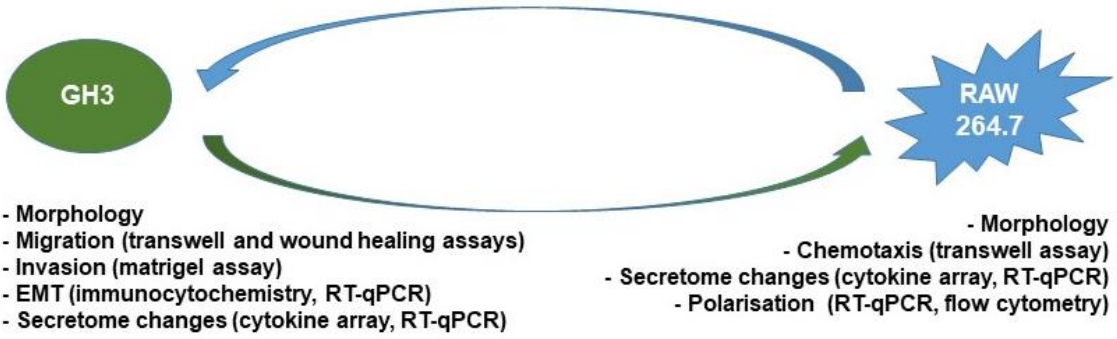

Figure 3.18: *In vitro* cell model using GH3 cells and RAW 264.7 macrophages

GH3 cell-derived factors increase macrophage chemotaxis and alter their morphology

To investigate the role of GH3 cell-derived factors in macrophage chemotaxis, I performed a transwell migration assay experiment in which I observed a remarkable 36-fold increase in macrophage migration towards GH3-CM in comparison to complete medium or recombinant CX3CL1 (Figure 3.19-A). This prominent macrophage chemoattractant effect of pituitary tumour cell-derived secretions is consistent with the association between high PA-derived chemokine levels and more infiltrating macrophages in human PAs (Figure 3.12).

Immune cell chemotaxis depends not only on tissue chemokine gradient, but also on chemokine receptor expression in trafficking cells[209]. My RNAscope data in human PA samples showed strong expression of chemokine receptors in perivascular immune cells, presumably contributing to their recruitment and transmigration into the TME in response to a gradient created by chemokines mainly synthesised by pituitary tumour cells (Figure 3.14). GH3-CM increased more than 12x the expression of *Cx3cr1* (chemokine receptor with specific affinity for CX3CL1 and highly expressed in RAW 264.7 macrophages[533]), and the *Ccr5* expression (p=0.051) (Figure 3.19-B). Thus, the GH3-CM chemoattractant effect can be explained, at least in part, by upregulation of chemokine receptor expression in RAW 264.7 macrophages.

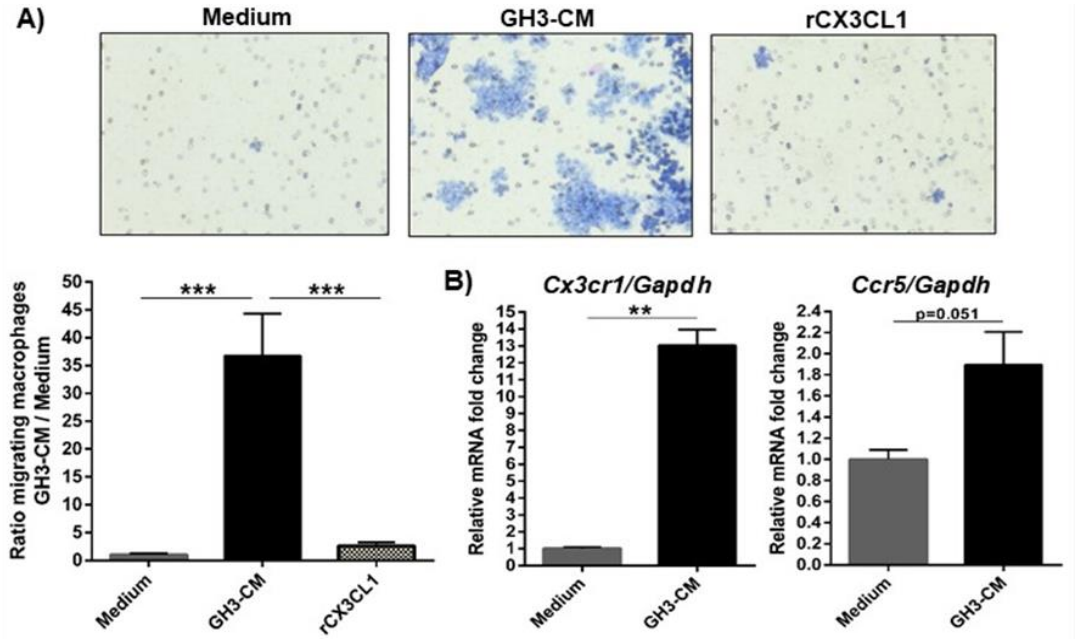

Figure 3.19: GH3-CM effect on macrophage chemotaxis and their chemokine receptor expression
A) Transwell chemotaxis assay performed on RAW 264.7 macrophages towards complete medium, GH3-CM and recombinant CX3CL1 (rCX3CL1) at concentration 100ng/mL for 72h. Data are shown as mean ±SEM for the ratio of migrated macrophages towards GH3-CM or rCX3CL1 in relation to migrated macrophages in complete medium. n=6. *, <0.05, **, <0.01, ***, <0.001 (one way-ANOVA with Bonferroni multiple comparison test). B) *Cx3cr1* and *Ccr5* expression in RAW 264.7 macrophages determined by RT-qPCR after treatment with GH3-CM for 24h *vs* complete medium. Data are shown as mean±SEM for *Cx3cr1* or *Ccr5* mRNA expression fold change relative to *Gapdh*, determined by the ΔΔCT method. n=3. *, <0.05, **, <0.01, ***, <0.001 (Mann Whitney U test).

Following GH3-CM treatment, macrophages showed morphological changes typical of activated macrophages: an increase in area, perimeter, Feret's diameter and spindle-shaped morphology[229,339] and a decrease in solidity, roundness and circularity (Figure 3.20), representing macrophages with an enhanced migration phenotype.

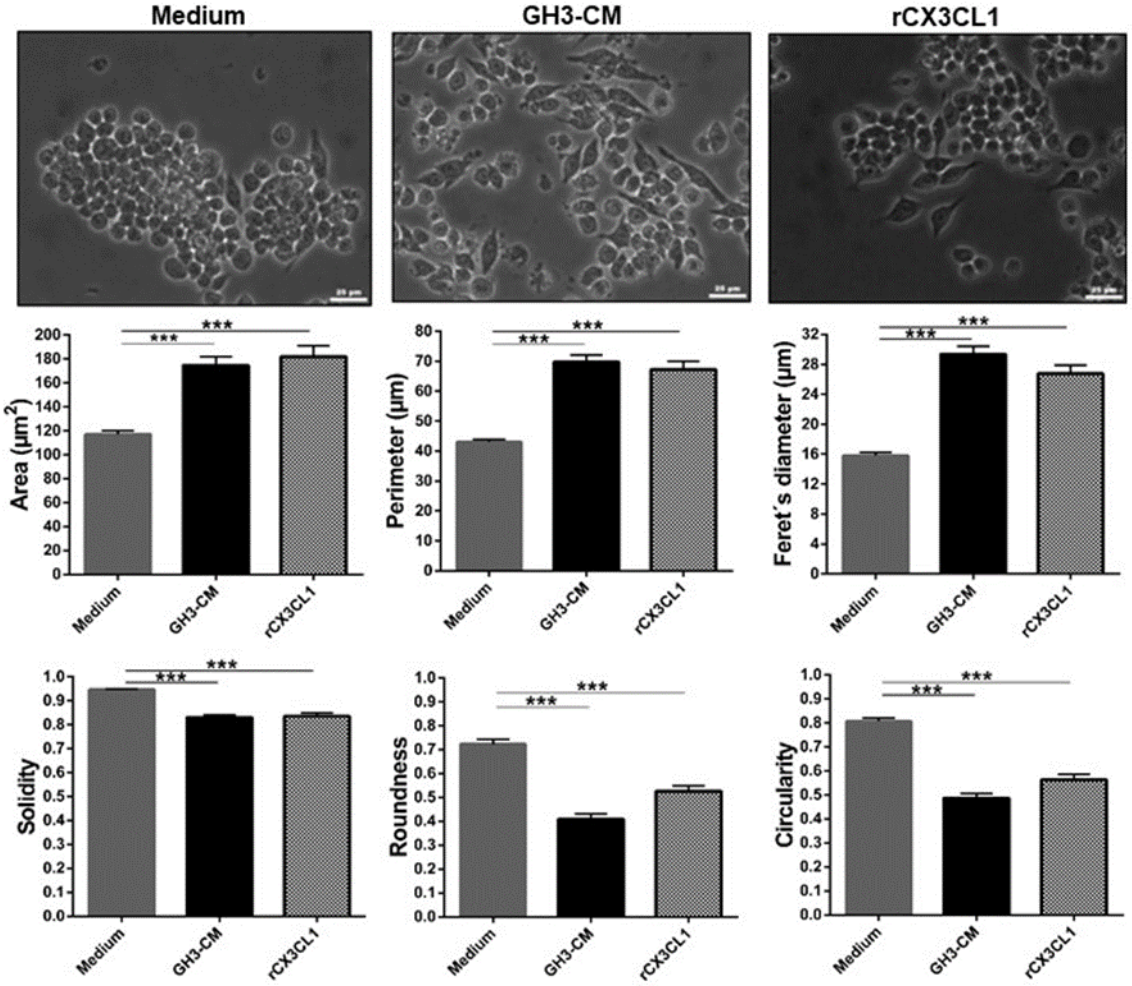

Figure 3.20: GH3-CM effect on macrophage morphology
Morphological evaluation of RAW 264.7 macrophages after treatment for 72h with complete medium (n=3), GH3-CM and recombinant CX3CL1 (rCX3CL1) at concentration of 100ng/mL. Data are shown as mean±SEM for the 6 morphological parameters evaluated by Image J: cell area (µm^2), Feret's diameter (µm), solidity (0-1), perimeter (µm), roundness (0-1) and circularity (0-1). Per experiment 75 cells were analysed, with a minimum of 3 experiments per treatment condition. Scale bar 25µm. *, <0.05, **, <0.01, ***, <0.001 (one-way ANOVA with Bonferroni multiple comparison test).

Recombinant CX3CL1 was used as positive control, as this was the chemokine with the highest concentration in GH3 supernatants (Appendix 5), and has a recognised potent chemoattractant effect on RAW 264.7 macrophages[533]. I could verify this CX3CL1 chemotaxis effect in my dose-response optimisation migration experiments (Figure 3.21-B), and I also noted that recombinant CX3CL1 induced morphology changes in RAW 264.7 macrophages (Figure 3.21-A), more markedly at 100ng/mL (this dose was then used in the chemotaxis and morphology studies).

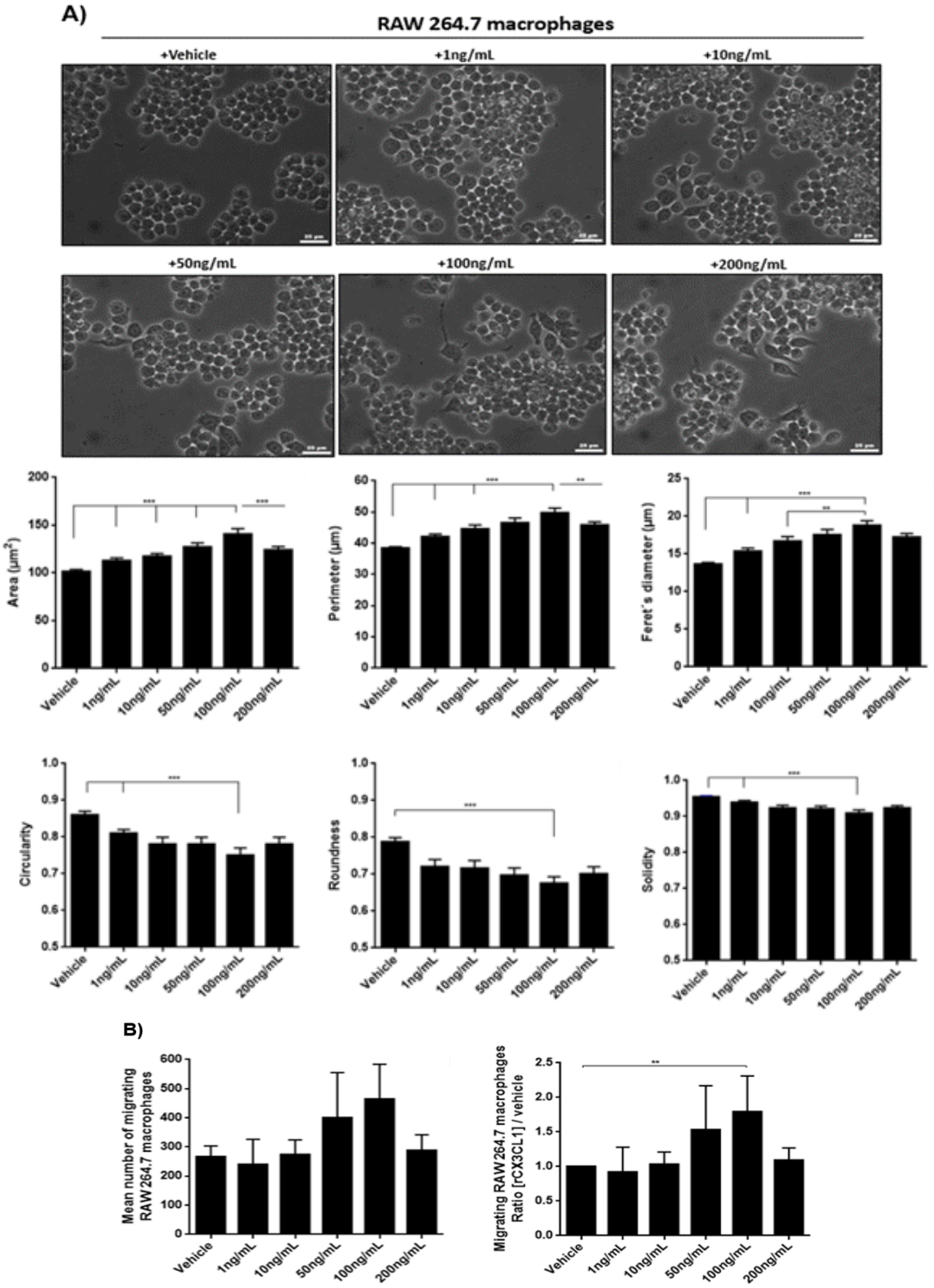

Figure 3.21: CX3CL1 dose-response optimisation for migration and morphological studies

A) Morphological evaluation of RAW 264.7 macrophages cells after treatment for 72h with different concentrations of recombinant CX3CL1 (rCX3CL1). Most prominent changes were seen at 100ng/mL. Data are shown as mean±SEM for the 6 morphological parameters evaluated by Image J: cell area (µm^2), Feret´s diameter (µm), solidity (0-1), perimeter (µm), roundness (0-1) and circularity (0-1). Per experiment 75 cells were analysed; n=3. Scale bar 25µm. B) Migration assays performed on RAW 264.7 macrophages through transwell chambers towards complete medium (vehicle) and different rCX3CL1 concentrations after 72h. Data are represented as number of cells migrating in the different conditions and as a ratio of migrating macrophages towards rCX3CL1 in relation to migrated cells towards vehicle, mean±SEM. n=4. *, <0.05, **, <0.01, ***, <0.001 (two-way ANOVA with Bonferroni multiple comparison test).

GH3 cell-derived factors induce secretome changes in RAW 264.7 macrophages

In different cancers, tumour cell-derived cytokines can modulate the surrounding TME non-neoplastic cells, including their cytokine secretome[220-222]. To investigate whether GH3 cells are able to induce changes in the macrophage cytokine secretome, I analysed the secretome in supernatants from RAW 264.7 macrophages treated with GH3 cell-CM (using CM from both GH3-NT and GH3-*Aip*-KD) and compared to untreated macrophages secretome (Appendix 5).

The first observation was that RAW 264.7 macrophages display a secretome considerably different from GH3 cells, secreting high amounts of chemokines, particularly CCL3 and CCL4, but low amounts of interleukins (Appendix 5). The second observation is that GH3 cell-CM was able to induce changes in the macrophage secretome, with 10 different cytokines being differentially secreted upon treatment with GH3 cell-CM, in most of cases resulting in higher concentrations after treatment (Appendix 5). The third observation is that GH3-*Aip*-KD-CM induced changes in more macrophage-derived cytokines, and more prominently than GH3-NT-CM, increasing most of the cytokines except IL-1β (Figure 3.22). Hence, GH3-*Aip*-KD cells displayed a more potent effect on macrophage secretome than GH3-NT cells. These findings suggest that AIP deficiency may modulate the surrounding TME, in particular the secretome from non-neoplastic cells such as macrophages, and thus the cytokine network in the TME, potentially leading to increased aggressiveness associated with *AIP*mut PAs[19,91,161], and the presence of more macrophages in *AIP*mut somatotrophinomas[513] (discussed in Chapter 6).

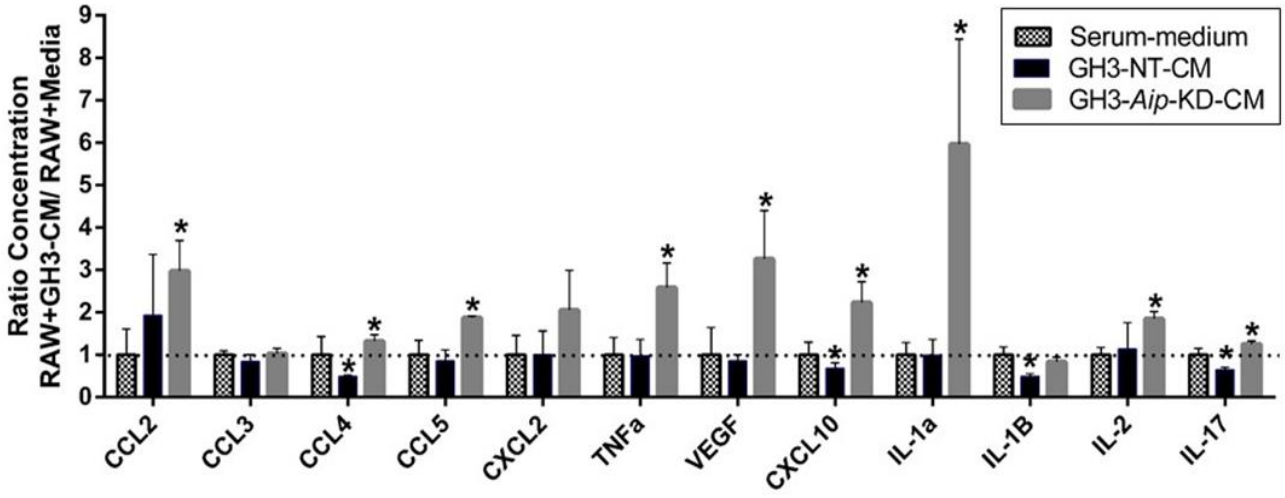

Figure 3.22: GH3-CM effect on macrophage cytokine secretome
RAW 264.7 macrophage secretome changes induced by GH3-CM (NT and *Aip*-KD) after treatment for 24h. Data are shown for the most significantly changed macrophage-derived cytokines or those cytokines found at higher concentrations in macrophage supernatants after GH3 cell-CM treatment in comparison to the baseline evaluation, and expressed as ratio between cytokine concentration after 24h of treatment with GH3 cell-CM and 24h of treatment with serum-medium. Cytokine were assessed by Millipore MILLIPLEX assay (mouse cytokine/chemokine array 32-plex). Data are shown as mean±SEM, n=3. *, <0.05, **, <0.01, ***, <0.001 (Mann-Whitney U test).

By RT-qPCR, the expression of some cytokines and growth factors identified by the cytokine array as differentially secreted upon GH3 cell-CM was studied. My RNA expression data did not overlap with the protein cytokine array data, except for VEGF which was found significantly overexpressed in macrophage treated with either GH3-NT and GH3-*Aip*-KD cell-CM, and also for IL-1α whose RNA was significantly upregulated in macrophages treated with GH3-NT cells and showing a trend to a 2-fold increase in those exposed to GH3-*Aip*-KD cells (Figure 3.23). *Cxcl10*, *Ccl2* and *Ccl4* mRNA (for macrophages treated with GH3-*Aip*-KD-CM) were downregulated contrary to the cytokine array data (Figure 3.23).

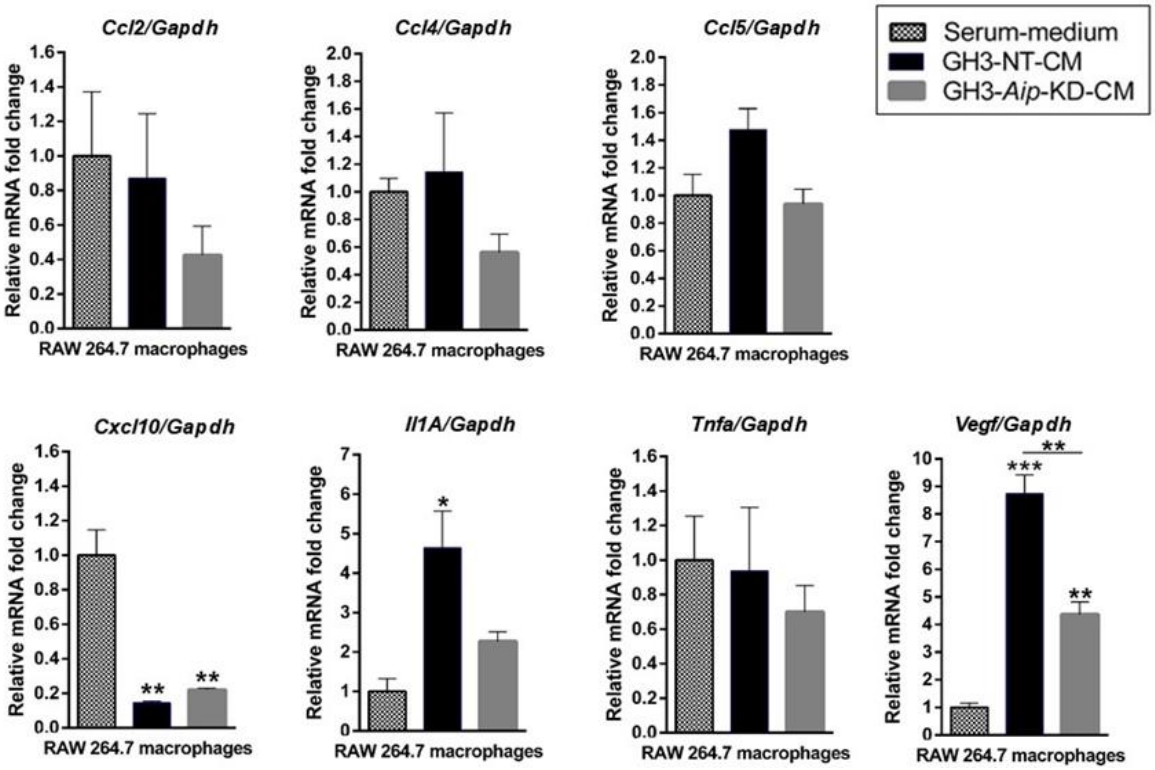

Figure 3.23: GH3-CM effect on macrophage cytokine gene expression
Cytokine expression changes on macrophages after treatment for 24h with GH3-NT and GH3-*Aip*-KD cell-CM, determined by RT-qPCR. The genes analysed are correspondent to those cytokines identified on the preliminary cytokine array data. Data are shown as mRNA expression fold change relative to *Gapdh*, mean±SEM, and determined by the ΔΔCT method. n=3. *, <0.05, **, <0.01, ***, <0.001 (one-way ANOVA test).

Thus, RNA and protein data not always correlate, and this is particularly valid for cytokines whose regulation is complex, with translation often mismatching transcription, and they are also subject to autocrine/paracrine feedback loops as a putative mechanism to prevent cell overstimulation[534,535]. GH3 cell-derived factors likely stimulate the release of pre-synthesised cytokines (stored in vesicles), whose concentration increases rapidly in the supernatants and over a 24h period and may exert a negative feedback effect supressing their own transcription.

GH3 cell-derived factors are unable to induce polarisation of RAW 264.7 macrophages

In different cancers, tumour cells are able to activate immune or stromal cells in the surrounding TME, including macrophages[229,332,334]. To investigate whether GH3 cell-derived factors could lead to RAW 264.7 macrophage polarisation into the pro-tumoural M2-like subtype[229], the predominant macrophage subtype in human PAs (Figure 3.10), I conducted a RT-qPCR study assessing the expression of *iNos* (M1-macrophage marker), *Arg1* and *CD206* (M2-macrophage marker) (Figure 3.24-A), as well as a flow cytometry experiment (Figure 3.24-B) after treating macrophages with GH3 cell-CM (from both GH3-*Aip*-KD and GH3-NT cells).

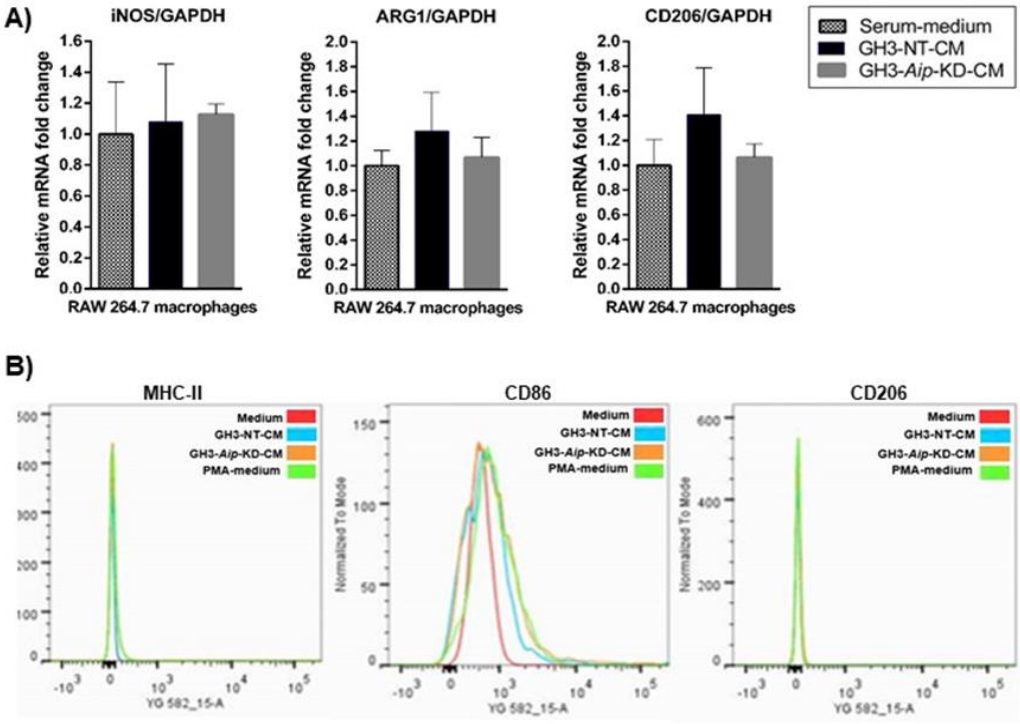

Percentage and median marker expression by RAW 264.7 macrophages per treatment condition			
Treatment condition	**MHC-II**	**CD86**	**CD206**
Medium %(median expression)	6.37% (308)	92.4% (783)	3.44% (13932)
GH3-NT cell–CM %(median expression)	6.3% (329)	79.3% (568)	16.4% (14754)
GH3-*Aip*-KD cell-CM %(median expression)	6.85% (328)	78.1% (551)	8.85% (15838)
PMA-medium %(median expression)	2.67% (336)	84.7% (575)	2.85% (14669)

Figure 3.24: GH3-CM effect on macrophage polarisation

A) M1 and M2 macrophage markers expression in RAW 264.7 macrophages after treatment with GH3-NT-CM and GH3-*Aip*-KD-CM for 24h vs untreated, determined by RT-qPCR. Data are shown as mRNA expression fold change to relative *Gapdh*, mean±SEM, determined by the ΔΔCT method. n=3. *, <0.05, **, <0.01, ***, <0.001 (one-way ANOVA test). B) MHC-II and CD86 (M1-like macrophage markers) and CD206 (M2-like macrophage markers) expression levels in RAW 264.7 macrophages treated with GH3-NT and GH3-*Aip*-KD cell-CM for 24h, assessed by flow cytometry. Fluorescent peaks of RAW 264.7 macrophages for different receptors after treatment with medium, GH3-NT or GH3-*Aip*-KD GH3 cell-CM and PMA (5nM)-medium, and a table with percentage and median marker expression per treatment condition, are shown.

These data showed that GH3 cell-CM was unable to fully polarise RAW 264.7 macrophages. Such findings are not surprising in the view of the low cytokine levels in GH3 supernatants (Appendix 5), particularly those leading to M2 polarisation (IL-4, IL-10 and IL-13)[229].

RAW 264.7 macrophage-derived factors affect the behaviour and invasiveness of GH3 cells

CM from untreated (-PMA_Raw-CM) or PMA-treated macrophages (+PMA_Raw-CM) increased GH3 cell area, perimeter and Feret's diameter and reduced their solidity, circularity and roundness (Figure 3.25) indicating that GH3 cells acquired an EMT-like phenotype. Macrophage-induced morphology changes in GH3 cells were confirmed with actin immunocytochemistry: GH3 cells treated with macrophage-CM developed a granular pattern of actin with prominent stress fibres and numerous spikes (Figure 3.25) representing an EMT-like cytoskeletal change[536].

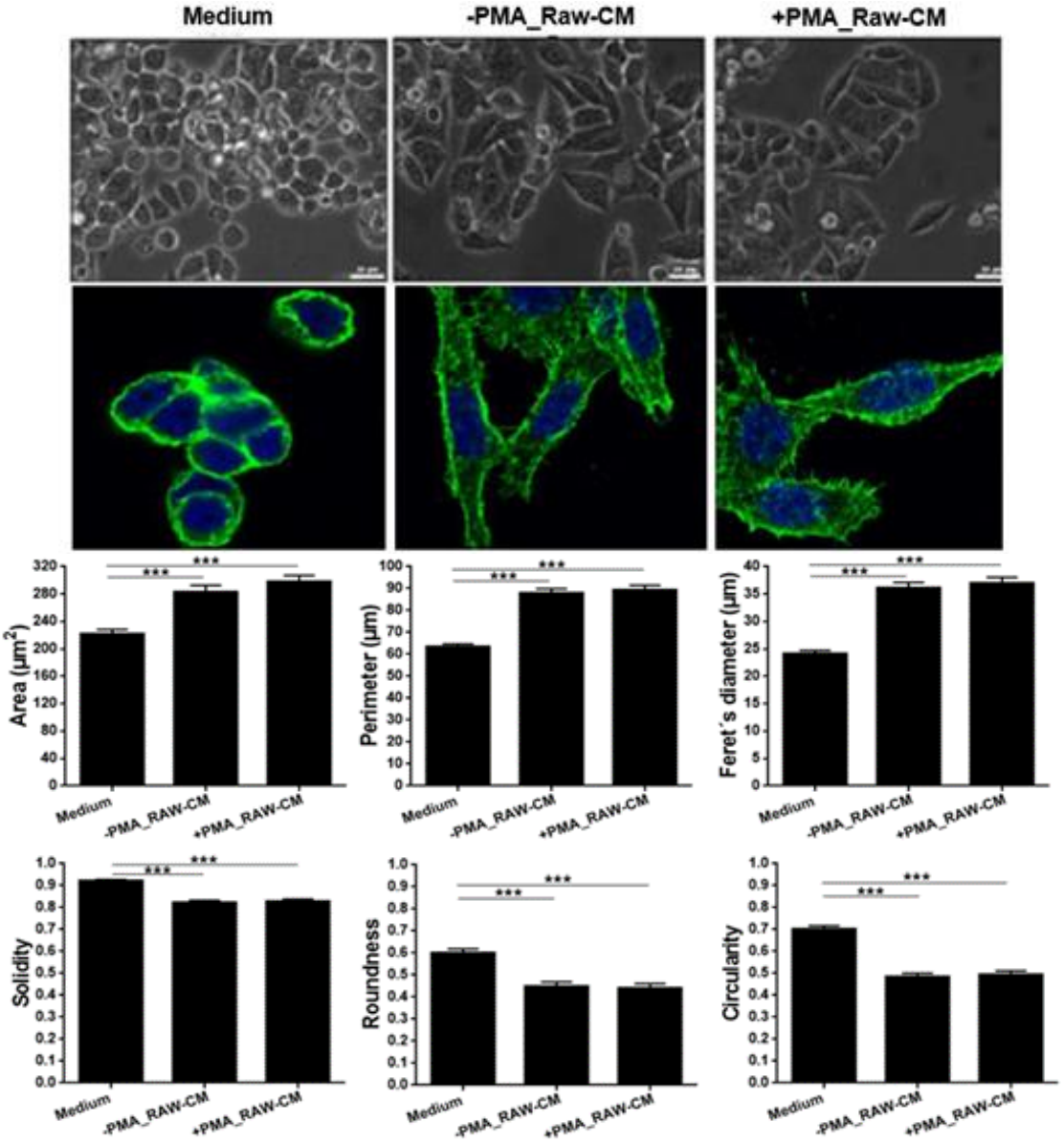

Figure 3.25: Macrophage-CM effect on GH3 cells morphology
Morphological evaluation of GH3 cells after treatment for 72h with serum-medium and RAW 264.7 macrophage-CM, either from untreated (-PMA_Raw-CM) or PMA-treated macrophages (+PMA_Raw-CM). Data are shown as mean±SEM for the 6 morphology parameters assessed by ImageJ. 75 cells were analysed per experiment, minimum of 3 experiments per condition. Scale bar 25µm. *,<0.05, **,<0.01, ***,<0.001 (one-way ANOVA with Bonferroni multiple comparison test). Alterations on actin fibers in GH3 cells after treatment with macrophage-CM for 72h in comparison to serum-medium are shown; representative images were taken on a confocal microscope at 63x; DAPI was used to stain the nuclei.

Migration is defined as any directed cell movement within the body, allowing cells to change position in a tissue, whereas invasion requires motility and ability to penetrate tissue barriers, i.e. to invade a cell needs degrade the surrounding ECM mainly by proteolysis and at same time migrate through its components[537]. GH3 cells showed increased invasion towards +PMA_Raw-CM and tended to invade more towards -PMA_Raw-CM (p=0.079) (Figure 3.26-A).

As invasion depends on cell ability to secrete proteases to degrade ECM, I hypothesised that macrophage-CM upregulates MMPs expression in GH3 cells allowing them to invade. MMP-9 is a key protease for type IV collagen (main component of matrigel[538], and of pituitary capsule and cavernous sinus wall[446-448]), as well as MMP-9 overexpression is associated with PA invasiveness[448]. Hence, *Mmp9* expression in GH3 cells was studied after treatment with macrophage-CM, and a significant *Mmp9* upregulation in GH3 cells exposed to macrophage-derived factors was observed (Figure 3.26-C).

In the transwell migration assay, GH3 cells demonstrated a non-significant trend for increased migration towards inactivated or PMA-activated macrophage-CM in comparison to complete medium (p=0.103 and p=0.119, respectively) (Figure 3.26-B).

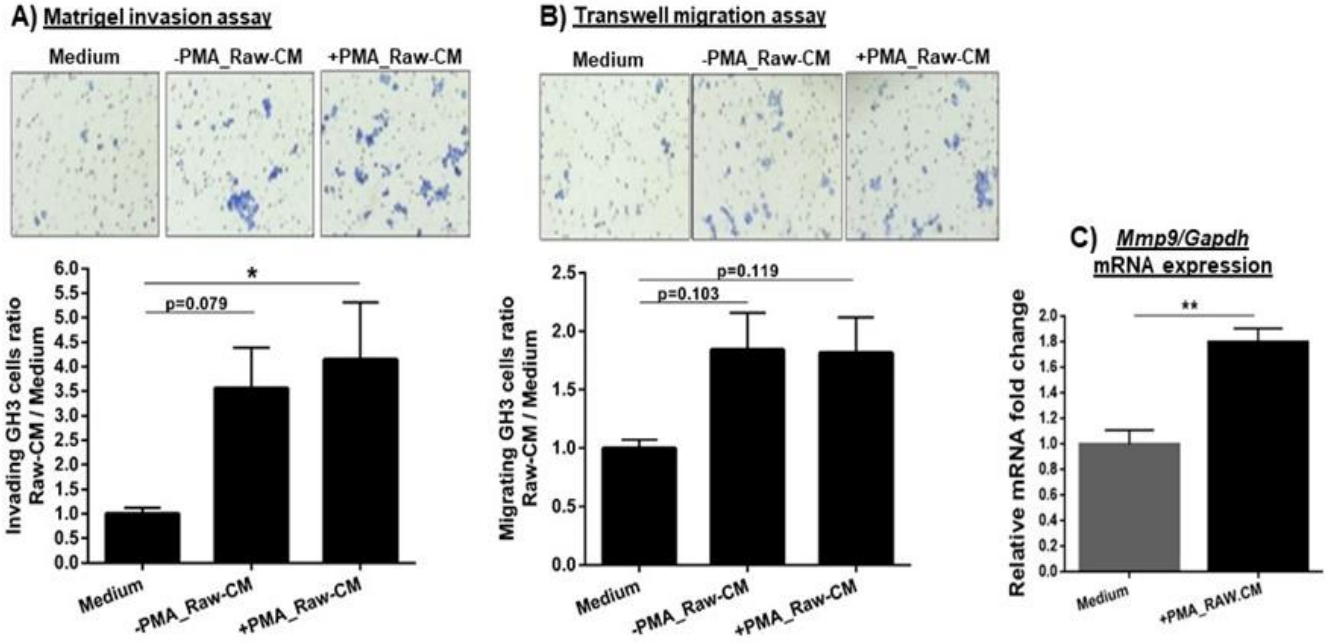

Figure 3.26: Macrophage-CM effect on GH3 cell invasion and migration
Matrigel-coated chamber invasion assays (B) and transwell migration assays (C) on GH3 cells towards serum-medium, -PMA_Raw-CM and +PMA_Raw-CM after 72h. Data are shown as mean±SEM for the ratio of invading/migrated GH3 cells towards -PMA_Raw-CM and +PMA_Raw-CM in relation to invading/ migrated GH3 cells in serum-medium. Invasion studies were repeated 4x in duplicate, and migration assays were repeated 3x in duplicate. *, <0.05, **, <0.01, ***, <0.001 (one-way ANOVA with Bonferroni multiple comparison test). C) *Mmp9* expression assessed by RT-qPCR in GH3 cells in medium or after treatment for 24h with +PMA_Raw-CM. Data are shown for *Mmp9* mRNA expression fold change relative to *Gapdh*, mean±SEM, as determined by ΔΔCT method. n=3. *, <0.05, **, <0.01, ***, <0.001 (Mann Whitney U test).

To further characterise the GH3 cells migration under macrophage-CM conditions, I performed a wound healing assay (Figure 3.27). After 24h there were no changes in the wound area closed, thus no significant GH3 cell migration was detected either in macrophage-CM but also in complete medium. Although after 24h wound healing assay does not differentiate properly migration vs cell proliferation/survival[537,539], the assay was run for up to 6 days due to poor GH3 cell migration at the 24h time-point. A small wound area was covered over this period, more prominently in complete medium than in macrophage-CM conditions, likely reflecting increased proliferation rather than cell motility as perceived by the cell density visible in the images (Figure 3.27). These results, as opposed to those obtained in the transwell migration assay, are not surprising as GH3 cells are unable to migrate properly on plain plastic surfaces (as shown in unpublished work from my group[540]). Wound healing assays may also poorly reflect migration and often have discordant results from those in transwell assays[539]. Moreover, migration and invasion are often uncoupled, with increased migration not constituting an inexorable consequence of EMT[539]. In fact, invasion rather than migration, is regarded as EMT hallmark[539], although cells undergoing EMT often show both features[467,537].

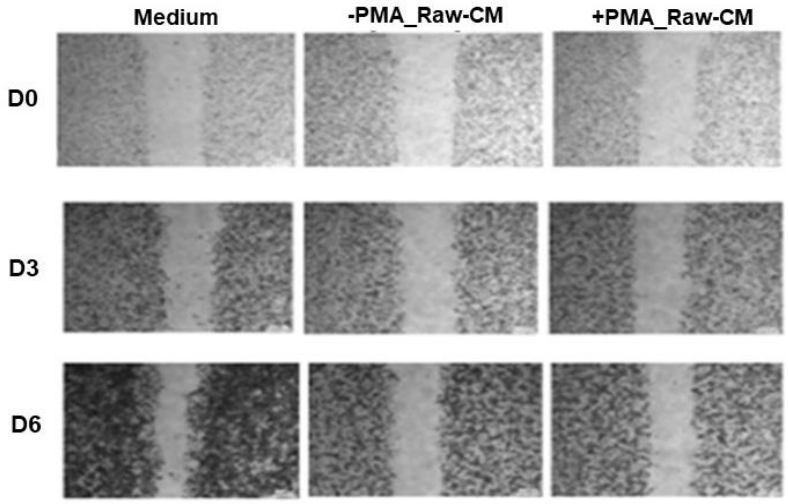

Figure 3.27: Macrophage-CM effect on GH3 cell migration assessed by wound healing assay
Wound healing assay (Ibidi culture-inserts chambers) performed on GH3 cells under complete medium, inactivated (-PMA_Raw-CM) or PMA-activated RAW 264.7 macrophage-CM (+PMA_Raw-CM), and assessed at different time-points. Representative of wound healing assay images are displayed at baseline, day 3 and day 6 showing the wound uncovered area.

The observed morphology changes and increased invasion/migration induced by macrophage-CM strongly suggest that macrophage-derived factors induce EMT in GH3 cells. I further studied the expression of classical markers of EMT (E-cadherin and ZEB1)[467] by immunocytochemistry in GH3 cells untreated vs treated with macrophage-CM. Macrophage-CM induced EMT activation in GH3 cells decreasing E-cadherin and increasing ZEB1 expression (Figure 3.28), two hallmarks of EMT activation[466].

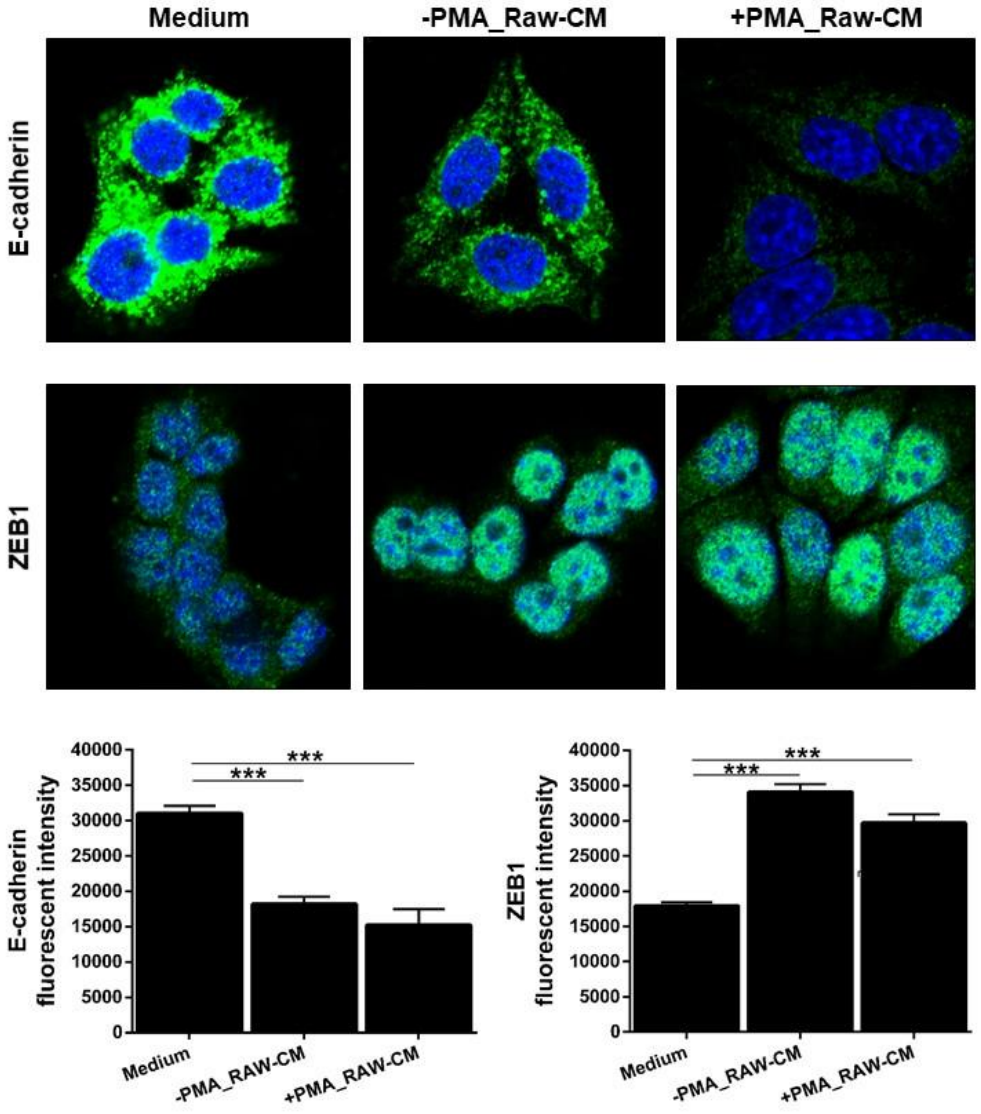

Figure 3.28: Macrophage-CM inducing EMT in GH3 cells assessed by immunocytochemistry
Alterations in E-cadherin and ZEB1 expression by GH3 cells after treatment for 72 hours with complete medium, -PMA_Raw-CM or +PMA_Raw-CM. Untreated GH3 cells show strong E-cadherin with membranous localisation but also in the cytoplasm as well as low nuclear ZEB1 expression, while macrophage-CM treated GH3 cells display decreased E-cadherin expression and increased nuclear ZEB1 expression. Pictures were taken on confocal microscope at 63x magnification. DAPI was used to stain the nuclei. E-cadherin and ZEB1 fluorescent intensities were quantified in 30 cells per treatment condition using Carl Zeiss Zen Blue Edition v2.3 software. Data are shown as fluorescent intensity, mean±SEM. n=30. *,<0.05, **,<0.01, ***,<0.001 (one-way ANOVA with Bonferroni multiple comparison test).

In order to validate the EMT immunocytochemistry data at the RNA level, I further conducted RT-qPCR assessing *Cdh1* and *Zeb1* expression in GH3 cells treated with macrophage-CM vs untreated. However, macrophage-CM did not show decreased expression of neither *Cdh1* nor upregulated *Zeb1* (p=0.150 and p=0.337, respectively) (Figure 3.29).

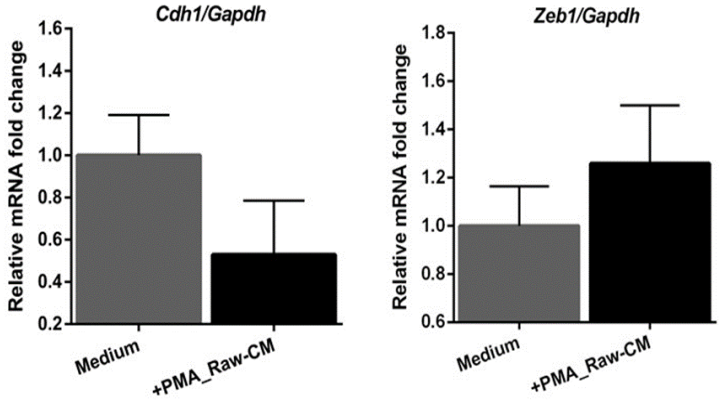

Figure 3.29: Macrophage-CM inducing EMT in GH3 cells assessed by RT-qPCR
E-cadherin (encoded by *Cdh1*) and *Zeb1* expression in GH3 cells untreated and treated with PMA-activated RAW 264.7 macrophage-CM (+PMA_Raw-CM) for 24h, determined by RT-qPCR. Data are shown as mRNA fold change expression relative to *Gapdh*, mean±SEM, determined by ΔΔCT method. n=6. *, <0.05, **, <0.01, ***, <0.001 (Mann-Whitney U test).

I also found that PMA-activated macrophage-CM is able to induce cytokine secretion changes in GH3 cells (both in GH3-*Aip*-KD and GH3-NT cells), increasing the release of CX3CL1, CCL3, CXCL1, CXCL10, IL-1β, IL-10, IL-13 and VEGF (Figure 3.30 and Appendix 5), peptides that play a role in different tumourigenic mechanisms[209,210,222,226].

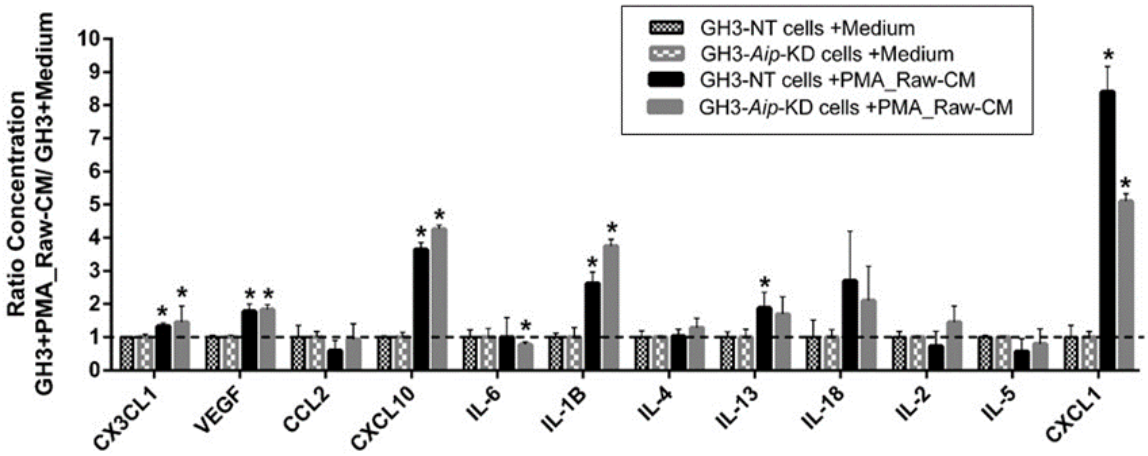

Figure 3.30: Macrophage-CM effect on GH3 cell cytokine secretome
GH3 cells secretome changes (in both NT and *Aip*-KD) induced by PMA-activated RAW 264.7 macrophage-CM after treatment for 24h. Data are shown for the most significantly changed cytokines after macrophage-CM treatment in comparison to the baseline evaluation and/or cytokines which were found at higher concentrations in the GH3 supernatants. Data are represented as ratio of cytokines after 24h of treatment with PMA (5nM)-activated RAW 264.7macrophage-CM, mean±SEM. Cytokine were assessed by the Millipore MILLIPLEX assay (rat cytokine/chemokine array 27-plex). n=3. *, <0.05, **, <0.01, ***, <0.001 (two-way ANOVA with Bonferroni multiple comparison test).

By RT-qPCR, I observed a tendency for overexpression of the different cytokines identified in the cytokine array after treating GH3 cells with macrophage-CM, although statistical significance was not reached (Figure 3.31), in part due to the considerable variability in the cytokine gene expression results from experiment to experiment.

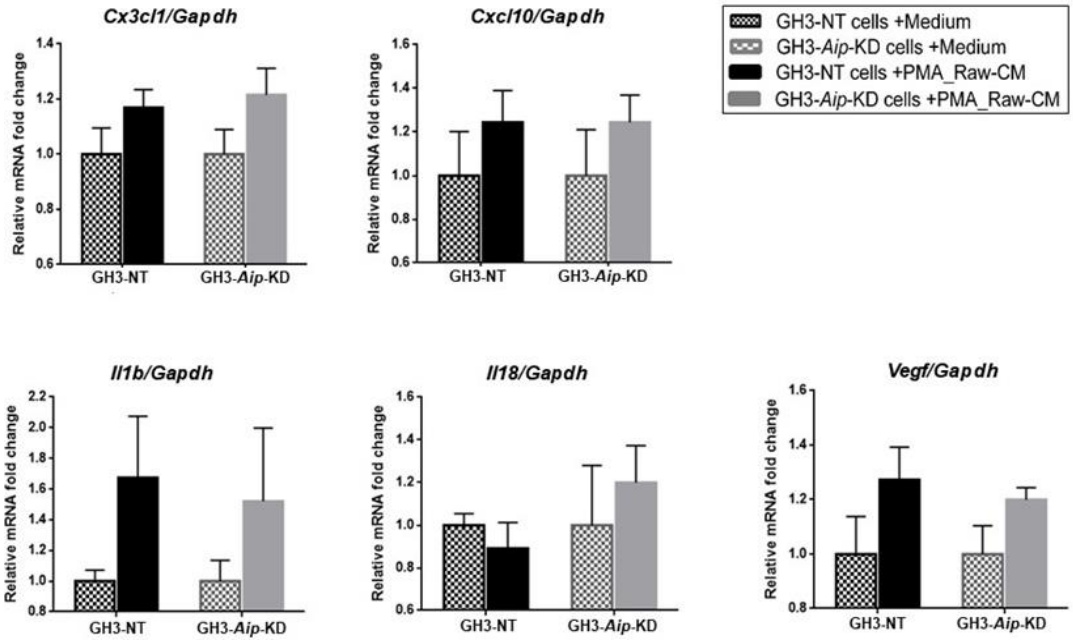

Figure 3.31: Macrophage-CM effect on GH3 cell cytokine expression
Cytokine expression changes from GH3-NT and GH3-*Aip*-KD cells treated with PMA-activated RAW 264.7 macrophage-CM for 24h, assessed by RT-qPCR. The cytokines analysed were the most significantly changed after macrophage-CM treatment in comparison to the baseline evaluation as identified by the cytokine array. Data are shown as mRNA fold change expression relative to *Gapdh*, mean±SEM, determined by ΔΔCT method. n=3. *, <0.05, **, <0.01, ***, <0.001 (two-way ANOVA with Bonferroni multiple comparison test).

Such lack of a correlation of RNA and protein data is typical in cytokine studies, as previously discussed, in part due to their physiological properties, strong bioactivity and secretion in low amounts. Cytokines are stored in cell vesicles and released upon stimulation, thus there is a mismatch with transcription, as well as they are subject of posttranslational changes. Moreover, cytokines can regulate their expression in a paracrine or autocrine manner, and thus the release of cytokines may signal its suppression via negative feedback loop of which one of the most well-studied mediator is SOCS (suppressors of cytokine signalling) able to suppress the transcription of the respective cytokine or others, as well as inhibit cytokine pathways such as JAK-STAT[534]. These findings suggest that macrophages can induce changes in the cytokine secretion from GH3 cells, which can potentially influence their own behaviour (via paracrine or autocrine loops) or other non-neoplastic surrounding cells in the TME. My data does not suggest a relevant role for AIP in terms of secretome changes following an external macrophage stimuli, although CXCL10 and IL-1β were secreted in higher amounts from macrophage-CM treated GH3-*Aip*-KD cells (not confirmed by RT-qPCR) but also secreted significantly less CXCL1 (Figure 3.30).

Circulating immune cells and inflammation-based scores in patients with PAs

Serum inflammatory-based scores NLR, PLR and LMR were calculated for each case of my cohort of 24 patients with PAs from pre-operative FBC data (Table 3.14). The relation between these ratios and clinico-pathological, biochemical, cytokine and immune infiltrates, was analysed.

Pre-operative haematological parameters	**Overall cohort PAs (n=24)** *Mean ± SD*	**NFPAs (n=16)** *Mean ± SD*	**Som (n=8)** *Mean ± SD*	***p* value** (NFPAs vs Som)
Red cell count (10^{12}/L) *[NR: M 4.4-5.8 / F 3.95-5.15]*	4.58 ± 0.46	4.63 ± 0.49	4.49 ± 0.40	0.482
Haemoglobin (g/L) *[NR: M 130-170 / F 115-155]*	132.46 ± 12.47	131.00 ± 12.01	135.38 ± 13.68	0.430
Haematocrit (%) *[NR: M 37-50 / F 33-45]*	40.24 ± 3.79	40.09 ± 3.99	40.54 ± 3.58	0.794
White cell count (10^9/L) *[NR: 3.0-10.0]*	7.08 ± 3.39	7.33 ± 3.81	6.58 ± 2.26	0.618
Neutrophil count (10^9/L) *[NR: 2.0-7.5]*	3.73 ± 1.51	3.87 ± 1.48	3.43 ± 1.63	0.512
Lymphocyte count (10^9/L) *[NR: 1.2-3.65]*	2.71 ± 2.25	2.86 ± 2.71	2.42 ± 0.86	0.660
Monocyte count (10^9/L) *[NR: 0.2-1.0]*	0.44 ± 0.13	0.43 ± 0.10	0.48 ± 0.19	0.413
Eosinophil count (10^9/L) *[NR: 0.0-0.4]*	0.17 ± 0.11	0.15 ± 0.11	0.23 ± 0.10	0.079
Basophil count (10^9/L) *[NR: 0.0-0.1]*	0.03 ± 0.02	0.02 ± 0.01	0.03 ± 0.02	0.233
Platelet count (10^9/L) *[NR: 150-400]*	234.96 ± 62.18	229.63 ± 59.92	245.63 ± 69.40	0.564
Pre-operative serum inflammation-based scores	**Overall cohort PAs (n=24)** *Mean ± SD*	**NFPAs (n=16)** *Mean ± SD*	**Som (n=8)** *Mean ± SD*	***p* value** (NFPAs vs Som)
Neutrophil-to-lymphocyte ratio (NLR)	1.63 ± 0.76	1.70 ± 0.76	1.51 ± 0.78	0.572
Lymphocyte-to-monocyte ratio (LMR)	6.53 ± 5.58	6.95 ± 1.67	5.68 ± 0.81	0.603
Platelet-to-lymphocyte ratio (PLR)	108.48 ± 45.03	104.99 ± 39.91	115.46 ± 56.27	0.609

Table 3.14: Pre-operative haematological parameters and scores of the 24 patients with PAs
Data are shown as mean±standard deviation (SD) for pre-operative haematological parameters and serum inflammation-based scores. Mann Whitney U test was used to calculate *p* value for the comparison NFPAs vs somatotrophinomas (NFPA vs Som). F, females; M, males; NFPA, non-functioning pituitary adenoma; NR, normal range; Som, somatotrophinoma.

Circulating immune cells and inflammation-based scores and clinical features

There were no significant associations between cavernous sinus invasion or a high Ki-67 (≥3%) in PAs and the pre-operative scores NLR, LMR or PLR, neither with the circulating immune cell counts (Table 3.15). However, there was a trend for patients with PAs invading cavernous sinus to have lower neutrophil counts than in patients with non-invasive PAs (p=0.06).

Pre-operative haematological parameters and ratios	Ki-67			Cavernous sinus invasion		
	<3% (n=19)	≥3% (n=5)	*p* value	No (n=14)	Yes (n=10)	*p* value
Red cell count (10^{12}/L)	4.56 ± 0.11	4.64 ± 0.19	0.757	4.60 ± 0.15	4.55 ± 0.10	0.765
White cell count (10^9/L)	7.26 ± 0.83	6.40 ± 0.96	0.622	7.90 ± 1.09	5.94 ± 0.43	0.161
Neutrophil count (10^9/L)	3.80 ± 0.34	3.45 ± 0.80	0.662	4.21 ± 0.44	3.05 ± 0.31	0.060
Lymphocyte count (10^9/L)	2.80 ± 2.52	2.35 ± 0.61	0.699	3.04 ± 0.77	2.26 ± 0.23	0.415
Monocyte count (10^9/L)	0.45 ± 0.14	0.40 ± 0.05	0.446	0.45 ± 0.11	0.43 ± 0.05	0.771
Eosinophil count (10^9/L)	0.18 ± 0.03	0.16 ± 0.05	0.814	0.17 ± 0.03	0.18 ± 0.03	0.897
Basophil count (10^9/L)	0.03 ± 0.00	0.03 ± 0.01	0.436	0.03 ± 0.01	0.03 ± 0.00	0.812
Platelet count (10^9/L)	227.79 ± 13.70	262.20 ± 31.64	0.281	219.07 ± 16.69	257.20 ± 18.19	0.142
NLR	1.65 ± 0.18	1.48 ± 0.30	0.623	1.74 ± 0.20	1.49 ± 0.24	0.434
LMR	6.69 ± 1.44	5.93 ± 0.43	0.793	7.05 ± 1.90	5.81 ± 0.74	0.603
PLR	106.09 ± 10.80	117.57 ± 17.64	0.623	97.24 ± 11.18	124.21 ± 14.77	0.152

Table 3.15: Haematological parameters/scores and Ki-67/cavernous sinus invasion
Data are shown as mean±SEM for the different haematological parameters and inflammation-based scores NLR, LMR and PLR. *p* values were non-significant for the comparative analysis between less vs more proliferative PAs, and for PAs without vs with cavernous sinus invasion (Mann-Whitney U test).

There were also no significant associations between pre-operative serum inflammation-based scores or circulating immune cells and PA grades as per Trouillas classification[43] (Table 3.16).

Pre-operative haematological parameters and ratios	Grade 1a (non-invasive) n=11	Grade 1b (non-invasive and proliferative) n= 3	Grade 2a (invasive) n=8	Grade 2b (invasive and proliferative) n=2	*p* value
Red cell count (10^{12}/L)	4.60 ± 0.18	4.63 ± 0.28	4.52 ± 0.10	4.66 ± 0.34	0.974
White cell count (10^9/L)	8.08 ± 1.36	7.21 ± 1.48	6.12 ± 0.51	5.20 ± 0.58	0.542
Neutrophil count (10^9/L)	4.17 ± 0.51	4.36 ± 1.06	3.29 ± 0.34	2.10 ± 0.09	0.215
Lymphocyte count (10^9/L)	3.24 ± 0.98	2.28 ± 0.36	2.21 ± 0.27	2.46 ± 0.58	0.790
Monocyte count (10^9/L)	0.47 ± 0.03	0.39 ± 0.08	0.44 ± 0.07	0.43 ± 0.02	0.829
Eosinophil count (10^9/L)	0.18 ± 0.04	0.14 ± 0.07	0.17 ± 0.03	0.20 ± 0.09	0.930
Basophil count (10^9/L)	0.03 ± 0.01	0.04 ± 0.01	0.03 ± 0.01	0.02 ± 0.01	0.313
Platelet count (10^9/L)	206.91 ± 14.71	263.67 ± 56.69	256.50 ± 22.77	260.00 ± 19.00	0.252
NLR	1.70 ± 0.25	1.87 ± 0.32	1.64 ± 0.28	0.90 ± 0.17	0.539
LMR	7.32 ± 2.44	6.06 ± 0.37	5.83 ± 0.91	5.74 ± 1.15	0.947
PLR	90.35 ± 11.65	122.53 ± 29.96	127.73 ± 18.17	110.14 ± 18.06	0.331

Table 3.16: Haematological parameters/scores and Trouillas grade classification
Data are shown as mean±SEM for the different haematological parameters and the inflammation-based scores NLR, LMR and PLR. *p* values were non-significant for the comparative analysis between the different PA grades as per Trouillas grade classification[43] (one-way ANOVA test).

Similarly, there were no significant correlations between pre-operative serum inflammation-based scores or circulating immune cells and the presence of headache, visual impairment or hypopituitarism at diagnosis (Table 3.17).

Pre-operative haematological parameters	Headache at diagnosis			Visual impairment at diagnosis			Hypopituitarism at diagnosis		
	No (n=16)	Yes (n=8)	*p*	No (n=11)	Yes (n=13)	*p*	No (n=13)	Yes (n=11)	*p*
Red cell count (10^{12}/L)	4.50 ± 0.10	4.75 ± 0.18	0.206	4.55 ± 0.11	4.61 ± 0.15	0.741	4.53 ± 0.12	4.64 ± 0.15	0.588
White cell count (10^9/L)	7.16 ± 0.98	6.92 ± 0.70	0.874	6.70 ± 0.64	7.40 ± 1.15	0.617	7.80 ± 1.20	6.23 ± 0.39	0.262
Neutrophil count (10^9/L)	3.55 ± 0.38	4.07 ± 0.53	0.441	3.70 ± 0.50	3.75 ± 0.40	0.940	4.07 ± 0.51	3.31 ± 0.27	0.225
Lymphocyte count (10^9/L)	2.94 ± 0.68	2.26 ± 0.28	0.498	2.32 ± 0.23	3.04 ± 0.83	0.442	3.06 ± 0.84	2.30 ± 0.19	0.424
Monocyte count (10^9/L)	0.46 ± 0.04	0.41 ± 0.04	0.378	0.46 ± 0.05	0.43 ± 0.03	0.681	0.46 ± 0.04	0.43 ± 0.04	0.633
Eosinophil count (10^9/L)	0.18 ± 0.03	0.16 ± 0.03	0.588	0.20 ± 0.03	0.15 ± 0.03	0.352	0.18 ± 0.03	0.16 ± 0.03	0.641
Basophil count (10^9/L)	0.03 ± 0.00	0.03 ± 0.01	0.362	0.03 ± 0.01	0.02 ± 0.00	0.274	0.03 ± 0.01	0.03 ± 0.00	0.570
Platelet count (10^9/L)	218.25 ± 10.62	268.38 ± 29.42	0.144	242.09 ± 19.22	228.92 ± 17.40	0.616	239.08 ± 21.74	230.09 ± 11.57	0.733
NLR	1.49 ± 0.18	1.92 ± 0.28	0.193	1.70 ± 0.25	1.58 ± 0.20	0.717	1.73 ± 0.25	1.53 ± 0.17	0.532
LMR	6.94 ± 1.69	5.72 ± 0.61	0.627	5.64 ± 0.63	7.28 ± 2.05	0.485	7.32 ± 2.07	5.60 ± 0.53	0.463
PLR	98.50 ± 10.40	128.45 ± 17.76	0.127	116.86 ± 15.45	101.39 ± 11.03	0.414	110.14 ± 15.28	106.52 ± 9.60	0.850

Table 3.17: Haematological parameters and headache, visual damage or hypopituitarism at diagnosis
Data are shown as mean±SEM for the different haematological parameters and inflammation-based scores NLR, LMR and PLR. *p* values were non-significant for the different comparative analysis (Mann-Whitney U test).

In general, there were no significant correlations between pre-operative serum inflammation-based scores or circulating immune cells and age at diagnosis, number of pituitary deficiencies at diagnosis or at last follow-up, and number of total treatments that patients have received (Table 3.18). However, significant correlations were noted for the basophil count which positively correlated with the number of pituitary deficiencies at diagnosis (p=0.047) and number of treatments received (p=0.036), as well as for neutrophil and red cell counts which correlated positively with age at diagnosis (p=0.043) and number of pituitary deficiencies at last follow-up (p=0.038), respectively (Table 3.18).

		Age at diagnosis (yrs)	n of pituitary deficiencies at diagnosis	n of total treatments	n of pituitary deficiencies at last follow-up
Red cell count	Pearson correlation *r*	-0.005	0.129	0.362	0.427
	p value	0.983	0.559	0.082	**0.038**
	N	24	23	24	24
White cell count	Pearson correlation *r*	0.356	-0.101	-0.045	-0.080
	p value	0.088	0.647	0.836	0.709
	N	24	23	24	24
Neutrophils count	Pearson correlation *r*	0.416	-0.152	0.072	0.067
	p value	**0.043**	0.488	0.738	0.756
	N	24	23	24	24
Lymphocytes count	Pearson correlation *r*	0.228	-0.063	-0.116	-0.161
	p value	0.284	0.774	0.588	0.453
	N	24	23	24	24
Monocytes count	Pearson correlation *r*	0.341	0.104	-0.032	0.115
	p value	0.103	0.637	0.882	0.594
	N	24	23	24	24
Eosinophils count	Pearson correlation *r*	0.060	0.052	0.006	-0.254
	p value	0.782	0.815	0.979	0.231
	N	24	23	24	24
Basophils count	Pearson correlation *r*	-0.324	0.418	0.430	0.280
	p value	0.123	**0.047**	**0.036**	0.184
	N	24	23	24	24
Platelet count	Pearson correlation *r*	-0.046	0.010	-0.055	-0.124
	p value	0.832	0.962	0.800	0.565
	N	24	23	24	24
NLR	Pearson correlation *r*	0.267	-0.256	0.087	0.120
	p value	0.207	0.239	0.686	0.577
	N	24	23	24	24
LMR	Pearson correlation *r*	0.162	-0.117	-0.138	-0.241
	p value	0.449	0.596	0.521	0.256
	N	24	23	24	24
PLR	Pearson correlation *r*	-0.126	-0.232	-0.020	-0.082
	p value	0.556	0.286	0.924	0.705
	N	24	23	24	24

Table 3.18: Haematological parameters and age at diagnosis, number of pituitary deficiencies and treatments
p values were determined by the Pearson correlation coefficient *r*.

Circulating immune cells and serum inflammation-based scores and pituitary function

In general, there were no correlations between pre-operative serum inflammation-based scores or circulating immune cells and pituitary hormone levels in NFPAs, or in GH/IGF-1 levels in somatotrophinomas (Appendix 6). However, within somatotrophinomas correlations were noted between FT4 and neutrophil (r=0.790, p=0.035), monocyte count (r=0.927; p=0.003) and NLR (r=0.865, p=0.012); LH and FSH correlated with NLR (r=0.907, p=0.005 and r=0.808, p=0.028, respectively), and LH and monocyte count also correlated (r=0.779, p=0.39) (Appendix 6).

Circulating immune cells and serum inflammation-based scores and PA cytokine secretome

In general, there were no significant correlations between pre-operative serum inflammation-based scores or circulating immune cells and the PA cytokine secretome assessed in the primary culture supernatants, except for the significant positive correlations between PA-derived FGF-2 and PLR (p=0.005), and between NLR and PDGF-AA (p=0.043) and IL-6 (p=0.037) (Figure 3.32 and Appendix 6).

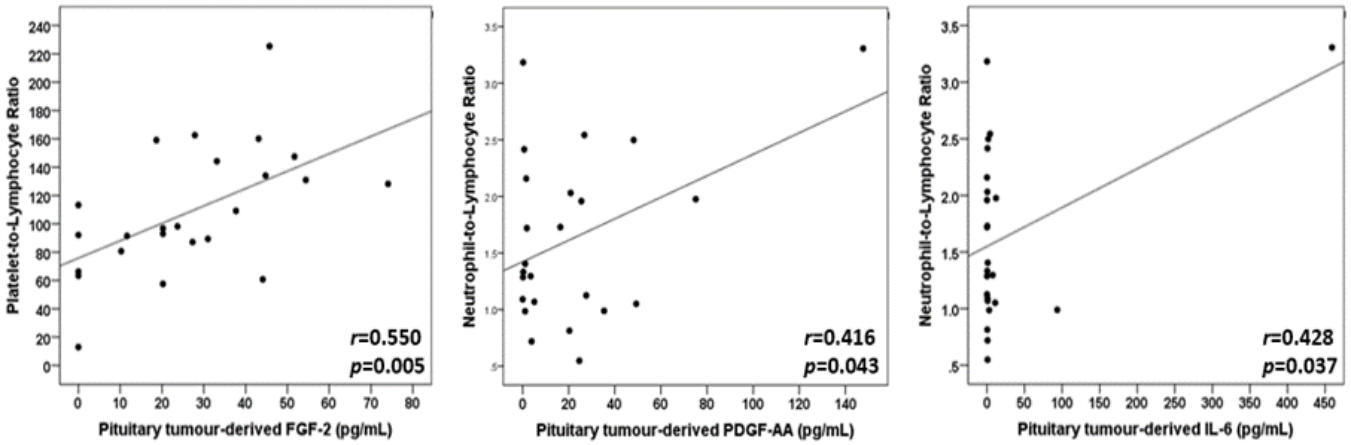

Figure 3.32: Correlation between serum inflammation-based scores and PA-derived cytokines
p values were determined by the Pearson correlation coefficient *r*.

When pre-operative serum inflammation-based scores or circulating immune cells and the PA cytokine secretome were analysed per histiotypes, additional significant correlations among NFPAs were noted: CCL22 with both NLR (r=0.670, p=0.005) and PLR (r=0.500, p=0.048); FGF-2 with both NLR (r=0.693, p=0.003) and PLR (r=0.712, p=0.002); IL-6 with NLR (r=0.509, p=0.044); PDGF-AA with NLR (r=0.560, p=0.024); VEGF-A with platelet count (r=501, p=0.048) (Appendix 6).

Among somatotrophinoma subgroup, PA-derived levels of CXLC1 negatively correlated with neutrophil (r=-0.754, p=0.031) and monocyte count (r=-0.733, p=0.039), while PA-derived CCL2 levels significantly correlated with the monocyte count (r=-0.723, p=0.043) (Appendix 6).

These data suggest that some of the PA-derived cytokines may reach the circulation and eventually influence the haematopoiesis and confer some degree of systemic inflammation (i.e. increased NLR and PLR), with FGF-2 and PDGF-AA emerging as possibly the most relevant ones. However, in the whole study cohort, most of the correlations between PA-derived cytokines and the haematological parameters here analysed were indeed non-significant, suggesting that the effects of PA-derived cytokines on the bone marrow may not be that relevant biologically.

Discussion

In this study, using a comprehensively phenotyped cohort of human PAs with cytokine array data from primary culture, immunohistochemical immune infiltrates and clinicopathological data, PAs were found to be an active source of chemokines which facilitate macrophage, neutrophil and lymphocyte recruitment into the TME. Infiltrating immune cells once in the TME of PAs may determine increased PA aggressiveness, particularly tumour proliferation. My human data are strengthened by my *in vitro* functional data providing mechanistic insights into the crosstalk pituitary tumour cells-macrophages. My *in vitro* data confirmed that pituitary tumour-derived factors promote macrophage chemotaxis, while macrophage factors influence tumour cell behaviour leading to morphology changes, increased invasion, cytokine secretome changes and EMT activation. Thus, the cytokine network in the TME of PAs, derived from both tumour and immune cells, as well as PA-associated fibroblasts (Chapter 4), may play a role in the modulation of the TME and aggressiveness of PAs (Figure 3.33).

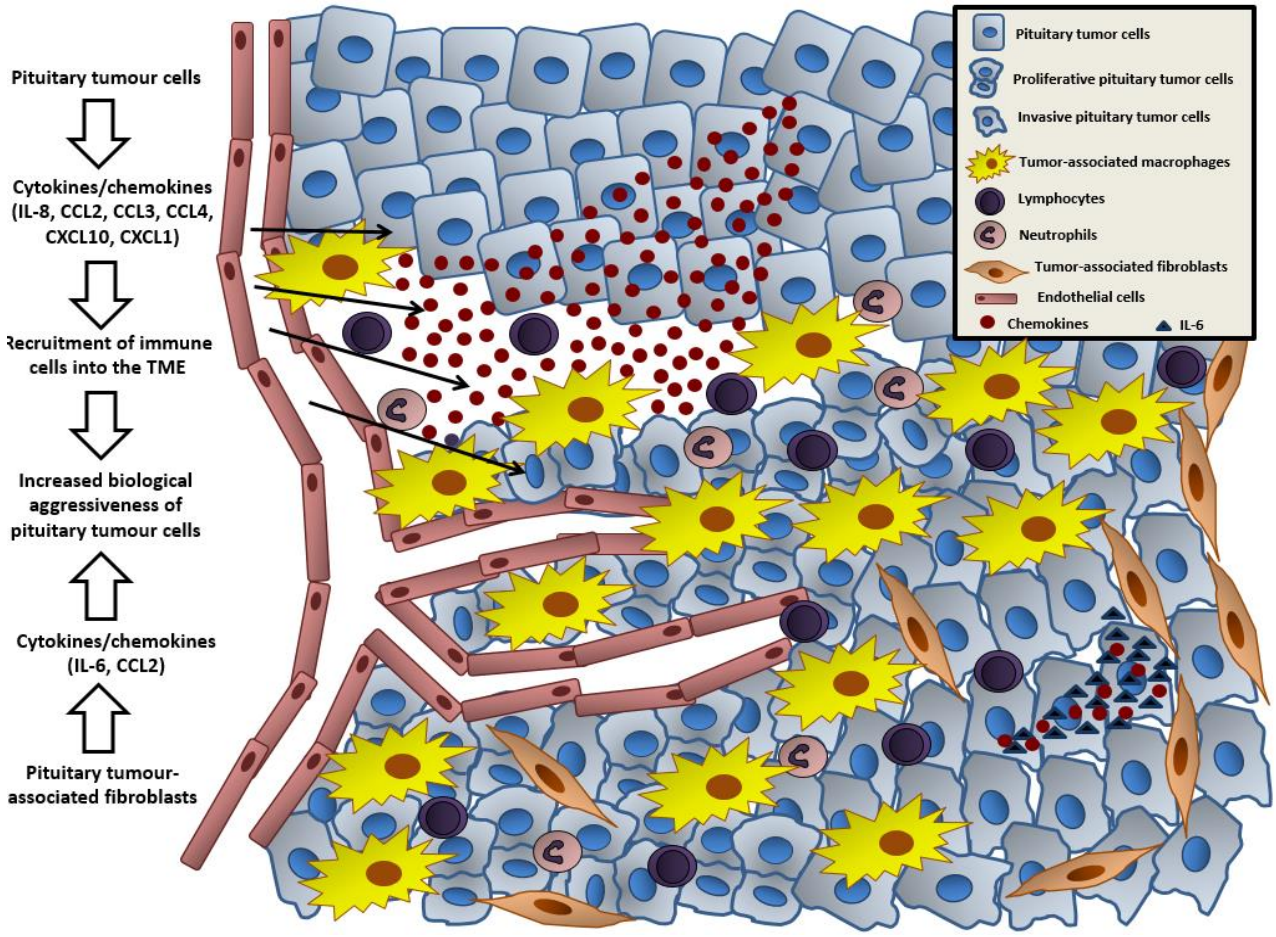

Figure 3.33: The tumour microenvironment of PAs
Pituitary tumour cells release different chemokines directly into the TME promoting the recruitment of immune cells, including macrophages, lymphocytes and neutrophils. PA-infiltrating immune cells change the behaviour of tumour cells, namely increasing their proliferative capacity. PA-associated fibroblasts also secrete cytokines, including IL-6 and other chemokines, which lead to increased invasion of tumour cells.

Pituitary tumour cells are an active source of chemokines which lead to immune cell recruitment into the TME of PAs

IL-8, CCL2, CCL3 and CCL4 were highly secreted by the great majority of PAs. A similar cytokine secretome analysis has not previously been performed in PAs, but interestingly cytokine array data from 48 human craniopharyngiomas identified CCL2 and IL-8 as the most secreted cytokines in plasma, primary culture supernatants, cell and tissue lysates[541]. There are no previous data on CCL2, CCL3 or CCL4 in PAs, but these chemokines are involved in tumour growth and invasion in other tumours[209,226], as well as in immune cell chemotaxis in cancer[209,226,333,517,529,530,542,543]. I found no association between CCL2, CCL3 or CCL4 levels and PA aggressiveness, but PAs with a high content of macrophages, CD8+ T cells and neutrophils secreted higher levels of these chemokines, supporting their role in recruiting such cells.

PAs with more macrophages were associated with higher levels of IL-8, and there was also a non-significant trend for PAs with increased neutrophil amounts to release more IL-8. IL-8 is a chemokine that recruits immune cells, classically neutrophils but also macrophages, as well as influencing several oncogenic pathways[236,528]. IL-8 mRNA was previously found in PAs, although different methods provide a wide range of expression levels[232-234]. I also identified other chemokines potentially relevant in PAs, namely CXCL10, CCL22, CXCL1 and CX3CL1, all well studied in other cancers[209,226], but not in PAs. My data suggest CXCL1 and CXCL10 as potential modulators of PA-infiltrating neutrophils and macrophages. CXCL1 and its receptor CXCR2 were previously identified in human PAs[279], but there are no data regarding CXCL10, CCL22 and CX3CL1. Together, these findings suggest a link between endocrine cells and chemokines reflecting their possible involvement in tumourigenesis and modulation of immune infiltrates, constituting a promising target for drugs affecting the PA cytokine network, as already explored for other cancers[210,226,544].

NFPAs secreted cytokines more often and in higher amounts than somatotrophinomas. These secretome differences are unlikely to be explained by pre-operative exposure to SSAs, as untreated or pre-treated somatotrophinoma patients had similar cytokine secretome. This phenomenon has not been reported before; however, in a study analysing IL-6 release from 100 primary cultures of human PAs, IL-6 levels in NFPAs reached higher absolute levels than in somatotrophinomas, with six NFPAs releasing >500U/L while only a single somatotrophinoma had IL-6 levels >500U/L[237]. In another study, CXCL12 expression was detected in more NFPAs (78%) than somatotrophinomas (63%)[268]. Despite these cytokine secretome differences between NFPAs and somatotrophinomas, there were no major differences regarding infiltrating immune cells or ratios among these. However, somatotrophinomas had significantly fewer neutrophils than NFPAs

which could be due to this prominently reduced chemokine release, particularly IL-8, but other aspects may be involved such as impaired neutrophil chemotaxis[545]; this difference is thought not to be attributable to haematopoietic differences among NFPAs and somatotrophinomas, as neutrophil counts did not differ between NFPA and somatotrophinoma patients.

Immune infiltrates in PAs differ from NP and potentially contribute to pituitary tumourigenesis

Macrophages are present in NP[344,345] and PAs[346,347,513]. My immunohistochemical and xCELL data showed that PAs contained 3-4x more macrophages than NPs, and they are the predominant immune cell type in PAs. I found no association between PA-infiltrating macrophages and cavernous sinus invasion, and correlation with high Ki-67 was borderline. Lu *et al.* reported that macrophage content was correlated with size and invasiveness[347]. *AIP*mut somatotrophinomas often more aggressive[19,167], have more macrophages than sporadic somatotrophinomas or NPs[513].

Next, I studied the phenotype of infiltrating macrophages in human PAs and NPs using the macrophage markers CD163 (M2) and HLA-DR (M1)[229,546,547]. I noted a 3-fold increased M2:M1 macrophage ratio in PAs compared to NPs, in line with my xCell data (M2-macrophage score was >4x higher in PAs). The predominance of M2-macrophages in PAs can be due, at least in part, to higher concentrations of PA-derived M2-polarising cytokines, namely IL-4, which was 5x higher than IFNγ, the main M1-polarising cytokine[229,339]. M1- and M2 macrophages have been described in normal rat pituitary and in DES-induced prolactinomas[346], with prolactinomas having remarkably more M2-macrophages than NP. M2-macrophage number increased during the first weeks of DES treatment, even before tumour formation, suggesting a role for M2-macrophages in initiating tumourigenesis. During DES treatment capillaries became more tortuous with increased calibre and developed haemorrhage areas suggesting a possible role for M2-macrophages in angiogenesis and vasculature modulation in PAs[346], in agreement with the observed correlations between M2:M1 ratio and PA microvessel density and area. These findings support a role for M2-macrophages in PA angiogenesis, as in other cancers[229,297,332,339,417,548].

Infiltrating immune cells may influence aggressiveness and tumourigenic mechanisms in PAs

I found that a low CD8:CD4 ratio is associated with a higher Ki-67, suggesting that relatively low CD8+ to high CD4+ T cells, rather than absolute CD8+ and CD4+ T cell amounts *per se*, represent a relative imbalance potentially affecting tumour proliferation. This has been described in gliomas, where the number of tumour-infiltrating CD8+ and CD4+ cells alone had no prognostic value, while

low CD8:CD4 ratio was an independent predictor of poor progression-free and survival[549]. Poor clinical outcome and persistence/recurrence was described in PAs with TILs[371]. Another study found no association between CD8+ T cell count and Ki-67, tumour size, gender or age[374]. I observed more CD4+ and fewer CD8+ cells, with a significant 2-fold decrease in CD8:CD4 ratio in comparison to NPs, supporting the known anti-tumour role of cytotoxic CD8+ T cells and the pro-tumour effect of CD4+ T cells, possibly Th2[516,532,549]. Indeed, downregulation of Th1 pathway-related genes was observed in aggressive PAs[550]. M2-macrophages support CD4+ Th2 cells and prevent the expression of cytokines required for Th1 cells[347,551], which may further contribute to a Th2 phenotype in PAs. *Vice versa*, Th2 cytokines in the TME sustain M2-macrophages[229,333,551] possibly contributing to the predominant M2-macrophage phenotype I observed in PAs.

Although I found generally low amounts of FOXP3+ T cells in PAs, as previously shown[370], PAs with a higher Ki-67 had significantly more FOXP3+ T cells. Moreover, a significant 3-fold reduced CD8:FOXP3 ratio was noted in PAs with a higher Ki-67, revealing that a deleterious imbalance between CD8+ and FOXP3+ T cells may increase proliferation and thereby aggressiveness, as described for other cancers[552,553]. In this study, all PAs with a "deleterious immune phenotype" (i.e. high content of macrophages, T helper lymphocytes, FOXP3+ T regulatory and B cells) had a Ki-67≥3%, which together with results regarding the ratios CD68:FOXP3, CD8:CD4 and CD8:FOXP3, highlights that the pooled inflammatory context integrating different immune subpopulations within the TME of PAs is more relevant for the biological behaviour and aggressiveness than each distinct PA-infiltrating immune cell *per se*.

There is some variability in the PA-infiltrating immune cells reported in literature[347,366,369,371,372,374]. This inconsistency can reflect the variable level of immunosurveillance from tumour to tumour[516,554,555], patient selection[347], or can be due to a lack of standardisation method reporting immune infiltrates[347,371,374], such as reporting hotspots or taking random HPFs, or reporting interstitial areas or perivascular inflammatory cells[347], use of different cell markers and antibodies to detect the same immune cell type[347,369,371], or assessment of full slides versus tissue microarrays, which can greatly influence the results. Despite these issues, the current immunohistochemical data are in line with the xCELL data, and with previous data[347,371,372,374].

The functional crosstalk between pituitary tumour cells and macrophages

My *in vitro* cell line experiments focused on macrophages as these are the predominant immune cell type in PAs, and I selected RAW 264.7 macrophages for the reasons previously stated. My *in vitro* observations, consistent with previous findings in a different cell model[513], show a

remarkable macrophage chemoattractant effect induced by GH3 cell-derived factors, an effect explained not only by the chemokine gradient but also by their ability to upregulate chemokine receptor expression. These findings are in line with the human data (association between PA-infiltrating macrophages and PA-derived chemokine levels), suggesting that pituitary tumour cells are able to attract immune cells, namely macrophages.

On the other hand, I confirmed that macrophage-derived factors induced numerous effects on GH3 cells, including changes in morphology, invasion, EMT activation and cytokine secretome alterations, suggesting that immune cell-derived factors can influence pituitary tumour mechanisms leading to increased aggressiveness of PAs, as seen in my cohort of human PAs (Figure 3.16) and in another *in vitro* model using GH3 cells and bone-derived rat macrophages[513], as well as in other cancers[209,210,222,226].

Circulating immune cells and inflammation-based scores do not predict aggressiveness of PAs

The serum inflammation-based scores, namely NLR, LMR and PLR, have been used in cancer as predictors of outcomes and prognosis[521-526], including in endocrine-related neoplasms such as thyroid cancer[556-558], neuroendocrine tumours[559-562] and craniopharyngiomas[563,564]. However, there are no data in PAs. Identifying any of these scores as predictors of aggressiveness and/or prognosis would provide significant advances in risk stratification and potentially in the management algorithms for patients with PAs.

Neutrophilia and thrombocytopenia in aggressive cancers occur due to myeloid-derived factors from cancer secondary to inflammation, tissue destruction or cytokine production, while the lymphopenia signify impaired innate cell immunity against malignancy. These cancer-related haematopoietic effects, typical in highly malignant/metastatic neoplasms, result in elevated NLR and PLR and decreased LMR which translate excessive but ineffective immune response to the tumour or imbalanced inflammatory state which can facilitate its growth[522,556]. In fact, the mean NLR and PLR scores in my cohort of PAs were relatively lower (1.6±0.8 and 108.5±45.0, respectively) than those reported for other aggressive malignant neoplasms[41,45,46], with NLR>5.0 and PLR>300 commonly indicating poor prognosis[522,565-569]. On the other hand, the mean LMR in PAs is relatively high (6.5±1.6), in keeping with less lymphopenia, low systemic inflammation and indolent biological disease in patients with PAs, in comparison to other malignant neoplasms where LMR<2.38-4.01 indicate aggressive disease and poor outcomes [525,526,570]. These finding are not surprising taking into account that PAs are benign, lacking major biological aggressiveness and metastatic potential. This is translated into little or no systemic inflammation in patients with PAs

driven by pituitary tumour-derived factors (if) released in low amounts into the circulation. In contrast, the systemic inflammation can be prominent in other highly malignant neoplasms, such as in breast, gastric, pancreas, colorectal cancer or melanoma, hence these inflammation-based ratios are valuable[41,45,46]. Nevertheless, some PA-derived cytokines may modulate the circulating immune cells and/or systemic inflammation in patients with PAs as suggested by the correlations between PA-derived FGF-2 and PDGF-AA and NLR or PLR ratios, or by the significant correlation between serum monocyte count and PA-derived levels of CCL22, and between neutrophil count and PA-derived CXLC1 among somatotrophinoma patients.

Overall, no association was seen between the inflammation-based scores NLR, LMR and PLR (nor white cell counts) and clinical (headache, visual damage or hypopituitarism) or aggressiveness (cavernous sinus invasion or high Ki-67) features in my cohort of patients with PAs suggesting that these tools may not be useful in predicting aggressiveness of PAs. There were also no correlations between pre-operative serum NLR, LMR and PLR or circulating immune cells and pituitary hormone levels in NFPAs or GH/IGF-1 levels in somatotrophinomas, suggesting that PA-related hormonal status may not be relevant in determining systemic inflammation in patients with PAs.

Limitations of this study

Limitations of my study include the fact that I have a relatively small cohort of cases, and thus these observations need to be validated in larger series, preferably including all different PA types. The small sample size is a particular issue for the assessment of inflammation-based scores in predicting aggressiveness of PAs, as provides insufficient statistical power to detect differences (for an α-error 0.05), also considering that NLR, PLR and LMR vary substantially from case to case, and thus the negative findings here reported may not reflect the lack of association but instead the few cases included for comparative subanalysis (for example, only had 5 PAs had a Ki-67≥3%). As the study was based on fresh primary culture, I inevitably had a relative short postoperative follow-up of patients, rendering data on recurrence unavailable.

In the *in vitro* cell model I used a rat rather than human cell line, as no suitable human pituitary cell line exists; moreover, my monolayer cell cultures are unable to investigate the complex paracrine and autocrine interactions occurring *in vivo* within the TME, which involves a wider range of immune cells besides macrophages, as well as stromal cells, endothelial cells, pericytes and ECM[204].

I used a distinction between macrophages based on CD163 and HLA-DR surface markers[229,332,339], and I acknowledge this is simplistic and may not comprehensively address the heterogeneous and complex macrophage phenotypes[571]. In fact, there is a notable heterogeneity on methods to study macrophages, particularly regarding the selection of surface markers. We selected CD68 that satisfactorily identify general macrophages, and CD163 for M2 macrophages[229,332,339]; however, studying M1 macrophages is more challenging, as a specific marker is lacking, but HLA-DR or iNOS are often used for this purpose[229,572,573]. Thus, the immunohistochemical findings may well be influenced by such elements; nevertheless, the data were reproduced on a separate set of samples using a different methodology (xCell), providing another layer of evidence regarding the macrophage phenotype of human PAs.

Conclusions

In summary, these data suggest that pituitary tumour cells are an active source of cytokines, particularly chemokines, which facilitate immune cell recruitment into the TME of PAs, which in turn may influence tumourigenic mechanisms such as tumour proliferation and angiogenesis. The *in vitro* findings confirm increased macrophage chemotaxis towards pituitary tumour cell-derived factors, and on the other hand, macrophage secreting-factors influence pituitary tumour cells inducing morphological changes, increasing invasion and migration, as well as inducing cytokine secretome changes and the EMT pathway. Serum inflammation-based scores or circulating immune cell counts appears to have no value in predicting aggressiveness of PAs.

Chapter 4: Fibroblasts in the tumour microenvironment of pituitary adenomas

Introduction

Tumour behaviour is influenced by the surrounding stromal cells, including fibroblasts, via crosstalk with neoplastic cells mediated by a complex cytokine network, which plays a key role in tumour initiation, progression, angiogenesis, invasion and metastasis[204,207,209-211]. Fibroblasts are present in tumours (TAFs)[383,384], and constitute an important source of cytokines and growth factors, mediators of their pro-tumour effects[384,391,574]. In numerous cancers, such as breast[386,387], prostate[388], lung[389], gastric[390] and pancreas cancer[385,391], increased density of TAFs are associated with aggressiveness and poor outcomes. The role of PA-derived TAFs in pituitary tumour behaviour remains unknown.

Somatostatin is a ubiquitous neuropeptide that interacts with G-protein coupled somatostatin receptors (SSTs), of which 5 types have been identified (SST1 to SST5), all binding somatostatin with high affinity[575]. Somatostatin inhibits numerous biological functions, including endocrine and exocrine secretion, cell proliferation and angiogenesis, as well as inducing apoptotic cell death[391,575].

These anti-proliferative and anti-secretory effects of somatostatin have generated interest in the oncology field, particularly in endocrine-related cancer. However, the usefulness of somatostatin is limited due to short half-life (~1.5min), which has led to the development of SSAs with higher stability and longer half-lives. Despite their lower affinity for SSTs in comparison to exogenous somatostatin, SSA have been effectively used to treat some neoplasms, including neuroendocrine tumours[576] and PAs, particularly in acromegaly and thyrotrophinomas, but also in Cushing´s disease[577].

Currently, there are 3 SSA available and approved for clinical practice: octreotide and lanreotide, both with high affinity for SST2, but lower affinities for SST3 or SST5 and none for SST1 and SST4[577]; and pasireotide (SOM230) a second-generation SSA, which is considered as an “universal” SSA as it binds with high affinity to SST1, SST2, SST4 and SST5 (Figure 4.1)[577-580].

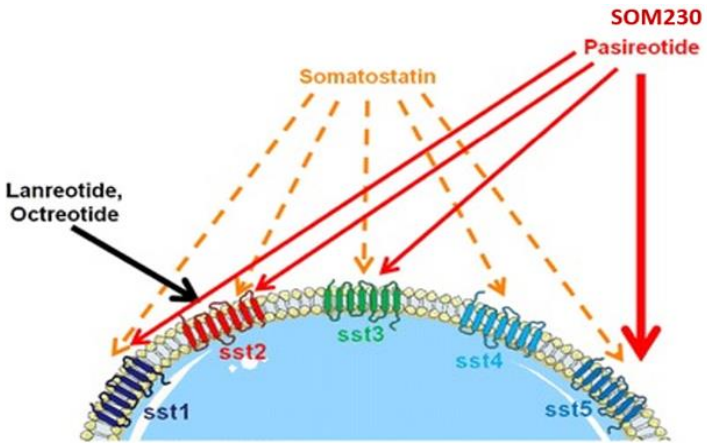

Figure 4.1: Somatostatin and SSA affinity for the different somatostatin receptors
Adapted from Fleseriu & Petersenn (2012)[578].

The effects of SSAs are initiated by their interaction with cell membrane SSTs, and mediated by different intracellular signalling pathways, including membrane-bound or cytoplasmic kinases, phosphatases, lipases, cyclic nucleotide synthases, ion channels, among others[575,577,580]. In addition to their direct inhibitory effects on tumour cells[577], SSAs may also display an indirect anti-tumour effect by targeting non-neoplastic cells within the TME, as shown in a recent study where the anti-proliferative, anti-invasive and anti-metastatic effects of pasireotide were mediated through pharmacological inhibition of stromal pancreas cancer fibroblasts[391].

Aims

Overall aim

To characterise the cytokine secretome of PA-associated TAFs and study its role in the clinical phenotype and pituitary tumour aggressiveness.

Specific aims

1. To confirm the presence of TAFs in PAs and isolate and characterise these cells *in vitro*
2. To characterise the PA-derived TAF cytokine secretome and define its role in the phenotype and aggressiveness of PAs
3. To assess the functional effect of TAF-derived factors in the behaviour, migration, invasion and EMT activation of pituitary tumour cells
4. To study the effect of SSAs in the TAF-derived cytokine secretome

Results

Detection and *in vitro* isolation of PA-derived tumour-associated fibroblasts

Vimentin-positive TAFs were identified in my experimental sample set of PAs both in the intra-tumoural area and in a rim of fibrous connective tissue (Figure 4.2 A-D), representing the tumour pseudo-capsule[581,582]. Isolated TAFs showed spindle-shaped morphology (Figure 4.2 E-F), stained for actin and vimentin in all TAFs with some expressing α-SMA (Figure 4.2 G-H), suggesting that only some TAFs display an active phenotype. TAF supernatants and CM was generated from this mixed TAF population (i.e. αSMA-positive and αSMA-negative TAFs). TAF morphology differed from the appearance of skin fibroblasts from healthy individuals (Figure 4.2 I-J), having a more prominent spindle-like shape with several cell projections, and being more irregularly distributed in the culture flasks.

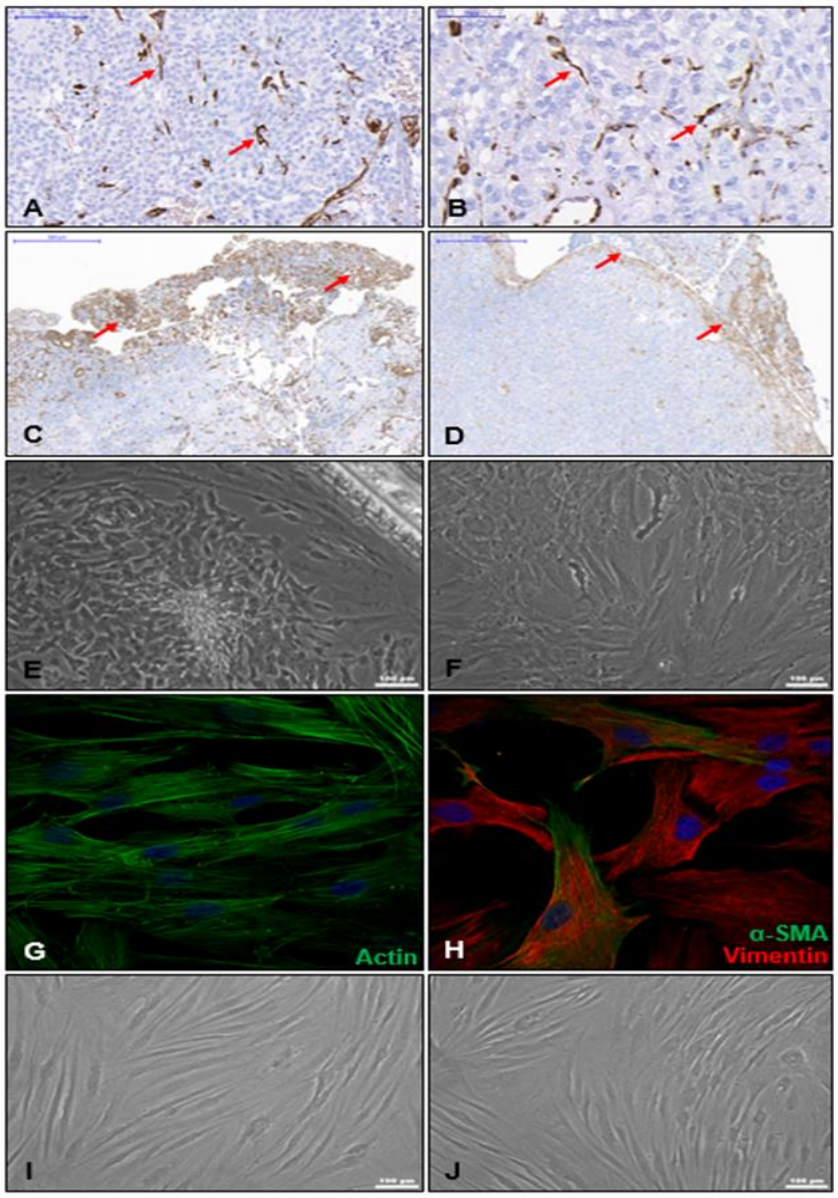

Figure 4.2: TAFs in PAs and their in vitro isolation
Immunohistochemical detection and *in vitro* isolation of PA-derived tumour-associated fibroblasts (TAFs). A-D: Vimentin immunostain of PAs shows positive staining in spindle-shaped and long cells with cytoplasmic projections (red arrows), located in the intra-tumoural areas (A-B) but also in a rim of fibrous connective tissue probably representing the tumour pseudo-capsule (C-D). Vimentin staining is also positive in endothelial cells, distinguishable from fibroblasts by their morphology and localisation in vessels lumen. Representative photographs at different magnifications are shown (A, 20x; B, 40x; C, 5x; D, 5x). E-F: TAFs isolated *in vitro* after migrating out from a debris tissue piece (E) and after reaching confluency in culture flasks (F). G-H: Immunofluorescent staining for actin (G) and for vimentin (red) and α-SMA (green) with vimentin expression seen in all TAFs, whereas α-SMA expression seen in many but not all TAFs (H), suggesting that only some TAFs have an active phenotype (63x). I-J: Morphological appearance of dermal fibroblasts from 2 different healthy individuals, having a less prominent spindle-like shape with shorter projections and being more regularly distributed in the culture flask surface.

The presence of TAFs was further assessed with the gene-signature based method xCell on a different set of samples including 7 PAs (4 NFPAs, 3 somatotrophinomas) with an estimated mean xCell fraction scores of 0.0196±0.017 (vs 0.007±0.007 in 5 NPs; p=0.572).

The role of TAF cytokine secretome in the phenotype and aggressiveness of PAs

I hypothesised that TAFs, as a relevant source of cytokines and growth factors, would influence PAs aggressiveness. To address this, I established primary cultures of TAFs from 16 human PAs (clinico-pathological features from these patients shown in Table 4.1), and then I further assessed their cytokine secretome (Table 4.2 and Appendix 7).

Patients clinico-pathological features	**TAFs (n=16)**
Gender Male *[n (%)]* Female	11 (68.8%) 5 (31.2%)
Age at first symptoms (yrs) *[mean± SD]*	50.1 (±13.9)
Age at diagnosis (yrs) *[mean±SD]*	51.8 (±13.6)
Clinical diagnosis Acromegaly *[n (%)]* NFPA	5 (31.2%) 11 (68.8%)
Headache at diagnosis *[n (%)]*	8 (50.0%)
Visual impairment at diagnosis *[n (%)]*	9 (56.3%)
Hypopituitarism at diagnosis *[n (%)]*	7 (43.8%)
Pituitary deficiencies at diagnosis *[mean±SD]*	0.9 (±1.2)
Macroadenoma *[n (%)]*	16 (100%)
Suprasellar extension *[n (%)]*	16 (100%)
Cavernous sinus invasion *[n (%)]*	6 (37.5%)
Ki-67 ≥ 3% *[n (%)]*	3 (18.8%)

Table 4.1: Baseline features of the 16 patients with PAs from whom TAFs were isolated

The most highly secreted cytokines/growth factors by TAFs were CCL2, CCL11, VEGF-A, CCL22, IL-6, FGF-2 and IL-8 (Table 4.2). IL-1α, IL-2, IL-3, IL-5, IL-7, IL-9, IL-10, IL-13, IL-1ra, CCL4, TNF-α and TGF-α were undetectable in TAF supernatants, and some cytokines were detected in low concentrations such as IL-17A, IL-1β, IFNγ and CCL3 (Appendix 7). TAF secretomes from NFPAs and somatotrophinomas did not significantly differ (Table 4.2), suggesting that TAFs may exert similar functions within the TME of both NFPAs and somatotrophinomas. I also analysed the cytokine secretome of skin fibroblasts from 2 healthy controls, demonstrating an overall tendency for lower cytokine concentrations, prominent for CCL2, VEGF-A, CCL22, IL-8, CX3CL1, and in the cases of CCL11 and PDGF-AA not detectable, suggesting that PA-derived TAFs and healthy skin fibroblast secretomes are distinct (Appendix 7).

Cytokine/ Chemokine/ Growth factor	Mean concentration (pg/mL) ± SEM			
	TAFs n=16	Serum-free medium	NFPA-TAFs (n=11)	Somatotrophinoma-TAFs (n=5)
CCL2	4786.86 ± 642.17	4.00	4782.87 ± 903.21	4795.62 ± 679.53
CCL11	836.27 ± 328.16	0	399.44 ± 168.63	1797.30 ± 894.43
VEGF-A	174.29 ± 80.60	0	70.06 ± 46.86	403.59 ± 240.29
CCL22	62.54 ± 21.50	20.78	74.17 ± 29.63	36.96 ± 21.92
IL-6	54.76 ± 6.50	0	50.60 ± 8.17	63.89 ± 10.45
FGF-2	42.93 ± 5.82	0	45.96 ± 8.24	36.29 ± 4.13
IL-8	42.20 ± 11.11	7.06	31.53 ± 7.10	65.69 ± 31.66
CXCL1	28.20 ± 6.56	20.78	26.23 ± 6.44	32.54 ± 16.78
CX3CL1	26.86 ± 8.34	6.73	29.86 ± 12.09	20.26 ± 3.86
CCL7	13.83 ± 5.97	8.20	9.43 ± 3.67	23.51 ± 17.89
PDGF-AA	11.64 ± 3.71	0.12	7.40 ± 3.44	20.98 ± 8.29
IFNα2	8.82 ± 2.40	1.79	10.25 ± 3.38	5.68 ± 1.54

Table 4.2: PA-derived TAF cytokine secretome
Top 12 highly secreted cytokines, chemokines and growth factors in primary culture supernatants from TAFs isolated from PAs. TAF supernatants were collected following 24h on serum-free medium conditions and the cytokine secretome determined with the human Millipore MILLIPLEX cytokine 42-plex array. Results are shown as concentration (pg/mL), mean±SEM. *p* values were non-significant for comparative analysis per cytokine between TAFs derived from NFPAs (NFPA-TAFs) or from somatotrophinomas (Somatotrophinoma-TAFs) (Mann Whitney U test).

TAF-derived IL-6 levels were higher in PAs with cavernous sinus invasion in comparison to non-invasive PAs (72.7±10.7 *vs* 43.9±6.3 pg/mL; p=0.027), while there was a trend (p=0.058) for TAFs isolated from PAs with a higher Ki-67 to secrete more CCL2 (Figure 4.3).

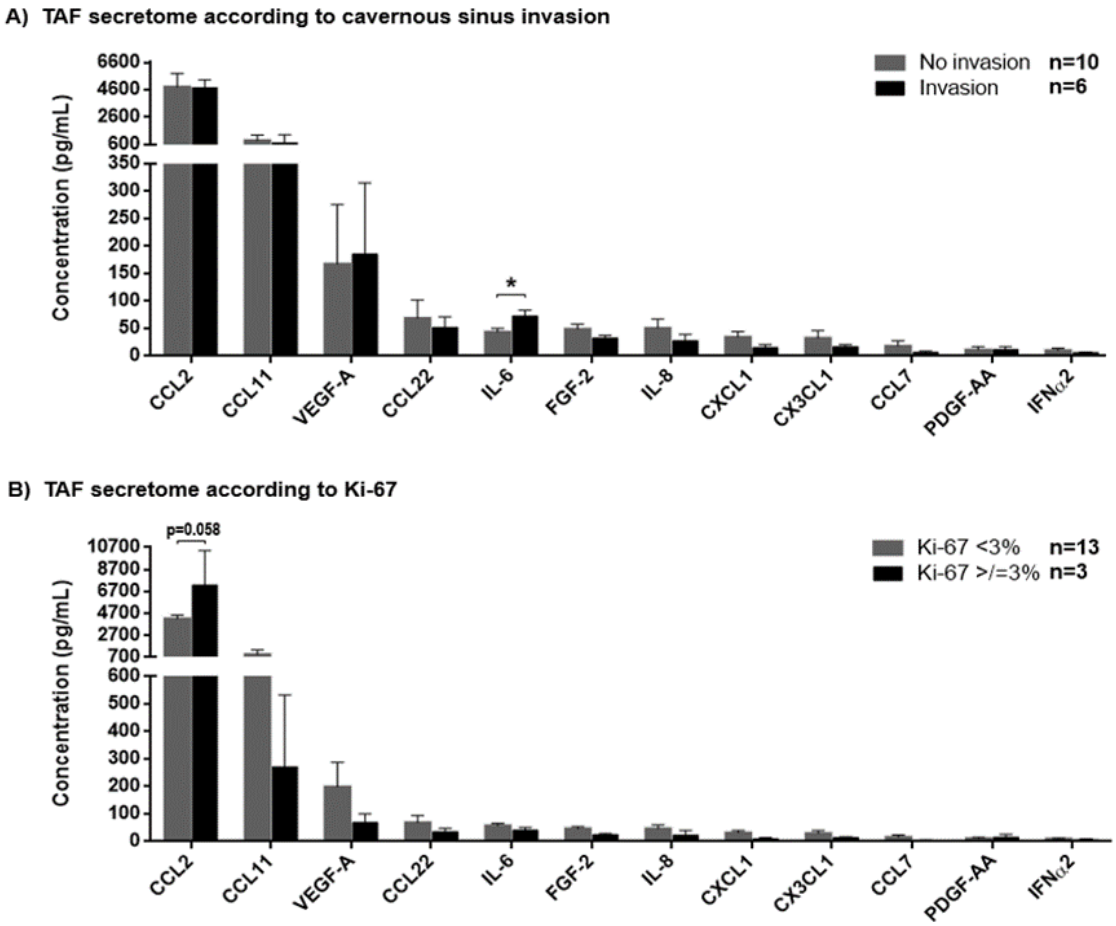

Figure 4.3: TAF cytokine secretome according to cavernous sinus invasion (A) or Ki-67 (B)
Data are shown as concentration (pg/mL), mean±SEM for the top 12 secreted cytokines, chemokines and growth factors, as determined in PA-derived TAF supernatants by the human Millipore MILLIPLEX cytokine 42-plex array. n=16. *, <0.05, **, <0.01, ***, <0.001 (Mann Whitney U test).

CCL2 secretion was higher in TAFs derived from females than males (6698±1831 *vs* 3918±220 pg/mL; p=0.04), but there were no gender differences regarding other cytokines (Figure 4.4). CCL2 secretion was not dependent on age or the females' pre or postmenopausal status.

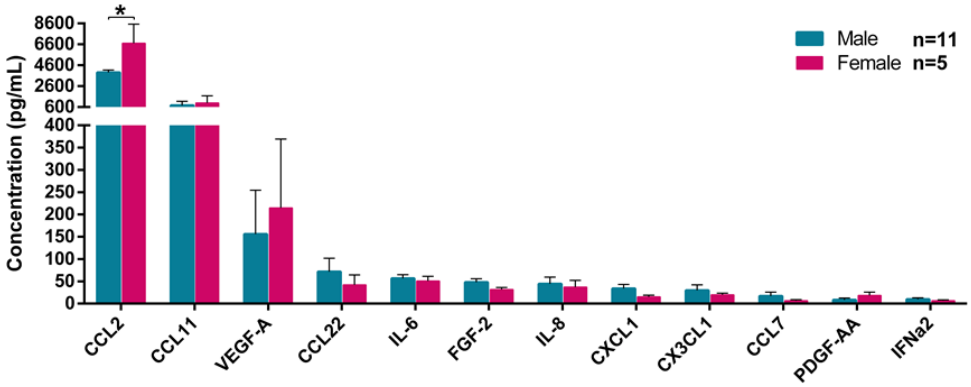

Figure 4.4: TAF cytokine secretome according to gender
Data are shown as concentration (pg/mL), mean±SEM for the top 12 secreted cytokines, chemokines and growth factors, as determined in PA-derived TAF supernatants by the human Millipore MILLIPLEX cytokine 42-plex array. n=16. *, <0.05, **, <0.01, ***, <0.001 (Mann-Whitney U test).

The presence of headache, hypopituitarism or visual impairment at diagnosis were not associated with differences in TAF cytokine release (Table 4.3).

Cytokine/ chemokine derived from TAFs	Presence of headache at diagnosis		*p* value
	No headache (n=8) Mean concentration (pg/mL) ± SEM	**Headache (n=8)** Mean concentration (pg/mL) ± SEM	
CCL2	5066.78 ± 1245.42	4506.93 ± 440.36	0.678
CCL11	256.07 ± 83.42	1416.48 ± 598.65	**0.095**
VEGF-A	42.99 ± 15.28	305.59 ± 150.60	**0.105**
CCL22	62.39 ± 15.45	62.70 ± 41.75	0.994
IL-6	50.64 ± 7.85	58.88 ± 10.69	0.545
FGF-2	38.66 ± 5.83	47.21 ± 10.29	0.482
IL-8	32.67 ± 9.18	51.73 ± 20.46	0.410
CXCL1	21.49 ± 4.18	34.92 ± 21.42	0.323
CX3CL1	21.66 ± 6.20	32.06 ± 15.87	0.551
CCL7	5.47 ± 2.27	22.18 ± 11.31	0.188
PDGF-AA	8.21 ± 5.40	15.07 ± 5.16	0.374
IFNα2	6.83 ± 1.84	10.81 ± 4.48	0.425
Cytokine/ chemokine derived from TAFs	**Presence of visual impairment at diagnosis**		***p* value**
	No visual impairment (n=7) Mean concentration (pg/mL) ± SEM	**Visual impairment (n=9)** Mean concentration (pg/mL) ± SEM	
CCL2	4533.52 ± 508.44	4983.90 ± 1101.24	0.741
CCL11	1556.89 ± 666.40	275.80 ± 100.76	0.104
VEGF-A	321.27 ± 174.25	59.98 ± 14.46	0.185
CCL22	88.94 ± 46.11	42.01 ± 13.44	0.294
IL-6	65.23 ± 10.31	46.61 ± 7.72	0.162
FGF-2	48.11 ± 11.00	38.91 ± 6.14	0.452
IL-8	59.81 ± 23.14	28.51 ± 6.73	0.235
CXCL1	39.58 ± 13.59	19.35 ± 3.67	0.195
CX3CL1	35.86 ± 18.03	19.86 ± 5.30	0.359
CCL7	4533.52 ± 508.44	4983.90 ± 1101.24	0.741
PDGF-AA	1556.89 ± 666.40	275.80 ± 100.76	0.104
IFNα2	321.27 ± 174.25	59.98 ± 14.46	0.185
Cytokine/ chemokine derived from TAFs	**Presence of hypopituitarism at diagnosis**		***p* value**
	Eupituitarism (n=9) Mean concentration (pg/mL) ± SEM	**Hypopituitarism (n=7)** Mean concentration (pg/mL) ± SEM	
CCL2	4400.58 ± 412.30	5283.49 ± 1411.38	0.514
CCL11	830.04 ± 408.12	844.28 ± 574.28	0.984
VEGF-A	139.57 ± 87.74	218.93 ± 152.75	0.642
CCL22	73.36 ± 32.27	48.64 ± 18.16	0.586
IL-6	49.70 ± 4.96	61.25 ± 13.65	0.396
FGF-2	45.55 ± 9.74	39.57 ± 5.25	0.627
IL-8	36.78 ± 9.41	49.17 ± 23.21	0.598
CXCL1	22.28 ± 8.02	35.82 ± 10.89	0.323
CX3CL1	31.74 ± 13.99	20.58 ± 7.06	0.526
CCL7	9.38 ± 4.38	19.55 ± 12.70	0.417
PDGF-AA	16.86 ± 5.71	4.94 ± 3.11	**0.092**
IFNα2	10.29 ± 4.06	6.93 ± 1.88	0.504

Table 4.3: TAF secretome according to headache, visual impairment or hypopituitarism at diagnosis
Cytokine secretome from TAF supernatants according to the presence of headache, visual impairment or hypopituitarism at diagnosis. Data are shown as concentration (pg/mL), mean±SEM for the top 12 secreted cytokines, chemokines and growth factors as identified by the human Millipore MILLIPLEX 42-plex assay. *p* values were non-significant for all cytokine comparisons per feature (Mann-Whitney U test).

There were some significant correlations between TAF cytokines and serum pituitary hormone levels (Appendix 8). Among NFPA-derived TAFs, significant correlations were noted between PDGF-AA and IGF-1 (r=0.658, p=0.039), FT4 (r=0.662, p=0.037) and FSH (r=0.677, p=0.032), and between IL-6 and FT4 (r=-0.747, p=0.013). Among somatotrophinoma-derived TAFs, there were correlations between IFNα2 and GH (r=-0.939, p=0.018), FGF-2 and TSH (r=-0.886, p=0.045), and between CCL22 and LH (r=0.968, p=0.007) and FSH (r=-0.969, p=0.006) (Appendix 8).

The levels of TAF-derived CCL2, a chemokine with angiogenic functions[583,584], were positively correlated with microvessel area (r=0.672; p=0.004) suggesting a possible role for TAF-derived factors in PA angiogenesis (Table 4.4), as shown in other cancers[384,585-587]. Further details regarding angiogenesis in PAs are discussed in the Chapter 5.

Cytokine/ Chemokine/ Growth factor TAFs n=16		Microvessel density	Microvessel area	E-cadherin immunoreactivity	ZEB1 immunoreactivity
CCL2	Pearson correlation *r*	0.440	0.672	-0.217	-0.039
	p value	0.088	**0.004**	0.419	0.887
CCL11	Pearson correlation *r*	-0.193	-0.347	0.174	-0.401
	p value	0.474	0.189	0.519	0.124
VEGF-A	Pearson correlation *r*	-0.173	-0.255	0.188	-0.318
	p value	0.521	0.340	0.486	0.230
CCL22	Pearson correlation *r*	-0.029	-0.051	0.331	0.071
	p value	0.915	0.852	0.211	0.793
IL-6	Pearson correlation *r*	-0.466	-0.318	0.278	-0.056
	p value	0.069	0.231	0.298	0.838
FGF-2	Pearson correlation *r*	0.177	-0.016	0.337	0.061
	p value	0.511	0.954	0.201	0.821
IL-8	Pearson correlation *r*	-0.079	-0.270	0.372	-0.228
	p value	0.772	0.311	0.156	0.396
CXCL1	Pearson correlation *r*	-0.100	-0.181	0.497	-0.246
	p value	0.713	0.503	0.050	0.359
CX3CL1	Pearson correlation *r*	-0.089	-0.161	0.173	-0.221
	p value	0.744	0.552	0.523	0.410
CCL7	Pearson correlation *r*	-0.076	-0.199	0.426	-0.248
	p value	0.779	0.460	0.100	0.354
PDGF-AA	Pearson correlation *r*	-0.267	-0.482	-0.564	-0.409
	p value	0.317	0.058	**0.023**	0.116
IFNα2	Pearson correlation *r*	-0.095	-0.143	0.175	-0.129
	p value	0.726	0.598	0.516	0.633

Table 4.4: TAF cytokine secretome and PA angiogenesis and EMT
Correlations between the cytokine secretome from PA-derived TAFs and microvessel density (number of vessels/HPF), microvessel area (μm^2/HPF), E-cadherin and ZEB1 immunoreactivities in PAs. Data are shown for the top 12 highly secreted cytokines, chemokines and growth factors in supernatants from TAFs. *p* values were determined by the Pearson correlation coefficient *r*.

PDGF-AA levels were negatively correlated with E-cadherin expression (r=-0.564, p=0.023), suggesting a possible role for the TAF secretome in promoting EMT by downregulating E-cadherin (Table 4.4 and Figure 4.5), an effect recognised to PDGFs and their receptors[588-590]. However, I

found no other correlation between E-cadherin or ZEB1 immunoreactivity in my cohort of PAs and TAF-derived cytokine levels (Table 4.4). This lack of significant association can be explained by the lack of an EMT signature in PAs as discussed in Chapter 5, or alternatively could be explained by the lack or only very mild effect of TAFs in the EMT in PAs.

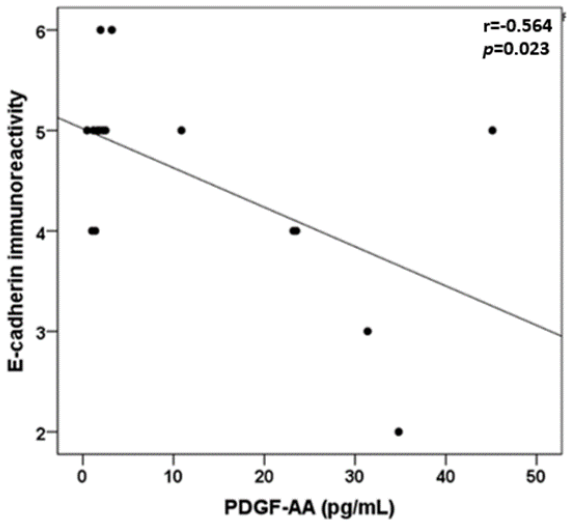

Figure 4.5: Correlation between TAF-derived FGF-2 levels and E-cadherin immunoreactivity in PAs
p value was determined by the Pearson correlation coefficient *r*. n=16.

TAFs have been implicated in the recruitment of immune cells into the TME[384,585,591]. I found a positive correlation between the PA-infiltrating macrophages content and TAF-derived FGF-2 (Figure 4.6), a protein with recognised macrophage chemotaxis properties[592-594].

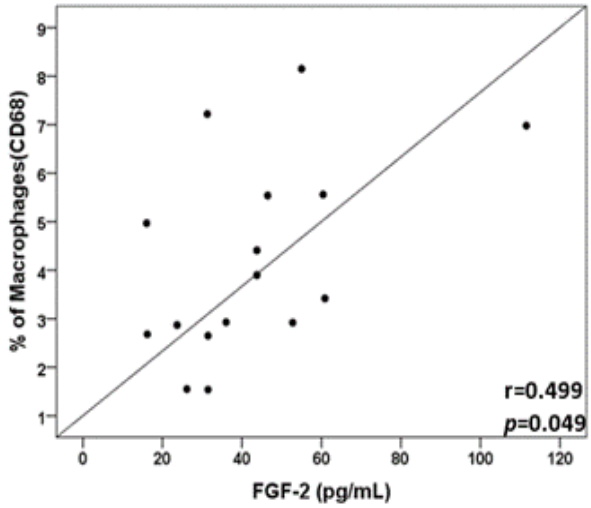

Figure 4.6: Correlation between PA-infiltrating macrophages and TAF-derived FGF-2
p value was determined by the Pearson correlation coefficient *r*.

PAs with a M2:M1 macrophage ratio ≥2 were associated with higher TAF-derived levels of FGF-2 and CXCL1 (Figure 4.7), two proteins able to promote M2-macrophage polarisation[595-597].

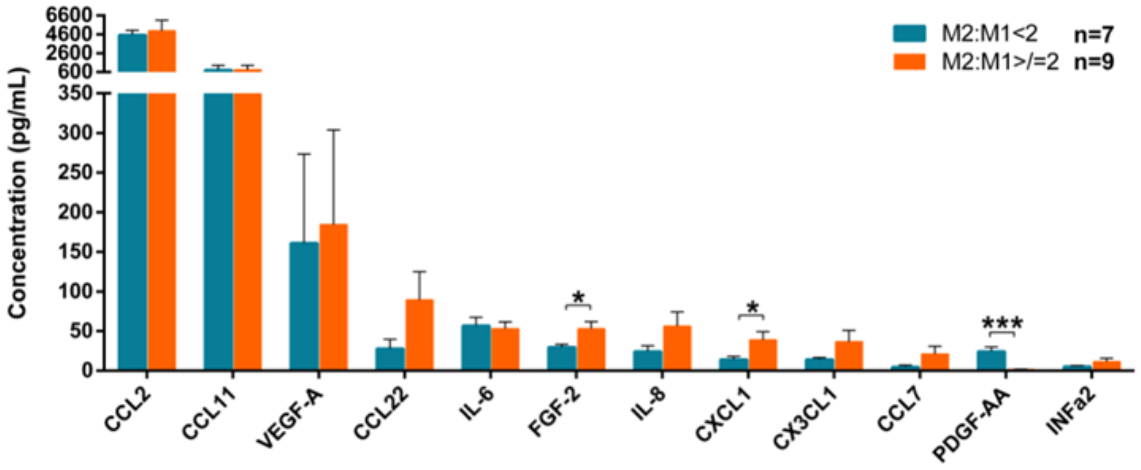

Figure 4.7: TAF cytokine secretome and M2:M1 macrophage ratio
Cytokine secretome profile of TAF supernatants according to lower (<2) vs higher (≥2) M2:M1 macrophage ratio. Data are shown as concentration (pg/mL), mean±SEM, and for the top secreted proteins as identified by the Millipore MILLIPLEX assay. *,<0.05, **,<0.01, ***,<0.001 (Mann-Whitney U test).

TAF-derived IL6 levels were also inversely correlated with CD4+ T cells, but there were no other correlations between TAF-derived cytokines and other PA immune cells (Table 4.5).

TAF-derived cytokine secretome (n=16)		% of macrophages	% of CD4+ T cells	% of CD8+ T cells	% of FOXP3+ T cells	% of neutrophils
CCL2	Pearson correlation *r*	.295	.110	-.080	-.158	-.323
	p value	.267	.684	.769	.560	.222
CCL11	Pearson correlation *r*	.098	-.414	-.036	-.197	-.270
	p value	.717	.110	.893	.464	.312
VEGF-A	Pearson correlation *r*	.055	-.328	.068	-.041	-.270
	p value	.841	.214	.801	.879	.312
CCL22	Pearson correlation *r*	.325	.058	.091	-.293	.410
	p value	.220	.831	.737	.271	.115
IL-6	Pearson correlation *r*	-.138	-.503	-.066	.149	-.203
	p value	.610	**.047**	.807	.582	.450
FGF-2	Pearson correlation *r*	.499	.064	.186	-.352	.437
	p value	**.049**	.813	.490	.182	.091
IL-8	Pearson correlation *r*	.359	-.385	.191	-.083	-.173
	p value	.172	.141	.478	.760	.522
CXCL1	Pearson correlation *r*	.422	-.199	.273	-.171	.110
	p value	.104	.461	.306	.527	.685
CX3CL1	Pearson correlation *r*	.329	-.016	-.048	-.358	.333
	p value	.213	.953	.861	.173	.208
CCL7	Pearson correlation *r*	.311	-.234	.242	-.047	-.073
	p value	.241	.383	.366	.862	.790
PDGF-AA	Pearson correlation *r*	-.413	.002	-.205	.380	-.408
	p value	.112	.995	.446	.147	.117
IFNα2	Pearson correlation *r*	.292	.010	.024	-.260	.405
	p value	.272	.970	.928	.331	.120

Table 4.5: TAF cytokine secretome and PA-infiltrating immune cells
p value was determined by the Pearson correlation coefficient *r*. n=16.

***In vitro* studies investigating the interactions between fibroblasts and pituitary tumour cells**

TAF-derived factors increase invasion, migration and induce EMT-like phenotype in GH3 cells

To study the effects of TAF-derived factors in pituitary tumour cells, in the absence of an appropriate human pituitary tumour cell line, I assessed morphology, migration, invasion and EMT activation of GH3 cells in response to TAF-CM or skin fibroblast-CM.

GH3 cells showed significantly higher migration and invasion towards TAF-CM compared to complete medium, but not towards normal skin fibroblast-conditioned medium. Skin fibroblasts were not able to increase invasion, while TAF-CM led to an 11-fold increased invasiveness in comparison to complete medium (Figure 4.8). Skin fibroblasts are also a source of cytokines and chemokines[598,599], hence it was not surprising to report the non-significant trend for increased GH3 cell migration observed in the presence of skin fibroblast-CM. However, skin fibroblasts were not able to increase GH3 cell invasion, while TAF-CM lead to an 11-fold increased invasiveness (Figure 4.8). In fact, invasion requires not only the capacity for cells to migrate, but also ability to secrete enzymes and proteases to degrade matrigel[600], which seems to be induced by TAF-derived factors, but not by skin fibroblast-derived factors.

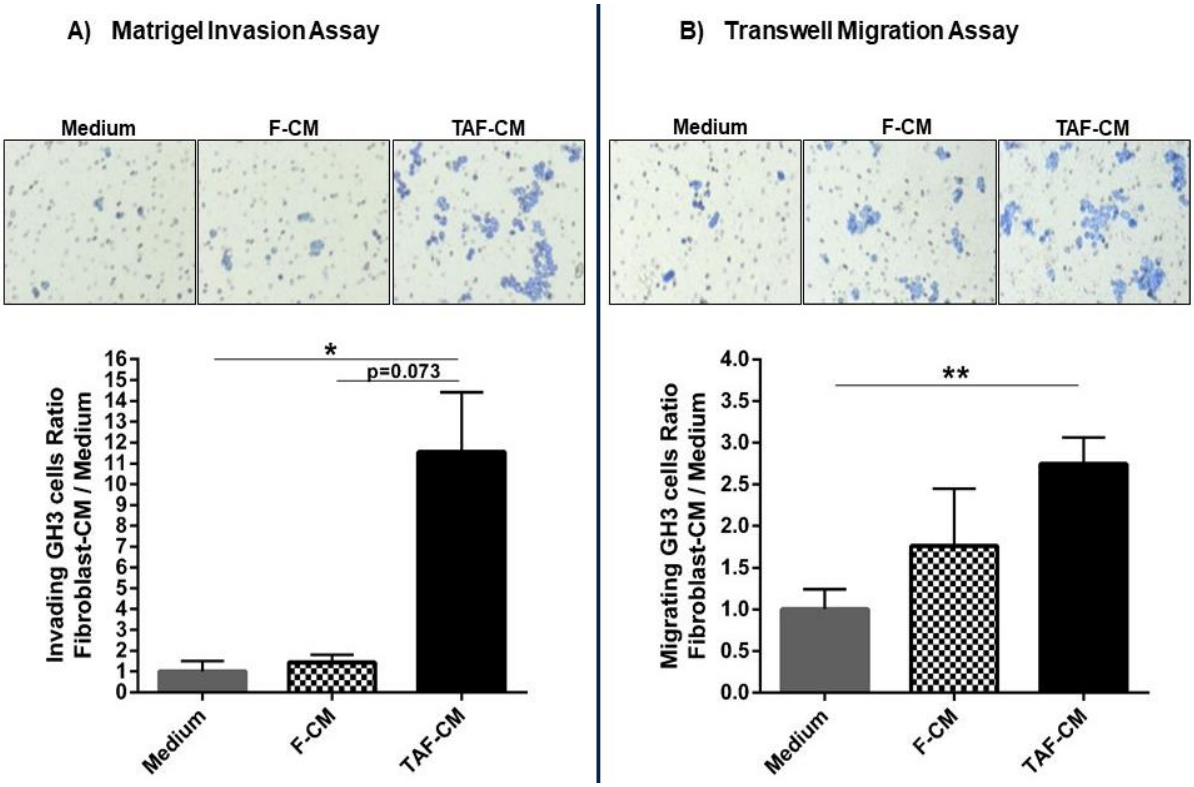

Figure 4.8: TAF-CM effect on GH3 cell invasion and migration

Matrigel-coated chamber invasion assays (A) and transwell migration assays (B) performed on GH3 cells towards complete medium, tumour-associated fibroblasts-conditioned medium (TAF-CM) and CM from dermal fibroblasts from healthy individuals (F-CM) after 72h. Data are represented as a ratio of invading or migrated GH3 cells towards TAF-CM or F-CM in relation to invading/migrated GH3 cells in serum-medium, mean±SEM. *,<0.05, **,<0.01, ***,<0.001 (one way-ANOVA with Bonferroni multiple comparison test).

TAF-CM, but not skin fibroblast-CM, induced EMT-like morphological changes in GH3 cells, leading to a significant increase in cell area, perimeter and Feret's diameter, with decreased solidity, roundness and circularity (Figure 4.9). These changes result in larger cells with an elongated shape which are more deformable and have a better ability to migrate and invade, in line with the migration and invasion experiments (Figure 4.8). These morphological changes were accompanied by granular actin staining with prominent stress fibres and spikes, characteristic of EMT-like cytoskeletal changes[536], while untreated GH3 cells showed actin distributed in a cortical ring (Figure 4.9).

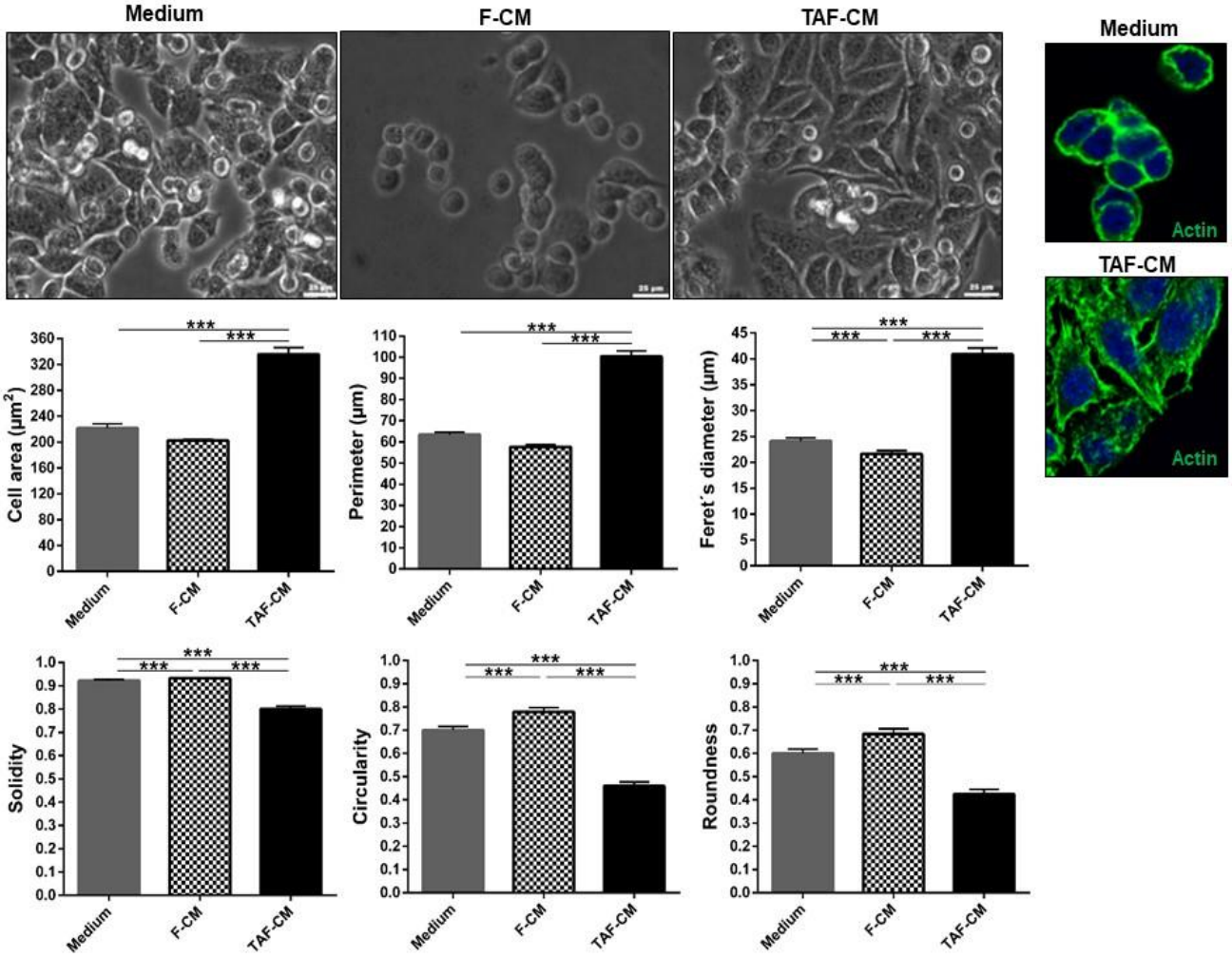

Figure 4.9: TAF-CM effect on GH3 cell morphology
Morphology of GH3 cells after treatment for 72h with serum-medium (n=3), tumour-associated fibroblasts-conditioned medium (TAF-CM) (n=4) and with CM from dermal fibroblasts from healthy individuals (F-CM) (n=3). GH3 cell morphology was evaluated for six parameters using ImageJ: cell area, Feret's diameter, solidity, perimeter, roundness and circularity. 75 cells were analysed per experiment, with a minimum of 3 experiments per treatment condition. Data are shown as mean±SEM. Scale bar: 25µm. *,<0.05, **,<0.01, ***,<0.001 (two-way ANOVA with Bonferroni multiple comparison test). On the right, actin immunostaining is shown of GH3 cells after treatment with TAF-CM for 72h in comparison to serum-medium, (63x) magnification; DAPI was used to stain the nuclei.

TAF-CM induced EMT in GH3 cells, significantly decreasing E-cadherin and increasing nuclear ZEB1 expression (hallmarks of EMT pathway activation[466]), while untreated GH3 cells showed strong E-cadherin with membranous localisation but also in the cytoplasm as well as low nuclear ZEB1 expression (Figure 4.10). Direct induction of EMT, in line with increased invasiveness, migration and altered cell shape, suggests that TAF-derived factors interact with pituitary tumour cells to influence their behaviour and invasiveness.

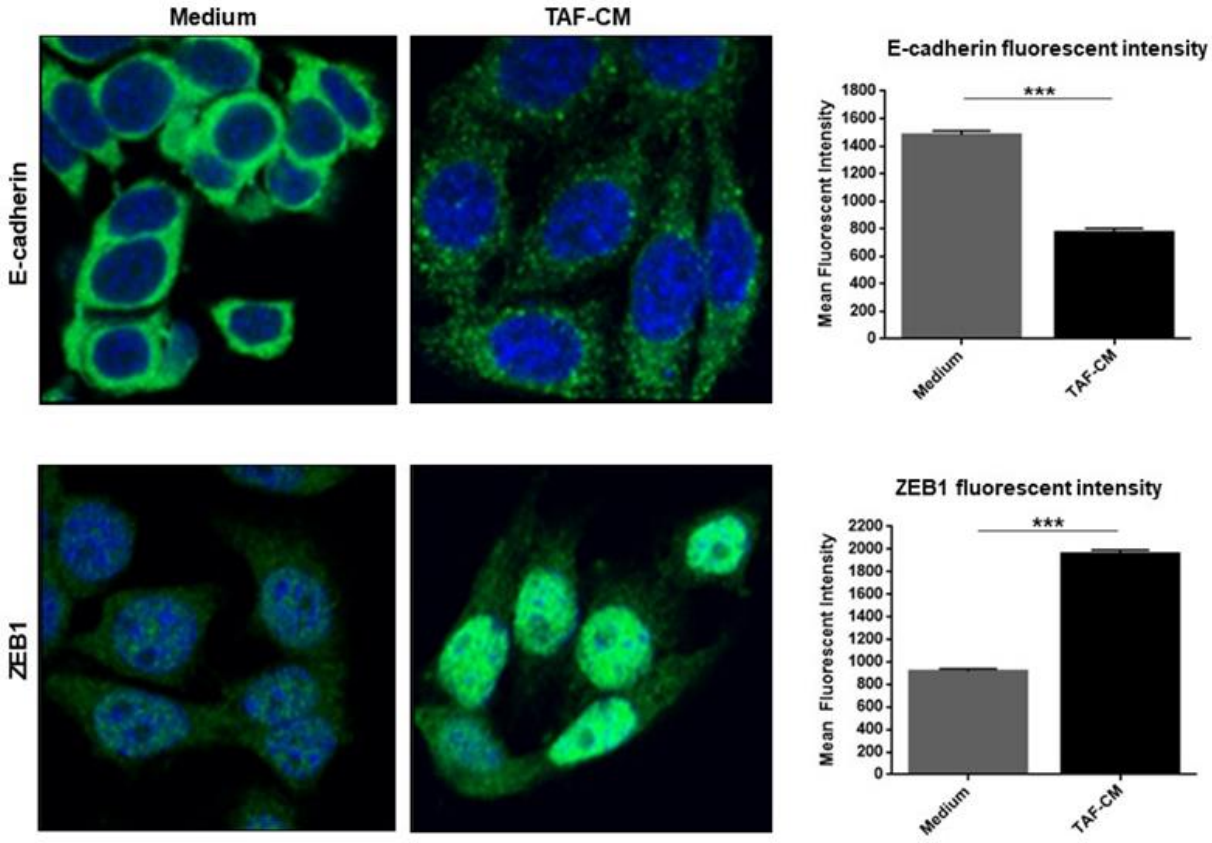

Figure 4.10: TAF-CM inducing EMT activation in GH3 cells
Alterations in the E-cadherin and ZEB1 expression by GH3 cells after treatment for 72h with TAF-CM or complete medium. Pictures were taken on confocal microscope at 63x magnification. DAPI was used to stain the nuclei. E-cadherin and ZEB1 fluorescent intensities were quantified in 30 different cells per treatment condition using the Carl Zeiss Zen Blue Edition version 2.3 software. Data are shown as fluorescent intensity, mean±SEM. *,<0.05, **,<0.01, ***,<0.001 (Mann-Whitney U test).

Somatostatin analogue effect in TAF cytokine secretome

TAFs express somatostatin receptors, predominantly the type 1

To investigate whether SSA affect TAF cytokine secretome, I first determined SST expression in TAFs. SST1 was the predominant type in TAFs (Figure 4.11), as it is in pancreatic cancer-associated fibroblasts[385,391], while the expression of SST2 and SST5 was minimal (Figure 4.11).

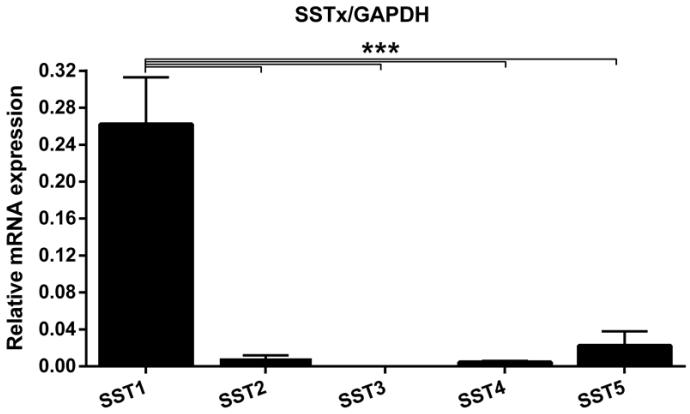

Figure 4.11: SST expression profile in TAFs
Somatostatin receptor expression profile in human PA-derived TAFs assessed by RT-qPCR. Data are shown as *SSTx* mRNA fold change expression relative to *GAPDH*, mean±SEM, determined by the standard curve method. n=16.*,<0.05, **,<0.01, ***,<0.001 (one way-ANOVA with Bonferroni multiple comparison test).

TAF expression of SSTx did not differ between NFPA-TAFs vs somatotrophinoma-TAFs, as well as between PAs with low vs high Ki-67 or with vs without cavernous sinus invasion (Figure 4.12).

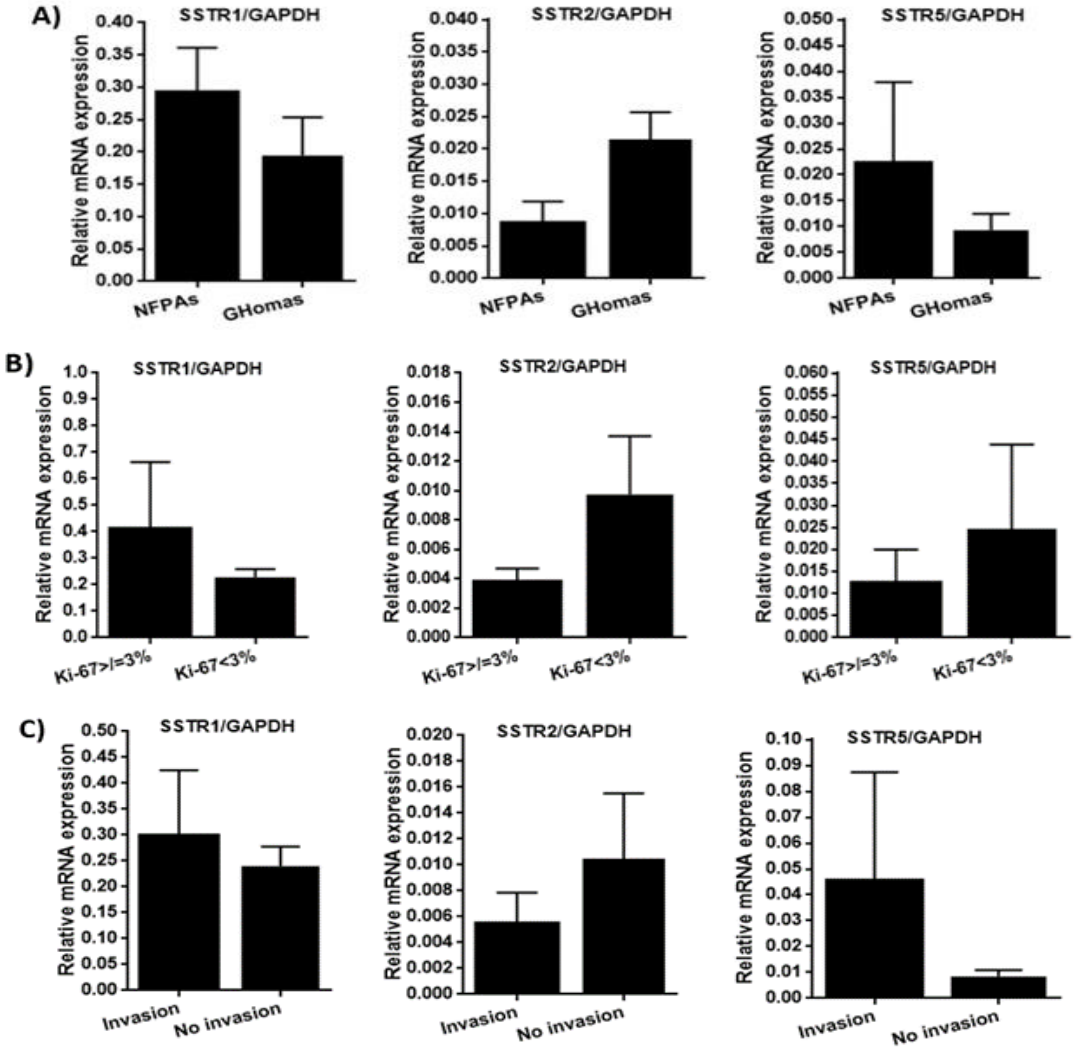

Figure 4.12: SST expression profile in TAFs according to PA subtype, Ki-67 or cavernous sinus invasion
Somatostatin receptor (SST) expression in human PA-derived TAFs assessed by RT-qPCR according to: A) PA type (NFPAs or somatotrophinomas (GHomas)); B) low vs high Ki-67; C) cavernous sinus invasion vs no invasion. Data shown as *SSTx* mRNA expression fold change relative to *GAPDH*, mean±SEM, determined by the standard curve method. NFPA-TAFs, n=11; Somatotrophinoma-TAFs, n=5. PAs with cavernous sinus invasion n=6; PAs without invasion, n=10. PAs with Ki-67<3%, n=13; PAs with Ki-67≥3%, n=3. *p* values were non-significant for all the comparative analysis (Mann-Whitney U test).

Pasireotide inhibits cytokine secretion from TAFs

As TAFs mainly expressed SST1, I used pasireotide (10^{-7}M) treatment[385,391] to assess TAF cytokine secretome responses to SSAs. Pasireotide treatment significantly decreased IL-6 release by 80% ($p<0.001$) and CCL2 by 35% ($p=0.038$), while the other factors showed a trend for reduction but this was not statistically significant (Figure 4.13-A and Appendix 7).

IL-6 secretion was reduced in all 16 TAFs treated with pasireotide, while CCL2 decreased in 10 out of 16 cases (62.5%) (Figure 4.13-B and Table 4.6). CCL2, CCL11, VEGF-A, IL-8, PDGF-AA, FGF-2 and IFNα2 decreased in more than 50% of treated TAFs (Figure 4.14), whereas CCL22, CX3CL1, CXCL1 and CCL7 decreased in less than 50% of the pasireotide-treated TAFs (Figure 4.15).

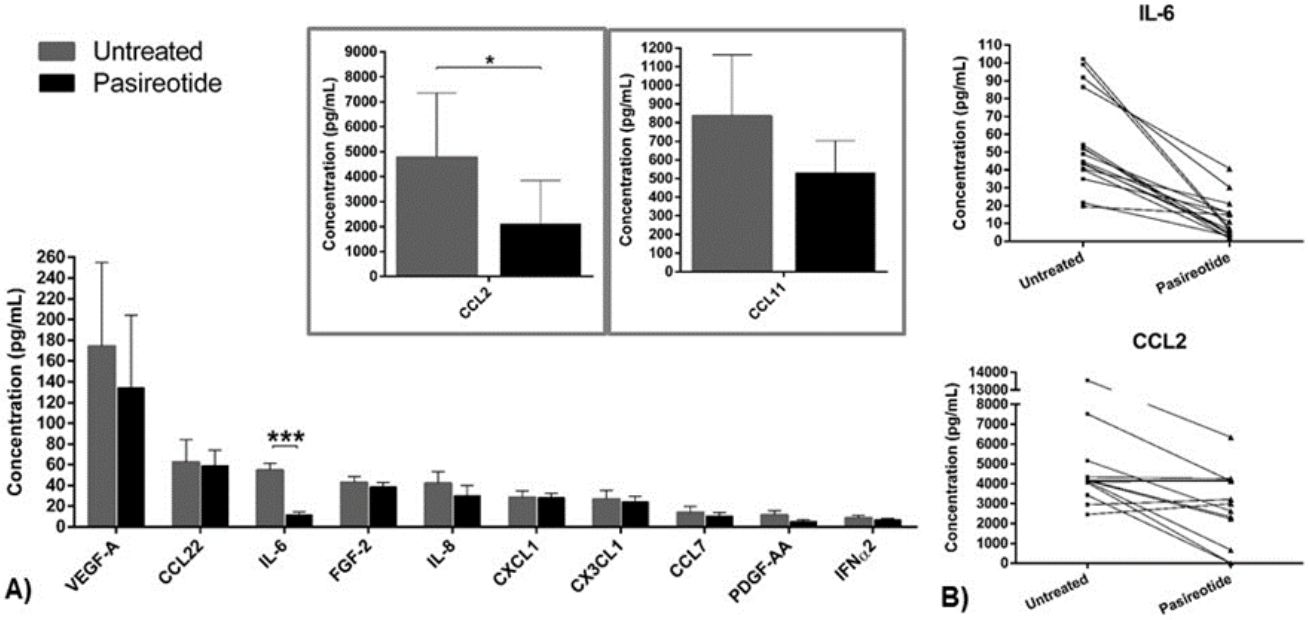

Figure 4.13: TAF cytokine secretome at baseline and after pasireotide treatment
Cytokine secretome from human PA-derived TAFs at baseline (untreated) and after treatment with pasireotide (10^{-7}M). Data are shown as concentration (pg/mL), mean±SEM for the top 12 highly secreted proteins in PA-derived TAF supernatants collected following 24h on serum-free medium conditions with pasireotide (10^{-7}M) or without (A). IL-6 and CCL2 levels before (left side, square mark) and after pasireotide treatment (right side, triangle mark) are shown per case individually (B). n=16. *,<0.05, **,<0.01, ***,<0.001 (Mann Whitney U test).

Cytokine/ Chemokine/ Growth factor	Number of cases with decreased levels after pasireotide n (%)	Concentrations difference untreated vs pasireotide (pg/mL, mean±SEM)	Mean fold-change after treatment pasireotide (% (±SEM))
CCL2	10 (62.5%)	- 1681.43 ± 547.05	-30.50% (±10.02)
CCL11	13 (81.3%)	-306.45 ± 241.92	-37.78% (±20.24)
VEGF-A	14 (87.5%)	-40.18 ± 21.72	-29.22% (±11.10)
CCL22	5 (31.3%)	-3.40 ± 13.07	+60% (±30.9)
IL-6	16 (100.0%)	-42.93 ± 6.16	-75.78% (±5.40)
FGF-2	11 (68.8%)	-4.31 ± 4.79	+6.13% (±16.27)
IL-8	10 (62.5%)	-12.00 ± 9.29	-21.97% (±14.89)
CXCL1	4 (25.0%)	-0.07 ± 4.60	+23.31% (±12.83)
CX3CL1	8 (50.0%)	-2.82 ± 4.78	+22.70% (±23.18)
CCL7	8 (50.0%)	-3.36 ± 3.60	+49.28% (52.44)
PDGF-AA	11 (68.8%)	-6.28 ± 2.82	-15.93% (±18.37)
IFNα2	10 (62.5%)	-2.06 ± 1.42	+8.88% (±24.87)

Table 4.6: Quantification of the TAF cytokine secretome responses to pasireotide
Number of cases which cytokine concentrations have decreased after treatment with pasireotide (10^{-7}M), and also mean concentration difference and mean-fold change between untreated and pasireotide-treated TAFs derived from 16 PAs. Data are shown as n(%) or expressed as concentration (pg/mL), mean±SEM, and for the top 12 secreted proteins as identified by the Millipore MILLIPLEX assay in TAF supernatants.

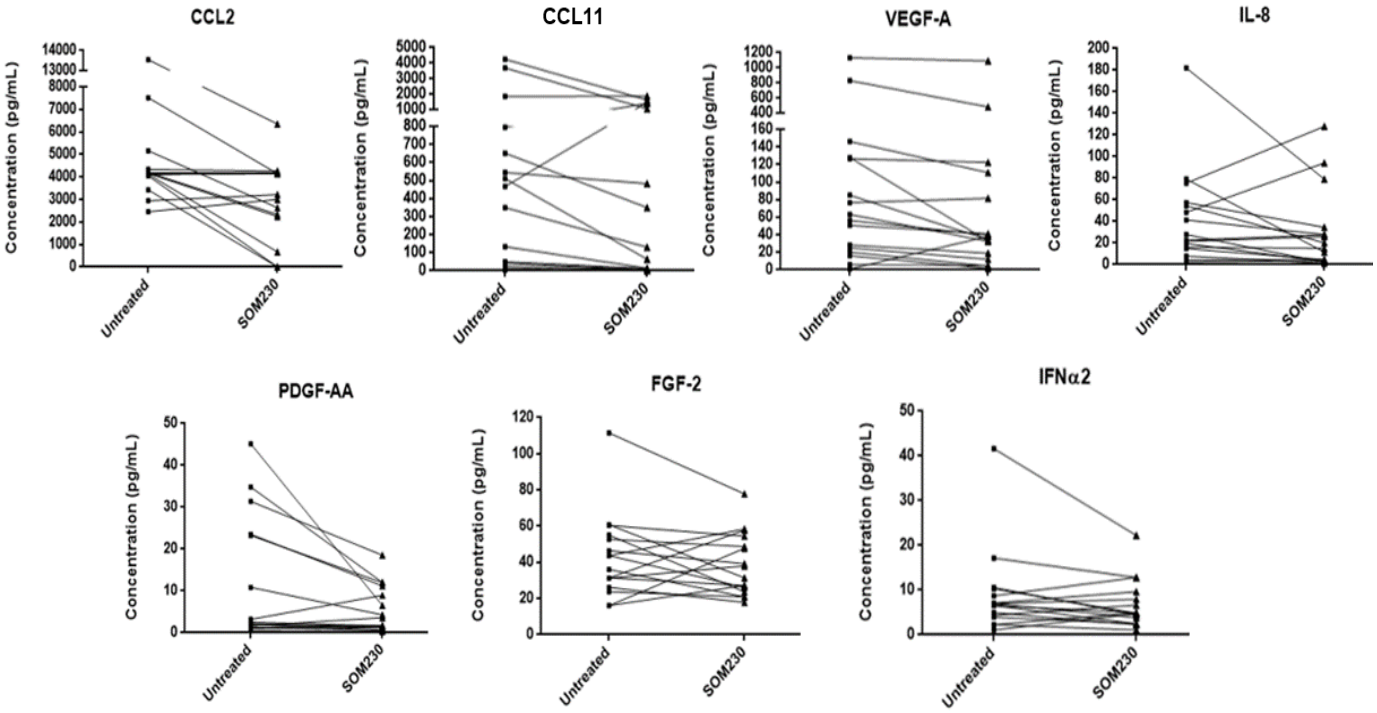

Figure 4.14: Cytokines decreased in more than half of pasireotide-treated TAFs
Cytokines that decreased in more than 50% (>8 out of 16) in the supernatants of TAFs after treatment with 10^{-7}M of pasireotide (SOM230). Data are shown in concentration (pg/mL) for each individual case before (on the left side, square mark) and after treatment with SOM230 (on the right side, triangle mark), per cytokine, chemokine or growth factor. n=16.

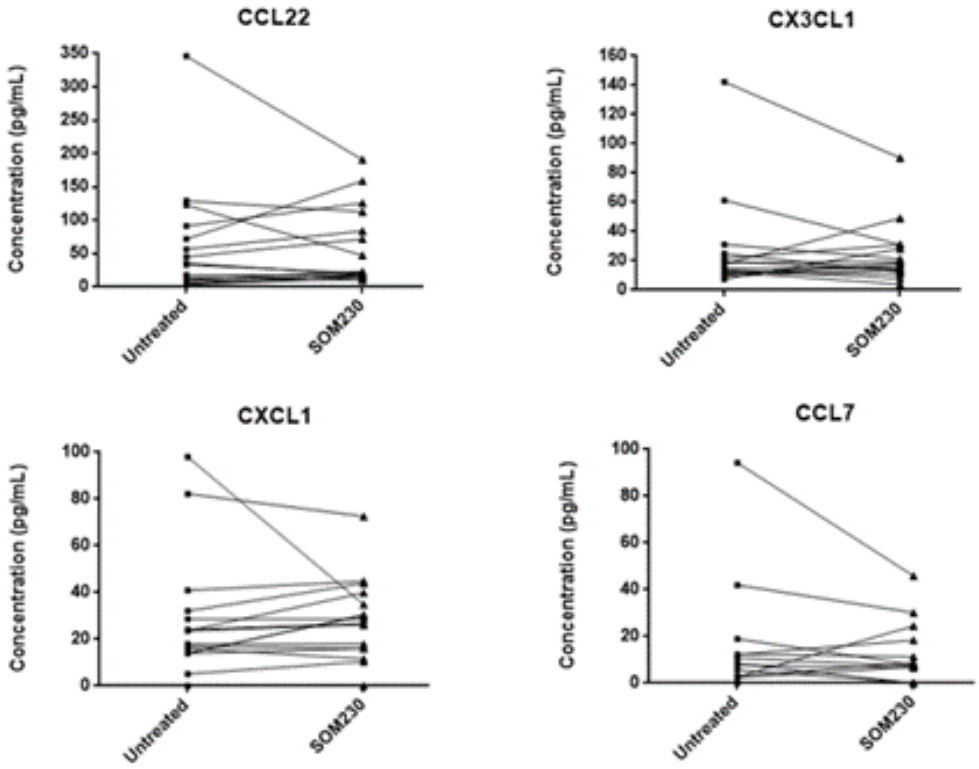

Figure 4.15: Cytokines decreased in less than half of pasireotide-treated TAFs
Cytokines that decreased in less than 50% (<8 out of 16) in the supernatants of TAFs after treatment with 10^{-7}M of pasireotide (SOM230). Data are shown in concentration (pg/mL) for each individual case before (on the left side, square mark) and after treatment with pasireotide (on the right side, triangle mark), per cytokine, chemokine or growth factor. n=16.

Interestingly, the TAF expression levels of SST2 increased after pasireotide treatment (p=0.020), although there were no changes in the expression of SST1 and SST5 (Figure 4.16).

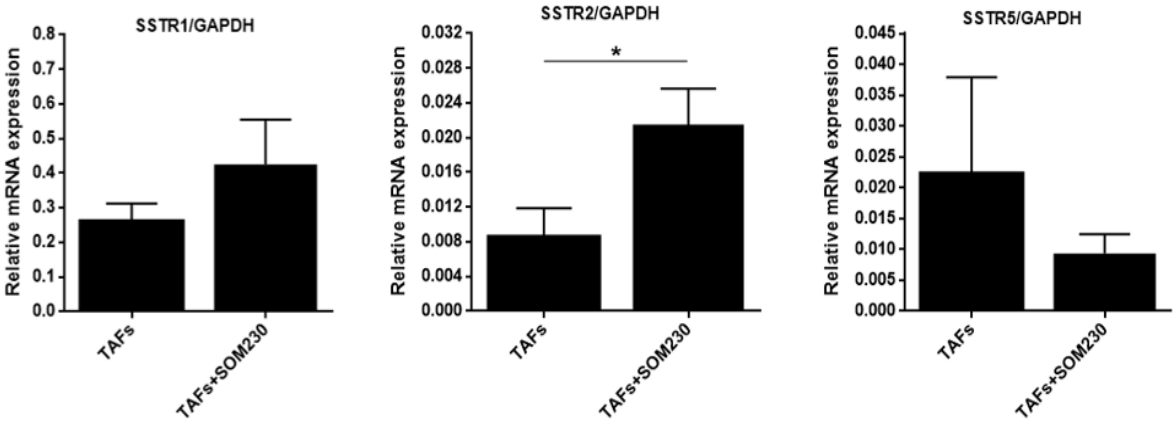

Figure 4.16: SST expression profile in TAFs at baseline and after pasireotide treatment
Somatostatin receptor (SST) expression profile in human PA-derived TAFs determined by RT-qPCR, at baseline and after treatment with pasireotide (SOM230). Data are shown as relative *SSTx* mRNA fold change expression to *GAPDH*, mean±SEM, determined using the standard curve method. n=16. *,<0.05, **,<0.01, ***,<0.001 (Mann Whitney U test).

Discussion

TAFs determine tumour initiation, proliferation, invasiveness and clinical outcomes for many types of tumours[383,384], but their role in PAs has never been studied. My data suggest that PA-derived TAFs are a source of cytokines which may impact on tumour behaviour. Of the TAF-derived cytokines studied, IL-6 and CCL2 emerged as potential mediators of PA invasiveness. My human data are strengthened by *in vitro* data providing mechanistic insights into the crosstalk between TAFs and pituitary tumour cells. In my *in vitro* cell model, I confirmed that TAF-derived factors influence pituitary tumour cells leading to morphological changes, increased invasion and migration, and EMT activation, effects not induced by normal skin fibroblast-derived factors. Hence, TAF-derived cytokines, together with factors released from tumour or immune cells (Chapter 3), may play a key role in TME modulation and in the aggressiveness of PAs (Figure 3.33). The observed inhibitory effect of pasireotide on TAF cytokine secretion highlights a promising indirect anti-tumoural effect of SSAs by targeting TAFs, in addition to any direct effect on tumour cells[391,577].

TAFs are an active source of cytokines which can influence PA phenotype and aggressiveness

TAFs are components of the TME in different tumours, including in PAs[395], and these cells are active sources of cytokines and growth factors[383,384,574]. I found highly secreted levels of CCL2, CCL11, VEGF-A, CCL22, IL-6, FGF-2 and IL-8 in TAF supernatants. The secretome from NFPA-TAFs and somatotrophinoma-TAFs did not differ suggesting that TAF intrinsic biology within the TME of PAs may not vary according to the PA histiotype.

CCL2 levels were higher from TAFs isolated from PAs with more proliferation and more capillaries, suggesting a role for TAF-derived CCL2 in PA aggressiveness and angiogenesis. The reason for the observed gender difference in CCL2 secretion is unclear, as no gender-specific effect has previously been described for CCL2 release[601,602]. CCL2 has a number of roles, including in angiogenesis, cell proliferation and invasion[583]. While CCL2 in PAs has not previously been described in the literature, cell culture supernatants and lysates of craniopharyngiomas show significant release of CCL2[541]. CCL2 was also one of the main chemokines released from primary cultured PA cells (Chapter 3).

IL-6 plays a role in the progression and aggressiveness of PAs[214,230,237-239]. Invasive PAs have a high proportion of IL-6 expression (67.5%), while non-invasive PAs expressed IL-6 only in 22.5% of cases[249]. Suppression of the cytokine transducer gp130, which usually results in inhibition of IL-6

secretion, impaired the development of transplanted GH3 cell tumours in nude mice[603]. In GH3 cells, IL-6 stimulates cell proliferation and DNA synthesis, as well as GH and PRL release[241]. IL-6 can also be secreted by non-tumoural folliculo-stellate cells, which can have paracrine effect on pituitary tumour cells causing increased proliferation and aggressiveness[230,248,253,254]. My study showed that TAF-derived IL-6 levels were higher in PAs with cavernous sinus invasion, supporting a possible role for the paracrine effects of IL-6 in PA invasiveness. Thus, IL-6 may represent a drug target for PAs to reduce the paracrine effects of TAFs.

Chemokines and growth factors, such as PDGFs[588,590], often secreted by TAFs or other non-tumoural cells of the TME, and are able to induce EMT[466-468]. In my study, TAF-derived PDGF-AA levels were negatively correlated with E-cadherin expression, suggesting a possible role for the TAF secretome in promoting EMT in PAs, in line with data from my *in vitro* experiments.

TAFs have been implicated in the recruitment of immune cells into the TME[591], including macrophages, and they can even promote macrophage polarisation into the M2 subtype[604], thus contributing for the remodeling of the TME[384,585]. In my study, I found a correlation between TAF-derived FGF-2 levels and the amount of PA-infiltrating macrophages, suggesting a potential chemotaxis role for some of the TAF-derived factors. FGF-2 is a growth factor secreted by different cells, including TAFs, and has a recognised role in macrophage chemotaxis[592-594] among other biological functions[605]. I also observed that PAs with relatively more M2-macrophages and fewer M1-macrophages (M2:M1 ratio ≥2) had higher TAF-derived FGF-2 and CXCL1 levels, two proteins able to induce M2-macrophage polarisation[595-597].

The functional crosstalk between pituitary tumour cells and fibroblasts

My *in vitro* data showed that TAF-derived factors, but not normal skin fibroblasts factors, are able to induce numerous effects on GH3 cells. Direct induction of EMT, in line with increased invasion, migration and altered cell shape, suggest that TAF-derived factors interact with pituitary tumour cells to influence their behaviour and invasiveness. I noted a non-significant trend for increased GH3 cell migration towards skin fibroblast-CM, less marked than in the presence of TAF-CM, which is not surprising considering that skin fibroblasts are also a source of cytokines and chemokines[598,599], suggesting that fibroblast factors in general may alter tumour cell migration. However, invasion requires not only the capacity for cells to migrate, but also their ability to secrete enzymes to degrade matrigel[537,606]; this seems to be induced only by TAF-derived factors, and not by factors derived from normal skin fibroblasts. In fact, skin fibroblast-CM was not able to increase invasion, whereas TAF-CM remarkably increased GH3 cell invasion in comparison to

complete medium, and almost significantly in comparison to skin fibroblast-CM. EMT induction by TAF-derived factors, a crucial process for migration and invasion of neoplastic cells[466], support my human data linking cavernous sinus invasion and TAF-derived cytokines, particularly IL-6, an interleukin of high importance for fibroblast biology[586,607].

Pasireotide inhibits cytokine secretion from TAFs

Considering that TAF-derived IL-6 can be involved in cavernous sinus invasion, and CCL2 may be relevant for proliferation and angiogenesis of PAs (as suggested by this study), the anti-secretory effect of pasireotide observed for these 2 particularly TAF-derived cytokines may be of most importance in the modulation of the TME and the aggressiveness of PAs.

Somatostatin controls hormone secretion and proliferation in normal and neoplastic pituitary, and reduced IL-6 and IL-8 in human somatotrophinoma cultures[234,608]. The inhibitory effect of somatostatin on IL-6 secretion was also shown in non-pituitary cells[609-611]. In a study using human NFPA primary cultures, it was demonstrated that pasireotide can inhibit tumour cell viability by inhibiting VEGF secretion[612]. Pasireotide, by activating SST1 expressed in pancreas cancer-associated fibroblasts, inhibited various cytokines including IL-6, with abrogation of metastasis and prevention of EMT[385,391]. The inhibitory effect of pasireotide on IL-6 release from PAs-derived TAFs observed here suggests that this effect may play a role in the effectiveness of pasireotide. Furthermore, the benefits of targeting TAFs with pasireotide likely extends beyond its role in inhibiting cytokine release. Fibroblasts are mediators of fibrosis due to their ability to secrete collagen, proteoglycans and other ECM proteins[383,585]. A correlation between collagen-producing cells and fibrous deposition was seen in PAs, with thyrotrophinomas having the highest number of collagen-producing cells and fibrous matrix[395], in line with their recognised firm consistency[613], which may hinder surgical resection[614]. Thus, a drug able to target TAFs and reduce fibrosis may be valuable in improving outcomes in patients with PAs. Emerging data support the anti-fibrotic properties of SSA, mainly by inhibition of fibroblast proliferation and induction of apoptosis[615-617]. Pasireotide was effective as methylprednisolone in patients with Graves´ orbitopathy[618], a condition in which SST-expressing orbital fibroblasts are key pathophysiological elements[616,617].

The anti-secretory and anti-proliferative effects of a specific SSA in a certain PA depends on its SST expression pattern and the SST binding profile of that SSA[164,577,619]. However, the mere abundance of a given SST does not necessarily correlate with the level of response to a SSA with strong affinity for that SST[619]. In fact, some studies found no correlation between the inhibitory effects of octreotide or pasireotide and a particular SST expression pattern, or even less prominent response

to pasireotide in pituitary tumour cells expressing high levels of SST5[619,620]. The reasons for such discrepancies are unknown, but may well be related to the extrapituitary effects of SSAs, such as their modulatory effect directly to non-tumour cells present in the TME, including TAFs. The pharmacological effect on TAFs might also explain why *in vivo* pasireotide efficacy is superior than octreotide in patients with acromegaly[621,622], while *in vitro* pasireotide and octreotide inhibit pituitary tumour cells similarly[619,620]. There are contradictory observations in NFPAs, where octreotide was able to stabilise the tumour size in most patients[623] whereas *in vitro* there was a poor response or even a paradoxical increase in cell viability after treatment with both octreotide and pasireotide[619].

Limitations of this study

The limitations of this study include the fact that I studied only a small cohort of cases with a relatively short postoperative follow-up, as this study is based on fresh primary cell culture, rendering data on longer term clinical outcomes and recurrence unavailable. The cytokine array experiments lack fresh fibroblasts derived from NP as controls, thus I used an alternative suitable control - normal skin fibroblasts. In the *in vitro* experiments I used a rat pituitary tumour cell line rather than a human cell line, as a human pituitary tumour cell line does not exist.

Conclusions

TAFs, as part of the TME of PAs, represent a source of cytokines influencing tumour proliferation, invasiveness and neovascularisation, with IL-6 and CCL2 emerging as key mediators. My *in vitro* findings confirm that TAF-derived factors, but not normal skin fibroblast-CM, influence pituitary tumour cells inducing EMT-like morphological changes, increasing invasion and migration, as well as activating EMT. My data also suggest that the inhibitory effects of pasireotide on cytokine release from TAFs may play a key role in its anti-tumoural effects.

Chapter 5: Other tumour microenvironment-related oncogenic mechanisms in pituitary adenomas

Introduction

The TME is determined by the non-tumour cells surrounding neoplastic cells, including immune cells (such as macrophages, lymphocytes and neutrophils) or stromal cells (such as fibroblasts), which determine not only the biological behaviour of tumour cells but also modulate different oncogenic mechanisms such as angiogenesis, ECM remodelling and EMT through a complex network of cytokines, chemokines and growth factors (Figure 5.1)[204,207,429].

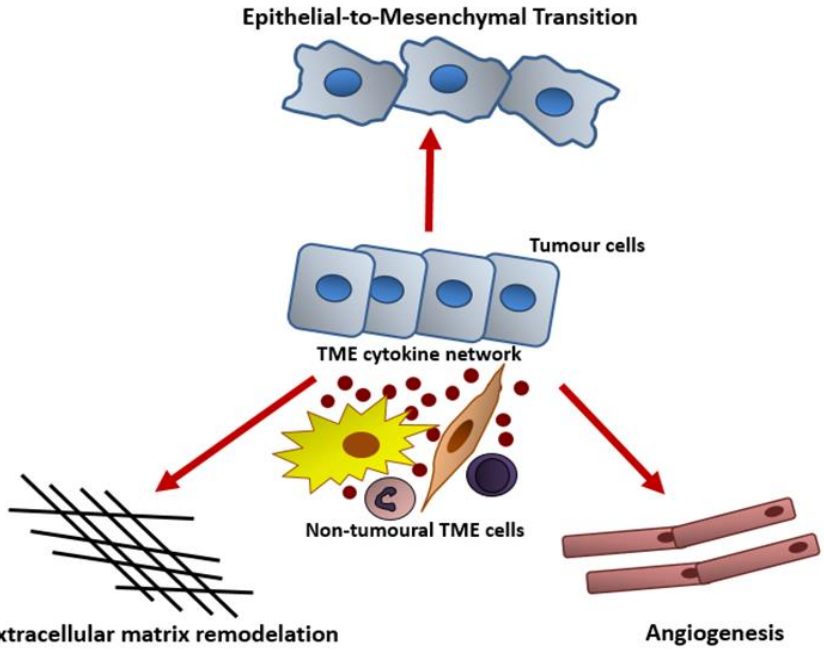

Figure 5.1: TME-related oncogenic mechanisms
Tumour cells release different cytokines and growth factors promoting the recruitment and modulation of immune cells (including macrophages, lymphocytes and neutrophils) and stromal cells (including fibroblasts) within the tumour microenvironment (TME). In turn, these TME elements and their crosstalk influence several oncogenic mechanisms, such as angiogenesis, extracellular matrix remodelling and epithelial-to-mesenchymal transition.

Angiogenesis is an essential process for tumour development, growth, invasion and metastasis and is regulated by different non-cellular TME components, such as cytokines, chemokines, growth factors or ECM-remodelling enzymes[297,304,421], as well as by different cells such as macrophages[339] or TAFs[469,585]. The degree of tumour angiogenesis is commonly assessed by the microvessel density, i.e. the number of vessels per given area which can be, for instance, a high-

power field, although other vascular parameters are also relevant[304]. Although angiogenesis has been studied to some extent in PAs[297,304,421], research exploring the relationship between angiogenic processes in PAs and its TME is lacking, contrasting with the extensive data available for other cancers[417,548,624].

Different proteases, including MMPs, are able to change the ECM in the TME[430-432], interfering with the tumour/non-tumour cell and ECM interactions[429]. ECM remodelling plays a role in several oncogenic mechanisms, such as angiogenesis, proliferation and metastasis, and thus ECM-degrading proteases have an important role in the modulation of the TME. MMPs are important ECM proteases in cancer[207,439], being upregulated and released into the TME either by neoplastic or non-neoplastic cells (Figure 5.2)[435-438]. Associations between MMP activity and invasiveness have been shown in different cancers[440-443]. Several studies described an association between MMP expression and invasive PAs, particularly MMP-2 and MMP-9 (type IV collagenases essentially to degrade type IV collagen present in the cavernous sinus)[448,450-453], but also MMP-14[460]. Nevertheless, the modulatory role of the different TME components in the expression of MMPs has never been addressed in PAs.

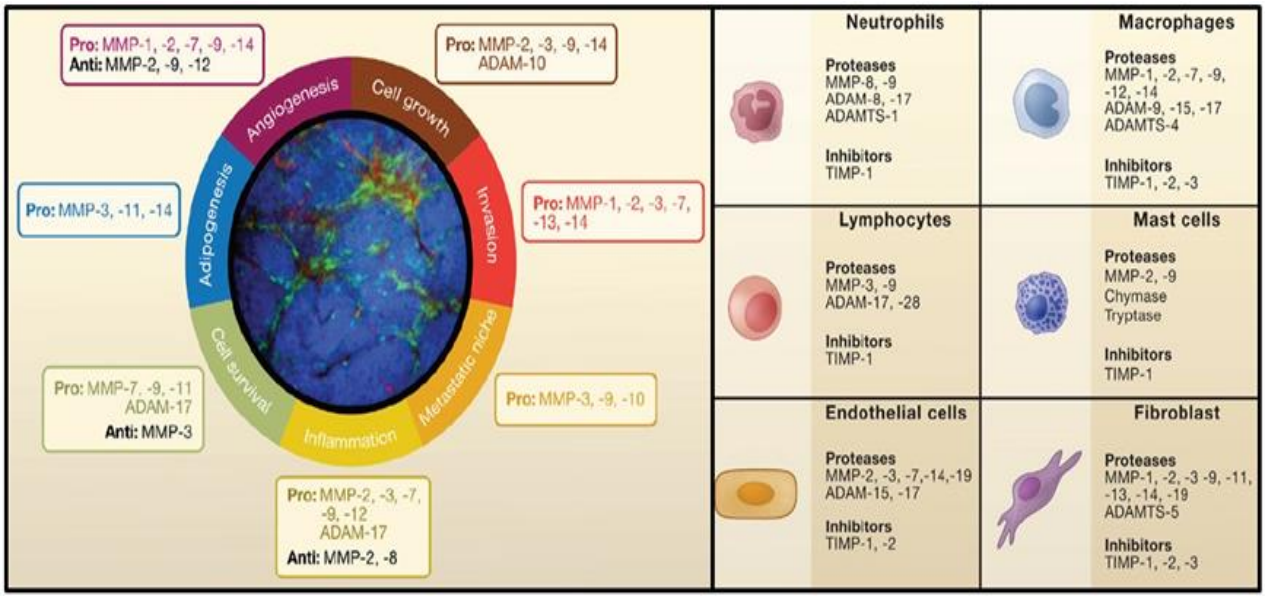

Figure 5.2: MMPs main sources within the TME and their role in the modulation of the TME
Several oncogenic mechanisms that are modulated by matrix metalloproteases (MMPs) in the tumour microenvironment (TME). In the figure are represented the most important families of ECM-degrading proteases: MMPs and ADAMs, both able to modulate and promote pro- or anti-tumoural effects within the TME. MMPs are mainly provided by non-malignant cells, such as inflammatory or stromal cells present in the TME, including neutrophils, macrophages, lymphocytes, mast cells, fibroblasts and endothelial cells, however neoplastic cells can also release MMPs into the TME. Adapted from Kessenbrock *et al.* (2010)[441].

EMT, a process that increases the invasiveness of a tumour, is characterised by the loss of E-cadherin and is determined by complex interactions between different TME elements, including cytokines, chemokines and growth factors, as well as different TME cells, playing a key role in tumourigenesis, invasion, progression and metastasis[466-468]. EMT and its complex regulation remain largely unexplored in PAs. It has been shown that PAs may undergo EMT, although they often they display a partial/incomplete EMT signature[505,513]. Research linking cellular and non-cellular TME elements and EMT in PAs is lacking.

Neural cell adhesion molecule (NCAM), also known as CD56, is a cell surface glycoprotein important for the mechanical stability and cohesion among cells, as well as between cells and the ECM. In addition, NCAM also participates in other cellular activities including proliferation, differentiation, mitogenesis and apoptosis[625,626]. NCAM multiple functions depend mainly on its various forms resulting from alternative splicing, glycosylation or polysialylation status, and expression patterns at different developmental stages[625,627]. NCAM, characterised by 5 extracellular immunoglobulin-like and 2 fibronectin III domains (explaining its adhesion properties), is mainly expressed by neural tissues (neurons and glia) where it mediates homophilic adhesion of neural cells, activating a number of intracellular signalling cascades and regulating neurite outgrowth (Figure 5.3)[625,626]. NCAM is also found in haematopoietic cells, including NK cells[628], muscle tissues and endocrine cells[625,629].

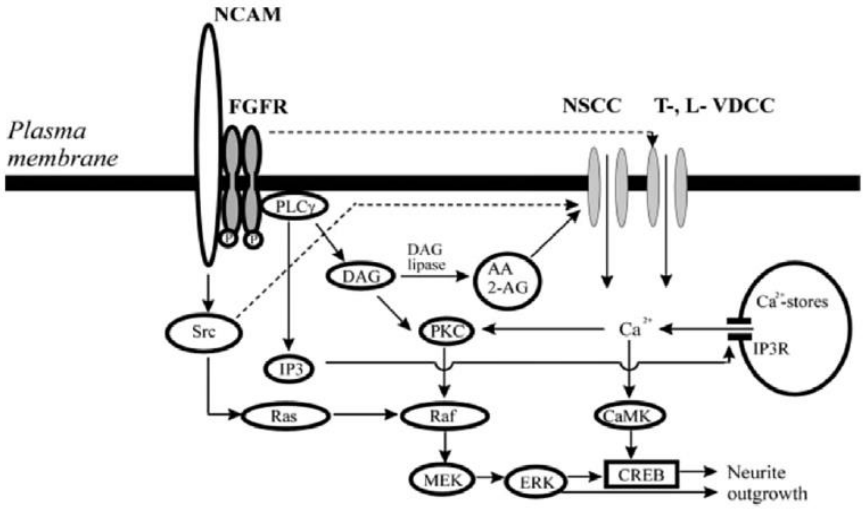

Figure 5.3: Molecular mechanisms of NCAM action in neuronal tissues
2-AG, 2-arachidonoylglycerol; AA, arachidonic acid; Ca, calcium; CaMK, calmodulin protein kinase; CREB, cAMP response element binding; DAG, diacylglycerol; ERK, extracellular-signal-regulated kinase; FGFR, fibroblast growth factor receptor; IP3, inositol triphosphate; IP3R, inositol triphosphate receptor; NCAM, neural cell adhesion molecule; NSCC, non-selective cationic channel; PKC, protein kinase C; PLC, phospholipase C; VDCC, voltage-dependent calcium channel. Weledji & Assob (2014)[625].

NCAM is overexpressed in many cancers, particularly in gliomas, neuroblastomas, astrocytomas, medulloblastomas, retinoblastomas, rhabdomyosarcomas, thyroid cancer, small cell lung cancer and haematological malignancies[625,630,631], with modest expression levels in other solid tumours (Figure 5.4). Increased NCAM expression is generally associated with poorer outcomes in cancer, which may result from the ectopic expression of NCAM and/or from the shed of its extracellular domain which stimulates migration, invasion and survival of tumour cells[625,630,632-634]. However, in some malignancies the NCAM loss has been linked with tumourigenesis, invasiveness and/or unfavourable cancer outcomes, most likely as a result of lacking NCAM adhesion properties[635,636].

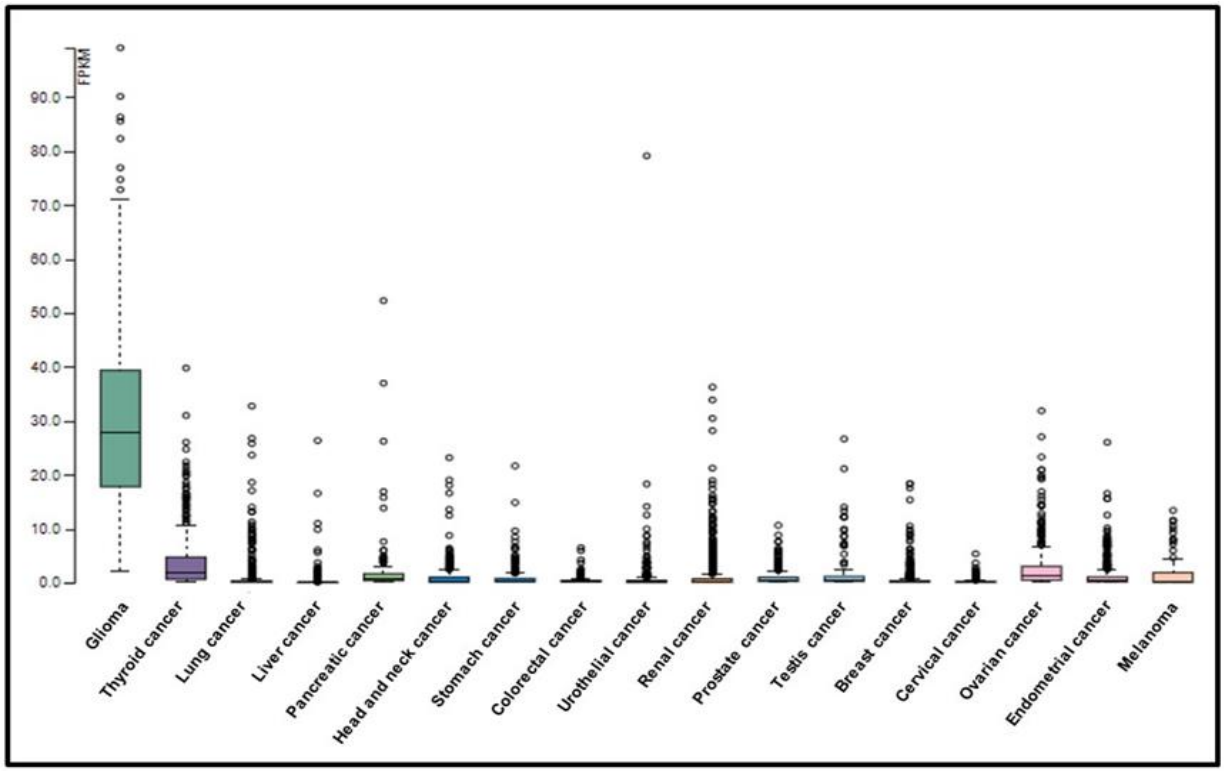

Figure 5.4: RNA expression levels of NCAM in different malignancies
Adapted from Protein Atlas (https://www.proteinatlas.org/ENSG00000149294-NCAM1/pathology).

NCAM is expressed by foetal and adult rat pituitary cells[637], and may regulate various pituitary functions including hormone secretion[626]. NCAM was expressed in most PAs, without major differences among PA subtypes, except for prolactinomas which express lower levels of NCAM[626,629,638-640]. The release of soluble NCAM was also observed in some PAs[640]. Increased NCAM was associated with PA invasion, particularly its polysialylated form, which was not detected in the NP[627,641]. However, other studies have reported no association between NCAM expression and tumour invasiveness[639,642]. The influence of the different elements of the TME in the expression of NCAM in PAs has not currently been studied.

Aims

Overall aim

To study the role of different TME components (cytokines, immune cells and TAFs) in the modulation of different oncogenic mechanisms in PAs.

Specific aims

1. To characterise angiogenesis in human PAs and in NP
2. To study PA microvessel density and vascular architecture in view of PA- and TAF-derived cytokines and PA-infiltrating immune cells
3. To study the expression of ECM-remodelling enzymes MMP-9 and MMP-14 in human PAs and in NP
4. To study the role of PA- and TAF-derived cytokines and PA-infiltrating immune cells in the modulation of MMP-9 and MMP-14 expression
5. To characterise EMT in human PAs and in NP
6. To study the role of the PA- and TAF-derived cytokines and PA-infiltrating immune cells in the modulation of EMT in PAs
7. To characterise the expression of NCAM in human PAs and in NP
8. To study the role of PA- and TAF-derived cytokines and PA-infiltrating immune cells in the modulation of NCAM expression in PAs

Results

Angiogenesis in human pituitary adenomas

I analysed my cohort of 24 PAs with clinico-pathological, cytokine and infiltrating immune cells data for microvessel density and vasculature architecture parameters, staining the vessels with the specific endothelial marker $CD31^{643}$, aiming to study the influence of the cytokine network and immune infiltrates in the TME of human PAs.

Angiogenesis in PAs vs NPs

The vasculature is significantly different between PAs and NP (Figure 5.5), as shown previously[297,304,421,427]. When compared to NP, PAs showed remarkably lower microvessel density (p=0.015) and microvessel area/HPF (p<0.001). In terms of vascular architecture parameters, there were no major differences except for the fact that vessels were less round in PAs than those seen in NPs (p<0.001) (Figure 5.5).

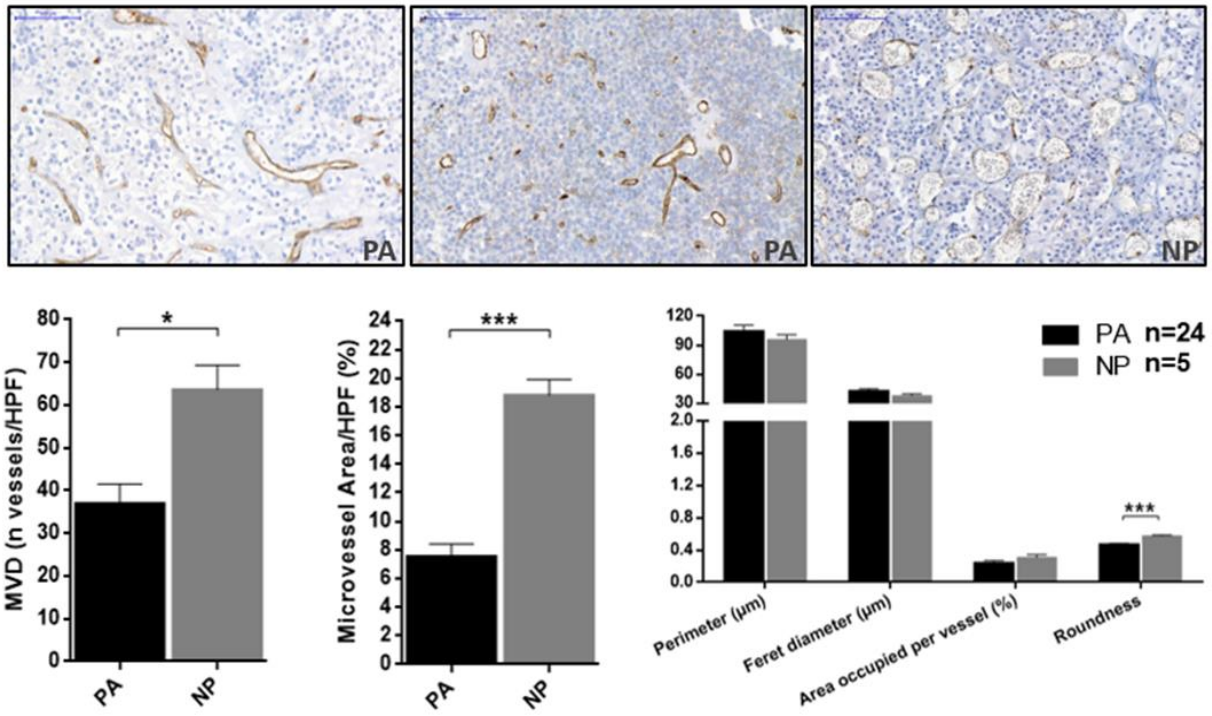

Figure 5.5: Angiogenesis in PAs and in NPs
Microvessel density (MVD) and vasculature architecture parameters differences between human pituitary adenomas (PA) and normal pituitary (NP) are shown. PA (n=24) and NP (n=5) tissue sections were stained for CD31. CD31-vessels were counted in 3 different high power fields (HPF) to obtain MVD (number of vessels/HPF). CD31-stained 20x magnification fields were analysed with ImageJ and vessel contour was manually traced in order to obtain the vasculature architecture parameters: total microvessel area, area occupied per vessel, vessel perimeter, vessel Feret's diameter and roundness. Data are shown as mean±SEM. Representative images of vessels from 2 PAs and 1 NP are shown (20x). *, <0.05, **, <0.01, ***, <0.001 (Mann Whitney U test).

Angiogenesis and clinical features in PAs

I found no association between microvessel density, total area or vascular architecture parameters and the different PA clinico-pathological features. In particular, there were no correlations with cavernous sinus invasion, Ki-67 or PA grades according to the Trouillas classification[43]. However, re-operated PAs tended to have increased microvessel density (p=0.072) and vessel roundness (p=0.074) than PAs operated for the first time (Table 5.1).

n PAs = 24	MVD Mean ± SEM	TMVA Mean ± SEM	Perimeter Mean ± SEM	Feret's diameter Mean ± SEM	Area per vessel Mean ± SEM	Roundness Mean ± SEM
Gender						
Male (n=16)	34.77 ± 5.18	6.84 ± 0.72	106.17 ± 8.46	43.15 ± 3.53	0.25 ± 0.49	0.47 ± 0.15
Female (n=8)	41.54 ± 8.88	8.96 ± 2.13	101.45 ± 6.57	41.06 ± 2.47	0.22 ± 0.36	0.47 ± 0.01
Headache at diagnosis						
Yes (n=8)	36.88 ± 8.96	6.37 ± 1.27	98.21 ± 6.62	39.69 ± 2.50	0.19 ± 0.02	0.45 ± 0.15
No (n=16)	37.11 ± 5.24	8.14 ± 1.11	107.79 ± 8.36	43.83 ± 3.48	0.27 ± 0.05	0.47 ± 0.01
Visual impairment at diagnosis						
Yes (n=13)	40.23 ± 7.43	8.51 ± 1.23	112.52 ± 8.97	46.05 ± 3.77	0.27 ± 0.06	0.46 ± 0.02
No (n=11)	33.24 ± 4.46	6.42 ± 1.13	95.23 ± 6.99	38.19 ± 2.63	0.20 ± 0.03	0.47 ± 0.01
Hypopituitarism at diagnosis						
Yes (n=11)	39.06 ± 6.42	8.72 ± 1.23	111.35 ± 9.27	45.09 ± 3.76	0.28 ± 0.07	0.47 ± 0.01
No (n=13)	35.31 ± 6.44	6.55 ± 1.15	98.88 ± 7.74	40.21 ± 3.26	0.21 ± 0.03	0.47 ± 0.02
Cavernous sinus invasion						
Yes (n=10)	32.00 ± 6.18	7.53 ± 1.14	115.30 ± 12.40	46.69 ± 5.10	0.31 ± 0.08	0.45 ± 0.02
No (n=14)	40.62 ± 6.30	7.56 ± 1.25	96.95 ± 4.64	39.42 ± 1.96	0.19 ± 0.01	0.48 ± 0.01
Ki-67						
< 3% (n=19)	37.18 ± 4.69	7.19 ± 0.81	101.13 ± 6.81	40.88 ± 2.77	0.23 ± 0.04	0.48 ± 0.01
≥ 3% (n=5)	36.47 ± 13.39	8.92 ± 2.87	117.75 ± 11.74	48.42 ± 5.03	0.27 ± 0.04	0.43 ± 0.03
Trouillas grade classification						
1a (n=11)	38.24 ± 6.47	6.65 ± 0.99	94.12 ± 5.53	38.23 ± 2.35	0.18 ± 0.02	0.49 ± 0.01
1b (n=3)	49.33 ± 19.73	10.90 ± 4.74	107.35 ± 4.85	43.77 ± 1.87	0.21 ± 0.01	0.45 ± 0.02
2a (n=8)	35.71 ± 7.17	7.93 ± 1.41	110.78 ± 14.16	44.52 ± 5.72	0.30 ± 0.10	0.46 ± 0.01
2b (n=2)	17.17 ± 1.84	5.95 ± 0.36	133.37 ± 30.03	55.39 ± 12.69	0.35 ± 0.06	0.40 ± 0.07
Re-operation						
Yes (n=5)	52.67 ± 11.66§	8.78 ± 1.77	85.88 ± 5.83	34.71 ± 2.76	0.17 ± 0.02	0.50 ± 0.01§
No (n=19)	32.91 ± 4.47	7.22 ± 0.98	109.52 ± 7.02	44.49 ± 2.87	0.26 ± 0.04	0.46 ± 0.01

Table 5.1: Angiogenesis and clinical features in PAs
Microvessel density (MVD), total microvessel area (TMVA) and vascular architecture parameters among the cohort of 24 PAs according to different clinical features. MVD is expressed as vessels/HPF. TMVA is expressed as percentage of microvessel area/HPF. Vascular architecture parameters are expressed as follows: perimeter and Feret's diameter in µm; area occupied per vessel in percentage of the HPF; roundness is expressed with a numeric value comprised between 0-1. Data are shown as mean±SEM, per feature. *p* values were non-significant for all comparisons. §, 0.05 < 0.1 (Mann Whitney U test were used for all comparisons, except for variable Trouillas grade classification where one-way ANOVA test was used).

Angiogenesis in NFPAs vs somatotrophinomas

Microvessel density did not differ among NFPAs and somatotrophinomas, but the total area, vessel perimeter and Feret's diameter were significantly higher in NFPAs in comparison to somatotrophinomas (Figure 5.6). The area occupied per vessel tended to be also higher in NFPAs in comparison to somatotrophinoma vessels (p=0.097).

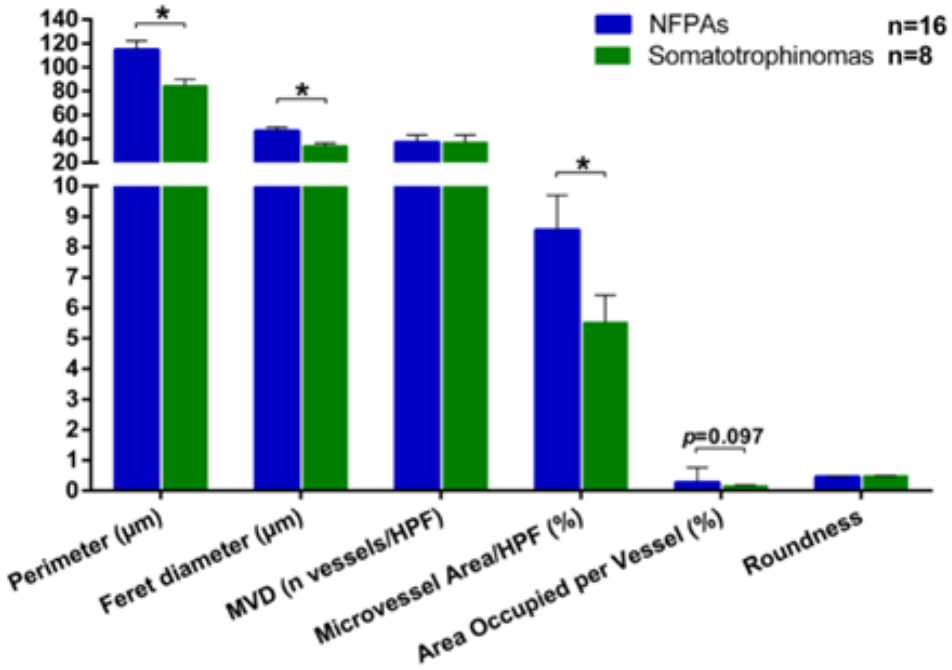

Figure 5.6: Angiogenesis in NFPAs and somatotrophinomas
Microvessel density (MVD) and vasculature architecture parameters differences between human NFPAs and somatotrophinomas are shown. NFPA (n=16) and somatotrophinoma (n=8) tissue sections were stained for CD31. CD31-vessels were counted in 3 different high power fields (HPF) to obtain MVD (number of vessels/HPF). CD31-stained 20x magnification fields were analysed with Image J and vessel contour was manually traced in order to obtain the vasculature architecture parameters: total microvessel area, area occupied per vessel, vessel perimeter, vessel Feret's diameter and roundness. Data are shown as mean±SEM. *, <0.05, **, <0.01, ***, <0.001 (Mann Whitney U test).

There were no differences between somatotrophinomas untreated (n=2) and those pre-treated with SSAs (n=6) regarding microvessel density (p=0.740), total microvessel area (p=0.221), vessel perimeter (p=0.637), Feret's diameter (p=0.496), area occupied per vessel (p=0.541) or microvessel roundness (p=0.539).

Overall, there were not many correlations between microvessel density, total microvessel area and the vascular architecture parameters, and pituitary hormonal levels in my cohort of PAs as a whole and per PA subtype (Appendix 9). However, I found a significant negative correlation between serum IGF-1 and both perimeter and Feret's diameter in the whole cohort of PAs (both NFPAs and somatotrophinomas) (Figure 5.7), suggesting a possible role for GH/IGF-1 levels in the differential modulation of the vessel architecture among NFPAs and somatotrophinomas. This statistical significance was lost when the different PA subtypes were analysed separately (Appendix 9), suggesting that the absolute GH/IGF-1 levels, or the extent of GH excess in somatotrophinomas, may not explain the vascular architecture heterogeneity observed within the same PA subgroup.

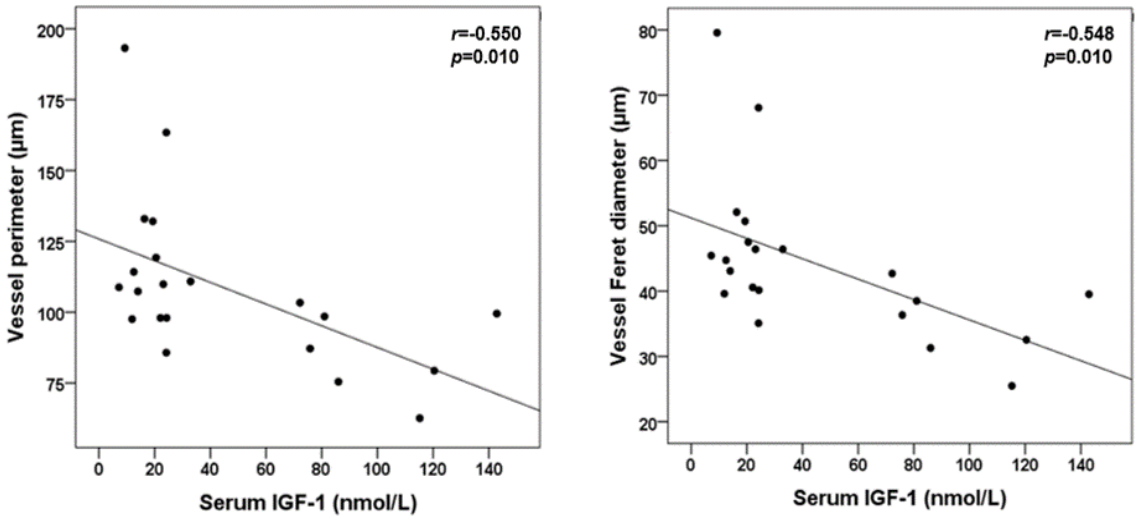

Figure 5.7: Correlation between serum IGF-1 levels and vessel perimeter and Feret's diameter in PAs
Number of PAs analysed = 24. *p* values were determined by the Pearson correlation coefficient *r*.

Within the somatotrophinoma subgroup, there was a correlation between serum PRL and area occupied per vessel (r=0.958, p=0.010, Figure 5.8-A), and within the NFPA subgroup I also noted a positive correlation between serum PRL and microvessel density (r=0.542, p=0.045, Figure 5.8-B), suggesting a possible role for PRL in the modulation of angiogenesis in both somatotrophinomas and NFPAs.

Serum levels of FT4 were also correlated with microvessel density among somatotrophinomas (r=0.875, p=0.010, Figure 5.8-C), consistent with the angiogenic properties of thyroid hormones[644-646], but not within the NFPA subgroup (Appendix 9).

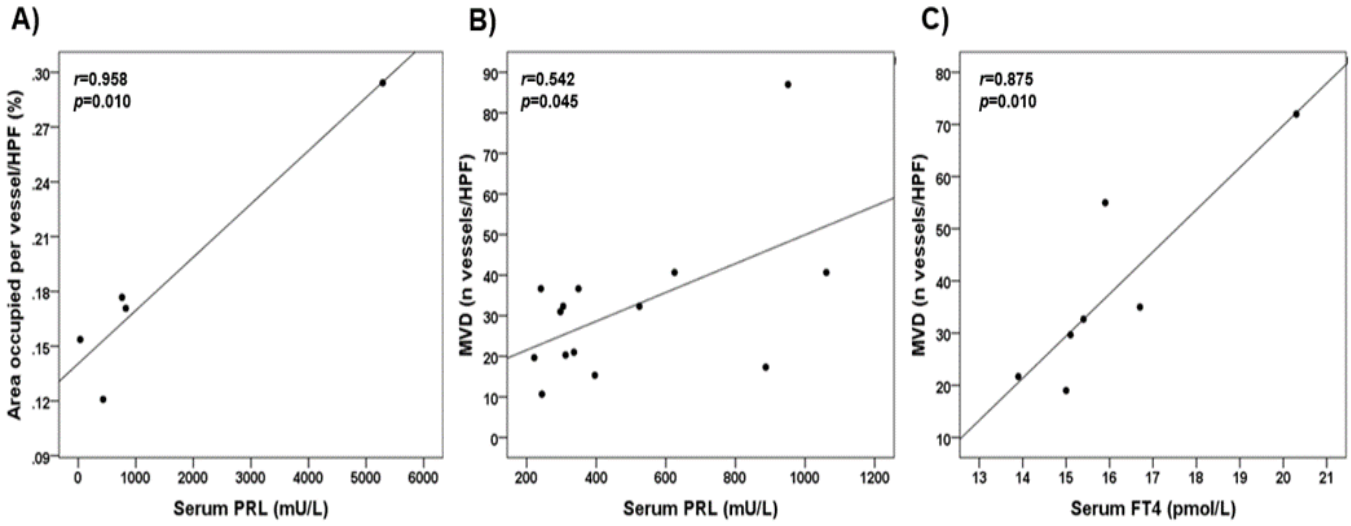

Figure 5.8: Serum pituitary hormone levels and vessel parameters in PAs
Statistical significant correlations between: A) serum PRL levels and area occupied per vessel/HPF within somatotrophinomas (n=8); B) serum PRL levels and microvessel density (MVD) within NFPAs (n=16); C) FT4 levels and MVD in somatotrophinomas (n=8). *p* values were determined by the Pearson correlation coefficient *r*.

Angiogenesis and PA-derived cytokine secretome

There were no significant correlations between PA-derived cytokines and microvessel density or microvessel area (Appendix 9), even for molecules with recognised angiogenic properties such as VEGF-A, IL-8, FGF-2 and CCL2[297,417]. However, there was a negative correlation between PA-derived FGF-2 levels and vessel perimeter (r=-0.407, p=0.048) (Figure 5.9-A). There was also as a significant correlation between PA-derived CXCL10 and the area occupied per vessel (r=0.407, p=0.049), but this statistical significance was driven by 2 outliers while the remaining 22 cases demonstrated no correlation (Figure 5.9-B). Nevertheless, these findings highlight the ability for some of these secreted proteins to affect PA vessel morphology, specifically FGF-2[365].

When the data were analysed separately per PA type, within the NFPA subgroup no correlations between PA-derived cytokines and microvessel density or any of the vasculature architecture parameters were seen (Appendix 9). Among somatotrophinomas, I observed a correlation between the area occupied per vessel and PA-derived IL-8 (r=0.725, p=0.042) (Figure 5.9-C) and FGF-2 (r=0.769, p=0.026) (Figure 5.9-D).

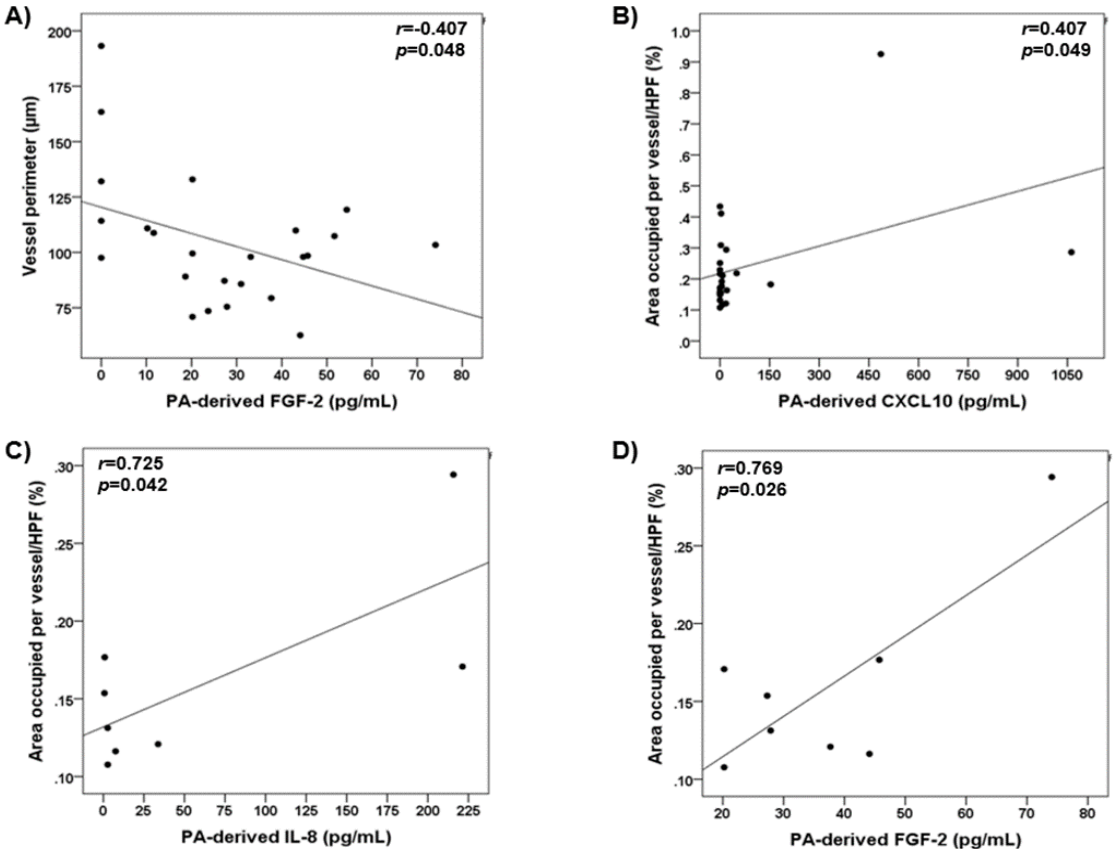

Figure 5.9: PA-derived cytokines and vessel parameters in PAs

Statistical significant correlations between: A) FGF-2 levels and vessel perimeter in the whole cohort of PAs (n=24); B) CXCL10 levels and area occupied per vessel/HPF in the whole cohort of PAs (n=24); C) IL-8 levels and area occupied per vessel/HPF within somatotrophinomas (n=8); D) FGF-2 levels and area occupied per vessel/HPF in somatotrophinomas (n=8). *p* values were determined by Pearson correlation coefficient *r*.

Angiogenesis and PA-infiltrating immune cells

Microvessel density was higher in PAs with lower FOXP3+ T cells content (Figure 5.10-A and Appendix 9) and also tended to be higher in PAs with more macrophages (Figure 5.10-B) and more CD4+ T cells (Figure 5.10-C). PAs with more CD4+T cells were significantly associated with increased total microvessel area (Figure 5.10-D). M2:M1 macrophage ratio was also positively correlated with microvessel density (p=0.015) and microvessel area (p<0.001) (Figure 3.17 in Chapter 3 and Appendix 9). Infiltrating immune cells do not seem to affect PA vessel morphology, as there were no correlations between different infiltrating immune cells and vessel architecture, except regarding B cells which content was associated with increased microvessel roundness (Figure 5.10-F and Appendix 9).

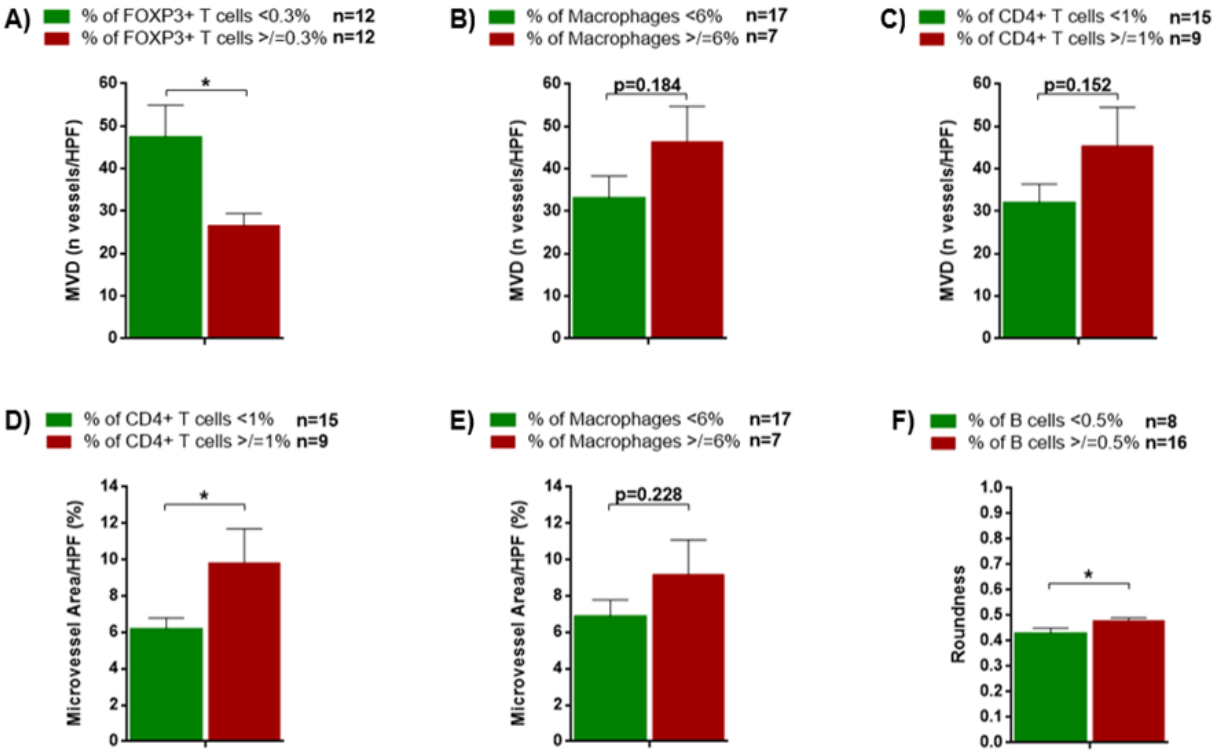

Figure 5.10: PA-infiltrating immune cells and angiogenesis in PAs
Microvessel density (MVD) and vascular architecture parameters in PAs with lower vs higher amounts of FOXP3+ T cells (A), macrophages (B and E), CD4+ T cells (C and D) and B cells (F). Data are shown as mean±SEM. *, <0.05, **, <0.01, ***, <0.001 (Mann Whitney U test).

NFPAs with a higher content of PA-infiltrating CD4+ T cells (≥1%) had increased microvessel density (50.67±10.93 vs 26.56±4.64 vessels/HPF, p=0.044), increased total microvessel area (6.47±0.68 vs 11.24±2.11%, p=0.032) and were more round (0.50±0.01 vs 0.43±0.02, p=0.004) than NFPAs with lower amounts of CD4+ T cells (<1%). Vessels were also more round in NFPAs with less PA-infiltrating B cells (0.38±0.14 vs 0.24±0.03, p=0.048). Vessels from NFPAs with more infiltrating FOXP3+ T cells had increased diameter (132.42±13.42 vs 53.80±5.61µm, p=0.029) and

Feret's diameter (53.80±5.61 vs 40.95±2.05µm, p=0.033) than those NFPAs with fewer FOXP3+ T cells. M2:M1 macrophage ratio was also positively correlated with total microvessel area (r=0.676; p=0.004) and tended to correlate with microvessel density (r=0.408; p=0.117) and area occupied per vessel (r=0.408; p=0.117) (Appendix 9).

Somatotrophinomas with increased amounts of macrophages (≥6%) had larger microvessels than those cases with lower PA-infiltrating macrophages (namely higher perimeter: 101.41±1.93 vs 78.98±5.14µm, p=0.007; higher Feret's diameter: 41.12±1.59 vs 31.90±2.06, p=0.019; each vessel occupied increased area: 0.23±0.06 vs 0.13±0.01%, p=0.031). Among somatotrophinomas there was also a positive correlation between M2:M1 ratio and microvessel density (r=0.801; p=0.017) and between CD8:CD4 ratio and microvessel area (r=0.718; p=0.045) (Appendix 9).

Angiogenesis and TAF-derived cytokine secretome

Within the whole TAF cohort (n=16), TAF-derived levels of CCL2 were positively correlated with microvessel area (r=0.672; p=0.004) (Table 4.4 in Chapter 4 and Appendix 9). However, there were no further correlations between microvessel density or area neither with vessel architecture parameters nor other TAF-derived cytokines (Appendix 9), including for VEGF-A, FGF-2 or PDGF-AA, proteins secreted by fibroblasts with known angiogenic functions[384].

The cytokine secretome analysis from TAFs derived from NFPAs showed significant correlations between CCL2 and total microvessel area (r=0.828; p=0.002), as well as between IL-6 levels and vessel perimeter (r=0.651; p=0.030), Feret's diameter (r=0.618; p=0.043) and area occupied per vessel (r=0.674; p=0.023) (Appendix 9).

There were some significant correlations between released cytokines from TAFs isolated from somatotrophinomas and angiogenic parameters: somatotrophinoma-TAF-derived IL-6 levels correlated with area occupied per vessel (r=0.912; p=0.031), CCL2 levels correlated with both microvessel density (r=0.937, p=0.019) and total microvessel area (r=0.916, p=0.029), and CCL11 concentrations correlated with area occupied per vessel (r=0.883, p=0.092) (Appendix 9).

ECM-remodeling matrix metalloproteinases in human pituitary adenomas

MMP-9 and MMP-14 expression in PAs vs NPs

The expression of both MMP-9 and MMP-14, as measured by immunohistochemistry, differed between PAs and NPs, being remarkably higher in the normal gland than in neoplastic pituitary (Figure 5.11). MMP-9 was expressed by 12 out of 24 PAs (50%) and MMP-14 was detected in 9 out of 24 PAs (37.5%), whereas in NP the MMP-9 and MMP-14 expression was detected in 100% (5/5) and 80% (4/5) respectively.

The expression levels of MMP-9 and MMP-14 did not correlate within the whole cohort of PAs (r=-0.119; p=0.578) or in the NPs alone (r=0.058; p=0.926).

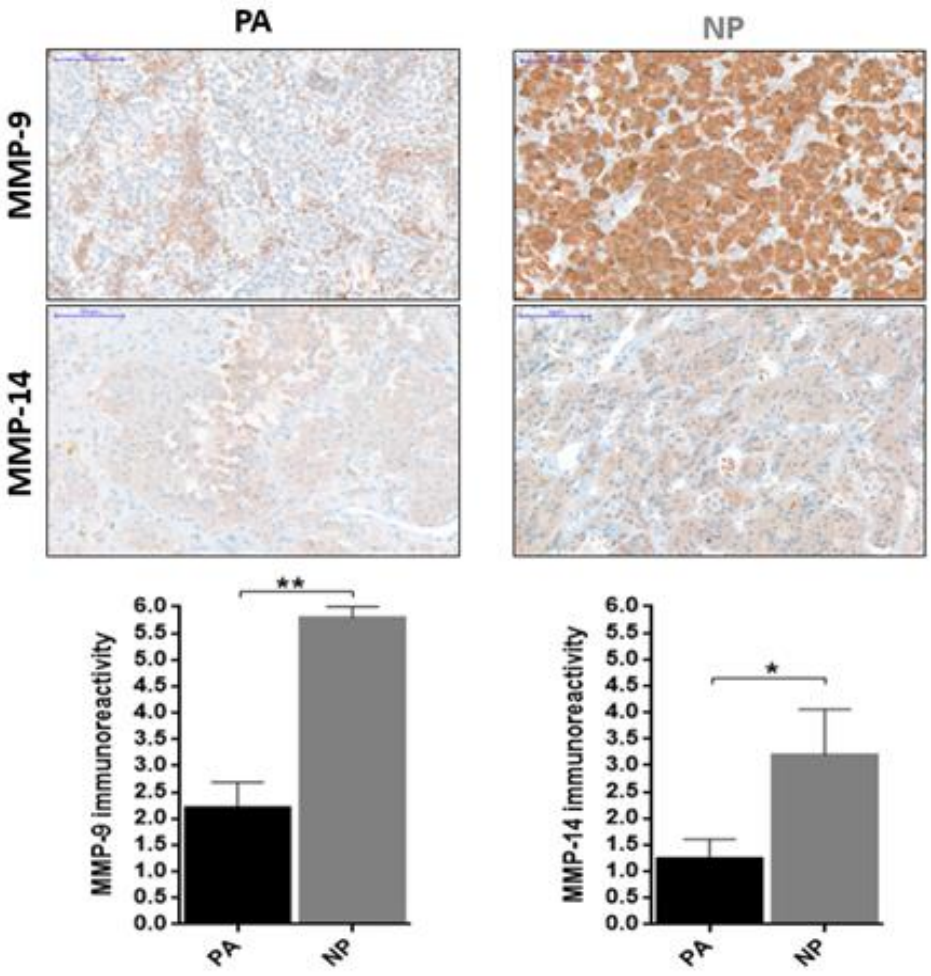

Figure 5.11: MMP-9 and MMP-14 expression in PAs and in NPs
MMP-9 and MMP-14 immunoreactivity differences between human pituitary adenomas (PAs) and normal pituitary (NPs) are shown. PA (n=24) and NP (n=5) tissue sections were stained for MMP-9 and MMP-14 and immunoreactivities measured using a semi-quantitative method. Representative images from MMP-9 and MMP-14 expression in a PA and in a NP are shown (20x). Data are shown as mean±SEM. *, <0.05, **, <0.01, ***, <0.001 (Mann Whitney U test).

MMP-9 and MMP-14 expression and clinical features in PAs

PAs with higher Ki-67 had significantly lower MMP-9 immunoreactivity (p=0.028) and in PAs from patients who presented with visual impairment (p=0.037). On the other hand, PAs from patients who had headache at diagnosis had increased MMP-9 expression (p=0.010). There were no correlation with cavernous sinus invasion or PA grade according to the Trouillas classification[43] and MMP-9 expression (Table 5.2). I found no associations between MMP-14 immunoreactivity and different clinical features (Table 5.2).

PA n = 24	**MMP-9 immunoreactivity** Mean ± SEM	**MMP-14 immunoreactivity** Mean ± SEM
Gender		
Male (n=16)	2.13 ± 0.63	1.56 ± 0.48
Female (n=8)	2.38 ± 0.73	0.63 ± 0.42
	p=0.799	*p*=0.158
Headache at diagnosis		
Yes (n=8)	3.88 ± 0.64	1.75 ± 0.68
No (n=16)	1.38 ± 0.54	1.00 ± 0.42
	***p*=0.010**	*p*=0.333
Visual impairment at diagnosis		
Yes (n=13)	1.31 ± 0.58	1.08 ± 0.50
No (n=11)	3.27 ± 0.68	1.45 ± 0.53
	***p*=0.037**	*p*=0.610
Hypopituitarism at diagnosis		
Yes (n=11)	1.73 ± 0.74	1.00 ± 0.45
No (n=13)	2.62 ± 0.63	1.46 ± 0.55
	p=0.923	*p*=0.635
Cavernous sinus invasion		
Yes (n=10)	2.00 ± 0.68	1.40 ± 0.62
No (n=14)	2.36 ± 0.68	1.14 ± 0.44
	p=0.721	*p*=0.731
Ki-67		
< 3% (n=19)	2.63 ± 0.55	1.21 ± 0.39
≥ 3% (n=5)	0.60 ± 0.60	1.40 ± 0.98
	***p*=0.028**	*p* =0.835
Trouillas grade classification		
1a (n=11)	2.73 ± 0.80	1.27 ± 0.54
1b (n=3)	1.00 ± 1.00	0.67 ± 0.67
2a (n=8)	2.50 ± 0.76	1.13 ± 0.58
2b (n=2)	0	2.50 ± 2.50
	p=0.374	*p*=0.733
Re-operation		
Yes (n=5)	2.80 ± 1.16	1.00 ± 0.63
No (n=19)	2.05 ± 0.53	1.32 ± 0.43
	p=0.537	*p*=0.728

Table 5.2: MMP-9 and MMP-14 expression and clinical features in PAs
MMP-9 and MMP-14 immunoreactivities according to different clinical features among the cohort of 24 PAs. Data are shown as mean±SEM for MMP-9 and MMP-14 immunoreactivities, per clinical feature. *, <0.05, **, <0.01, ***, <0.001 (Mann Whitney U test were used for all comparisons, except regarding the Trouillas grade classification variable where one-way ANOVA test was used).

Consistent with the above observations, PAs with no expression of MMP-9 were associated more often with visual impairment at diagnosis (75.0 vs 33.3%, p=0.041) and less headache at diagnosis (8.3 vs 58.3%, p=0.009) (Table 5.3). There were no differences regarding these different clinical features in PAs with or without expression of MMP-14 (Table 5.3).

	MMP-9 immunoreactivity			MMP-14 immunoreactivity		
	Positive (n=12)	**Negative (n=12)**	***p* value**	**Positive (n=9)**	**Negative (n=15)**	***p* value**
Gender						
Male (n=16)	7 (58.3%)	9 (75.0%)	0.386	7 (77.8%)	9 (60.0%)	0.371
Female (n=8)	5 (41.7%)	3 (25.0%)		2 (22.2%)	6 (40.0%)	
Headache at diagnosis						
Yes (n=8)	7 (58.3%)	1 (8.3%)	**0.009**	5 (55.6%)	4 (26.7%)	0.371
No (n=16)	5 (41.7%)	11 (91.7%)		4 (44.4%)	11 (73.3%)	
Visual impairment at diagnosis						
Yes (n=13)	4 (33.3%)	9 (75.0%)	**0.041**	4 (44.4%)	9 (60.0%)	0.459
No (n=11)	8 (66.7%)	3 (25.0%)		5 (55.6%)	6 (40.0%)	
Hypopituitarism at diagnosis						
Yes (n=11)	4 (33.3%)	7 (58.3%)	0.219	4 (44.4%)	7 (46.7%)	0.916
No (n=13)	8 (66.7%)	5 (41.7%)		5 (55.6%)	8 (53.3%)	
Cavernous sinus invasion						
Yes (n=10)	7 (58.3%)	7 (58.3%)	1.000	5 (55.6%)	9 (60.0%)	0.831
No (n=14)	5 (41.7%)	5 (41.7%)		4 (44.4%)	6 (40.0%)	
Ki-67						
< 3% (n=19)	11 (91.7%)	8 (66.7%)	0.132	7 (77.8%)	12 (80.0%)	0.897
≥ 3% (n=5)	1 (8.3%)	4 (33.3%)		2 (22.2%)	3 (20.0%)	
Trouillas grade classification						
1a (n=11)	6 (50.0%)	5 (41.7%)	0.403	4 (44.4%)	7 (46.7%)	0.984
1b (n=3)	1 (8.3%)	2 (16.7%)		1 (11.1%)	2 (13.3%)	
2a (n=8)	5 (41.7%)	3 (25.0%)		3 (33.3%)	5 (33.3%)	
2b (n=2)	0	2 (16.7%)		1 (11.1%)	1 (6.7%)	
Re-operation						
Yes (n=5)	3 (25.0%)	2 (16.7%)	0.615	2 (22.2%)	3 (20.0%)	0.897
No (n=19)	9 (75.0%)	10 (83.3%)		7 (77.8%)	12 (80.0%)	

Table 5.3: Positive/negative MMP-9 and MMP-14 expression and clinical features in PAs
Positive vs negative MMP-9 and MMP-14 immunoreactivities in PAs according to the respective different clinical features among the cohort of 24 PAs. Data are shown as n(%) per clinical feature. *p* values were calculated using the Chi-square test.

MMP-9 and MMP-14 expression in NFPAs vs somatotrophinomas

Somatotrophinomas had significantly increased MMP-9 immunoreactivity compared to NFPAs, while there were no differences regarding the expression of MMP-14 (Figure 5.12).

MMP-9 was expressed by 7 out of 8 (87.5%) somatotrophinomas and in only 5 out 16 (31.2%) of the studied NFPAs (p=0.009), whereas positive expression of MMP-14 was observed in 43.8% (7/16) and in 25.0% (2/8) of NFPAs and somatotrophinomas respectively (p=0.371).

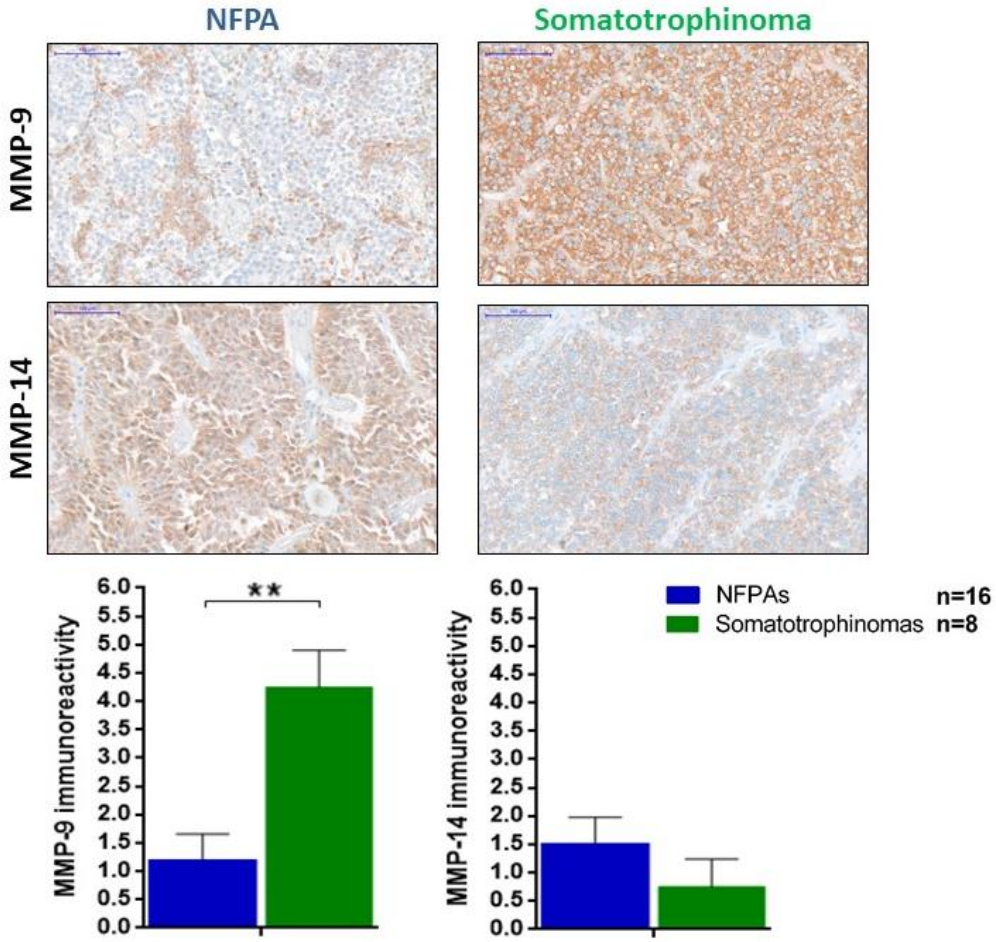

Figure 5.12: Expression of MMP-9 and MMP-14 in NFPAs and somatotrophinomas
MMP-9 and MMP-14 immunoreactivity differences between NFPAs (n=16) and somatotrophinomas (n=8). Tissue sections were stained for MMP-9 and MMP-14 and immunoreactivities measured using a semi-quantitative method. Representative images from MMP-9 and MMP-14 expression in a NFPA and in a somatotrophinoma are shown (20x). Data are shown as mean±SEM for MMP-9 and MMP-14 immunoreactivities. *, <0.05, **, <0.01, ***, <0.001 (Mann Whitney U test).

There were no significant correlations between MMP-9 and MMP-14 immunoreactivities and serum pituitary hormones, except in the case of serum IGF-1 and IGF-1 index and MMP-9 (Figures 5.13-A and 5.13-B, and Appendix 9). This association may suggest a possible role for GH/IGF-1 in the differential expression of MMP-9 between NFPAs and somatotrophinomas, or the different MMP-9 expression may be a consequence of different IGF-1 levels in NFPAs and in somatotrophinomas. This association between MMP-9 and serum IGF-1 was not observed in the separate analysis within the NFPA and somatotrophinoma subgroups (Figures 5.13-C and 5.13-D), suggesting that GH/IGF-1 levels may not *per se* determine the extent of MMP-9 expression in each of these PA subtypes. Of the somatotrophinomas, I observed a negative correlation between serum PRL and MMP-9 immunoreactivity (r=-0.963, p=0.009) (Appendix 9), but this significance was driven by an outlier case that had elevated PRL at 5289 mU/L and no expression of MMP-9.

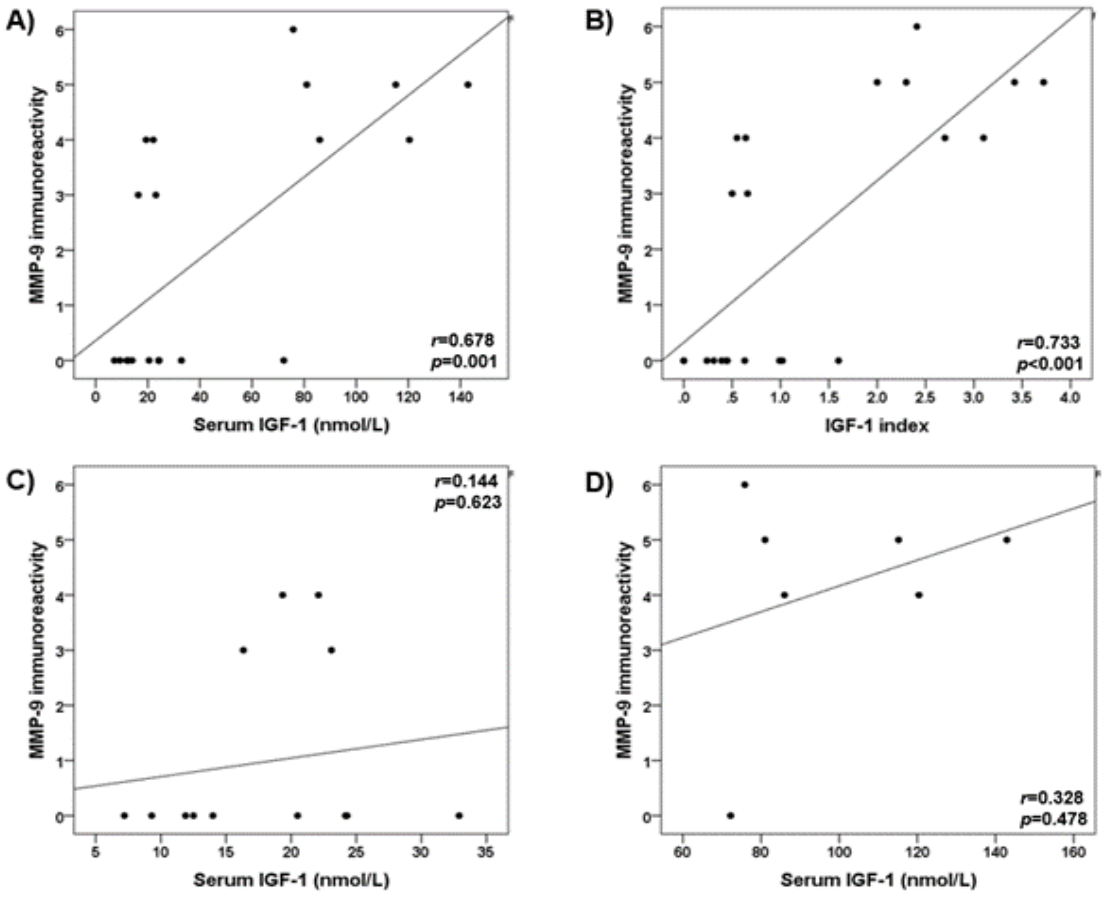

Figure 5.13: Serum IGF-1 and MMP-9 expression
Correlation between: MMP-9 immunoreactivity and serum IGF-1 and IGF-1 index in the cohort of 24 PAs (A and B); MMP-9 immunoreactivity and serum IGF-1 among the 16 NFPAs (C); MMP-9 immunoreactivity and serum IGF-1 among the 8 somatotrophinomas (D). *p* values were determined by the Pearson correlation coefficient *r*.

MMP-9 and MMP-14 expression and PA-derived cytokine secretome

There were no significant correlations between PA-derived cytokines and MMP-9 and MMP-14 immunoreactivities among the whole cohort of PAs (Appendix 9), except between PA-derived CCL2 levels and MMP-9 immunoreactivity (r=-0.450; p=0.027).

When the data were analysed separately per PA subtype, within the NFPA subgroup there were no correlations between NFPA-derived cytokines and MMP-9 and MMP-14 expression (Appendix 9); however, among somatotrophinomas, I observed negative correlations between MMP-9 immunoreactivity and PA-derived CCL4 (r=-0.864; p=0.006), CXCL10 (r=-0.747; p=0.033), FGF-2 (r=-0.809; p=0.015) and IL-6 (r=-0.738; p=0.037) (Figure 5.14 and Appendix 9).

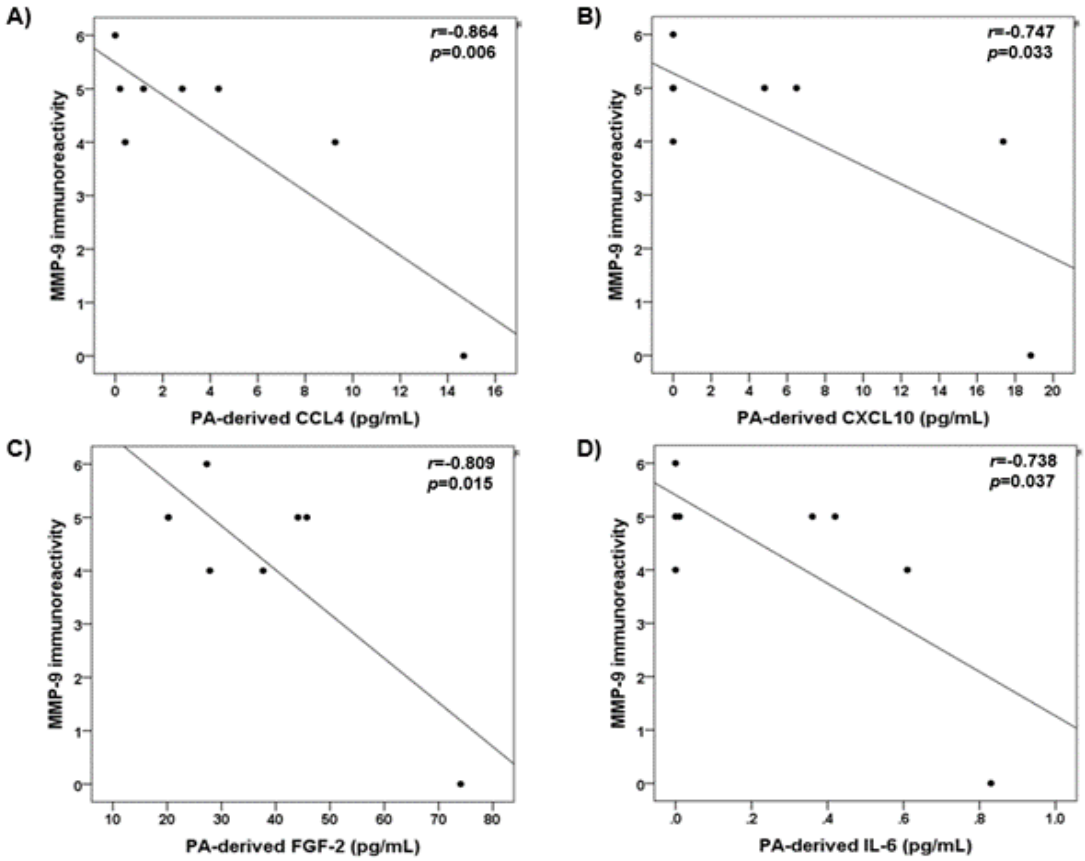

Figure 5.14: PA-derived cytokines and MMP-9 expression in somatotrophinomas
Correlation between MMP-9 immunoreactivity and PA-derived levels of CCL4 (A), CXCL10 (B), FGF-2 (C) and IL-6 (D) among somatotrophinomas (n=8). *p* values were determined by Pearson correlation coefficient *r*.

These findings suggest that some PA-derived cytokines may influence the MMP-9 expression in somatotrophinomas, downregulating its expression, an effect possibly not occurring in NFPAs. If PA-derived cytokines indeed inhibit MMP-9 expression in PAs, the differential expression of MMP-9 between somatotrophinomas and NFPAs could be potentially explained by the fact that NFPAs released significantly higher amounts of cytokines than somatotrophinomas (Figure 3.1 in Chapter 3) which may have downregulated MMP-9 in NFPAs.

MMP-9 and MMP-14 expression and PA-infiltrating immune cells

PAs with more macrophages (≥6%) were associated with lower expression of MMP-9 (0.71±0.71 vs 2.82±0.55, p=0.042) (Appendix 9) and displayed more often no MMP-9 expression (50.0 vs 8.3%; p=0.025) (Table 5.4). PAs with more neutrophils (≥0.5%) had increased expression of MMP-14 (2.18±0.59 vs 0.46±0.31, p=0.020) (Appendix 9) and had more often positive MMP-14 immunoreactivity (Table 5.4). There were no other associations between MMP-9 or MMP-14 immunoreactivity and immune cell ratios in the whole cohort of PAs (Appendix 9 and Table 5.4).

	MMP-9 immunoreactivity			MMP-14 immunoreactivity		
	Positive (n=12)	**Negative (n=12)**	***p* value**	**Positive (n=9)**	**Negative (n=15)**	***p* value**
Infiltrating macrophages						
<6% (n=17)	11 (91.7%)	6 (50.0%)	**0.025**	6 (66.7%)	11 (73.3%)	0.728
≥6% (n=7)	1 (8.3%)	6 (50.0%)		3 (33.3%)	4 (26.7%)	
Infiltrating CD8+ T cells						
<1% (n=6)	2 (16.7%)	4 (33.3%)	0.346	2 (22.2%)	4 (26.7%)	0.808
≥1% (n=18)	10 (83.3%)	8 (66.7%)		7 (77.8%)	11 (73.3%)	
Infiltrating CD4+ T cells						
<1% (n=15)	8 (66.7%)	7 (58.3%)	0.673	5 (55.6%)	10 (66.7%)	0.459
≥1% (n=9)	4 (33.3%)	5 (41.7%)		4 (44.4%)	5 (33.3%)	
Infiltrating B cells						
<0.5% (n=8)	5 (41.7%)	3 (25.0%)	0.386	2 (22.2%)	6 (40.0%)	0.371
≥0.5% (n=16)	7 (58.3%)	9 (75.0%)		7 (77.8%)	9 (60.0%)	
Infiltrating neutrophils						
<0.5% (n=13)	8 (66.7%)	5 (41.7%)	0.219	2 (22.2%)	11 (73.3%)	**0.015**
≥0.5% (n=11)	4 (33.3%)	7 (58.3%)		7 (77.8%)	4 (26.7%)	
Infiltrating FOXP3+ T cells						
<0.3% (n=12)	5 (41.7%)	7 (58.3%)	0.414	3 (33.3%)	9 (60.0%)	0.206
≥0.3% (n=12)	7 (58.3%)	5 (41.7%)		6 (66.7%)	6 (40.0%)	
Immune cell ratios						
M2:M1	2.09 ± 0.20	2.28 ± 0.24	0.570	1.88 ± 0.18	2.37 ± 0.21	0.133
CD8:CD4	2.25 ± 0.43	1.80 ± 0.41	0.456	1.50 ± 0.19	2.34 ± 0.44	0.097
CD8:FOXP3	5.99 ± 1.11	5.29 ± 1.03	0.650	5.82 ± 1.64	5.54 ± 0.73	0.862
CD68:FOXP3	11.63 ± 2.59	22.18 ± 5.77	0.116	16.89 ± 6.84	16.91 ± 3.51	0.997

Table 5.4: Positive/negative MMP-9 and MMP-14 expression and PA-infiltrating immune cells
Positive vs negative MMP-9 and MMP-14 immunoreactivities in PAs according to the infiltrating immune cells and immune cell ratios among the cohort of 24 PAs. Data are shown as n(%) per PA-infiltrating immune cells and as mean±SEM for immune cell ratios. *p* values were calculated using the Chi-square test for PA-infiltrating immune cells and Mann Whitney U test for immune cell ratios.

NFPAs with increased contents of macrophages (≥6%) and lower amounts of B cells (<0.5%) had negative expression of MMP-9, while NFPAs with lower contents of neutrophils (<0.5%) were associated with absent MMP-14 immunoreactivity (Appendix 9). No significant associations were noted among the subgroup of somatotrophinomas (Appendix 9). Overall, these data suggest that some infiltrating immune cells may influence the expression of MMP-9 and MMP-14, namely macrophages and neutrophils, and thus may have a modulatory role in the remodelling of the ECM within the TME of PAs, as shown in other cancers[435-438].

MMP-9 and MMP-14 expression and TAF-derived cytokine secretome

Overall, there were no associations between TAF-derived cytokines and MMP-9 and MMP-14 immunoreactivity in the cohort of 24 PAs. However, within somatotrophinomas I observed significant correlations between MMP-14 immunoreactivity and TAF-derived CX3CL1 levels (r=-0.901; p=0.037) and IFNα2 (r=-0.911; p=0.031) (Appendix 9).

Epithelial-to-mesenchymal transition in human pituitary adenomas

EMT and its regulatory mechanisms remain largely unexplored in PAs. It was previously shown that PAs may have a partial EMT phenotype[505], which is consistent with the fact that PAs are benign and rarely metastasise. Data from Dr. Barry suggest that somatotrophinomas - particularly those due to an *AIP* mutation - undergo EMT (Figure 5.15), but her gene expression data showed no upregulation of some classical mesenchymal markers such as vimentin or N-cadherin in *AIP*mut somatotrophinomas, which indeed suggest an incomplete EMT signature[513].

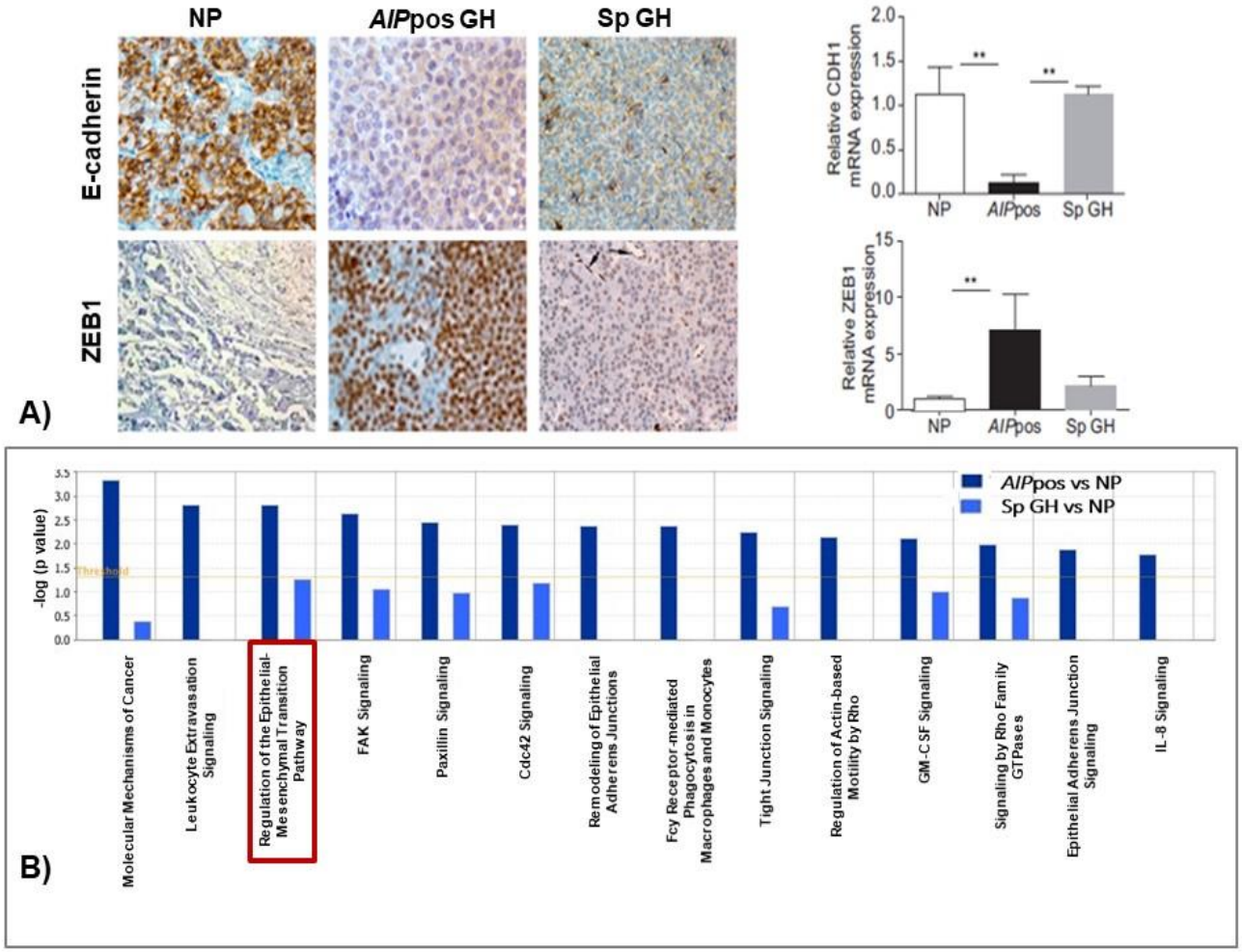

Figure 5.15: EMT in human *AIP*mut and *AIP*neg somatotrophinomas
A) Immunohistochemical analysis of E-cadherin and ZEB1 (EMT markers) in *AIP* mutation-positive somatotrophinomas (*AIP*pos GH), sporadic somatotrophinomas (Sp GH) and normal pituitary (NP), and its respective validation with RT-qPCR. Representative immunohistochemistry images at x20 magnification are shown, and for RT-qPCR experiment data are shown as relative mRNA expression. *, <0.05, **, <0.01, ***, <0.001 (Kruskal-Wallis test followed by Conover–Inman test for individual comparisons). B) Ingenuity pathway analysis of canonical pathways significantly altered in *AIP*pos and sporadic somatotrophinomas in comparison to NP. The differentially expressed genes in these 2 comparisons were analysed using Ingenuity pathway multiple comparison analysis. The top significant canonical pathways are shown, and was noted that "Regulation of the Epithelial-Mesenchymal Transition Pathway" is one of the most significantly altered pathways in *AIP*pos compared to sporadic somatotrophinomas. The horizontal line parallel to the X axis indicates a threshold for p=0.05 (Dr. Sayka Barry´s data[513]).

EMT in PAs vs NPs

In my study, E-cadherin immunoreactivity did not differ between PAs and NPs, whereas the expression of ZEB1 was significantly higher in PAs than in NP which did not express ZEB1 in any of the studied specimens (Figure 5.16). In general, normal pituitary cells and most PA cells showed uniform moderate to strong membranous staining for E-cadherin and cytoplasmic positivity. Regarding ZEB1, normal pituitary cells were completely negative in all 10 cases, whereas some NFPAs and somatotrophinomas (not all) exhibited weak to moderate positive nuclear staining in some cells (not all), suggesting that those cells may be undergoing EMT, a process heterogeneously occurring in the PA tissue (Figure 5.16).

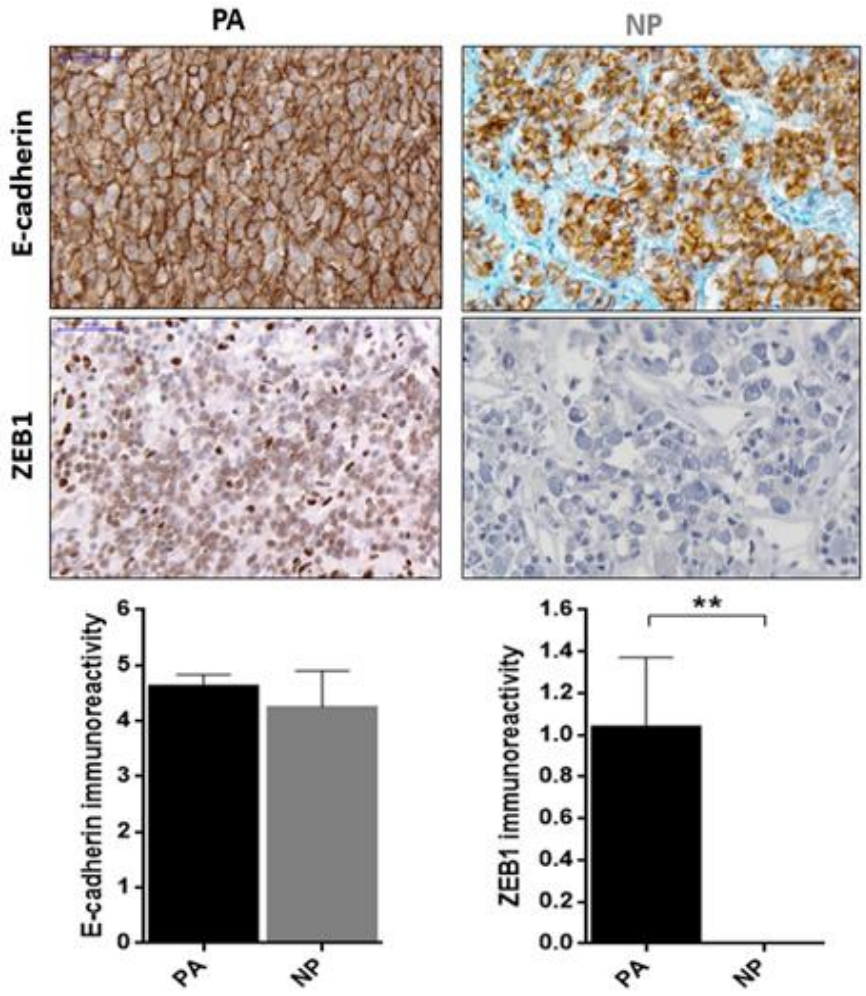

Figure 5.16: E-cadherin expression in PAs and in NPs
Immunohistochemical analysis of E-cadherin and ZEB1 in human pituitary adenomas (PAs, n=24) and in normal pituitaries (NPs, n=10). The stained sections were scored using a semi-quantitative method on the basis of both extent and intensity of the immunoreactivity. The extent of immunoreactivity was scored according to the percentage of stained cells in relation to the entire section as 0 points for no staining, 1 point for <20%, 2 points for 20-50% and 3 points for >50% of the cells. Staining intensity was graded on a scale including 0 (no staining), 1 (weak), 2 (moderate) and 3 (strong). The sum of the intensity and extent scores was used as final score. E-cadherin and ZEB1 expression are shown as mean±SEM. Representative images of a PA and in a NP are shown. *, <0.05, **, <0.01, ***, <0.001 (Mann Whitney U test).

Unexpectedly, E-cadherin and ZEB1 immunoreactivities correlated positively (r=0.404; p=0.041) (Figure 5.17).

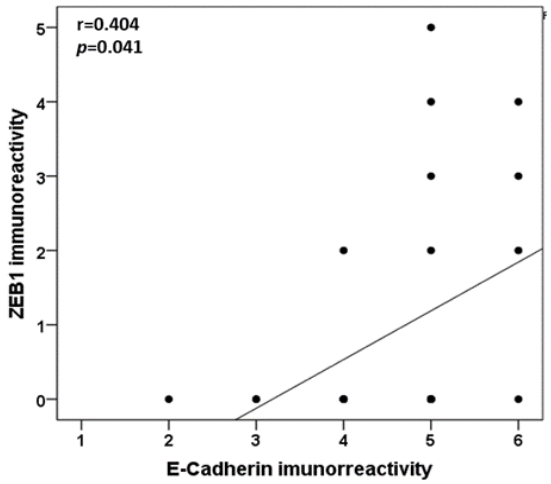

Figure 5.17: Correlation between E-cadherin and ZEB1 immunoreactivity in PAs
N PAs analysed = 24. *p* value was determined by the Pearson correlation coefficient *r*.

EMT and clinical features in PAs

E-cadherin and ZEB1 expression were not associated with PA aggressiveness, as determined by the presence of cavernous sinus invasion or by higher Ki-67; however, PAs with Ki-67≥3% tended to display lower levels of E-cadherin expression (4.00±0.60 vs 4.79±0.21, p=0.123) (Table 5.5). There were no associations between E-cadherin or ZEB1 immunoreactivities and other clinical features at presentation (Table 5.5).

n PAs = 24	**E-cadherin immunoreactivity** Mean ± SEM	**ZEB1 immunoreactivity** Mean ± SEM
Gender		
Male (n=16)	4.88 ± 0.20	1.19 ± 0.43
Female (n=8)	4.13 ± 0.44	0.75 ± 0.53
	p=0.087	*p*=0.547
Headache at diagnosis		
Yes (n=8)	4.25 ± 0.45	0.63 ± 0.42
No (n=16)	4.81 ± 0.21	1.25 ± 0.45
	p=0.207	*p*=0.387
Visual Impairment at diagnosis		
Yes (n=13)	4.38 ± 0.29	1.15 ± 0.48
No (n=11)	4.91 ± 0.29	0.91 ± 0.48
	p=0.214	*p*=0.722
Hypopituitarism at diagnosis		
Yes (n=11)	4.55 ± 0.28	0.64 ± 0.34
No (n=13)	4.69 ± 0.31	1.38 ± 0.54
	p=0.732	*p*=0.253

Cavernous sinus invasion		
Yes (n=10)	4.80 ± 0.29	1.30 ± 0.56
No (n=14)	4.50 ± 0.29	0.86 ± 0.42
	p=0.487	*p*=0.523
Ki-67		
< 3% (n=19)	4.79 ± 0.21	1.00 ± 0.38
≥ 3% (n=5)	4.00 ± 0.60	1.20 ± 0.80
	p=0.123	*p* =0.813
Trouillas grade classification		
1a (n=11)	4.82 ± 0.26	0.91 ± 0.51
1b (n=3)	3.33 ± 0.67	0.67 ± 0.67
2a (n=8)	4.75 ± 0.37	1.13 ± 0.58
2b (n=2)	5.00 ± 0.00	2.00 ± 2.00
	p=0.122	*p*=0.835
Re-operation		
Yes (n=5)	5.00 ± 0.48	1.40 ± 0.60
No (n=19)	4.53 ± 0.23	0.95 ± 0.39
	p=0.364	*p*=0.591

Table 5.5: E-cadherin and ZEB1 expression and clinical features in PAs
E-cadherin and ZEB1 immunoreactivities according to different clinical features among the cohort of 24 PAs. Data are shown as mean±SEM per feature. *,<0.05, **,<0.01, ***,<0.001 (Mann Whitney U test were used for all comparisons, except for Trouillas grade classification where one-way ANOVA test was used).

EMT in NFPAs vs somatotrophinomas

There were no differences in E-cadherin or ZEB1 immunoreactivities between NFPAs and somatotrophinomas (Figure 5.18), suggesting that the EMT signature may not differ between these 2 PA subtypes.

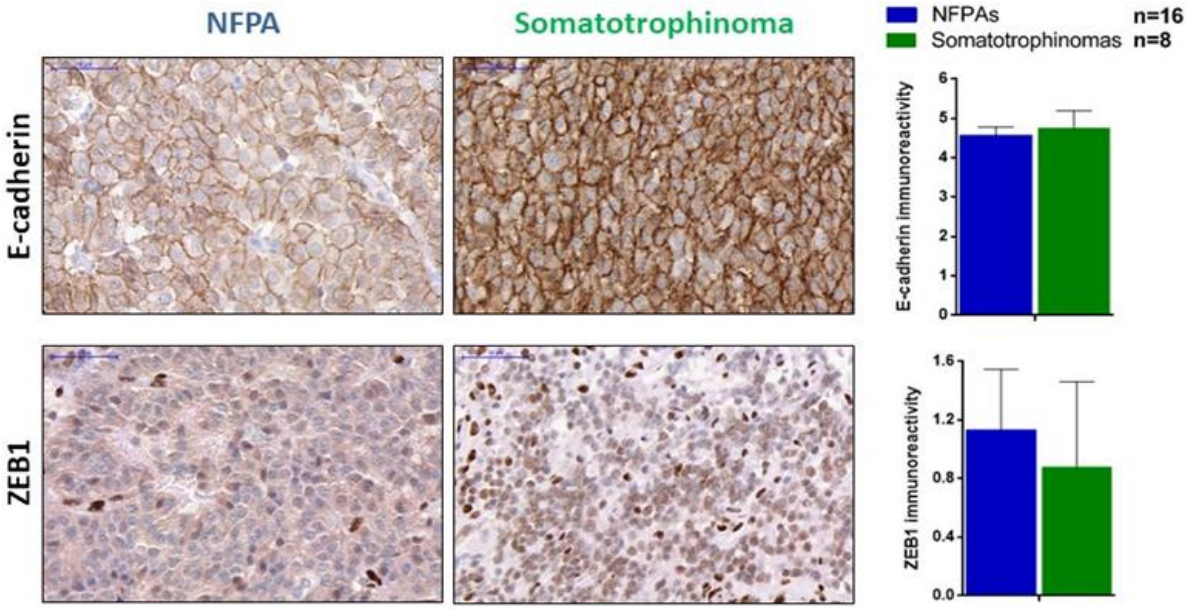

Figure 5.18: Expression of E-cadherin and ZEB1 in NFPAs and somatotrophinomas
E-cadherin and ZEB1 immunoreactivity differences between NFPAs (n=16) and somatotrophinomas (n=8). Representative images from E-cadherin and ZEB1 expression in a NFPA and in a somatotrophinoma are shown (20x). Data are shown as mean±SEM. *, <0.05, **, <0.01, ***, <0.001 (Mann Whitney U test).

There were no significant correlations between E-cadherin and ZEB1 immunoreactivities and serum pituitary hormones in the whole cohort of 24 PAs, and also among NFPAs (Appendix 9). However, within the subgroup of somatotrophinomas I observed a significant negative correlation between E-cadherin immunoreactivity and serum GH levels (r=-0.801; p=0.031), as well as a trend for negative correlation between E-cadherin immunoreactivity and serum IGF-1 (r=-0.719; p=0.069) (Figure 5.19), suggesting a potential effect for GH/IGF-1 excessive levels in patients with somatotrophinomas to promote EMT.

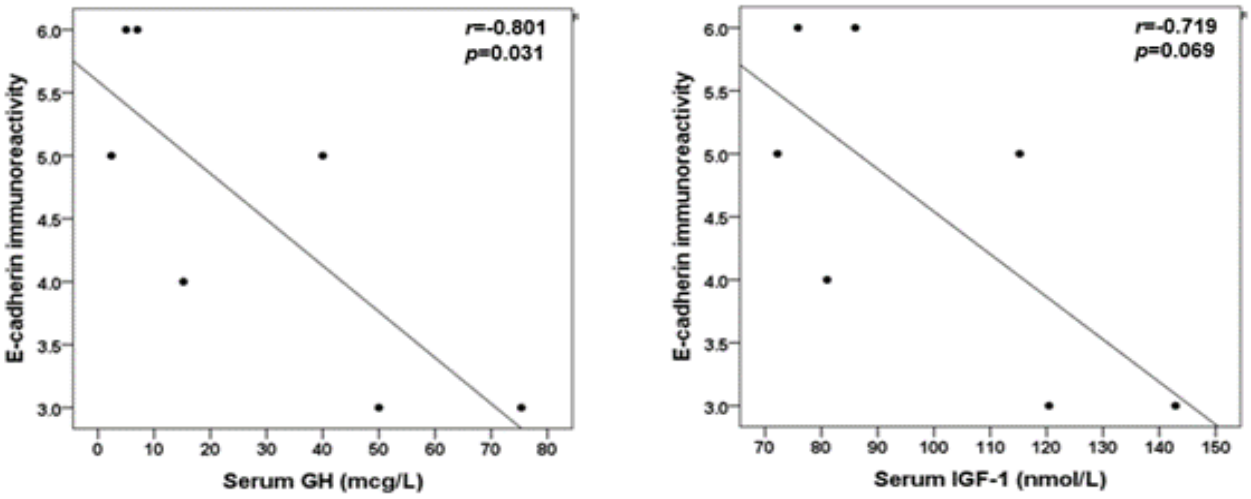

Figure 5.19: Serum GH and IGF-1 and E-cadherin expression in somatotrophinomas
Correlation between E-cadherin immunoreactivity and serum levels of GH and IGF-1 within the subgroup of somatotrophinomas (n=8). *p* values were determined by the Pearson correlation coefficient *r*.

EMT and PA-derived cytokine secretome

In general, there were no significant correlations between E-cadherin immunoreactivity and PA-derived cytokine levels in the primary culture supernatants of the 24 PAs, except for VEGF-A which negatively correlated with E-cadherin expression (r=-0.476; p=0.019) (Figure 5.20 and Appendix 9). VEGF-A is a growth factor known to induce EMT[647], in part by repressing E-cadherin expression in tumour cells, in a similar manner to other cytokines/growth factors[467,647].

Regarding ZEB1 expression, I observed an overall tendency for negative correlations between all PA-derived cytokines and ZEB1 immunoreactivity, but statistical significance was only reached for PA-derived FGF-2 (*r*=-0.543; p=0.006) (Figure 5.20 and Appendix 9).

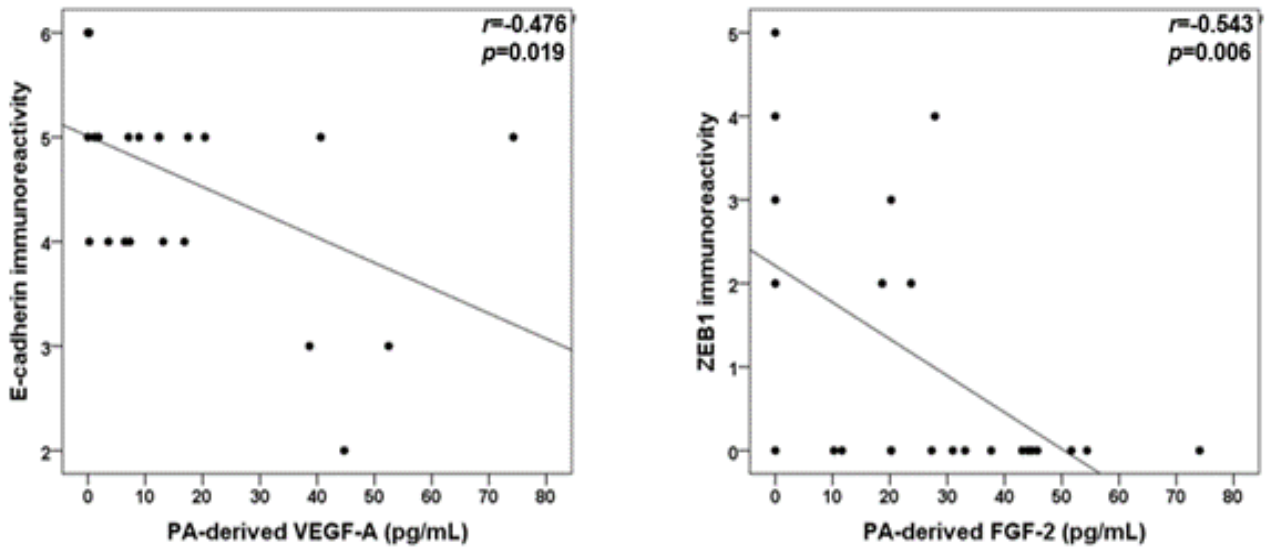

Figure 5.20: PA-derived VEGF-A and FGF-2 and E-cadherin/ZEB1 expression in PAs
N PAs analysed = 24. *p* values were determined by the Pearson correlation coefficient *r*.

Considering the marked differences between NFPA and somatotrophinoma cytokine secretomes (Figure 3.1 in Chapter 3), I performed a separate subanalysis between E-cadherin and ZEB1 immunoreactivities and cytokine levels among these PA subtypes. Within somatotrophinomas CCL3 and VEGF-A levels were negatively correlated with E-cadherin immunoreactivity (r=-0.817; p=0.013 and r=-0.886; p=0.003 respectively), while for NFPAs no correlation between cytokines and E-cadherin immunoreactivity was noted. On other hand, among NFPAs a negative correlation between FGF-2 levels and ZEB1 immunoreactivity was noted (r=-0.612; p=0.012) while no significant correlations were seen in somatotrophinomas (Appendix 9).

EMT and PA-infiltrating immune cells

I did not observe correlations between PA-infiltrating immune cells and E-cadherin or ZEB1 expression, which can again be explained, at least in part, by the lack of true EMT signature in my cohort of PAs, as discussed. However, there was a significant correlation between M2:M1 ratio and ZEB1 expression among somatotrophinomas (r=0.773; p=0.024) (Appendix 9), suggesting that the relative imbalance of more M2-macrophages and less M1-macrophages may promote EMT by upregulating ZEB1 in patients with somatotrophinomas.

EMT and TAF-derived cytokine secretome

In different cancer models, cancer-associated fibroblasts have been shown to induce EMT[387,388,390]. TAF-derived PDGF-AA levels were negatively correlated with E-cadherin expression (r=-0.564, p=0.023), suggesting a possible role for TAF secretome in promoting EMT by downregulating E-cadherin (Figure 4.5 in Chapter 4 and Appendix 9). ZEB1 expression was also negatively correlated with TAF-derived FGF-2 levels (r=-0.543; p=0.006) (Appendix 9). I found no other correlations between TAF-derived cytokine levels and E-cadherin or ZEB1 immunoreactivities (Table 4.4 in Chapter 4 and Appendix 9).

Neural cell adhesion molecule in human pituitary adenomas

NCAM expression in PAs vs NPs

The expression of NCAM was not different between PAs and NPs (4.96±0.14 vs 5.40±0.25; p=0.192) (Figure 5.21). All PA and NP cases displayed NCAM intense immunoreactivity mainly visible in the cell membrane but also in the cytoplasm, consistent with previous descriptions[639].

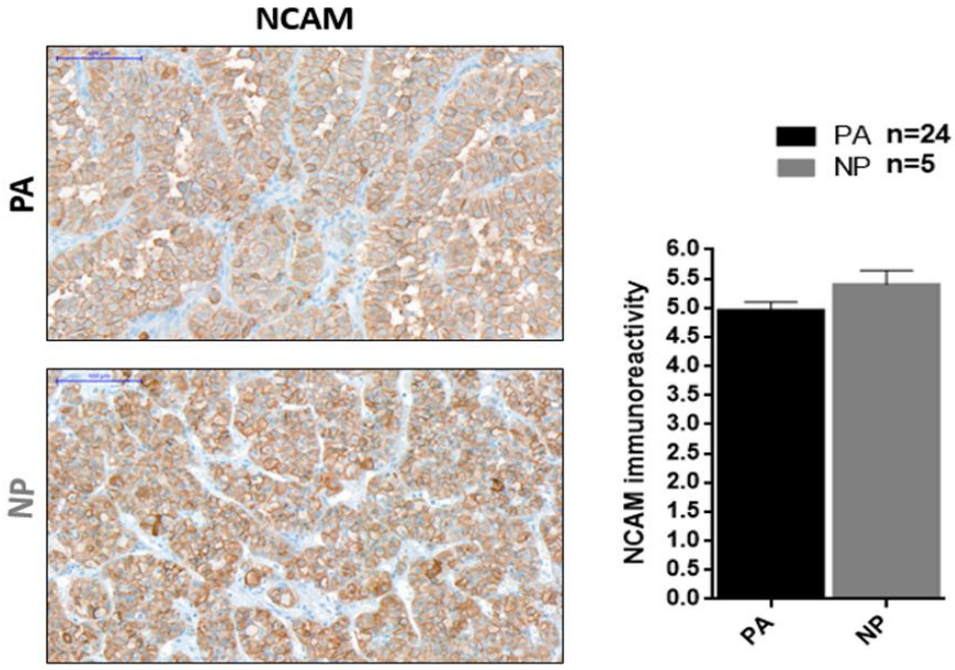

Figure 5.21: NCAM expression in PAs and in NPs
NCAM immunoreactivity differences between human pituitary adenomas (PAs) and normal pituitary (NPs) are shown. NCAM immunoreactivity was measured using a semi-quantitative method. Representative images from NCAM expression in a PA and in a NP are shown (20x). Data are shown as mean±SEM for NCAM immunoreactivity. *, <0.05, **, <0.01, ***, <0.001 (Mann Whitney U test).

NCAM expression and clinical features in PAs

There was no association between different clinico-pathological features and NCAM immunoreactivity in my cohort of 24 PAs (Table 5.6).

n PAs = 24	**NCAM immunoreactivity** Mean ± SEM
Gender	
Male (n=16)	4.88 ± 0.16
Female (n=8)	5.13 ± 0.30
	p=0.415
Headache at diagnosis	
Yes (n=8)	4.88 ± 0.23
No (n=16)	5.00 ± 0.18
	p=0.685
Visual impairment at diagnosis	
Yes (n=13)	4.92 ± 0.18
No (n=11)	5.00 ± 0.23
	p=0.792
Hypopituitarism at diagnosis	
Yes (n=11)	4.82 ± 0.12
No (n=13)	5.08 ± 0.23
	p=0.372
Cavernous sinus invasion	
Yes (n=10)	5.20 ± 0.20
No (n=14)	4.79 ± 0.19
	p=0.151
Ki-67	
< 3% (n=19)	4.95 ± 0.14
≥ 3% (n=5)	5.00 ± 0.48
	p=0.883
Trouillas grade classification	
1a (n=11)	4.73 ± 0.20
1b (n=3)	5.00 ± 0.58
2a (n=8)	5.25 ± 0.16
2b (n=2)	5.00 ± 1.00
	p=0.469
Re-operation	
Yes (n=5)	4.80 ± 0.37
No (n=19)	5.00 ± 0.15
	p=0.576

Table 5.6: NCAM expression and clinical features in PAs
NCAM immunoreactivity according to different clinical features among the cohort of 24 PAs. Data are shown as mean±SEM for NCAM immunoreactivity, per feature. *,<0.05, **,<0.01, ***,<0.001 (Mann Whitney U test were used for all comparisons, except for Trouillas grade classification where one-way ANOVA test was used).

NCAM expression in NFPAs vs somatotrophinomas

NCAM expression did not differ among NFPAs and somatotrophinomas (p=0.415) (Figure 5.22).

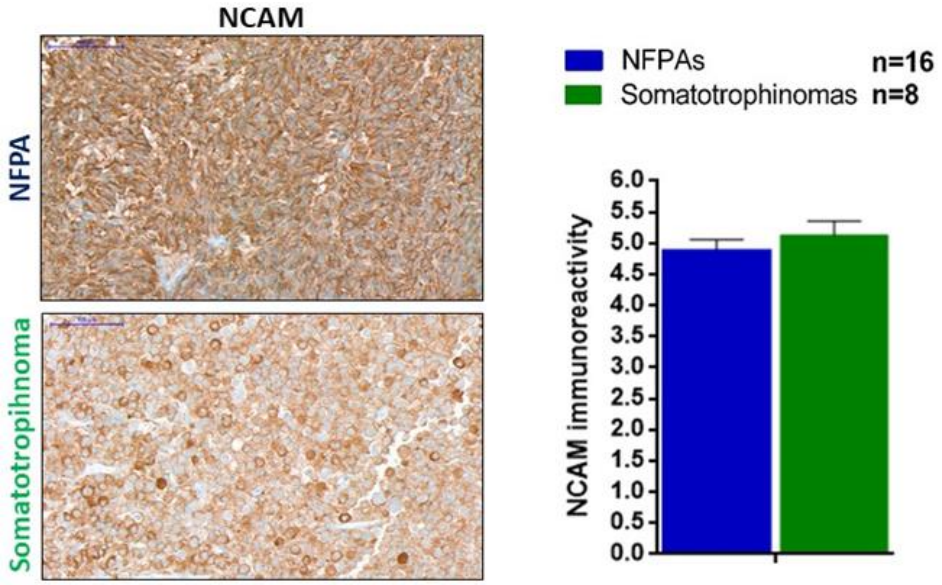

Figure 5.22: NCAM expression in NFPAs and in somatotrophinomas
NCAM immunoreactivity differences between human NFPAs (n=16) and NPs (n=8) are shown. NCAM immunoreactivity was measured using a semi-quantitative method. Representative images from NCAM expression in a NFPA and in a somatotrophinomas are shown (20x). Data are shown as mean±SEM for NCAM immunoreactivity. *, <0.05, **, <0.01, ***, <0.001 (Mann Whitney U test).

There was a correlation between NCAM expression and serum LH (r=0.518; p=0.016) and FSH (r=0.487; p=0.025) in the whole cohort of PAs (Figures 5.23-A and 5.23-B), but there were no other significant correlations between serum pituitary hormones including GH/IGF-1 and PRL and NCAM expression (Appendix 9). Within the NFPA subgroup there were also no correlation between pituitary hormones and NCAM immunoreactivity, and in somatotrophinomas PRL correlated with NCAM expression (r=-0.989; p=0.001) but this was driven by an outlier case (Figure 5.23-C); there was however no correlation with GH/IGF-1 levels (Appendix 9).

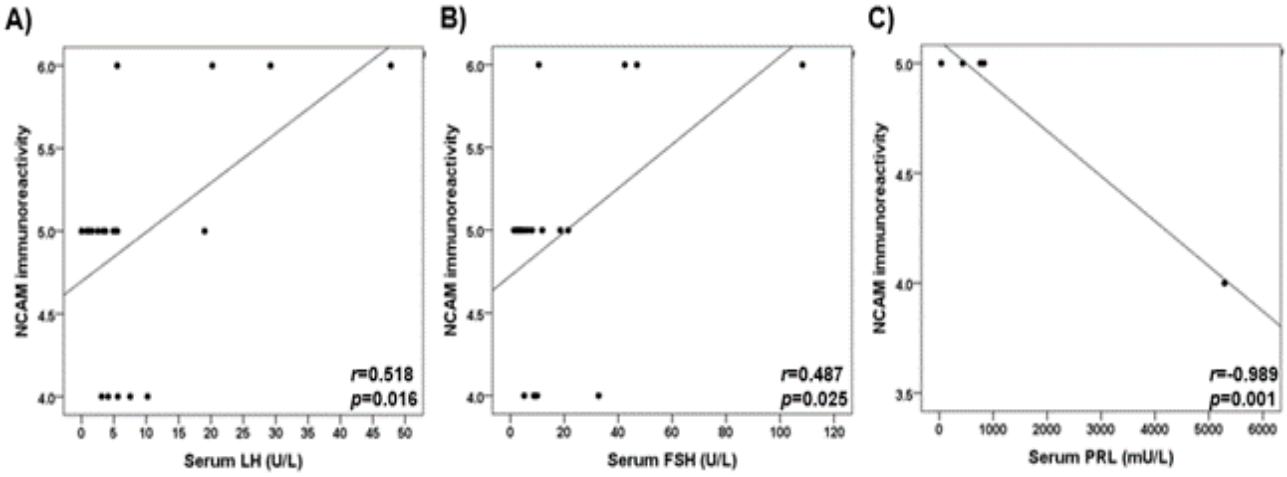

Figure 5.23: Serum pituitary hormones and NCAM expression in PAs
Statistical significant correlations between: A) serum LH levels and NCAM immunoreactivity within the cohort of 24 PAs; B) serum FSH levels and NCAM immunoreactivity within the cohort of 24 PAs; C) serum PRL levels and NCAM immunoreactivity within somatotrophinomas (n=8). *p* values were determined by the Pearson correlation coefficient *r*.

NCAM expression and PA-derived cytokine secretome

There were no correlation between PA-derived cytokine levels and NCAM immunoreactivity in the overall cohort of PAs (Appendix 9). As NFPA and somatotrophinoma secretomes differed (Figure 3.1 in Chapter 3), these PA types were analysed individually. In NFPAs there were no correlations (Appendix 9), but somatotrophinomas with lower NCAM expression had higher levels of CCL4 (p=0.026), CXCL1 (p=0.045), FGF-2 (p=0.021) and IL-6 (p=0.030) (Figure 5.24 and Appendix 9).

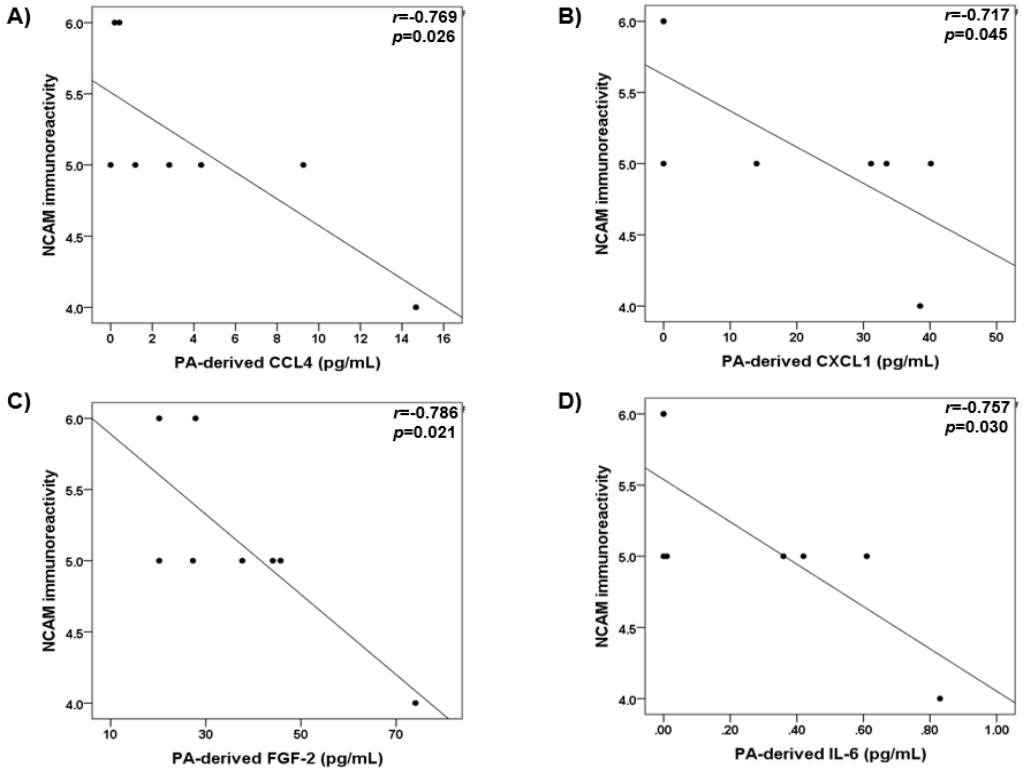

Figure 5.24: PA-derived cytokines and NCAM expression in somatotrophinomas
Number of somatotrophinomas = 8. *p* values were determined by the Pearson correlation coefficient *r*.

NCAM expression and PA-infiltrating immune cells

Overall, there was no association between the NCAM immunoreactivity and PA-infiltrating immune cell contents, neither with immune cell ratios (Appendix 9).

NCAM expression and TAF-derived cytokine secretome

TAF-derived FGF-2 was negatively correlated with NCAM immunoreactivity in overall cohort of 24 PAs (r=-0.631; p=0.009) (Appendix 9). Among NFPAs, NCAM negatively correlated also with TAF-derived FGF-2 levels (r=-0.716; p=0.013), as well as with CXCL1 (r=-0.661; p=0.027) and CCL7 (r=-0.609; p=0.047). In the somatotrophinomas subgroup, I found a positive correlation between TAF-derived CCL22 levels and NCAM expression (r=0.978; p=0.004) (Appendix 9).

Discussion

Using a comprehensively phenotyped cohort of human PAs with cytokine data from primary cultures of PA cells and TAFs as well as immunohistochemical immune infiltrates data, I found that some elements within the TME of PAs may modulate different oncogenic mechanisms, as summarised in Figure 5.25.

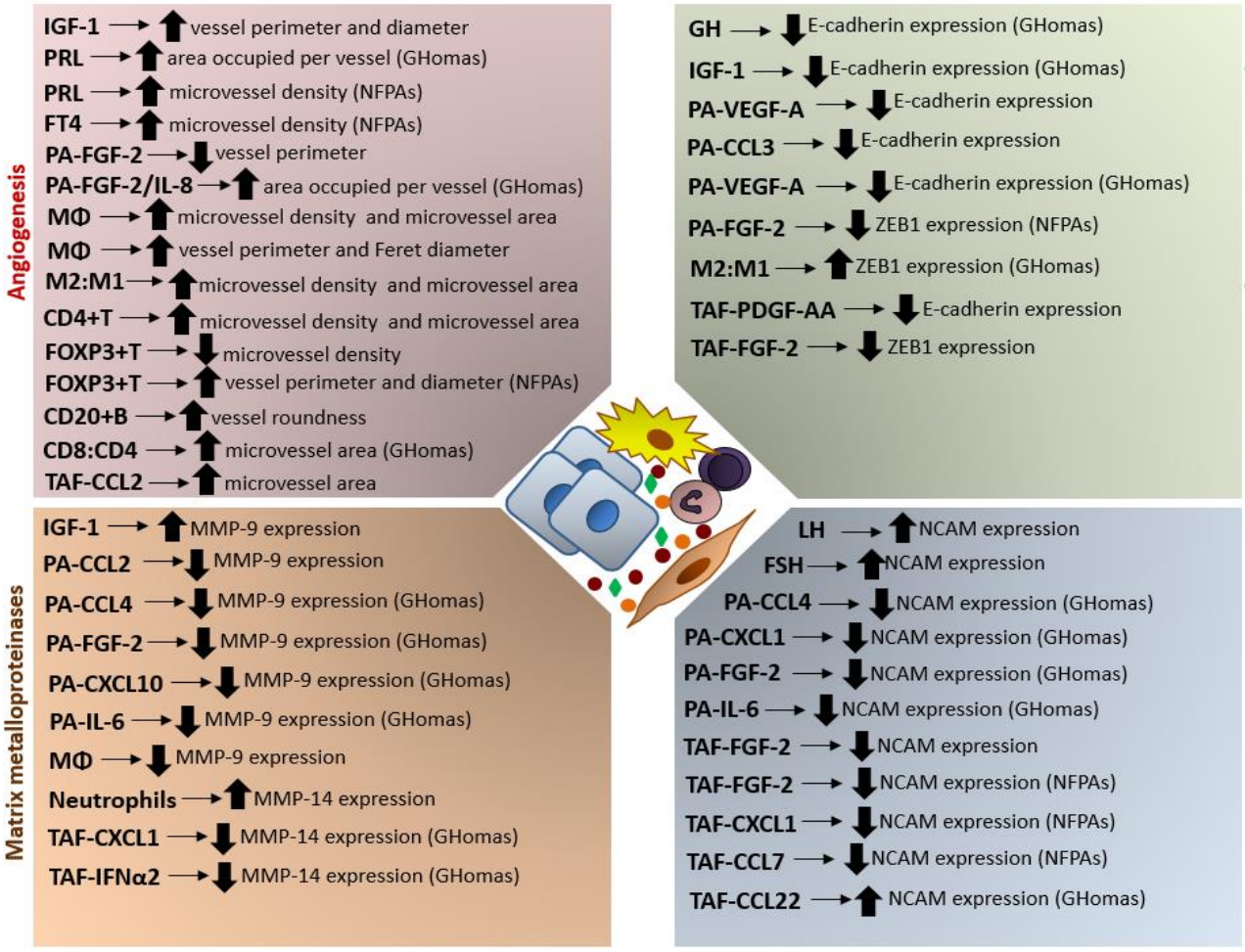

Figure 5.25: Modulation of oncogenic mechanisms in PAs by different TME components
Different proteins are secreted by the non-neoplastic tumour-associated fibroblasts (TAFs) and infiltrating immune cells, as well as from pituitary adenoma (PA) cells into the tumour microenvironment (TME). These proteins are able to influence and modulate distinct oncogenic mechanisms, including angiogenesis, matrix metalloproteinases expression, epithelial-to-mesenchymal transition activation (E-cadherin downregulation and/or ZEB1 upregulation) and expression of the neural cell adhesion molecule (NCAM). CD4+T, CD4+ T cells; CD8:CD4, CD8+ T cytotoxic –CD4+ T helper cell ratio; CD20+B, CD20+ B lymphocytes; FOXP3+T, FOXP3+ T regulatory cells; FSH, follicle-stimulating hormone; FT4, free thyroxine; GH, growth hormone; GHomas, somatotrophinomas; IGF-1, insulin-like growth factor-1; LH, luteinising hormone; MΦ, CD68+ macrophages; M2:M1, M2-M1 macrophage ratio; MMP, matrix metalloproteinase; NCAM, neural cell adhesion molecule; NFPA, non-functioning pituitary adenoma; PA, pituitary adenoma; PRL, prolactin; TAF, tumour associated fibroblast.

Angiogenesis in pituitary adenomas

Angiogenesis provides tumour cells with energy supply and oxygen necessary for tumour growth, and increased requirements are needed for aggressive tumour growth[416,417]. Angiogenesis has been studied in the neoplastic and normal pituitary in the past, but little is known about the role of different cellular and non-cellular TME elements in pituitary angiogenesis[297,416].

PAs are less vascularised than NP[302,421,427], and in general previous studies have shown that there is no association between PA vascularisation and invasiveness[297,303,416], consistent with my own observations. These observations raise uncertainty about the role of angiogenesis in PAs, as opposed to other malignancies in which the neovascularisation correlates with tumour growth, invasion and metastasis[297,417,648]. However, the lack of increased angiogenesis in PAs in comparison to NP, and the lack of association between vascularisation and PA aggressiveness, may underlie the low growth rate and benign nature of PAs which uncommonly metastasise[297,303,416]. This apparent paradox can be partially explained by the lower oxygen consumption rate of PA cells. Tumour vessels can themselves be hypoxic and carry little oxygen, or can have oscillating rather than directed blood flows and thus be ineffective at transporting oxygen. Moreover, tumour cells are known to tolerate oxygen deprivation and be resistant to apoptosis under hypoxia, which allows for increased intercapillary distance[643]. Nevertheless, increased microvessel density was described for pituitary carcinomas compared to PAs and NP suggesting that angiogenesis may be a relevant mechanism, at least for highly aggressive pituitary tumours[303].

I observed that somatotrophinomas were less vascularised than NFPAs, in line with previous observations[303,649], and have smaller vessels (lower perimeter and Feret's diameter). However, some other series have reported no differences between distinct PA subtypes[304,421,422]. The observed difference is unlikely due to pre-operative SSA treatment as there were no angiogenic differences between untreated vs pre-treated somatotrophinomas. This corresponds to previous studies showing that SSA or dopamine agonists do not affect PA microvessel density[303,422,425]. I found a negative correlation between serum IGF-1 levels and perimeter and Feret's diameter suggesting that GH/IGF-1 hypersecretion may decrease vessel size and area occupied by vessels in PAs possibly explaining the differences between NFPAs and somatotrophinomas. These findings are somewhat surprising owing the angiogenic properties of IGF-1[650,651].

I noted a positive correlation between PRL and area occupied per vessel in somatotrophinomas, and between PRL and microvessel density among NFPAs, suggesting a possible role for PRL in stimulating angiogenesis in both somatotrophinomas and NFPAs. PRL has recognised angiogenic

properties[652,653], and previous studies showed that prolactinomas have higher microvessel density than other PA types[304,421,422], which can be at least in part due to PRL hypersecretion.

PA-derived FGF-2 levels were associated with smaller vessels in PAs, and in somatotrophinomas FGF-2 and IL-8 correlated with increased area occupied per vessel. FGF-2 and IL-8 are expressed in PAs by both somatotroph and gonadotroph cells[232,416] and have angiogenic properties[297,417], thus may be able to modulate PA angiogenesis. However, most of my data correlating PA-derived secretome and angiogenic parameters were negative, including for VEGF-A (strong angiogenic factor in PAs[301,304]), suggesting that cytokines released by PA cells *per se* may play a limited role in tumoural angiogenesis. Other factors such as the hormonal milieu in PAs or secreted pro-inflammatory cytokines from TME non-neoplastic cells, as described for other cancers[648,654,655], may be more relevant for the regulation of PA angiogenesis, as discussed below.

Increased microvessel density and area were associated with more macrophages in the TME of PAs and correlated with the M2:M1 ratio. My data together with a recent study showing more M2-macrophages in rat prolactinomas than in NP, and that tumour M2-macrophage content increase as capillaries became more tortuous and of increased calibre[346], suggest an angiogenic role for M2-macrophages in PAs, as shown for other cancers[229,297,332,339,417,548,648,656]. Increased microvessel density/area were also associated with more PA-infiltrating CD4+ T cells, whereas PAs with more FOXP3+ T cells showed decreased microvessel density. Among NFPAs, increased amount of PA-infiltrating CD4+ and FOXP3+ T cells were associated to bigger vessels while in somatotrophinomas larger vessels were associated with more macrophages. The crosstalk between tumour and immune cells in hypoxic and cytokine-rich TME result in the induction of pro-angiogenic behaviour in both cell types and thus promoting tumour neovascularisation[648,657]. Macrophages, CD4+ T and FOXP3+ T cells are strong promoters of angiogenesis in tumours[648,655,657], in line with my data. However, the FOXP3+ T cell immunosuppressive activity directly to macrophages and CD4+ T cells may impair their angiogenic functions resulting in vascularisation suppression[658], possibly explaining why PAs with more FOXP3+ T cells had lower vessel density. Overall, these data suggest that immune cells may influence the angiogenesis in PAs, particularly macrophages and T lymphocytes, active sources of angiogenic cytokines and growth factors in the TME[648,654,655]. However, the modest infiltration of immune cell seen in PAs, and thus the lower degree of tumour inflammation resulting in lower pro-inflammatory and pro-angiogenic factors compared to malignant tumours, may explain the reduced angiogenesis in PAs.

In addition to inflammatory cell-derived angiogenic compounds, TAF-derived levels of CCL2, a chemokine with known angiogenic functions[583,584], correlated with microvessel area, suggesting a

possible role for some TAF-derived factors in PA angiogenesis as described in other cancers[384,585-587]. Thus, together with immune cells, stromal cells may influence PA neovascularisation.

Angiogenesis is commonly evaluated by immunohistochemistry assessing microvessel density and vasculature morphology by examining CD31- or CD34-stained tissue sections in image analyser systems[297,304,643], a method I used in my study. However, immunohistochemical assessment of angiogenesis has a number of shortcomings that can explain some inconsistencies among previous studies and represent limitations to my study. Firstly, as in any tumour, PAs have a complex biology and irregular geometry of the vascular system, which vary from case to case and also among different subtypes[304,416], leading to variable results. Secondly, some tumours, including PAs, have lower microvessel density than the corresponding normal tissues, hence the assessment of microvessel density may not be sufficient to reveal the functional or angiogenic status of a tumour[643]. Thirdly, is important to take into account vessel topography in the selection of the fields to assess, differentiating vessels into those supplying invading tumour edges, those serving the inner tumour area and those in the peripheral tumour areas usually composed of capillaries with endothelial cells derived from pre-existing vessels[643]. Fourthly, attention should be paid to vessel diameter, where tumours with high metabolic rate usually have small vessel diameter and high vascular density; in contrast, tumours of low metabolic rate have larger vessels with many cell layers and a relatively low vascular density. Fifthly, variability in the results can be also due to the lack of standardised protocols in manual or automated vessel counting or due to technical aspects such as observer subjectivity, choice to count vessels in hot spot areas vs randomly chosen fields, field magnification, and the selection of the endothelial marker to use on immunohistochemical studies[643].

Matrix metalloproteinases in pituitary adenomas

MMP-9 and MMP-14 have been studied in PAs, particularly their role in PA aggressiveness and phenotype[450-453,460,659]. However, studies analysing MMP-9 and MMP-14 expression in PAs vs NP are scarcer, and there are no series assessing the role of TME elements in MMP regulation.

I observed that MMP-9 and MMP-14 expression were remarkably more prominent in NPs than in PAs, in line with Knappe *et al.* findings[660]. However, Turner *et al.* reported no MMP-9 expression in all the 4 NPs analysed[421], and Pereda *et al.* found MMP-2 expression only in some PAs but not in the NPs studied[454]. I noted positive MMP-9 expression in half of the PAs, which is line with Knappe study reporting positive MMP-9 expression in 41 out of 84 PAs[660]; on other hand, only 37.5% of my PAs expressed MMP-14.

In my cohort of PAs, there were no association between MMP-9 and MMP-14 and cavernous sinus invasion or PA angiogenesis, suggesting that MMP-9's differential expression may not be that relevant or the leading mechanism to determine PA invasiveness. These findings are in line with some reports which found no association between MMPs and PA invasiveness[660,661]. However, other studies, including a large meta-analysis, showed that MMP-9 expression is associated with PA invasiveness[313,448,450,452-454]. I found that patients who had headache at diagnosis had significantly more expression of MMP-9. MMP-9 has never been implicated in the aetiology of headache in patients with PAs, although it has been linked with neuropathic pain and migraines in other settings[662-665]; moreover, MMP-9 is involved in the development of haemorrhage or apoplexy within PAs, phenomenon that can itself elicit headache[666].

Serum IGF-1 and MMP-9 expression levels correlated which may explain the increased MMP-9 immunoreactivity observed in somatotrophinomas in my study and elsewhere[660], consistent with the fact that expression and enzymatic activity of MMPs can be upregulated by IGF-1[667,668] or by other related mitogenic factors such as insulin[433,441,669]. Nevertheless, other series reported no MMP-9 expression differences among PA types, including NFPAs and somatotrophinomas[448,450,452]. Cytokines can upregulate MMP expression and activity. Hence, the negative correlations I observed between MMP-9 and PA-derived CCL2 levels in my cohort of PAs, and with CCL4, CXCL10, FGF-2 and IL-6 among somatotrophinomas, the lack of correlation between PA-derived cytokines and MMP-14 expression and the lack of association between TAF-derived cytokines and MMPs expression, were rather unexpected. Nevertheless, cytokines within the TME are also derived from other cell types, including immune cells, which can strongly modulate the expression of MMPs[433,441], possibly explaining the observed correlation between MMP-14 expression and PA-infiltrating neutrophils.

MMP activity is balanced by tissue inhibitors of metalloproteinases[433,441,453,454], which I have not analysed in my study, hence the relative imbalance between MMPs and their tissue inhibitors, cannot be fully assessed in my study. Moreover, my cohort of PAs and NPs is probably too small to properly assess differences between PAs and NPs, as well as to define the role of MMPs in PA phenotype and invasiveness, previously shown in larger studies[313,448,450,452-454,460,659]. Another aspect to consider is that tumour cells are not the only source of MMPs, which can also be derived from stromal or immune cells present in the TME[433], and thus the assessed MMP-9 and MMP-14 immunoreactivities in my study (and others) account not only PA cells but also non-neoplastic cells. Together, these reasons may explain some of my unexpected findings such as higher expression of MMP-9 and MMP-14 in NPs than in PAs, the association between higher Ki-67 and low MMP-9 expression and the lack of correlation between MMPs expression and cavernous sinus

invasion, taking into account that MMPs are involved in early stages of tumour development and mechanisms including proliferation, survival, invasion and angiogenesis[433,441]. Moreover, these reasons can also partially explain the lack of association between PA-derived or TAF-derived cytokines, PA-infiltrating immune cells and MMPs expression generally observed in my study, despite the known role for these TME elements in the regulation of MMP expression[433,441].

EMT in pituitary adenomas

EMT is determined by the interactions between different TME elements, including cytokines, as well as different non-tumour cells, and play a key role in the tumourigenesis, tumour progression and invasion[466-468]. There are no studies assessing the role of the TME in the EMT in PAs. PAs may have a partial/incomplete EMT phenotype[505,513], consistent with the fact that PAs are benign and rarely metastasise. My data corroborate this, as I observed no differences between PAs and NPs in terms of E-cadherin expression (the main EMT hallmark[466]), but a significant upregulation of ZEB1 (a marker whose over-expression suggests EMT activation[466]) in PAs in comparison to NP (none of the 10 studied NPs expressed ZEB1). The observed positive correlation between E-cadherin and ZEB1 expression was unexpected considering that ZEB1 represses E-cadherin, further supporting the notion of a partial EMT signature in PAs. My data also suggest that ZEB1 may be superior to E-cadherin to identify (early) EMT activation in PAs; in fact, factors promoting mesenchymal phenotype, such as ESRP1[505] or indeed ZEB1[513], seemed more adequate to assess EMT in PAs than epithelial markers which can be due to the fact that PA cells difficultly lose epithelial phenotype in keeping with their inability to metastasize.

In my study, there were no significant associations between E-cadherin or ZEB1 expression and clinico-pathological features, but I observed that PAs with higher Ki-67 tended to have lower E-cadherin expression, as expected, because E-cadherin downregulation and hence EMT activation, is associated with increased aggressiveness in cancer[466-468], and in PAs[449,460,461].

There were no differences regarding E-cadherin or ZEB1 immunoreactivities between NFPAs and somatotrophinomas. However, within somatotrophinomas E-cadherin expression and serum GH and IGF-1 correlated negatively, suggesting a potential effect for GH/IGF-1 excessive levels to induce EMT in patients with somatotrophinomas by downregulating E-cadherin, an effect already described for GH which is regarded as a strong EMT inducer[499]. However, my data contrast with those from Lekva's study showing positive correlation between E-cadherin and GH/IGF-1 levels[505].

Cytokines and growth factors are recognised EMT promoters due to their repressive effect on E-cadherin expression, but also by upregulating mesenchymal markers such as ZEB1[466]. E-cadherin downregulation was correlated with VEGF-A, a growth factor known to induce EMT[647], in part by repressing E-cadherin expression in tumour cells[467,647]. TAF-derived PDGF-AA also correlated negatively with E-cadherin expression suggesting a possible role for TAF secretome in promoting EMT by downregulating E-cadherin. PDGFs are growth factors secreted by different cells, including fibroblasts, and has been shown that different PDGF isoforms and their receptors have important roles in the regulation of tumourigenesis, proliferation and survival of tumour cells, angiogenesis and in promoting EMT[588-590].

Despite the fact that immune cells within the TME are well-known promoters of EMT[466], I found no associations between PA-infiltrating immune cells and E-cadherin/ZEB1 expression, suggesting the lack or (very) mild effect of these non-neoplastic TME cells in the EMT modulation in PAs *in vivo*, although *in vitro* macrophage-derived factors were able to induce EMT in GH3 cells (Chapter 3). The lack of a true EMT signature in my cohort of PAs may actually explain, at least in part, these negative data and the contrast findings between my *in vitro* and human data. There was, however, a positive correlation between M2:M1 ratio and ZEB1 expression in somatotrophinomas, suggesting that, at least in this subtype, the predominance of M2 over M1-macrophages may activate EMT, an effect well-recognised to M2-macrophages[229,334,466,670].

NCAM in pituitary adenomas

In my study, there were no NCAM expression differences between NFPAs and somatotrophinomas, as described in another study[37]. While there were no associations with clinico-pathological features, PAs with cavernous sinus tended to exhibit increased NCAM expression in line with data linking NCAM expression to aggressiveness and poor outcome in cancer[36,40,42-44] and to higher PA invasion[627,641]. However, other studies showed no relation between NCAM expression and PA invasiveness[639,642].

In my study, I found no association between NCAM expression and GH/IGF-1 levels, despite the fact that NCAM increase GH release from foetal pituitary cultures and cultured somatotrophinoma cells[626]. However, NCAM expression correlated with serum LH and FSH, which may be due to a direct effect on gonadotropin secretion taking into account that pituitary hormone secretion is regulated by cell-cell contact (as shown for GH[626] and PRL[671]). I noted a negative correlation between serum PRL and NCAM expression only in somatotrophinomas, but this result was driven by an outlier, thus is unlikely that PRL have any effect in NCAM expression, or the other way

around (i.e. NCAM overexpression unlikely decrease PRL secretion). In fact, as for GH[626], NCAM may stimulate PRL secretion, as shown in GH4 pituitary tumour cells in which NCAM induction increased 40-fold PRL secretion[671]. However, in rat transplantable pituitary tumours polysialylated-NCAM expression did not correlate with GH or PRL secretion[641].

The role of cytokines in the modulation of cell adhesion molecules, including NCAM, has been described[672], but in my study I generally found no correlation between PA-derived cytokines and NCAM expression in PAs. However, among somatotrophinomas increased levels of PA-derived CCL4, CXCL1, FGF-2 and IL-6 correlated with lower NCAM expression. Regarding TAF-derived cytokines, NCAM expression correlated only with FGF-2. These data suggest that cytokines derived from PA cells or TAFs may not have a major role in the modulation of NCAM in PAs. However, FGF-2 may indeed modulate NCAM expression in PAs taking into account that NCAM intracellular signalling and physiological effects are mediated by FGF-receptors[673,674].

The role of immune cells in modulating cell adhesion molecules expression, including NCAM, is well-known. Immune cells can down or upregulate cell adhesion molecules, depending on many factors, including the surrounding TME. On the other hand, cell adhesion molecules can also influence immune infiltrates in tissues, including in the TME, as they play important roles in immune cell recruitment and transmigration[675-678]. Nevertheless, I found no association between NCAM expression and PA-infiltrating immune cells, suggesting that immune infiltrates in the TME of PAs may not play a crucial role in the modulation of NCAM expression.

Overall, my data suggest that NCAM expression in PAs may not be dependent of cellular or non-cellular TME elements, as PA-infiltrating immune cells and PA- or TAF-derived cytokines do not affect NCAM expression. However, I have only analysed the general form of NCAM and these data cannot be extrapolated to its different isoforms, including the polysialylated form, which may be more relevant to the PA biology considering that hypersialylation is a mechanism that confer increased aggressiveness to tumours[679] and polysialylated-NCAM was associated with PA invasiveness[627,641].

Conclusions

In summary, my data suggest that some of the different cellular and non-cellular TME elements within PAs may have a modulatory role in distinct oncogenic mechanisms. PA-derived cytokines (namely FGF-2 and IL-8), as well as TAF-derived cytokines (namely CCL2) may influence the PA

angiogenesis, although the modulatory angiogenic effect of immune cells seems to prevail, with macrophages (M2), CD4+ T and FOXP3+ T cells appearing particularly relevant. PA- and TAF-derived cytokines (CCL2, CCL4, FGF-2, IL-6, CXCL1) influenced MMP and NCAM expression in PAs, more prominently among somatotrophinomas than in NFPAs, with PA-infiltrating immune cells showing little or no correlation with MMP and NCAM. In terms of EMT, my human PA data showed no association between immune cells and E-cadherin or ZEB1 expression, as well as minor influence from PA or TAF-derived factors in the expression of EMT markers, supporting a lacking or mild effect exerted by these cells in EMT modulation in PAs, contrasting with *in vitro* data showing that macrophage-derived factors induce EMT in pituitary tumour cells (Chapter 3). The partial EMT signature in my cohort of PAs (ZEB1 upregulated but no E-cadherin downregulation in comparison to NP) may explain, at least in part, some of my negative or unexpected results, as well as the discrepancies between my human PA and *in vitro* data.

Chapter 6: The effect of AIP deficiency in the pituitary tumour cytokine secretome

Introduction

The AIP protein is an ubiquitously expressed co-chaperone binding to several partners (Figure 1.4 in Chapter 1), including the AHR which is one of the main AIP partners[152,176]. AHR is a ligand-activated transcription factor classically involved in the toxic effects of the environmental toxin TCDD[152,177]. However, AHR has been involved in immune system regulation[177,680,681], such as regulating the production of cytokines and reactive oxygen species[682], controlling the differentiation and activity of T helper 17 cells[683], modulating adaptive immune responses[681,684], influencing biological processes in immune cells[681] including polarisation of macrophages[685] or the development of germinal centre B cells[686], as well as interacting with some components of the NF-kβ signalling pathway[687,688], an important pathway for the regulation and activation of immune responses including cytokine secretion[689].

The cytokine network in cancer is complex and predisposes to tumour initiation and growth, particularly in highly or chronic inflammatory conditions. However, not only does inflammation promote tumourigenesis, but also tumours can produce inflammation as a result of tumour cell secretion of mediators as cytokines, chemokines and growth factors into the TME, which can be a direct consequence of a certain oncogenic change such as a oncogene or tumour suppressor gene mutation[209,210]. Borrello *et al.* provided the first evidence for this showing that the rearrangement of the RET tyrosine kinase (recognised partner of AIP[152]) in thyrocytes represent a frequent, early and causative genetic event in the pathogenesis of papillary thyroid carcinoma, with the oncogenic change RET/PTC in primary human thyrocytes resulting in inflammation activation, including a number of different inflammatory mediators such as CCL2, CCL20 and IL-8[690]. Currently, other oncogenic changes affecting different genes (such as *VHL*, *TP53, MYC*) are known to modulate the cytokine network in the TME and thus tumour-related inflammation[209,210]. In fact, oncogenic changes in tumour cells may disrupt the cytokine/chemokine system: in some cancers, there is overexpression of certain chemokines leading to increased inflammatory cell contents and creating a tumour supportive TME, whereas in others chemokine downregulation impair anti-tumour immune responses[209,227].

Hence, I hypothesised that AIP loss could influence the pituitary tumour cytokine secretome, and if so, perhaps differential cytokine secretory activities among AIP deficiency vs AIP normal tumour cells may constitute an explanation for the increased *AIP*mut PA aggressiveness[19,91,161,691] and high number of macrophages and FOXP3+ T cells observed in *AIP*mut PAs[513].

Aims

Overall aim

To investigate the role of AIP deficiency in the pituitary tumour cell cytokine secretome.

Specific aims

1. To determine the role of AIP deficiency in the pituitary tumour cell cytokine secretome
2. To determine the role of AIP deficiency in the cytokine secretome of non-neoplastic cells, in particular tumour-associated fibroblasts and dermal fibroblasts
3. To assess the role of AIP deficiency in the cytokine secretome response to somatostatin analogues

Results

Detecting differences in the cytokine secretome between *AIP*mut PAs and *AIP*neg PAs could explain some of the biological and phenotype differences among them, namely, the increased aggressiveness of *AIP*mut PAs[19,152] (discussed in detail in Chapters 7 and 8). Differential *AIP*mut PA-associated cytokine and chemokine secreting abilities could also explain the higher amount of macrophages seen in human (Figure 6.1-A) and mouse (Figure 6.1-B) *AIP*mut somatotrophinomas[513], as well as the increased chemotaxis induced by GH3-*Aip*-KD cells in RAW264.7 macrophages observed in my own *in vitro* functional experiments (Figure 6.1-C) and in bone marrow-derived rat macrophages as reported by Dr. Barry[513] (Figure 6.1-D), findings that indeed prompted me to assess the cytokine secretome differences among pituitary tumour cells with and without AIP deficiency.

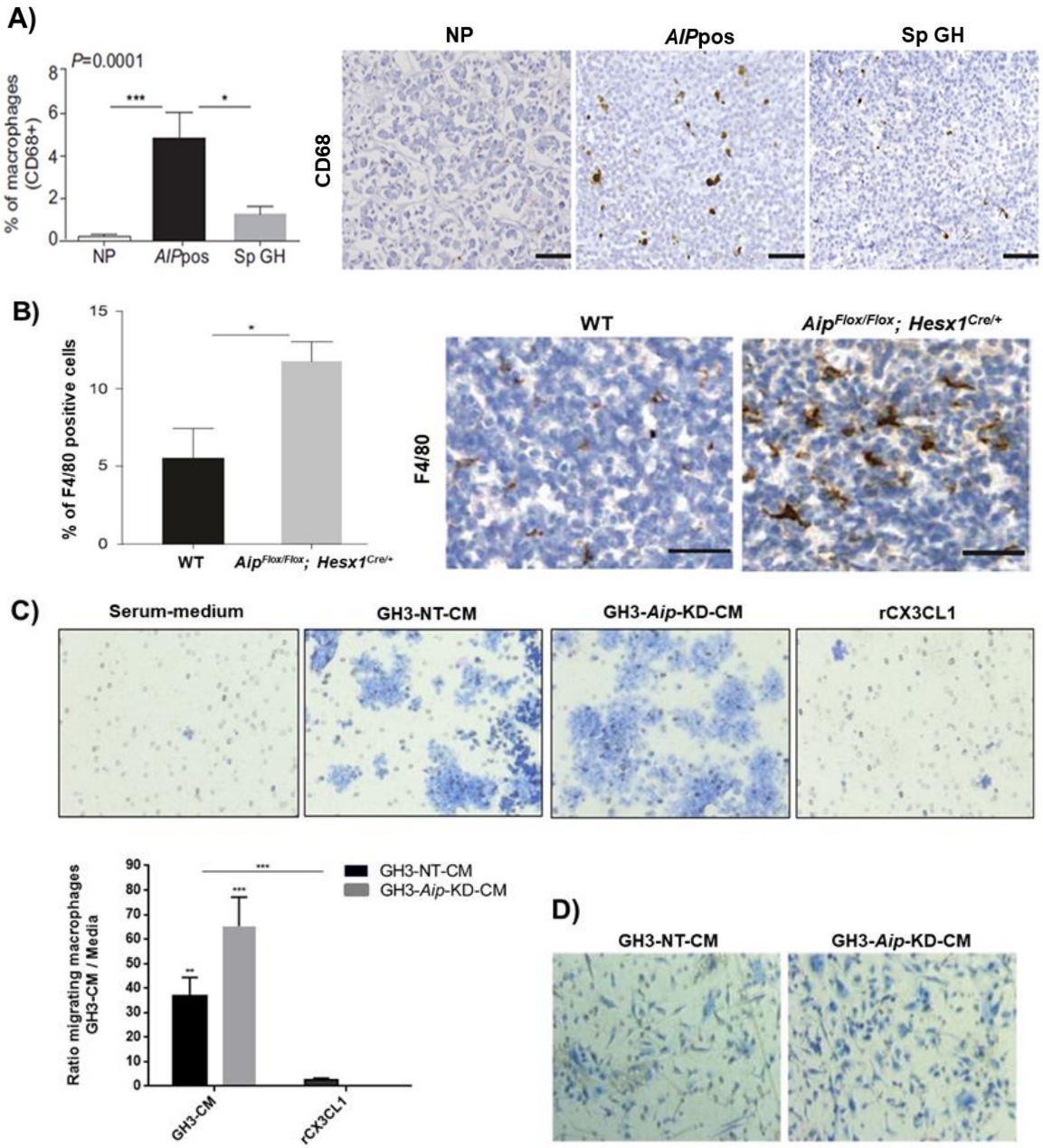

Figure 6.1: Increased macrophage infiltrates and chemotaxis in *AIP* mutation-positive tumours
A) Immunohistochemical analysis of macrophages in human *AIP* mutation-positive somatotrophinomas (*AIP*pos), sporadic somatotrophinomas (Sp GH) and normal pituitary (NP). Data are shown as mean±SEM for the percentage of CD68+ cells per high power magnification field, counted on 3-5 random fields; n=5 in each subgroup. Representative images are shown, at x200 magnification. Scale bar=100µm. *, <0.05, **, <0.01, ***, <0.001 (Kruskal-Wallis test followed by Conover–Inman test for individual comparisons) – Dr. Sayka Barry´s data[513]. B) The graph bar shows the increased number of macrophages in *Aip*-knockout mice (*Aip*$^{Flox/Flox}$;*Hesx1*$^{Cre/+}$) compared to wild type (WT). Representative images of macrophage infiltration in WT and homozygote *Aip*-knockout mice as determined by F4/80 staining (mouse macrophage marker) and quantified as percentage of F4/80+ cells. n=4 per genotype. Scale bar = 50µm. *, <0.05, **, <0.01, ***, <0.001 (Mann Whitney U test) (Dr. Sayka Barry´s data[513]). C) Transwell assay performed on RAW 264.7 macrophages towards serum-medium, GH3-NT-CM, GH3-*Aip*-KD-CM and recombinant CX3CL1 (rCX3CL1) at 100ng/mL for 72h. Data are shown as mean±SEM for the ratio of migrated macrophages towards GH3-NT-CM or GH3-*Aip*-KD-CM or rCX3CL1 in relation to migrated macrophages in serum-medium. n=6. *, <0.05, **, <0.01, ***, <0.001 (two way-ANOVA with Bonferroni multiple comparison test). D) Transwell migration assay representative images showing that bone-derived rat macrophages migration was more prominent towards GH3-*Aip*-KD-CM compared to GH3-NT-CM (Dr. Sayka Barry´s data[513]).

Considering the extreme rarity of *AIP*mut PAs available as a fresh sample for culture, it was not possible to conduct a proper cytokine study on freshly cultured human *AIP*mut PAs in order to investigate the effects of AIP deficiency in the pituitary tumour cytokine secretome. However, I had a single sample available. As a model, therefore, I have assessed the cytokine profile in supernatants from a stably lentiviral-transduced shRNA knockdown of *Aip* in the rat pituitary somatomammotroph cell line GH3 (GH3-*Aip*-KD), which was available in our laboratory, and compare this to the cytokine secretome from non-targeting GH3 cells (GH3-NT) with normal AIP levels. These GH3-*Aip*-KD cells show 80% reduced AIP protein in comparison to the GH3-NT cells (Figure 6.2).

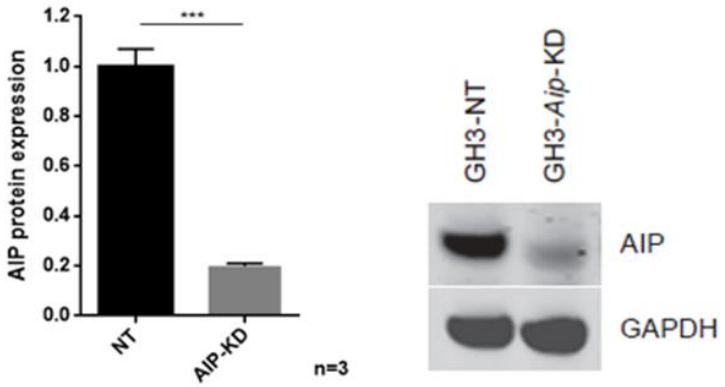

Figure 6.2: GH3-*Aip*-KD cells have 80% reduced levels of AIP comparing to GH3-NT cells
AIP protein expression in shRNA transduced GH3 cells (GH3-*Aip*-KD) compared to NT shRNA GH3 cells (GH3-NT), assessed by immunoblotting. A representative image is shown. Data are shown as mean±SEM, is normalised to GAPDH and compared to GH3-NT cells, n=8 (Mann Whitney U test). Data from Dr. Stiles.

During the time of this study, I had one *AIP*mut somatotrophinoma operated from which I could set up primary cultures of both PA cells and TAFs, and then assess their cytokine secretome in culture supernatants. I also had the opportunity to culture skin fibroblasts derived from subjects carrying germline *AIP* mutations in homozygosity and heterozygosity (unpublished patients), and then being able to analyse their secretomes and compare it to those from skin fibroblasts collected from healthy subjects. These unique data will be shown here, despite the fact that the low number of cases does not allow a proper statistical analysis of the results.

The role of *AIP* deficiency in the cytokine secretome of GH3 cells

Supernatants from GH3-*Aip*-KD and from GH3-NT cells were collected at different time-points (24, 48 and 72h) and then assessed by the rat cytokine Millipore MILLIPLEX 27-plex assay. Of the 27 cytokines measured simultaneously by this assay (Appendix 5), CX3CL1 was the only significantly

increased in the GH3-*Aip*-KD supernatants at both 24h and 48h when compared to GH3-NT cell supernatants (Figure 6.3-A). Increased CX3CL1 expression in GH3-*Aip*-KD was validated by RT-qPCR (Figure 6.3-B). CX3CL1 receptor (CX3CR1) is not expressed by GH3-*Aip*-KD or GH3-NT cells, as confirmed by RT-qPCR.

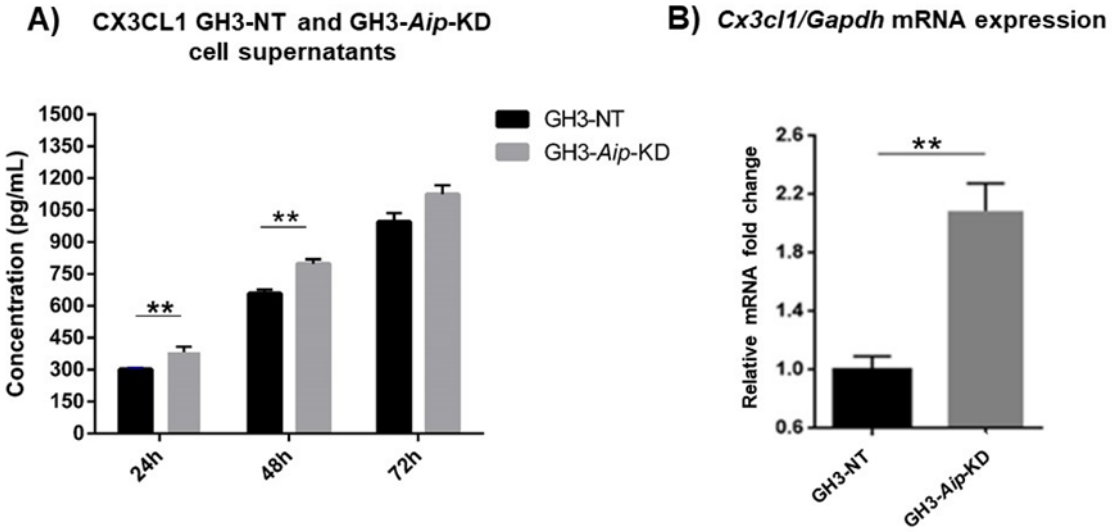

Figure 6.3: CX3CL1 in GH3-*Aip*-KD vs GH3-NT cells
A) CX3CL1 (fractalkine) concentration in GH3-NT *vs* GH3 *Aip*-KD cells. Millipore MILLIPLEX assay measured simultaneously 27 different cytokines, chemokines and growth factors. CX3CL1 levels were significantly higher in GH3-*Aip*-KD supernatants than in GH3-NT cells supernatants at 24 and 48h. Data are shown as mean±SEM for concentration (pg/mL), n=6. *, <0.05, **, <0.01, ***, <0.001 (Mann Whitney U test) B) *Cx3cl1* expression in GH3-NT and GH3-*Aip*-KD cells determined by RT-qPCR. GH3-*Aip*-KD cells have higher *Cx3cl1* expression than GH3-NT cells. Data are shown as relative *Cx3cl1* mRNA expression fold change relative to *Gapdh*, mean±SEM, determined by ΔΔCT method. n=3. *, <0.05, **, <0.01, ***, <0.001 (Mann Whitney U test).

Increased CX3CL1 levels in GH3-*Aip*-KD cells supernatants seems to be due its increased synthesis, rather than due to increased cleavage in its shed form, as no differences were noted in ADAM10, ADAM17 and MMP-9 expression among GH3-*Aip*-KD and GH3-NT cells (Figure 6.4).

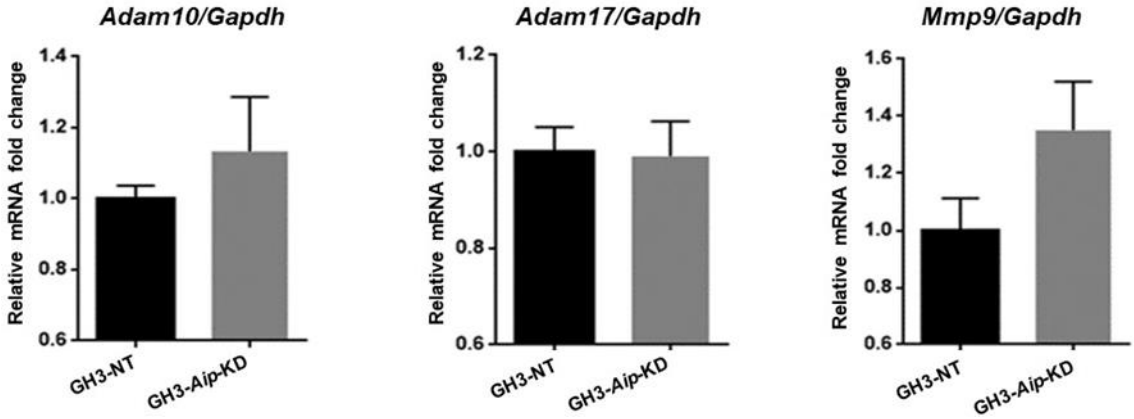

Figure 6.4: CX3CL1 cleavage-related proteases expression in GH3-NT and GH3-*Aip*-KD cells
Data are shown as *Adam10*, *Adam17* and *Mmp9* mRNA fold expression relative to *Gapdh*, mean±SEM, determined by RT-qPCR using ΔΔCT method. n=3. *, <0.05, **, <0.01, ***, <0.001 (Mann Whitney U test).

However, the association AIP deficiency and differential CX3CL1 expression/secretion was not confirmed in the gene expression data previously generated by my colleagues Dr. Craig Stiles and Dr. Sayka Barry, in both human PAs (Figure 6.5-A) and in GH3 cells transiently knockdown for AIP (Figure 6.5-B). I performed an ELISA experiment measuring CX3CL1 levels on GH3-*Aip*-KD and GH3-NT cell supernatants at both 24h and 48h (Figure 6.5-C), which failed to validate the differences seen in the cytokine array and in the RT-qPCR experiment.

A)

LIMMA comparison	Probe ID	Map	Symbol	LogFC	*p* value
***AIP*pos vs NP**	823_at	16q13	CX3CL1	-0.460	0.365
***AIP*neg vs NP**	823_at	16q13	CX3CL1	-0.769	0.200
***AIP*pos vs *AIP*neg**	823_at	16q13	CX3CL1	0.308	0.854

LIMMA comparison	Probe ID	Map	Symbol	LogFC	*p* value
***AIP*pos vs NP**	203687_at	16q13	CX3CL1	-0.028	0.943
***AIP*neg vs NP**	823_at	16q13	CX3CL1	-0.080	0.858
***AIP*pos vs *AIP*neg**	823_at	16q13	CX3CL1	0.052	0.989

B) ***Cx3cl1* expression in siRNA GH3-*Aip*-KD vs GH3-NT cells**

siRNA GH3-*Aip*-KD cells vs GH3-NT cells (n=2)	*Cx3cl1*
Average expression	6.952165
LogFC	0.3247
***p* value**	0.0526396

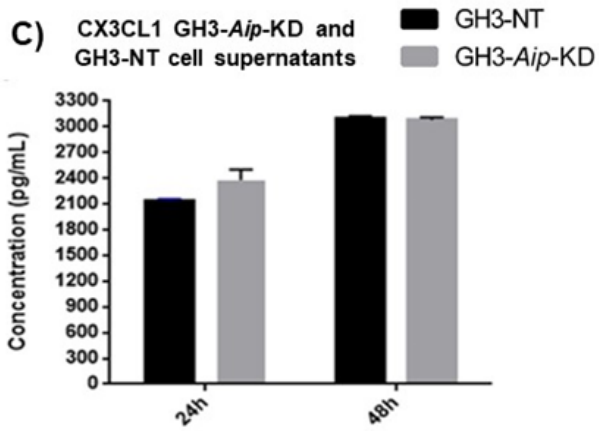

Figure 6.5: Effect of *AIP* mutation or *AIP* knockdown in CX3CL1 expression
A) Affymetrix gene expression data regarding mRNA *CX3CL1* expression in human pituitary adenoma samples. Two CX3CL1 probes were available in Affymetrix assay (823_at and 203687_at). There were no differences in *CX3CL1* expression between *AIP* mutation-positive PAs (*AIP*pos, n=6) *vs* normal pituitary (NP, n=5), or *vs AIP* mutation-negative PAs (*AIP*neg, n=5). B) Affymetrix gene expression data regarding mRNA *Cx3cl1* expression in siRNA GH3-*Aip*-KD cells (transient knockdown) *vs* GH3-NT cells (n=2). No statistical difference in *Cx3cl1* expression between GH3-NT and transient GH3-*Aip*-KD cells was noted (Dr. Craig Stiles´ data). C) CX3CL1 concentration in GH3-NT *vs* GH3-*Aip*-KD cells quantified by ELISA. No differences in CX3CL1 levels were seen in GH3-*Aip*-KD supernatants in comparison to GH3-NT at both 24 and 48h. Data are shown as mean±SEM (n=3). *p* values were non-significant (Mann Whitney U test).

CX3CL1 levels in the PA cell supernatant from the cultured human *AIP*mut somatotrophinoma were less than those observed in *AIP*neg somatotrophinomas (3.98 vs 13.23±4.12pg/mL, Table 6.1). *AIP*mut somatotrophinoma-associated TAFs had lower CX3CL1 concentration (22.96 pg/mL)

in their supernatants than the CX3CL1 levels seen in sporadic PA-associated TAF supernatants (26.86±8.34pg/mL, Table 6.2). CX3CL1 levels were also lower in supernatants from skin fibroblast from individuals carrying an *AIP* mutation in homozygosity and in heterozygosity in comparison to those seen in healthy skin fibroblast (Table 6.3). These data, together with those summarised in Figure 6.3, contradicted the hypothesis raised by my preliminary cytokine and RT-qPCR data that AIP deficiency could lead to increased expression and secretion of CX3CL1 from *AIP*mut pituitary tumour cells (Figure 6.3).

Considering these inconsistent findings regarding CX3CL1, a recognised macrophage-attracting chemokine[477,692], differential secretion of other chemokines/factors derived from tumour cells with and without AIP deficiency could then potentially explain, at least in part, the increased amount of infiltrating macrophages in *AIP*mut PAs and the increased macrophage chemotaxis promoted by tumour cells with AIP deficiency (Figure 6.1), including CCL2, CCL5 or CCL17.

From the cytokine data, I noted that the absolute CCL2 concentrations were higher in GH3-*Aip*-KD than in GH3-NT cells at 24, 48 and 72h (non-significantly), but statistical significance was almost reached for the time-point 24h (141.52±18.86 *vs* 82.61±25.47, p=0.088) (Appendix 5). Of note, CCL2 levels were marginally increased in the *AIP*mut somatotrophinoma supernatant in comparison to *AIP*neg somatotrophinomas (62.55 *vs* 54.27±23.69 pg/mL) (Table 6.1), but CCL2 levels were higher in *AIP*mut somatotrophinoma-TAF supernatants (14354.69 pg/mL) than in sporadic somatotrophinoma-TAFs (4795.62±679.53 pg/mL) or in the overall TAFs (4786.86± 642.17pg/mL) (Table 6.2).

Dr. Barry's previous study found increased CCL5 levels in GH3-*Aip*-KD cells in comparison to GH3-NT cells[513], but I did not observe this difference in my cytokine bead array data on GH3-*Aip*-KD and GH3-NT cells supernatants, in which CCL5 levels did not differ among them, and were even slightly higher in GH3-NT supernatants at both 24h and 48h (Appendix 5). Moreover, CCL5 levels in the human *AIP*mut somatotrophinoma were lower than the mean CCL5 concentration observed in supernatants from *AIP*neg ones (1.28 vs 2.84±0.81pg/mL) (Table 6.1). Hence, according to these data, differential CCL5 release may not explain the macrophage infiltrates differences between *AIP*mut and *AIP*neg PAs.

Although CCL17 was upregulated in GH3-*Aip*-KD cells in comparison to GH3-NT cells in Dr. Stiles' Affymetrix gene expression data (Figure 6.6-A), I failed to identify differences in CCL17 expression between GH3-NT and GH3-*Aip*-KD cells in my RT-qPCR experiments (Figure 6.6-B), suggesting that differential CCL17 secretion among *AIP*mut and *AIP*neg PAs may also not be the explanation for more infiltrating macrophages in *AIP*mut PAs.

A) *Ccl17* expression in siRNA GH3-*Aip*-KD vs GH3-NT cells

siRNA GH3-*Aip*-KD cells vs GH3-NT cells (n=2)	*Ccl17*
LogFC	1.01661
p value	0.00052

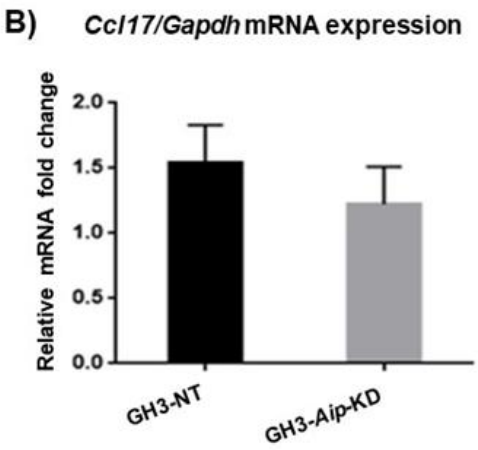

Figure 6.6: Effect of AIP knockdown in CCL17 expression in GH3 cells
A) Affymetrix gene expression data regarding mRNA *Ccl17* expression in siRNA GH3-*Aip*-KD cells (transient knockdown) vs GH3-NT cells (n=2). No statistical difference in Cx3cl1 expression between GH3-NT and transient GH3-*Aip*-KD cells was noted (Dr. Craig Stiles data). B) CCL17 expression in GH3-NT and GH3-*Aip*-KD cells determined by RT-qPCR. GH3-*Aip*-KD cells have increased CCL17 expression in comparison to GH3-NT cells. Data are shown as relative CCL17 mRNA expression fold change to GAPDH, mean±SEM, determined by ΔΔCT method. n=3. *p* value was non-significant (Mann Whitney U test).

Tumour cells with AIP deficiency may have differential cytokine secretion after stimulation than those with normal AIP levels. Although the GH3 cell secretome was not assessed after stimulation with a specific cytokine or growth factor, GH3-NT and GH3-*Aip*-KD secretomes were determined after treatment with RAW 264.7 macrophage-CM and compared to baseline. This macrophage-CM was able to induce GH3 cytokine release, namely CX3CL1, CCL3, CXCL1, CXCL10, IL-1β, IL-10, IL-13 and VEGF, in general more prominently for GH3-*Aip*-KD cells (statistical significance noted for CXCL10 and IL-1β) (Appendix 5 and Figure 3.30 in Chapter 3).

On other hand, GH3-*Aip*-KD-CM induced more prominent changes in the RAW 264.7 macrophage secretome than GH3-NT-CM, raising the secretion of most cytokines, notably CCL2, CCL4, CCL5, TNF-α, VEGF, CXCL10, IL-1α, IL-2 and IL-17 (Appendix 5 and Figure 3.22 in Chapter 3). This suggest that GH3-*Aip*-KD cell-CM may have a more potent effect in releasing macrophage cytokines and chemokines which in turn will act further as chemoattractant for immune cells including macrophages (explaining the increased immune infiltrates in *AIP*mut PAs[513]) and may confer increased aggressiveness (explaining the invasive phenotype recognised to *AIP*mut PAs[19,152]).

The role of *AIP* deficiency in the cytokine secretome of a human *AIP*mut somatotrophinoma

Due to the rarity of *AIP*mut PAs[19,152], I have cytokine secretome data from only one human *AIP*mut somatotrophinoma (*AIP*mut c.910C>T; p.R304*), rendering these data unique, but at the same time limited to properly infer secretome differences among *AIP*mut and *AIP*neg PAs.

Observing the *AIP*mut somatotrophinoma cytokine data, I cannot identify striking differences in comparison to *AIP* mutation-negative somatotrophinomas. The levels of most cytokines were actually lower in the *AIP*mut somatotrophinoma, except for CCL2, CCL3 and PDGF-AA which were slightly elevated than in the *AIP*neg cases (Table 6.1).

Cytokine	*AIP* mutation-positive somatotrophinoma (n=1)	*AIP* mutation-negative somatotrophinomas (n=8)
IL-8	26.28	60.65 ± 34.68 [0.67, 220.70]
CCL2	**62.55**	54.27 ± 23.69 [0, 153.71]
CCL3	**8.94**	3.57 ± 0.86 [0, 7.62]
CCL4	2.58	4.11 ± 1.86 [0, 14.67]
CXCL10	0	5.94 ± 2.80 [0, 18.82]
CCL22	13.17	65.03 ± 19.25 [11.50, 138.28]
CXCL1	13.96	19.65 ± 6.39 [0, 40.13]
CX3CL1	3.98	13.23 ± 4.12 [0, 31.14]
FGF-2	23.70	37.15 ± 6.32 [20.22, 74.07]
IL-6	0	0.28 ± 0.12 [0, 0.83]
PDGF-AA	**8.57**	6.89 ± 3.83 [0, 27.58]
VEGF-A	10.15	15.51 ± 7.01 [0, 52.49]
PDGF-BB	0.25	3.41 ± 1.34 [0, 10.79]
INFα2	0.87	5.48 ± 1.68 [0.18, 11.14]
IL-4	0	5.74 ± 2.62 [0, 20.18]
G-CSF	2.15	3.61 ±0.88 [0.64, 8.40]
GM-CSF	0.48	1.79 ± 0.62 [0.07, 4.34]
CCL5	1.28	2.84 ± 0.81 [0, 5.69]
IL-12 p40	0	3.98 ± 1.58 [0, 11.69]
TNF-α	0.15	0.37 ± 0.09 [0.08, 0.76]
Flt3L	0.3	2.74 ± 0.44 [1.40, 4.50]
IL-18	0	3.06 ± 1.14 [0, 7.15]
CCL11	3.28	2.66 ± 1.02 [0, 6.39]
EGF	2.21	2.33 ± 0.75 [0, 5.52]

Table 6.1: Cytokine secretome from an *AIP* mutation-positive vs 8 *AIP*neg somatotrophinomas
Cytokine secretomes were determined by the human Millipore MILLIPLEX 42-plex assay in supernatants from a human *AIP* mutation-positive somatotrophinoma (n=1) in comparison to *AIP* mutation-negative somatotrophinomas (n=8). Only detectable cytokines, chemokines or growth factors are represented in the table. Data are shown as concentration (pg/mL), mean±SEM. Minimum and maximum cytokine levels are shown in square brackets for the subgroup of *AIP* mutation-negative somatotrophinomas.

The role of *AIP* deficiency in the cytokine secretome of *AIP*mut somatotrophinoma TAFs

In order to study loss of heterozygosity these TAFs isolated from this *AIP*mut somatotrophinoma with proven germline *AIP*mut (c.910C>T; p.R304*), I extracted DNA and amplified the region of interest by PCR and then sequenced this genomic region. I confirmed that these TAFs were heterozygous for this *AIP* mutation, hence there was no loss of heterozygosity (Figure 6.7).

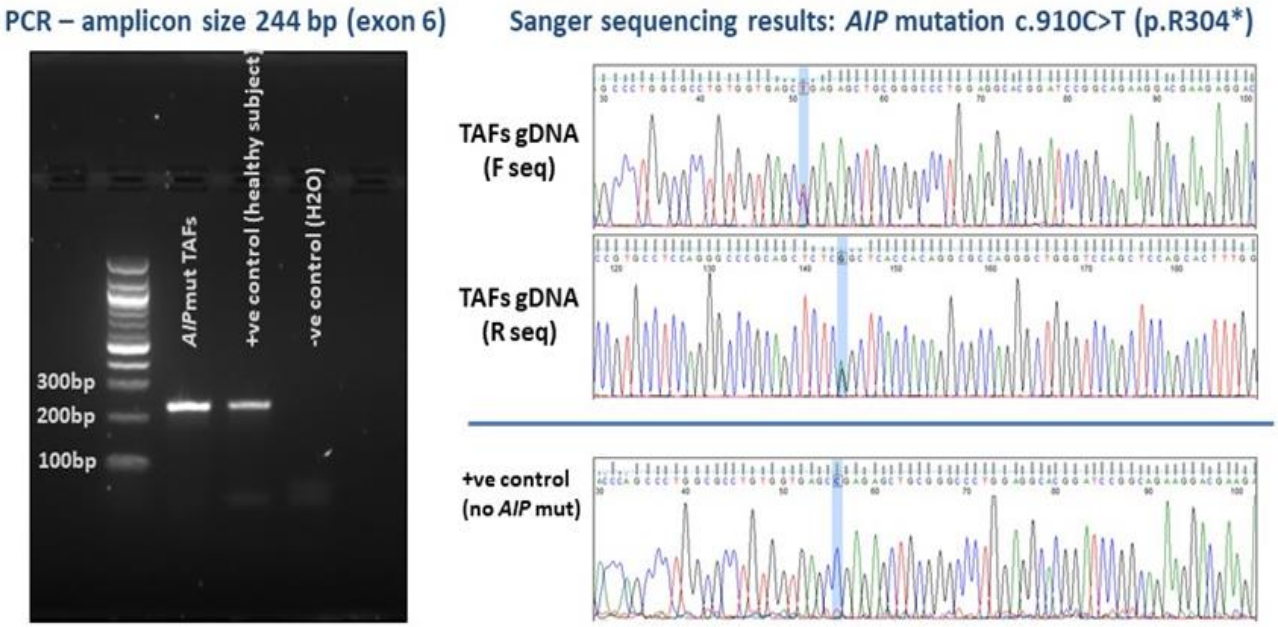

Figure 6.7: *AIP*mut PA-associated TAFs had no loss of heterozygosity at the AIP locus
On the left panel is shown the DNA amplified band with 244bp (as expected) in a DNA sample from AIPmut PA-associated TAFs and from a healthy subject (positive control confirming that the PCR reaction worked), and the negative control (water instead of DNA excluding genomic contamination in the PCR reaction). On the right panel is shown the Sanger sequencing results (GATC company) as displayed by FinchTV software showing the heterozygous status of the known *AIP* mutation.

My cytokine array data on supernatants from *AIP*mut somatotrophinoma-derived TAFs showed remarkably high CCL2 levels, 3x times more than those seen in sporadic somatotrophinoma TAFs or in sporadic overall PA-derived TAFs. *AIP*mut TAF-derived levels of CCL7 were 4-fold increased comparing to sporadic somatotrophinoma-derived TAFs and 6-fold increased than in the sporadic PA-derived TAFs. CCL22, FGF-2, CXCL1 were also modestly higher in *AIP*mut TAFs (Table 6.2).

Cytokine/ chemokine/ growth factor	***AIP*mut somatotrophinoma-derived TAFs (n=1)** Mean concentration (pg/mL) ± SEM	**Sporadic somatotrophinoma-derived TAFs (n=5)** Mean concentration (pg/mL) ± SEM	**Overall sporadic PA-derived TAFs (n=16)** Mean concentration (pg/mL) ± SEM
CCL2	**14354.69**	4795.62 ± 679.53	4786.86 ± 642.17
CCL11	1038.78	1797.30 ± 894.43	836.27 ± 328.16
VEGF-A	220.49	403.59 ± 240.29	174.29 ± 80.60
CCL22	**78.02**	36.96 ± 21.92	62.54 ± 21.50
IL-6	36.14	63.89 ± 10.45	54.76 ± 6.50
FGF-2	**52.23**	36.29 ± 4.13	42.93 ± 5.82
IL-8	32.93	65.69 ± 31.66	42.20 ± 11.11
CXCL1	**37.04**	32.54 ± 16.78	28.20 ± 6.56
CX3CL1	22.96	20.26 ± 3.86	26.86 ± 8.34

CCL7	**91.48**	23.51 ± 17.89	13.83 ± 5.97
PDGF-AA	7.89	20.98 ± 8.29	11.64 ± 3.71
IFNα2	7.08	5.68 ± 1.54	8.82 ± 2.40

Table 6.2: *AIP*mut PA-derived TAF cytokine secretome and comparison to sporadic PA-associated TAFs
Top 12 highly secreted cytokines, chemokines and growth factors in primary culture supernatants from tumour-associated fibroblasts (TAFs) isolated from PAs, including from the *AIP*mut somatotrophinoma case and from other sporadic somatotrophinomas (n=5) and overall PAs (n=16, 5 from somatotrophinomas and 11 from NFPAs). PA-derived TAF supernatants were collected following 24h on serum-free medium conditions and the cytokine secretome determined with the human Millipore MILLIPLEX cytokine 42-plex array. Data are shown as concentration (pg/mL), mean ±SEM.

The role of *AIP* deficiency in the cytokine secretome of skin fibroblasts from *AIP*mut subjects

During the course of this study, our lab obtained skin fibroblasts from a kindred with seven *AIP*mut individuals, encoded as "Family F487". Interestingly, there were 2 individuals (M1 and M8) who died in the first few months of life for unclear reasons and who carried an *AIP* mutation in homozygosity. The complete lack of AIP protein in their skin fibroblasts, as shown in the Figure 6.7, suggest that this missense change resulted in an instable protein, as shown by our laboratory using cycloheximide chase study (data not shown). We also received skin fibroblasts from 2 members carrying *AIP* mutation in heterozygosity (M2 and M3) with detectable AIP but, as expected, in less amount than wild-type skin fibroblasts (Figure 6.8).

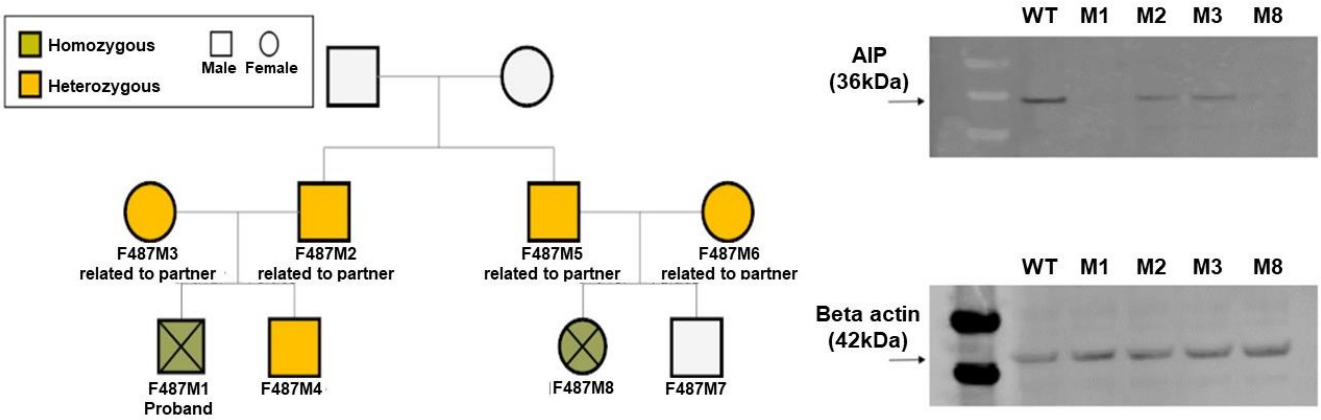

Figure 6.8: *AIP*mut kindred with subjects carrying *AIP* mutation in homozygosity and in heterozygosity
AIP mutation-positive kindred including 2 individuals with *AIP* mutations in homozygosity (F487M1 and M8) leading to lack of AIP protein in skin fibroblasts, and 2 members carrying an *AIP* mutation in heterozygosity (F487M2 and M3) expressing less amounts of AIP protein in their skin fibroblasts than in wild-type fibroblasts, as demonstrated by immunoblotting. The western blot shown was performed by Dr. Chung Lim.

When I compared the mean concentration of each cytokine measured in the supernatants from skin fibroblasts from homozygous *AIP*mut (n=2) vs heterozygous *AIP*mut (n=2) vs wild-type (n=2) subjects, there were no significant differences except for EGF (0 vs 0 vs 2.16±0.40pg/mL, $p<0.05$) (Table 6.3). The low number of samples limit conclusions from these data.

However, some observations can be made. For most cytokines, the lowest concentrations were seen in the heterozygous *AIP*mut subgroup vs homozygous *AIP*mut vs healthy subgroup, which had in general similar concentrations, with a pattern notable for CCL2 (269.62±28.92 vs 1310.22± 705.11 vs 2756.56±28.92pg/mL, respectively), VEGF-A (30.38±7.73 vs 117.81±15.72 vs 96.09± 29.12pg/mL, respectively), CCL7 (7.02±5.83 vs 29.96±16.94 vs 26.18 ±15.71pg/mL, respectively) and FGF-2 (20.07±6.08 vs 33.86±7.71 vs 28.40±0 pg/mL respectively).

In the case of IL-8, *AIP*mut status was associated with a higher concentration (homozygosity: 64.29±43.35; heterozygosity: 21.84±1.31; wild-type: 1.89±0.27pg/mL), but not consistent with data from cultured *AIP*mut somatotrophinoma cells.

In the case of IL-6, *AIP*mut status was associated to lower levels (homozygosity: 34.60±30.52; heterozygosity: 17.18±3.42; wild-type: 68.42±7.82pg/mL) (Table 6.3).

Cytokine/ chemokine/ growth factor	Homozygous *AIP*mut (M1)	Homozygous *AIP*mut (M8)	Heterozygous *AIP*mut (M2)	Heterozygous *AIP*mut (M3)	Wild-type male skin fibroblasts	Wild-type female skin fibroblasts	Serum-free medium
CCL2	605.11	2015.33	298.53	240.70	1171.34	4341.78	4.00
CXCL1	51.68	498.59	26.79	33.81	56.87	0	20.78
VEGF-A	102.09	133.52	22.65	38.10	66.97	125.21	0
IL-8	18.94	109.64	20.53	23.14	2.15	1.62	7.06
IL-6	4.08	65.11	13.76	20.59	60.60	76.24	0
FGF-2	41.57	26.15	26.15	13.99	28.4	28.4	0
CCL7	10.02	43.90	12.84	1.19	10.47	41.88	8.20
CCL22	16.00	13.73	17.15	9.30	13.73	16.00	20.78
CX3CL1	7.86	5.53	0	2.42	7.86	10.96	6.73
Flt3L	2.95	2.69	2.12	0	2.69	2.69	1.72
IL-15	1.31	2.53	0.31	0.08	2.09	1.98	0.55
G-CSF	1.22	1.90	0.25	0.16	1.16	1.05	0
IFNα2	2.49	0	0.18	1.33	2.25	0.18	1.79
GM-CSF	0.85	1.47	0.02	0.64	1.16	1.05	0
IFNγ	1.56	0.64	0.64	1.1	2.25	0.87	0.34
EGF	0	0	0	0	2.57*	1.78*	0

Table 6.3: Cytokine secretome from *AIP*mut skin fibroblasts
Cytokine secretome results determined by Millipore MILLIPLEX human 42-plex assay in supernatants from skin fibroblasts derived from 2 individuals with *AIP* mutations in homozygosity (M1, M8), 2 members carrying an *AIP* mutation in heterozygosity (M2, M3) and 2 healthy controls. Undetectable cytokines (i.e. readings below the assay quantification) were: CCL11, CCL3, CCL4, CCL5, CXCL10, IL-1A, IL-1B, IL-2, IL-3, IL-4, IL-5, IL-7, IL-9, IL-10, IL-12p40, IL-12p70, IL-13, IL-17A, IL-18, PDGF-AA, PDGF-BB, sCD40L, TNF-α, TNF-β, TGF-α. Data are shown as concentration (pg/mL). Mean of each one of the 3 subgroups (each n=2) were calculated with no statistical significance obtained for any subgroup comparison except for the significantly higher levels of EGF in healthy fibroblasts comparing to both homozygous and heterozygous *AIP*mut cases.

AIP mutation-positive fibroblasts cytokine secretome response to pasireotide

As seen for sporadic PA-derived TAFs (data shown in more detail in the Chapter 4 in Figure 4.13-A and Table 4.6, and in Appendix 7), the *AIP*mut somatotrophinoma-derived TAF cytokine secretome showed remarkable responsiveness to pasireotide, with the levels from all cytokines decreasing significantly after 24h of pasireotide treatment (10^{-7}M), except in the case of FGF-2 whose levels doubled after treatment (Table 6.4).

In sporadic PA-derived TAFs, pasireotide secretome responses were most noted for IL-6 and CCL2 reduction by 80% ($p<0.001$) and by 35% ($p=0.038$), respectively (Figure 4.13-A and Appendix 7). In the case of *AIP*mut TAFs the degree of pasireotide responsiveness was even higher, with IL-6 reducing by 90% and CCL2 by 80%. This pasireotide inhibitory effect in *AIP*mut TAFs was also prominent for CCL11 (reduced by 90%), CCL7 (reduced by 89%), PDGF-AA (reduced by 84%), IL-8 (reduced by 62%) and VEGF-A (reduced by 60%) (Table 6.4).

Cytokine/ chemokine/ growth factor	***AIP*mut somatotrophinoma-derived TAFs (n=1)** Mean concentration (pg/mL) ± SEM		**Overall sporadic PA-derived TAFs (n=16)** Mean concentration (pg/mL) ± SEM	
	UNTREATED	**PASIREOTIDE**	**UNTREATED**	**PASIREOTIDE**
CCL2	14354.69	**2919.48**	4786.86 ± 642.17	**3105.43 ± 434.95**
CCL11	1038.78	**117.39**	836.27 ± 328.16	**529.82 ± 173.32**
VEGF-A	220.49	**81.79**	174.29 ± 80.60	**134.11 ± 69.96**
CCL22	78.02	**61.47**	62.54 ± 21.50	**59.15 ± 14.64**
IL-6	36.14	**4.25**	54.76 ± 6.50	**11.83 ± 2.77**
FGF-2	52.23	**111.30**	42.93 ± 5.82	**38.62 ± 4.32**
IL-8	32.93	**12.35**	42.20 ± 11.11	**30.21 ± 9.38**
CXCL1	37.04	**23.93**	28.20 ± 6.56	**28.13 ± 4.32**
CX3CL1	22.96	**20.29**	26.86 ± 8.34	**24.04 ± 5.21**
CCL7	91.48	**10.46**	13.83 ± 5.97	**10.47 ± 3.29**
PDGF-AA	7.89	**1.28**	11.64 ± 3.71	**5.37 ± 1.38**
IFNα2	7.08	**4.09**	8.82 ± 2.40	**6.76 ± 1.35**

Table 6.4: *AIP*mut TAF cytokine secretome at baseline and after pasireotide treatment
Cytokine secretome from the human *AIP*mut somatotrophinoma-derived TAFs at baseline (untreated) and after treatment with pasireotide (10^{-7}M), and from the overall sporadic PA-derived TAFs (n=16). Data are shown as concentration (pg/mL), mean±SEM for the top 12 highly secreted proteins in PA-derived TAF supernatants collected following 24h on serum-free medium conditions with pasireotide or without. In the pasireotide treatment column, the cytokines which levels decreased after treatment with pasireotide are represented in green, whereas the cytokines that increased are represented in red.

As seen in PA-associated TAFs (Figure 4.11 in Chapter 4), SST1 was the predominant receptor type in skin fibroblasts (Figure 6.9). Hence, I have used pasireotide treatment in a similar manner and in the same dose (10^{-7}M) to assess the pasireotide cytokine secretome responsiveness of skin wild-type and *AIP*mut fibroblasts (Table 6.4).

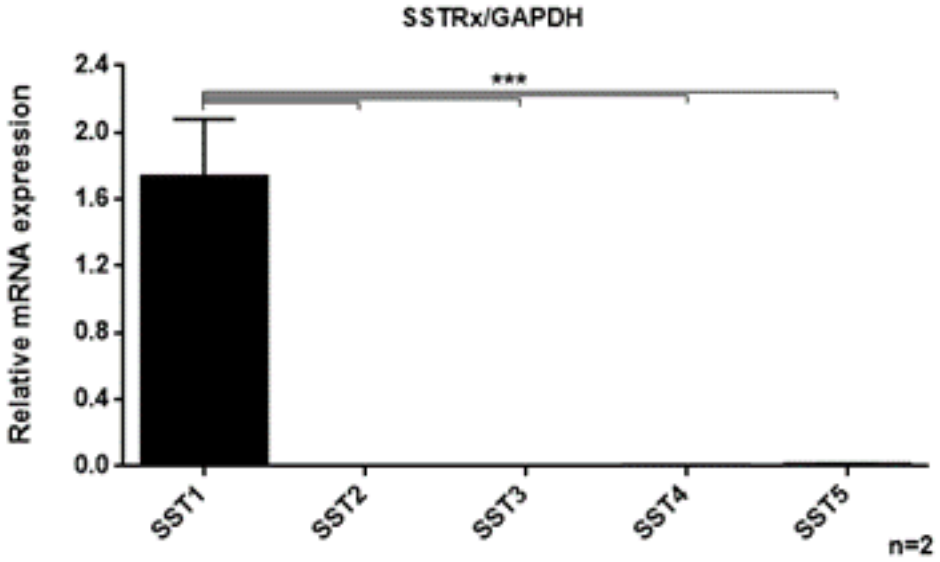

Figure 6.9: SST expression profile in human skin fibroblasts
Somatostatin receptor (SST) expression profile in human PA-derived TAFs assessed by RT-qPCR. Data are shown as *SSTx* mRNA fold change expression relative to *GAPDH*, mean±SEM, determined by the standard curve method. n=2. *,<0.05, **,<0.01, ***,<0.001 (one way-ANOVA with Bonferroni multiple comparison test).

In general, homozygous and heterozygous *AIP*mut skin fibroblasts showed marked responsiveness to pasireotide in terms of cytokine secretome inhibition, with most cytokines decreasing following pasireotide treatment, with IL-6 decreasing by and CCL2 decreasing by 52% and by 95%. Among heterozygous *AIP*mut skin fibroblasts, the IL-6 and CCL2 decrease was almost statistically significant (p=0.051 and p=0.072 respectively), despite the low number of cases analysed (Table 6.5 and Figure 6.10).

In contrast, wild-type skin fibroblasts the pasireotide-induced cytokine concentrations reductions were smaller, for instance for CCL2 with a very modest reduction by 4%. The release of some cytokines from wild-type skin fibroblasts increased after pasireotide treatment including CXCL1, VEGF-A, FGF-2 (p<0.05), CCL7, CCL22, Flt3L, GM-CSF (p=0.087) and IL-15 (Table 6.5 and Figure 6.10).

Cytokine/ chemokine / growth factor	Homozygous *AIP*mut skin fibroblasts (n=2) Mean concentration (pg/mL) ± SEM		Heterozygous *AIP*mut skin fibroblasts (n=2) Mean concentration (pg/mL) ± SEM		Wild-type skin fibroblasts (n=2) Mean concentration (pg/mL) ± SEM	
	UNTREATED	PASIREOTIDE	UNTREATED	PASIREOTIDE	UNTREATED	PASIREOTIDE
CCL2	1310.22 ± 705.11	637.17 ± 303.80	2756.56 ± 1585.22	127.22 ± 17.55	269.62 ± 28.92	259.73 ± 88.14
CXCL1	275.14 ± 223.46	132.71 ± 54.58	28.44 ± 28.44	37.24 ± 7.97	30.30 ± 3.51	33.90 ± 22.25
VEGF-A	117.81 ± 15.72	80.35 ± 19.53	96.09 ± 29.12	25.92 ± 6.01	30.38 ± 7.73	48.75 ± 2.43
IL-8	64.29 ± 43.35	17.18 ± 3.96	1.89 ± 0.27	8.20 ± 2.94	21.84 ± 1.31	2.39 ± 0.30
IL-6	34.60 ± 30.52	2.89 ± 2.05	68.42 ± 7.82	1.96 ± 1.09	17.18 ± 3.42	4.45 ± 0.89
FGF-2	33.86 ± 7.71	28.53 ± 4.83	28.40 ± 0.00	26.58 ± 2.88	20.07 ± 6.08	22.33 ± 1.37
CCL7	26.96 ± 16.94	12.70 ± 12.70	26.18 ± 15.71	0	7.02 ± 5.83	7.89 ± 0.61
CCL22	14.87 ± 1.13	19.53 ± 3.53	14.87 ± 1.14	10.45 ± 4.41	13.23 ± 3.93	18.93 ± 2.93
CX3CL1	6.70 ± 1.17	3.98 ± 2.33	9.41 ± 1.55	5.53 ± 1.55	1.21 ± 1.21	0.83 ± 0.82
Flt3L	2.82 ± 0.13	2.19 ±0.22	2.69 ± 0.00	1.95 ± 0.46	1.06 ± 1.06	1.69 ± 1.00
IL-15	1.92 ± 0.61	2.28 ± 0.42	2.04 ± 0.06	0.51 ± 0.19	0.20 ± 0.12	1.42 ± 0.22
G-CSF	1.56 ± 0.34	0.35 ±0.19	1.10 ± 0.06	0.23 ± 0.22	0.21 ± 0.05	0.18 ± 0.18
IFNα2	1.25 ± 1.25	0.78 ± 0.78	1.22 ± 1.04	0.41 ± 0.23	0.76 ± 0.58	0.41 ± 0.23
GM-CSF	1.16 ± 0.31	0.89 ± 0.89	1.10 ± 0.06	0.28 ± 0.16	0.33 ± 0.31	0.44 ± 0.20
IFNy	1.10 ± 0.46	0.55 ± 0.55	1.56 ± 0.69	0.70 ± 0.29	0.87 ± 0.23	0.64 ± 0.23
EGF	0	0	2.18 ± 0.40	0.89 ± 0.89	0	0

Table 6.5: *AIP*mut skin fibroblasts cytokine secretome at baseline and after pasireotide treatment
Cytokine secretome from skin fibroblasts derived from subjects with *AIP* mutations in homozygosity (n=2), in heterozygosity (n=2) and wild-type controls (n=2) at baseline and after pasireotide treatment. Undetectable cytokines were: CCL11, CCL3, CCL4, CCL5, CXCL10, IL-1A, IL-1B, IL-2, IL-3, IL-4, IL-5, IL-7, IL-9, IL-10, IL-12p40, IL-12p70, IL-13, IL-17A, IL-18, PDGF-AA, PDGF-BB, sCD40L, TNF-α, TNF-β, TGF-α. Data are shown as concentration (pg/mL), mean±SEM. In pasireotide treatment column, cytokines which levels decreased after treatment are represented in green, whereas those cytokines that increased are shown in red.

On an individual basis (i.e. subject by subject), the levels of IL-6, CCL2, VEGF-A, IL-8, CCL7 and INFy decreased consistently in all the *AIP*mut (homozygous and heterozygous) and wild-type skin fibroblasts following pasireotide treatment (Figures 6.11). For other cytokines there were inconsistent responses variable from subject to subject regardless genotype (Figure 6.12).

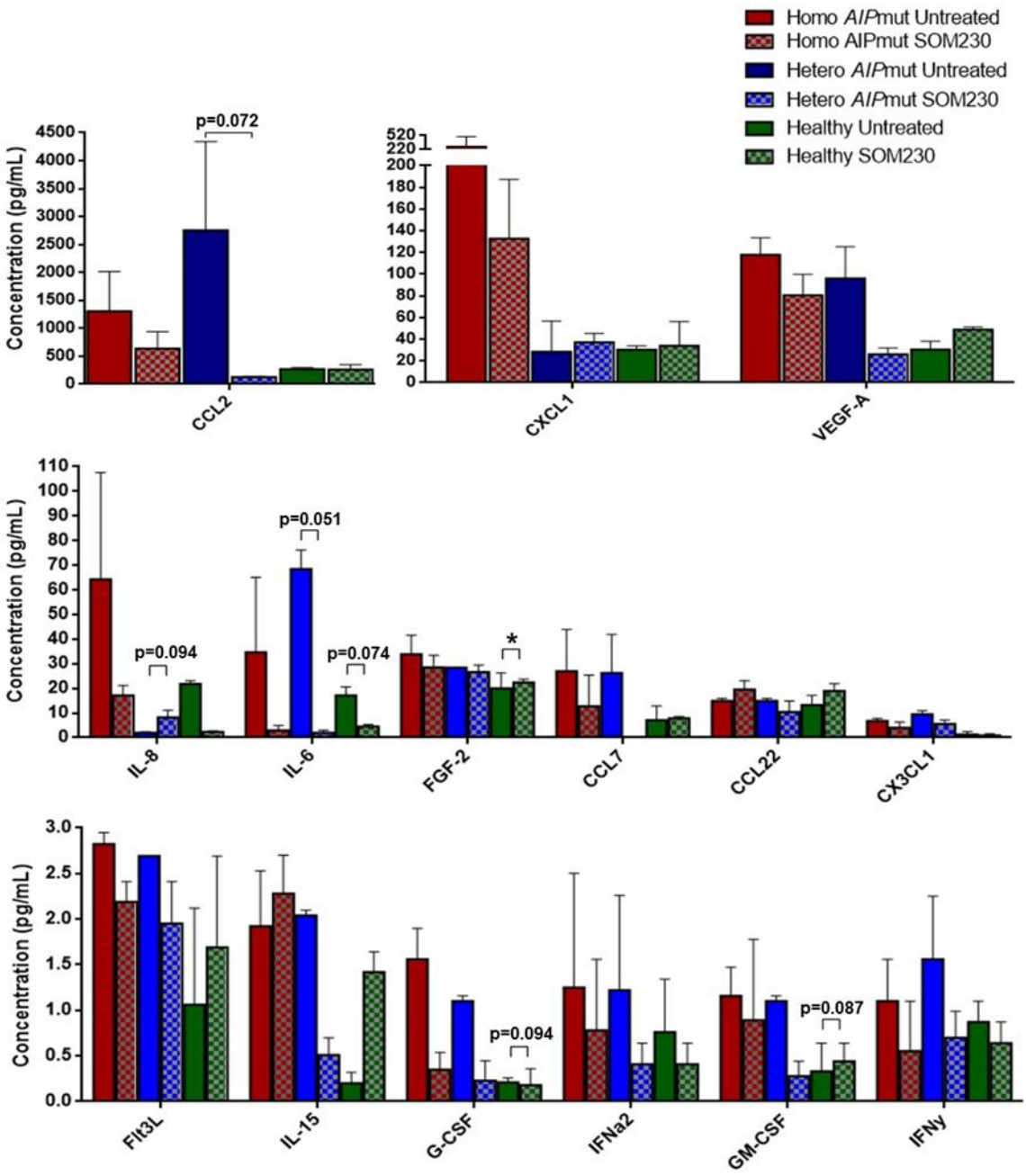

Figure 6.10: *AIP*mut skin fibroblasts cytokine secretome responsiveness to pasireotide
Cytokine secretome results at baseline and after treatment with 10^{-7}M pasireotide (SOM230) as assessed by the human Millipore MILLIPLEX 42-plex assay in supernatants from skin fibroblasts derived from subjects with *AIP* mutations in homozygosity (n=2, red), in heterozygosity (n=2, blue) and wild-type controls (n=2, green). Only detectable cytokines are shown in the figure. Data are shown as concentration (pg/mL), mean±SEM. n=2 per skin fibroblast subgroup, identified with different colours. *,<0.05, **,<0.01, ***,<0.001 (Mann Whitney U test was used to compare baseline vs pasireotide within each subgroup).

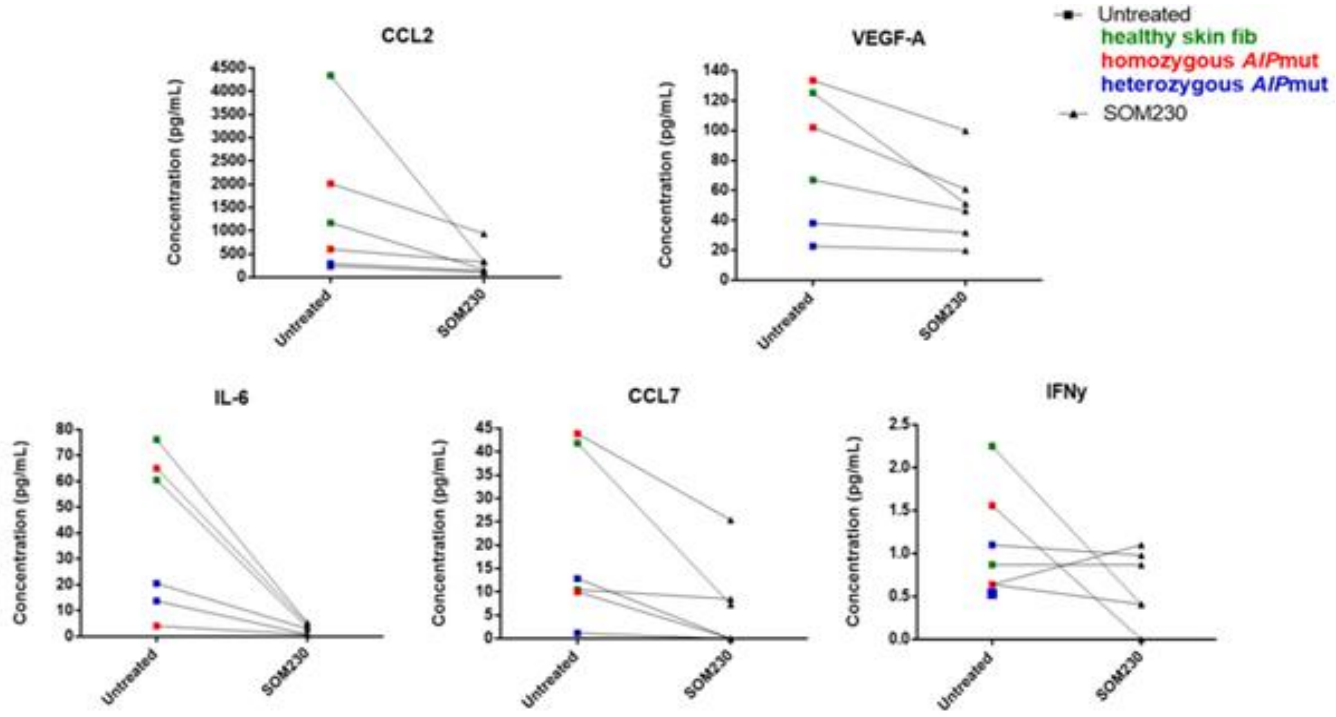

Figure 6.11: Cytokines decreased in all pasireotide-treated skin fibroblasts
Cytokines that decreased consistently in supernatants of skin fibroblasts after treatment with 10^{-7}M of pasireotide (SOM230). Data are shown as concentration (pg/mL), per case before (left, square mark) and after pasireotide (right, triangle mark), per cytokine. Subjects with *AIP* mutations in homozygosity (n=2), in heterozygosity (n=2) and wild-type controls (n=2) are identified in red, blue and green, respectively.

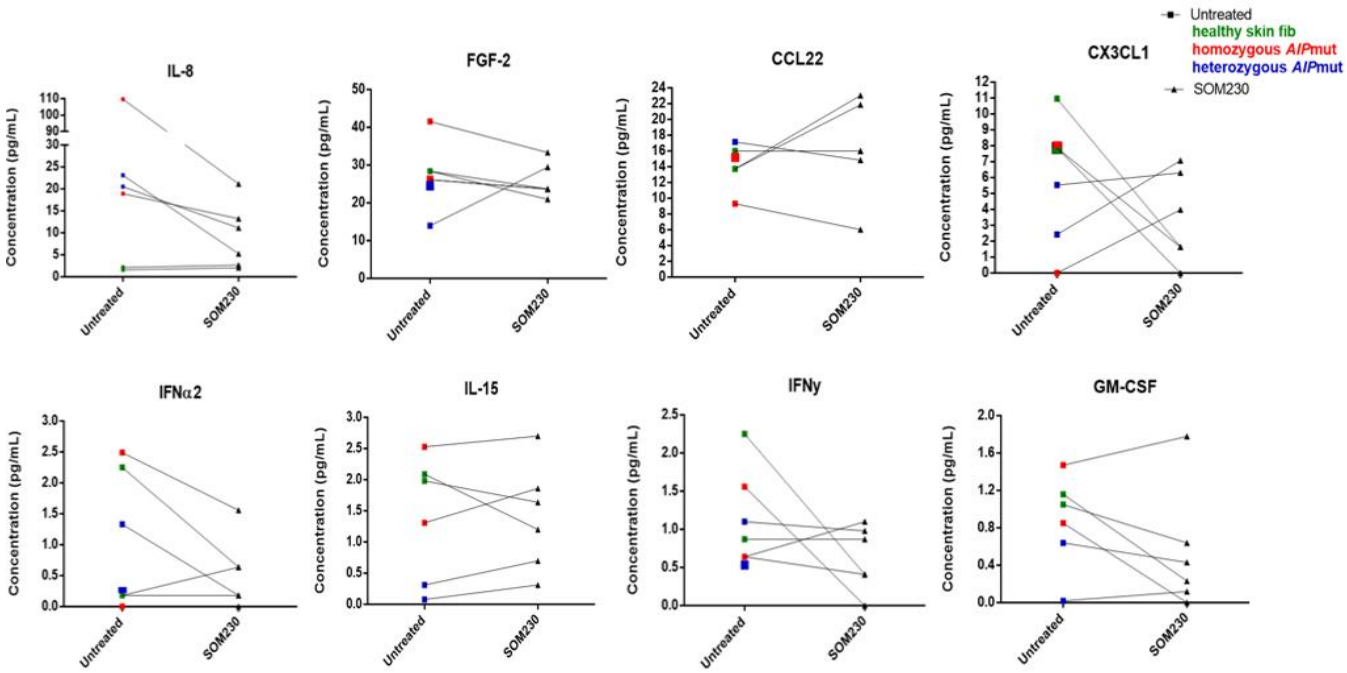

Figure 6.12: Cytokines responding inconsistently to pasireotide among the skin fibroblast subgroups
Cytokines with inconsistent responses to 10^{-7}M pasireotide (SOM230) treatment (i.e. in some cases decreased and others increased). Data are shown as concentration (pg/mL) per case before (left, square mark) and after SOM230 (right, triangle mark), per cytokine. Subjects with *AIP* mutations in homozygosity (n=2), heterozygosity (n=2) and wild-type controls (n=2) are identified in red, blue and green, respectively.

Discussion

The cytokine secretome from different cells with AIP deficiency was studied and compared to the corresponding cell types with normal AIP levels: GH3-*Aip*-KD vs GH3-NT rat pituitary tumour cells; human *AIP*mut somatotroph adenoma cells vs sporadic *AIP*neg somatotrophinoma cells; human *AIP*mut somatotrophinoma-associated TAFs vs TAFs derived from sporadic PAs and namely from somatotrophinomas; and human *AIP*mut skin fibroblasts vs wild-type fibroblasts.

CX3CL1 in *AIP*mut vs *AIP*neg pituitary tumour cells

CX3CL1 was found in higher concentrations in supernatants from GH3-*Aip*-KD cells than in GH3-NT cells, and the CX3CL1 mRNA expression was also increased in GH3-*Aip*-KD cells. These data suggested that CX3CL1 could be differentially secreted between pituitary tumour cells with and without AIP deficiency.

CX3CL1 is a chemokine that promotes tumour growth[223], macrophage chemotaxis and polarisation to the M2-macrophage phenotype, EMT pathway[477,692], and also leukocyte adhesion to activated endothelial cells, thus having important roles in the TME. CX3CL1 and its receptor CX3CR1 are expressed in different cancers and have well-known pro-tumourigenic effects, for instance in nervous system malignancies[228]; however, owing to its adhesive properties, CX3CL1 can also exert anti-tumour effects[228,693] (Appendix 10).

CX3CL1 comprises 5 domains (Figure 6.13-A), including a mucin-like stalk structure similar to some ECM proteins indicating its ability to interact with ECM, thus explaining some its functions as leukocyte transmigration or cell adhesion[694]. CX3CL1 exists in 2 forms: membrane-attached and shed forms. Shedding of the membrane CX3CL1 into soluble forms represents a regulatory mechanism for CX3CL1 signalling. The liberation of soluble CX3CL1 is mainly done by the metalloproteinases ADAM10, ADAM17, but other MMPs can be involved (Figure 6.13-B)[693,695]. This prompted me to assess the *Adam10*, *Adam17* and *Mmp9* expression in GH3-*Aip*-KD and GH3-NT cells to understand whether the increased CX3CL1 levels in GH3-*Aip*-KD supernatants seen in my cytokine array data could reflect an increased CX3CL1 cleavage rather than increased production. There were no differences in the expression of these metalloproteinases between GH3-*Aip*-KD and GH3-NT cells, suggesting that GH3-*Aip*-KD cells may release more CX3CL1 due to increased synthesis rather than increased cleavage associated to metalloproteinase enzymatic activity.

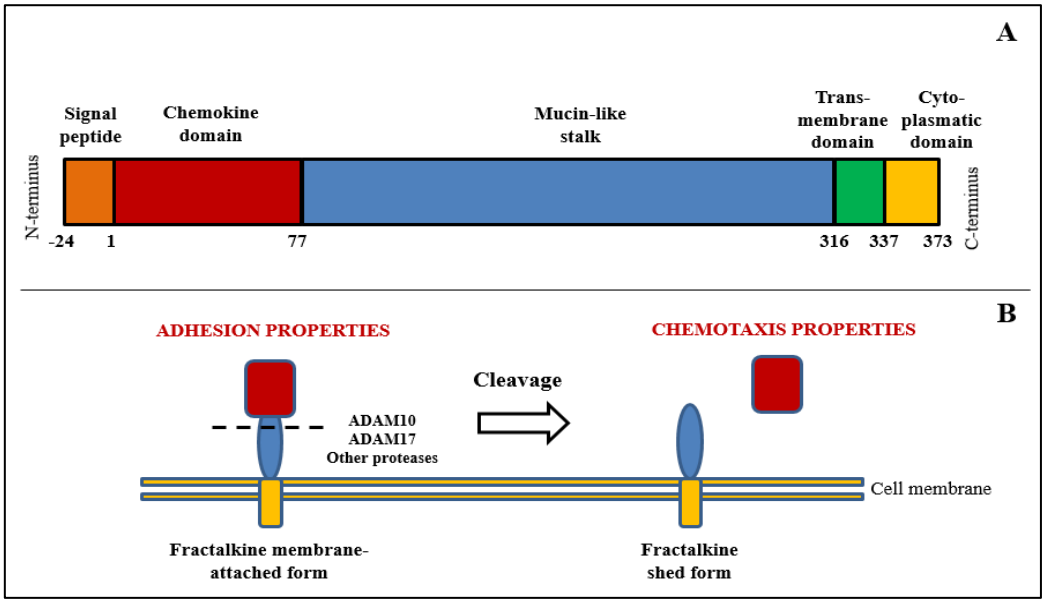

Figure 6.13: CX3CL1 structure and its location to the membrane and cleavage
Fractalkine (CX3CL1), the only member of the chemokine subgroup CX3C, is a large 373 amino-acids protein containing five domains: signal peptide sequence; N-terminal chemokine domain (residues 1-76); unique mucin-like stalk (residues 77-317); transmembrane domain (residues 337-373) (A). The mature transmembrane CX3CL1 can be cleaved from the cell surface by proteases, mainly ADAM10 and ADAM17, producing a soluble fractalkine fragment that contains the chemokine domain (B).

My preliminary findings suggesting increased expression and release of CX3CL1 in GH3-*Aip*-KD cells were not validated further by ELISA, and my primary culture cytokine array data from human *AIP*mut somatotrophinoma, *AIP*mut somatotrophinoma-TAFs and *AIP*mut skin fibroblasts (either in homozygosity or heterozygosity) actually showing lower CX3CL1 levels in these cell supernatants than in the corresponding normal cell types, contradicting my initial hypothesis established from my preliminary cytokine and RT-qPCR data. Hence, taking these data together, the *AIP* mutational status may not be determining for the CX3CL1 synthesis/release in PAs.

The role of AIP deficiency in the cytokine secretome from tumour and non-tumoural cells

The initial hypothesis that AIP deficiency would increase the release of (some) cytokines and chemokines was in general not consistently seen in my cytokine data, except in the case of CCL2 (although I analysed a very low number of samples which is a major limitation of my study). CCL2 levels were higher in the GH3-*Aip*-KD supernatants (non-significantly, but nearly significant at 72h), in the *AIP*mut somatotroph adenoma cells and respective TAFs culture supernatants, and also in *AIP*mut skin fibroblast supernatants. These findings suggest that AIP deficiency may affect CCL2 release, the main macrophage chemoattractant[696], which could explain the increased content of macrophages in *AIP*mut PAs[513].

The levels of CCL5, another relevant macrophage-related chemokine[333,339], were lower in both GH3-*Aip*-KD cell and in the human *AIP*mut somatotrophinoma supernatants. However, my colleague Dr. Barry has shown increased CCL5 expression in human *AIP*mut PAs compared to normal pituitary, and higher secreted levels of CCL5 in GH3-*Aip*-KD than in GH3-NT cell supernatants as determined by ELISA[513]. Dr. Barry's *in vitro* data showed that the CCL5-dependent macrophage chemotaxis increased significantly towards GH3-*Aip*-KD-CM compared to GH3-NT-CM and disruption of this signalling with maraviroc (CCR5 antagonist[697]) reduced macrophage migration by 50%[513]. Dr. Barry also described higher expression of FLI-1 (Friend leukaemia virus integration 1) in human *AIP*mut somatotrophinomas at both RNA and protein levels[513], a transcription regulator able to upregulate different cytokines and chemokines, including CCL5 and CCL2[698-700]. Dr. Barry´s data strongly implicate CCL5/CCR5 axis, as well as FLI-1, in *AIP*-related pituitary tumourigenesis and possibly in the recruitment of macrophages into their TME, explaining the higher macrophage content seen in *AIP*mut PAs[513].

As a co-chaperone, AIP may interact with FLI-1, and loss of AIP may well result in FLI-1 overexpression with subsequent FLI-1-mediated upregulation of different cytokines, an effect previously described for FLI-1 which is able to increase cytokine expression, including CCL5[699] supporting Dr. Barry´s findings, as well as CCL2[698] which could explain my own observations of higher CCL2 levels secreted from AIP deficient cells.

AIP inactivation by mutation can also interfere with the STAT3 pathway, which potentially induces further alterations in cytokine (namely IL-6) and hormone (namely GH) production[701,702]. In fact, it was recently shown that *AIP* mutation-positive GH3 cells have increased level of phosphorylated STAT3 and secrete higher amounts of IL-6 than wild-type GH3 cells[701]. In AIP deficient PA cell supernatants (GH3 and *AIP*mut somatotrophinoma cells), IL-6 was practically undetectable, but IL-6 levels were higher in *AIP*mut skin fibroblast supernatants (homozygous and heterozygous) than in wild-type skin fibroblasts, which is not consistent with the reported higher secretion of IL-6 in *AIP* mutation-positive GH3 cells[701].

AIP can theoretically modulate the cytokine secretome via other mechanisms unrelated to FLI-1 or STAT3. The other obvious candidate would be via AHR, which is a recognised AIP partner and a modulator of several immune-related processes including cytokine secretion[177,680,681,689]. AIP can also modulate cytokine secretome by interacting with other cytokine transcription factors, including the IRF7 (interferon regulatory factor 7). IRF7 is a key regulator of type 1 interferon and its activation prevent excessive inflammation and autoimmunity. AIP inhibits IRF7 suppressing the induction of interferon. In fact, knocking down AIP has led to increased production of IFNα/β[703].

Overall, I was not able to find major cytokine secretome differences among GH3 cells, human somatotroph adenoma cells, TAFs and skin fibroblasts with different *AIP* mutational status. There were no specific cytokines or groups of cytokines released by the AIP deficient cells that were not secreted by wild-type cells. I observed differences in absolute levels for some cytokines, some of them possibly related to the assay variability or technical issues. In general, the cytokine secretome from *AIP*mut primary cells (pituitary tumour cells and fibroblasts) showed a decreased number of cytokines with higher concentrations than the respective sporadic wild-type cells.

My cell line and primary cell culture cytokine data suggest a limited role for AIP in defining the cytokine secretome of pituitary tumour cells, at least in basal/unstimulated conditions. Nevertheless, the AIP loss may instead (or mainly) affect the cytokine secretome under stimulatory circumstances (but not in basal conditions) which may differentially modulate the secretory ability of non-neoplastic cells in the TME (such as macrophages), as supported by my *in vitro* data regarding the secretome changes induced by macrophage-derived factors in both GH3-*Aip*-KD and GH3-NT cells.

This lack of major cytokine secretome differences between (unstimulated) *AIP*mut and *AIP*neg cells is in line with the fact that immune-related diseases such as autoimmune diseases, haematological malignancies, or immunosuppression-related issues such as frequent or atypical infections, are not reported in *AIP*mut patients who are at risk only for isolated PAs[91,152,161]. Moreover, gene expression data generated from Dr. Barry revealed no differential expression of cytokine genes between *AIP*mut (n=6) and sporadic *AIP*neg (n=4) somatotrophinomas [513].

The role of AIP deficiency in the cytokine secretome responsiveness to pasireotide

The concentrations from all cytokines decreased after pasireotide treatment in *AIP*mut somatotrophinoma-derived TAFs (except FGF-2), and the degree of pasireotide cytokine response tended to be higher in *AIP*mut TAFs than in sporadic PA-associated TAFs, with prominent pasireotide-induced reduction in the secretion of IL-6 (by 90%), CCL2 (by 80%), CCL11 (by 90%), CCL7 (by 89%), PDGF-AA (by 84%), IL-8 (by 62%) and VEGF-A (by 60%).

Similar trends were observed in *AIP*mut skin fibroblasts, where pasireotide remarkably decreased the secretion of most cytokines, with prominent reductions noted for IL-6, CCL2, VEGF-A, CCL7, whereas in wild-type skin fibroblasts the reductions were more modest and in some cases pasireotide even increased the cytokine levels (e.g. for VEGF-A and CCL7).

This study data suggest that AIP deficiency may not confer resistance to the inhibitory effect of pasireotide in terms of cytokine release, at least in fibroblasts. In fact, the opposite notion transpires from my data, which suggest that AIP loss may facilitate pasireotide's inhibitory effect on cytokine secretion, but the number of samples here analysed are far too small to allow any valid conclusions and further studies, with larger number of samples and including other cell types lacking AIP, are needed. Interestingly, pasireotide controlled GH excess in 2 patients with *AIP*mut acromegaly resistant to first-generation somatostatin analogues[704]. Overall, these data suggest that AIP deficiency may not impair pasireotide anti-secretory activity, in contrast to the reduced octreotide effectiveness in inhibiting GH secretion in *AIP*mut somatotrophinomas[161,575,577].

Conclusions

In summary, my cell line and primary cell culture cytokine data suggest a limited role for AIP in determining the cytokine secretome of pituitary tumour cells. In fact, my data suggest that AIP deficiency is unlikely to induce major stimulatory (or inhibitory) effects on the cell cytokine secretome, at least under basal/unstimulated conditions. AIP deficiency also seems to create no resistance to (and indeed possibly enhances) the inhibitory pasireotide effect in terms of cytokine release, at least in fibroblasts, in contrast with the well-known reduced effectiveness of SSAs in inhibiting GH secretion in *AIP*mut somatotrophinomas.

Chapter 7: Characterisation of *AIP* mutation-positive pituitary adenomas and screening for *AIP* mutations: benefits of the genetic and clinical screening of *AIP* mutation carriers

Introduction

Most PAs occur sporadically, but about 5% of all PAs are familial[7,691]. FIPA is a heterogeneous condition that involves the presence of PAs in 2 or more members of the same family in the absence of other syndromic manifestations, such as those seen in MEN1, MEN4 or Carney complex[691]. Up to 20% of all FIPA and 50% of familial acromegaly kindreds carry germline mutations in the *AIP* gene[91,152,161]. These mutations are also seen in sporadically diagnosed PAs (simplex cases), particularly in young patients, where the lack of a family history is usually due to incomplete penetrance rather than *de novo* mutations[110,155,705,706]. The typical *AIP* mutation-positive (*AIP*mut) phenotype is characterised by a young patient presenting with a large invasive GH-secreting PA that is refractory to conventional treatments[91,152,153,161,169,705,707], with *AIP*mut somatotrophinomas being responsible in one study for 29% of pituitary gigantism cases[196].

Family members at risk of inheriting an *AIP* mutation are recommended to undergo genetic testing and carriers should be referred for clinical screening of pituitary disease[91,152,167,168,708]. The rationale behind this strategy is that identifying PAs in *AIP*mut carriers with otherwise unrecognised disease at an early stage increases the likelihood of effective treatment and remission[91,152,167]. The assumption is that screening-discovered PAs are diagnosed at a less advanced stage and are less invasive than PAs with a clinical presentation, and thus should show a more favourable response to treatment and better clinical outcomes. However, these predicted advantages have never been actually shown.

Aims

Overall aim

To study the benefits of genetic and clinical screening of *AIP* mutation carriers by characterising prospectively-diagnosed *AIP*mut PAs and to compare to those with a clinical presentation.

Specific aims

1. To characterise prospectively-diagnosed *AIP*mut PAs and compare to clinically-presenting *AIP*mut PAs in order to assess the benefits of screening *AIP*mut carriers
2. To expand the knowledge regarding the clinical features, disease course and outcomes of patients with *AIP*mut PAs, providing a comparison with *AIP*neg cases
3. To study phenotype-genotype correlations in patients with *AIP*mut PAs
4. To describe *AIP*mut vs *AIP*neg FIPA kindreds

Methods

Study population

I selected my study population from our cohort (2079 patients with PAs and their 1029 unaffected relatives) recruited via the collaborative research network of the International FIPA Consortium (http://www.fipapatients.org/fipaconsortium/) between February 2007 and April 2019. All participants gave written informed consent approved by the local Ethics Committee.

Indications for *AIP* genetic testing were: i) FIPA patients; ii) sporadic macroadenomas with disease onset ≤30 years; and iii) sporadic microadenomas with disease onset ≤18 years. First-degree family members of individuals carrying *AIP*mut were offered genetic testing. We included in our analysis all patients with known *AIP* mutational status matching these criteria (n=1477). We excluded patients with undetermined affected status (i.e. proven *AIP*mut carriers who did not undergo clinical screening or had pending clinical test results by the time of data analysis). Patients with XLAG, MEN1, MEN4, Carney complex, SDHx-related, McCune-Albright and DICER1 syndromes, identified on the basis of clinical, biochemical and genetic testing as appropriate, were excluded.

Of 1477 patients included in the study, 167 were *AIP*mut, 154 with documented germline *AIP* pathogenic/likely pathogenic variant and 13 affected subjects with predicted *AIP*mut status (obligate carriers in *AIP*mut kindreds but not formally tested, including subjects already deceased). The variant pathogenicity was assessed using Mutation Taster (http://www.mutationtaster.org/), Annovar[709] and Variant Effect Predictor *in silico* prediction programmes[710], as well as published clinical and experimental data on these variants[169]. Only pathogenic/likely pathogenic variants were considered as 'mutations'. The *AIP*neg subgroup included 1310 patients with PAs in which a

germline *AIP* mutation was excluded by genetic testing of all simplex probands and of the youngest affected member in the families.

AIP genetic testing and clinical screening

AIP testing was performed using either Sanger sequencing and multiplex ligation-dependent probe amplification, or targeted next generation sequencing on genomic DNA obtained from blood or saliva samples[91,169,711]. All the unaffected individuals with positive genetic screening for *AIP* were advised to undergo clinical, biochemical and image screening tests by their local physician for the early diagnosis of possible pituitary disease. Follow-up was advised on an annual basis or as appropriate[91,152,168].

Definition of *AIP* mutation-positive (*AIP*mut) and *AIP* mutation-negative (*AIP*neg) subgroups

Out of 1477 patients, 167 were *AIP*mut, 154 with documented germline *AIP* pathogenic/likely pathogenic variant and 13 predicted *AIP*mut (obligate carriers in *AIP*mut kindreds but not formally tested, including subjects already deceased or that refused genetic test). The *AIP*neg subgroup included 1310 patients with PAs, in which a germline *AIP* mutation was excluded by genetic testing in 1062 patients, while 248 subjects were predicted *AIP*neg (patients who had at least one affected relative tested negative for *AIP* mutation and who had individual or familial phenotypes not suggestive of *AIP*mut, i.e. subjects not affected with young-onset somatotrophinomas or prolactinomas and not deriving from homogeneous somatotrophinoma families or with relatives with gigantism).

Study groups and clinical parameters

The familial cohort was comprised of FIPA patients. The sporadic cohort included patients with young onset PAs (≤30yr) with no known family history of PAs or syndromic disease. The clinical diagnoses were established as GH excess (acromegaly and gigantism), prolactinomas (PRLomas), NFPAs, Cushing's disease (ACTHomas) and thyrotrophinomas (TSHomas), as previously described[91]. Cases where the diagnosis was not specified due to unavailability of histopathological, clinical or biochemical data, were termed as "PA not specified" (PA-NS). Age of onset was defined as the age of presentation of first symptoms. Macroadenomas were defined as tumour size ≥10mm. Hypopituitarism at diagnosis and at last follow-up was defined as the presence of at least

one pituitary deficiency documented biochemically. The number of treatments included the number of individual treatments given (each medication, surgery and radiotherapy). Multimodal treatment was defined as the employment of two or more distinct forms of treatment in patient management. The reoperation subgroup involved patients who had at least one additional surgery following their first operation. Active disease was considered in patients with secretory PAs displaying the respective pituitary hormone above the normal assay range, and/or evidence of persistent or recurrent progressive tumour remnants in the surveillance pituitary MRI scan for both secretory PAs and NFPAs. Small persistent tumour remnants after operation, stable over a period of time and requiring no further intervention, were considered as not active NFPAs.

Results

General characterisation of the study population

Of the 1477 patients with PAs, 167 were *AIP*mut (11.3%) and 1310 were *AIP*neg patients (FIPA or age ≤30yr at onset). Demographic and clinical characteristics and comparative analysis of *AIP*mut vs *AIP*neg PAs are presented in Table 7.1 and Figure 7.1.

	***AIP*mut vs *AIP*neg PAs**			**Study population** n=1477
	***AIP*mut** n=167	***AIP*neg** n=1310	***p* value**	
Cohort type based on family history of PAs Familial cohort Sporadic cohort	 114 (68.3%) 53 (31.7%) [n=167]	 586 (44.7%) 724 (55.3%) [n=1310]	**<0.001**	 700 (47.4%) 777 (52.6%) [n=1477]
Gender Male Female	 102 (61.1%) 65 (38.9%) [n=167]	 591 (45.2%) 716 (54.8%) [n=1307]	**<0.001**	 693 (47.0%) 781 (53.0%) [n=1474]
Age at disease onset ≤ 18 yr	94 (64.8%) [n=145]	311 (28.8%) [n=1080]	**<0.001**	405 (33.1%) [n=1225]
Age at first symptoms (yr)	19.0 ± 9.5 [n=139]	26.8 ± 13.1 [n=1058]	**<0.001**	25.9 ± 13.0 [n=1197]
Age at diagnosis (yr)	24.3 ± 11.9 [n=160]	30.0 ± 13.5 [n=1187]	**<0.001**	29.4 ± 13.5 [n=1347]
Delay in diagnosis (yr)	4.1 ± 6.6 [n=138]	3.2 ± 4.9 [n=1058]	0.212	3.3 ± 5.1 [n=1196]
GH excess	136 (81.4%) [n=167]	650 (49.6%) [n=1310]	**<0.001**	786 (53.2%) [n=1477]
Pituitary apoplexy	12 (8.2%) [n=146]	37 (3.6%) [n=1032]	**0.009**	49 (4.2%) [n=1173]
Hypopituitarism at diagnosis	32 (42.7%) [n=75]	173 (49.0%) [n=353]	0.318	205 (47.9%) [n=428]
Number of pituitary deficiencies at diagnosis	0.84 ± 1.11 [n=75]	0.79 ± 1.03 [n=353]	0.841	0.80 ± 1.05 [n=428]

Macroadenoma	124 (83.2%) [n=149]	844 (79.2%) [n=1065]	0.259	968 (79.7%) [n=1214]
Maximum tumour diameter (mm)	20.1 ± 13.0 [n=74]	22.8 ± 16.0 [n=575]	0.281	22.5 ± 15.7 [n=649]
Suprasellar extension	44 (54.3%) [n=81]	253 (42.4%) [n=596]	**0.043**	297 (43.9%) [n=677]
Cavernous sinus invasion	29 (36.7%) [n=79]	164 (28.3%) [n=580]	0.122	193 (29.3%) [n=659]
Ki-67 > 3%	12 (41.4%) [n=29]	48 (41.0%) [n=117]	0.972	60 (41.1%) [n=146]
Number of treatments	2.07 ± 1.66 [n=160]	1.87 ± 1.32 [n=934]	0.228	1.90 ± 1.38 [n=1094]
Number of surgeries	0.93 ± 0.79 [n=162]	0.87 ± 0.72 [n=980]	0.468	0.88 ± 0.73 [n=1142]
Re-operation	27 (23.1%) [n=117]	119 (16.9%) [n=704]	0.106	146 (17.8%) [n=821]
Radiotherapy	53 (32.9%) [n=161]	201 (21.5%) [n=933]	**0.002**	254 (23.2%) [n=1094]
Multimodal treatment	90 (67.2%) [n=134]	414 (47.0%) [n=880]	**<0.001**	504 (49.7%) [n=1014]
≥ 3 treatments	54 (40.3%) [n=134]	229 (25.8%) [n=886]	**<0.001**	283 (27.7%) [n=1020]
Active disease at last follow-up	31 (25.0%) [n=124]	203 (34.5%) [n=589]	**0.041**	234 (32.8%) [n=713]
Hypopituitarism at last follow-up	16 (29.6%) [n=54]	80 (33.6%) [n=238]	0.574	96 (32.9%) [n=292]
Number of pituitary deficiencies at last follow-up	0.45 ± 0.96 [n=49]	0.77 ± 1.27 [n=224]	0.148	0.71 ± 1.22 [n=273]
Follow-up duration (yr)	11.2 ± 12.3 [n=128]	7.8 ± 9.5 [n=703]	**0.008**	8.4 ± 10.1 [n=831]

Table 7.1: Characteristics of the study population and comparative analysis of AIPmut vs AIPneg PAs
Categorical data are shown as n(%); continuous variables are shown as mean±SD. In square brackets is indicated the number of cases where data was available regarding each parameter/variable.

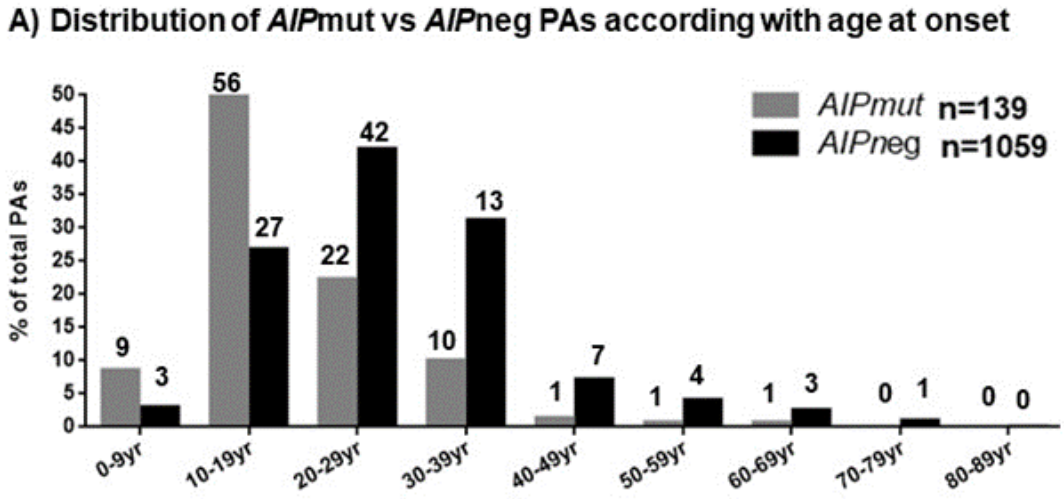

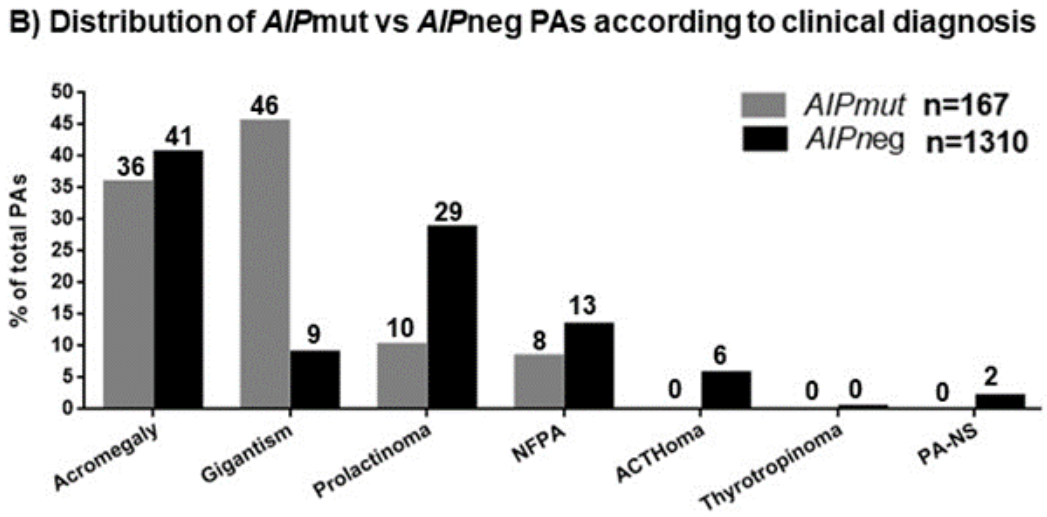

Figure 7.1: Distribution of AIPmut vs AIPneg PAs according to age at onset (A) and clinical diagnosis (B) Numbers above the columns represent percentage of patients. We note that the two *AIP*mut cases with first symptoms in the 5th and 6th decade, both had macroprolactinomas, one presenting with apoplexy. ACTHoma, ACTH-secreting adenoma or Cushing´s disease; *AIP*mut, *AIP* mutation-positive; *AIP*neg, *AIP* mutation-negative; NFPA, non-functioning pituitary adenoma; PA-NS, pituitary adenoma not specified; yr, years.

The familial cohort (355 families, 700 patients, 47% of the whole study population) consisted of 37 *AIP*mut kindreds (114 patients) and 318 *AIP*neg families (586 patients). Of the 37 *AIP*mut families, 36 (97.8%) had at least one somatotrophinoma case, 19 were homogeneous somatotrophinoma kindreds and one was homogeneous prolactinoma family. Of the 318 *AIP*neg families, 146 (46%) were homogeneous and 172 were heterogeneous, with detailed subtypes shown in Table 7.2. In the sporadic cohort (n=777), 53 (6.8%) had an *AIP* mutation. Within the sporadic tumour subgroup, 10.5% (50 out of 477) of somatotrophinomas, 1.5% (3 out of 197) of prolactinomas and none (0 out of 54) of the NFPA cases were found to harbor a germline *AIP* mutation (Tables 7.3 and 7.4).

PA types within the same kindred	***AIP*mut kindreds** n=37	***AIP*neg kindreds** n=318	**Total** n=355
ACTHoma only	0	7 (2.2%)	7 (2.0%)
ACTHoma + FSHoma	0	1 (0.3%)	1 (0.3%)
ACTHoma + Somatotrophinoma	0	7 (2.2%)	7 (2.0%)
ACTHoma + NFPA	0	1 (0.3%)	1 (0.3%)
ACTHoma + NFPA + PA-NS	0	1 (0.3%)	1 (0.3%)
ACTHoma + NFPA + Prolactinoma	0	1 (0.3%)	1 (0.3%)
ACTHoma + PA-NS	0	2 (0.6%)	2 (0.6%)
ACTHoma + PRLoma	0	8 (2.5%)	8 (2.3%)
Somatotrophinoma only	19 (51.4%)	68 (21.4%)	87 (24.5%)
Somatotrophinoma + NFPA	8 (21.6%)	25 (7.9%)	33 (9.3%)
Somatotrophinoma + NFPA + Prolactinoma	1 (2.7%)	4 (1.3%)	5 (1.4%)

Somatotrophinoma + PA-NS	0	19 (6.0%)	19 (5.3%)
Somatotrophinoma + PA-NS + Prolactinoma	0	1 (0.3%)	1 (0.3%)
Somatotrophinoma + Prolactinoma	8 (21.6%)	45 (14.2%)	53 (14.9%)
NFPA only	0	24 (7.5%)	24 (6.8%)
NFPA + PA-NS	0	14 (4.4%)	14 (3.9%)
NFPA + Prolactinoma	0	24 (7.5%)	24 (6.8%)
Prolactinoma only	1 (2.7%)	47 (14.8%)	48 (13.5%)
Prolactinoma + FSHoma	0	1 (0.3%)	1 (0.3%)
Prolactinoma + PA-NS	0	18 (5.7%)	18 (5.1%)

Table 7.2: *AIP*mut and *AIP*neg FIPA kindreds according to PA types
Data are shown as n(%). ACTHoma, ACTH-secreting adenoma or Cushing´s disease; *AIP*mut, *AIP* mutation-positive; *AIP*neg, *AIP* mutation-negative; FSHoma, FSH-secreting adenoma; NFPA, non-functioning pituitary adenoma; PA-NS, pituitary adenoma not specified.

Comparative analysis between *AIP*mut and *AIP*neg PAs

*AIP*mut patients were more frequently males (61% vs 45%; p<0.001) compared to *AIP*neg patients, 8yr younger at first symptoms (19±10 vs 27±13yr; p<0.001) and 6yr younger at diagnosis (24±12 vs 30±14yr; p<0.001), with disease onset ≤18yr in 65% and <30yr in 87%, in contrast to the *AIP*neg subgroup with 29% (p<0.001) and 72% (p<0.001) (Table 7.1 and Figure 7.1-A). *AIP*mut PAs were more often associated with GH excess (81% vs 50%; p<0.001), with gigantism being the predominant diagnosis (Figure 7.1-B and Figure 7.2). *AIP*mut PAs had a higher rate of apoplexy (8% vs 4%; p=0.009) and suprasellar extension (54% vs 42%; p=0.043). *AIP*mut patients required radiotherapy (33% vs 22%; p=0.002) and multimodal treatment (67% vs 47%; p<0.001) more often, with ≥3 treatments given in 40% of *AIP*mut patients vs 26% in *AIP*neg ones (p<0.001) (Table 1). *AIP*mut patients had lower rates of active disease at last follow-up (25% vs 35%; p=0.041). As *AIP*mut had a longer follow-up, I analysed only patients with no longer than 10yr follow-up, and then there was no difference in the rate of active disease at last follow-up (39% vs 43%; p=0.642).

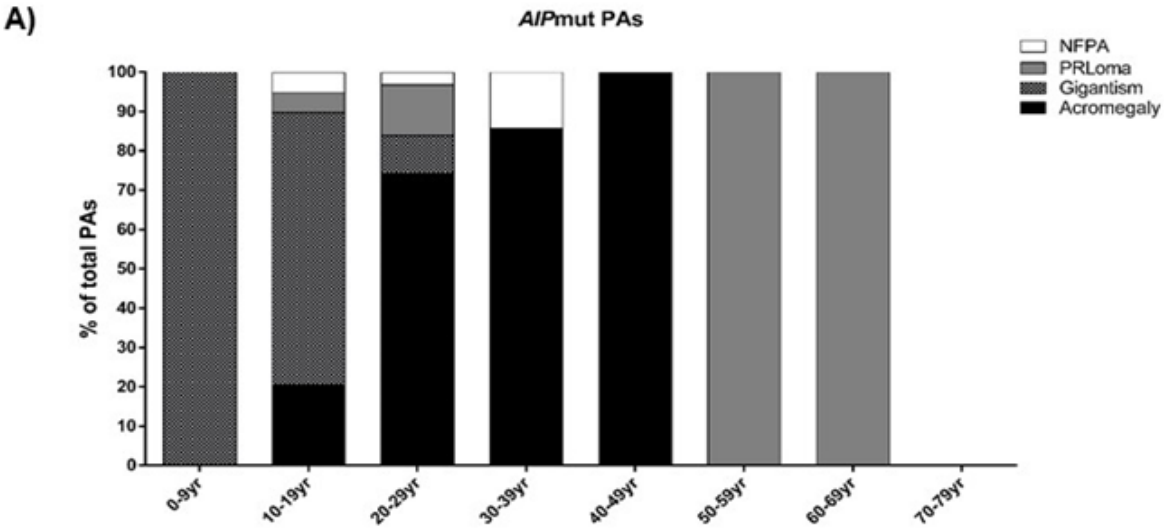

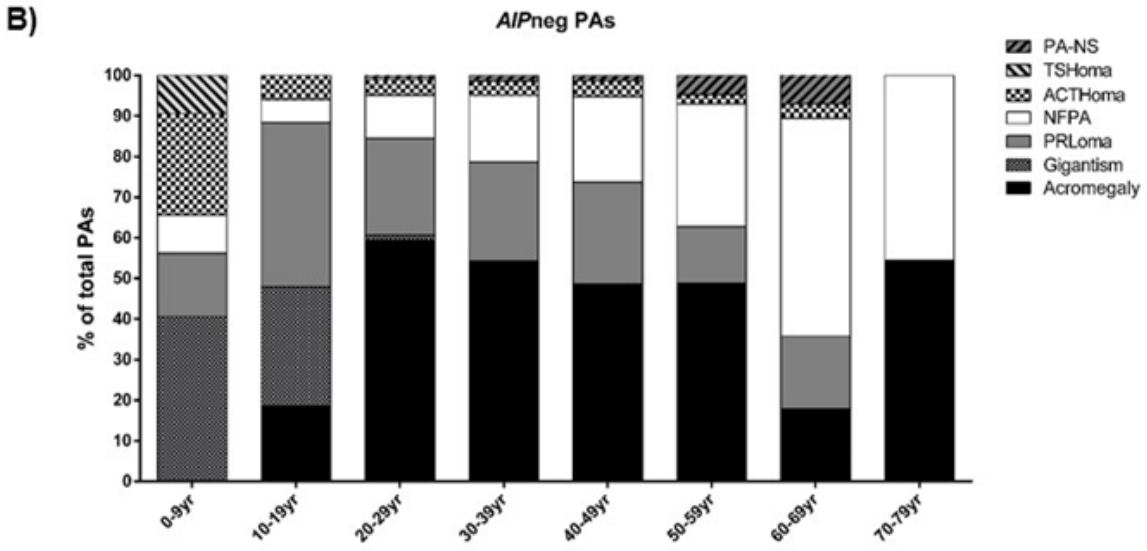

Figure 7.2: Clinical diagnosis according to age of onset among *AIP*mut (A) and *AIP*neg (B) PA patients
In this comparison, GH/PRL positive pituitary adenomas were added to the gigantism or acromegaly group, as appropriate. ACTHoma, ACTH-secreting adenoma or Cushing´s disease; *AIP*mut, *AIP* mutation-positive; *AIP*neg, *AIP* mutation-negative; NFPA, non-functioning pituitary adenoma; PA-NS, pituitary adenoma not specified; PRLoma, prolactinoma; TSHoma, thyrotrophinomas; yr, years.

Comparisons of *AIP*mut vs *AIP*neg patients by tumour type

*AIP*mut patients with GH excess (n=136) were younger at first symptoms (18±8 vs 26±12yr; p<0.001) and at diagnosis (23±11 *vs* 30±12yr; p<0.001) than *AIP*neg cases (n=650) (Table 4). The predominant clinical diagnosis of *AIP*mut cases was gigantism (56% vs 18%, p<0.001). There was no difference in IGF-1 levels at diagnosis between clinically-presenting *AIP*mut and *AIP*neg patients (p=0.696, Table 7.3). All *AIP*mut somatotrophinomas were sparsely-granulated in contrast to 68% of the *AIP*neg ones (p<0.001); similar ratios were seen only considering *AIP*mut and *AIP*neg giants. *AIP*mut somatotrophinomas were associated to higher rates of apoplexy (8% vs 3%; p<0.001), suprasellar extension (60% vs 46%; p=0.042), radiotherapy (39 vs 28%; p=0.018) and reoperation (25% vs 16%; p=0.025), and showed trends for an increased need for multimodal therapy (p=0.076) and ≥3 treatments (p=0.079). The mean final height was higher in the *AIP*mut somatotrophinoma subgroup (p<0.001) both for males (193±18 vs 185±14 cm; p=0.004) and females (175±13 vs 169±9 cm; p=0.017) (Table 4). *AIP*mut somatotrophinoma patients had lower rates of active disease at last follow-up (28% vs 43%; p=0.005).

	***AIP*mut vs *AIP*neg somatotrophinomas**			**Overall somato-trophinomas** n=786
	***AIP*mut** n=136	***AIP*neg** n=650	***p* value**	
Cohort type based on family history of PAs Familial cohort Sporadic cohort	 86 (63.2%) 50 (36.8%) [n=136]	 223 (34.3%) 427 (65.7%) [n=650]	**<0.001**	 309 (39.3%) 477 (60.7%) [n=786]
Gender Male Female	 84 (61.8%) 52 (38.2%) [n=136]	 332 (51.3%) 315 (48.7%) [n=647]	**0.026**	 416 (53.1%) 367 (46.9%) [n=783]
Age at disease onset ≤ 18 yr	85 (67.5%) [n=126]	142 (25.0%) [n=569]	**<0.001**	227 (32.7%) [n=695]
Age at first symptoms (yr)	18.1 ± 8.4 [n=122]	26.1 ± 11.8 [n=563]	**<0.001**	24.7 ± 11.7 [n=685]
Age at diagnosis (yr)	23.2 ± 10.8 [n=133]	30.2 ± 12.2 [n=609]	**<0.001**	28.9 ± 12.3 [n=742]
Delay in diagnosis (yr)	4.3 ± 6.5 [n=120]	4.2 ± 5.4 [n=563]	0.371	4.2 ± 5.6 [n=683]
Gigantism	76 (55.9%) [n=136]	118 (18.2%) [n=650]	**<0.001**	194 (24.7%) [n=786]
Pituitary apoplexy	10 (8.3%) [n=121]	15 (2.8%) [n=533]	**0.005**	25 (3.8%) [n=654]
Height at diagnosis (cm) Males [n=250] Females [n=196]	 188.8 ± 19.7 170.4 ± 11.2	 183.5 ± 14.7 168.9 ± 9.0	 0.054 0.392	 184.8 ± 16.2 169.3 ± 9.5
Height Z-score at diagnosis	2.7 ± 2.4 [n=103]	1.5 ± 1.9 [n=339]	**<0.001**	1.8 ± 2.1 [n=442]
IGF-1 xULN at diagnosis	2.5 ± 3.5 [n=41] *2.7 ± 3.8*	2.9 ± 2.3 [n=195] *2.9 ± 2.3*	**<0.001** *0.696*	2.8 ± 2.5 [n=236] *2.9 ± 2.5*
Hypopituitarism at diagnosis	26 (46.4%) [n=56]	74 (49.0%) [n=151]	0.742	100 (48.3%) [n=207]
Number of pituitary deficiencies at diagnosis	0.89 ± 1.12 [n=56]	0.71 ± 0.90 [n=151]	0.565	0.76 ± 0.97 [n=207]
Macroadenoma	108 (90.0%) [n=120]	487 (89.2%) [n=546]	0.796	595 (89.3%) [n=666]
Maximum tumour diameter (mm)	23.0 ± 11.9 [n=56]	24.8 ± 13.6 [n=303]	0.403	24.5 ± 13.3 [n=359]
Suprasellar extension	38 (60.3%) [n=63]	133 (46.2%) [n=288]	**0.042**	171 (48.7%) [n=351]
Cavernous sinus invasion	26 (41.9%) [n=62]	101 (35.7%) [n=283]	0.356	127 (36.8%) [n=345]
Granulation pattern Densely -granulated Sparsely-granulated	 0 (0%) 32 (100%) [n=32]	 23 (31.9%) 49 (68.1%) [n=72]	**<0.001**	 23 (22.1%) 81 (77.9%) [n=104]
Ki-67 > 3%	11 (44.0%) [n=25]	25 (35.7%) [n=70]	0.519	36 (37.9%) [n=95]
Number of treatments	2.35 ± 1.68 [n=130]	2.30 ± 1.41 [n=490]	0.821	2.31 ± 1.47 [n=620]
Number of surgeries	1.06 ± 0.78 [n=132]	1.07 ± 0.61 [n=516]	0.606	1.07 ± 0.65 [n=648]
Re-operation	27 (25.2%) [n=107]	74 (16.1%) [n=461]	**0.025**	101 (17.8%) [n=568]
Radiotherapy	51 (38.9%) [n=131]	138 (28.2%) [n=489]	**0.018**	189 (30.5%) [n=620]
Somatostatin analogues	59 (45.4%) [n=130]	264 (54.2%) [n=487]	0.073	323 (52.4%) [n=617]

Dopamine agonists	31 (23.8%) [n=130]	128 (26.3%) [n=487]	0.572	159 (25.8%) [n=617]
Pegvisomant	14 (10.8%) [n=130]	33 (6.8%) [n=487]	0.127	47 (7.6%) [n=617]
Multimodal treatment	84 (72.4%) [n=116]	305 (63.7%) [n=479]	0.076	389 (65.4%) [n=595]
≥ 3 treatments	53 (45.7%) [n=116] *47.7%*	178 (36.9%) [n=483] *36.9%*	0.079 ***0.039***	231 (38.6%) [n=599] *39.0%*
Active disease at last follow-up	28 (27.7%) [n=101]	139 (43.3%) [n=321]	**0.005**	167 (39.6%) [n=422]
Hypopituitarism at last follow-up	13 (36.1%) [n=36]	36 (39.1%) [n=92]	0.752	49 (38.3%) [n=128]
Number of pituitary deficiencies at last follow-up	0.48 ± 0.93 [n=31]	0.79 ± 1.22 [n=85]	0.288	0.71 ± 1.15 [n=116]
Final height (cm)	185.9 ± 18.3 [n=95]	177.9 ± 14.3 [n=329]	**<0.001**	179.7 ± 15.6 [n=424]
Final height (cm) by gender				
Males [n=241]	192.8 ± 17.6	185.2 ± 13.8	**0.004**	187.1 ± 15.1
Females [n=183]	174.8 ± 13.4	168.9 ± 8.7	**0.017**	170.1 ± 10.0
Follow-up duration (yr)	11.4 ± 12.8 [n=103]	7.4 ± 8.9 [n=388]	**0.027**	8.3 ± 10.0 [n=491]

Table 7.3: Comparative analysis between *AIP*mut vs *AIP*neg somatotrophinomas
Categorical data are shown as n(%); continuous variables are shown as mean±SD. In square brackets is indicated the number of cases where data was available regarding each parameter/variable. Data for clinically-presenting somatotrophinomas comparison are added in italics where showing different results. *AIP*mut, *AIP* mutation-positive; *AIP*neg, *AIP* mutation-negative; PA, pituitary adenoma; ULN, upper limit of the normal; yr, years.

Patients with *AIP*mut prolactinomas had higher rates of apoplexy (17% vs 3%; p=0.009) and a more frequent family history of PAs (82% vs 49%; p=0.006) than *AIP*neg counterparts, and these remained significant when considering only clinically-presenting cases (Table 7.4). *AIP*mut NFPAs had lower rates of macroadenomas (31% vs 85%; p<0.001), hypopituitarism at last follow-up (10% vs 46%; p=0.040), lower tumour diameter (9±10 vs 23±16mm; p=0.001) and pituitary deficiencies at diagnosis (0.2±0.6 vs 1.0±1.4; p=0.045), and required fewer treatments (0.5±0.8 vs 1.2±1.0; p=0.005) and surgery (0.3±0.5 vs 0.9±0.7; p=0.001). However, when excluding the 10 prospectively-diagnosed NFPA patients these significant differences were lost (Table 7.4).

	Prolactinomas			**NFPAs**		
	***AIP*mut** n=17	***AIP*neg** n=377	***p* value**	***AIP*mut** n=14	***AIP*neg** n=172	***p* value**
Cohort type Familial cohort	14 (82.4%)	183 (48.5%)	**0.006**	14 (100%)	118 (68.6%)	**0.013**
Sporadic cohort	3 (17.6%) [n=17]	194 (51.5%) [n=377]		0 (0%) [n=14]	54 (31.4%) [n=172]	
Gender Male	9 (52.9%)	125 (33.2%)	0.092	9 (64.3%)	98 (57.0%)	0.595
Female	8 (47.1%) [n=17]	252 (66.8%) [n=377]		5 (35.7%) [n=14]	74 (43.0%) [n=172]	
Age at disease onset ≤ 18 yr	5 (45.5%) [n=11] *40.0%*	123 (40.6%) [n=303]	0.747 *0.970*	4 (50.0%) [n=8] *33.3%*	17 (12.4%) [n=137]	**0.003** *0.291*

Age at first symptoms (yr)	27.5 ± 17.9 [n=10]	24.1 ± 10.8 [n=290]	0.959	22.6 ± 7.7 [n=7]	36.6 ± 17.3 [n=136]	**0.016**
Age at diagnosis (yr)	30.7 ± 16.5 [n=15] *32.0 ± 16.4*	26.2 ± 11.2 [n=340]	0.619 *0.346*	29.2 ± 14.8 [n=12] *27.0 ± 11.5*	39.4 ± 17.3 [n=159]	**0.038** *0.189*
Delay in diagnosis (yr)	4.5 ± 8.8 [n=11]	2.4 ± 4.6 [n=290]	0.665	1.1 ± 2.3 [n=7]	1.5 ± 3.3 [n=136]	0.761
Pituitary apoplexy	2 (16.7%) [n=12] *20.0%*	8 (2.8%) [n=283]	**0.009** ***0.003***	0 [n=13]	12 (8.6%) [n=139]	0.270
Hypopituitarism at diagnosis	5 (62.5%) [n=8] *83.3%*	72 (59.0%) [n=132]	0.846 *0.235*	1 (9.1%) [n=11] *100%*	22 (41.5%) [n=53]	**0.041** *0.238*
Number of pituitary deficiencies at diagnosis	1.38 ± 1.51 [n=8] *1.83 ± 1.47*	0.93 ± 1.04 [n=122]	0.470 *0.088*	0.18 ± 0.60 [n=11] *2.00 ± 0*	1.00 ± 1.40 [n=53]	**0.045** *0.344*
Macroadenoma	12 (75.0%) [n=16]	193 (63.7%) [n=303]	0.358	4 (30.8%) [n=13]	130 (85.0%) [n=153]	**<0.001**
Maximum tumour diameter (mm)	14.4 ± 16.1 [n=7] *16.3 ± 16.8*	20.6 ± 19.7 [n=161]	0.270 *0.591*	9.0 ± 9.8 [n=11] *35.0*	22.8 ± 15.9 [n=86]	**0.001** *0.330*
Suprasellar extension	3 (42.9%) [n=7] *60.0%*	67 (34.9%) [n=192]	0.665 *0.247*	3 (27.3%) [n=11] *100%*	45 (56.2%) [n=80]	0.071 *0.245*
Cavernous sinus invasion	1 (16.7%) [n=6] *25.0%*	42 (22.7%) [n=185]	0.728 *0.914*	2 (18.2%) [n=11] *50.0%*	17 (22.4%) [n=76]	0.753 *0.391*
Ki-67 > 3%	0 [n=1]	9 (52.9%) [n=17]	0.303	1 (33.3%) [n=3] *50.0%*	7 (63.2%) [n=19]	0.907 *0.716*
Number of treatments	1.12 ± 0.78 [n=17] *1.20 ± 0.78*	1.39 ± 0.90 [n=247]	0.212 *0.479*	0.46 ± 0.78 [n=13] *1.33 ± 0.58*	1.19 ± 1.01 [n=127]	**0.005** *0.648*
Number of surgeries	0.35 ± 0.49 [n=17] *0.40 ± 0.51*	0.35 ± 0.68 [n=253]	0.609 *0.396*	0.31 ± 0.48 [n=13] *1.00 ± 0*	0.89 ± 0.66 [n=141]	**0.001** *0.728*
Re-operation	0 [n=6]	13 (18.6%) [n=70]	0.246	0 [n=4]	15 (13.9%) [n=108]	0.423
Radiotherapy	1 (5.9%) [n=17] *6.7%*	18 (7.2%) [n=250]	0.838 *0.938*	1 (7.7%) [n=13] *33.3%*	26 (20.8%) [n=125]	0.257 *0.864*
Dopamine agonists	12 (70.6%) [n=17] *73.3%*	214 (86.6%) [n=247]	0.068 *0.362*	1 (7.7%) [n=13] 0	9 (7.2%) [n=125]	0.948 *0.622*
Multimodal treatment	4 (28.6%) [n=14] *30.8%*	54 (22.8%) [n=237]	0.618 *0.507*	2 (50.0%) [n=4] *33.3%*	28 (28.9%) [n=97]	0.365 *0.867*
≥ 3 treatments	1 (7.1%) [n=14] *7.7%*	19 (8.0%) [n=237]	0.907 *0.966*	0 [n=4]	13 (13.3%) [n=98]	0.435 *0.499*
Active disease at last follow-up	2 (15.4%) [n=13] *16.7%*	44 (29.1%) [n=151]	0.289 *0.356*	1 (10.0%) [n=10] *50.0%*	13 (18.8%) [n=69]	0.494 *0.274*
Hypopituitarism at last follow-up	2 (25.0%) [n=8] *33.3%*	23 (23.0%) [n=100]	0.897 *0.563*	1 (10.0%) [n=10] *100%*	16 (45.7%) [n=35]	**0.040** *0.310*
Number of pituitary deficiencies at last follow-up	0.75 ± 1.49 [n=8] *1.00 ± 1.67*	0.58 ± 1.16 [n=98]	0.847 *0.515*	0.10 ± 0.31 [n=10] *1.00 ± 0*	1.16 ± 1.50 [n=33]	0.067 *0.771*

Follow-up duration (yr)	13.6 ± 12.5 [n=13] *14.3 ± 12.8*	9.3 ± 10.1 [n=172]	0.150 *0.131*	7.5 ± 7.1 [n=12] *19.5 ± 0.7*	8.1 ± 11.3 [n=94]	0.551 *0.094*

Table 7.4: Comparative analysis between *AIP*mut vs *AIP*neg prolactinomas and NFPAs
Categorical data are shown as n(%); continuous variables as mean±SD. In square brackets is indicated the number of cases where data was available regarding each parameter/variable. Data for clinically-presenting *AIP*mut prolactinomas (n=15) and NFPAs (n=4) comparison are added in italics. *AIP*mut, *AIP* mutation-positive; *AIP*neg, *AIP* mutation-negative; NFPA, non-functioning pituitary adenoma; yr, years.

Prospectively-diagnosed vs clinically-presenting *AIP*mut PAs

Genetic testing of *AIP*mut kindreds identified 187 apparently unaffected *AIP*mut carriers. 165 *AIP*mut carriers were disease-free at both baseline screening and at last follow-up assessment (mean follow-up duration 5.9 ±3.3yr, ranging between 1-11yr), while 22 subjects (11.8%) were prospectively-diagnosed with a PAs. The mean age at diagnosis of prospectively-diagnosed *AIP*mut PA patients (30.4±15.7yr) and the age at genetic testing of unaffected *AIP*mut carriers (35.9±24.1yr) did not differ (p=0.453). There was no significant difference in the gender distribution either: 49.7% prospectively-diagnosed males vs 63.6% unaffected carrier males (p=0.219).

Three of these prospectively-diagnosed cases had normal biochemistry and contrast-enhanced pituitary MRI at baseline screening, but went on to develop a PA during the subsequent follow-up: 2 small NFPAs and 1 microprolactinoma, being stable since their initial detection and none requiring intervention to date. Eight of these 22 cases (36%) had retrospectively symptoms that could be attributed to pituitary disease. Prospectively-diagnosed PAs were smaller than clinically-presenting PAs (10±7 vs 24±13mm; p<0.001), and 68% vs 8% were microadenomas (p<0.001, Table 7.5). Prospectively-diagnosed PAs were associated with lower rates of hypopituitarism at diagnosis (0 vs 58%; p<0.001), suprasellar extension (11% vs 68%; p<0.001), and cavernous sinus invasion (11% vs 44%; p=0.010), and none had pituitary apoplexy (vs 10%; p=0.118, Table 3). Prospectively-diagnosed PAs required fewer treatments (0.7±1.0 vs 2.3±1.7; p<0.001) and operations (0.4±0.5 vs 1.0±0.8; p<0.001), none required radiotherapy (vs 38%; p<0.001) and had decreased rates of active disease (6 vs 28%; p=0.039) and hypopituitarism at last follow-up (0 vs 41%; p=0.003, Table 7.5).

	*AIP*mut PAs		
	Prospectively-diagnosed n=22	**Clinically-presenting** n=145	***p* value**
Gender Male Female	 14 (63.6%) 8 (36.4%) [n=22]	 88 (60.7%) 57 (39.3%) [n=145]	0.792
Age at diagnosis (yr)	30.4 ± 15.7 [n=20]	23.5 ± 11.1 [n=140]	0.065
Clinical diagnosis Acromegaly Gigantism Prolactinoma NFPA	 8 (36.4%) 2 (9.1%) 2 (9.1%) 10 (45.4%) [n=22]	 52 (35.9%) 74 (51.0%) 15 (10.3%) 4 (2.8%) [n=145]	**<0.001**
GH excess	10 (45.5%) [n=22]	126 (86.9%) [n=145]	**<0.001**
Pituitary apoplexy	0 (0%) [n=22]	12 (9.7%) [n=124]	0.118
Hypopituitarism at diagnosis	0 (0%) [n=20]	32 (58.2%) [n=55]	**<0.001**
Number of pituitary deficiencies at diagnosis	0 [n=20]	1.15 ± 1.19 [n=55]	**<0.001**
Macroadenoma	7 (31.8%) [n=22]	117 (92.1%) [n=127]	**<0.001**
Maximum tumour diameter (mm)	9.5 ± 7.2 [n=19]	23.8 ± 12.6 [n=55]	**<0.001**
Suprasellar extension	2 (10.5%) [n=19]	42 (67.7%) [n=62]	**<0.001**
Cavernous sinus invasion	2 (11.1%) [n=18]	27 (44.3%) [n=61]	**0.010**
Ki-67 > 3%	1 (16.7%) [n=6]	11 (47.8%) [n=23]	0.168
Number of treatments	0.68 ± 0.95 [n=22]	2.29 ± 1.65 [n=138]	**<0.001**
Number of surgeries	0.36 ± 0.49 [n=22]	1.01 ± 0.79 [n=140]	**<0.001**
Re-operation	0 [n=8]	27 (24.8%) [n=109]	0.108
Radiotherapy	0 [n=22]	53 (38.1%) [n=139]	**<0.001**
Multimodal treatment	5 (55.6%) [n=9]	85 (68.0%) [n=125]	0.443
≥ 3 treatments	1 (11.1%) [n=9]	53 (42.4%) [n=125]	0.065
Active disease at last follow-up	1 (5.6%) [n=18]	30 (28.3%) [n=106]	**0.039**
Hypopituitarism at last follow-up	0 [n=15]	16 (41.0%) [n=39]	**0.003**
Number of pituitary deficiencies at last follow-up	0 [n=15]	0.65 ± 1.10 [n=34]	**0.014**
Follow-up duration (yr)	5.3 ± 4.5 [n=21]	12.4 ± 13.0 [n=107]	0.067

Table 7.5: Comparative analysis between prospectively-diagnosed vs clinically-presenting *AIP*mut PAs
Categorical data are shown as n(%); continuous variables are shown as mean±SD. In square brackets is indicated the number of cases where data was available regarding each parameter/variable. *AIP*mut, *AIP* mutation-positive; *AIP*neg, *AIP* mutation-negative; GH, growth hormone; PA, pituitary adenoma; yr, years.

Prospectively-diagnosed PAs (10 somatotrophinomas, 10 NFPAs and 2 prolactinomas) had lower rates of hypopituitarism at diagnosis, macroadenomas and suprasellar extension, requiring fewer treatments than those clinically presented (Table 7.6). Prospectively-diagnosed *AIP*mut somatotrophinomas were also significantly smaller and none had radiotherapy (p=0.009). None of the prospectively-diagnosed *AIP*mut NFPAs had hypopituitarism or active disease at last follow-up (Table 7.6). Two *AIP*mut patients had prospectively-diagnosed microprolactinomas with no suprasellar extension or cavernous sinus invasion, and were eupituitary at diagnosis and at last follow-up: one responded well to dopamine agonist and the other is under observation (described in detail as case 5 in my recent publication[167]).

	***AIP*mut somatotrophinomas**			***AIP*mut NFPAs**		
	Prospectively-diagnosed n=10	**Clinically-presenting** n=126	***p* value**	**Prospectively-diagnosed** n=10	**Clinically-presenting** n=4	***p* value**
Gender Male Female	7 (70.0%) 3 (30.0%) [n=10]	77 (61.1%) 49 (38.9%) [n=126]	0.578	6 (60.0%) 4 (40.0%) [n=10]	3 (75.0%) 1 (25.0%) [n=4]	0.597
Age at diagnosis (yr)	32.6 ± 15.7 [n=10]	22.4 ± 10.0 [n=123]	**0.022**	29.9 ± 16.3 [n=9]	27.0 ± 11.5 [n=3]	1.000
Pituitary apoplexy	0 [n=10]	10 (9.0%) [n=111]	0.322	0 [n=10]	0 [n=3]	1.000
Hypopituitarism at diagnosis	0 [n=10]	26 (54.2%) [n=48]	**0.004**	0 [n=10]	1 (100.0%) [n=1]	**0.001**
Number of pituitary deficiencies at diagnosis	0 [n=8]	1.04 ± 1.15 [n=48]	**0.008**	0 [n=10]	2 [n=1]	**0.002**
Macroadenoma	6 (60.0%) [n=10]	102 (92.7%) [n=110]	**0.001**	1 (10.0%) [n=10]	3 (100.0%) [n=3]	**0.003**
Maximum tumour diameter (mm)	14.1 ± 7.6 [n=8]	24.5 ± 11.9 [n=48]	**0.015**	6.4 ± 5.0 [n=10]	35.0 [n=1]	0.113
Suprasellar extension	1 (12.5%) [n=8]	37 (67.3%) [n=55]	**0.003**	1 (11.1%) [n=9]	2 (100.0%) [n=2]	**0.011**
Cavernous sinus invasion	1 (14.3%) [n=7]	25 (45.5%) [n=55]	0.115	1 (11.1%) [n=9]	1 (50.0%) [n=2]	0.197
Ki-67 > 3%	1 (20.0%) [n=5]	10 (50.0%) [n=20]	0.227	0 [n=1]	1 (50.0%) [n=2]	0.386
Number of treatments	1.20 ± 1.03 [n=10]	2.45 ± 1.69 [n=120]	**0.015**	0.20 ± 6.32 [n=10]	1.33 ± 0.58 [n=3]	**0.010**
Number of surgeries	0.70 ± 0.48 [n=10]	1.09 ± 0.79 [n=122]	0.105	0.10 ± 0.32 [n=10]	1.33 ± 0.58 [n=3]	**0.004**
Re-operation	0 [n=7]	27 (27.0%) [n=100]	0.112	0 [n=1]	0 [n=3]	1.000
Radiotherapy	0 [n=10]	51 (42.1%) [n=121]	**0.009**	0 [n=10]	1 (33.3%) [n=3]	0.057
Multimodal treatment	4 (57.1%) [n=7]	80 (73.4%) [n=109]	0.351	1 (100.0%) [n=1]	1 (33.3%) [n=3]	0.248
≥ 3 treatments	1 (14.3%) [n=7]	52 (47.7%) [n=109]	0.085	0 [n=1]	1 (33.3%) [n=3]	1.000
Active disease at last follow-up	1 (11.1%) [n=9]	27 (29.3%) [n=92]	0.243	0 [n=8]	1 (50.0%) [n=2]	**0.035**
Hypopituitarism at last follow-up	0 [n=4]	13 (40.6%) [n=32]	0.111	0 [n=9]	1 (100.0%) [n=1]	**0.002**

Number of pituitary deficiencies at last follow-up	0 [n=4]	0.56 ± 0.97 [n=27]	0.220	0 [n=9]	1.00 [n=1]	**0.003**
Follow-up duration (yr)	5.5 ± 4.8 [n=10]	12.0 ± 13.2 [n=93]	0.276	5.1 ± 4.7 [n=10]	19.5 ± 0.7 [n=2]	**0.030**

Table 7.6: Prospectively-diagnosed vs clinically-presenting *AIP*mut somatotrophinomas or NFPAs
Categorical data are shown as n(%); continuous variables are shown as mean±SD. In square brackets is indicated the number of cases where data was available regarding each parameter/variable. *AIP*mut, *AIP* mutation-positive; *AIP*neg, *AIP* mutation-negative; NFPA, non-functioning pituitary adenoma; yr, years.

AIP mutations in the study population and genotype-phenotype correlation

Forty-four germline pathogenic/likely pathogenic *AIP* mutations were identified, including 5 mutations not previously described (exon 1 deletion; c.344delT (p.L115fs*41); c.773T>G (p.L258R); c.779delA (p.K260fs*44); c.863_864del (p.F288Cfs*?)), among the 167 *AIP*mut patients (Table 7.7). The most common mutation types were nonsense (27%) and frameshift mutations (25%), followed by missense (18%), splice site (7%), in-frame insertions/deletions (9%) and large genomic deletions (7%). Of 167 *AIP*mut PAs, 127 (76%) were due to a truncating mutation, and the most frequent *AIP* mutation was c.910C>T (p.R304*), which was detected in 57 patients.

In the study population, I identified 17 different *AIP* variants classified as *benign*, *likely benign* or *variants of uncertain significance* according to American College of Medical Genetics and Genomics and the Association for Molecular Pathology criteria[712] (Table 7.8). Of note, one of the most common *AIP* variants identified, p.R304Q, although controversial, is currently classified as variant of uncertain significance[713], so patients from these kindreds were considered *AIP*neg.

Of 167 *AIP*mut PAs, 126 were due to a truncating mutation, and the most frequent *AIP* mutation was c.910C>T (p.R304*) detected in 57 patients. No differences were found regarding proportion of gigantism or GH excess cases, age at onset or at diagnosis, pituitary apoplexy, hypopituitarism at diagnosis, macroadenomas, suprasellar extension, cavernous sinus invasion, radiotherapy, active disease at last follow-up and hypopituitarism at last follow-up between PAs due to truncating vs non-truncating *AIP* mutations, or between PAs associated with p.R304* vs non-p.R304* *AIP* mutation (Table 7.9). However, fewer treatments (p=0.026) and operations (p<0.001) were seen in p.R304**AIP*mut patients, as well as in *AIP*mut patients with truncating mutation (p=0.040 and p=0.014, respectively). Truncating *AIP*mut PAs had less frequently multimodal treatment and SSAs, fewer males and shorter diagnosis delay in comparison with the non-truncating mutation subgroup (Table 7.9).

***AIP* mutation**	**Prevalence within *AIP*mut PAs (n=167)**	**Mutation type**	**Location in the AIP protein**	**References to previously published mutations / brief description of patients with novel *AIP* mutations**
g.4856_4857CG>AA (p.?)	2 (1.2%)	*Promoter*	5-UTR (not in protein)	[156,175,187]
c.1-?_993+?del- (p.0?) (whole gene deletion)	8 (4.8%)	*Large genomic deletion*	Absence of whole protein	[187]
c.(?-50)_(99+1_100-1)del (p.0?) (exon 1 deletion)	1 (0.6%)	*Large genomic deletion*	Absence of whole protein	**Female, age at onset 17yr, age at diagnosis 19yr, acromegaly, macroadenoma**
c.3G>A (p.?)	2 (1.2%)	*Start codon*	N-terminus	[192]
c.40C>T (p.Q14*)	2 (1.2%)	*Nonsense*	N-terminus	[91,153,714,715]
c.70G>T (p.E24*)	7 (4.2%)	*Nonsense*	N-terminus	[156,174]
c.74_81delins7 (p.L25Pfs*130)	4 (2.4%)	*Frameshift*	PPIase domain	[187,716]
c.100-1025_279+357del (p.A34_K93del) (exon 2 deletion)	6 (3.6%)	*Large genomic deletion*	PPIase domain	[717]
c.140_163del (p.G47_R54del)	1 (0.6%)	In-frame deletion	PPIase domain	[161]
c.240_241delinsTG (p.M80_R81delinsIG)	1 (0.6%)	In-frame deletion insertion	PPIase domain	[169]
c.241C>T (p.R81*)	7 (4.2%)	*Nonsense*	PPIase domain	[156,175,718-720]
c.249G>T (p.G83Afs*15)	3 (1.8%)	*Splice site*	PPIase domain	[187]
c.333delC (p.K112Rfs*44)	1 (0.6%)	*Frameshift*	PPIase domain	[169]
c.338_341dup (p.L115Pfs*16)	2 (1.2%)	*Frameshift*	PPIase domain	[91,721]
c.344delT (p.L115Rfs*41)	**1 (0.6%)**	***Frameshift***	**PPIase domain**	**Male, age at onset 15yr, age at diagnosis 16yr, prolactinoma, microadenoma**
c.376_377delCA (p.Q126Dfs*3)	1 (0.6%)	*Frameshift*	PPIase domain	[169]
c.427C>T (p.Q143*)	2 (1.2%)	*Nonsense*	Between PPIase and TPR1 domains	[91]
c.469-2A>G (p.E158_Q184del)	1 (0.6%)	*Splice site (resulting in in-frame deletion)*	TPR1 domain	[705,722,723]
c.490C>T (p.Q164*)	2 (1.2%)	*Nonsense*	Between PPIase and TPR1 domains	[187]
c.504G>A (p.W168*)	1 (0.6%)	*Nonsense*	TPR1 domain	[724]
c.562C>T(p.R188W)	1 (0.6%)	Missense	TPR1 domain	[191]
c.570C>G (p.Y190*)	4 (2.4%)	*Nonsense*	TPR1 domain	[91]
c.605A>G (p.Y202C)	1 (0.6%)	Missense	TPR1 domain	[169]
c.645+1G>C (p.?)	1 (0.6%)	*Splice site*	TPR1 domain	[169]

c.662dupC (p.E222*)	2 (1.2%)	*Frameshift*	Between TPR1 and TPR2 domains	[187]
c.713G>A (p.C238Y)	3 (1.8%)	Missense	TPR2 domain	[156,174]
c.760T>C (p.C254R)	1 (0.6%)	Missense	TPR2 domain	[191]
c.762C>G (p.C254W)	2 (1.2%)	Missense	TPR2 domain	[191]
c.773T>G (p.L258R)	**1 (0.6%)**	**Missense[#]**	**TPR2 domain**	**Male, age at onset 21yr, age at diagnosis 29yr, prolactinoma, macroadenoma**
c.779delA (p.K260Sfs*44)	**1 (0.6%)**	***Frameshift***	**PPIase domain**	**Male, age at onset 8yr, age at diagnosis 12yr, gigantism, macroadenoma**
c.783C>G (p.Y261*)	2 (1.2%)	*Nonsense*	TPR2 domain	[91,110,705]
c.804C>A (p.Y268*)	3 (1.8%)	*Nonsense*	TPR3 domain	[91,720,725]
c.805_825dup (p.F269_H275dup)	16 (9.6%)	In-frame insertion	TPR3 domain	[156,175,705]
c.811C>T (p.R271W)	8 (4.8%)	Missense	TPR3 domain	[155,187,707,726]
c.815G>A (p.G272D)	1 (0.6%)	Missense	TPR3 domain	[192,727]
c.816delC (p.K273Rfs*30)	1 (0.6%)	*Frameshift*	TPR3 domain	[91]
c.863_864del (p.F288Cfs*?)	**1 (0.6%)**	***Frameshift***	**TPR3 domain**	**Female, age at onset 16yr, age at diagnosis 31yr, acromegaly, macroadenoma**
c.868A>T (p.K290*)	1 (0.6%)	*Nonsense*	TPR3 domain	[91]
c.872_877delTGCTGG (p.V291_L292del)	1 (0.6%)	In-frame deletion	TPR3 domain	[728]
c.910C>T (p.R304*)	57 (34.1%)	*Nonsense*	C-terminal α-helix	[110,153,155,156,705,707,722,729]
c.967delC (p.R323Gfs*39)	1 (0.6%)	*Frameshift*	C-terminal α-helix	[91]
c.976_977insC (p.G326Afs*?)	1 (0.6%)	*Frameshift*	C-terminal α-helix	[91]
c.978dupG (p.I327Dfs*?)	1 (0.6%)	*Frameshift*	C-terminal α-helix	[91]
c.991T>C (p.*331R)	1 (0.6%)	Stop-loss	C-terminal α-helix	[169]

Table 7.7: List of AIP pathogenic/likely pathogenic mutations identified in our cohort

Mutations in bold are novel mutations not previously described. None of these were found in GnomAD (https://gnomad.broadinstitute.org/gene/ENSG00000110711). All 5 patients with novel mutations were simplex cases. [#]Revel score[730] of this variant is 0.989 out of the maximum 1, strongly suggesting pathogenic status and Gavin score[731] is 'pathogenic'. *AIP*mut, *AIP* mutation-positive; PA, pituitary adenoma; PPIase, peptidylprolyl isomerase; TPR, tetratricopeptide repeat; UTR, untranslated region.

Variant HGVS nomenclature: DNA (protein)	dbSNP ID	American College of Medical Genetics and Genomics and the Association for Molecular Pathology category	Revel and Gavin scores	Number of subjects in our study population	MAF in our cohort - affected individuals (n=1216) (%)	MAF in GnomAD exomes and genomes (%)
c.47G>A (p.R16H)	rs145047094	benign	0.777 / benign	4 (all affected)	0.3289	0.2082
c.100-18C>T (p?)	rs202156895	likely benign	*n/a / benign	7 (all affected)	0.5757	0.3147
c.132C>T (p.D44=)	rs11822907	benign	*n/a / benign	3 (all affected)	0.2467	0.7984
c.144C>T (p.T48=)	rs772658134	benign	*n/a / benign	1 (affected)	0.0822	0.0064
c.468+9C>T (p?)	rs373159347	likely benign	*n/a / benign	1 (affected)	0.0822	0.0066
c.469-13C>T (p?)	n/a	VUS	*n/a / benign	1 (affected)	0.0822	n/a
c.516C>T (p.D172=)	rs2276020	benign	*n/a / benign	22 (nineteen affected, three unaffected [one homozygous])	1.56	3.4314
c.579G>T (p.G193=)	rs1194122725	likely benign	*n/a / benign	1 (unaffected)	0	n/a
c.682A>C (p.K228Q) †	rs641081	likely benign	0.117 / benign	18 (all affected)	1.4803	5.0202
c.787+9C>T (p?)	rs749392143	VUS	*n/a / benign	1 (affected)	0.0822	0.0047
c.807C>T (p.F269=)	rs139407567	VUS	*n/a / benign	11 (five affected)	0.4112	0.0550
c.831C>T (p.A277=)	rs531331351	VUS	*n/a / pathogenic	1 (affected)	0.0822	0.0016
c.891C>A (p.A297=)	rs35665586	benign	*n/a / benign	2 (affected)	0.1645	0.1813
c.896C>T (p.A299V)	rs148986773	likely benign	0.292 / pathogenic	5 (one affected)[#]	0.0822	0.0544
c.906G>A (p.V302=)	rs142912418	benign	*n/a / benign	2 (one affected)	0.0822	0.0086
c.911G>A (p.R304Q)	rs104894190	VUS	0.31 / benign	32 (sixteen affected)	1.32	0.1568

Table 7.8: List of non-pathogenic *AIP* variants identified in the study population

n/a, not available; VUS, variant of uncertain significance. *n/a, Revel score not available as this scoring system only consider missense variants. †There is a Q at this position in the AIP reference sequence, but we consider K as the wild-type amino-acid, due to its higher prevalence in the population screened so far (GnomAD, 1000Genomes); we considered A at this position as the reference allele when analysing GnomAD data. [#]Two of the unaffected subjects carry the R304* and the A299V variants on 2 different alleles, strongly suggesting that the A299V variant is benign[708]. Variant nomenclature was based on transcript NM_003977.4. Categorisation of variants was based on the combination of multiple *in silico* prediction tools, clinical and experimental data.

	*AIP*mut PAs: truncating vs non-truncating mutation			*AIP*mut PAs: p.R304* vs non-p.R304*		
	Truncating *AIP*mut n=126	**Non-truncating *AIP*mut** n=41	***p* value**	**p.R304* *AIP*mut** n=57	**non-p.R304* *AIP*mut** n=110	***p* value**
Cohort type based on family history of PAs						
Familial cohort	95 (75.4%)	19 (46.3%)	**0.001**	44 (77.2%)	70 (63.6%)	0.074
Sporadic cohort	31 (24.6%) [n=126]	22 (53.7%) [n=41]		13 (22.8%) [n=57]	40 (36.4%) [n=110]	
Gender						
Male	69 (54.8%)	33 (80.5%)	**0.003**	33 (57.9%)	69 (62.7%)	0.544
Female	57 (45.2%) [n=126]	8 (19.5%) [n=41]		24 (42.1%) [n=57]	41 (37.3%) [n=110]	
Age at disease onset ≤18 yr	70 (65.4%) [n=107]	24 (63.2%) [n=38]	0.802	31 (67.4%) [n=46]	63 (63.6%) [n=99]	0.659
Age at first symptoms (yr)	19.3 ± 10.2 [n=104]	18.2 ± 7.4 [n=35]	0.940	19.4 ± 10.1 [n=44]	18.8 ± 9.3 [n=95]	0.834
Age at diagnosis (yr)	24.8 ± 12.6 [n=121]	22.9 ± 9.6 [n=39]	0.700	24.9 ± 12.5 [n=54]	24.0 ± 11.7 [n=106]	0.632
Delay in diagnosis (yr)	3.8 ± 6.7 [n=103]	5.0 ± 6.3 [n=35]	**0.013**	3.4 ± 6.0 [n=44]	4.5 ± 6.9 [n=94]	0.221
GH excess	99 (78.6%) [n=126]	37 (90.2%) [n=41]	0.095	43 (75.4%) [n=57]	93 (84.5%) [n=110]	0.151
Gigantism	56 (44.5%) [n=126]	20 (48.8%) [n=41]	0.273	25 (43.9%) [n=57]	51 (46.4%) [n=110]	0.688
Pituitary apoplexy	9 (8.0%) [n=112]	3 (8.8%) [n=34]	0.884	5 (10.0%) [n=50]	7 (7.3%) [n=96]	0.572
Height at diagnosis (cm)	180.1 ± 18.9 [n=89]	180.4 ± 19.7 [n=27]	0.759	181.7 ± 16.9 [n=38]	179.4 ± 20.4 [n=78]	0.508
Height Z-score at diagnosis	2.5 ± 2.4 [n=89]	1.9 ± 2.6 [n=26]	0.243	2.7 ± 2.0 [n=38]	2.3 ± 2.7 [n=71]	0.151
IGF-1 xULN at diagnosis	2.4 ± 3.7 [n=37]	1.7 ± 0.8 [n=13]	0.691	1.5 ± 1.0 [n=14]	2.5 ± 3.7 [n=36]	0.191
Hypopituitarism at diagnosis	24 (40.0%) [n=60]	8 (53.3%) [n=15]	0.350	14 (45.2%) [n=31]	18 (40.9%) [n=44]	0.714
Number of pituitary deficiencies at diagnosis	0.78 ± 1.12 [n=60]	1.07 ± 1.22 [n=15]	0.348	1.00 ± 1.29 [n=31]	0.73 ± 1.02 [n=44]	0.464
Macroadenoma	93 (81.6%) [n=114]	31 (88.6%) [n=35]	0.333	40 (80.0%) [n=50]	84 (84.8%) [n=99]	0.455
Maximum tumour diameter (mm)	18.7 ± 12.4 [n=58]	25.2 ± 14.8 [n=16]	0.109	18.0 ± 12.3 [n=28]	21.4 ± 13.4 [n=46]	0.315
Suprasellar extension	32 (52.5%) [n=61]	12 (60.0%) [n=20]	0.557	13 (48.1%) [n=27]	31 (57.4%) [n=54]	0.430
Cavernous sinus invasion	21 (36.8%) [n=57]	8 (36.4%) [n=22]	0.968	8 (34.8%) [n=23]	21 (37.5%) [n=56]	0.820
Ki-67 > 3%	11 (47.8%) [n=23]	1 (16.7%) [n=6]	0.168	3 (27.3%) [n=11]	9 (50.0%) [n=18]	0.228
Number of treatments	1.90 ± 1.73 [n=122]	2.61 ± 1.33 [n=38]	**0.002**	1.75 ± 1.72 [n=56]	2.24 ± 1.62 [n=104]	**0.026**
Number of surgeries	0.86 ± 0.82 [n=124]	1.13 ± 0.62 [n=38]	**0.014**	0.61 ± 0.62 [n=56]	1.09 ± 0.81 [n=106]	**<0.001**
Re-operation	19 (22.9%) [n=83]	8 (23.5%) [n=34]	0.941	4 (13.3%) [n=30]	23 (26.4%) [n=87]	0.142
Radiotherapy	39 (31.7%) [n=123]	14 (36.8%) [n=38]	0.556	18 (32.1%) [n=56]	35 (33.3%) [n=105]	0.878

Somatostatin analogues	38 (31.1%) [n=122]	21 (55.3%) [n=38]	**0.007**	17 (30.4%) [n=56]	42 (40.4%) [n=104]	0.210
Pegvisomant	8 (6.6%) [n=122]	6 (15.8%) [n=38]	0.079	4 (7.1%) [n=56]	10 (9.6%) [n=104]	0.598
Dopamine agonists	32 (26.2%) [n=122]	12 (31.6%) [n=38]	0.519	19 (33.9%) [n=56]	25 (24.0%) [n=104]	0.181
Multimodal treatment	60 (61.9%) [n=97]	30 (81.1%) [n=37]	**0.034**	25 (59.5%) [n=42]	65 (70.7%) [n=92]	0.203
≥ 3 treatments	35 (36.1%) [n=97]	19 (51.4%) [n=37]	0.107	16 (38.1%) [n=42]	38 (41.3%) [n=92]	0.725
Active disease at last follow-up	21 (22.1%) [n=95]	10 (34.5%) [n=29]	0.178	8 (17.4%) [n=46]	23 (29.5%) [n=78]	0.133
Hypopituitarism at last follow-up	8 (21.6%) [n=37]	8 (47.1%) [n=17]	0.057	3 (14.3%) [n=21]	13 (39.4%) [n=33]	**0.049**
Number of pituitary deficiencies at last follow-up	0.49 ± 1.04 [n=37]	0.33 ± 0.65 [n=12]	0.975	0.43 ± 1.12 [n=21]	0.46 ± 0.84 [n=28]	0.361
Final height (cm)	185.6 ± 17.2 [n=79]	180.4 ± 19.7 [n=27]	0.759	188.0 ± 16.9 [n=34]	183.3 ± 18.3 [n=71]	0.151
Follow-up duration (yr)	11.7 ± 12.9 [n=102]	9.3 ± 9.5 [n=26]	0.593	14.0 ± 13.7 [n=47]	9.6 ± 11.2 [n=81]	0.054

Table 7.9: *AIP*mut PAs due to truncating vs non-truncating mutations or due to p.R304* vs non-p.R304*
Categorical data are shown as n(%); continuous variables are shown as mean±SD. In square brackets is indicated the number of cases where data was available regarding each specific parameter/variable. *AIP*mut, *AIP* mutation-positive; PA, pituitary adenoma; ULN, upper limit of the normal; yr, years.

Discussion

In this study, I analysed a large cohort of patients with familial and young-onset PAs, of whom 11.3% had germline *AIP* mutations, focusing on the prospectively-diagnosed *AIP*mut PAs as characterisation of this particular subgroup, crucial to assess the potential benefits of genetic screening for *AIP* mutations, is lacking. I also aimed to expand the current knowledge on *AIP*mut PAs clinical, therapeutic and outcome characteristics.

My data suggest that the clinical phenotypic spectrum of *AIP*-related pituitary disease is wide, wider than previously thought. Characteristic patients present with aggressive PAs requiring a complex therapeutical approach; however, prospectively-diagnosed *AIP*mut PAs are less invasive and usually require a less complex treatment due to their intrinsic less aggressiveness and/or detection in an early stage facilitating its management.

Hence, prospectively-diagnosed *AIP*mut PAs are those most likely benefiting from early detection via genetic and clinical screening, highlighting the role for genetic screening of at-risk family members in *AIP*mut families and emphasise the benefits of screening *AIP*mut carriers (Figure 7.3).

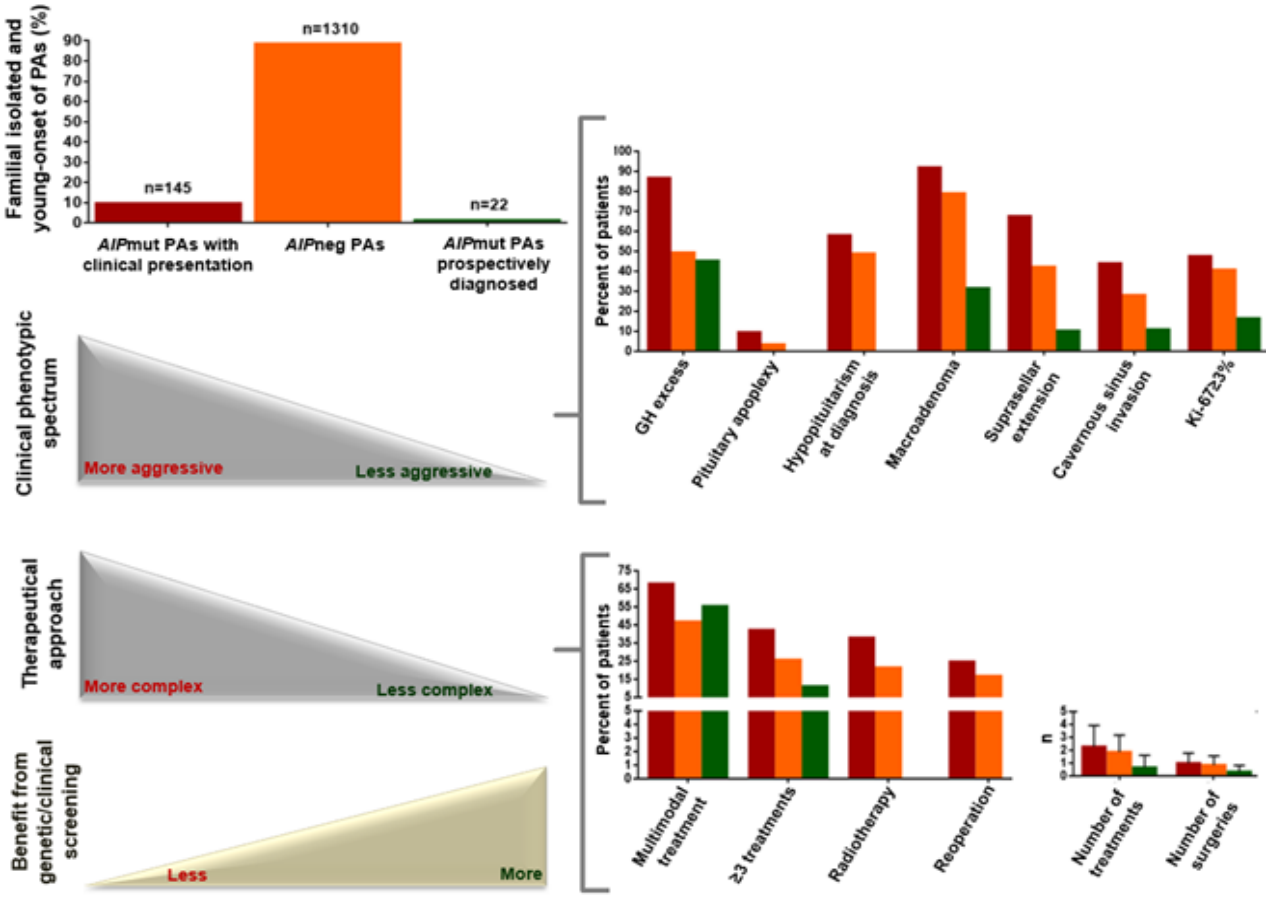

Figure 7.3: Heterogeneous clinical phenotype and management of patients with *AIP*mut PAs, and the benefits of their early detection by genetic and clinical screening

*AIP*mut PAs are more aggressive and refractory to conventional therapy, but *AIP*-related pituitary disease can be controlled with multimodal therapeutical approach

In the *AIP*mut and *AIP*neg comparison, *AIP*mut tumours presented earlier and more aggressively than *AIP*neg ones. Multimodal treatment, including radiotherapy and three or more treatments, were required more often in the *AIP*mut setting. Such observations reflect the more aggressive nature and poorer responsiveness of *AIP*mut PAs, as seen in previous studies[91,161,705,707,732], but the inclusion of aggressive or therapy resistant pituitary disease did not improve the identification of *AIP* mutations in a recent study[733]. In fact, our data show that some *AIP*mut PAs will not display an aggressive phenotype[155,161,196,734]. Moreover, the rate of active disease at last follow-up was 10% lower in the *AIP*mut PAs group, suggesting that *AIP*mut PAs can be satisfactorily controlled despite requiring more complex and multimodal therapeutic schemes[196,310,704,735,736]. Although these data may seem paradoxical (more aggressive disease at presentation in the *AIP*mut patients, but better controlled disease at last follow-up), they could be explained by a more aggressive treatment approach in *AIP*mut cases, especially the use of radiotherapy. Another possibility is that

the follow-up of *AIP*neg cases in our cohort was somewhat shorter; indeed, considering a cut-off of maximum 10yr follow-up, there was no difference in rate of active disease between the 2 groups. Rostomyan *et al.* also reported higher rates of biochemical control at last follow-up and a trend for increased long-term controlled disease in patients with *AIP*mut pituitary gigantism in comparison to those with genetically-negative gigantism[196]. Thus, these data suggest that management of *AIP*mut PA patients can be challenging, but the disease is controllable in a significant proportion of cases.

_AIP_mut somatotrophinomas present earlier, are more aggressive and require more often radiotherapy, with patients ending up taller than those with _AIP_neg somatotrophinomas

Among *AIP*mut patients, somatotrophinomas were the main PA subtype and gigantism the predominant diagnosis, as previously shown[161,169]. *AIP*mut somatotrophinoma patients were younger at first symptoms and at diagnosis, and had higher rates of apoplexy and suprasellar extension, consistent with previous studies[91,161,196,728]. IGF-1 levels at diagnosis did not differ between clinically-presenting *AIP*mut and *AIP*neg somatotrophinoma patients, suggesting that *AIP*mut somatotrophinomas are not biochemically more active at presentation than their *AIP*neg counterparts, similar to earlier data[161]. *AIP*mut patients with gigantism also showed similar IGF-1 levels in our cohort[92], although *AIP*neg giants had higher IGF-1 in another cohort[196]. *AIP*mut somatotrophinoma patients tended to require multimodal and multiple therapy, and had significantly more radiotherapy than *AIP*neg patients, for which a nonsignificant trend had been observed previously[161]. Stature and final adult height are regarded as markers for disease course, aggressiveness and effective management in patients with pituitary gigantism[737,738]. The mean final height in my cohort was higher in the *AIP*mut somatotrophinoma subgroup, with both *AIP*mut males and females ending up taller than *AIP*neg counterparts, although this has not been consistently shown in other series[196]. The taller final height in the *AIP*mut somatotrophinoma patients is likely due to earlier onset of disease, but may reflect the management difficulties, as suggested by the high proportion of patients requiring radiotherapy and multiple therapy.

_AIP_mut prolactinomas present more often with apoplexy than _AIP_neg prolactinomas

Patients with *AIP*mut prolactinomas had higher rates of pituitary apoplexy and more frequently had a family history of PAs than *AIP*neg prolactinomas. We found no differences regarding

treatment and clinical outcomes in the comparative analysis of *AIP*mut vs *AIP*neg prolactinomas. Although the numbers are relatively small, this suggests that *AIP*mut prolactinomas may not be more refractory to medical therapy, in line with the previous report showing that presence of an *AIP* mutation in children or adolescents with macroprolactinomas does not influence the response/resistance to dopamine agonists[734]. Of the 13 *AIP*mut prolactinoma patients reported by Daly *et al.*, 12 received primary dopamine agonist therapy, with initial normalisation of PRL in 5 cases, 1 with initial response but resistance later, and 6 uncontrolled with dopamine agonists requiring surgery, together with radiotherapy given to 3 patients[161]. In Daly *et al. AIP*mut prolactinoma cohort, long-term control was achieved in 61.5% (8 out of 13 patients)[161], which is lower than the rates of controlled disease we found in our cohort (84.6%).

_AIP_mut NFPAs may display an indolent course of disease and have similar features and clinical outcomes as _AIP_neg NFPAs, some of these possibly representing incidentalomas

*AIP*mut NFPAs had lower rates of macroadenomas, hypopituitarism at last follow-up, lower maximum tumour diameter, number of pituitary deficiencies at diagnosis and required fewer treatments and operations than *AIP*neg NFPAs. However, these differences were lost when the 10 prospectively-diagnosed cases were excluded from the analysis, highlighting the remarkable difference in terms of aggressiveness between clinically-presenting and prospectively-diagnosed *AIP*mut NFPAs. In fact, clinically-presenting *AIP*mut NFPAs were macroadenomas, had suprasellar extension and hypopituitarism at diagnosis/last follow-up, and half remain uncontrolled at last follow-up. Clinically-presenting *AIP*mut NFPAs reported previously were also noted for their aggressive behaviour[161]. Some of the small prospectively-diagnosed *AIP*mut NFPAs may represent incidentalomas similar to those often observed in the general population, although incidentalomas are more common in older subjects[7,23]. *MEN1*mut prospectively-diagnosed NFPAs also display an indolent behaviour, do not progress to macroadenomas and often require no intervention[99,101]. Nevertheless, some of these patients will have aggressive *AIP*mut NFPAs which will benefit from early detection by genetic testing and clinical screening.

Phenotype spectrum of _AIP_mut PA patients is heterogeneous: not all _AIP_mut PAs are associated with aggressive behaviour or poor clinical outcomes

My data show that not all *AIP*mut PAs are aggressive or difficult to manage, particularly those prospectively-diagnosed, as some patients have stable or indolent course of disease, including

very early cases of acromegaly with no/mild symptoms and subtle biochemical burden as well as microprolactinomas or small NFPAs (possibly incidentalomas) requiring no treatment. *AIP*mut prolactinomas were not more difficult to manage than *AIP*neg prolactinomas and the rates of active disease at last follow-up were lower in patients with *AIP*mut somatotrophinomas suggesting that *AIP*mut PAs can respond to treatment. Hence, my findings do not fully support the increased aggressiveness or necessarily poor prognosis recognised to *AIP*mut PAs, highlighting that the phenotypic spectrum of *AIP*-related pituitary disease is wider than previously suggested[91,161,705]. Interestingly, the inclusion of aggressive or therapy resistant pituitary disease did not increase the frequency of *AIP* mutations in a recent study[733]. This also supports the current recommendations for managing familial PAs in a similar manner as sporadic *AIP*neg PAs[23,167,170,171].

Prospectively-diagnosed *AIP*mut PAs are less aggressive and have better outcomes than clinically-presenting PAs highlighting the benefits of testing *AIP*mut carriers

In this study, I focused on prospectively-diagnosed *AIP*mut patients, as the clinical and therapeutic characterisation of this subgroup, crucial to assess the potential benefits of genetic testing and clinical screening, is lacking. The clinical screening of carrier family members of *AIP*mut probands has been recommended on the assumption that the early detection of PAs might be associated with more favourable outcomes[91,152,167,168]; however, these predicted advantages had not been previously demonstrated. Among the 187 apparently unaffected *AIP*mut carriers, 22 (11.8%) were identified with a prospectively-diagnosed PA by clinical, biochemical and imaging screening. Prospectively-diagnosed PAs were not present at baseline assessment in 3 *AIP*mut carriers (2 cases previously reported[167]) but emerged during the follow-up (5 to 7 years after the initial screening), reinforcing the need for long-term surveillance of unaffected *AIP*mut carriers as currently recommended[91,152,167,168]. Tichomirowa *et al.* identified 2 patients with PAs among the 21 *AIP*mut carriers screened (9.5%), both clinically silent microadenomas requiring no intervention[155]. In this series, as a group, prospectively-diagnosed *AIP*mut PAs were mainly microadenomas, smaller and associated with lower rates of suprasellar extension, cavernous sinus invasion, hypopituitarism at diagnosis, and required fewer treatments, operations, no radiotherapy, and had reduced rates of active disease and hypopituitarism at last follow-up when compared to their clinically-presenting counterparts. Similar results were obtained when prospectively-diagnosed *AIP*mut somatotrophinomas and *AIP*mut NFPAs were analysed separately. Overall, prospectively-diagnosed *AIP*mut PAs are significantly less invasive and associated with better outcomes than those with a clinical presentation, highlighting the benefits of *AIP* genetic testing of family members at risk and the

screening of individuals carrying an *AIP* mutation, thus providing strong evidence to justify current screening recommendations[152,154,168,169].

Considering the relatively low penetrance of PAs among *AIP*mut carriers (20-23%)[91,152] and the benign nature of their potential condition, *AIP*mut carriers can be reassured and informed about the benefits of early disease detection clearly demonstrated in this study. The advantages of genetic testing and clinical screening are recognised for many familial endocrine tumours, including phaeochromocytomas/paragangliomas[739,740], medullary thyroid cancer[741], parathyroid tumours[116] and MEN1[99]. Some of the screening-detected *MEN1*-related PAs are non-functioning microadenomas[99], similarly to what we have identified in our cohort. Both *AIP*mut and *MEN1*mut prospectively-diagnosed PAs are suggested to be managed according to current guidelines[23,98,99,170,742-744]. As most clinically-presenting *AIP*mut cases show symptoms by the age of 30[91,152,167,168], and no patient has been described to date with normal findings at age 30yr and developing disease later, the surveillance of *AIP*mut carriers could be relaxed after this age[91,167].

Three key questions for clinicians managing PA patients regarding *AIP* testing

(1) Which clinically-presenting PA patient should be tested for *AIP* mutations? Four simple factors (age of onset, family history, tumor type and size), may predict the risk of carrying an *AIP* mutation in a patient with a PA[169]. As mutation status correlates with age of disease onset better than age of diagnosis[91], careful history taking is key. For example, the age at onset between 19-30yr is an independent risk factor for sporadic PA patients to carry an *AIP* mutation; however, patients in this age group without GH excess or an absence of family history have a lower risk[169]. Hence, risk prediction should take several parameters into account, and for patients with fewer risk factors the age cut-off for *AIP* testing could be lower than 30yr[169,733]. My study shows that many sporadic PA patients who undergo *AIP* analysis based on age at onset ≤30yr[91,169] will have negative results. In the young-onset sporadic PA cohort 6.8% were *AIP*mut with slightly higher rates in the sporadic somatotrophinoma group (10.5%) this is at the level of usual risk recommendation for genetic testing, but I identified low rates in sporadic prolactinomas (1.5%) with no cases of NFPAs or corticotrophinomas.

(2) When to initiate genetic screening for family members of a proband? Germline *AIP* mutation genetic testing should be offered at the earliest opportunity to first-degree relatives including children, because the disease may manifest by the age of 4 yr[310].

(3) What should be the clinical follow-up of *AIP*mut carriers? Based on this study, careful baseline assessment of *AIP*mut carriers (including clinical examination, measurement of serum IGF-1 and PRL, and pituitary MRI scan) picks up the largest number of pituitary abnormalities. As *AIP* mutation testing has only been established just over a decade ago, the age range of establishing carrier status was wide in my cohort. However, as testing is now routinely available, we predict that a larger number of carriers will be followed starting at an early age. As the age of disease onset has an inverted U shape, the recommendation for *AIP*mut carrier follow-up could be different for the various age groups. For *AIP*mut carriers until the age of 20yr, annual clinical assessment with measurement of serum IGF-1 and PRL and baseline MRI (starting at 10yr for younger carriers) followed by 5-yearly scans could be appropriate. Follow-up between 21-30yr, if assessment is normal at age 20yr, probably could be relaxed. My data would also raise the possibility that adult *AIP*mut carriers with a normal baseline assessment could be followed with clinical and biochemical assessment, with further pituitary MRI scan only indicated in case of symptoms or biochemical abnormalities. Most clinically-presenting cases show symptoms before the age of 30yr[91,152], and I am not aware of any case with a normal full assessment at age ≥30yr who later developed a PA. However, a cost-effectiveness analysis evaluating the economic burden of genetic and clinical screening programs in this setting, while weighing the benefits of early detection of *AIP*mut PAs, is currently lacking.

Limitations of this study

There are some limitations in my study. Firstly, I used the onset of symptoms age cut-off ≤30yr as a criterion to guide *AIP* genetic testing in patients with young-onset sporadic PAs, as in previous *AIP*-related studies[91,161,169,705]. This age cut-off relies on age of onset which can be subjective; however, age of onset rather than age at diagnosis is suggested to be a better option to guide genetic testing as PAs are often diagnosed with significant delay[169]. Secondly, our patients were recruited from different countries and thus their characteristics and outcomes may be affected by their different genetic backgrounds and/or different local clinical practice. Thirdly, I assigned, based on current experimental, clinical and *in silico* data, the *AIP* variants into pathogenic/likely

pathogenic, or variant of uncertain significance/likely benign/benign groups; however, these categories may change as these variants are better characterised. Fourthly, clinico-therapeutical features and outcome data were not accessible/available for all patients, limiting statistical power of some of my comparative analysis. Fifthly, since the apparently unaffected participants of our study were genetically and clinically screened at various ages, we cannot determine, at this point, the disease penetrance for the prospectively-diagnosed cohort per age group. We also cannot fully exclude that any of the predicted *AIP*neg patients could eventually carry an *AIP* mutation; however, as these cases had at least one affected relative tested negative for *AIP* mutation and their familial phenotypes are not suggestive of *AIP*mut, it is very unlike that we have missed phenocopy families in this study.

Conclusions

Genetic testing followed by clinical screening in *AIP*mut kindreds can detect clinically-relevant pituitary disease, where earlier intervention results in better outcomes. While clinically-presenting *AIP*mut PAs occur in younger patients with more advanced disease, complex treatment strategies can result in well-controlled disease. There is a wider spectrum of disease severity in *AIP*mut PA patients, even within the same family, than previously suspected. When considering patients for *AIP* mutation testing, key clinical factors help to predict the risk level to guide decision making.

Chapter 8: Characterisation of *MEN1* mutation-positive pituitary adenomas and comparison with *AIP* mutation-positive ones: remarkable phenotypic differences in patients with distinct forms of familial pituitary adenomas

Introduction

Familial forms of PAs can occur as part of a complex syndrome, such as in the MEN1 syndrome[19,691], an autosomal dominant disorder usually associated with *MEN1* gene mutations that predisposes mainly to PHPT, PAs and pNETs[97,98]. The prevalence of PAs in MEN1 vary from 10-76% depending on the series[100-102], and pituitary involvement can be the first manifestation in up to a third of MEN1 patients[99,745]. Studies analysing PAs in MEN1 patients are relatively scarce[99,101,103,109,746-748], nevertheless *MEN1*mut PAs are recognised in young patients, more invasive and large as well as is often more challenging to normalise pituitary hypersecretion than in *MEN1* mutation-negative PAs [100,103,109].

AIP and *MEN1* mutations are the main cause of familial forms of PAs, thus genetic analysis of these genes is recommended in PA screening algorithms[97,98,110,168,691]. The order of genes to test in a patient with a suspected familial PA is often dictated by the presence of syndromic manifestations; however, isolated PAs can occur in MEN1, either as first MEN1 manifestation and/or cases where may be the only penetrant condition at that point in time, raising challenges in terms of which gene to test first (*AIP* or *MEN1*) and being misleading if only *AIP* is tested[110].

A comparative analysis between *AIP*mut and *MEN1*mut PAs may provide insights in terms of genetic analysis prioritisation in familial PA cases, besides providing further knowledge on these 2 rare inherited forms of PAs.

Aims

General

To characterise *AIP*mut and *MEN1*mut PA patients in general and by subtype and to provide a comparative analysis between *AIP*mut and *MEN1*mut PAs.

Specific

1. To characterise PAs in *AIP*mut and *MEN1*mut patients in general and by PA subtype
2. To provide a comparative analysis between *AIP*mut and *MEN1*mut PAs
3. To determine phenotypic or clinical features that may aid prioritising genetic analysis in young patients presenting with isolated PAs

Methods

Study population

Patients were selected from The International FIPA Consortium research group database (http://www.fipapatients.org/fipaconsortium/). Data from each case was collected from medical records and clinical letters as provided by referral clinicians. In this database, we have a total of 99 MEN1 individuals genetically confirmed, including 70 patients with PAs, 18 patients with non-pituitary MEN1-related manifestations and 11 asymptomatic *MEN1*mut carriers. We also have 2079 FIPA patients of which 167 are due to a germline *AIP* mutation (details about the cases included in the *AIP*mut subgroup in Chapter 7). My study population consisted of 70 patients with *MEN1*mut PAs and 167 patients with *AIP*mut PAs.

MEN1 and *AIP* genetic analysis

MEN1 genetic testing was offered to index patients with MEN1 (two or more MEN1-related endocrine tumours) or patients with suspicious or atypical MEN1 phenotype (PHPT before the age of 30, multigland parathyroid disease, gastrinoma or multiple pNET at any age, individuals with isolated young-onset *AIP*neg PAs particularly prolactinomas, or individuals who have 2 or more MEN1-related tumours not part of the classical MEN1 triad), as previously recommended[98]. Indications for *AIP* genetic testing are described in Chapter 7.

AIP and *MEN1* genetic testing and pathogenicity determination of *MEN1* or *AIP* variants were performed as described in the Chapter 7. First-degree family members of individuals carrying *MEN1* or *AIP* mutations were offered genetic testing, and mutation carriers then had a baseline clinical, biochemical and imaging screening, in line with current recommendations[98,152,167,168].

Definition of *MEN1*mut and *AIP*mut PA subgroups

*MEN1*mut subgroup consisted of 70 patients with PAs identified with a *MEN1* mutation: 68 had a documented germline *MEN1* mutation and 2 were predicted *MEN1*mut (both obligate carriers affected with PA, PHPT and pNET, and both belonging to a *MEN1*mut kindred with at least one *MEN1*mut relative). *AIP*mut subgroup consisted of 167 patients with familial isolated and young-onset PAs with known *AIP* mutation, defined as described in Chapter 7. I excluded patients with PAs with unknown *AIP* or *MEN1* genetic status, including those with a diagnosis of MEN1 based on clinical criteria, but without documented *MEN1* mutation. Individuals carrying *AIP* or *MEN1* mutations but with undetermined PA status (*AIP*mut or *MEN1*mut carriers who did not undergo clinical screening or had pending results by the time of data analysis) were also excluded.

Definitions of MEN1-related diseases and the study clinical parameters

PAs were defined based on histopathology and/or radiological examination (MRI showing a PA) and/or symptoms caused by elevated anterior pituitary hormone levels in accordance to current guidelines[23,170,171]. The clinical diagnoses were categorised as prolactinoma, acromegaly or gigantism and clinically NFPAs. There were no Cushing´s disease or thyrotrophinomas in the *MEN1*mut or *AIP*mut PA subgroups. PHPT, pNETs, thymic carcinoid tumours, adrenocortical tumours and other MEN1-related tumours were defined and diagnosed according to corresponding guidelines[98,749-752]. The definition of clinical parameters and outcomes are described in detail in Chapter 7.

Results

General characterisation of the *MEN1*mut cohort

Out of 99 individuals carrying a *MEN1*mut included in the database, 56 were initially diagnosed based on clinical criteria, 13 had a familial MEN1 diagnosis, while 30 individuals were diagnosed via genetic testing. Eleven *MEN1*mut carriers remain free-of-disease, whereas 88 individuals had at least one MEN1 manifestation at last observation (mean number of manifestations 2.4±1.4). PA was the most prevalent manifestation affecting 70 subjects (70.7%), followed by PHPT and pNETs seen in 66 and 56 subjects, with 35.4% being affected simultaneously by a PA+PHPT+pNET (Figure 8.1). Less commonly, adrenal tumours (26.3%), lipomas (14.1%), carcinoid tumours (9.1%), thyroid tumours (7.1%), angiofibromas/collagenomas (3%) and meningiomas (1%) were seen.

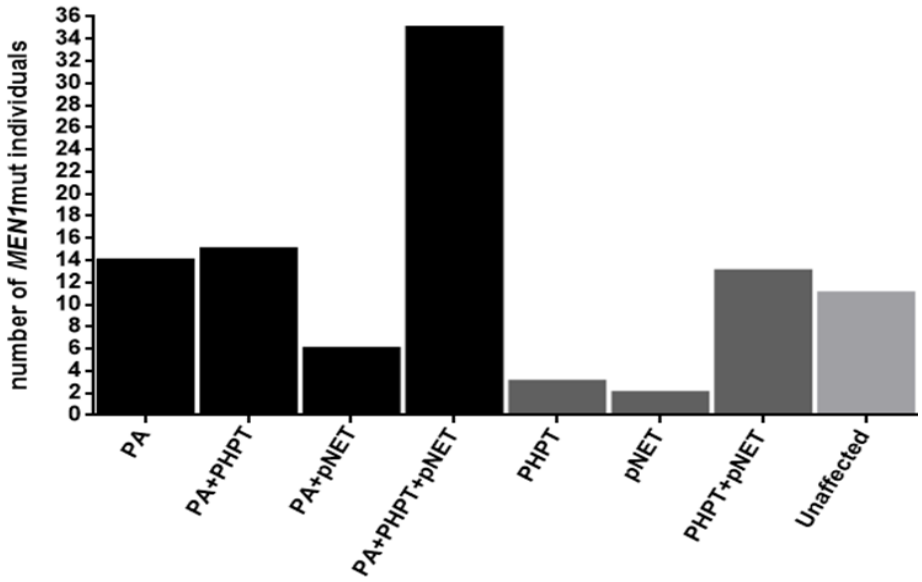

Figure 8.1: Main MEN1-related manifestations among the cohort of 99 MEN1 patients
*MEN1*mut, *MEN1* mutation-positive; PA, pituitary adenoma; PHPT, primary hyperparathyroidism; pNET, pancreatic neuroendocrine tumour.

The mean current age of *MEN1*mut individuals is 42.2±14.2yr (29 subjects below the age of 30), differing considerably among subjects unaffected or subjects affected with one or more MEN1 manifestations (p<0.001): 13 patients affected only with PAs had a current mean age of 29.9±14.3yr, similar to unaffected subjects (29.3±20.3yr), whereas patients with PA+PHPT+pNET had a mean current age of 53.4±15.7yr (Figure 8.2).

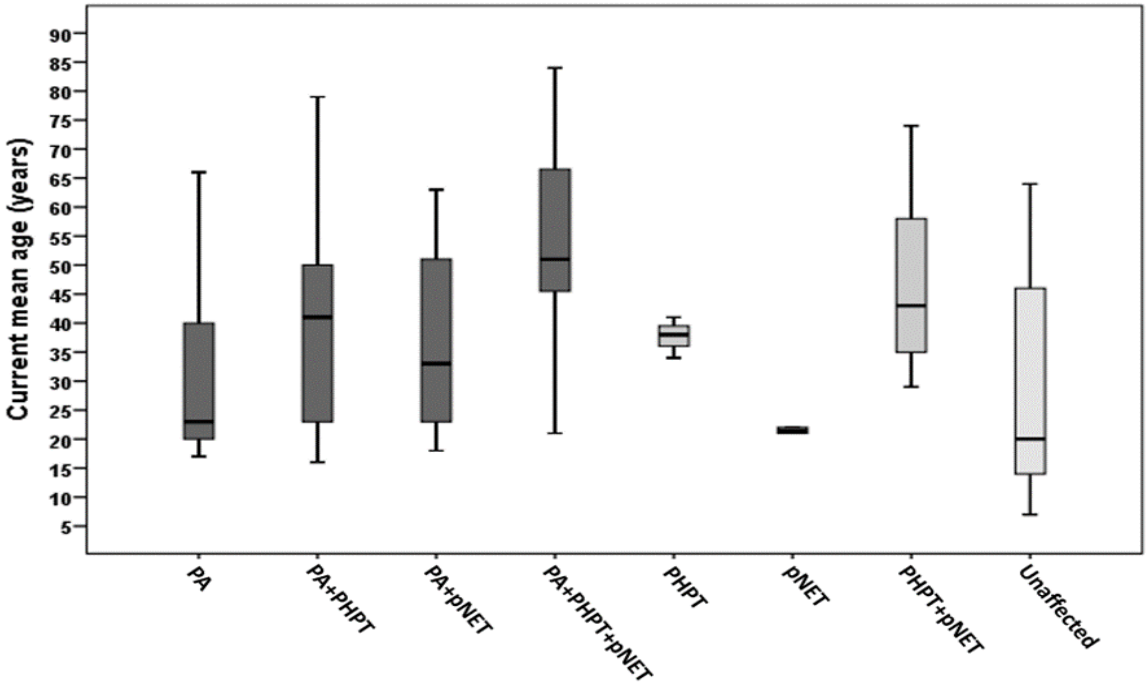

Figure 8.2: Current age among the cohort of 99 MEN1 patients according to main manifestations
Data are shown as mean±SD. *MEN1*mut, *MEN1* mutation-positive; PA, pituitary adenoma; PHPT, primary hyperparathyroidism; pNET, pancreatic neuroendocrine tumour.

Twenty-one different germline *MEN1* mutations were identified in my study population, and are listed in Table 8.1 (*AIP* mutations in the study population are listed in Table 7.7 in Chapter 7).

c.231C>G (p.Y77*)
c.249_252delGTCT (p.I85Sfs)
c.292del (p.R98fs)
317ins5
c.378G>A (p.W126*)
c.406del (p.D136fs)
c.446-1G>A (p.?)
c.461G>T (p.S154I)
c.478G>C (p.A160P)
c.490G>C (p.A164P)
c.590C>T (p.T197I)
c.628_631delACAG (p.T210Sfs)
c.738_741delACAG
c.784-9G>A (p.?)
c.784-15_784-14delTC
c.1243C>T (p.R415*)
c.1328C>A (p.S443Y)
c.1350+1_1350+11delGTGAGGGACAG (p.?)
c.1452delG
c.1546dupC (p.Arg516Profs)
1657insC

Table 8.1: List of *MEN1* mutations identified in the study population

*MEN1*mut PAs characterisation and comparative subanalysis by PA type

In the *MEN1*mut PA cohort, PAs were the most frequent first MEN1-related manifestation (58.8%), followed by PHPT (27.5%) and pNET (13.7%); PHPT and pNETs were the most common second and third manifestations respectively (Table 8.2).

Main MEN1-related manifestations	First MEN1 manifestation	Second MEN1 manifestation	Third MEN1 manifestation
PA	30 (58.8%)	11 (35.5%)	7 (43.7%)
PHPT	14 (27.5%)	12 (38.7%)	1 (6.3%)
pNET	7 (13.7%)	8 (25.8%)	8 (50.0%)
	[n=51]	[n=31]	[n=16]

Table 8.2: Main MEN1-related manifestations order of onset in patients with *MEN1*mut PAs
Categorical data are shown as n (%). In square brackets is indicated the number of cases where data was available. MEN1, multiple endocrine neoplasia type 1; PHPT, primary hyperparathyroidism; PA, pituitary adenoma; pNET, pancreatic neuroendocrine tumour.

The mean age at PA diagnosis was lower in patients with PA only than in patients with PA and additional MEN1-related manifestations (Figure 8.3).

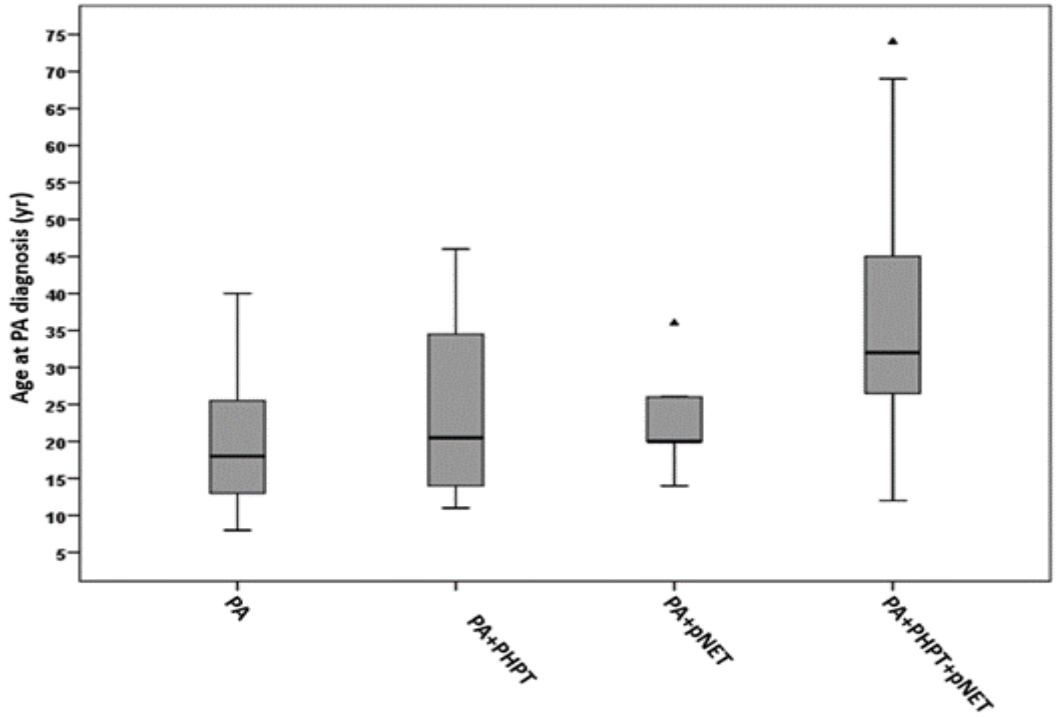

Figure 8.3: Age at PA diagnosis among 70 MEN1 patients with PAs according to different combination of MEN1 manifestations

Data are shown as mean±SD. *MEN1*mut, *MEN1* mutation-positive; PA, pituitary adenoma; PHPT, primary hyperparathyroidism; pNET, pancreatic neuroendocrine tumour; yr, years.

Male:female ratio was 1:1.12 with a mean age at first symptoms and at diagnosis of PA of 21.6±11.7 and 29.6±16.6yr respectively. There were no cases of apoplexy among *MEN1*mut PA patients, and the rates of hypopituitarism at diagnosis, macroadenoma, extrasellar/suprasellar extension and cavernous sinus invasion were 21, 42, 29 and 27% respectively. *MEN1*mut PAs required a relatively low number of treatments and surgeries, radiotherapy was used in 13%, and only 3% were active at last follow-up (Table 8.3).

	***MEN1*mut vs *AIP*mut PAs**		
	***MEN1*mut** n=70	***AIP*mut** n=167	***p* value**
Clinical diagnosis			
Acromegaly	8 (11.4%)	60 (35.9%)	**<0.001**
Gigantism	1 (1.4%)	76 (45.5%)	
NFPA	20 (28.6%)	14 (8.4%)	
Prolactinoma	41 (58.6%)	17 (10.2%)	
	[n=70]	[n=167]	
GH excess	9 (12.9%) [n=70]	136 (81.4%) [n=167]	**<0.001**
Gender			
Male	33 (47.1%)	102 (61.1%)	**0.048**
Female	37 (52.9%)	65 (38.9%)	
	[n=70]	[n=167]	
Age at disease onset ≤ 18 yr	13 (44.8%) [n=29]	94 (64.8%) [n=145]	**0.043**

Age at first symptoms (yr)	21.6 ± 11.7 [n=29]	19.0 ± 9.5 [n=139]	0.420
Age at diagnosis (yr)	29.6 ± 16.6 [n=51]	24.3 ± 11.9 [n=160]	0.063
Delay in diagnosis (yr)	2.0 ± 2.7 [n=138]	4.1 ± 6.6 [n=138]	0.097
Prospective diagnosis	7 (10.6%) [n=66]	22 (13.2%) [n=167]	0.593
Pituitary apoplexy	0 [n=57]	12 (8.2%) [n=146]	**0.026**
Hypopituitarism at diagnosis	12 (21.4%) [n=56]	32 (42.7%) [n=75]	**0.011**
Number of pituitary deficiencies at diagnosis	0.34 ± 0.77 [n=56]	0.84 ± 1.11 [n=75]	**0.006**
Macroadenoma	25 (42.4%) [n=59]	124 (83.2%) [n=149]	**<0.001**
Maximum tumour diameter (mm)	14.6 ± 15.0 [n=39]	20.1 ± 13.0 [n=74]	**0.005**
Extrasellar extension	14 (28.6%) [n=49]	60 (66.7%) [n=90]	**<0.001**
Suprasellar extension	14 (28.6%) [n=49]	44 (54.3%) [n=81]	**0.004**
Cavernous sinus invasion	13 (26.5%) [n=49]	29 (36.7%) [n=79]	0.233
Number of treatments	1.01 ± 0.95 [n=67]	2.07 ± 1.66 [n=160]	**<0.001**
Number of surgeries	0.21 ± 0.45 [n=67]	0.93 ± 0.79 [n=162]	**<0.001**
Re-operation	1 (7.7%) [n=13]	27 (23.1%) [n=117]	0.201
Radiotherapy	9 (13.4%) [n=67]	53 (32.9%) [n=161]	**0.003**
Multimodal treatment	14 (30.4%) [n=46]	90 (67.2%) [n=134]	**<0.001**
≥ 3 treatments	4 (8.7%) [n=46]	54 (40.3%) [n=134]	**<0.001**
Active disease at last follow-up	2 (4.7%) [n=43]	31 (25.0%) [n=124]	**0.004**
Hypopituitarism at last follow-up	14 (25.9%) [n=54]	16 (29.6%) [n=54]	0.667
Number of pituitary deficiencies at last follow-up	0.60 ± 1.34 [n=5]	0.45 ± 0.96 [n=49]	0.984
Follow-up duration (yr)	10.7 ± 10.0 [n=40]	11.2 ± 12.3 [n=128]	0.480

Table 8.3: Comparative analysis between *MEN1*mut vs *AIP*mut PAs
Categorical data are shown as n(%); continuous variables are shown as mean±SD. In square brackets is indicated the number of cases where data was available regarding each specific parameter/variable. *AIP*mut, *AIP* mutation-positive; GH, growth hormone; *MEN1*mut, *MEN1* mutation-positive; PA, pituitary adenoma; yr, years.

Within our *MEN1*mut PA subgroup, 41 (58.6%) patients had prolactinomas, 20 (28.6%) had NFPAs and 9 (12.8%) had somatotrophinomas. Demographic, clinical, treatment and disease outcome parameters, as well as a comparative analysis by PA type among *MEN1*mut PA patients, are shown in the Table 8.4. *MEN1*mut prolactinomas were diagnosed on average 14 and 5 years earlier than

NFPAs and somatotrophinomas (p=0.026), with a tendency for higher rates of hypopituitarism at diagnosis than *MEN1*mut NFPAs or somatotrophinomas (30.3 vs 5.9 vs 16.7%; p=0.131). *MEN1*mut prolactinomas occurred more in females (63.5%), in contrast to *MEN1*mut somatotrophinomas (45%) and *MEN1*mut NFPAs (22.2%) both more predominant in males (p=0.057). *MEN1*mut prolactinomas when compared to NFPAs and somatotrophinomas were larger (21.8±17.1 vs 5.0±3.6 vs 13.0±11.2mm; p=0.003) and had higher rates of cavernous sinus invasion (41.4 vs 6.2 vs 0%; p=0.017). *MEN1*mut prolactinomas required less frequently multimodal treatment than NFPAs and somatotrophinomas (17.6 vs 60 vs 71.4%; p=0.006). *MEN1*mut NFPAs were diagnosed at older ages, were smaller and predominantly microadenomas, and required fewer treatments (0.4±0.8) than both *MEN1*mut prolactinomas (1.2±0.8) and *MEN1*mut somatotrophinomas (1.7±1.3). *MEN1*mut somatotrophinomas required more often multimodal treatment (p=0.006) than *MEN1*mut prolactinomas and *MEN1*mut NFPAs (Table 8.4).

	***MEN1*mut prolactinomas** n=41	***MEN1*mut NFPAs** n=20	***MEN1*mut somatotrophinomas** n=9	***p* value**
Gender Male Female	 15 (36.6%) 26 (63.4%) [n=41]	 11 (55.0%) 9 (45.0%) [n=20]	 7 (77.8%) 2 (22.2%) [n=9]	0.057*[a]
Age at disease onset ≤ 18 yr	12 (52.2%) [n=23]	0 [n=2]	1 (25.0%) [n=4]	0.251
Age at first symptoms (yr)	18.9 ± 8.2 [n=23]	53.5 ± 5.0 [n=2]	21.8 ± 6.9 [n=4]	**<0.001***[b]
Age at diagnosis (yr)	24.9 ± 15.4 [n=29]	38.9 ± 17.9 [n=15]	29.6 ± 10.9 [n=7]	**0.026***[c]
Delay in diagnosis (yr)	1.6 ± 2.2 [n=22]	4.0 [n=1]	4.0 ± 4.3 [n=4]	0.183
Prospective diagnosis	5 (13.2%) [n=38]	2 (10.5%) [n=19]	0 [n=9]	0.515
Pituitary apoplexy	0 [n=33]	0 [n=16]	0 [n=8]	1.000
Hypopituitarism at diagnosis	10 (30.3%) [n=33]	1 (5.9%) [n=17]	1 (16.7%) [n=6]	0.131*[c]
Number of pituitary deficiencies at diagnosis	0.52 ± 0.94 [n=33]	0.06 ± 0.24 [n=17]	0.17 ± 0.41 [n=6]	0.117
Macroadenoma	19 (54.3%) [n=35]	2 (11.8%) [n=17]	4 (57.1%) [n=7]	**0.010***[b]
Maximum tumour diameter (mm)	21.8 ± 17.1 [n=20]	5.0 ± 3.6 [n=14]	13.0 ± 11.2 [n=5]	**0.003***[c]
Extrasellar extension	11 (37.9%) [n=29]	2 (12.5%) [n=16]	1 (25.0%) [n=4]	0.193
Suprasellar extension	11 (37.9%) [n=29]	2 (12.5%) [n=16]	1 (25.0%) [n=4]	0.193
Cavernous sinus invasion	12 (41.4%) [n=29]	1 (6.2%) [n=16]	0 [n=4]	**0.017***[c]
Number of treatments	1.18 ± 0.77 [n=38]	0.40 ± 0.75 [n=20]	1.67 ± 1.32 [n=9]	**<0.001***[b]
Number of surgeries	0.16 ± 0.44 [n=38]	0.20 ± 0.41 [n=20]	0.44 ± 0.53 [n=9]	0.223

Re-operation	1 (20.0%) [n=5]	0 [n=4]	0 [n=4]	0.420
Radiotherapy	5 (13.2%) [n=38]	1 (5.0%) [n=20]	3 (33.3%) [n=9]	0.117*[d]
Multimodal treatment	6 (17.6%) [n=34]	3 (60.0%) [n=5]	5 (71.4%) [n=7]	**0.006***[e]
≥ 3 treatments	2 (5.9%) [n=34]	0 [n=5]	2 (28.6%) [n=7]	0.117
Active disease at last follow-up	2 (8.3%) [n=24]	0 [n=14]	0 [n=5]	0.436
Hypopituitarism at last follow-up	9 (28.1%) [n=32]	2 (12.5%) [n=16]	3 (50.0%) [n=6]	0.183
Follow-up duration (yr)	10.9 ± 9.0 [n=20]	9.0 ± 10.8 [n=14]	14.0 ± 12.2 [n=6]	0.599

Table 8.4: Comparative analysis by subtype among *MEN1*mut PAs
Categorical data are shown as n(%); continuous variables are shown as mean±SD. In square brackets is indicated the number of cases where data was available regarding each specific parameter. *[a] $p<0.05$ only between prolactinomas and somatotrophinomas. *[b] $p<0.05$ between NFPAs and both prolactinomas and somatotrophinomas, but no differences between prolactinoma and somatotrophinomas. *[c] $p<0.05$ only between prolactinomas and NFPAs. *[d] $p<0.05$ only between somatotrophinomas and NFPAs. *[e] $p<0.05$ between prolactinomas and both NFPAs and somatotrophinomas, but no differences between NFPAs and somatotrophinomas. NFPA, non-functioning pituitary adenoma; yr, years.

*AIP*mut PAs characterisation and comparative subanalysis by PA type

Out of 167 *AIP*mut PA patients, 102 were males (male:female ratio 1.57:1) and 94 had disease onset ≤18yr with a mean age at first symptoms and at diagnosis of 19.0±9.5 and 24.3±11.9yr respectively. Twelve *AIP*mut PA patients suffered apoplexy, 43% had hypopituitarism at diagnosis, 83% had a macroadenoma, and the rates of extrasellar, suprasellar extension and cavernous sinus invasion were 67, 54 and 37% respectively. *AIP*mut PAs required a relatively high number of treatments and surgeries (2.07±1.66 and 0.93±0.79 respectively), multimodal therapy was given in 67%, radiotherapy in 33%, and the rate of active disease at last follow-up was 25% (Table 8.3).

Within the *AIP*mut PA subgroup, 136 (81.4%) patients had somatotrophinomas, 17 (10.2%) had prolactinomas and 14 (8.4%) had NFPAs. Demographic, clinical, treatment and disease outcome parameters, as well as a comparative analysis by PA type among *AIP*mut PA patients, are shown in the Table 8.5. *AIP*mut somatotrophinomas had lower ages at first symptoms and at diagnosis, and also required more frequently multimodal (p=0.003) and multiple treatments (p=0.005) than *AIP*mut prolactinomas (but not *AIP*mut NFPAs). *AIP*mut somatotrophinomas when compared to both NFPAs and prolactinomas were associated to higher rates of extrasellar extension (p=0.002), and required more treatments (p<0.001), surgeries (p<0.001) and radiotherapy (p=0.003). *AIP*mut NFPAs had significantly less hypopituitarism at diagnosis, lower rates of macroadenomas and were smaller than *AIP*mut somatotrophinomas (p=0.035, p<0.001 and p=0.002) but did not differ from *AIP*mut prolactinomas (Table 8.5).

	***AIP*mut prolactinomas** n=17	***AIP*mut NFPAs** n=14	***AIP*mut somatotrophinomas** n=136	***p* value**
Gender Male Female	9 (52.9%) 8 (47.1%) [n=17]	9 (64.3%) 5 (35.7%) [n=14]	84 (61.8%) 52 (38.2%) [n=136]	0.755
Age at disease onset ≤ 18 yr	5 (45.5%) [n=11]	4 (50.0%) [n=8]	85 (67.5%) [n=126]	0.227
Age at first symptoms (yr)	27.5 ± 17.9 [n=10]	22.6 ± 7.7 [n=7]	18.1 ± 8.4 [n=122]	**0.006***[a]
Age at diagnosis (yr)	30.7 ± 16.5 [n=15]	29.2 ± 14.8 [n=12]	23.2 ± 10.8 [n=133]	**0.022***[a]
Delay in diagnosis (yr)	4.5 ± 8.8 [n=11]	1.14 ± 2.3 [n=7]	4.3 ± 6.5 [n=120]	0.469
Prospective diagnosis	2 (11.8%) [n=17]	10 (71.4%) [n=14]	10 (7.4%) [n=136]	**<0.001***[b]
Pituitary apoplexy	2 (16.7%) [n=12]	0 [n=13]	10 (8.3%) [n=121]	0.317
Hypopituitarism at diagnosis	5 (62.5%) [n=8]	1 (9.1%) [n=11]	26 (46.4%) [n=56]	**0.035***[b]
Number of pituitary deficiencies at diagnosis	1.38 ± 1.51 [n=8]	0.18 ± 0.60 [n=11]	0.89 ± 1.12 [n=56]	0.060
Macroadenoma	12 (75.0%) [n=16]	4 (30.8%) [n=13]	108 (90.0%) [n=120]	**<0.001***[b]
Maximum tumour diameter (mm)	14.4 ± 16.1 [n=7]	9.0 ± 9.8 [n=11]	23.0 ± 11.9 [n=56]	**0.002***[c]
Extrasellar extension	4 (44.4%) [n=9]	3 (27.3%) [n=11]	53 (75.7%) [n=70]	**0.002***[d]
Suprasellar extension	3 (42.9%) [n=7]	3 (27.3%) [n=11]	38 (60.3%) [n=63]	0.104*[c]
Cavernous sinus invasion	1 (16.7%) [n=6]	2 (18.2%) [n=11]	26 (41.9%) [n=62]	0.183
Number of treatments	1.12 ± 0.78 [n=17]	0.46 ± 0.78 [n=13]	2.35 ± 1.68 [n=130]	**<0.001***[d]
Number of surgeries	0.35 ± 0.49 [n=17]	0.31 ± 0.48 [n=13]	1.06 ± 0.78 [n=132]	**<0.001***[d]
Re-operation	0 [n=6]	0 [n=4]	27 (25.2%) [n=107]	0.194
Radiotherapy	1 (5.9%) [n=17]	1 (7.7%) [n=13]	51 (38.9%) [n=131]	**0.003***[d]
Multimodal treatment	4 (28.6%) [n=14]	2 (50.0%) [n=4]	84 (72.4%) [n=116]	**0.003***[a]
≥ 3 treatments	4 (28.6%) [n=14]	2 (50.0%) [n=4]	84 (72.4%) [n=116]	**0.005***[a]
Active disease at last follow-up	2 (15.4%) [n=13]	1 (10.0%) [n=10]	28 (27.7%) [n=101]	0.326
Hypopituitarism at last follow-up	2 (25.0%) [n=8]	1 (10.0%) [n=10]	13 (36.1%) [n=36]	0.265
Number of pituitary deficiencies at last follow-up	0.75 ± 1.49 [n=8]	0.10 ± 0.32 [n=10]	0.48 ± 0.93 [n=31]	0.348
Follow-up duration (yr)	13.6 ± 12.5 [n=13]	7.5 ± 7.1 [n=12]	11.4 ± 12.8 [n=103]	0.453

Table 8.5: Comparative analysis by subtype among AIPmut PAs

Categorical data are shown as n(%); continuous variables are shown as mean±SD. In square brackets is indicated the number of cases where data was available regarding each specific parameter. *[a] $p<0.05$ only between prolactinomas and somatotrophinomas. *[b] $p<0.05$ between NFPAs and both prolactinomas and somatotrophinomas, but no differences between prolactinomas and somatotrophinomas. *[c] $p<0.05$ only between somatotrophinomas and NFPAs. *[d] $p<0.05$ between somatotrophinomas and both prolactinomas and NFPAs, but no differences between prolactinomas and NFPAs.

Comparative analysis *MEN1*mut vs *AIP*mut PAs

*MEN1*mut PAs were less often associated with GH excess (12.9% vs 81.4%; p<0.001) with prolactinoma being the predominant diagnosis (58.6%), in contrast to the *AIP*mut PA subgroup where gigantism and acromegaly (45.5 and 35.9% respectively) were the most frequent diagnoses (Table 8.3). In comparison to patients with *AIP*mut PAs, *MEN1*mut PA patients were more frequently females (52.9% vs 38.9%; p=0.048), had less commonly disease onset ≤18yr (44.8% vs 64.8%; p=0.043) and a trend for older age at diagnosis (29.6±16.6 vs 24.3±11.9yr; p=0.063). *MEN1*mut PAs had also lower rates of hypopituitarism at diagnosis (21.4% vs 42.7%; p=0.011), macroadenomas (42.4% vs 83.2%; p<0.001), extrasellar extension (28.6% vs 66.7%; p<0.001), suprasellar extension (28.6% vs 54.3%; p=0.004), as well as fewer pituitary deficits (0.3±0.8 vs 0.8±1.1; p=0.006) and smaller tumours (14.6±15.0 vs 20.1±13.0mm; p=0.005) at diagnosis, and none had pituitary apoplexy (vs 8.2%; p=0.026).

*MEN1*mut PA patients required fewer treatments (1.01±0.95 vs 2.07±1.66; p<0.001) and surgeries (0.21±0.45 vs 0.93±0.79; p<0.001), less often radiotherapy (13.4% vs 32.9%; p=0.003) and multimodal treatment (30.4% vs 67.2%; p<0.001), and a smaller proportion were active at last follow-up (4.7% vs 25%; p=0.004) in comparison to *AIP*mut PAs (Table 8.3).

Taking into account the significant differences in terms of clinical diagnoses distribution among *MEN1*mut and *AIP*mut PAs, a comparative subanalysis per PA subtypes was then conducted (Table 8.6 and Table 8.7).

In comparison to *AIP*mut prolactinomas, *MEN1*mut prolactinomas had lower rate of pituitary apoplexy (0 vs 16.7%; p=0.016), and a tendency for older ages at onset (27.5±17.9 vs 18.9±8.2yr; p=0.158), lower rates of macroadenoma (54.3% vs 75%; p=0.160) and hypopituitarism at diagnosis (30.3% vs 62.5%; p=0.090) with fewer pituitary deficiencies (0.5±0.9 vs 1.4±1.51; p=0.066). *MEN1*mut prolactinomas also tended to require fewer surgeries than *AIP*mut prolactinomas (0.16±0.44 vs 0.35±0.49; p=0.072) (Table 8.6).

*MEN1*mut NFPA features, treatment and outcome parameters did not differ from *AIP*mut NFPAs, except for higher age at first symptoms (53.5±5.0 vs 22.6±7.7yr; p=0.040) and tendency for smaller tumours (5.0±3.6 vs 9.0±9.8mm; p=0.126) among *MEN1*mut NFPAs. Both *MEN1*mut and *AIP*mut NFPAs had relatively low rates of hypopituitarism at diagnosis (5.9% and 9.1%), macroadenoma (11.8% and 30.8%), extrasellar/suprasellar extension (12.5% and 27.3%), cavernous sinus invasion (6.2% and 18.2%), low number of treatments (0.4±0.8 and 0.5±0.8) and surgeries (0.2±0.4 and 0.3±0.5), and low rates of active disease (0 and 10%) and hypopituitarism at last-follow-up (12.5% and 10%) (Table 8.6).

	Prolactinomas			NFPAs		
	***MEN1*mut** n=41	***AIP*mut** n=17	***p* value**	***MEN1*mut** n=20	***AIP*mut** n=14	***p* value**
Gender Male Female	15 (36.6%) 26 (63.4%) [n=41]	9 (52.9%) 8 (47.1%) [n=17]	0.250	11 (55.0%) 9 (45.0%) [n=20]	9 (64.3%) 5 (35.7%) [n=14]	0.588
Age at disease onset ≤ 18 yr	12 (52.2%) [n=23]	5 (45.5%) [n=11]	0.714	2 (100.0%) [n=2]	4 (50.0%) [n=8]	0.197
Age at first symptoms (yr)	18.9 ± 8.2 [n=23]	27.5 ± 17.9 [n=10]	0.158	53.5 ± 5.0 [n=2]	22.6 ± 7.7 [n=7]	**0.040**
Age at diagnosis (yr)	24.9 ± 15.4 [n=29]	30.7 ± 16.5 [n=15]	0.244	38.9 ± 17.9 [n=15]	29.2 ± 14.8 [n=12]	0.136
Delay in diagnosis (yr)	1.6 ± 2.2 [n=22]	4.5 ± 8.8 [n=11]	0.773	4.0 [n=1]	1.1 ± 2.3 [n=7]	0.211
Pituitary apoplexy	0 (0%) [n=33]	2 (16.7%) [n=12]	**0.016**	0 [n=16]	0 [n=13]	1.000
Hypopituitarism at diagnosis	10 (30.3%) [n=33]	5 (62.5%) [n=8]	0.090	1 (5.9%) [n=17]	1 (9.1%) [n=11]	0.747
Number of pituitary deficiencies at diagnosis	0.52 ± 0.94 [n=33]	1.38 ± 1.51 [n=8]	0.066	0.06 ± 0.24 [n=17]	0.18 ± 0.60 [n=11]	0.712
Macroadenoma	19 (54.3%) [n=35]	12 (75.0%) [n=16]	0.160	2 (11.8%) [n=17]	4 (30.8%) [n=13]	0.197
Maximum tumour diameter (mm)	21.8 ± 17.1 [n=20]	14.4 ± 16.1 [n=7]	0.375	5.0 ± 3.6 [n=14]	9.0 ± 9.8 [n=11]	0.126
Extrasellar extension	11 (37.9%) [n=29]	4 (44.4%) [n=9]	0.727	2 (12.5%) [n=16]	3 (27.3%) [n=11]	0.332
Suprasellar extension	11 (37.9%) [n=29]	3 (42.9%) [n=7]	0.810	2 (12.5%) [n=16]	3 (27.3%) [n=11]	0.332
Cavernous sinus invasion	12 (41.4%) [n=29]	1 (16.7%) [n=6]	0.254	1 (6.2%) [n=16]	2 (18.2%) [n=11]	0.332
Number of treatments	1.18 ± 0.77 [n=38]	1.12 ± 0.78 [n=17]	0.804	0.40 ± 0.75 [n=20]	0.46 ± 0.78 [n=13]	0.759
Number of surgeries	0.16 ± 0.44 [n=38]	0.35 ± 0.49 [n=17]	0.072	0.20 ± 0.41 [n=20]	0.31 ± 0.48 [n=13]	0.487
Re-operation	1 (20.0%) [n=5]	0 [n=6]	0.251	0 [n=4]	0 [n=4]	1.000
Radiotherapy	5 (13.2%) [n=38]	1 (5.9%) [n=17]	0.424	1 (5.0%) [n=20]	1 (7.7%) [n=13]	0.751
Dopamine agonists	31 (81.6%) [n=38]	12 (70.6%) [n=17]	0.362	3 (15.0%) [n=20]	1 (7.7%) [n=13]	0.530
Multimodal treatment	6 (17.6%) [n=34]	4 (28.6%) [n=14]	0.397	3 (60.0%) [n=5]	2 (50.0%) [n=4]	0.764
≥ 3 treatments	2 (5.9%) [n=34]	1 (7.1%) [n=14]	0.907	0 [n=5]	0 [n=4]	1.000
Active disease at last follow-up	2 (8.3%) [n=24]	2 (15.4%) [n=13]	0.510	0 [n=14]	1 (10.0%) [n=10]	0.227
Hypopituitarism at last follow-up	9 (28.1%) [n=32]	2 (25.0%) [n=8]	0.859	2 (12.5%) [n=16]	1 (10.0%) [n=10]	0.846
Number of pituitary deficiencies at last follow-up	0 [n=3]	0.75 ± 1.49 [n=8]	0.364	0 [n=1]	0.10 ± 0.31 [n=10]	0.752
Follow-up duration (yr)	10.9 ± 9.0 [n=20]	13.6 ± 12.5 [n=13]	0.671	9.0 ± 10.8 [n=14]	7.5 ± 7.1 [n=12]	0.959

Table 8.6: Comparison between MEN1mut vs AIPmut prolactinomas and MEN1mut vs AIPmut NFPAs
Categorical data are shown as n(%); continuous variables are shown as mean±SD. In square brackets is indicated the number of cases where data was available regarding each specific parameter. *AIP*mut, *AIP* mutation-positive; *MEN1*mut, *MEN1* mutation-positive; NFPA, non-functioning pituitary adenoma; yr, years.

*AIP*mut somatotrophinoma patients were commonly diagnosed with gigantism (55.9%), whereas only 1 out of 9 *MEN1*mut somatotrophinoma patients had gigantism (p=0.052). In comparison to *AIP*mut somatotrophinomas*, MEN1*mut somatotrophinomas had lower rates of macroadenoma (57.1% vs 90%; p=0.009) and extrasellar extension (25% vs 75.7%; p=0.026), and required fewer surgeries (0.4±0.5 vs 1.1±0.8; p=0.009). *MEN1*mut somatotrophinomas also showed a tendency for less cavernous sinus invasion (0 vs 41.9%; p=0.096), and none were active at last follow-up (vs 27.7% in *AIP*mut somatotrophinoma subgroup; p=0.170) (Table 8.7).

	***MEN1*mut somatotrophinomas** n=9	***AIP*mut somatotrophinomas** n=136	***p* value**
Gender Male Female	7 (77.8%) 2 (22.2%) [n=9]	84 (61.8%) 52 (38.2%) [n=136]	0.336
Age at disease onset ≤ 18 yr	1 (25.0%) [n=4]	85 (67.5%) [n=126]	0.077
Age at first symptoms (yr)	21.8 ± 7.0 [n=4]	18.1 ± 8.4 [n=122]	0.291
Age at diagnosis (yr)	29.6 ± 10.9 [n=7]	23.2 ± 10.8 [n=133]	0.101
Delay in diagnosis (yr)	4.0 ± 4.3 [n=4]	4.3 ± 6.5 [n=120]	0.708
Gigantism	1 (11.1%) [n=9]	76 (55.9%) [n=136]	0.052
Pituitary apoplexy	0 [n=8]	10 (8.3%) [n=121]	0.397
Height at diagnosis (cm)	172.0 ± 6.1 [n=4]	181.5 ± 19.1 [n=103]	0.221
Hypopituitarism at diagnosis	1 (16.7%) [n=6]	26 (46.4%) [n=56]	0.162
Number of pituitary deficiencies at diagnosis	0.17 ± 0.41 [n=6]	0.89 ± 1.12 [n=56]	0.125
Macroadenoma	4 (57.1%) [n=7]	108 (90.0%) [n=120]	**0.009**
Maximum tumour diameter (mm)	13.0 ± 11.2 [n=5]	23.0 ± 11.9 [n=56]	0.123
Extrasellar extension	1 (25.0%) [n=4]	53 (75.7%) [n=70]	**0.026**
Suprasellar extension	1 (25.0%) [n=4]	38 (60.3%) [n=63]	0.165
Cavernous sinus invasion	0 [n=4]	26 (41.9%) [n=62]	0.096
Number of treatments	1.67 ± 1.32 [n=9]	2.35 ± 1.68 [n=130]	0.252
Number of surgeries	0.44 ± 0.53 [n=9]	1.06 ± 0.78 [n=132]	**0.009**
Re-operation	0 [n=4]	27 (25.2%) [n=107]	0.248
Radiotherapy	3 (33.3%) [n=9]	51 (38.9%) [n=131]	0.739
Somatostatin analogues	3 (33.3%) [n=9]	59 (45.4%) [n=130]	0.482
Dopamine agonists	5 (55.6%) [n=9]	31 (23.8%) [n=130]	**0.036**

Pegvisomant	0 [n=9]	14 (10.8%) [n=130]	0.299
Multimodal treatment	5 (71.4%) [n=7]	84 (72.4%) [n=116]	0.955
≥ 3 treatments	2 (28.6%) [n=7]	53 (45.7%) [n=116]	0.376
Active disease at last follow-up	0 [n=5]	28 (27.7%) [n=101]	0.170
Hypopituitarism at last follow-up	3 (50.0%) [n=6]	13 (36.1%) [n=36]	0.517
Number of pituitary deficiencies at last follow-up	3.00 [n=1]	0.48 ± 0.93 [n=31]	**0.047**
Final height (cm)	177.0 ± 13.3 [n=4]	185.9 ± 18.3 [n=95]	0.290
Follow-up duration (yr)	14.0 ± 12.2 [n=6]	11.4 ± 12.8 [n=103]	0.296

Table 8.7: Comparative analysis between MEN1mut vs AIPmut somatotrophinomas
Categorical data are shown as n(%); continuous variables are shown as mean±SD. In square brackets is indicated the number of cases where data was available regarding each specific parameter. *AIP*mut, *AIP* mutation-positive; *MEN1*mut, *MEN1* mutation-positive; ULN, upper limit of the normal; yr, years.

Discussion

In this study, I analysed a cohort of patients with two distinct familial forms of PAs aiming to expand the current knowledge on *AIP*mut and *MEN1*mut PAs and to provide the first detailed comparative analysis between *AIP*mut and *MEN1*mut PAs, in general and by PA type.

PAs are common in MEN1 and often the first MEN1-related manifestation

PA was the most prevalent manifestation in my MEN1 cohort, seen in 70.7% of the *MEN1*mut individuals, notably higher than previously reported (30-40%[98,99,102]). PAs were also the most frequent first manifestation in *MEN1*mut PA patients (58.8%), contrarily to previous series reporting PHPT as the predominant first manifestation[99,101,102,745,753]. On the other hand, the prevalence of PHPT in our cohort (66.7%) was lower than the previously reported incidences of approximately 90%[98,102,103,746]; however, a recent MEN1 series focused in PAs described a similarly low PHPT prevalence of 68.5%[101]. This relatively high PA prevalence and low PHPT prevalence, as well as the high frequency of PA as first MEN1 manifestation, may reflect a referral bias to the International FIPA Consortium study which is focused on PAs. Additionally, it may also be explained by the fact that some MEN1 manifestations (namely PHPT) may not yet penetrated in my relatively young cohort of MEN1 patients (mean current age 42.2yr) particularly in those affected only with PAs (mean current age 29.9yr). This might also explain the relatively low

proportion of MEN1 patients with combined PA+PHPT+pNET in my study (35.4%) when compared to other series[101,103,746,754]. The mean age at PA diagnosis in my *MEN1*mut cohort (29.6±16.6yr) was relatively lower than reported by most series, usually describing age at diagnosis well above the age of 30[102,103,746], and some above 40[754] or even 50 years[101]. The mean age at PA diagnosis was lower in the subgroup of MEN1 affected only with PAs. Hence, suspicion for MEN1 should be raised in young patients presenting with isolated PAs (often the first MEN1 manifestation), and thus genetic analysis of *MEN1* should be offered to young patients with sporadic PAs[110] particularly the *AIP*neg ones.

MEN1-related PAs occur more in females and are often prolactinomas, in contrast with *AIP*mut PAs which affect mostly males and are somatotrophinomas

We observed a higher proportion of females among the *MEN1*mut PA group, namely among *MEN1*mut prolactinomas, in line with previous studies[101-103,755]. The explanation for female predomi-nance in MEN1 is unknown, although it has been postulated that oestrogens may exert a stimulus for cell proliferation leading to pituitary tumourigenesis[103,105] taking into account the well-known stimulatory effects of oestrogens on pituitary lactotroph secretion and proliferation[106,107]. In contrast, *AIP*mut PAs occur predominantly in males consistent with previous reports[156,161,187], although this male predominance might be influenced by an ascertainment bias for gigantism, a condition more prevalent in men in part due to later puberty and later growth cessation[19,196].

Diagnosis among *MEN1*mut and *AIP*mut PA patients differed significantly, with the former group composed mainly by prolactinomas (58.6%), while 81.4% of *AIP*mut patients had a somatotrophi-noma (45.5% gigantism; 35.9% acromegaly), in line with previous reports[91,102,103,161,169,746].

Hence, such differences regarding gender and clinical diagnoses between patients with *MEN1*mut and *AIP*mut PAs may guide clinicians deciding which gene test first in young patients with isolated PAs: a young female presenting with isolated prolactinoma may be a candidate for *MEN1* genetic analysis first, whereas *AIP* should be first tested in a young male with gigantism/acromegaly.

***MEN1*mut PAs are not particularly aggressive and can be controlled with conventional therapy**

Within my cohort of patients with *MEN1*mut PAs, 42% had macroadenomas, 29% had extrasellar and suprasellar extension, 27% had cavernous sinus invasion, and they required a relatively low number of treatments and surgeries, with 97% having cured/controlled disease at last follow-up.

My findings do not support the increased aggressiveness recognised of *MEN1*mut PAs and are divergent from previous series reporting higher rates of macroadenomas up to 85% (vs 42% in non-MEN1 PAs)[103], higher rates of cavernous sinus invasion up to 31.3% (vs 14% in non-MEN1 PAs)[109] or less frequent normalisation of pituitary hypersecretion of about 42% (vs 90% in non-MEN1 PAs)[103] in patients with *MEN1*mut PAs. However, similar to my findings, some other studies also debate the previous notion of increased aggressiveness to *MEN1*mut PAs reporting lower rates of macroadenomas (18.5-37.1%)[99,101,746] with high dopamine agonist response rate of >90% in patients with *MEN1*mut prolactinomas[99]. Ki-67 and mitotic count were not higher in *MEN1*mut PAs in comparison to sporadic PAs[109], and *MEN1*mut non-functioning microadenomas have an indolent behaviour, do not progress to macroadenomas and most often require no treatment[99,101].

_AIP_mut PAs are more aggressive than _MEN1_mut PAs, with somatotrophinomas imposing most of the management challenges

*AIP*mut PAs were remarkably more aggressive than *MEN1*mut PAs, showing significantly higher rates of macroadenomas (larger tumour diameter), extrasellar extension, suprasellar extension, hypopituitarism at diagnosis (more pituitary deficiencies) and apoplexy. Moreover, *AIP*mut PAs required significantly more treatments, surgeries, radiotherapy, multimodal treatment and a higher proportion of cases were active at last follow-up in comparison to *MEN1*mut PAs. Aggressive PAs and/or PAs with poor response to therapy should raise suspicion for an *AIP*mut particularly in young subjects with GH-secreting PAs and family history of PAs[169]. In *AIP*neg PA patients with aggressive or unresponsive to therapy, *MEN1* analysis unlikely will identify mutation carriers, as shown in a recent study[733]. Thus, an individual-based approach focused on clinical elements should prevail for genetic screening of patients with aggressive and refractory PAs.

Considering that clinical diagnoses differed between *MEN1*mut and *AIP*mut PAs, which may grossly explain their distinct clinical features and outcomes, I further conducted a comparative analysis per PA subtype within and between these subgroups.

*MEN1*mut prolactinomas, diagnosed earlier than *MEN1*mut NFPAs and somatotrophinomas and predominantly in females, were larger, had higher rates of cavernous sinus invasion, and had a trend for higher rates of hypopituitarism at diagnosis and more extrasellar/suprasellar extension, displaying overall a more aggressive phenotype than *MEN1*mut NFPAs or *MEN1*mut somatotrophinomas. However, the management of *MEN1*mut somatotrophinomas was more challenging than *MEN1*mut prolactinomas requiring more often multimodal and ≥3 treatments, including surgeries, and a greater tendency for hypopituitarism at last follow-up despite the fact

that all *MEN1*mut somatotrophinoma cases were cured/controlled at last assessment. On the other hand, *MEN1*mut NFPAs were predominantly microadenomas, smaller and required fewer treatments than both *MEN1*mut prolactinomas and *MEN1*mut somatotrophinomas, thus being the most indolent *MEN1*mut PA subtype, in line with previous reports[99,101].

Within the *AIP*mut setting, somatotrophinomas was the most detrimental *AIP*mut PA subtype, displaying higher rates of extrasellar extension, cavernous sinus invasion and requiring more treatments, surgeries and radiotherapy than both *AIP*mut prolactinomas and *AIP*mut NFPAs; conversely, *AIP*mut NFPAs were the less detrimental *AIP*mut subtype.

*MEN1*mut prolactinomas had lower rate of pituitary apoplexy and showed trend for lower rates of macroadenoma, hypopituitarism at diagnosis and for requiring fewer surgeries than *AIP*mut prolactinomas. These findings suggest that *AIP*mut prolactinomas may be more aggressive than *MEN1*mut prolactinomas, contrasting with the findings of increased dopamine agonists associated to *MEN1* mutation status, but not with *AIP* mutations, recently shown in young patients with macroprolactinomas[734]. *MEN1*mut somatotrophinomas had less aggressive phenotype than *AIP*mut somatotrophinomas displaying lower rates of macroadenoma and extrasellar extension, required fewer surgeries, and a tendency for less hypopituitarism at diagnosis and less cavernous sinus invasion. M*EN1*mut and *AIP*mut NFPAs did not differ and both displayed an indolent behaviour and disease course, as previously shown for M*EN1*mut NFPAs[99,101], as well as for *AIP*mut NFPAs (Chapter 7). In fact, some of these small NFPAs may represent prospectively-diagnosed pituitary incidentalomas similar to those often observed in the general population[7,23].

Main highlights from this study

The comparative analysis *MEN1*mut vs *AIP*mut PAs highlights the following points: 1) different familial forms of PAs may be associated with different degrees of aggressiveness; 2) *AIP*mut PAs display, in general, a more aggressive phenotype and poorer clinical course than *MEN1*mut PAs; 3) *AIP*mut prolactinomas and somatotrophinomas were associated with increased aggressiveness and poorer outcomes than *MEN1*mut prolactinomas and somatotrophinomas respectively; 4) both *AIP*mut and *MEN1*mut NFPAs had a indolent course of disease; 5) not all familial forms of PAs are inexorably aggressive, with some cases being particularly indolent (e.g. *AIP*mut and *MEN1*mut NFPAs) and responsive to treatment (e.g. *MEN1*mut prolactinomas and *MEN1*mut somatotrophinomas); 6) the PA subtype may be more determinant for the clinical course than the specific *AIP* or *MEN1* gene mutation.

This study not only expands the knowledge and characterisation of these 2 rare familial forms of PAs, but provides, for the first time, a comparison between *MEN1*mut and *AIP*mut PAs, in general and by PA subtype, which may be useful for redefinition of genetic screening guidance in patients with PAs. Firstly, my study show that a significant proportion (71%) of MEN1 patients may present a PA as first manifestation, needing differentiation from *AIP*mut FIPA patients, which raises the question of what gene analyse first, however many centres are currently offering genetic testing panels which include all, or at least the most relevant PA-predisposing genes such as *AIP* and *MEN1*. In fact, suspicion for MEN1 should be raised in young patients presenting with isolated PAs, and thus *MEN1* genetic test should be offered even in the absence of syndromic manifestations. Secondly, the gender and clinical diagnosis differences among our young *MEN1*mut and *AIP*mut PA patients support that young females with isolated prolactinomas could be considered for *MEN1* genetic testing in the first place, while young males with gigantism/acromegaly should be first tested for *AIP* mutations. Thirdly, PAs with aggressive behaviour and/or poor responsiveness to therapy may raise suspicion for a familial form, particularly for *AIP*-related disease, taking into account other clinical elements (such as age of onset, family history, GH excess and tumour size[169]). Our data also support the current recommendations for managing familial PAs in a similar manner as non-*MEN1*mut and non-*AIP*mut PAs[23,170,171]. In fact, not all *MEN1*mut and *AIP*mut PAs are aggressive, with some being particularly responsive to treatment such as *MEN1*mut prolactinomas while others have indolent disease course such as *MEN1*mut and *AIP*mut NFPAs, thus requiring an approach as recommended for patients with sporadic non-familial PAs.

Limitations of this study

There are some limitations associated with my study. Firstly, the study population was recruited from different countries as part of The International FIPA Consortium study, and thus patients' characteristics and outcomes may be affected by their distinct genetic backgrounds and/or different local clinical practise. Secondly, the MEN1 cohort is most likely affected by a referral bias as clinicians more likely refer us MEN1 patients with PAs to our International multicentric pituitary study, as reflected by the relatively high PA and low PHPT proportions in my cohort. I indeed acknowledge that my MEN1 cohort may not represent the most typical setting of MEN1 patients, being more closely to a MEN1 setting from a dedicated pituitary centre; however, it does provide a unique population of MEN1 patients with predominant pituitary involvement ideal to specifically study PAs in MEN1. Thirdly, clinical and outcome data were not available for all the patients,

which, together with the relative small size of some subgroups, limited the statistical power of some of my comparative subanalysis.

Conclusions

*MEN1*mut and *AIP*mut PAs are different familial forms of PA with distinct genetic basis, clinical features, disease courses, outcomes and aggressiveness profile. *AIP*mut PAs are in general more aggressive than *MEN1*mut PAs, which are in turn probably not as aggressive as previously reported. Both *AIP*mut prolactinomas and *AIP*mut somatotrophinomas have more unfavourable course of disease and clinical outcomes than *MEN1*mut prolactinomas and *MEN1*mut somatotrophinomas. Not all *AIP*mut and *MEN1*mut PAs are inexorably aggressive and poorly responsive to therapy, particularly *AIP*mut and *MEN1*mut NFPAs which showed an indolent course of disease and often require no treatment, or *MEN1*mut prolactinomas and *MEN1*mut somatotrophinomas which may respond well to the conventional forms of treatment.

Chapter 9: General conclusions and future research directions

The studies presented in this thesis aimed to understand the role of the different TME elements, including the cytokine network (Chapter 3), infiltrating immune cells (Chapter 3) and tumour-associated fibroblasts (Chapter 4), in the clinical phenotype and aggressiveness of PAs, as well as in different TME-related tumourigenic mechanisms (Chapter 5). In general, the data from these studies support the concept that different cellular and non-cellular TME components may affect the biological behaviour, oncogenic mechanisms and aggressiveness of PAs; however, many questions remain still open and represent excellent avenues for future research.

On the topic of familial PAs, particularly those due to germline *AIP* mutations, I developed a project exploring the role of AIP deficiency in the cytokine secretome of pituitary tumour (and non-neoplastic) cells (Chapter 6), and a project studying the clinical phenotype and outcomes of patients with familial PAs. Specifically those due to mutations in the PA-predisposing genes *AIP* (Chapter 7) and *MEN1* (Chapter 8). In general, my data suggest that AIP deficiency may not be determinant to the cytokine secretome, and does not affect the inhibitory effect of pasireotide in terms of cytokine release. From the clinical study, it is clear that the phenotypes of *AIP*mut and *MEN1*mut PAs are variable and heterogeneous, including highly aggressive cases, but also cases with indolent behaviour such as prospectively-diagnosed *AIP*mut PAs or *MEN1*mut NFPAs; my data also highlight the benefits of genetic screening of family members at risk for inheriting a PA-predisposing gene mutation and the clinical assessment of mutation carriers.

In the following paragraphs, I will summarise the main results from my research projects presented in this thesis, emphasising the novel findings as well as pointing out different aspects and questions that could be addressed in future studies.

The role of the TME in the phenotype of PAs

Pituitary tumour cell-derived chemokines recruit immune cells into the TME

Using a 42-multiplex cytokine array, I comprehensively assessed the cytokine secretome from primary cultured pituitary tumour cells. My data suggest that pituitary tumour cells are an active source of chemokines, namely IL-8, CCL2, CCL3 and CCL4, which have not previously been described in PAs apart from IL-8[232-234]. PA-derived chemokines may facilitate the immune cell recruitment into the TME of PAs, as higher contents of PA-infiltrating macrophages, neutrophils

and CD8+ T cells correlated with higher chemokine levels. My *in vitro* functional data confirmed increased macrophage chemotaxis driven by pituitary tumour cell-derived factors.

Infiltrating immune cells in the TME affect the biology and aggressiveness of PAs

Immune cell infiltrates differ between PAs and NPs, with PAs displaying higher content of macrophages and CD4+ T cells and fewer neutrophils and CD8+ T cells. Moreover, the macrophage phenotype in PAs is primarily M2-like with a 3-fold increased M2:M1 macrophage ratio in PAs compared to NP. A higher content of the immunosuppressive FOXP3+ T cells *per se*, lower CD8:CD4 and CD8:FOXP3 ratios, and a deleterious immune cell phenotype (higher content of macrophages, T-helper lymphocytes, FOXP3+ T regulatory and B cells) were associated with increased tumour proliferation. My *in vitro* cell line data confirmed that macrophage secreted-factors influence pituitary tumour cells, being able to induce morphological changes, cytokine secretome changes and EMT, as well as an increased invasion/migration from tumour cells.

TAFs release cytokines which influence the phenotype and aggressiveness of PAs

My data support the concept that TAFs are a component of the TME of PAs and can be isolated *in vitro*. They represent an important source of cytokines, with IL-6 and CCL2 emerging as key mediators for cavernous sinus invasion, proliferation and neovascularisation. My *in vitro* data confirm that TAF-derived factors, but not normal skin fibroblast factors, influence pituitary tumour cells, inducing morphological changes, increasing invasion and migration and activating EMT.

Pasireotide inhibits the cytokine secretion from TAFs

My data support the inhibitory effect of pasireotide on cytokine release from TAFs, particularly IL-6 and CCL2, which may play a key role in its recognised anti-tumoural effects in patients with PAs. This pasireotide cytokine inhibitory effect is most likely mediated by SST1, the predominant SST in TAFs, in line with the findings reported in pancreatic cancer-associated fibroblasts[385,391].

Cytokine network and infiltrating immune cells in the TME modulate PA oncogenic mechanisms

PA-derived cytokines (namely FGF-2 and IL-8) as well as TAF-derived cytokines (namely CCL2) may influence angiogenesis in PAs, although the modulatory effect of infiltrating immune cells in PA angiogenesis seems more prominent, with M2-macrophages, CD4+ T and FOXP3+ T cells emerging

as the most relevant immune cell types influencing neovascularisation and vessel morphology in PAs. Certain PA- and TAF-derived cytokines (CCL2, CCL4, FGF-2, IL-6, CXCL1), but not infiltrating immune cells, influence the expression of MMPs and NCAM in PAs, more remarkably in somatotrophinomas. In terms of EMT, my human data showed no association between PA-infiltrating immune cells and E-cadherin or ZEB1 expression, as well as little influence from PA or TAF-derived factors in the expression of these EMT markers, supporting a lack or only a mild effect exerted by these cells in EMT modulation in PAs: the partial or incomplete EMT signature in PAs may explain, at least in part, some of these negative/unexpected findings. In contrast, *in vitro* macrophage-derived factors induced EMT in pituitary tumour cells.

Avenues for future research

The role of the main PA-derived chemokines CCL2 and IL-8 (as identified in my cytokine array study) could be further studied, particularly their effects in immune cell chemotaxis (macrophages and neutrophils essentially) and on tumour proliferation and invasion, as well as in other tumourigenic mechanisms such as in angiogenesis, EMT and ECM-remodelling, possibly using similar methods used in my research projects but in a larger cohort of cases.

Attempting to further characterise the cellular components of TME of PAs, the immune cell types could be performed by immunohistochemical analysis, possibly combined with other laboratory techniques such as FACS sorting, magnetic beads for immune cell separation, *in situ hybridization* with RNAscope or gene-signature methodologies such as xCell, in a much larger cohort of PAs; other immune cell types could also be assessed such as NK cells, Th17 cells, dendritic cells and mast cells, among others. The phenotype of PA-infiltrating macrophages (M2 or M1 macrophages) could be further assessed, and possibly using double immunohistochemistry for CD68 and CD163 or CD206 (marking M2-macrophages) and for CD68 and HLA-DR or iNOS (marking M1-macrophages). Stromal cells such as TAFs (using a combination of markers such as FAP, vimentin, α-SMA, CD90) or pericytes (CD31 and α-SMA) could be characterised in the same cohort of cases, quantified in the tissue sections and then correlated with the amounts of PA-infiltrating immune cells, with angiogenesis, EMT activation or for instance with tumour fibrosis, cell proliferation or apoptosis. Correlation with clinical features including resistance to medical therapy could be assessed for both immune cell and stromal cell infiltrates among the same large cohort of PAs.

The potential direct effects on pituitary tumour cells resulting from pasireotide's inhibitory effect on TAF cytokine secretome requires further research. Studies assessing proliferation, migration, invasion, EMT, apoptosis in pituitary tumour cells (GH3 cells and primary PA cells) after exposure

to pasireotide vs untreated TAFs (eventually using simultaneously antibodies neutralising IL-6 or blocking IL-6 receptor), using CM or co-cultures, may prove that the benefits of pasireotide on PA cells depend on the TAF secretome, observed in my studies. Perhaps it would be better to conduct studies in rodents implanting pituitary tumourlets under different conditions (untreated vs pasireotide treated vs pasireotide treated plus IL-6 neutralising antibodies), as reported in previous studies investigating the pasireotide effect in pancreas cancer fibroblasts[385,391].

Functional *in vitro* experiments are needed to investigate some of the modulatory effects from factors derived from pituitary tumour cells, immune cells and TAFs in different tumourigenic mechanisms such as angiogenesis, EMT and ECM remodelling. To investigate the interactions between pituitary tumour cells and immune/stromal cells, *in vitro* functional studies using 3D culturing techniques and/or co-culture, where tumour cells are able to form cohesive structures with ECM deposition (more similar to TME) and are in more physiological contact with surrounding cells, would be more appropriate than the 2D culture methods that I have used in my research projects. In fact, in the studies I conducted *in vitro* cells are grown in a 2D environment in non-physiological conditions (plastic growth surfaces, culture medium and lack of cell-cell contact in all directions) and do not entirely resemble the complex crosstalk between tumour cells and non-neoplastic cells within the TME (acknowledging that the *in vivo* TME is nearly impossible to replicate *in vitro*), despite the fact that 2D culture methods are still widely used.

A more physiological way to assess the crosstalk between pituitary tumour cells and surrounding TME non-neoplastic cells would be to innoculate into rodents tumourlets of pituitary tumour cells (primary PA cells and/or GH3 cells), either in isolation, combined with immune/stromal cells (e.g. macrophages or fibroblasts), or eventually after being co-cultured or treated with CM from some of these non-neoplastic cells. Tumourlets could be allowed to grow to verify the effects of immune/stromal cell-derived factors in terms of cell proliferation, with the animals eventually sacrificed to measure tumour size/weight, and to collect the tumourlet for further immunohistochemical studies assessing for instance Ki-67, EMT, MMPs expression, fibrosis, angiogenesis and apoptosis, among others.

The role of AIP deficiency in the pituitary tumour cytokine secretome

My cell line and primary cell culture cytokine data suggested overall a limited role for AIP in determining the cytokine secretome of pituitary tumour cells and fibroblasts. Indeed, my data suggest that AIP deficiency unlikely induce major stimulatory (or inhibitory) effects in the cytokine secretory function, at least under basal/unstimulated conditions. CX3CL1 first emerged from my

cytokine array and RT-qPCR data on GH3 cells as differentially secreted between GH3-*Aip*-KD vs GH3-NT cells, but other lines of evidence from my experiments and from available data from my laboratory does not support the suggestion that CX3CL1 expression and release is enhanced by AIP deficiency. CCL2 would be a possible chemokine differentially secreted between *AIP*mut and *AIP*neg, and the AIP-induced overexpression of FLI-1 could be the underlying mechanism by which CCL2 and also CCL5[513] expression would be increased in *AIP*mut pituitary tumour cells.

AIP deficiency seems to create no resistance to (and possibly enhances) the inhibitory effect of pasireotide in terms of cytokine release, at least in fibroblasts, in contrast to the well-known reduced effectiveness of pasireotide in inhibiting GH secretion in *AIP*mut somatotrophinomas.

Avenues for future research

From my data, CCL2 appears an interesting candidate to explain why *AIP*mut PAs have increased amount of macrophages than *AIP*neg PAs[513], as well as why *AIP*mut are in general more aggressive and refractory to treatment[19]. The role of AIP deficiency in the expression of CCL2 could be then further investigated using similar *in vitro* studies, as well as immunohistochemical studies (or RNAscope) in human *AIP*mut and *AIP*neg somatotrophinoma tissue sections, likewise the studies recently conducted from Dr. Barry to investigate CCL5 in *AIP*mut vs *AIP*neg PAs. Further cytokine arrays could be done in supernatants from other cell types (e.g. mouse-embryonic fibroblasts or HEK293 cells) after knocking down and/or overexpressing *AIP* and compare to the respective wild-type; cytokines differentially secreted could be further validated with RT-qPCR, Western blotting or by ELISA, and by immunohistochemistry or RNAscope in human PA samples. Cytokine arrays could also be done on supernatants after stimulation for instance with TNF-α, IFN-γ or IGF-1 to assess the role of AIP deficiency in the cytokine secretome under stimulatory circumstances.

Phenotype of *AIP*mut and *MEN1*mut familial PAs and the benefits of genetic/clinical screening

In this study, I analysed a large cohort of patients with familial and young-onset PAs, of whom 167 had germline *AIP* mutations and 70 had *MEN1* mutations, aiming to expand the current knowledge on characteristics and outcomes of familial forms of PAs, but at the same time greatly focusing on the prospectively-diagnosed *AIP*mut PAs as a characterisation of this particular group, crucial to assess the potential benefits of genetic screening for *AIP* mutations, is lacking.

My study allowed some interesting observations, some of them not previously reported in the literature: i) *AIP*mut PAs were in general more aggressive and refractory to conventional therapy,

requiring more complex and multimodal management approaches; however *AIP*-related pituitary disease can be controlled in a significant proportion of cases; ii) *AIP*mut somatotrophinomas present earlier, are more aggressive and require more often radiotherapy, with patients ending up taller than those with *AIP*neg somatotrophinomas; iii) *AIP*mut prolactinomas present more often with apoplexy, but are not necessarily more invasive or refractory to conventional therapy, in comparison with *AIP*neg prolactinomas; iv) *AIP*mut NFPAs may display an indolent course of disease and have similar features and clinical outcomes (or even more favourable) than *AIP*neg NFPAs, highlighting that the clinical phenotypic spectrum of *AIP*-related pituitary disease is wider than previously reported, including also indolent and non-aggressive PAs sometimes requiring no treatment at all; v) prospectively-diagnosed *AIP*mut PAs are less aggressive and have better outcomes than clinically-presenting PAs, highlighting the benefits of genetic analysis and clinical screening of *AIP*mut carriers; vi) PAs are common in MEN1 and are often the first MEN1-related manifestation; vii) *MEN1*mut PAs affect more frequently females and are often prolactinomas, contrasting with *AIP*mut PAs which occur more in males and are usually somatotrophinomas; viii) *MEN1*mut PAs are not particularly aggressive and can be controlled with conventional therapy, contrasting with the previous notion that *MEN1*mut PAs was more aggressive and refractory to therapy; ix) *MEN1*mut NFPAs display indolent behaviour and little invasiveness, as the *AIP*mut NFPAs; x) *AIP*mut PAs are in general more aggressive than MEN1mut PAs, but not all familial PA forms are inexorably aggressive, with some cases being indolent (*AIP*mut and *MEN1*mut NFPAs) and responding well to treatment (*MEN1*mut prolactinomas and *MEN1*mut somatotrophinomas).

Avenues for future research

Much data are now available regarding the characteristics of *AIP*mut and *MEN*1mut PAs, and this study expands the phenotypic spectrum of these 2 familial forms of PAs and illustrate the benefits of genetic and clinical screening in particular for *AIP*mut carriers. Probably future studies (clinical and experimental *in vitro* studies) should focus in the *AIP* (and *MEN1*) variants of uncertain significance in order to clarify their role in the pathogenesis of PAs. This is definitely an important direction of future research as it will allow clinicians to better advise their PA patients carrying a variant of uncertain significance as to whether that variant indeed caused the PA and whether family members need to be genetically tested and mutation carriers clinically assessed. Confirming the lack pathogenicity from some of these variants will spare the psychological distress and unnecessary assessment of patients' relatives, as well as will limit the economic burden associated with unneeded medical, clinical, genetic, biochemical and imaging assessments in this setting.

Reference list

1. Hong GK, Payne SC & Jane JA, Jr. Anatomy, Physiology, and Laboratory Evaluation of the Pituitary Gland. *Otolaryngol Clin North Am* 2016 **49** 21-32.
2. Swartz JD, Russell KB, Basile BA, O'Donnell PC & Popky GL. High-resolution computed tomographic appearance of the intrasellar contents in women of childbearing age. *Radiology* 1983 **147** 115-117.
3. Chanson P, Daujat F, Young J, Bellucci A, Kujas M, Doyon D & Schaison G. Normal pituitary hypertrophy as a frequent cause of pituitary incidentaloma: a follow-up study. *J Clin Endocrinol Metab* 2001 **86** 3009-3015.
4. Tekiner H, Acer N & Kelestimur F. Sella turcica: an anatomical, endocrinological, and historical perspective. *Pituitary* 2015 **18** 575-578.
5. Lechan RM. Neuroendocrinology of pituitary hormone regulation. *Endocrinol Metab Clin North Am* 1987 **16** 475-501.
6. Goncalves MB, de Oliveira JG, Williams HA, Alvarenga RM & Landeiro JA. Cavernous sinus medial wall: dural or fibrous layer? Systematic review of the literature. *Neurosurg Rev* 2012 **35** 147-153; discussion 153-144.
7. Molitch ME. Diagnosis and Treatment of Pituitary Adenomas: A Review. *JAMA* 2017 **317** 516-524.
8. Marques P, Mafra M, Calado C, Martins A, Monteiro J & Leite V. Aggressive pituitary lesion with a remarkably high Ki-67. *Arq Bras Endocrinol Metabol* 2014 **58** 656-660.
9. Yeung CM, Chan CB, Leung PS & Cheng CH. Cells of the anterior pituitary. *Int J Biochem Cell Biol* 2006 **38** 1441-1449.
10. Allaerts W & Vankelecom H. History and perspectives of pituitary folliculo-stellate cell research. *Eur J Endocrinol* 2005 **153** 1-12.
11. Devnath S & Inoue K. An insight to pituitary folliculo-stellate cells. *J Neuroendocrinol* 2008 **20** 687-691.
12. Ooi GT, Tawadros N & Escalona RM. Pituitary cell lines and their endocrine applications. *Mol Cell Endocrinol* 2004 **228** 1-21.
13. Harris GW. Neural control of the pituitary gland. *Physiol Rev* 1948 **28** 139-179.
14. Marques P, Skorupskaite K, Rozario KS, Anderson RA & George JT. Physiology of Gnrh and Gonadotropin Secretion. In *Endotext*. Eds LJ De Groot, G Chrousos, K Dungan, KR Feingold, A Grossman, JM Hershman, C Koch, M Korbonits, R McLachlan, M New, J Purnell, R Rebar, F Singer & A Vinik. South Dartmouth (MA), 2000.
15. Ben-Shlomo A & Melmed S. Hypothalamic regulation of anterior pituitary function. In *The Pituitary*, edn 3rd, pp 21-45. Ed M S. San Diego, CA, USA: Academic Press, 2011.
16. Borba VV, Zandman-Goddard G & Shoenfeld Y. Prolactin and Autoimmunity. *Front Immunol* 2018 **9** 73.
17. Brand JM, Frohn C, Cziupka K, Brockmann C, Kirchner H & Luhm J. Prolactin triggers pro-inflammatory immune responses in peripheral immune cells. *Eur Cytokine Netw* 2004 **15** 99-104.
18. Pereira Suarez AL, Lopez-Rincon G, Martinez Neri PA & Estrada-Chavez C. Prolactin in inflammatory response. *Adv Exp Med Biol* 2015 **846** 243-264.
19. Marques P & Korbonits M. Genetic Aspects of Pituitary Adenomas. *Endocrinol Metab Clin North Am* 2017 **46** 335-374.
20. Asa SL, Casar-Borota O, Chanson P, Delgrange E, Earls P, Ezzat S, Grossman A, Ikeda H, Inoshita N, Karavitaki N, Korbonits M, Laws ER, Jr., Lopes MB, Maartens N, McCutcheon IE, Mete O, Nishioka H, Raverot G, Roncaroli F, Saeger W, Syro LV, Vasiljevic A, Villa C, Wierinckx A, Trouillas J & attendees of 14th Meeting of the International Pituitary Pathology Club AFN. From pituitary adenoma to pituitary neuroendocrine tumor (PitNET): an International Pituitary Pathology Club proposal. *Endocr Relat Cancer* 2017 **24** C5-C8.

21. Ho KKY, Fleseriu M, Wass J, van der Lely A, Barkan A, Giustina A, Casanueva FF, Heaney AP, Biermasz N, Strasburger C & Melmed S. A tale of pituitary adenomas: to NET or not to NET : Pituitary Society position statement. *Pituitary* 2019.
22. Aflorei ED & Korbonits M. Epidemiology and etiopathogenesis of pituitary adenomas. *J Neurooncol* 2014 **117** 379-394.
23. Freda PU, Beckers AM, Katznelson L, Molitch ME, Montori VM, Post KD, Vance ML & Endocrine S. Pituitary incidentaloma: an endocrine society clinical practice guideline. *J Clin Endocrinol Metab* 2011 **96** 894-904.
24. Vasilev V, Rostomyan L, Daly AF, Potorac I, Zacharieva S, Bonneville JF & Beckers A. MANAGEMENT OF ENDOCRINE DISEASE: Pituitary "incidentaloma": Neuroradiological assessment and differential diagnosis. *Eur J Endocrinol* 2016.
25. Raverot G, Castinetti F, Jouanneau E, Morange I, Figarella-Branger D, Dufour H, Trouillas J & Brue T. Pituitary carcinomas and aggressive pituitary tumours: merits and pitfalls of temozolomide treatment. *Clin Endocrinol (Oxf)* 2012 **76** 769-775.
26. Melmed S. Pituitary tumors. *Endocrinol Metab Clin North Am* 2015 **44** 1-9.
27. Daly AF, Rixhon M, Adam C, Dempegioti A, Tichomirowa MA & Beckers A. High prevalence of pituitary adenomas: a cross-sectional study in the province of Liege, Belgium. *J Clin Endocrinol Metab* 2006 **91** 4769-4775.
28. Fernandez A, Karavitaki N & Wass JA. Prevalence of pituitary adenomas: a community-based, cross-sectional study in Banbury (Oxfordshire, UK). *Clin Endocrinol (Oxf)* 2010 **72** 377-382.
29. Gruppetta M, Mercieca C & Vassallo J. Prevalence and incidence of pituitary adenomas: a population based study in Malta. *Pituitary* 2013 **16** 545-553.
30. Raappana A, Koivukangas J, Ebeling T & Pirila T. Incidence of pituitary adenomas in Northern Finland in 1992-2007. *J Clin Endocrinol Metab* 2010 **95** 4268-4275.
31. Fontana E & Gaillard R. [Epidemiology of pituitary adenoma: results of the first Swiss study]. *Rev Med Suisse* 2009 **5** 2172-2174.
32. Lloyd RO, R.; Klöppel, G.; Rosai, J. WHO classification of tumours of endocrine organs, 4th edn. *Lyon, IARC, Press* 2017.
33. Drummond J, Roncaroli F, Grossman AB & Korbonits M. Clinical and Pathological Aspects of Silent Pituitary Adenomas. *J Clin Endocrinol Metab* 2019 **104** 2473-2489.
34. Lopes MBS. The 2017 World Health Organization classification of tumors of the pituitary gland: a summary. *Acta Neuropathol* 2017 **134** 521-535.
35. Mete O & Lopes MB. Overview of the 2017 WHO Classification of Pituitary Tumors. *Endocr Pathol* 2017 **28** 228-243.
36. Lloyd RY, W.; Farrel, W.; Asa, S.; Trouillas, J.; Kontogeorgos, G.; Sano, T.; Scheithaeur, B.; Horvath, E.; DeLellis, R.; Heitz, P. Pituitary tumors; in WHO Classification of Tumors of the Endocrine Organs: Pathology and Genetics of Endocrine Organs. *Lyon, IARC, Press* 2004.
37. Chatzellis E, Alexandraki KI, Androulakis, II & Kaltsas G. Aggressive pituitary tumors. *Neuroendocrinology* 2015 **101** 87-104.
38. Chiloiro S, Doglietto F, Trapasso B, Iacovazzo D, Giampietro A, Di Nardo F, de Waure C, Lauriola L, Mangiola A, Anile C, Maira G, De Marinis L & Bianchi A. Typical and atypical pituitary adenomas: a single-center analysis of outcome and prognosis. *Neuroendocrinology* 2015 **101** 143-150.
39. Zaidi HA, Cote DJ, Dunn IF & Laws ER, Jr. Predictors of aggressive clinical phenotype among immunohistochemically confirmed atypical adenomas. *J Clin Neurosci* 2016 **34** 246-251.
40. Knosp E, Steiner E, Kitz K & Matula C. Pituitary adenomas with invasion of the cavernous sinus space: a magnetic resonance imaging classification compared with surgical findings. *Neurosurgery* 1993 **33** 610-617; discussion 617-618.
41. Hardy J. Transphenoidal microsurgery of the normal and pathological pituitary. *Clin Neurosurg* 1969 **16** 185-217.

42. Raverot G, Dantony E, Beauvy J, Vasiljevic A, Mikolasek S, Borson-Chazot F, Jouanneau E, Roy P & Trouillas J. Risk of Recurrence in Pituitary Neuroendocrine Tumors: A Prospective Study Using a Five-Tiered Classification. *J Clin Endocrinol Metab* 2017 **102** 3368-3374.
43. Trouillas J, Roy P, Sturm N, Dantony E, Cortet-Rudelli C, Viennet G, Bonneville JF, Assaker R, Auger C, Brue T, Cornelius A, Dufour H, Jouanneau E, Francois P, Galland F, Mougel F, Chapuis F, Villeneuve L, Maurage CA, Figarella-Branger D, Raverot G, members of H, Barlier A, Bernier M, Bonnet F, Borson-Chazot F, Brassier G, Caulet-Maugendre S, Chabre O, Chanson P, Cottier JF, Delemer B, Delgrange E, Di Tommaso L, Eimer S, Gaillard S, Jan M, Girard JJ, Lapras V, Loiseau H, Passagia JG, Patey M, Penfornis A, Poirier JY, Perrin G & Tabarin A. A new prognostic clinicopathological classification of pituitary adenomas: a multicentric case-control study of 410 patients with 8 years post-operative follow-up. *Acta Neuropathol* 2013 **126** 123-135.
44. Herman V, Fagin J, Gonsky R, Kovacs K & Melmed S. Clonal origin of pituitary adenomas. *J Clin Endocrinol Metab* 1990 **71** 1427-1433.
45. Zhou Y, Zhang X & Klibanski A. Genetic and epigenetic mutations of tumor suppressive genes in sporadic pituitary adenoma. *Mol Cell Endocrinol* 2014 **386** 16-33.
46. Alexander JM, Biller BM, Bikkal H, Zervas NT, Arnold A & Klibanski A. Clinically nonfunctioning pituitary tumors are monoclonal in origin. *J Clin Invest* 1990 **86** 336-340.
47. Biller BM, Alexander JM, Zervas NT, Hedley-Whyte ET, Arnold A & Klibanski A. Clonal origins of adrenocorticotropin-secreting pituitary tissue in Cushing's disease. *J Clin Endocrinol Metab* 1992 **75** 1303-1309.
48. Gicquel C, Le Bouc Y, Luton JP, Girard F & Bertagna X. Monoclonality of corticotroph macroadenomas in Cushing's disease. *J Clin Endocrinol Metab* 1992 **75** 472-475.
49. Jacoby LB, Hedley-Whyte ET, Pulaski K, Seizinger BR & Martuza RL. Clonal origin of pituitary adenomas. *J Neurosurg* 1990 **73** 731-735.
50. Heaney AP. Clinical review: Pituitary carcinoma: difficult diagnosis and treatment. *J Clin Endocrinol Metab* 2011 **96** 3649-3660.
51. Gadelha MR, Trivellin G, Hernandez Ramirez LC & Korbonits M. Genetics of pituitary adenomas. *Front Horm Res* 2013 **41** 111-140.
52. Chesnokova V, Zonis S, Ben-Shlomo A, Wawrowsky K & Melmed S. Molecular mechanisms of pituitary adenoma senescence. *Front Horm Res* 2010 **38** 7-14.
53. Alexandraki KI, Khan MM, Chahal HS, Dalantaeva NS, Trivellin G, Berney DM, Caron P, Popovic V, Pfeifer M, Jordan S, Korbonits M & Grossman AB. Oncogene-induced senescence in pituitary adenomas and carcinomas. *Hormones (Athens)* 2012 **11** 297-307.
54. Asa SL & Ezzat S. The pathogenesis of pituitary tumors. *Annu Rev Pathol* 2009 **4** 97-126.
55. Yoshida S, Kato T & Kato Y. EMT Involved in Migration of Stem/Progenitor Cells for Pituitary Development and Regeneration. *J Clin Med* 2016 **5**.
56. Cannavo S, Ragonese M, Puglisi S, Romeo PD, Torre ML, Alibrandi A, Scaroni C, Occhi G, Ceccato F, Regazzo D, De Menis E, Sartorato P, Arnaldi G, Trementino L, Trimarchi F & Ferrau F. Acromegaly Is More Severe in Patients With AHR or AIP Gene Variants Living in Highly Polluted Areas. *J Clin Endocrinol Metab* 2016 **101** 1872-1879.
57. Cannavo S, Ferrau F, Ragonese M, Curto L, Torre ML, Magistri M, Marchese A, Alibrandi A & Trimarchi F. Increased prevalence of acromegaly in a highly polluted area. *Eur J Endocrinol* 2010 **163** 509-513.
58. Ueno M, Inano H, Onoda M, Murase H, Ikota N, Kagiya TV & Anzai K. Modification of mortality and tumorigenesis by tocopherol-mono-glucoside (TMG) administered after X irradiation in mice and rats. *Radiat Res* 2009 **172** 519-524.
59. Sapochnik M, Nieto LE, Fuertes M & Arzt E. Molecular Mechanisms Underlying Pituitary Pathogenesis. *Biochem Genet* 2016 **54** 107-119.
60. Jordan S, Lidhar K, Korbonits M, Lowe DG & Grossman AB. Cyclin D and cyclin E expression in normal and adenomatous pituitary. *Eur J Endocrinol* 2000 **143** R1-6.

61. Moreno CS, Evans CO, Zhan X, Okor M, Desiderio DM & Oyesiku NM. Novel molecular signaling and classification of human clinically nonfunctional pituitary adenomas identified by gene expression profiling and proteomic analyses. *Cancer Res* 2005 **65** 10214-10222.
62. Vandeva S, Jaffrain-Rea ML, Daly AF, Tichomirowa M, Zacharieva S & Beckers A. The genetics of pituitary adenomas. *Best Pract Res Clin Endocrinol Metab* 2010 **24** 461-476.
63. Bamberger CM, Fehn M, Bamberger AM, Ludecke DK, Beil FU, Saeger W & Schulte HM. Reduced expression levels of the cell-cycle inhibitor p27Kip1 in human pituitary adenomas. *Eur J Endocrinol* 1999 **140** 250-255.
64. Ogino A, Yoshino A, Katayama Y, Watanabe T, Ota T, Komine C, Yokoyama T & Fukushima T. The p15(INK4b)/p16(INK4a)/RB1 pathway is frequently deregulated in human pituitary adenomas. *J Neuropathol Exp Neurol* 2005 **64** 398-403.
65. Pease M, Ling C, Mack WJ, Wang K & Zada G. The role of epigenetic modification in tumorigenesis and progression of pituitary adenomas: a systematic review of the literature. *PLoS One* 2013 **8** e82619.
66. Simpson DJ, Hibberts NA, McNicol AM, Clayton RN & Farrell WE. Loss of pRb expression in pituitary adenomas is associated with methylation of the RB1 CpG island. *Cancer Res* 2000 **60** 1211-1216.
67. Simpson DJ, Frost SJ, Bicknell JE, Broome JC, McNicol AM, Clayton RN & Farrell WE. Aberrant expression of G(1)/S regulators is a frequent event in sporadic pituitary adenomas. *Carcinogenesis* 2001 **22** 1149-1154.
68. Hibberts NA, Simpson DJ, Bicknell JE, Broome JC, Hoban PR, Clayton RN & Farrell WE. Analysis of cyclin D1 (CCND1) allelic imbalance and overexpression in sporadic human pituitary tumors. *Clin Cancer Res* 1999 **5** 2133-2139.
69. Saeger W, Schreiber S & Ludecke DK. Cyclins D1 and D3 and topoisomerase II alpha in inactive pituitary adenomas. *Endocr Pathol* 2001 **12** 39-47.
70. Dworakowska D, Wlodek E, Leontiou CA, Igreja S, Cakir M, Teng M, Prodromou N, Goth MI, Grozinsky-Glasberg S, Gueorguiev M, Kola B, Korbonits M & Grossman AB. Activation of RAF/MEK/ERK and PI3K/AKT/mTOR pathways in pituitary adenomas and their effects on downstream effectors. *Endocr Relat Cancer* 2009 **16** 1329-1338.
71. Lin Y, Jiang X, Shen Y, Li M, Ma H, Xing M & Lu Y. Frequent mutations and amplifications of the PIK3CA gene in pituitary tumors. *Endocr Relat Cancer* 2009 **16** 301-310.
72. Schiemann U, Assert R, Moskopp D, Gellner R, Hengst K, Gullotta F, Domschke W & Pfeiffer A. Analysis of a protein kinase C-alpha mutation in human pituitary tumours. *J Endocrinol* 1997 **153** 131-137.
73. Palmieri D, Valentino T, De Martino I, Esposito F, Cappabianca P, Wierinckx A, Vitiello M, Lombardi G, Colao A, Trouillas J, Pierantoni GM, Fusco A & Fedele M. PIT1 upregulation by HMGA proteins has a role in pituitary tumorigenesis. *Endocr Relat Cancer* 2012 **19** 123-135.
74. Pellegrini I, Barlier A, Gunz G, Figarella-Branger D, Enjalbert A, Grisoli F & Jaquet P. Pit-1 gene expression in the human pituitary and pituitary adenomas. *J Clin Endocrinol Metab* 1994 **79** 189-196.
75. Fedele M, Visone R, De Martino I, Troncone G, Palmieri D, Battista S, Ciarmiello A, Pallante P, Arra C, Melillo RM, Helin K, Croce CM & Fusco A. HMGA2 induces pituitary tumorigenesis by enhancing E2F1 activity. *Cancer Cell* 2006 **9** 459-471.
76. Gadelha MR, Kasuki L, Denes J, Trivellin G & Korbonits M. MicroRNAs: Suggested role in pituitary adenoma pathogenesis. *J Endocrinol Invest* 2013 **36** 889-895.
77. Di Ieva A, Butz H, Niamah M, Rotondo F, De Rosa S, Sav A, Yousef GM, Kovacs K & Cusimano MD. MicroRNAs as biomarkers in pituitary tumors. *Neurosurgery* 2014 **75** 181-189; discussion 188-189.

78. Li XH, Wang EL, Zhou HM, Yoshimoto K & Qian ZR. MicroRNAs in Human Pituitary Adenomas. *Int J Endocrinol* 2014 **2014** 435171.
79. Melmed S. Pathogenesis of pituitary tumors. *Nat Rev Endocrinol* 2011 **7** 257-266.
80. Reincke M, Sbiera S, Hayakawa A, Theodoropoulou M, Osswald A, Beuschlein F, Meitinger T, Mizuno-Yamasaki E, Kawaguchi K, Saeki Y, Tanaka K, Wieland T, Graf E, Saeger W, Ronchi CL, Allolio B, Buchfelder M, Strom TM, Fassnacht M & Komada M. Mutations in the deubiquitinase gene USP8 cause Cushing's disease. *Nat Genet* 2015 **47** 31-38.
81. Ma ZY, Song ZJ, Chen JH, Wang YF, Li SQ, Zhou LF, Mao Y, Li YM, Hu RG, Zhang ZY, Ye HY, Shen M, Shou XF, Li ZQ, Peng H, Wang QZ, Zhou DZ, Qin XL, Ji J, Zheng J, Chen H, Wang Y, Geng DY, Tang WJ, Fu CW, Shi ZF, Zhang YC, Ye Z, He WQ, Zhang QL, Tang QS, Xie R, Shen JW, Wen ZJ, Zhou J, Wang T, Huang S, Qiu HJ, Qiao ND, Zhang Y, Pan L, Bao WM, Liu YC, Huang CX, Shi YY & Zhao Y. Recurrent gain-of-function USP8 mutations in Cushing's disease. *Cell Res* 2015 **25** 306-317.
82. Murat CB, Braga PB, Fortes MA, Bronstein MD, Correa-Giannella ML & Giorgi RR. Mutation and genomic amplification of the PIK3CA proto-oncogene in pituitary adenomas. *Braz J Med Biol Res* 2012 **45** 851-855.
83. Cai WY, Alexander JM, Hedley-Whyte ET, Scheithauer BW, Jameson JL, Zervas NT & Klibanski A. ras mutations in human prolactinomas and pituitary carcinomas. *J Clin Endocrinol Metab* 1994 **78** 89-93.
84. Karga HJ, Alexander JM, Hedley-Whyte ET, Klibanski A & Jameson JL. Ras mutations in human pituitary tumors. *J Clin Endocrinol Metab* 1992 **74** 914-919.
85. Christoforidis A, Maniadaki I & Stanhope R. McCune-Albright syndrome: growth hormone and prolactin hypersecretion. *J Pediatr Endocrinol Metab* 2006 **19 Suppl 2** 623-625.
86. Collins MT, Singer FR & Eugster E. McCune-Albright syndrome and the extraskeletal manifestations of fibrous dysplasia. *Orphanet J Rare Dis* 2012 **7 Suppl 1** S4.
87. Weinstein LS, Yu S, Warner DR & Liu J. Endocrine manifestations of stimulatory G protein alpha-subunit mutations and the role of genomic imprinting. *Endocr Rev* 2001 **22** 675-705.
88. Lumbroso S, Paris F, Sultan C & European Collaborative S. Activating Gsalpha mutations: analysis of 113 patients with signs of McCune-Albright syndrome--a European Collaborative Study. *J Clin Endocrinol Metab* 2004 **89** 2107-2113.
89. Daly AF, Castermans E, Oudijk L, Guitelman MA, Beckers P, Potorac I, Neggers S, Sacre N, van der Lely AJ, Bours V, de Herder WW & Beckers A. Pheochromocytomas and pituitary adenomas in three patients with MAX exon deletions. *Endocr Relat Cancer* 2018 **25** L37-L42.
90. Roszko KL, Blouch E, Blake M, Powers JF, Tischler AS, Hodin R, Sadow P & Lawson EA. Case Report of a Prolactinoma in a Patient With a Novel MAX Mutation and Bilateral Pheochromocytomas. *J Endocr Soc* 2017 **1** 1401-1407.
91. Hernandez-Ramirez LC, Gabrovska P, Denes J, Stals K, Trivellin G, Tilley D, Ferrau F, Evanson J, Ellard S, Grossman AB, Roncaroli F, Gadelha MR, Korbonits M & International FC. Landscape of Familial Isolated and Young-Onset Pituitary Adenomas: Prospective Diagnosis in AIP Mutation Carriers. *J Clin Endocrinol Metab* 2015 **100** E1242-1254.
92. Iacovazzo D, Caswell R, Bunce B, Jose S, Yuan B, Hernandez-Ramirez LC, Kapur S, Caimari F, Evanson J, Ferrau F, Dang MN, Gabrovska P, Larkin SJ, Ansorge O, Rodd C, Vance ML, Ramirez-Renteria C, Mercado M, Goldstone AP, Buchfelder M, Burren CP, Gurlek A, Dutta P, Choong CS, Cheetham T, Trivellin G, Stratakis CA, Lopes MB, Grossman AB, Trouillas J, Lupski JR, Ellard S, Sampson JR, Roncaroli F & Korbonits M. Germline or somatic GPR101 duplication leads to X-linked acrogigantism: a clinico-pathological and genetic study. *Acta Neuropathol Commun* 2016 **4** 56.
93. Trivellin G, Daly AF, Faucz FR, Yuan B, Rostomyan L, Larco DO, Schernthaner-Reiter MH, Szarek E, Leal LF, Caberg JH, Castermans E, Villa C, Dimopoulos A, Chittiboina P, Xekouki P, Shah N, Metzger D, Lysy PA, Ferrante E, Strebkova N, Mazerkina N, Zatelli MC, Lodish

M, Horvath A, de Alexandre RB, Manning AD, Levy I, Keil MF, Sierra Mde L, Palmeira L, Coppieters W, Georges M, Naves LA, Jamar M, Bours V, Wu TJ, Choong CS, Bertherat J, Chanson P, Kamenicky P, Farrell WE, Barlier A, Quezado M, Bjelobaba I, Stojilkovic SS, Wess J, Costanzi S, Liu P, Lupski JR, Beckers A & Stratakis CA. Gigantism and acromegaly due to Xq26 microduplications and GPR101 mutation. *N Engl J Med* 2014 **371** 2363-2374.

94. Hernandez-Ramirez LC, Gam R, Valdes N, Lodish MB, Pankratz N, Balsalobre A, Gauthier Y, Faucz FR, Trivellin G, Chittiboina P, Lane J, Kay DM, Dimopoulos A, Gaillard S, Neou M, Bertherat J, Assie G, Villa C, Mills JL, Drouin J & Stratakis CA. Loss-of-function mutations in the CABLES1 gene are a novel cause of Cushing's disease. *Endocr Relat Cancer* 2017 **24** 379-392.
95. Zhang Q, Peng C, Song J, Zhang Y, Chen J, Song Z, Shou X, Ma Z, Peng H, Jian X, He W, Ye Z, Li Z, Wang Y, Ye H, Zhang Z, Shen M, Tang F, Chen H, Shi Z, Chen C, Chen Z, Shen Y, Wang Y, Lu S, Zhang J, Li Y, Li S, Mao Y, Zhou L, Yan H, Shi Y, Huang C & Zhao Y. Germline Mutations in CDH23, Encoding Cadherin-Related 23, Are Associated with Both Familial and Sporadic Pituitary Adenomas. *Am J Hum Genet* 2017 **100** 817-823.
96. Cohen M, Persky R, Stegemann R, Hernandez-Ramirez LC, Zeltser D, Lodish MB, Chen A, Keil MF, Tatsi C, Faucz FR, Buchner DA, Stratakis CA & Tiosano D. Germline USP8 Mutation Associated With Pediatric Cushing Disease and Other Clinical Features: A New Syndrome. *J Clin Endocrinol Metab* 2019 **104** 4676-4682.
97. Thakker RV. Multiple endocrine neoplasia type 1 (MEN1) and type 4 (MEN4). *Mol Cell Endocrinol* 2014 **386** 2-15.
98. Thakker RV, Newey PJ, Walls GV, Bilezikian J, Dralle H, Ebeling PR, Melmed S, Sakurai A, Tonelli F, Brandi ML & Endocrine S. Clinical practice guidelines for multiple endocrine neoplasia type 1 (MEN1). *J Clin Endocrinol Metab* 2012 **97** 2990-3011.
99. de Laat JM, Dekkers OM, Pieterman CR, Kluijfhout WP, Hermus AR, Pereira AM, van der Horst-Schrivers AN, Drent ML, Bisschop PH, Havekes B, de Herder WW & Valk GD. Long-Term Natural Course of Pituitary Tumors in Patients With MEN1: Results From the DutchMEN1 Study Group (DMSG). *J Clin Endocrinol Metab* 2015 **100** 3288-3296.
100. Syro LV, Scheithauer BW, Kovacs K, Toledo RA, Londono FJ, Ortiz LD, Rotondo F, Horvath E & Uribe H. Pituitary tumors in patients with MEN1 syndrome. *Clinics (Sao Paulo)* 2012 **67 Suppl 1** 43-48.
101. Wu Y, Gao L, Guo X, Wang Z, Lian W, Deng K, Lu L, Xing B & Zhu H. Pituitary adenomas in patients with multiple endocrine neoplasia type 1: a single-center experience in China. *Pituitary* 2019 **22** 113-123.
102. Marini F, Giusti F & Brandi ML. Multiple endocrine neoplasia type 1: extensive analysis of a large database of Florentine patients. *Orphanet J Rare Dis* 2018 **13** 205.
103. Verges B, Boureille F, Goudet P, Murat A, Beckers A, Sassolas G, Cougard P, Chambe B, Montvernay C & Calender A. Pituitary disease in MEN type 1 (MEN1): data from the France-Belgium MEN1 multicenter study. *J Clin Endocrinol Metab* 2002 **87** 457-465.
104. Stratakis CA, Schussheim DH, Freedman SM, Keil MF, Pack SD, Agarwal SK, Skarulis MC, Weil RJ, Lubensky IA, Zhuang Z, Oldfield EH & Marx SJ. Pituitary macroadenoma in a 5-year-old: an early expression of multiple endocrine neoplasia type 1. *J Clin Endocrinol Metab* 2000 **85** 4776-4780.
105. Shull JD, Birt DF, McComb RD, Spady TJ, Pennington KL & Shaw-Bruha CM. Estrogen induction of prolactin-producing pituitary tumors in the Fischer 344 rat: modulation by dietary-energy but not protein consumption. *Mol Carcinog* 1998 **23** 96-105.
106. Ishida M, Takahashi W, Itoh S, Shimodaira S, Maeda S & Arita J. Estrogen actions on lactotroph proliferation are independent of a paracrine interaction with other pituitary cell types: a study using lactotroph-enriched cells. *Endocrinology* 2007 **148** 3131-3139.
107. Zarate S & Seilicovich A. Estrogen receptors and signaling pathways in lactotropes and somatotropes. *Neuroendocrinology* 2010 **92** 215-223.

108. Schernthaner-Reiter MH, Trivellin G & Stratakis CA. MEN1, MEN4, and Carney Complex: Pathology and Molecular Genetics. *Neuroendocrinology* 2016 **103** 18-31.
109. Trouillas J, Labat-Moleur F, Sturm N, Kujas M, Heymann MF, Figarella-Branger D, Patey M, Mazucca M, Decullier E, Verges B, Chabre O, Calender A & Groupe d'etudes des Tumeurs E. Pituitary tumors and hyperplasia in multiple endocrine neoplasia type 1 syndrome (MEN1): a case-control study in a series of 77 patients versus 2509 non-MEN1 patients. *Am J Surg Pathol* 2008 **32** 534-543.
110. Cuny T, Pertuit M, Sahnoun-Fathallah M, Daly A, Occhi G, Odou MF, Tabarin A, Nunes ML, Delemer B, Rohmer V, Desailloud R, Kerlan V, Chabre O, Sadoul JL, Cogne M, Caron P, Cortet-Rudelli C, Lienhardt A, Raingeard I, Guedj AM, Brue T, Beckers A, Weryha G, Enjalbert A & Barlier A. Genetic analysis in young patients with sporadic pituitary macroadenomas: besides AIP don't forget MEN1 genetic analysis. *Eur J Endocrinol* 2013 **168** 533-541.
111. Newey PJ & Thakker RV. Role of multiple endocrine neoplasia type 1 mutational analysis in clinical practice. *Endocr Pract* 2011 **17 Suppl 3** 8-17.
112. Gan HW, Bulwer C, Jeelani O, Levine MA, Korbonits M & Spoudeas HA. Treatment-resistant pediatric giant prolactinoma and multiple endocrine neoplasia type 1. *Int. J. Pediatr. Endocrinol* 2015 **2015** 15.
113. Chandrasekharappa SC, Guru SC, Manickam P, Olufemi SE, Collins FS, Emmert-Buck MR, Debelenko LV, Zhuang Z, Lubensky IA, Liotta LA, Crabtree JS, Wang Y, Roe BA, Weisemann J, Boguski MS, Agarwal SK, Kester MB, Kim YS, Heppner C, Dong Q, Spiegel AM, Burns AL & Marx SJ. Positional cloning of the gene for multiple endocrine neoplasia-type 1. *Science* 1997 **276** 404-407.
114. Lemmens I, Van de Ven WJ, Kas K, Zhang CX, Giraud S, Wautot V, Buisson N, De Witte K, Salandre J, Lenoir G, Pugeat M, Calender A, Parente F, Quincey D, Gaudray P, De Wit MJ, Lips CJ, Hoppener JW, Khodaei S, Grant AL, Weber G, Kytola S, Teh BT, Farnebo F, Thakker RV & et al. Identification of the multiple endocrine neoplasia type 1 (MEN1) gene. The European Consortium on MEN1. *Hum Mol Genet* 1997 **6** 1177-1183.
115. Lemos MC & Thakker RV. Multiple endocrine neoplasia type 1 (MEN1): analysis of 1336 mutations reported in the first decade following identification of the gene. *Hum Mutat* 2008 **29** 22-32.
116. Thakker RV. Genetics of parathyroid tumours. *J Intern Med* 2016.
117. Yuan Z, Sanchez Claros C, Suzuki M, Maggi EC, Kaner JD, Kinstlinger N, Gorecka J, Quinn TJ, Geha R, Corn A, Pastoriza J, Jing Q, Adem A, Wu H, Alemu G, Du YC, Zheng D, Greally JM & Libutti SK. Loss of MEN1 activates DNMT1 implicating DNA hypermethylation as a driver of MEN1 tumorigenesis. *Oncotarget* 2016 **7** 12633-12650.
118. Fontaniere S, Tost J, Wierinckx A, Lachuer J, Lu J, Hussein N, Busato F, Gut I, Wang ZQ & Zhang CX. Gene expression profiling in insulinomas of Men1 beta-cell mutant mice reveals early genetic and epigenetic events involved in pancreatic beta-cell tumorigenesis. *Endocr Relat Cancer* 2006 **13** 1223-1236.
119. La P, Schnepp RW, C DP, A CS & Hua X. Tumor suppressor menin regulates expression of insulin-like growth factor binding protein 2. *Endocrinology* 2004 **145** 3443-3450.
120. Hughes CM, Rozenblatt-Rosen O, Milne TA, Copeland TD, Levine SS, Lee JC, Hayes DN, Shanmugam KS, Bhattacharjee A, Biondi CA, Kay GF, Hayward NK, Hess JL & Meyerson M. Menin associates with a trithorax family histone methyltransferase complex and with the hoxc8 locus. *Mol Cell* 2004 **13** 587-597.
121. Wu T & Hua X. Menin represses tumorigenesis via repressing cell proliferation. *Am J Cancer Res* 2011 **1** 726-739.
122. Concolino P, Costella A & Capoluongo E. Multiple endocrine neoplasia type 1 (MEN1): An update of 208 new germline variants reported in the last nine years. *Cancer Genet* 2016 **209** 36-41.

123. Machens A, Schaaf L, Karges W, Frank-Raue K, Bartsch DK, Rothmund M, Schneyer U, Goretzki P, Raue F & Dralle H. Age-related penetrance of endocrine tumours in multiple endocrine neoplasia type 1 (MEN1): a multicentre study of 258 gene carriers. *Clin Endocrinol (Oxf)* 2007 **67** 613-622.
124. Cavaco BM, Domingues R, Bacelar MC, Cardoso H, Barros L, Gomes L, Ruas MM, Agapito A, Garrao A, Pannett AA, Silva JL, Sobrinho LG, Thakker RV & Leite V. Mutational analysis of Portuguese families with multiple endocrine neoplasia type 1 reveals large germline deletions. *Clin Endocrinol (Oxf)* 2002 **56** 465-473.
125. Bassett JH, Forbes SA, Pannett AA, Lloyd SE, Christie PT, Wooding C, Harding B, Besser GM, Edwards CR, Monson JP, Sampson J, Wass JA, Wheeler MH & Thakker RV. Characterization of mutations in patients with multiple endocrine neoplasia type 1. *Am J Hum Genet* 1998 **62** 232-244.
126. Thevenon J, Bourredjem A, Faivre L, Cardot-Bauters C, Calender A, Le Bras M, Giraud S, Niccoli P, Odou MF, Borson-Chazot F, Barlier A, Lombard-Bohas C, Clauser E, Tabarin A, Pasmant E, Chabre O, Castermans E, Ruszniewski P, Bertherat J, Delemer B, Christin-Maitre S, Beckers A, Guilhem I, Rohmer V, Goichot B, Caron P, Baudin E, Chanson P, Groussin L, Du Boullay H, Weryha G, Lecomte P, Schillo F, Bihan H, Archambeaud F, Kerlan V, Bourcigaux N, Kuhn JM, Verges B, Rodier M, Renard M, Sadoul JL, Binquet C & Goudet P. Unraveling the intrafamilial correlations and heritability of tumor types in MEN1: a Groupe d'etude des Tumeurs Endocrines study. *Eur J Endocrinol* 2015 **173** 819-826.
127. Agarwal SK, Mateo CM & Marx SJ. Rare germline mutations in cyclin-dependent kinase inhibitor genes in multiple endocrine neoplasia type 1 and related states. *J Clin Endocrinol Metab* 2009 **94** 1826-1834.
128. Bertherat J, Horvath A, Groussin L, Grabar S, Boikos S, Cazabat L, Libe R, Rene-Corail F, Stergiopoulos S, Bourdeau I, Bei T, Clauser E, Calender A, Kirschner LS, Bertagna X, Carney JA & Stratakis CA. Mutations in regulatory subunit type 1A of cyclic adenosine 5'-monophosphate-dependent protein kinase (PRKAR1A): phenotype analysis in 353 patients and 80 different genotypes. *J Clin Endocrinol Metab* 2009 **94** 2085-2091.
129. Matyakhina L, Pack S, Kirschner LS, Pak E, Mannan P, Jaikumar J, Taymans SE, Sandrini F, Carney JA & Stratakis CA. Chromosome 2 (2p16) abnormalities in Carney complex tumours. *J Med Genet* 2003 **40** 268-277.
130. Forlino A, Vetro A, Garavelli L, Ciccone R, London E, Stratakis CA & Zuffardi O. PRKACB and Carney complex. *N Engl J Med* 2014 **370** 1065-1067.
131. Correa R, Salpea P & Stratakis CA. Carney complex: an update. *Eur J Endocrinol* 2015 **173** M85-97.
132. Boikos SA & Stratakis CA. Pituitary pathology in patients with Carney Complex: growth-hormone producing hyperplasia or tumors and their association with other abnormalities. *Pituitary* 2006 **9** 203-209.
133. Courcoutsakis NA, Tatsi C, Patronas NJ, Lee CC, Prassopoulos PK & Stratakis CA. The complex of myxomas, spotty skin pigmentation and endocrine overactivity (Carney complex): imaging findings with clinical and pathological correlation. *Insights Imaging* 2013 **4** 119-133.
134. Pack SD, Kirschner LS, Pak E, Zhuang Z, Carney JA & Stratakis CA. Genetic and histologic studies of somatomammotropic pituitary tumors in patients with the "complex of spotty skin pigmentation, myxomas, endocrine overactivity and schwannomas" (Carney complex). *J Clin Endocrinol Metab* 2000 **85** 3860-3865.
135. Stratakis CA, Matyakhina L, Courkoutsakis N, Patronas N, Voutetakis A, Stergiopoulos S, Bossis I & Carney JA. Pathology and molecular genetics of the pituitary gland in patients with the 'complex of spotty skin pigmentation, myxomas, endocrine overactivity and schwannomas' (Carney complex). *Front Horm Res* 2004 **32** 253-264.

136. Hernandez-Ramirez LC, Tatsi C, Lodish MB, Faucz FR, Pankratz N, Chittiboina P, Lane J, Kay DM, Valdes N, Dimopoulos A, Mills JL & Stratakis CA. Corticotropinoma as a Component of Carney Complex. *J Endocr Soc* 2017 **1** 918-925.
137. Kiefer FW, Winhofer Y, Iacovazzo D, Korbonits M, Wolfsberger S, Knosp E, Trautinger F, Hoftberger R, Krebs M, Luger A & Gessl A. PRKAR1A mutation causing pituitary-dependent Cushing disease in a patient with Carney complex. *Eur J Endocrinol* 2017 **177** K7-K12.
138. Benn DE, Gimenez-Roqueplo AP, Reilly JR, Bertherat J, Burgess J, Byth K, Croxson M, Dahia PL, Elston M, Gimm O, Henley D, Herman P, Murday V, Niccoli-Sire P, Pasieka JL, Rohmer V, Tucker K, Jeunemaitre X, Marsh DJ, Plouin PF & Robinson BG. Clinical presentation and penetrance of pheochromocytoma/paraganglioma syndromes. *J Clin Endocrinol Metab* 2006 **91** 827-836.
139. Lopez-Jimenez E, de Campos JM, Kusak EM, Landa I, Leskela S, Montero-Conde C, Leandro-Garcia LJ, Vallejo LA, Madrigal B, Rodriguez-Antona C, Robledo M & Cascon A. SDHC mutation in an elderly patient without familial antecedents. *Clin Endocrinol (Oxf)* 2008 **69** 906-910.
140. Denes J, Swords F, Rattenberry E, Stals K, Owens M, Cranston T, Xekouki P, Moran L, Kumar A, Wassif C, Fersht N, Baldeweg SE, Morris D, Lightman S, Agha A, Rees A, Grieve J, Powell M, Boguszewski CL, Dutta P, Thakker RV, Srirangalingam U, Thompson CJ, Druce M, Higham C, Davis J, Eeles R, Stevenson M, O'Sullivan B, Taniere P, Skordilis K, Gabrovska P, Barlier A, Webb SM, Aulinas A, Drake WM, Bevan JS, Preda C, Dalantaeva N, Ribeiro-Oliveira A, Jr., Garcia IT, Yordanova G, Iotova V, Evanson J, Grossman AB, Trouillas J, Ellard S, Stratakis CA, Maher ER, Roncaroli F & Korbonits M. Heterogeneous genetic background of the association of pheochromocytoma/paraganglioma and pituitary adenoma: results from a large patient cohort. *J Clin Endocrinol Metab* 2015 **100** E531-541.
141. Papathomas TG, Gaal J, Corssmit EP, Oudijk L, Korpershoek E, Heimdal K, Bayley JP, Morreau H, van Dooren M, Papaspyrou K, Schreiner T, Hansen T, Andresen PA, Restuccia DF, van Kessel I, van Leenders GJ, Kros JM, Looijenga LH, Hofland LJ, Mann W, van Nederveen FH, Mete O, Asa SL, de Krijger RR & Dinjens WN. Non-pheochromocytoma (PCC)/paraganglioma (PGL) tumors in patients with succinate dehydrogenase-related PCC-PGL syndromes: a clinicopathological and molecular analysis. *Eur J Endocrinol* 2014 **170** 1-12.
142. Xekouki P, Pacak K, Almeida M, Wassif CA, Rustin P, Nesterova M, de la Luz Sierra M, Matro J, Ball E, Azevedo M, Horvath A, Lyssikatos C, Quezado M, Patronas N, Ferrando B, Pasini B, Lytras A, Tolis G & Stratakis CA. Succinate dehydrogenase (SDH) D subunit (SDHD) inactivation in a growth-hormone-producing pituitary tumor: a new association for SDH? *J Clin Endocrinol Metab* 2012 **97** E357-366.
143. Xekouki P, Szarek E, Bullova P, Giubellino A, Quezado M, Mastroyannis SA, Mastorakos P, Wassif CA, Raygada M, Rentia N, Dye L, Cougnoux A, Koziol D, Sierra Mde L, Lyssikatos C, Belyavskaya E, Malchoff C, Moline J, Eng C, Maher LJ, 3rd, Pacak K, Lodish M & Stratakis CA. Pituitary adenoma with paraganglioma/pheochromocytoma (3PAs) and succinate dehydrogenase defects in humans and mice. *J Clin Endocrinol Metab* 2015 **100** E710-719.
144. O'Toole SM, Denes J, Robledo M, Stratakis CA & Korbonits M. 15 YEARS OF PARAGANGLIOMA: The association of pituitary adenomas and phaeochromocytomas or paragangliomas. *Endocr Relat Cancer* 2015 **22** T105-122.
145. Comino-Mendez I, Gracia-Aznarez FJ, Schiavi F, Landa I, Leandro-Garcia LJ, Leton R, Honrado E, Ramos-Medina R, Caronia D, Pita G, Gomez-Grana A, de Cubas AA, Inglada-Perez L, Maliszewska A, Taschin E, Bobisse S, Pica G, Loli P, Hernandez-Lavado R, Diaz JA, Gomez-Morales M, Gonzalez-Neira A, Roncador G, Rodriguez-Antona C, Benitez J, Mannelli M, Opocher G, Robledo M & Cascon A. Exome sequencing identifies MAX mutations as a cause of hereditary pheochromocytoma. *Nat Genet* 2011 **43** 663-667.

146. de Kock L, Sabbaghian N, Plourde F, Srivastava A, Weber E, Bouron-Dal Soglio D, Hamel N, Choi JH, Park SH, Deal CL, Kelsey MM, Dishop MK, Esbenshade A, Kuttesch JF, Jacques TS, Perry A, Leichter H, Maeder P, Brundler MA, Warner J, Neal J, Zacharin M, Korbonits M, Cole T, Traunecker H, McLean TW, Rotondo F, Lepage P, Albrecht S, Horvath E, Kovacs K, Priest JR & Foulkes WD. Pituitary blastoma: a pathognomonic feature of germ-line DICER1 mutations. *Acta Neuropathol* 2014 **128** 111-122.
147. Sahakitrungruang T, Srichomthong C, Pornkunwilai S, Amornfa J, Shuangshoti S, Kulawonganunchai S, Suphapeetiporn K & Shotelersuk V. Germline and somatic DICER1 mutations in a pituitary blastoma causing infantile-onset Cushing's disease. *J Clin Endocrinol Metab* 2014 **99** E1487-1492.
148. Bahubeshi A, Bal N, Rio Frio T, Hamel N, Pouchet C, Yilmaz A, Bouron-Dal Soglio D, Williams GM, Tischkowitz M, Priest JR & Foulkes WD. Germline DICER1 mutations and familial cystic nephroma. *J Med Genet* 2010 **47** 863-866.
149. Foulkes WD, Bahubeshi A, Hamel N, Pasini B, Asioli S, Baynam G, Choong CS, Charles A, Frieder RP, Dishop MK, Graf N, Ekim M, Bouron-Dal Soglio D, Arseneau J, Young RH, Sabbaghian N, Srivastava A, Tischkowitz MD & Priest JR. Extending the phenotypes associated with DICER1 mutations. *Hum Mutat* 2011 **32** 1381-1384.
150. Hill DA, Ivanovich J, Priest JR, Gurnett CA, Dehner LP, Desruisseau D, Jarzembowski JA, Wikenheiser-Brokamp KA, Suarez BK, Whelan AJ, Williams G, Bracamontes D, Messinger Y & Goodfellow PJ. DICER1 mutations in familial pleuropulmonary blastoma. *Science* 2009 **325** 965.
151. Scheithauer BW, Kovacs K, Horvath E, Kim DS, Osamura RY, Ketterling RP, Lloyd RV & Kim OL. Pituitary blastoma. *Acta Neuropathol* 2008 **116** 657-666.
152. Beckers A, Aaltonen LA, Daly AF & Karhu A. Familial isolated pituitary adenomas (FIPA) and the pituitary adenoma predisposition due to mutations in the aryl hydrocarbon receptor interacting protein (AIP) gene. *Endocr Rev* 2013 **34** 239-277.
153. Vierimaa O, Georgitsi M, Lehtonen R, Vahteristo P, Kokko A, Raitila A, Tuppurainen K, Ebeling TM, Salmela PI, Paschke R, Gundogdu S, De Menis E, Makinen MJ, Launonen V, Karhu A & Aaltonen LA. Pituitary adenoma predisposition caused by germline mutations in the AIP gene. *Science* 2006 **312** 1228-1230.
154. Daly AF & Beckers A. Familial isolated pituitary adenomas (FIPA) and mutations in the aryl hydrocarbon receptor interacting protein (AIP) gene. *Endocrinol Metab Clin North Am* 2015 **44** 19-25.
155. Tichomirowa MA, Barlier A, Daly AF, Jaffrain-Rea ML, Ronchi C, Yaneva M, Urban JD, Petrossians P, Elenkova A, Tabarin A, Desailloud R, Maiter D, Schurmeyer T, Cozzi R, Theodoropoulou M, Sievers C, Bernabeu I, Naves LA, Chabre O, Montanana CF, Hana V, Halaby G, Delemer B, Aizpun JI, Sonnet E, Longas AF, Hagelstein MT, Caron P, Stalla GK, Bours V, Zacharieva S, Spada A, Brue T & Beckers A. High prevalence of AIP gene mutations following focused screening in young patients with sporadic pituitary macroadenomas. *Eur J Endocrinol* 2011 **165** 509-515.
156. Leontiou CA, Gueorguiev M, van der Spuy J, Quinton R, Lolli F, Hassan S, Chahal HS, Igreja SC, Jordan S, Rowe J, Stolbrink M, Christian HC, Wray J, Bishop-Bailey D, Berney DM, Wass JA, Popovic V, Ribeiro-Oliveira A, Jr., Gadelha MR, Monson JP, Akker SA, Davis JR, Clayton RN, Yoshimoto K, Iwata T, Matsuno A, Eguchi K, Musat M, Flanagan D, Peters G, Bolger GB, Chapple JP, Frohman LA, Grossman AB & Korbonits M. The role of the aryl hydrocarbon receptor-interacting protein gene in familial and sporadic pituitary adenomas. *J Clin Endocrinol Metab* 2008 **93** 2390-2401.
157. Villa C, Lagonigro MS, Magri F, Koziak M, Jaffrain-Rea ML, Brauner R, Bouligand J, Junier MP, Di Rocco F, Sainte-Rose C, Beckers A, Roux FX, Daly AF & Chiovato L. Hyperplasia-adenoma sequence in pituitary tumorigenesis related to aryl hydrocarbon receptor interacting protein gene mutation. *Endocr Relat Cancer* 2011 **18** 347-356.

158. Xekouki P, Mastroyiannis SA, Avgeropoulos D, de la Luz Sierra M, Trivellin G, Gourgari EA, Lyssikatos C, Quezado M, Patronas N, Kanaka-Gantenbein C, Chrousos GP & Stratakis CA. Familial pituitary apoplexy as the only presentation of a novel AIP mutation. *Endocr Relat Cancer* 2013 **20** L11-14.
159. Kasuki Jomori de Pinho L, Vieira Neto L, Armondi Wildemberg LE, Gasparetto EL, Marcondes J, de Almeida Nunes B, Takiya CM & Gadelha MR. Low aryl hydrocarbon receptor-interacting protein expression is a better marker of invasiveness in somatotropinomas than Ki-67 and p53. *Neuroendocrinology* 2011 **94** 39-48.
160. Kasuki L, Vieira Neto L, Wildemberg LE, Colli LM, de Castro M, Takiya CM & Gadelha MR. AIP expression in sporadic somatotropinomas is a predictor of the response to octreotide LAR therapy independent of SSTR2 expression. *Endocr Relat Cancer* 2012 **19** L25-29.
161. Daly AF, Tichomirowa MA, Petrossians P, Heliovaara E, Jaffrain-Rea ML, Barlier A, Naves LA, Ebeling T, Karhu A, Raappana A, Cazabat L, De Menis E, Montanana CF, Raverot G, Weil RJ, Sane T, Maiter D, Neggers S, Yaneva M, Tabarin A, Verrua E, Eloranta E, Murat A, Vierimaa O, Salmela PI, Emy P, Toledo RA, Sabate MI, Villa C, Popelier M, Salvatori R, Jennings J, Longas AF, Labarta Aizpun JI, Georgitsi M, Paschke R, Ronchi C, Valimaki M, Saloranta C, De Herder W, Cozzi R, Guitelman M, Magri F, Lagonigro MS, Halaby G, Corman V, Hagelstein MT, Vanbellinghen JF, Barra GB, Gimenez-Roqueplo AP, Cameron FJ, Borson-Chazot F, Holdaway I, Toledo SP, Stalla GK, Spada A, Zacharieva S, Bertherat J, Brue T, Bours V, Chanson P, Aaltonen LA & Beckers A. Clinical characteristics and therapeutic responses in patients with germ-line AIP mutations and pituitary adenomas: an international collaborative study. *J Clin Endocrinol Metab* 2010 **95** E373-383.
162. Chahal HS, Trivellin G, Leontiou CA, Alband N, Fowkes RC, Tahir A, Igreja SC, Chapple JP, Jordan S, Lupp A, Schulz S, Ansorge O, Karavitaki N, Carlsen E, Wass JA, Grossman AB & Korbonits M. Somatostatin analogs modulate AIP in somatotroph adenomas: the role of the ZAC1 pathway. *J Clin Endocrinol Metab* 2012 **97** E1411-1420.
163. Jaffrain-Rea ML, Rotondi S, Turchi A, Occhi G, Barlier A, Peverelli E, Rostomyan L, Defilles C, Angelini M, Oliva MA, Ceccato F, Maiorani O, Daly AF, Esposito V, Buttarelli F, Figarella-Branger D, Giangaspero F, Spada A, Scaroni C, Alesse E & Beckers A. Somatostatin analogues increase AIP expression in somatotropinomas, irrespective of Gsp mutations. *Endocr Relat Cancer* 2013 **20** 753-766.
164. Iacovazzo D, Carlsen E, Lugli F, Chiloiro S, Piacentini S, Bianchi A, Giampietro A, Mormando M, Clear AJ, Doglietto F, Anile C, Maira G, Lauriola L, Rindi G, Roncaroli F, Pontecorvi A, Korbonits M & De Marinis L. Factors predicting pasireotide responsiveness in somatotroph pituitary adenomas resistant to first-generation somatostatin analogues: an immunohistochemical study. *Eur J Endocrinol* 2016 **174** 241-250.
165. Khoo SK, Pendek R, Nickolov R, Luccio-Camelo DC, Newton TL, Massie A, Petillo D, Menon J, Cameron D, Teh BT & Chan SP. Genome-wide scan identifies novel modifier loci of acromegalic phenotypes for isolated familial somatotropinoma. *Endocr. Relat. Cancer* 2009 **16** 1057-1063.
166. Lecoq AL, Bouligand J, Hage M, Cazabat L, Salenave S, Linglart A, Young J, Guiochon-Mantel A, Chanson P & Kamenicky P. Very low frequency of germline GPR101 genetic variation and no biallelic defects with AIP in a large cohort of patients with sporadic pituitary adenomas. *Eur J Endocrinol* 2016 **174** 523-530.
167. Marques P, Barry S, Ronaldson A, Ogilvie A, Storr HL, Goadsby PJ, Powell M, Dang MN, Chahal HS, Evanson J, Kumar AV, Grieve J & Korbonits M. Emergence of Pituitary Adenoma in a Child during Surveillance: Clinical Challenges and the Family Members' View in an AIP Mutation-Positive Family. *Int J Endocrinol* 2018 **2018** 8581626.
168. Korbonits M, Storr H & Kumar AV. Familial pituitary adenomas - who should be tested for AIP mutations? *Clin Endocrinol (Oxf)* 2012 **77** 351-356.

169. Caimari F, Hernandez-Ramirez LC, Dang MN, Gabrovska P, Iacovazzo D, Stals K, Ellard S, Korbonits M & International Fc. Risk category system to identify pituitary adenoma patients with AIP mutations. *J Med Genet* 2018 **55** 254-260.
170. Katznelson L, Laws ER, Jr., Melmed S, Molitch ME, Murad MH, Utz A, Wass JA & Endocrine S. Acromegaly: an endocrine society clinical practice guideline. *J Clin Endocrinol Metab* 2014 **99** 3933-3951.
171. Melmed S, Casanueva FF, Hoffman AR, Kleinberg DL, Montori VM, Schlechte JA, Wass JA & Endocrine S. Diagnosis and treatment of hyperprolactinemia: an Endocrine Society clinical practice guideline. *J Clin Endocrinol Metab* 2011 **96** 273-288.
172. Kuzhandaivelu N, Cong YS, Inouye C, Yang WM & Seto E. XAP2, a novel hepatitis B virus X-associated protein that inhibits X transactivation. *Nucleic Acids Res* 1996 **24** 4741-4750.
173. Thakker RV, Pook MA, Wooding C, Boscaro M, Scanarini M & Clayton RN. Association of somatotrophinomas with loss of alleles on chromosome 11 and with gsp mutations. *J Clin Invest* 1993 **91** 2815-2821.
174. Gadelha MR, Prezant TR, Une KN, Glick RP, Moskal SF, 2nd, Vaisman M, Melmed S, Kineman RD & Frohman LA. Loss of heterozygosity on chromosome 11q13 in two families with acromegaly/gigantism is independent of mutations of the multiple endocrine neoplasia type I gene. *J Clin Endocrinol Metab* 1999 **84** 249-256.
175. Soares BS, Eguchi K & Frohman LA. Tumor deletion mapping on chromosome 11q13 in eight families with isolated familial somatotropinoma and in 15 sporadic somatotropinomas. *J Clin Endocrinol Metab* 2005 **90** 6580-6587.
176. Trivellin G & Korbonits M. AIP and its interacting partners. *J Endocrinol* 2011 **210** 137-155.
177. Stockinger B, Di Meglio P, Gialitakis M & Duarte JH. The aryl hydrocarbon receptor: multitasking in the immune system. *Annu Rev Immunol* 2014 **32** 403-432.
178. Aflorei ED, Klapholz B, Chen C, Radian S, Dragu AN, Moderau N, Prodromou C, Ribeiro PS, Stanewsky R & Korbonits M. In vivo bioassay to test the pathogenicity of missense human AIP variants. *J Med Genet* 2018 **55** 522-529.
179. Lahvis GP, Pyzalski RW, Glover E, Pitot HC, McElwee MK & Bradfield CA. The aryl hydrocarbon receptor is required for developmental closure of the ductus venosus in the neonatal mouse. *Mol Pharmacol* 2005 **67** 714-720.
180. Lin BC, Nguyen LP, Walisser JA & Bradfield CA. A hypomorphic allele of aryl hydrocarbon receptor-associated protein-9 produces a phenocopy of the AHR-null mouse. *Mol Pharmacol* 2008 **74** 1367-1371.
181. Fernandez-Salguero PM, Hilbert DM, Rudikoff S, Ward JM & Gonzalez FJ. Aryl-hydrocarbon receptor-deficient mice are resistant to 2,3,7,8-tetrachlorodibenzo-p-dioxin-induced toxicity. *Toxicol Appl Pharmacol* 1996 **140** 173-179.
182. Gonzalez FJ & Fernandez-Salguero P. The aryl hydrocarbon receptor: studies using the AHR-null mice. *Drug Metab Dispos* 1998 **26** 1194-1198.
183. Peng L, Mayhew CN, Schnekenburger M, Knudsen ES & Puga A. Repression of Ah receptor and induction of transforming growth factor-beta genes in DEN-induced mouse liver tumors. *Toxicology* 2008 **246** 242-247.
184. Barhoover MA, Hall JM, Greenlee WF & Thomas RS. Aryl hydrocarbon receptor regulates cell cycle progression in human breast cancer cells via a functional interaction with cyclin-dependent kinase 4. *Mol Pharmacol* 2010 **77** 195-201.
185. Heliovaara E, Raitila A, Launonen V, Paetau A, Arola J, Lehtonen H, Sane T, Weil RJ, Vierimaa O, Salmela P, Tuppurainen K, Makinen M, Aaltonen LA & Karhu A. The expression of AIP-related molecules in elucidation of cellular pathways in pituitary adenomas. *Am J Pathol* 2009 **175** 2501-2507.
186. Jaffrain-Rea ML, Angelini M, Gargano D, Tichomirowa MA, Daly AF, Vanbellinghen JF, D'Innocenzo E, Barlier A, Giangaspero F, Esposito V, Ventura L, Arcella A, Theodoropoulou M, Naves LA, Fajardo C, Zacharieva S, Rohmer V, Brue T, Gulino A, Cantore G, Alesse E &

Beckers A. Expression of aryl hydrocarbon receptor (AHR) and AHR-interacting protein in pituitary adenomas: pathological and clinical implications. *Endocr Relat Cancer* 2009 **16** 1029-1043.

187. Igreja S, Chahal HS, King P, Bolger GB, Srirangalingam U, Guasti L, Chapple JP, Trivellin G, Gueorguiev M, Guegan K, Stals K, Khoo B, Kumar AV, Ellard S, Grossman AB, Korbonits M & International FC. Characterization of aryl hydrocarbon receptor interacting protein (AIP) mutations in familial isolated pituitary adenoma families. *Hum Mutat* 2010 **31** 950-960.
188. Tuominen I, Heliovaara E, Raitila A, Rautiainen MR, Mehine M, Katainen R, Donner I, Aittomaki V, Lehtonen HJ, Ahlsten M, Kivipelto L, Schalin-Jantti C, Arola J, Hautaniemi S & Karhu A. AIP inactivation leads to pituitary tumorigenesis through defective Galphai-cAMP signaling. *Oncogene* 2015 **34** 1174-1184.
189. Lloyd C & Grossman A. The AIP (aryl hydrocarbon receptor-interacting protein) gene and its relation to the pathogenesis of pituitary adenomas. *Endocrine* 2014 **46** 387-396.
190. Raitila A, Lehtonen HJ, Arola J, Heliovaara E, Ahlsten M, Georgitsi M, Jalanko A, Paetau A, Aaltonen LA & Karhu A. Mice with inactivation of aryl hydrocarbon receptor-interacting protein (Aip) display complete penetrance of pituitary adenomas with aberrant ARNT expression. *Am J Pathol* 2010 **177** 1969-1976.
191. Hernandez-Ramirez LC, Martucci F, Morgan RM, Trivellin G, Tilley D, Ramos-Guajardo N, Iacovazzo D, D'Acquisto F, Prodromou C & Korbonits M. Rapid proteasomal degradation of mutant proteins is the primary mechanism leading to tumorigenesis in patients with missense AIP mutations. *J Clin Endocrinol Metab* 2016 jc20161307.
192. Radian S, Diekmann Y, Gabrovska P, Holland B, Bradley L, Wallace H, Stals K, Bussell AM, McGurren K, Cuesta M, Ryan AW, Herincs M, Hernandez-Ramirez LC, Holland A, Samuels J, Aflorei ED, Barry S, Denes J, Pernicova I, Stiles CE, Trivellin G, McCloskey R, Ajzensztejn M, Abid N, Akker SA, Mercado M, Cohen M, Thakker RV, Baldeweg S, Barkan A, Musat M, Levy M, Orme SM, Unterlander M, Burger J, Kumar AV, Ellard S, McPartlin J, McManus R, Linden GJ, Atkinson B, Balding DJ, Agha A, Thompson CJ, Hunter SJ, Thomas MG, Morrison PJ & Korbonits M. Increased Population Risk of AIP-Related Acromegaly and Gigantism in Ireland. *Hum Mutat* 2017 **38** 78-85.
193. Chahal HS, Stals K, Unterlander M, Balding DJ, Thomas MG, Kumar AV, Besser GM, Atkinson AB, Morrison PJ, Howlett TA, Levy MJ, Orme SM, Akker SA, Abel RL, Grossman AB, Burger J, Ellard S & Korbonits M. AIP mutation in pituitary adenomas in the 18th century and today. *N Engl J Med* 2011 **364** 43-50.
194. Occhi G, Jaffrain-Rea ML, Trivellin G, Albiger N, Ceccato F, De Menis E, Angelini M, Ferasin S, Beckers A, Mantero F & Scaroni C. The R304X mutation of the aryl hydrocarbon receptor interacting protein gene in familial isolated pituitary adenomas: Mutational hot-spot or founder effect? *J Endocrinol Invest* 2010 **33** 800-805.
195. Salvatori R, Radian S, Diekmann Y, Iacovazzo D, David A, Gabrovska P, Grassi G, Bussell AM, Stals K, Weber A, Quinton R, Crowne EC, Corazzini V, Metherell L, Kearney T, Du Plessis D, Sinha AK, Baborie A, Lecoq AL, Chanson P, Ansorge O, Ellard S, Trainer PJ, Balding D, Thomas MG & Korbonits M. In-frame seven amino-acid duplication in AIP arose over the last 3000 years, disrupts protein interaction and stability and is associated with gigantism. *Eur J Endocrinol* 2017 **177** 257-266.
196. Rostomyan L, Daly AF, Petrossians P, Nachev E, Lila AR, Lecoq AL, Lecumberri B, Trivellin G, Salvatori R, Moraitis AG, Holdaway I, Kranenburg-van Klaveren DJ, Chiara Zatelli M, Palacios N, Nozieres C, Zacharin M, Ebeling T, Ojaniemi M, Rozhinskaya L, Verrua E, Jaffrain-Rea ML, Filipponi S, Gusakova D, Pronin V, Bertherat J, Belaya Z, Ilovayskaya I, Sahnoun-Fathallah M, Sievers C, Stalla GK, Castermans E, Caberg JH, Sorkina E, Auriemma RS, Mittal S, Kareva M, Lysy PA, Emy P, De Menis E, Choong CS, Mantovani G, Bours V, De Herder W, Brue T, Barlier A, Neggers SJ, Zacharieva S, Chanson P, Shah NS, Stratakis CA,

Naves LA & Beckers A. Clinical and genetic characterization of pituitary gigantism: an international collaborative study in 208 patients. *Endocr Relat Cancer* 2015 **22** 745-757.

197. Beckers A, Lodish MB, Trivellin G, Rostomyan L, Lee M, Faucz FR, Yuan B, Choong CS, Caberg JH, Verrua E, Naves LA, Cheetham TD, Young J, Lysy PA, Petrossians P, Cotterill A, Shah NS, Metzger D, Castermans E, Ambrosio MR, Villa C, Strebkova N, Mazerkina N, Gaillard S, Barra GB, Casulari LA, Neggers SJ, Salvatori R, Jaffrain-Rea ML, Zacharin M, Santamaria BL, Zacharieva S, Lim EM, Mantovani G, Zatelli MC, Collins MT, Bonneville JF, Quezado M, Chittiboina P, Oldfield EH, Bours V, Liu P, W WdH, Pellegata N, Lupski JR, Daly AF & Stratakis CA. X-linked acrogigantism syndrome: clinical profile and therapeutic responses. *Endocr Relat Cancer* 2015 **22** 353-367.
198. Daly AF, Yuan B, Fina F, Caberg JH, Trivellin G, Rostomyan L, de Herder WW, Naves LA, Metzger D, Cuny T, Rabl W, Shah N, Jaffrain-Rea ML, Zatelli MC, Faucz FR, Castermans E, Nanni-Metellus I, Lodish M, Muhammad A, Palmeira L, Potorac I, Mantovani G, Neggers SJ, Klein M, Barlier A, Liu P, Ouafik L, Bours V, Lupski JR, Stratakis CA & Beckers A. Somatic mosaicism underlies X-linked acrogigantism syndrome in sporadic male subjects. *Endocr Relat Cancer* 2016 **23** 221-233.
199. Rodd C, Millette M, Iacovazzo D, Stiles CE, Barry S, Evanson J, Albrecht S, Caswell R, Bunce B, Jose S, Trouillas J, Roncaroli F, Sampson J, Ellard S & Korbonits M. Somatic GPR101 Duplication Causing X-Linked Acrogigantism (XLAG)-Diagnosis and Management. *J Clin Endocrinol Metab* 2016 **101** 1927-1930.
200. Naves LA, Daly AF, Dias LA, Yuan B, Zakir JC, Barra GB, Palmeira L, Villa C, Trivellin G, Junior AJ, Neto FF, Liu P, Pellegata NS, Stratakis CA, Lupski JR & Beckers A. Aggressive tumor growth and clinical evolution in a patient with X-linked acro-gigantism syndrome. *Endocrine* 2016 **51** 236-244.
201. Albani A, Theodoropoulou M & Reincke M. Genetics of Cushing's disease. *Clin Endocrinol (Oxf)* 2018 **88** 3-12.
202. Oshima A, Jaijo T, Aller E, Millan JM, Carney C, Usami S, Moller C & Kimberling WJ. Mutation profile of the CDH23 gene in 56 probands with Usher syndrome type I. *Hum Mutat* 2008 **29** E37-46.
203. Marques P, Spencer R, Morrison PJ, Carr IM, Dang MN, Bonthron DT, Hunter S & Korbonits M. Cantu syndrome with coexisting familial pituitary adenoma. *Endocrine* 2018 **59** 677-684.
204. Balkwill FR, Capasso M & Hagemann T. The tumor microenvironment at a glance. *J Cell Sci* 2012 **125** 5591-5596.
205. Paget S. The distribution of secondary growths in cancer of the breast. 1889. *Cancer Metastasis Rev* 1989 **8** 98-101.
206. Fidler IJ. Critical determinants of metastasis. *Semin Cancer Biol* 2002 **12** 89-96.
207. Bissell MJ & Radisky D. Putting tumours in context. *Nat Rev Cancer* 2001 **1** 46-54.
208. Drake LE & Macleod KF. Tumour suppressor gene function in carcinoma-associated fibroblasts: from tumour cells via EMT and back again? *J Pathol* 2014 **232** 283-288.
209. Balkwill FR. The chemokine system and cancer. *J Pathol* 2012 **226** 148-157.
210. Balkwill FR & Mantovani A. Cancer-related inflammation: common themes and therapeutic opportunities. *Semin Cancer Biol* 2012 **22** 33-40.
211. Grizzi F, Borroni EM, Vacchini A, Qehajaj D, Liguori M, Stifter S, Chiriva-Internati M & Di Ieva A. Pituitary Adenoma and the Chemokine Network: A Systemic View. *Front Endocrinol (Lausanne)* 2015 **6** 141.
212. Wilson J & Balkwill F. The role of cytokines in the epithelial cancer microenvironment. *Semin Cancer Biol* 2002 **12** 113-120.
213. Turner MD, Nedjai B, Hurst T & Pennington DJ. Cytokines and chemokines: At the crossroads of cell signalling and inflammatory disease. *Biochim Biophys Acta* 2014 **1843** 2563-2582.

214. Arzt E, Pereda MP, Castro CP, Pagotto U, Renner U & Stalla GK. Pathophysiological role of the cytokine network in the anterior pituitary gland. *Front Neuroendocrinol* 1999 **20** 71-95.
215. Tsagarakis S, Kontogeorgos G & Kovacs K. The role of cytokines in the normal and neoplastic pituitary. *Crit Rev Oncol Hematol* 1998 **28** 73-90.
216. Ray D & Melmed S. Pituitary cytokine and growth factor expression and action. *Endocr Rev* 1997 **18** 206-228.
217. Dinarello CA. Historical insights into cytokines. *Eur J Immunol* 2007 **37 Suppl 1** S34-45.
218. Kelso A. Cytokines: principles and prospects. *Immunol Cell Biol* 1998 **76** 300-317.
219. Lin WW & Karin M. A cytokine-mediated link between innate immunity, inflammation, and cancer. *J Clin Invest* 2007 **117** 1175-1183.
220. Lippitz BE. Cytokine patterns in patients with cancer: a systematic review. *Lancet Oncol* 2013 **14** e218-228.
221. Lewis AM, Varghese S, Xu H & Alexander HR. Interleukin-1 and cancer progression: the emerging role of interleukin-1 receptor antagonist as a novel therapeutic agent in cancer treatment. *J Transl Med* 2006 **4** 48.
222. Mantovani A, Allavena P, Sica A & Balkwill F. Cancer-related inflammation. *Nature* 2008 **454** 436-444.
223. Rostene W, Guyon A, Kular L, Godefroy D, Barbieri F, Bajetto A, Banisadr G, Callewaere C, Conductier G, Rovere C, Melik-Parsadaniantz S & Florio T. Chemokines and chemokine receptors: new actors in neuroendocrine regulations. *Front Neuroendocrinol* 2011 **32** 10-24.
224. Murdoch C & Finn A. Chemokine receptors and their role in inflammation and infectious diseases. *Blood* 2000 **95** 3032-3043.
225. Bestebroer J, De Haas CJ & Van Strijp JA. How microorganisms avoid phagocyte attraction. *FEMS Microbiol Rev* 2010 **34** 395-414.
226. Mantovani A, Savino B, Locati M, Zammataro L, Allavena P & Bonecchi R. The chemokine system in cancer biology and therapy. *Cytokine Growth Factor Rev* 2010 **21** 27-39.
227. Yapa S, Mulla O, Green V, England J & Greenman J. The Role of Chemokines in Thyroid Carcinoma. *Thyroid* 2017 **27** 1347-1359.
228. Marchesi F, Locatelli M, Solinas G, Erreni M, Allavena P & Mantovani A. Role of CX3CR1/CX3CL1 axis in primary and secondary involvement of the nervous system by cancer. *J Neuroimmunol* 2010 **224** 39-44.
229. Mantovani A, Sozzani S, Locati M, Allavena P & Sica A. Macrophage polarization: tumor-associated macrophages as a paradigm for polarized M2 mononuclear phagocytes. *Trends Immunol* 2002 **23** 549-555.
230. Haedo MR, Gerez J, Fuertes M, Giacomini D, Paez-Pereda M, Labeur M, Renner U, Stalla GK & Arzt E. Regulation of pituitary function by cytokines. *Horm Res* 2009 **72** 266-274.
231. Barbieri F, Thellung S, Wurth R, Gatto F, Corsaro A, Villa V, Nizzari M, Albertelli M, Ferone D & Florio T. Emerging Targets in Pituitary Adenomas: Role of the CXCL12/CXCR4-R7 System. *Int J Endocrinol* 2014 **2014** 753524.
232. Green VL, Atkin SL, Speirs V, Jeffreys RV, Landolt AM, Mathew B, Hipkin L & White MC. Cytokine expression in human anterior pituitary adenomas. *Clin Endocrinol (Oxf)* 1996 **45** 179-185.
233. Suliman ME, Royds JA, Baxter L, Timperley WR, Cullen DR & Jones TH. IL-8 mRNA expression by in situ hybridisation in human pituitary adenomas. *Eur J Endocrinol* 1999 **140** 155-158.
234. Vindelov SD, Hartoft-Nielsen ML, Rasmussen AK, Bendtzen K, Kosteljanetz M, Andersson AM & Feldt-Rasmussen U. Interleukin-8 production from human somatotroph adenoma cells is stimulated by interleukin-1beta and inhibited by growth hormone releasing hormone and somatostatin. *Growth Horm IGF Res* 2011 **21** 134-139.

235. Salomon MP, Wang X, Marzese DM, Hsu SC, Nelson N, Zhang X, Matsuba C, Takasumi Y, Ballesteros-Merino C, Fox BA, Barkhoudarian G, Kelly DF & Hoon DSB. The Epigenomic Landscape of Pituitary Adenomas Reveals Specific Alterations and Differentiates Among Acromegaly, Cushing's Disease and Endocrine-Inactive Subtypes. *Clin Cancer Res* 2018 **24** 4126-4136.
236. Waugh DJ & Wilson C. The interleukin-8 pathway in cancer. *Clin Cancer Res* 2008 **14** 6735-6741.
237. Jones TH, Daniels M, James RA, Justice SK, McCorkle R, Price A, Kendall-Taylor P & Weetman AP. Production of bioactive and immunoreactive interleukin-6 (IL-6) and expression of IL-6 messenger ribonucleic acid by human pituitary adenomas. *J Clin Endocrinol Metab* 1994 **78** 180-187.
238. Kurotani R, Yasuda M, Oyama K, Egashira N, Sugaya M, Teramoto A & Osamura RY. Expression of interleukin-6, interleukin-6 receptor (gp80), and the receptor's signal-transducing subunit (gp130) in human normal pituitary glands and pituitary adenomas. *Mod Pathol* 2001 **14** 791-797.
239. Velkeniers B, Vergani P, Trouillas J, D'Haens J, Hooghe RJ & Hooghe-Peters EL. Expression of IL-6 mRNA in normal rat and human pituitaries and in human pituitary adenomas. *J Histochem Cytochem* 1994 **42** 67-76.
240. Borg SA, Kerry KE, Baxter L, Royds JA & Jones TH. Expression of interleukin-6 and its effects on growth of HP75 human pituitary tumor cells. *J Clin Endocrinol Metab* 2003 **88** 4938-4944.
241. Arzt E, Buric R, Stelzer G, Stalla J, Sauer J, Renner U & Stalla GK. Interleukin involvement in anterior pituitary cell growth regulation: effects of IL-2 and IL-6. *Endocrinology* 1993 **132** 459-467.
242. Lyson K & McCann SM. The effect of interleukin-6 on pituitary hormone release in vivo and in vitro. *Neuroendocrinology* 1991 **54** 262-266.
243. Pereda MP, Lohrer P, Kovalovsky D, Perez Castro C, Goldberg V, Losa M, Chervin A, Berner S, Molina H, Stalla GK, Renner U & Arzt E. Interleukin-6 is inhibited by glucocorticoids and stimulates ACTH secretion and POMC expression in human corticotroph pituitary adenomas. *Exp Clin Endocrinol Diabetes* 2000 **108** 202-207.
244. Renner U, Gloddek J, Arzt E, Inoue K & Stalla GK. Interleukin-6 is an autocrine growth factor for folliculostellate-like TtT/GF mouse pituitary tumor cells. *Exp Clin Endocrinol Diabetes* 1997 **105** 345-352.
245. Sawada T, Koike K, Kanda Y, Ikegami H, Jikihara H, Maeda T, Osako Y, Hirota K & Miyake A. Interleukin-6 stimulates cell proliferation of rat pituitary clonal cell lines in vitro. *J Endocrinol Invest* 1995 **18** 83-90.
246. Graciarena M, Carbia-Nagashima A, Onofri C, Perez-Castro C, Giacomini D, Renner U, Stalla GK & Arzt E. Involvement of the gp130 cytokine transducer in MtT/S pituitary somatotroph tumour development in an autocrine-paracrine model. *Eur J Endocrinol* 2004 **151** 595-604.
247. Gloddek J, Pagotto U, Paez Pereda M, Arzt E, Stalla GK & Renner U. Pituitary adenylate cyclase-activating polypeptide, interleukin-6 and glucocorticoids regulate the release of vascular endothelial growth factor in pituitary folliculostellate cells. *J Endocrinol* 1999 **160** 483-490.
248. Renner U, Gloddek J, Pereda MP, Arzt E & Stalla GK. Regulation and role of intrapituitary IL-6 production by folliculostellate cells. *Domest Anim Endocrinol* 1998 **15** 353-362.
249. Wu JL, Qiao JY & Duan QH. Significance of TNF-alpha and IL-6 expression in invasive pituitary adenomas. *Genet Mol Res* 2016 **15**.
250. Paoletta A, Arnaldi G, Papa R, Boscaro M & Tirabassi G. Intrapituitary cytokines in Cushing's disease: do they play a role? *Pituitary* 2011 **14** 236-241.

251. Watanobe H, Tamura T, Habu S, Kakizaki Y, Kohsaka A & Suda T. Measurement of cytokines in the cavernous sinus plasma from patients with Cushing's disease. *Neuropeptides* 1998 **32** 119-123.
252. Shah N, Ruiz HH, Zafar U, Post KD, Buettner C & Geer EB. Proinflammatory cytokines remain elevated despite long-term remission in Cushing's disease: a prospective study. *Clin Endocrinol (Oxf)* 2017 **86** 68-74.
253. Sapochnik M, Fuertes M & Arzt E. Programmed cell senescence: role of IL-6 in the pituitary. *J Mol Endocrinol* 2017 **58** R241-R253.
254. Sapochnik M, Haedo MR, Fuertes M, Ajler P, Carrizo G, Cervio A, Sevlever G, Stalla GK & Arzt E. Autocrine IL-6 mediates pituitary tumor senescence. *Oncotarget* 2017 **8** 4690-4702.
255. Bristulf J, Simoncsits A & Bartfai T. Characterization of a neuronal interleukin-1 receptor and the corresponding mRNA in the mouse anterior pituitary cell line AtT-20. *Neurosci Lett* 1991 **128** 173-176.
256. Sweep CG, van der Meer MJ, Hermus AR, Smals AG, van der Meer JW, Pesman GJ, Willemsen SJ, Benraad TJ & Kloppenborg PW. Chronic stimulation of the pituitary-adrenal axis in rats by interleukin-1 beta infusion: in vivo and in vitro studies. *Endocrinology* 1992 **130** 1153-1164.
257. Sapolsky R, Rivier C, Yamamoto G, Plotsky P & Vale W. Interleukin-1 stimulates the secretion of hypothalamic corticotropin-releasing factor. *Science* 1987 **238** 522-524.
258. Bernton EW, Beach JE, Holaday JW, Smallridge RC & Fein HG. Release of multiple hormones by a direct action of interleukin-1 on pituitary cells. *Science* 1987 **238** 519-521.
259. Wassen FW, Moerings EP, Van Toor H, De Vrey EA, Hennemann G & Everts ME. Effects of interleukin-1 beta on thyrotropin secretion and thyroid hormone uptake in cultured rat anterior pituitary cells. *Endocrinology* 1996 **137** 1591-1598.
260. Kovalovsky D, Paez Pereda M, Labeur M, Renner U, Holsboer F, Stalla GK & Arzt E. Nur77 induction and activation are necessary for interleukin-1 stimulation of proopiomelanocortin in AtT-20 corticotrophs. *FEBS Lett* 2004 **563** 229-233.
261. Gong FY, Deng JY & Shi YF. Stimulatory effect of interleukin-1beta on growth hormone gene expression and growth hormone release from rat GH3 cells. *Neuroendocrinology* 2005 **81** 217-228.
262. Ueland T, Fougner SL, Godang K, Lekva T, Schurgers LJ, Scholz H, Halvorsen B, Schreiner T, Aukrust P & Bollerslev J. Associations between body composition, circulating interleukin-1 receptor antagonist, osteocalcin, and insulin metabolism in active acromegaly. *J Clin Endocrinol Metab* 2010 **95** 361-368.
263. Renner U, Newton CJ, Pagotto U, Sauer J, Arzt E & Stalla GK. Involvement of interleukin-1 and interleukin-1 receptor antagonist in rat pituitary cell growth regulation. *Endocrinology* 1995 **136** 3186-3193.
264. Stepien H, Zerek-Melen G, Mucha S, Winczyk K & Fryczak J. Interleukin-1 beta stimulates cell proliferation in the intermediate lobe of the rat pituitary gland. *J Endocrinol* 1994 **140** 337-341.
265. Burger JA & Kipps TJ. CXCR4: a key receptor in the crosstalk between tumor cells and their microenvironment. *Blood* 2006 **107** 1761-1767.
266. Banisadr G, Dicou E, Berbar T, Rostene W, Lombet A & Haour F. Characterization and visualization of [125I] stromal cell-derived factor-1alpha binding to CXCR4 receptors in rat brain and human neuroblastoma cells. *J Neuroimmunol* 2000 **110** 151-160.
267. Barbieri F, Bajetto A, Porcile C, Pattarozzi A, Schettini G & Florio T. Role of stromal cell-derived factor 1 (SDF1/CXCL12) in regulating anterior pituitary function. *J Mol Endocrinol* 2007 **38** 383-389.
268. Barbieri F, Bajetto A, Stumm R, Pattarozzi A, Porcile C, Zona G, Dorcaratto A, Ravetti JL, Minuto F, Spaziante R, Schettini G, Ferone D & Florio T. Overexpression of stromal cell-

derived factor 1 and its receptor CXCR4 induces autocrine/paracrine cell proliferation in human pituitary adenomas. *Clin Cancer Res* 2008 **14** 5022-5032.
269. Horiguchi K, Ilmiawati C, Fujiwara K, Tsukada T, Kikuchi M & Yashiro T. Expression of chemokine CXCL12 and its receptor CXCR4 in folliculostellate (FS) cells of the rat anterior pituitary gland: the CXCL12/CXCR4 axis induces interconnection of FS cells. *Endocrinology* 2012 **153** 1717-1724.
270. Lee YH, Noh TW, Lee MK, Jameson JL & Lee EJ. Absence of activating mutations of CXCR4 in pituitary tumours. *Clin Endocrinol (Oxf)* 2010 **72** 209-213.
271. Florio T, Casagrande S, Diana F, Bajetto A, Porcile C, Zona G, Thellung S, Arena S, Pattarozzi A, Corsaro A, Spaziante R, Robello M & Schettini G. Chemokine stromal cell-derived factor 1alpha induces proliferation and growth hormone release in GH4C1 rat pituitary adenoma cell line through multiple intracellular signals. *Mol Pharmacol* 2006 **69** 539-546.
272. Massa A, Casagrande S, Bajetto A, Porcile C, Barbieri F, Thellung S, Arena S, Pattarozzi A, Gatti M, Corsaro A, Robello M, Schettini G & Florio T. SDF-1 controls pituitary cell proliferation through the activation of ERK1/2 and the Ca2+-dependent, cytosolic tyrosine kinase Pyk2. *Ann N Y Acad Sci* 2006 **1090** 385-398.
273. Lee Y, Kim JM & Lee EJ. Functional expression of CXCR4 in somatotrophs: CXCL12 activates GH gene, GH production and secretion, and cellular proliferation. *J Endocrinol* 2008 **199** 191-199.
274. Kim JM, Lee YH, Ku CR & Lee EJ. The cyclic pentapeptide d-Arg3FC131, a CXCR4 antagonist, induces apoptosis of somatotrope tumor and inhibits tumor growth in nude mice. *Endocrinology* 2011 **152** 536-544.
275. Yoshida D, Koketshu K, Nomura R & Teramoto A. The CXCR4 antagonist AMD3100 suppresses hypoxia-mediated growth hormone production in GH3 rat pituitary adenoma cells. *J Neurooncol* 2010 **100** 51-64.
276. Xing B, Kong YG, Yao Y, Lian W, Wang RZ & Ren ZY. Study on the expression levels of CXCR4, CXCL12, CD44, and CD147 and their potential correlation with invasive behaviors of pituitary adenomas. *Biomed Environ Sci* 2013 **26** 592-598.
277. Nomura R, Yoshida D & Teramoto A. Stromal cell-derived factor-1 expression in pituitary adenoma tissues and upregulation in hypoxia. *J Neurooncol* 2009 **94** 173-181.
278. Yoshida D, Nomura R & Teramoto A. Signalling pathway mediated by CXCR7, an alternative chemokine receptor for stromal-cell derived factor-1alpha, in AtT20 mouse adrenocorticotrophic hormone-secreting pituitary adenoma cells. *J Neuroendocrinol* 2009 **21** 481-488.
279. Tecimer T, Dlott J, Chuntharapai A, Martin AW & Peiper SC. Expression of the chemokine receptor CXCR2 in normal and neoplastic neuroendocrine cells. *Arch Pathol Lab Med* 2000 **124** 520-525.
280. Recouvreux MV, Camilletti MA, Rifkin DB & Diaz-Torga G. The pituitary TGFbeta1 system as a novel target for the treatment of resistant prolactinomas. *J Endocrinol* 2016 **228** R73-83.
281. Sarkar DK, Kim KH & Minami S. Transforming growth factor-beta 1 messenger RNA and protein expression in the pituitary gland: its action on prolactin secretion and lactotropic growth. *Mol Endocrinol* 1992 **6** 1825-1833.
282. De A, Morgan TE, Speth RC, Boyadjieva N & Sarkar DK. Pituitary lactotrope expresses transforming growth factor beta (TGF beta) type II receptor mRNA and protein and contains 125I-TGF beta 1 binding sites. *J Endocrinol* 1996 **149** 19-27.
283. Ruebel KH, Leontovich AA, Tanizaki Y, Jin L, Stilling GA, Zhang S, Coonse K, Scheithauer BW, Lombardero M, Kovacs K & Lloyd RV. Effects of TGFbeta1 on gene expression in the HP75 human pituitary tumor cell line identified by gene expression profiling. *Endocrine* 2008 **33** 62-76.

284. Zhenye L, Chuzhong L, Youtu W, Xiaolei L, Lei C, Lichuan H, Hongyun W, Yonggang W, Fei W & Yazhuo Z. The expression of TGF-beta1, Smad3, phospho-Smad3 and Smad7 is correlated with the development and invasion of nonfunctioning pituitary adenomas. *J Transl Med* 2014 **12** 71.
285. Gu YH & Feng YG. Down-regulation of TGF-beta RII expression is correlated with tumor growth and invasion in non-functioning pituitary adenomas. *J Clin Neurosci* 2018 **47** 264-268.
286. Candolfi M, Jaita G, Pisera D, Ferrari L, Barcia C, Liu C, Yu J, Liu G, Castro MG & Seilicovich A. Adenoviral vectors encoding tumor necrosis factor-alpha and FasL induce apoptosis of normal and tumoral anterior pituitary cells. *J Endocrinol* 2006 **189** 681-690.
287. Gaillard RC, Turnill D, Sappino P & Muller AF. Tumor necrosis factor alpha inhibits the hormonal response of the pituitary gland to hypothalamic releasing factors. *Endocrinology* 1990 **127** 101-106.
288. Nash AD, Brandon MR & Bello PA. Effects of tumour necrosis factor-alpha on growth hormone and interleukin 6 mRNA in ovine pituitary cells. *Mol Cell Endocrinol* 1992 **84** R31-37.
289. Milenkovic L, Rettori V, Snyder GD, Beutler B & McCann SM. Cachectin alters anterior pituitary hormone release by a direct action in vitro. *Proc Natl Acad Sci U S A* 1989 **86** 2418-2422.
290. Xiao Z, Liu Q, Mao F, Wu J & Lei T. TNF-alpha-induced VEGF and MMP-9 expression promotes hemorrhagic transformation in pituitary adenomas. *Int J Mol Sci* 2011 **12** 4165-4179.
291. Arita K, Kurisu K, Tominaga A, Sugiyama K, Eguchi K, Hama S, Yoshioka H, Yamasaki F & Kanou Y. Relationship between intratumoral hemorrhage and overexpression of vascular endothelial growth factor (VEGF) in pituitary adenoma. *Hiroshima J Med Sci* 2004 **53** 23-27.
292. Fukui S, Otani N, Nawashiro H, Yano A, Nomura N, Tokumaru AM, Miyazawa T, Ohnuki A, Tsuzuki N, Katoh H, Ishihara S, Shima K & Ooigawa H. The association of the expression of vascular endothelial growth factor with the cystic component and haemorrhage in pituitary adenoma. *J Clin Neurosci* 2003 **10** 320-324.
293. Takada K, Yamada S & Teramoto A. Correlation between tumor vascularity and clinical findings in patients with pituitary adenomas. *Endocr Pathol* 2004 **15** 131-139.
294. Zhu H, Guo J, Shen Y, Dong W, Gao H, Miao Y, Li C & Zhang Y. Functions and Mechanisms of Tumor Necrosis Factor-alpha and Noncoding RNAs in Bone-Invasive Pituitary Adenomas. *Clin Cancer Res* 2018 **24** 5757-5766.
295. Kim K, Yoshida D & Teramoto A. Expression of hypoxia-inducible factor 1alpha and vascular endothelial growth factor in pituitary adenomas. *Endocr Pathol* 2005 **16** 115-121.
296. Onofri C, Theodoropoulou M, Losa M, Uhl E, Lange M, Arzt E, Stalla GK & Renner U. Localization of vascular endothelial growth factor (VEGF) receptors in normal and adenomatous pituitaries: detection of a non-endothelial function of VEGF in pituitary tumours. *J Endocrinol* 2006 **191** 249-261.
297. Turner HE, Harris AL, Melmed S & Wass JA. Angiogenesis in endocrine tumors. *Endocr Rev* 2003 **24** 600-632.
298. McCabe CJ, Boelaert K, Tannahill LA, Heaney AP, Stratford AL, Khaira JS, Hussain S, Sheppard MC, Franklyn JA & Gittoes NJ. Vascular endothelial growth factor, its receptor KDR/Flk-1, and pituitary tumor transforming gene in pituitary tumors. *J Clin Endocrinol Metab* 2002 **87** 4238-4244.
299. Lloyd RV, Scheithauer BW, Kuroki T, Vidal S, Kovacs K & Stefaneanu L. Vascular Endothelial Growth Factor (VEGF) Expression in Human Pituitary Adenomas and Carcinomas. *Endocr Pathol* 1999 **10** 229-235.

300. Sanchez-Ortiga R, Sanchez-Tejada L, Moreno-Perez O, Riesgo P, Niveiro M & Pico Alfonso AM. Over-expression of vascular endothelial growth factor in pituitary adenomas is associated with extrasellar growth and recurrence. *Pituitary* 2013 **16** 370-377.
301. Cristina C, Perez-Millan MI, Luque G, Dulce RA, Sevlever G, Berner SI & Becu-Villalobos D. VEGF and CD31 association in pituitary adenomas. *Endocr Pathol* 2010 **21** 154-160.
302. Jugenburg M, Kovacs K, Stefaneanu L & Scheithauer BW. Vasculature in Nontumorous Hypophyses, Pituitary Adenomas, and Carcinomas: A Quantitative Morphologic Study. *Endocr Pathol* 1995 **6** 115-124.
303. Vidal S, Kovacs K, Horvath E, Scheithauer BW, Kuroki T & Lloyd RV. Microvessel density in pituitary adenomas and carcinomas. *Virchows Arch* 2001 **438** 595-602.
304. Takano S, Akutsu H, Hara T, Yamamoto T & Matsumura A. Correlations of vascular architecture and angiogenesis with pituitary adenoma histotype. *Int J Endocrinol* 2014 **2014** 989574.
305. Lohrer P, Gloddek J, Hopfner U, Losa M, Uhl E, Pagotto U, Stalla GK & Renner U. Vascular endothelial growth factor production and regulation in rodent and human pituitary tumor cells in vitro. *Neuroendocrinology* 2001 **74** 95-105.
306. Komorowski J, Jankewicz J & Stepien H. Vascular endothelial growth factor (VEGF), basic fibroblast growth factor (bFGF) and soluble interleukin-2 receptor (sIL-2R) concentrations in peripheral blood as markers of pituitary tumours. *Cytobios* 2000 **101** 151-159.
307. Lombardero M, Vidal S, Hurta R, Roman A, Kovacs K, Lloyd RV & Scheithauer BW. Modulation of VEGF/Flk-1 receptor expression in the rat pituitary GH3 cell line by growth factors. *Pituitary* 2006 **9** 137-143.
308. Lawnicka H & Kunert-Radek J. Stimulatory effect of GH3 cell line conditioned medium on the proliferation of the endothelial cell line (HECa10) in vitro. *Neuro Endocrinol Lett* 2005 **26** 413-418.
309. Alfer J, Neulen J & Gaumann A. Lactotrophs: the new and major source for VEGF secretion and the influence of ECM on rat pituitary function in vitro. *Oncol Rep* 2015 **33** 2129-2134.
310. Dutta P, Reddy KS, Rai A, Madugundu AK, Solanki HS, Bhansali A, Radotra BD, Kumar N, Collier D, Iacovazzo D, Gupta P, Raja R, Gowda H, Pandey A, Devgun JS & Korbonits M. Surgery, Octreotide, Temozolomide, Bevacizumab, Radiotherapy, and Pegvisomant Treatment of an AIP MutationPositive Child. *J Clin Endocrinol Metab* 2019 **104** 3539-3544.
311. Touma W, Hoostal S, Peterson RA, Wiernik A, SantaCruz KS & Lou E. Successful treatment of pituitary carcinoma with concurrent radiation, temozolomide, and bevacizumab after resection. *J Clin Neurosci* 2017 **41** 75-77.
312. Ilie MD, Vasiljevic A, Raverot G & Bertolino P. The Microenvironment of Pituitary Tumors-Biological and Therapeutic Implications. *Cancers (Basel)* 2019 **11**.
313. Qiu L, He D, Fan X, Li Z, Liao C, Zhu Y & Wang H. The expression of interleukin (IL)-17 and IL-17 receptor and MMP-9 in human pituitary adenomas. *Pituitary* 2011 **14** 266-275.
314. Glebauskiene B, Liutkeviciene R, Vilkeviciute A, Gudinaviciene I, Rocyte A, Simonaviciute D, Mazetyte R, Kriauciuniene L & Zaliuniene D. Association of Ki-67 Labelling Index and IL-17A with Pituitary Adenoma. *Biomed Res Int* 2018 **2018** 7490585.
315. Qiu L, Yang J, Wang H, Zhu Y, Wang Y & Wu Q. Expression of T-helper-associated cytokines in the serum of pituitary adenoma patients preoperatively and postperatively. *Med Hypotheses* 2013 **80** 781-786.
316. Arzt E, Stelzer G, Renner U, Lange M, Muller OA & Stalla GK. Interleukin-2 and interleukin-2 receptor expression in human corticotrophic adenoma and murine pituitary cell cultures. *J Clin Invest* 1992 **90** 1944-1951.
317. Denicoff KD, Durkin TM, Lotze MT, Quinlan PE, Davis CL, Listwak SJ, Rosenberg SA & Rubinow DR. The neuroendocrine effects of interleukin-2 treatment. *J Clin Endocrinol Metab* 1989 **69** 402-410.

318. Karanth S & McCann SM. Anterior pituitary hormone control by interleukin 2. *Proc Natl Acad Sci U S A* 1991 **88** 2961-2965.
319. Arzt E, Sauer J, Buric R, Stalla J, Renner U & Stalla GK. Characterization of Interleukin-2 (IL-2) receptor expression and action of IL-2 and IL-6 on normal anterior pituitary cell growth. *Endocrine* 1995 **3** 113-119.
320. Cannavo S, Ferrau F, Cotta OR, Saitta S, Barresi V, Cristani MT, Saija A, Ruggeri RM, Trimarchi F & Gangemi S. Increased serum interleukin-22 levels in patients with PRL-secreting and non-functioning pituitary macroadenomas. *Pituitary* 2014 **17** 76-80.
321. Labeur M, Refojo D, Wolfel B, Stalla J, Vargas V, Theodoropoulou M, Buchfelder M, Paez-Pereda M, Arzt E & Stalla GK. Interferon-gamma inhibits cellular proliferation and ACTH production in corticotroph tumor cells through a novel janus kinases-signal transducer and activator of transcription 1/nuclear factor-kappa B inhibitory signaling pathway. *J Endocrinol* 2008 **199** 177-189.
322. Vankelecom H, Andries M, Billiau A & Denef C. Evidence that folliculo-stellate cells mediate the inhibitory effect of interferon-gamma on hormone secretion in rat anterior pituitary cell cultures. *Endocrinology* 1992 **130** 3537-3546.
323. Yagnik G, Rutowski MJ, Shah SS & Aghi MK. Stratifying nonfunctional pituitary adenomas into two groups distinguished by macrophage subtypes. *Oncotarget* 2019 **10** 2212-2223.
324. Pyle ME, Korbonits M, Gueorguiev M, Jordan S, Kola B, Morris DG, Meinhardt A, Powell MP, Claret FX, Zhang Q, Metz C, Bucala R & Grossman AB. Macrophage migration inhibitory factor expression is increased in pituitary adenoma cell nuclei. *J Endocrinol* 2003 **176** 103-110.
325. Wang Z, Ren SG & Melmed S. Hypothalamic and pituitary leukemia inhibitory factor gene expression in vivo: a novel endotoxin-inducible neuro-endocrine interface. *Endocrinology* 1996 **137** 2947-2953.
326. Stefana B, Ray DW & Melmed S. Leukemia inhibitory factor induces differentiation of pituitary corticotroph function: an immuno-neuroendocrine phenotypic switch. *Proc Natl Acad Sci U S A* 1996 **93** 12502-12506.
327. Tomida M, Yoshida U, Mogi C, Maruyama M, Goda H, Hatta Y & Inoue K. Leukaemia inhibitory factor and interleukin 6 inhibit secretion of prolactin and growth hormone by rat pituitary MtT/SM cells. *Cytokine* 2001 **14** 202-207.
328. Kontogeorgos G, Patralexis H, Tran A, Kovacs K & Melmed S. Expression of leukemia inhibitory factor in human pituitary adenomas: a morphologic and immunocytochemical study. *Pituitary* 2000 **2** 245-251.
329. Paez-Pereda M, Giacomini D, Refojo D, Nagashima AC, Hopfner U, Grubler Y, Chervin A, Goldberg V, Goya R, Hentges ST, Low MJ, Holsboer F, Stalla GK & Arzt E. Involvement of bone morphogenetic protein 4 (BMP-4) in pituitary prolactinoma pathogenesis through a Smad/estrogen receptor crosstalk. *Proc Natl Acad Sci U S A* 2003 **100** 1034-1039.
330. Giacomini D, Paez-Pereda M, Theodoropoulou M, Gerez J, Nagashima AC, Chervin A, Berner S, Labeur M, Refojo D, Renner U, Stalla GK & Arzt E. Bone morphogenetic protein-4 control of pituitary pathophysiology. *Front Horm Res* 2006 **35** 22-31.
331. Giacomini D, Paez-Pereda M, Theodoropoulou M, Labeur M, Refojo D, Gerez J, Chervin A, Berner S, Losa M, Buchfelder M, Renner U, Stalla GK & Arzt E. Bone morphogenetic protein-4 inhibits corticotroph tumor cells: involvement in the retinoic acid inhibitory action. *Endocrinology* 2006 **147** 247-256.
332. Hao NB, Lu MH, Fan YH, Cao YL, Zhang ZR & Yang SM. Macrophages in tumor microenvironments and the progression of tumors. *Clin Dev Immunol* 2012 **2012** 948098.
333. Mantovani A, Sica A, Sozzani S, Allavena P, Vecchi A & Locati M. The chemokine system in diverse forms of macrophage activation and polarization. *Trends Immunol* 2004 **25** 677-686.

334. Zhang J, Yao H, Song G, Liao X, Xian Y & Li W. Regulation of epithelial-mesenchymal transition by tumor-associated macrophages in cancer. *Am J Transl Res* 2015 **7** 1699-1711.
335. Bonde AK, Tischler V, Kumar S, Soltermann A & Schwendener RA. Intratumoral macrophages contribute to epithelial-mesenchymal transition in solid tumors. *BMC Cancer* 2012 **12** 35.
336. Lawrence T & Natoli G. Transcriptional regulation of macrophage polarization: enabling diversity with identity. *Nat Rev Immunol* 2011 **11** 750-761.
337. Mosser DM & Edwards JP. Exploring the full spectrum of macrophage activation. *Nat Rev Immunol* 2008 **8** 958-969.
338. Ong SM, Tan YC, Beretta O, Jiang D, Yeap WH, Tai JJ, Wong WC, Yang H, Schwarz H, Lim KH, Koh PK, Ling KL & Wong SC. Macrophages in human colorectal cancer are pro-inflammatory and prime T cells towards an anti-tumour type-1 inflammatory response. *Eur J Immunol* 2012 **42** 89-100.
339. Mantovani A, Schioppa T, Porta C, Allavena P & Sica A. Role of tumor-associated macrophages in tumor progression and invasion. *Cancer Metastasis Rev* 2006 **25** 315-322.
340. Ryder M, Ghossein RA, Ricarte-Filho JC, Knauf JA & Fagin JA. Increased density of tumor-associated macrophages is associated with decreased survival in advanced thyroid cancer. *Endocr Relat Cancer* 2008 **15** 1069-1074.
341. Steidl C, Lee T, Shah SP, Farinha P, Han G, Nayar T, Delaney A, Jones SJ, Iqbal J, Weisenburger DD, Bast MA, Rosenwald A, Muller-Hermelink HK, Rimsza LM, Campo E, Delabie J, Braziel RM, Cook JR, Tubbs RR, Jaffe ES, Lenz G, Connors JM, Staudt LM, Chan WC & Gascoyne RD. Tumor-associated macrophages and survival in classic Hodgkin's lymphoma. *N Engl J Med* 2010 **362** 875-885.
342. Wei IH, Harmon CM, Arcerito M, Cheng DF, Minter RM & Simeone DM. Tumor-associated macrophages are a useful biomarker to predict recurrence after surgical resection of nonfunctional pancreatic neuroendocrine tumors. *Ann Surg* 2014 **260** 1088-1094.
343. Hagemann T, Wilson J, Kulbe H, Li NF, Leinster DA, Charles K, Klemm F, Pukrop T, Binder C & Balkwill FR. Macrophages induce invasiveness of epithelial cancer cells via NF-kappa B and JNK. *J Immunol* 2005 **175** 1197-1205.
344. Hume DA, Halpin D, Charlton H & Gordon S. The mononuclear phagocyte system of the mouse defined by immunohistochemical localization of antigen F4/80: macrophages of endocrine organs. *Proc Natl Acad Sci U S A* 1984 **81** 4174-4177.
345. Mander TH & Morris JF. Development of microglia and macrophages in the postnatal rat pituitary. *Cell Tissue Res* 1996 **286** 347-355.
346. Fujiwara K, Yatabe M, Tofrizal A, Jindatip D, Yashiro T & Nagai R. Identification of M2 macrophages in anterior pituitary glands of normal rats and rats with estrogen-induced prolactinoma. *Cell Tissue Res* 2017 **368** 371-378.
347. Lu JQ, Adam B, Jack AS, Lam A, Broad RW & Chik CL. Immune Cell Infiltrates in Pituitary Adenomas: More Macrophages in Larger Adenomas and More T Cells in Growth Hormone Adenomas. *Endocr Pathol* 2015 **26** 263-272.
348. Sato M, Tamura R, Tamura H, Mase T, Kosugi K, Morimoto Y, Yoshida K & Toda M. Analysis of Tumor Angiogenesis and Immune Microenvironment in Non-Functional Pituitary Endocrine Tumors. *J Clin Med* 2019 **8**.
349. Asgharzadeh S, Salo JA, Ji L, Oberthuer A, Fischer M, Berthold F, Hadjidaniel M, Liu CW, Metelitsa LS, Pique-Regi R, Wakamatsu P, Villablanca JG, Kreissman SG, Matthay KK, Shimada H, London WB, Sposto R & Seeger RC. Clinical significance of tumor-associated inflammatory cells in metastatic neuroblastoma. *J Clin Oncol* 2012 **30** 3525-3532.
350. Carron EC, Homra S, Rosenberg J, Coffelt SB, Kittrell F, Zhang Y, Creighton CJ, Fuqua SA, Medina D & Machado HL. Macrophages promote the progression of premalignant mammary lesions to invasive cancer. *Oncotarget* 2017.

351. Colvin EK. Tumor-associated macrophages contribute to tumor progression in ovarian cancer. *Front Oncol* 2014 **4** 137.
352. Lan C, Huang X, Lin S, Huang H, Cai Q, Wan T, Lu J & Liu J. Expression of M2-polarized macrophages is associated with poor prognosis for advanced epithelial ovarian cancer. *Technol Cancer Res Treat* 2013 **12** 259-267.
353. Maolake A, Izumi K, Shigehara K, Natsagdorj A, Iwamoto H, Kadomoto S, Takezawa Y, Machioka K, Narimoto K, Namiki M, Lin WJ, Wufuer G & Mizokami A. Tumor-associated macrophages promote prostate cancer migration through activation of the CCL22-CCR4 axis. *Oncotarget* 2017 **8** 9739-9751.
354. Fang W, Ye L, Shen L, Cai J, Huang F, Wei Q, Fei X, Chen X, Guan H, Wang W, Li X & Ning G. Tumor-associated macrophages promote the metastatic potential of thyroid papillary cancer by releasing CXCL8. *Carcinogenesis* 2014 **35** 1780-1787.
355. Fridman WH, Pages F, Sautes-Fridman C & Galon J. The immune contexture in human tumours: impact on clinical outcome. *Nat Rev Cancer* 2012 **12** 298-306.
356. Le Bitoux MA & Stamenkovic I. Tumor-host interactions: the role of inflammation. *Histochem Cell Biol* 2008 **130** 1079-1090.
357. Uppaluri R, Dunn GP & Lewis JS, Jr. Focus on TILs: prognostic significance of tumor infiltrating lymphocytes in head and neck cancers. *Cancer Immun* 2008 **8** 16.
358. Balkwill F, Montfort A & Capasso M. B regulatory cells in cancer. *Trends Immunol* 2013 **34** 169-173.
359. Mauri C & Bosma A. Immune regulatory function of B cells. *Annu Rev Immunol* 2012 **30** 221-241.
360. Olkhanud PB, Damdinsuren B, Bodogai M, Gress RE, Sen R, Wejksza K, Malchinkhuu E, Wersto RP & Biragyn A. Tumor-evoked regulatory B cells promote breast cancer metastasis by converting resting CD4(+) T cells to T-regulatory cells. *Cancer Res* 2011 **71** 3505-3515.
361. Schioppa T, Moore R, Thompson RG, Rosser EC, Kulbe H, Nedospasov S, Mauri C, Coussens LM & Balkwill FR. B regulatory cells and the tumor-promoting actions of TNF-alpha during squamous carcinogenesis. *Proc Natl Acad Sci U S A* 2011 **108** 10662-10667.
362. Tachibana T, Onodera H, Tsuruyama T, Mori A, Nagayama S, Hiai H & Imamura M. Increased intratumor Valpha24-positive natural killer T cells: a prognostic factor for primary colorectal carcinomas. *Clin Cancer Res* 2005 **11** 7322-7327.
363. Bando H, Iguchi G, Fukuoka H, Taniguchi M, Yamamoto M, Matsumoto R, Suda K, Nishizawa H, Takahashi M, Kohmura E & Takahashi Y. The prevalence of IgG4-related hypophysitis in 170 consecutive patients with hypopituitarism and/or central diabetes insipidus and review of the literature. *Eur J Endocrinol* 2014 **170** 161-172.
364. Guaraldi F, Giordano R, Grottoli S, Ghizzoni L, Arvat E & Ghigo E. Pituitary Autoimmunity. *Front Horm Res* 2017 **48** 48-68.
365. Lin HH, Gutenberg A, Chen TY, Tsai NM, Lee CJ, Cheng YC, Cheng WH, Tzou YM, Caturegli P & Tzou SC. In Situ Activation of Pituitary-Infiltrating T Lymphocytes in Autoimmune Hypophysitis. *Sci Rep* 2017 **7** 43492.
366. Rossi ML, Jones NR, Esiri MM, Havas L, al Izzi M & Coakham HB. Mononuclear cell infiltrate and HLA-Dr expression in 28 pituitary adenomas. *Tumori* 1990 **76** 543-547.
367. Gerli R, Rambotti P, Nicoletti I, Orlandi S, Migliorati G & Riccardi C. Reduced number of natural killer cells in patients with pathological hyperprolactinemia. *Clin Exp Immunol* 1986 **64** 399-406.
368. Ishibashi M, Kuzuya N, Sawada S, Kitamura K, Kamoi K & Yamaji T. Anti-thyroid antibodies in patients with hyperprolactinemia. *Endocrinol Jpn* 1991 **38** 517-522.
369. Heshmati HM, Kujas M, Casanova S, Wollan PC, Racadot J, Van Effenterre R, Derome PJ & Turpin G. Prevalence of lymphocytic infiltrate in 1400 pituitary adenomas. *Endocr J* 1998 **45** 357-361.

370. Jacobs JF, Idema AJ, Bol KF, Nierkens S, Grauer OM, Wesseling P, Grotenhuis JA, Hoogerbrugge PM, de Vries IJ & Adema GJ. Regulatory T cells and the PD-L1/PD-1 pathway mediate immune suppression in malignant human brain tumors. *Neuro Oncol* 2009 **11** 394-402.
371. Lupi I, Manetti L, Caturegli P, Menicagli M, Cosottini M, Iannelli A, Acerbi G, Bevilacqua G, Bogazzi F & Martino E. Tumor infiltrating lymphocytes but not serum pituitary antibodies are associated with poor clinical outcome after surgery in patients with pituitary adenoma. *J Clin Endocrinol Metab* 2010 **95** 289-296.
372. Mei Y, Bi WL, Greenwald NF, Du Z, Agar NY, Kaiser UB, Woodmansee WW, Reardon DA, Freeman GJ, Fecci PE, Laws ER, Jr., Santagata S, Dunn GP & Dunn IF. Increased expression of programmed death ligand 1 (PD-L1) in human pituitary tumors. *Oncotarget* 2016 **7** 76565-76576.
373. Gandini S, Massi D & Mandala M. PD-L1 expression in cancer patients receiving anti PD-1/PD-L1 antibodies: A systematic review and meta-analysis. *Crit Rev Oncol Hematol* 2016 **100** 88-98.
374. Wang PF, Wang TJ, Yang YK, Yao K, Li Z, Li YM & Yan CX. The expression profile of PD-L1 and CD8(+) lymphocyte in pituitary adenomas indicating for immunotherapy. *J Neurooncol* 2018 **139** 89-95.
375. Kemeny HR, Elsamadicy AA, Farber SH, Champion CD, Lorrey SJ, Chongsathidkiet P, Woroniecka KI, Cui X, Shen SH, Rhodin KE, Tsvankin V, Everitt J, Sanchez-Perez L, Healy P, McLendon RE, Codd P, Dunn IF & Fecci PE. Targeting PD-L1 initiates effective anti-tumor immunity in a murine model of Cushing's Disease. *Clin Cancer Res* 2019.
376. Lin AL, Jonsson P, Tabar V, Yang TJ, Cuaron J, Beal K, Cohen M, Postow M, Rosenblum M, Shia J, DeAngelis LM, Taylor BS, Young RJ & Geer EB. Marked Response of a Hypermutated ACTH-Secreting Pituitary Carcinoma to Ipilimumab and Nivolumab. *J Clin Endocrinol Metab* 2018 **103** 3925-3930.
377. Gabrilovich DI, Ostrand-Rosenberg S & Bronte V. Coordinated regulation of myeloid cells by tumours. *Nat Rev Immunol* 2012 **12** 253-268.
378. Huang B, Pan PY, Li Q, Sato AI, Levy DE, Bromberg J, Divino CM & Chen SH. Gr-1+CD115+ immature myeloid suppressor cells mediate the development of tumor-induced T regulatory cells and T-cell anergy in tumor-bearing host. *Cancer Res* 2006 **66** 1123-1131.
379. Sinha P, Clements VK, Bunt SK, Albelda SM & Ostrand-Rosenberg S. Cross-talk between myeloid-derived suppressor cells and macrophages subverts tumor immunity toward a type 2 response. *J Immunol* 2007 **179** 977-983.
380. Satpathy AT, Kc W, Albring JC, Edelson BT, Kretzer NM, Bhattacharya D, Murphy TL & Murphy KM. Zbtb46 expression distinguishes classical dendritic cells and their committed progenitors from other immune lineages. *J Exp Med* 2012 **209** 1135-1152.
381. Fridlender ZG, Sun J, Kim S, Kapoor V, Cheng G, Ling L, Worthen GS & Albelda SM. Polarization of tumor-associated neutrophil phenotype by TGF-beta: "N1" versus "N2" TAN. *Cancer Cell* 2009 **16** 183-194.
382. Granot Z, Henke E, Comen EA, King TA, Norton L & Benezra R. Tumor entrained neutrophils inhibit seeding in the premetastatic lung. *Cancer Cell* 2011 **20** 300-314.
383. Cirri P & Chiarugi P. Cancer-associated-fibroblasts and tumour cells: a diabolic liaison driving cancer progression. *Cancer Metastasis Rev* 2012 **31** 195-208.
384. Shiga K, Hara M, Nagasaki T, Sato T, Takahashi H & Takeyama H. Cancer-Associated Fibroblasts: Their Characteristics and Their Roles in Tumor Growth. *Cancers (Basel)* 2015 **7** 2443-2458.
385. Duluc C, Moatassim-Billah S, Chalabi-Dchar M, Perraud A, Samain R, Breibach F, Gayral M, Cordelier P, Delisle MB, Bousquet-Dubouch MP, Tomasini R, Schmid H, Mathonnet M, Pyronnet S, Martineau Y & Bousquet C. Pharmacological targeting of the protein synthesis

mTOR/4E-BP1 pathway in cancer-associated fibroblasts abrogates pancreatic tumour chemoresistance. *EMBO Mol Med* 2015 **7** 735-753.
386. Sappino AP, Skalli O, Jackson B, Schurch W & Gabbiani G. Smooth-muscle differentiation in stromal cells of malignant and non-malignant breast tissues. *Int J Cancer* 1988 **41** 707-712.
387. Soon PS, Kim E, Pon CK, Gill AJ, Moore K, Spillane AJ, Benn DE & Baxter RC. Breast cancer-associated fibroblasts induce epithelial-to-mesenchymal transition in breast cancer cells. *Endocr Relat Cancer* 2013 **20** 1-12.
388. Giannoni E, Bianchini F, Masieri L, Serni S, Torre E, Calorini L & Chiarugi P. Reciprocal activation of prostate cancer cells and cancer-associated fibroblasts stimulates epithelial-mesenchymal transition and cancer stemness. *Cancer Res* 2010 **70** 6945-6956.
389. Liao Y, Ni Y, He R, Liu W & Du J. Clinical implications of fibroblast activation protein-alpha in non-small cell lung cancer after curative resection: a new predictor for prognosis. *J Cancer Res Clin Oncol* 2013 **139** 1523-1528.
390. Wu X, Tao P, Zhou Q, Li J, Yu Z, Wang X, Li J, Li C, Yan M, Zhu Z, Liu B & Su L. IL-6 secreted by cancer-associated fibroblasts promotes epithelial-mesenchymal transition and metastasis of gastric cancer via JAK2/STAT3 signaling pathway. *Oncotarget* 2017.
391. Moatassim-Billah S, Duluc C, Samain R, Jean C, Perraud A, Decaup E, Cassant-Sourdy S, Bakri Y, Selves J, Schmid H, Martineau Y, Mathonnet M, Pyronnet S & Bousquet C. Anti-metastatic potential of somatostatin analog SOM230: Indirect pharmacological targeting of pancreatic cancer-associated fibroblasts. *Oncotarget* 2016 **7** 41584-41598.
392. Chen WL, Huang CH, Chiou LL, Chen TH, Huang YY, Jiang CC, Lee HS & Dong CY. Multiphoton imaging and quantitative analysis of collagen production by chondrogenic human mesenchymal stem cells cultured in chitosan scaffold. *Tissue Eng Part C Methods* 2010 **16** 913-920.
393. Gudjonsson T, Ronnov-Jessen L, Villadsen R, Rank F, Bissell MJ & Petersen OW. Normal and tumor-derived myoepithelial cells differ in their ability to interact with luminal breast epithelial cells for polarity and basement membrane deposition. *J Cell Sci* 2002 **115** 39-50.
394. Sundberg C, Ivarsson M, Gerdin B & Rubin K. Pericytes as collagen-producing cells in excessive dermal scarring. *Lab Invest* 1996 **74** 452-466.
395. Tofrizal A, Fujiwara K, Yashiro T & Yamada S. Alterations of collagen-producing cells in human pituitary adenomas. *Med Mol Morphol* 2016 **49** 224-232.
396. Lv L, Zhang S, Hu Y, Zhou P, Gao L, Wang M, Sun Z, Chen C, Yin S, Wang X & Jiang S. Invasive Pituitary Adenoma-Derived Tumor-Associated Fibroblasts Promote Tumor Progression both In Vitro and In Vivo. *Exp Clin Endocrinol Diabetes* 2018 **126** 213-221.
397. Navarro R, Compte M, Alvarez-Vallina L & Sanz L. Immune Regulation by Pericytes: Modulating Innate and Adaptive Immunity. *Front Immunol* 2016 **7** 480.
398. Cooke VG, LeBleu VS, Keskin D, Khan Z, O'Connell JT, Teng Y, Duncan MB, Xie L, Maeda G, Vong S, Sugimoto H, Rocha RM, Damascena A, Brentani RR & Kalluri R. Pericyte depletion results in hypoxia-associated epithelial-to-mesenchymal transition and metastasis mediated by met signaling pathway. *Cancer Cell* 2012 **21** 66-81.
399. O'Keeffe MB, Devlin AH, Burns AJ, Gardiner TA, Logan ID, Hirst DG & McKeown SR. Investigation of pericytes, hypoxia, and vascularity in bladder tumors: association with clinical outcomes. *Oncol Res* 2008 **17** 93-101.
400. Yonenaga Y, Mori A, Onodera H, Yasuda S, Oe H, Fujimoto A, Tachibana T & Imamura M. Absence of smooth muscle actin-positive pericyte coverage of tumor vessels correlates with hematogenous metastasis and prognosis of colorectal cancer patients. *Oncology* 2005 **69** 159-166.
401. Fujiwara K, Jindatip D, Kikuchi M & Yashiro T. In situ hybridization reveals that type I and III collagens are produced by pericytes in the anterior pituitary gland of rats. *Cell Tissue Res* 2010 **342** 491-495.

402. Perez-Castro C, Renner U, Haedo MR, Stalla GK & Arzt E. Cellular and molecular specificity of pituitary gland physiology. *Physiol Rev* 2012 **92** 1-38.
403. Hofler H, Walter GF & Denk H. Immunohistochemistry of folliculo-stellate cells in normal human adenohypophyses and in pituitary adenomas. *Acta Neuropathol* 1984 **65** 35-40.
404. Iwaki T, Kondo A, Takeshita I, Nakagaki H, Kitamura K & Tateishi J. Proliferating potential of folliculo-stellate cells in human pituitary adenomas. Immunohistochemical and electron microscopic analysis. *Acta Neuropathol* 1986 **71** 233-242.
405. Lauriola L, Cocchia D, Sentinelli S, Maggiano N, Maira G & Michetti F. Immunohistochemical detection of folliculo-stellate cells in human pituitary adenomas. *Virchows Arch B Cell Pathol Incl Mol Pathol* 1984 **47** 189-197.
406. Sbarbati A, Fakhreddine A, Zancanaro C, Bontempini L & Cinti S. Ultrastructural morphology of folliculo-stellate cells in human pituitary adenomas. *Ultrastruct Pathol* 1991 **15** 241-248.
407. Tachibana O & Yamashima T. Immunohistochemical study of folliculo-stellate cells in human pituitary adenomas. *Acta Neuropathol* 1988 **76** 458-464.
408. Voit D, Saeger W & Ludecke DK. Folliculo-stellate cells in pituitary adenomas of patients with acromegaly. *Pathol Res Pract* 1999 **195** 143-147.
409. Tortosa F, Pires M & Ortiz S. [Prognostic implications of folliculo-stellate cells in pituitary adenomas: relationship with tumoral behavior]. *Rev Neurol* 2016 **63** 297-302.
410. Horiguchi K, Kikuchi M, Kusumoto K, Fujiwara K, Kouki T, Kawanishi K & Yashiro T. Living-cell imaging of transgenic rat anterior pituitary cells in primary culture reveals novel characteristics of folliculo-stellate cells. *J Endocrinol* 2010 **204** 115-123.
411. Horiguchi K, Fujiwara K, Higuchi M, Yoshida S, Tsukada T, Ueharu H, Chen M, Hasegawa R, Takigami S, Ohsako S, Yashiro T, Kato T & Kato Y. Expression of chemokine CXCL10 in dendritic-cell-like S100beta-positive cells in rat anterior pituitary gland. *Cell Tissue Res* 2014 **357** 757-765.
412. Ueta Y, Levy A, Chowdrey HS & Lightman SL. S-100 antigen-positive folliculostellate cells are not the source of IL-6 gene expression in human pituitary adenomas. *J Neuroendocrinol* 1995 **7** 467-474.
413. Vajtai I, Sahli R & Kappeler A. Pituitary prolactinoma with T cell rich inflammatory infiltrate: a possible example of antitumoral immune response to be differentiated from lymphocytic hypophysitis. *Acta Neuropathol* 2006 **111** 397-399.
414. Matsumoto H, Ishibashi Y, Ohtaki T, Hasegawa Y, Koyama C & Inoue K. Newly established murine pituitary folliculo-stellate-like cell line (TtT/GF) secretes potent pituitary glandular cell survival factors, one of which corresponds to metalloproteinase inhibitor. *Biochem Biophys Res Commun* 1993 **194** 909-915.
415. Schechter J, Ahmad N & Weiner R. Activation of anterior pituitary folliculo-stellate cells in the formation of estrogen-induced prolactin-secreting tumors. *Neuroendocrinology* 1988 **48** 569-576.
416. Cristina C, Luque GM, Demarchi G, Lopez Vicchi F, Zubeldia-Brenner L, Perez Millan MI, Perrone S, Ornstein AM, Lacau-Mengido IM, Berner SI & Becu-Villalobos D. Angiogenesis in pituitary adenomas: human studies and new mutant mouse models. *Int J Endocrinol* 2014 **2014** 608497.
417. Carmeliet P & Jain RK. Molecular mechanisms and clinical applications of angiogenesis. *Nature* 2011 **473** 298-307.
418. Jain RK. Normalization of tumor vasculature: an emerging concept in antiangiogenic therapy. *Science* 2005 **307** 58-62.
419. Alitalo A & Detmar M. Interaction of tumor cells and lymphatic vessels in cancer progression. *Oncogene* 2012 **31** 4499-4508.
420. Swartz MA & Lund AW. Lymphatic and interstitial flow in the tumour microenvironment: linking mechanobiology with immunity. *Nat Rev Cancer* 2012 **12** 210-219.

421. Turner HE, Nagy Z, Gatter KC, Esiri MM, Harris AL & Wass JA. Angiogenesis in pituitary adenomas and the normal pituitary gland. *J Clin Endocrinol Metab* 2000 **85** 1159-1162.
422. Turner HE, Nagy Z, Gatter KC, Esiri MM, Harris AL & Wass JA. Angiogenesis in pituitary adenomas - relationship to endocrine function, treatment and outcome. *J Endocrinol* 2000 **165** 475-481.
423. Perez-Millan MI, Berner SI, Luque GM, De Bonis C, Sevlever G, Becu-Villalobos D & Cristina C. Enhanced nestin expression and small blood vessels in human pituitary adenomas. *Pituitary* 2013 **16** 303-310.
424. Itoh J, Serizawa A, Kawai K, Ishii Y, Teramoto A & Osamura RY. Vascular networks and endothelial cells in the rat experimental pituitary glands and in the human pituitary adenomas. *Microsc Res Tech* 2003 **60** 231-235.
425. Stefaneanu L, Kovacs K, Scheithauer BW, Kontogeorgos G, Riehle DL, Sebo TJ, Murray D, Vidal S, Tran A, Buchfelder M & Fahlbusch R. Effect of Dopamine Agonists on Lactotroph Adenomas of the Human Pituitary. *Endocr Pathol* 2000 **11** 341-352.
426. Turner HE, Nagy Z, Gatter KC, Esiri MM, Wass JA & Harris AL. Proliferation, bcl-2 expression and angiogenesis in pituitary adenomas: relationship to tumour behaviour. *Br J Cancer* 2000 **82** 1441-1445.
427. Vidal S, Scheithauer BW & Kovacs K. Vascularity in Nontumorous Human Pituitaries and Incidental Microadenomas: A Morphometric Study. *Endocr Pathol* 2000 **11** 215-227.
428. Ortiz LD, Syro LV, Scheithauer BW, Ersen A, Uribe H, Fadul CE, Rotondo F, Horvath E & Kovacs K. Anti-VEGF therapy in pituitary carcinoma. *Pituitary* 2012 **15** 445-449.
429. DeClerck YA, Mercurio AM, Stack MS, Chapman HA, Zutter MM, Muschel RJ, Raz A, Matrisian LM, Sloane BF, Noel A, Hendrix MJ, Coussens L & Padarathsingh M. Proteases, extracellular matrix, and cancer: a workshop of the path B study section. *Am J Pathol* 2004 **164** 1131-1139.
430. Krishnamachary B, Stasinopoulos I, Kakkad S, Penet MF, Jacob D, Wildes F, Mironchik Y, Pathak AP, Solaiyappan M & Bhujwalla ZM. Breast cancer cell cyclooxygenase-2 expression alters extracellular matrix structure and function and numbers of cancer associated fibroblasts. *Oncotarget* 2017.
431. Asimakopoulos F, Hope C, Johnson MG, Pagenkopf A, Gromek K & Nagel B. Extracellular matrix and the myeloid-in-myeloma compartment: balancing tolerogenic and immunogenic inflammation in the myeloma niche. *J Leukoc Biol* 2017.
432. Smith YE, Vellanki SH & Hopkins AM. Dynamic interplay between adhesion surfaces in carcinomas: Cell-cell and cell-matrix crosstalk. *World J Biol Chem* 2016 **7** 64-77.
433. Egeblad M & Werb Z. New functions for the matrix metalloproteinases in cancer progression. *Nat Rev Cancer* 2002 **2** 161-174.
434. Sounni NE, Janssen M, Foidart JM & Noel A. Membrane type-1 matrix metalloproteinase and TIMP-2 in tumor angiogenesis. *Matrix Biol* 2003 **22** 55-61.
435. van der Steen SC, Bulten J, Van de Vijver KK, van Kuppevelt TH & Massuger LF. Changes in the Extracellular Matrix Are Associated With the Development of Serous Tubal Intraepithelial Carcinoma Into High-Grade Serous Carcinoma. *Int J Gynecol Cancer* 2017.
436. Kudo D, Suto A & Hakamada K. The Development of a Novel Therapeutic Strategy to Target Hyaluronan in the Extracellular Matrix of Pancreatic Ductal Adenocarcinoma. *Int J Mol Sci* 2017 **18**.
437. Wang M, Zhao J, Zhang L, Wei F, Lian Y, Wu Y, Gong Z, Zhang S, Zhou J, Cao K, Li X, Xiong W, Li G, Zeng Z & Guo C. Role of tumor microenvironment in tumorigenesis. *J Cancer* 2017 **8** 761-773.
438. Rainero E. Extracellular matrix endocytosis in controlling matrix turnover and beyond: emerging roles in cancer. *Biochem Soc Trans* 2016 **44** 1347-1354.
439. Visse R & Nagase H. Matrix metalloproteinases and tissue inhibitors of metalloproteinases: structure, function, and biochemistry. *Circ Res* 2003 **92** 827-839.

440. Hofmann UB, Eggert AA, Blass K, Brocker EB & Becker JC. Expression of matrix metalloproteinases in the microenvironment of spontaneous and experimental melanoma metastases reflects the requirements for tumor formation. *Cancer Res* 2003 **63** 8221-8225.
441. Kessenbrock K, Plaks V & Werb Z. Matrix metalloproteinases: regulators of the tumor microenvironment. *Cell* 2010 **141** 52-67.
442. Hrabec E, Strek M, Nowak D, Greger J, Suwalski M & Hrabec Z. Activity of type IV collagenases (MMP-2 and MMP-9) in primary pulmonary carcinomas: a quantitative analysis. *J Cancer Res Clin Oncol* 2002 **128** 197-204.
443. Nakagawa T, Kubota T, Kabuto M, Sato K, Kawano H, Hayakawa T & Okada Y. Production of matrix metalloproteinases and tissue inhibitor of metalloproteinases-1 by human brain tumors. *J Neurosurg* 1994 **81** 69-77.
444. Wang H, Li WS, Shi DJ, Ye ZP, Tai F, He HY, Liang CF, Gong J & Guo Y. Correlation of MMP(1) and TIMP (1) expression with pituitary adenoma fibrosis. *J Neurooncol* 2008 **90** 151-156.
445. Jarzembowski J, Lloyd R & McKeever P. Type IV collagen immunostaining is a simple, reliable diagnostic tool for distinguishing between adenomatous and normal pituitary glands. *Arch Pathol Lab Med* 2007 **131** 931-935.
446. Ceylan S, Anik I, Koc K, Kokturk S, Ceylan S, Cine N, Savli H, Sirin G, Sam B & Gazioglu N. Microsurgical anatomy of membranous layers of the pituitary gland and the expression of extracellular matrix collagenous proteins. *Acta Neurochir (Wien)* 2011 **153** 2435-2443; discussion 2443.
447. Kawamoto H, Uozumi T, Kawamoto K, Arita K, Yano T & Hirohata T. Type IV collagenase activity and cavernous sinus invasion in human pituitary adenomas. *Acta Neurochir (Wien)* 1996 **138** 390-395.
448. Liu HY, Gu WJ, Wang CZ, Ji XJ & Mu YM. Matrix metalloproteinase-9 and -2 and tissue inhibitor of matrix metalloproteinase-2 in invasive pituitary adenomas: A systematic review and meta-analysis of case-control trials. *Medicine (Baltimore)* 2016 **95** e3904.
449. Azorin E, Solano-Agama C & Mendoza-Garrido ME. The invasion mode of GH(3) cells is conditioned by collagen subtype, and its efficiency depends on cell-cell adhesion. *Arch Biochem Biophys* 2012 **528** 148-155.
450. Liu W, Matsumoto Y, Okada M, Miyake K, Kunishio K, Kawai N, Tamiya T & Nagao S. Matrix metalloproteinase 2 and 9 expression correlated with cavernous sinus invasion of pituitary adenomas. *J Med Invest* 2005 **52** 151-158.
451. Turner HE, Nagy Z, Esiri MM, Harris AL & Wass JA. Role of matrix metalloproteinase 9 in pituitary tumor behavior. *J Clin Endocrinol Metab* 2000 **85** 2931-2935.
452. Gong J, Zhao Y, Abdel-Fattah R, Amos S, Xiao A, Lopes MB, Hussaini IM & Laws ER. Matrix metalloproteinase-9, a potential biological marker in invasive pituitary adenomas. *Pituitary* 2008 **11** 37-48.
453. Gultekin GD, Cabuk B, Vural C & Ceylan S. Matrix metalloproteinase-9 and tissue inhibitor of matrix metalloproteinase-2: Prognostic biological markers in invasive prolactinomas. *J Clin Neurosci* 2015 **22** 1282-1287.
454. Paez Pereda M, Ledda MF, Goldberg V, Chervin A, Carrizo G, Molina H, Muller A, Renner U, Podhajcer O, Arzt E & Stalla GK. High levels of matrix metalloproteinases regulate proliferation and hormone secretion in pituitary cells. *J Clin Endocrinol Metab* 2000 **85** 263-269.
455. Malik MT & Kakar SS. Regulation of angiogenesis and invasion by human Pituitary tumor transforming gene (PTTG) through increased expression and secretion of matrix metalloproteinase-2 (MMP-2). *Mol Cancer* 2006 **5** 61.
456. Li S, Zhang Z, Xue J, Guo X, Liang S & Liu A. Effect of Hypoxia on DDR1 Expression in Pituitary Adenomas. *Med Sci Monit* 2015 **21** 2433-2438.

457. Yoshida D & Teramoto A. Enhancement of pituitary adenoma cell invasion and adhesion is mediated by discoidin domain receptor-1. *J Neurooncol* 2007 **82** 29-40.
458. Yoshida D, Nomura R & Teramoto A. Regulation of cell invasion and signalling pathways in the pituitary adenoma cell line, HP-75, by reversion-inducing cysteine-rich protein with kazal motifs (RECK). *J Neurooncol* 2008 **89** 141-150.
459. Zhao C, Zhang M, Liu W, Wang C, Zhang Q & Li W. beta-Catenin knockdown inhibits pituitary adenoma cell proliferation and invasion via interfering with AKT and gelatinases expression. *Int J Oncol* 2015 **46** 1643-1650.
460. Hui P, Xu X, Xu L, Hui G, Wu S & Lan Q. Expression of MMP14 in invasive pituitary adenomas: relationship to invasion and angiogenesis. *Int J Clin Exp Pathol* 2015 **8** 3556-3567.
461. Di Meo A, Rotondo F, Kovacs K, Cusimano MD, Syro LV, Di Ieva A, Diamandis EP & Yousef GM. Human kallikrein 10 expression in surgically removed human pituitary corticotroph adenomas: an immunohistochemical study. *Appl Immunohistochem Mol Morphol* 2015 **23** 433-437.
462. Rotondo F, Di Ieva A, Kovacs K, Cusimano MD, Syro LV, Diamandis EP & Yousef GM. Human kallikrein 10 in surgically removed human pituitary adenomas. *Hormones (Athens)* 2015 **14** 272-279.
463. Tanase C, Albulescu R, Codrici E, Calenic B, Popescu ID, Mihai S, Necula L, Cruceru ML & Hinescu ME. Decreased expression of APAF-1 and increased expression of cathepsin B in invasive pituitary adenoma. *Onco Targets Ther* 2015 **8** 81-90.
464. Farnoud MR, Veirana N, Derome P, Peillon F & Li JY. Adenomatous transformation of the human anterior pituitary is associated with alterations in integrin expression. *Int J Cancer* 1996 **67** 45-53.
465. Farnoud MR, Farhadian F, Samuel JL, Derome P, Peillon F & Li JY. Fibronectin isoforms are differentially expressed in normal and adenomatous human anterior pituitaries. *Int J Cancer* 1995 **61** 27-34.
466. De Craene B & Berx G. Regulatory networks defining EMT during cancer initiation and progression. *Nat Rev Cancer* 2013 **13** 97-110.
467. Thiery JP, Acloque H, Huang RY & Nieto MA. Epithelial-mesenchymal transitions in development and disease. *Cell* 2009 **139** 871-890.
468. Lee JM, Dedhar S, Kalluri R & Thompson EW. The epithelial-mesenchymal transition: new insights in signaling, development, and disease. *J Cell Biol* 2006 **172** 973-981.
469. Bhowmick NA, Neilson EG & Moses HL. Stromal fibroblasts in cancer initiation and progression. *Nature* 2004 **432** 332-337.
470. Knutson KL, Lu H, Stone B, Reiman JM, Behrens MD, Prosperi CM, Gad EA, Smorlesi A & Disis ML. Immunoediting of cancers may lead to epithelial to mesenchymal transition. *J Immunol* 2006 **177** 1526-1533.
471. Lebret SC, Newgreen DF, Thompson EW & Ackland ML. Induction of epithelial to mesenchymal transition in PMC42-LA human breast carcinoma cells by carcinoma-associated fibroblast secreted factors. *Breast Cancer Res* 2007 **9** R19.
472. Reiman JM, Knutson KL & Radisky DC. Immune promotion of epithelial-mesenchymal transition and generation of breast cancer stem cells. *Cancer Res* 2010 **70** 3005-3008.
473. Bakin AV, Tomlinson AK, Bhowmick NA, Moses HL & Arteaga CL. Phosphatidylinositol 3-kinase function is required for transforming growth factor beta-mediated epithelial to mesenchymal transition and cell migration. *J Biol Chem* 2000 **275** 36803-36810.
474. Gocheva V, Zeng W, Ke D, Klimstra D, Reinheckel T, Peters C, Hanahan D & Joyce JA. Distinct roles for cysteine cathepsin genes in multistage tumorigenesis. *Genes Dev* 2006 **20** 543-556.

475. Lu Z, Ghosh S, Wang Z & Hunter T. Downregulation of caveolin-1 function by EGF leads to the loss of E-cadherin, increased transcriptional activity of beta-catenin, and enhanced tumor cell invasion. *Cancer Cell* 2003 **4** 499-515.
476. Orlichenko LS & Radisky DC. Matrix metalloproteinases stimulate epithelial-mesenchymal transition during tumor development. *Clin Exp Metastasis* 2008 **25** 593-600.
477. Tang J, Xiao L, Cui R, Li D, Zheng X, Zhu L, Sun H, Pan Y, Du Y & Yu X. CX3CL1 increases invasiveness and metastasis by promoting epithelial-to-mesenchymal transition through the TACE/TGF-alpha/EGFR pathway in hypoxic androgen-independent prostate cancer cells. *Oncol Rep* 2016 **35** 1153-1162.
478. Vincent T, Neve EP, Johnson JR, Kukalev A, Rojo F, Albanell J, Pietras K, Virtanen I, Philipson L, Leopold PL, Crystal RG, de Herreros AG, Moustakas A, Pettersson RF & Fuxe J. A SNAIL1-SMAD3/4 transcriptional repressor complex promotes TGF-beta mediated epithelial-mesenchymal transition. *Nat Cell Biol* 2009 **11** 943-950.
479. Mitselou A, Galani V, Skoufi U, Arvanitis DL, Lampri E & Ioachim E. Syndecan-1, Epithelial-Mesenchymal Transition Markers (E-cadherin/beta-catenin) and Neoangiogenesis-related Proteins (PCAM-1 and Endoglin) in Colorectal Cancer. *Anticancer Res* 2016 **36** 2271-2280.
480. Szatmari T, Otvos R, Hjerpe A & Dobra K. Syndecan-1 in Cancer: Implications for Cell Signaling, Differentiation, and Prognostication. *Dis Markers* 2015 **2015** 796052.
481. De Craene B, Gilbert B, Stove C, Bruyneel E, van Roy F & Berx G. The transcription factor snail induces tumor cell invasion through modulation of the epithelial cell differentiation program. *Cancer Res* 2005 **65** 6237-6244.
482. Batlle E, Sancho E, Franci C, Dominguez D, Monfar M, Baulida J & Garcia De Herreros A. The transcription factor snail is a repressor of E-cadherin gene expression in epithelial tumour cells. *Nat Cell Biol* 2000 **2** 84-89.
483. Cano A, Perez-Moreno MA, Rodrigo I, Locascio A, Blanco MJ, del Barrio MG, Portillo F & Nieto MA. The transcription factor snail controls epithelial-mesenchymal transitions by repressing E-cadherin expression. *Nat Cell Biol* 2000 **2** 76-83.
484. Comijn J, Berx G, Vermassen P, Verschueren K, van Grunsven L, Bruyneel E, Mareel M, Huylebroeck D & van Roy F. The two-handed E box binding zinc finger protein SIP1 downregulates E-cadherin and induces invasion. *Mol Cell* 2001 **7** 1267-1278.
485. Eger A, Aigner K, Sonderegger S, Dampier B, Oehler S, Schreiber M, Berx G, Cano A, Beug H & Foisner R. DeltaEF1 is a transcriptional repressor of E-cadherin and regulates epithelial plasticity in breast cancer cells. *Oncogene* 2005 **24** 2375-2385.
486. Moreno-Bueno G, Cubillo E, Sarrio D, Peinado H, Rodriguez-Pinilla SM, Villa S, Bolos V, Jorda M, Fabra A, Portillo F, Palacios J & Cano A. Genetic profiling of epithelial cells expressing E-cadherin repressors reveals a distinct role for Snail, Slug, and E47 factors in epithelial-mesenchymal transition. *Cancer Res* 2006 **66** 9543-9556.
487. Vandewalle C, Comijn J, De Craene B, Vermassen P, Bruyneel E, Andersen H, Tulchinsky E, Van Roy F & Berx G. SIP1/ZEB2 induces EMT by repressing genes of different epithelial cell-cell junctions. *Nucleic Acids Res* 2005 **33** 6566-6578.
488. Burk U, Schubert J, Wellner U, Schmalhofer O, Vincan E, Spaderna S & Brabletz T. A reciprocal repression between ZEB1 and members of the miR-200 family promotes EMT and invasion in cancer cells. *EMBO Rep* 2008 **9** 582-589.
489. Siemens H, Jackstadt R, Hunten S, Kaller M, Menssen A, Gotz U & Hermeking H. miR-34 and SNAIL form a double-negative feedback loop to regulate epithelial-mesenchymal transitions. *Cell Cycle* 2011 **10** 4256-4271.
490. Varambally S, Cao Q, Mani RS, Shankar S, Wang X, Ateeq B, Laxman B, Cao X, Jing X, Ramnarayanan K, Brenner JC, Yu J, Kim JH, Han B, Tan P, Kumar-Sinha C, Lonigro RJ, Palanisamy N, Maher CA & Chinnaiyan AM. Genomic loss of microRNA-101 leads to

overexpression of histone methyltransferase EZH2 in cancer. *Science* 2008 **322** 1695-1699.
491. Reinke LM, Xu Y & Cheng C. Snail represses the splicing regulator epithelial splicing regulatory protein 1 to promote epithelial-mesenchymal transition. *J Biol Chem* 2012 **287** 36435-36442.
492. Warzecha CC, Jiang P, Amirikian K, Dittmar KA, Lu H, Shen S, Guo W, Xing Y & Carstens RP. An ESRP-regulated splicing programme is abrogated during the epithelial-mesenchymal transition. *EMBO J* 2010 **29** 3286-3300.
493. Warzecha CC, Sato TK, Nabet B, Hogenesch JB & Carstens RP. ESRP1 and ESRP2 are epithelial cell-type-specific regulators of FGFR2 splicing. *Mol Cell* 2009 **33** 591-601.
494. Warzecha CC, Shen S, Xing Y & Carstens RP. The epithelial splicing factors ESRP1 and ESRP2 positively and negatively regulate diverse types of alternative splicing events. *RNA Biol* 2009 **6** 546-562.
495. Chaudhury A, Hussey GS, Ray PS, Jin G, Fox PL & Howe PH. TGF-beta-mediated phosphorylation of hnRNP E1 induces EMT via transcript-selective translational induction of Dab2 and ILEI. *Nat Cell Biol* 2010 **12** 286-293.
496. Evdokimova V, Tognon C, Ng T, Ruzanov P, Melnyk N, Fink D, Sorokin A, Ovchinnikov LP, Davicioni E, Triche TJ & Sorensen PH. Translational activation of snail1 and other developmentally regulated transcription factors by YB-1 promotes an epithelial-mesenchymal transition. *Cancer Cell* 2009 **15** 402-415.
497. Wang SP, Wang WL, Chang YL, Wu CT, Chao YC, Kao SH, Yuan A, Lin CW, Yang SC, Chan WK, Li KC, Hong TM & Yang PC. p53 controls cancer cell invasion by inducing the MDM2-mediated degradation of Slug. *Nat Cell Biol* 2009 **11** 694-704.
498. Vinas-Castells R, Beltran M, Valls G, Gomez I, Garcia JM, Montserrat-Sentis B, Baulida J, Bonilla F, de Herreros AG & Diaz VM. The hypoxia-controlled FBXL14 ubiquitin ligase targets SNAIL1 for proteasome degradation. *J Biol Chem* 2010 **285** 3794-3805.
499. Brittain AL, Basu R, Qian Y & Kopchick JJ. Growth Hormone and the Epithelial-to-Mesenchymal Transition. *J Clin Endocrinol Metab* 2017 **102** 3662-3673.
500. Christiansen JJ & Rajasekaran AK. Reassessing epithelial to mesenchymal transition as a prerequisite for carcinoma invasion and metastasis. *Cancer Res* 2006 **66** 8319-8326.
501. Brabletz T. To differentiate or not--routes towards metastasis. *Nat Rev Cancer* 2012 **12** 425-436.
502. Cheung LY, Davis SW, Brinkmeier ML, Camper SA & Perez-Millan MI. Regulation of pituitary stem cells by epithelial to mesenchymal transition events and signaling pathways. *Mol Cell Endocrinol* 2017 **445** 14-26.
503. Qian ZR, Li CC, Yamasaki H, Mizusawa N, Yoshimoto K, Yamada S, Tashiro T, Horiguchi H, Wakatsuki S, Hirokawa M & Sano T. Role of E-cadherin, alpha-, beta-, and gamma-catenins, and p120 (cell adhesion molecules) in prolactinoma behavior. *Mod Pathol* 2002 **15** 1357-1365.
504. Qian ZR, Sano T, Yoshimoto K, Asa SL, Yamada S, Mizusawa N & Kudo E. Tumor-specific downregulation and methylation of the CDH13 (H-cadherin) and CDH1 (E-cadherin) genes correlate with aggressiveness of human pituitary adenomas. *Mod Pathol* 2007 **20** 1269-1277.
505. Lekva T, Berg JP, Fougner SL, Olstad OK, Ueland T & Bollerslev J. Gene expression profiling identifies ESRP1 as a potential regulator of epithelial mesenchymal transition in somatotroph adenomas from a large cohort of patients with acromegaly. *J Clin Endocrinol Metab* 2012 **97** E1506-1514.
506. Chen X, Pang B, Liang Y, Xu SC, Xin T, Fan HT, Yu YB & Pang Q. Overexpression of EpCAM and Trop2 in pituitary adenomas. *Int J Clin Exp Pathol* 2014 **7** 7907-7914.
507. Barry S, Carlsen E, Marques P, Stiles CE, Gadaleta E, Berney DM, Roncaroli F, Chelala C, Solomou A, Herincs M, Caimari F, Grossman AB, Crnogorac-Jurcevic T, Haworth O, Gaston-

Massuet C & Korbonits M. Tumor microenvironment defines the invasive phenotype of AIP-mutation-positive pituitary tumors. *Oncogene* 2019 **38** 5381-5395.
508. Stenken JA & Poschenrieder AJ. Bioanalytical chemistry of cytokines--a review. *Anal Chim Acta* 2015 **853** 95-115.
509. Prichard JW. Overview of automated immunohistochemistry. *Arch Pathol Lab Med* 2014 **138** 1578-1582.
510. Wang F, Flanagan J, Su N, Wang LC, Bui S, Nielson A, Wu X, Vo HT, Ma XJ & Luo Y. RNAscope: a novel in situ RNA analysis platform for formalin-fixed, paraffin-embedded tissues. *J Mol Diagn* 2012 **14** 22-29.
511. Anderson CM, Zhang B, Miller M, Butko E, Wu X, Laver T, Kernag C, Kim J, Luo Y, Lamparski H, Park E, Su N & Ma XJ. Fully Automated RNAscope In Situ Hybridization Assays for Formalin-Fixed Paraffin-Embedded Cells and Tissues. *J Cell Biochem* 2016 **117** 2201-2208.
512. Hickman SE, Kingery ND, Ohsumi TK, Borowsky ML, Wang LC, Means TK & El Khoury J. The microglial sensome revealed by direct RNA sequencing. *Nat Neurosci* 2013 **16** 1896-1905.
513. Barry S, Carlsen E, Marques P, Stiles CE, Gadaleta E, Berney DM, Roncaroli F, Chelala C, Solomou A, Herincs M, Caimari F, Grossman AB, Crnogorac-Jurcevic T, Haworth O, Gaston-Massuet C & Korbonits M. Tumor microenvironment defines the invasive phenotype of AIP-mutation-positive pituitary tumors. *Oncogene* 2019.
514. Aran D, Hu Z & Butte AJ. xCell: digitally portraying the tissue cellular heterogeneity landscape. *Genome Biol* 2017 **18** 220.
515. Newman AM, Liu CL, Green MR, Gentles AJ, Feng W, Xu Y, Hoang CD, Diehn M & Alizadeh AA. Robust enumeration of cell subsets from tissue expression profiles. *Nat Methods* 2015 **12** 453-457.
516. Barnes TA & Amir E. HYPE or HOPE: the prognostic value of infiltrating immune cells in cancer. *Br J Cancer* 2017 **117** 451-460.
517. Coffelt SB, Wellenstein MD & de Visser KE. Neutrophils in cancer: neutral no more. *Nat Rev Cancer* 2016 **16** 431-446.
518. Powell DR & Huttenlocher A. Neutrophils in the Tumor Microenvironment. *Trends Immunol* 2016 **37** 41-52.
519. Marques P BS, Carlsen E, Collier D, Ronaldson A, Awad S, Dorward N, Grieve J, Balkwill F, Korbonits M. Cytokine network in pituitary adenomas and its role in the tumor microenvironment: focus on macrophages. *J Endocr Soc* 2019 **ENDO 2019, 5321, MON 25 Mar**.
520. Hazrati SM, Aghazadeh J, Mohtarami F, Abouzari M & Rashidi A. Immunotherapy of prolactinoma with a T helper 1 activator adjuvant and autoantigens: a case report. *Neuroimmunomodulation* 2006 **13** 205-208.
521. Ahmad J, Grimes N, Farid S & Morris-Stiff G. Inflammatory response related scoring systems in assessing the prognosis of patients with pancreatic ductal adenocarcinoma: a systematic review. *Hepatobiliary Pancreat Dis Int* 2014 **13** 474-481.
522. Bugada D, Allegri M, Lavand'homme P, De Kock M & Fanelli G. Inflammation-based scores: a new method for patient-targeted strategies and improved perioperative outcome in cancer patients. *Biomed Res Int* 2014 **2014** 142425.
523. Chang X, Zhang F, Liu T, Wang W & Guo H. Neutrophil-to-lymphocyte ratio as an independent predictor for survival in patients with localized clear cell renal cell carcinoma after radiofrequency ablation: a propensity score matching analysis. *Int Urol Nephrol* 2017 **49** 967-974.
524. Tang H, Lu W, Li B, Li C, Xu Y & Dong J. Prognostic significance of neutrophil-to-lymphocyte ratio in biliary tract cancers: a systematic review and meta-analysis. *Oncotarget* 2017 **8** 36857-36868.

525. Chan JC, Chan DL, Diakos CI, Engel A, Pavlakis N, Gill A & Clarke SJ. The Lymphocyte-to-Monocyte Ratio is a Superior Predictor of Overall Survival in Comparison to Established Biomarkers of Resectable Colorectal Cancer. *Ann Surg* 2017 **265** 539-546.
526. Yang T, Zhu J, Zhao L, Mai K, Ye J, Huang S & Zhao Y. Lymphocyte to monocyte ratio and neutrophil to lymphocyte ratio are superior inflammation-based predictors of recurrence in patients with hepatocellular carcinoma after hepatic resection. *J Surg Oncol* 2017 **115** 718-728.
527. Di Ieva A, Rotondo F, Syro LV, Cusimano MD & Kovacs K. Aggressive pituitary adenomas--diagnosis and emerging treatments. *Nat Rev Endocrinol* 2014 **10** 423-435.
528. Alfaro C, Sanmamed MF, Rodriguez-Ruiz ME, Teijeira A, Onate C, Gonzalez A, Ponz M, Schalper KA, Perez-Gracia JL & Melero I. Interleukin-8 in cancer pathogenesis, treatment and follow-up. *Cancer Treat Rev* 2017 **60** 24-31.
529. Reichel CA, Rehberg M, Lerchenberger M, Berberich N, Bihari P, Khandoga AG, Zahler S & Krombach F. Ccl2 and Ccl3 mediate neutrophil recruitment via induction of protein synthesis and generation of lipid mediators. *Arterioscler Thromb Vasc Biol* 2009 **29** 1787-1793.
530. Zhang X, Zhang W, Yuan X, Fu M, Qian H & Xu W. Neutrophils in cancer development and progression: Roles, mechanisms, and implications (Review). *Int J Oncol* 2016 **49** 857-867.
531. deLeeuw RJ, Kost SE, Kakal JA & Nelson BH. The prognostic value of FoxP3+ tumor-infiltrating lymphocytes in cancer: a critical review of the literature. *Clin Cancer Res* 2012 **18** 3022-3029.
532. Hadrup S, Donia M & Thor Straten P. Effector CD4 and CD8 T cells and their role in the tumor microenvironment. *Cancer Microenviron* 2013 **6** 123-133.
533. Gevrey JC, Isaac BM & Cox D. Syk is required for monocyte/macrophage chemotaxis to CX3CL1 (Fractalkine). *J Immunol* 2005 **175** 3737-3745.
534. Hanada T & Yoshimura A. Regulation of cytokine signaling and inflammation. *Cytokine Growth Factor Rev* 2002 **13** 413-421.
535. Stone MJ, Hayward JA, Huang C, Z EH & Sanchez J. Mechanisms of Regulation of the Chemokine-Receptor Network. *Int J Mol Sci* 2017 **18**.
536. McKayed KK & Simpson JC. Actin in action: imaging approaches to study cytoskeleton structure and function. *Cells* 2013 **2** 715-731.
537. Kramer N, Walzl A, Unger C, Rosner M, Krupitza G, Hengstschlager M & Dolznig H. In vitro cell migration and invasion assays. *Mutat Res* 2013 **752** 10-24.
538. Kleinman HK & Martin GR. Matrigel: basement membrane matrix with biological activity. *Semin Cancer Biol* 2005 **15** 378-386.
539. Schaeffer D, Somarelli JA, Hanna G, Palmer GM & Garcia-Blanco MA. Cellular migration and invasion uncoupled: increased migration is not an inexorable consequence of epithelial-to-mesenchymal transition. *Mol Cell Biol* 2014 **34** 3486-3499.
540. Stiles CEB, S.; Gadaleta, E.; Chelala, C.; Shoulders, C.; Korbonits, M. Investigation of the invasive phenotype of AIP-mutated pituitary adenomas. *Endocrine Abstracts* 2015 **38;P301**.
541. Nie J, Huang GL, Deng SZ, Bao Y, Liu YW, Feng ZP, Wang CH, Chen M, Qi ST & Pan J. The purine receptor P2X7R regulates the release of pro-inflammatory cytokines in human craniopharyngioma. *Endocr Relat Cancer* 2017 **24** 287-296.
542. Brown CE, Vishwanath RP, Aguilar B, Starr R, Najbauer J, Aboody KS & Jensen MC. Tumor-derived chemokine MCP-1/CCL2 is sufficient for mediating tumor tropism of adoptively transferred T cells. *J Immunol* 2007 **179** 3332-3341.
543. Slaney CY, Kershaw MH & Darcy PK. Trafficking of T cells into tumors. *Cancer Res* 2014 **74** 7168-7174.
544. Sandhu SK, Papadopoulos K, Fong PC, Patnaik A, Messiou C, Olmos D, Wang G, Tromp BJ, Puchalski TA, Balkwill F, Berns B, Seetharam S, de Bono JS & Tolcher AW. A first-in-human,

first-in-class, phase I study of carlumab (CNTO 888), a human monoclonal antibody against CC-chemokine ligand 2 in patients with solid tumors. *Cancer Chemother Pharmacol* 2013 **71** 1041-1050.

545. Fornari MC, Palacios MF, Diez RA & Intebi AD. Decreased chemotaxis of neutrophils in acromegaly and hyperprolactinemia. *Eur J Endocrinol* 1994 **130** 463-468.
546. Singhal S, Stadanlick J, Annunziata MJ, Rao AS, Bhojnagarwala PS, O'Brien S, Moon EK, Cantu E, Danet-Desnoyers G, Ra HJ, Litzky L, Akimova T, Beier UH, Hancock WW, Albelda SM & Eruslanov EB. Human tumor-associated monocytes/macrophages and their regulation of T cell responses in early-stage lung cancer. *Sci Transl Med* 2019 **11**.
547. Troiano G, Caponio VCA, Adipietro I, Tepedino M, Santoro R, Laino L, Lo Russo L, Cirillo N & Lo Muzio L. Prognostic significance of CD68(+) and CD163(+) tumor associated macrophages in head and neck squamous cell carcinoma: A systematic review and meta-analysis. *Oral Oncol* 2019 **93** 66-75.
548. Tjiu JW, Chen JS, Shun CT, Lin SJ, Liao YH, Chu CY, Tsai TF, Chiu HC, Dai YS, Inoue H, Yang PC, Kuo ML & Jee SH. Tumor-associated macrophage-induced invasion and angiogenesis of human basal cell carcinoma cells by cyclooxygenase-2 induction. *J Invest Dermatol* 2009 **129** 1016-1025.
549. Han S, Zhang C, Li Q, Dong J, Liu Y, Huang Y, Jiang T & Wu A. Tumour-infiltrating CD4(+) and CD8(+) lymphocytes as predictors of clinical outcome in glioma. *Br J Cancer* 2014 **110** 2560-2568.
550. Richardson TE, Shen ZJ, Kanchwala M, Xing C, Filatenkov A, Shang P, Barnett S, Abedin Z, Malter JS, Raisanen JM, Burns DK, White CL & Hatanpaa KJ. Aggressive Behavior in Silent Subtype III Pituitary Adenomas May Depend on Suppression of Local Immune Response: A Whole Transcriptome Analysis. *J Neuropathol Exp Neurol* 2017 **76** 874-882.
551. Muraille E, Leo O & Moser M. TH1/TH2 paradigm extended: macrophage polarization as an unappreciated pathogen-driven escape mechanism? *Front Immunol* 2014 **5** 603.
552. Semeraro M, Adam J, Stoll G, Louvet E, Chaba K, Poirier-Colame V, Sauvat A, Senovilla L, Vacchelli E, Bloy N, Humeau J, Buque A, Kepp O, Zitvogel L, Andre F, Mathieu MC, Delaloge S & Kroemer G. The ratio of CD8(+)/FOXP3 T lymphocytes infiltrating breast tissues predicts the relapse of ductal carcinoma in situ. *Oncoimmunology* 2016 **5** e1218106.
553. Suzuki H, Chikazawa N, Tasaka T, Wada J, Yamasaki A, Kitaura Y, Sozaki M, Tanaka M, Onishi H, Morisaki T & Katano M. Intratumoral CD8(+) T/FOXP3 (+) cell ratio is a predictive marker for survival in patients with colorectal cancer. *Cancer Immunol Immunother* 2010 **59** 653-661.
554. Stoll G, Bindea G, Mlecnik B, Galon J, Zitvogel L & Kroemer G. Meta-analysis of organ-specific differences in the structure of the immune infiltrate in major malignancies. *Oncotarget* 2015 **6** 11894-11909.
555. Stoll G, Zitvogel L & Kroemer G. Differences in the composition of the immune infiltrate in breast cancer, colorectal carcinoma, melanoma and non-small cell lung cancer: A microarray-based meta-analysis. *Oncoimmunology* 2016 **5** e1067746.
556. Liu CL, Lee JJ, Liu TP, Chang YC, Hsu YC & Cheng SP. Blood neutrophil-to-lymphocyte ratio correlates with tumor size in patients with differentiated thyroid cancer. *J Surg Oncol* 2013 **107** 493-497.
557. Ari A & Gunver F. Comparison of neutrophil-lymphocyte ratio and platelet-lymphocyte ratio in patients with thyroiditis and papillary tumors. *J Int Med Res* 2019 300060519838392.
558. Ozmen S, Timur O, Calik I, Altinkaynak K, Simsek E, Gozcu H, Arslan A & Carlioglu A. Neutrophil-lymphocyte ratio (NLR) and platelet-lymphocyte ratio (PLR) may be superior to C-reactive protein (CRP) for predicting the occurrence of differentiated thyroid cancer. *Endocr Regul* 2017 **51** 131-136.

559. Luo G, Liu C, Cheng H, Jin K, Guo M, Lu Y, Long J, Xu J, Ni Q, Chen J & Yu X. Neutrophil-lymphocyte ratio predicts survival in pancreatic neuroendocrine tumors. *Oncol Lett* 2017 **13** 2454-2458.
560. McDermott SM, Saunders ND, Schneider EB, Strosberg D, Onesti J, Dillhoff M, Schmidt CR & Shirley LA. Neutrophil Lymphocyte Ratio and Transarterial Chemoembolization in Neuroendocrine Tumor Metastases. *J Surg Res* 2018 **232** 369-375.
561. Okui M, Yamamichi T, Asakawa A, Harada M, Saito M & Horio H. Prognostic significance of neutrophil-lymphocyte ratios in large cell neuroendocrine carcinoma. *Gen Thorac Cardiovasc Surg* 2017 **65** 633-639.
562. Salman T, Kazaz SN, Varol U, Oflazoglu U, Unek IT, Kucukzeybek Y, Alacacioglu A, Atag E, Semiz HS, Cengiz H, Oztop I & Tarhan MO. Prognostic Value of the Pretreatment Neutrophil-to-Lymphocyte Ratio and Platelet-to-Lymphocyte Ratio for Patients with Neuroendocrine Tumors: An Izmir Oncology Group Study. *Chemotherapy* 2016 **61** 281-286.
563. Chen M, Zheng SH, Yang M, Chen ZH & Li ST. The diagnostic value of preoperative inflammatory markers in craniopharyngioma: a multicenter cohort study. *J Neurooncol* 2018 **138** 113-122.
564. Zhang J, He M, Liu Z, Song Y, Wang Y, Liang R, Chen H & Xu J. Impact of neutrophil-lymphocyte ratio on long-term outcome in patients with craniopharyngioma. *Medicine (Baltimore)* 2018 **97** e12375.
565. Halazun KJ, Aldoori A, Malik HZ, Al-Mukhtar A, Prasad KR, Toogood GJ & Lodge JP. Elevated preoperative neutrophil to lymphocyte ratio predicts survival following hepatic resection for colorectal liver metastases. *Eur J Surg Oncol* 2008 **34** 55-60.
566. Hung HY, Chen JS, Yeh CY, Changchien CR, Tang R, Hsieh PS, Tasi WS, You JF, You YT, Fan CW, Wang JY & Chiang JM. Effect of preoperative neutrophil-lymphocyte ratio on the surgical outcomes of stage II colon cancer patients who do not receive adjuvant chemotherapy. *Int J Colorectal Dis* 2011 **26** 1059-1065.
567. Stotz M, Gerger A, Eisner F, Szkandera J, Loibner H, Ress AL, Kornprat P, AlZoughbi W, Seggewies FS, Lackner C, Stojakovic T, Samonigg H, Hoefler G & Pichler M. Increased neutrophil-lymphocyte ratio is a poor prognostic factor in patients with primary operable and inoperable pancreatic cancer. *Br J Cancer* 2013 **109** 416-421.
568. He W, Yin C, Guo G, Jiang C, Wang F, Qiu H, Chen X, Rong R, Zhang B & Xia L. Initial neutrophil lymphocyte ratio is superior to platelet lymphocyte ratio as an adverse prognostic and predictive factor in metastatic colorectal cancer. *Med Oncol* 2013 **30** 439.
569. Sakka N, Smith RA, Whelan P, Ghaneh P, Sutton R, Raraty M, Campbell F & Neoptolemos JP. A preoperative prognostic score for resected pancreatic and periampullary neuroendocrine tumours. *Pancreatology* 2009 **9** 670-676.
570. Wang X, Su S & Guo Y. The clinical use of the platelet to lymphocyte ratio and lymphocyte to monocyte ratio as prognostic factors in renal cell carcinoma: a systematic review and meta-analysis. *Oncotarget* 2017 **8** 84506-84514.
571. Nahrendorf M & Swirski FK. Abandoning M1/M2 for a Network Model of Macrophage Function. *Circ Res* 2016 **119** 414-417.
572. Lima L, Oliveira D, Tavares A, Amaro T, Cruz R, Oliveira MJ, Ferreira JA & Santos L. The predominance of M2-polarized macrophages in the stroma of low-hypoxic bladder tumors is associated with BCG immunotherapy failure. *Urol Oncol* 2014 **32** 449-457.
573. Medrek C, Ponten F, Jirstrom K & Leandersson K. The presence of tumor associated macrophages in tumor stroma as a prognostic marker for breast cancer patients. *BMC Cancer* 2012 **12** 306.
574. De Boeck A, Hendrix A, Maynard D, Van Bockstal M, Daniels A, Pauwels P, Gespach C, Bracke M & De Wever O. Differential secretome analysis of cancer-associated fibroblasts

and bone marrow-derived precursors to identify microenvironmental regulators of colon cancer progression. *Proteomics* 2013 **13** 379-388.
575. Gadelha MR, Kasuki L & Korbonits M. Novel pathway for somatostatin analogs in patients with acromegaly. *Trends Endocrinol Metab* 2013 **24** 238-246.
576. Barbieri F, Albertelli M, Grillo F, Mohamed A, Saveanu A, Barlier A, Ferone D & Florio T. Neuroendocrine tumors: insights into innovative therapeutic options and rational development of targeted therapies. *Drug Discov Today* 2014 **19** 458-468.
577. Ibanez-Costa A & Korbonits M. AIP and the somatostatin system in pituitary tumours. *J Endocrinol* 2017 **235** R101-R116.
578. Fleseriu M & Petersenn S. Medical management of Cushing's disease: what is the future? *Pituitary* 2012 **15** 330-341.
579. Schmid HA. Pasireotide (SOM230): development, mechanism of action and potential applications. *Mol Cell Endocrinol* 2008 **286** 69-74.
580. Gunther T, Tulipano G, Dournaud P, Bousquet C, Csaba Z, Kreienkamp HJ, Lupp A, Korbonits M, Castano JP, Wester HJ, Culler M, Melmed S & Schulz S. International Union of Basic and Clinical Pharmacology. CV. Somatostatin Receptors: Structure, Function, Ligands, and New Nomenclature. *Pharmacol Rev* 2018 **70** 763-835.
581. Jagannathan J, Smith R, DeVroom HL, Vortmeyer AO, Stratakis CA, Nieman LK & Oldfield EH. Outcome of using the histological pseudocapsule as a surgical capsule in Cushing disease. *J Neurosurg* 2009 **111** 531-539.
582. Taylor DG, Jane JA & Oldfield EH. Resection of pituitary macroadenomas via the pseudocapsule along the posterior tumor margin: a cohort study and technical note. *J Neurosurg* 2018 **128** 422-428.
583. Yadav A, Saini V & Arora S. MCP-1: chemoattractant with a role beyond immunity: a review. *Clin Chim Acta* 2010 **411** 1570-1579.
584. Yoshimura T. The production of monocyte chemoattractant protein-1 (MCP-1)/CCL2 in tumor microenvironments. *Cytokine* 2017.
585. Kalluri R & Zeisberg M. Fibroblasts in cancer. *Nat Rev Cancer* 2006 **6** 392-401.
586. Nagasaki T, Hara M, Nakanishi H, Takahashi H, Sato M & Takeyama H. Interleukin-6 released by colon cancer-associated fibroblasts is critical for tumour angiogenesis: anti-interleukin-6 receptor antibody suppressed angiogenesis and inhibited tumour-stroma interaction. *Br J Cancer* 2014 **110** 469-478.
587. Di Maggio F, Arumugam P, Delvecchio FR, Batista S, Lechertier T, Hodivala-Dilke K & Kocher HM. Pancreatic stellate cells regulate blood vessel density in the stroma of pancreatic ductal adenocarcinoma. *Pancreatology* 2016 **16** 995-1004.
588. Heldin CH. Targeting the PDGF signaling pathway in tumor treatment. *Cell Commun Signal* 2013 **11** 97.
589. Kong D, Wang Z, Sarkar SH, Li Y, Banerjee S, Saliganan A, Kim HR, Cher ML & Sarkar FH. Platelet-derived growth factor-D overexpression contributes to epithelial-mesenchymal transition of PC3 prostate cancer cells. *Stem Cells* 2008 **26** 1425-1435.
590. Wu Q, Hou X, Xia J, Qian X, Miele L, Sarkar FH & Wang Z. Emerging roles of PDGF-D in EMT progression during tumorigenesis. *Cancer Treat Rev* 2013 **39** 640-646.
591. Takahashi H, Sakakura K, Kudo T, Toyoda M, Kaira K, Oyama T & Chikamatsu K. Cancer-associated fibroblasts promote an immunosuppressive microenvironment through the induction and accumulation of protumoral macrophages. *Oncotarget* 2017 **8** 8633-8647.
592. Numata Y, Terui T, Okuyama R, Hirasawa N, Sugiura Y, Miyoshi I, Watanabe T, Kuramasu A, Tagami H & Ohtsu H. The accelerating effect of histamine on the cutaneous wound-healing process through the action of basic fibroblast growth factor. *J Invest Dermatol* 2006 **126** 1403-1409.

593. Tang P, Jerebtsova M, Przygodzki R & Ray PE. Fibroblast growth factor-2 increases the renal recruitment and attachment of HIV-infected mononuclear cells to renal tubular epithelial cells. *Pediatr Nephrol* 2005 **20** 1708-1716.
594. Kouwenhoven EA, Stein-Oakley AN, Maguire JA, Jablonski P, de Bruin RW & Thomson NM. Increased expression of basic fibroblast growth factor during chronic rejection in intestinal transplants is associated with macrophage infiltrates. *Transpl Int* 1999 **12** 42-49.
595. Chikazu D, Katagiri M, Ogasawara T, Ogata N, Shimoaka T, Takato T, Nakamura K & Kawaguchi H. Regulation of osteoclast differentiation by fibroblast growth factor 2: stimulation of receptor activator of nuclear factor kappaB ligand/osteoclast differentiation factor expression in osteoblasts and inhibition of macrophage colony-stimulating factor function in osteoclast precursors. *J Bone Miner Res* 2001 **16** 2074-2081.
596. Singla DK, Singla RD, Abdelli LS & Glass C. Fibroblast growth factor-9 enhances M2 macrophage differentiation and attenuates adverse cardiac remodeling in the infarcted diabetic heart. *PLoS One* 2015 **10** e0120739.
597. Valeta-Magara A, Gadi A, Volta V, Walters B, Arju R, Giashuddin S, Zhong H & Schneider RJ. Inflammatory Breast Cancer Promotes Development of M2 Tumor-Associated Macrophages and Cancer Mesenchymal Cells through a Complex Chemokine Network. *Cancer Res* 2019 **79** 3360-3371.
598. Kubo K & Kuroyanagi Y. A study of cytokines released from fibroblasts in cultured dermal substitute. *Artif Organs* 2005 **29** 845-849.
599. Nolte SV, Xu W, Rennekampff HO & Rodemann HP. Diversity of fibroblasts--a review on implications for skin tissue engineering. *Cells Tissues Organs* 2008 **187** 165-176.
600. !!! INVALID CITATION !!!
601. Arakelyan A, Petrkova J, Hermanova Z, Boyajyan A, Lukl J & Petrek M. Serum levels of the MCP-1 chemokine in patients with ischemic stroke and myocardial infarction. *Mediators Inflamm* 2005 **2005** 175-179.
602. Wu M, Baron M, Pedroza C, Salazar GA, Ying J, Charles J, Agarwal SK, Hudson M, Pope J, Zhou X, Reveille JD, Fritzler MJ, Mayes MD & Assassi S. CCL2 in the Circulation Predicts Long-Term Progression of Interstitial Lung Disease in Patients With Early Systemic Sclerosis: Data From Two Independent Cohorts. *Arthritis Rheumatol* 2017 **69** 1871-1878.
603. Castro CP, Giacomini D, Nagashima AC, Onofri C, Graciarena M, Kobayashi K, Paez-Pereda M, Renner U, Stalla GK & Arzt E. Reduced expression of the cytokine transducer gp130 inhibits hormone secretion, cell growth, and tumor development of pituitary lactosomatotrophic GH3 cells. *Endocrinology* 2003 **144** 693-700.
604. Zhang A, Qian Y, Ye Z, Chen H, Xie H, Zhou L, Shen Y & Zheng S. Cancer-associated fibroblasts promote M2 polarization of macrophages in pancreatic ductal adenocarcinoma. *Cancer Med* 2017 **6** 463-470.
605. Bikfalvi A, Klein S, Pintucci G & Rifkin DB. Biological roles of fibroblast growth factor-2. *Endocr Rev* 1997 **18** 26-45.
606. Benton G, Arnaoutova I, George J, Kleinman HK & Koblinski J. Matrigel: from discovery and ECM mimicry to assays and models for cancer research. *Adv Drug Deliv Rev* 2014 **79-80** 3-18.
607. Kinoshita H, Hirata Y, Nakagawa H, Sakamoto K, Hayakawa Y, Takahashi R, Nakata W, Sakitani K, Serizawa T, Hikiba Y, Akanuma M, Shibata W, Maeda S & Koike K. Interleukin-6 mediates epithelial-stromal interactions and promotes gastric tumorigenesis. *PLoS One* 2013 **8** e60914.
608. Thiele JO, Lohrer P, Schaaf L, Feirer M, Stummer W, Losa M, Lange M, Tichomirowa M, Arzt E, Stalla GK & Renner U. Functional in vitro studies on the role and regulation of interleukin-6 in human somatotroph pituitary adenomas. *Eur J Endocrinol* 2003 **149** 455-461.

609. Andoh A, Hata K, Shimada M, Fujino S, Tasaki K, Bamba S, Araki Y, Fujiyama Y & Bamba T. Inhibitory effects of somatostatin on tumor necrosis factor-alpha-induced interleukin-6 secretion in human pancreatic periacinar myofibroblasts. *Int J Mol Med* 2002 **10** 89-93.
610. Grimaldi M, Florio T & Schettini G. Somatostatin inhibits interleukin 6 release from rat cortical type I astrocytes via the inhibition of adenylyl cyclase. *Biochem Biophys Res Commun* 1997 **235** 242-248.
611. Spangelo BL, Horrell S, Goodwin AL, Shroff S & Jarvis WD. Somatostatin and gamma-aminobutyric acid inhibit interleukin-1 beta-stimulated release of interleukin-6 from rat C6 glioma cells. *Neuroimmunomodulation* 2004 **11** 332-340.
612. Zatelli MC, Piccin D, Vignali C, Tagliati F, Ambrosio MR, Bondanelli M, Cimino V, Bianchi A, Schmid HA, Scanarini M, Pontecorvi A, De Marinis L, Maira G & degli Uberti EC. Pasireotide, a multiple somatostatin receptor subtypes ligand, reduces cell viability in non-functioning pituitary adenomas by inhibiting vascular endothelial growth factor secretion. *Endocr Relat Cancer* 2007 **14** 91-102.
613. Yamada S, Fukuhara N, Horiguchi K, Yamaguchi-Okada M, Nishioka H, Takeshita A, Takeuchi Y, Ito J & Inoshita N. Clinicopathological characteristics and therapeutic outcomes in thyrotropin-secreting pituitary adenomas: a single-center study of 90 cases. *J Neurosurg* 2014 **121** 1462-1473.
614. Chentli F & Safer-Tabi A. Pituitary Stone or Calcified Pituitary Tumor? Three Cases and Literature Review. *Int J Endocrinol Metab* 2015 **13** e28383.
615. Borie R, Fabre A, Prost F, Marchal-Somme J, Lebtahi R, Marchand-Adam S, Aubier M, Soler P & Crestani B. Activation of somatostatin receptors attenuates pulmonary fibrosis. *Thorax* 2008 **63** 251-258.
616. Pasquali D, Vassallo P, Esposito D, Bonavolonta G, Bellastella A & Sinisi AA. Somatostatin receptor gene expression and inhibitory effects of octreotide on primary cultures of orbital fibroblasts from Graves' ophthalmopathy. *J Mol Endocrinol* 2000 **25** 63-71.
617. Priestley GC, Aldridge RD, Sime PJ & Wilson D. Skin fibroblast activity in pretibial myxoedema and the effect of octreotide (Sandostatin) in vitro. *Br J Dermatol* 1994 **131** 52-56.
618. Le Moli R CC, Mouritz M, Souters M. Pasireotide and Graves´ orbitopathy: outcome in terms of efficacy compared to parental metilprednisolone; a pilot study. *Endocrine Abstracts* 2018 **56; P1113**.
619. Ibanez-Costa A, Rivero-Cortes E, Vazquez-Borrego MC, Gahete MD, Jimenez-Reina L, Venegas-Moreno E, de la Riva A, Arraez MA, Gonzalez-Molero I, Schmid HA, Maraver-Selfa S, Gavilan-Villarejo I, Garcia-Arnes JA, Japon MA, Soto-Moreno A, Galvez MA, Luque RM & Castano JP. Octreotide and pasireotide (dis)similarly inhibit pituitary tumor cells in vitro. *J Endocrinol* 2016 **231** 135-145.
620. Gatto F, Feelders RA, Franck SE, van Koetsveld PM, Dogan F, Kros JM, Neggers S, van der Lely AJ, Lamberts SWJ, Ferone D & Hofland LJ. In Vitro Head-to-Head Comparison Between Octreotide and Pasireotide in GH-Secreting Pituitary Adenomas. *J Clin Endocrinol Metab* 2017 **102** 2009-2018.
621. Colao A, Bronstein MD, Freda P, Gu F, Shen CC, Gadelha M, Fleseriu M, van der Lely AJ, Farrall AJ, Hermosillo Resendiz K, Ruffin M, Chen Y, Sheppard M & Pasireotide CSG. Pasireotide versus octreotide in acromegaly: a head-to-head superiority study. *J Clin Endocrinol Metab* 2014 **99** 791-799.
622. Gadelha MR, Bronstein MD, Brue T, Coculescu M, Fleseriu M, Guitelman M, Pronin V, Raverot G, Shimon I, Lievre KK, Fleck J, Aout M, Pedroncelli AM, Colao A & Pasireotide CSG. Pasireotide versus continued treatment with octreotide or lanreotide in patients with inadequately controlled acromegaly (PAOLA): a randomised, phase 3 trial. *Lancet Diabetes Endocrinol* 2014 **2** 875-884.

623. Fusco A, Giampietro A, Bianchi A, Cimino V, Lugli F, Piacentini S, Lorusso M, Tofani A, Perotti G, Lauriola L, Anile C, Maira G, Pontecorvi A & De Marinis L. Treatment with octreotide LAR in clinically non-functioning pituitary adenoma: results from a case-control study. *Pituitary* 2012 **15** 571-578.
624. Ueno T, Toi M, Saji H, Muta M, Bando H, Kuroi K, Koike M, Inadera H & Matsushima K. Significance of macrophage chemoattractant protein-1 in macrophage recruitment, angiogenesis, and survival in human breast cancer. *Clin Cancer Res* 2000 **6** 3282-3289.
625. Weledji EP & Assob JC. The ubiquitous neural cell adhesion molecule (N-CAM). *Ann Med Surg (Lond)* 2014 **3** 77-81.
626. Rubinek T, Yu R, Hadani M, Barkai G, Nass D, Melmed S & Shimon I. The cell adhesion molecules N-cadherin and neural cell adhesion molecule regulate human growth hormone: a novel mechanism for regulating pituitary hormone secretion. *J Clin Endocrinol Metab* 2003 **88** 3724-3730.
627. Trouillas J, Daniel L, Guigard MP, Tong S, Gouvernet J, Jouanneau E, Jan M, Perrin G, Fischer G, Tabarin A, Rougon G & Figarella-Branger D. Polysialylated neural cell adhesion molecules expressed in human pituitary tumors and related to extrasellar invasion. *J Neurosurg* 2003 **98** 1084-1093.
628. Van Acker HH, Capsomidis A, Smits EL & Van Tendeloo VF. CD56 in the Immune System: More Than a Marker for Cytotoxicity? *Front Immunol* 2017 **8** 892.
629. Langley OK, Aletsee-Ufrecht MC, Grant NJ & Gratzl M. Expression of the neural cell adhesion molecule NCAM in endocrine cells. *J Histochem Cytochem* 1989 **37** 781-791.
630. Cavallaro U & Christofori G. Multitasking in tumor progression: signaling functions of cell adhesion molecules. *Ann N Y Acad Sci* 2004 **1014** 58-66.
631. Cavallaro U & Christofori G. Cell adhesion and signalling by cadherins and Ig-CAMs in cancer. *Nat Rev Cancer* 2004 **4** 118-132.
632. Raveh S, Gavert N & Ben-Ze'ev A. L1 cell adhesion molecule (L1CAM) in invasive tumors. *Cancer Lett* 2009 **282** 137-145.
633. Daniel L, Bouvier C, Chetaille B, Gouvernet J, Luccioni A, Rossi D, Lechevallier E, Muracciole X, Coulange C & Figarella-Branger D. Neural cell adhesion molecule expression in renal cell carcinomas: relation to metastatic behavior. *Hum Pathol* 2003 **34** 528-532.
634. Prag S, Lepekhin EA, Kolkova K, Hartmann-Petersen R, Kawa A, Walmod PS, Belman V, Gallagher HC, Berezin V, Bock E & Pedersen N. NCAM regulates cell motility. *J Cell Sci* 2002 **115** 283-292.
635. Crnic I, Strittmatter K, Cavallaro U, Kopfstein L, Jussila L, Alitalo K & Christofori G. Loss of neural cell adhesion molecule induces tumor metastasis by up-regulating lymphangiogenesis. *Cancer Res* 2004 **64** 8630-8638.
636. Pyo JS, Kim DH & Yang J. Diagnostic value of CD56 immunohistochemistry in thyroid lesions. *Int J Biol Markers* 2018 **33** 161-167.
637. Berardi M, Hindelang C, Laurent-Huck FM, Langley K, Rougon G, Felix JM & Stoeckel ME. Expression of neural cell adhesion molecules, NCAMs, and their polysialylated forms, PSA-NCAMs, in the developing rat pituitary gland. *Cell Tissue Res* 1995 **280** 463-472.
638. Aletsee-Ufrecht MC, Langley K, Gratzl O & Gratzl M. Differential expression of the neural cell adhesion molecule NCAM 140 in human pituitary tumors. *FEBS Lett* 1990 **272** 45-49.
639. Kleinschmidt-DeMasters BK, Conway DR, Franklin WA, Lillehei KO & Kruse CA. Neural cell adhesion molecule expression in human pituitary adenomas. *J Neurooncol* 1995 **25** 205-213.
640. De Jong I, Aylwin SJ, Olabiran Y, Geddes JF, Monson JP, Wood DF & Burrin JM. Expression and secretion of neural cell adhesion molecules by human pituitary adenomas. *Ann Clin Biochem* 1999 **36 (Pt 5)** 660-665.
641. Daniel L, Trouillas J, Renaud W, Chevallier P, Gouvernet J, Rougon G & Figarella-Branger D. Polysialylated-neural cell adhesion molecule expression in rat pituitary transplantable

tumors (spontaneous mammotropic transplantable tumor in Wistar-Furth rats) is related to growth rate and malignancy. *Cancer Res* 2000 **60** 80-85.
642. Mendes G, Haag T, Trott G, Rech C, Ferreira N, Oliveira M, Kohek M & Pereira-Lima. Expression of E-cadherin, Slug and NCAM and its relationship to tumor invasiveness in patients with acromegaly. *Braz J Med Biol Res* 2018 **51(2)**.
643. Nico B, Benagiano V, Mangieri D, Maruotti N, Vacca A & Ribatti D. Evaluation of microvascular density in tumors: pro and contra. *Histol Histopathol* 2008 **23** 601-607.
644. Davis PJ, Davis FB & Mousa SA. Thyroid hormone-induced angiogenesis. *Curr Cardiol Rev* 2009 **5** 12-16.
645. Luidens MK, Mousa SA, Davis FB, Lin HY & Davis PJ. Thyroid hormone and angiogenesis. *Vascul Pharmacol* 2010 **52** 142-145.
646. Zhang L, Cooper-Kuhn CM, Nannmark U, Blomgren K & Kuhn HG. Stimulatory effects of thyroid hormone on brain angiogenesis in vivo and in vitro. *J Cereb Blood Flow Metab* 2010 **30** 323-335.
647. Gonzalez-Moreno O, Lecanda J, Green JE, Segura V, Catena R, Serrano D & Calvo A. VEGF elicits epithelial-mesenchymal transition (EMT) in prostate intraepithelial neoplasia (PIN)-like cells via an autocrine loop. *Exp Cell Res* 2010 **316** 554-567.
648. Bruno A, Pagani A, Pulze L, Albini A, Dallaglio K, Noonan DM & Mortara L. Orchestration of angiogenesis by immune cells. *Front Oncol* 2014 **4** 131.
649. Pawlikowski M, Pisarek H & Jaranowska M. Immunocytochemical Investigations on the Vascularization of Pituitary Adenomas. *Endocr Pathol* 1997 **8** 189-193.
650. Arthur WT, Vernon RB, Sage EH & Reed MJ. Growth factors reverse the impaired sprouting of microvessels from aged mice. *Microvasc Res* 1998 **55** 260-270.
651. Lin S, Zhang Q, Shao X, Zhang T, Xue C, Shi S, Zhao D & Lin Y. IGF-1 promotes angiogenesis in endothelial cells/adipose-derived stem cells co-culture system with activation of PI3K/Akt signal pathway. *Cell Prolif* 2017 **50**.
652. Reuwer AQ, Nowak-Sliwinska P, Mans LA, van der Loos CM, von der Thusen JH, Twickler MT, Spek CA, Goffin V, Griffioen AW & Borensztajn KS. Functional consequences of prolactin signalling in endothelial cells: a potential link with angiogenesis in pathophysiology? *J Cell Mol Med* 2012 **16** 2035-2048.
653. Yang X, Meyer K & Friedl A. STAT5 and prolactin participate in a positive autocrine feedback loop that promotes angiogenesis. *J Biol Chem* 2013 **288** 21184-21196.
654. Rahat MA, Hemmerlein B & Iragavarapu-Charyulu V. The regulation of angiogenesis by tissue cell-macrophage interactions. *Front Physiol* 2014 **5** 262.
655. Ribatti D & Crivellato E. Immune cells and angiogenesis. *J Cell Mol Med* 2009 **13** 2822-2833.
656. Owen JL & Mohamadzadeh M. Macrophages and chemokines as mediators of angiogenesis. *Front Physiol* 2013 **4** 159.
657. Riabov V, Gudima A, Wang N, Mickley A, Orekhov A & Kzhyshkowska J. Role of tumor associated macrophages in tumor angiogenesis and lymphangiogenesis. *Front Physiol* 2014 **5** 75.
658. Chaudhary B & Elkord E. Regulatory T Cells in the Tumor Microenvironment and Cancer Progression: Role and Therapeutic Targeting. *Vaccines (Basel)* 2016 **4**.
659. Wang J, Voellger B, Benzel J, Schlomann U, Nimsky C, Bartsch JW & Carl B. Metalloproteinases ADAM12 and MMP-14 are associated with cavernous sinus invasion in pituitary adenomas. *Int J Cancer* 2016 **139** 1327-1339.
660. Knappe UJ, Hagel C, Lisboa BW, Wilczak W, Ludecke DK & Saeger W. Expression of serine proteases and metalloproteinases in human pituitary adenomas and anterior pituitary lobe tissue. *Acta Neuropathol* 2003 **106** 471-478.

661. Yokoyama S, Hirano H, Moroki K, Goto M, Imamura S & Kuratsu JI. Are nonfunctioning pituitary adenomas extending into the cavernous sinus aggressive and/or invasive? *Neurosurgery* 2001 **49** 857-862; discussion 862-853.
662. Gupta VK. CSD, BBB and MMP-9 elevations: animal experiments versus clinical phenomena in migraine. *Expert Rev Neurother* 2009 **9** 1595-1614.
663. Imamura K, Takeshima T, Fusayasu E & Nakashima K. Increased plasma matrix metalloproteinase-9 levels in migraineurs. *Headache* 2008 **48** 135-139.
664. Lakhan SE & Avramut M. Matrix metalloproteinases in neuropathic pain and migraine: friends, enemies, and therapeutic targets. *Pain Res Treat* 2012 **2012** 952906.
665. Leira R, Sobrino T, Rodriguez-Yanez M, Blanco M, Arias S & Castillo J. Mmp-9 immunoreactivity in acute migraine. *Headache* 2007 **47** 698-702.
666. Gupta P & Dutta P. Landscape of Molecular Events in Pituitary Apoplexy. *Front Endocrinol (Lausanne)* 2018 **9** 107.
667. Lorenc VE, Jaldin-Fincati JR, Luna JD, Chiabrando GA & Sanchez MC. IGF-1 Regulates the Extracellular Level of Active MMP-2 and Promotes Muller Glial Cell Motility. *Invest Ophthalmol Vis Sci* 2015 **56** 6948-6960.
668. Saikali Z, Setya H, Singh G & Persad S. Role of IGF-1/IGF-1R in regulation of invasion in DU145 prostate cancer cells. *Cancer Cell Int* 2008 **8** 10.
669. Fischoeder A, Meyborg H, Stibenz D, Fleck E, Graf K & Stawowy P. Insulin augments matrix metalloproteinase-9 expression in monocytes. *Cardiovasc Res* 2007 **73** 841-848.
670. Liu CY, Xu JY, Shi XY, Huang W, Ruan TY, Xie P & Ding JL. M2-polarized tumor-associated macrophages promoted epithelial-mesenchymal transition in pancreatic cancer cells, partially through TLR4/IL-10 signaling pathway. *Lab Invest* 2013 **93** 844-854.
671. Ramsdell JS & Tashjian AH, Jr. GH4 pituitary cell variants selected as nonresponsive to thyrotropin-releasing hormone-enhanced substratum adhesion are nonresponsive to epidermal growth factor: evidence for a common signaling defect. *J Cell Physiol* 1989 **141** 565-572.
672. Meager A. Cytokine regulation of cellular adhesion molecule expression in inflammation. *Cytokine Growth Factor Rev* 1999 **10** 27-39.
673. Kiselyov VV, Soroka V, Berezin V & Bock E. Structural biology of NCAM homophilic binding and activation of FGFR. *J Neurochem* 2005 **94** 1169-1179.
674. Walmod PS, Kolkova K, Berezin V & Bock E. Zippers make signals: NCAM-mediated molecular interactions and signal transduction. *Neurochem Res* 2004 **29** 2015-2035.
675. Chae YK, Choi WM, Bae WH, Anker J, Davis AA, Agte S, Iams WT, Cruz M, Matsangou M & Giles FJ. Overexpression of adhesion molecules and barrier molecules is associated with differential infiltration of immune cells in non-small cell lung cancer. *Sci Rep* 2018 **8** 1023.
676. Crawford JM & Watanabe K. Cell adhesion molecules in inflammation and immunity: relevance to periodontal diseases. *Crit Rev Oral Biol Med* 1994 **5** 91-123.
677. Goridis C & Brunet JF. NCAM: structural diversity, function and regulation of expression. *Semin Cell Biol* 1992 **3** 189-197.
678. Ren G, Roberts AI & Shi Y. Adhesion molecules: key players in Mesenchymal stem cell-mediated immunosuppression. *Cell Adh Migr* 2011 **5** 20-22.
679. Rodrigues E & Macauley MS. Hypersialylation in Cancer: Modulation of Inflammation and Therapeutic Opportunities. *Cancers (Basel)* 2018 **10**.
680. Cella M & Colonna M. Aryl hydrocarbon receptor: Linking environment to immunity. *Semin Immunol* 2015 **27** 310-314.
681. Nguyen NT, Hanieh H, Nakahama T & Kishimoto T. The roles of aryl hydrocarbon receptor in immune responses. *Int Immunol* 2013 **25** 335-343.
682. Barroso A, Gualdron-Lopez M, Esper L, Brant F, Araujo RR, Carneiro MB, Avila TV, Souza DG, Vieira LQ, Rachid MA, Tanowitz HB, Teixeira MM & Machado FS. The Aryl Hydrocarbon Receptor Modulates Production of Cytokines and Reactive Oxygen Species and

Development of Myocarditis during Trypanosoma cruzi Infection. *Infect Immun* 2016 **84** 3071-3082.
683. Quintana FJ & Sherr DH. Aryl hydrocarbon receptor control of adaptive immunity. *Pharmacol Rev* 2013 **65** 1148-1161.
684. Simones T & Shepherd DM. Consequences of AhR activation in steady-state dendritic cells. *Toxicol Sci* 2011 **119** 293-307.
685. Climaco-Arvizu S, Dominguez-Acosta O, Cabanas-Cortes MA, Rodriguez-Sosa M, Gonzalez FJ, Vega L & Elizondo G. Aryl hydrocarbon receptor influences nitric oxide and arginine production and alters M1/M2 macrophage polarization. *Life Sci* 2016 **155** 76-84.
686. Sun D, Stopka-Farooqui U, Barry S, Aksoy E, Parsonage G, Vossenkamper A, Capasso M, Wan X, Norris S, Marshall JL, Clear A, Gribben J, MacDonald TT, Buckley CD, Korbonits M & Haworth O. Aryl Hydrocarbon Receptor Interacting Protein Maintains Germinal Center B Cells through Suppression of BCL6 Degradation. *Cell Rep* 2019 **27** 1461-1471 e1464.
687. Ravasi T, Suzuki H, Cannistraci CV, Katayama S, Bajic VB, Tan K, Akalin A, Schmeier S, Kanamori-Katayama M, Bertin N, Carninci P, Daub CO, Forrest AR, Gough J, Grimmond S, Han JH, Hashimoto T, Hide W, Hofmann O, Kamburov A, Kaur M, Kawaji H, Kubosaki A, Lassmann T, van Nimwegen E, MacPherson CR, Ogawa C, Radovanovic A, Schwartz A, Teasdale RD, Tegner J, Lenhard B, Teichmann SA, Arakawa T, Ninomiya N, Murakami K, Tagami M, Fukuda S, Imamura K, Kai C, Ishihara R, Kitazume Y, Kawai J, Hume DA, Ideker T & Hayashizaki Y. An atlas of combinatorial transcriptional regulation in mouse and man. *Cell* 2010 **140** 744-752.
688. Schimmack G, Eitelhuber AC, Vincendeau M, Demski K, Shinohara H, Kurosaki T & Krappmann D. AIP augments CARMA1-BCL10-MALT1 complex formation to facilitate NF-kappaB signaling upon T cell activation. *Cell Commun Signal* 2014 **12** 49.
689. Zhang Q, Lenardo MJ & Baltimore D. 30 Years of NF-kappaB: A Blossoming of Relevance to Human Pathobiology. *Cell* 2017 **168** 37-57.
690. Borrello MG, Alberti L, Fischer A, Degl'innocenti D, Ferrario C, Gariboldi M, Marchesi F, Allavena P, Greco A, Collini P, Pilotti S, Cassinelli G, Bressan P, Fugazzola L, Mantovani A & Pierotti MA. Induction of a proinflammatory program in normal human thyrocytes by the RET/PTC1 oncogene. *Proc Natl Acad Sci U S A* 2005 **102** 14825-14830.
691. Caimari F & Korbonits M. Novel Genetic Causes of Pituitary Adenomas. *Clin Cancer Res* 2016 **22** 5030-5042.
692. Wang Y, Fu Y, Xue S, Ai A, Chen H, Lyu Q & Kuang Y. The M2 polarization of macrophage induced by fractalkine in the endometriotic milieu enhances invasiveness of endometrial stromal cells. *Int J Clin Exp Pathol* 2014 **7** 194-203.
693. Liu W, Jiang L, Bian C, Liang Y, Xing R, Yishakea M & Dong J. Role of CX3CL1 in Diseases. *Arch Immunol Ther Exp (Warsz)* 2016 **64** 371-383.
694. Rossi DL, Hardiman G, Copeland NG, Gilbert DJ, Jenkins N, Zlotnik A & Bazan JF. Cloning and characterization of a new type of mouse chemokine. *Genomics* 1998 **47** 163-170.
695. Clark AK & Malcangio M. Fractalkine/CX3CR1 signaling during neuropathic pain. *Front Cell Neurosci* 2014 **8** 121.
696. Deshmane SL, Kremlev S, Amini S & Sawaya BE. Monocyte chemoattractant protein-1 (MCP-1): an overview. *J Interferon Cytokine Res* 2009 **29** 313-326.
697. Rossi R, Lichtner M, De Rosa A, Sauzullo I, Mengoni F, Massetti AP, Mastroianni CM & Vullo V. In vitro effect of anti-human immunodeficiency virus CCR5 antagonist maraviroc on chemotactic activity of monocytes, macrophages and dendritic cells. *Clin Exp Immunol* 2011 **166** 184-190.
698. Lennard Richard ML, Nowling TK, Brandon D, Watson DK & Zhang XK. Fli-1 controls transcription from the MCP-1 gene promoter, which may provide a novel mechanism for chemokine and cytokine activation. *Mol Immunol* 2015 **63** 566-573.

699. Lennard Richard ML, Sato S, Suzuki E, Williams S, Nowling TK & Zhang XK. The Fli-1 transcription factor regulates the expression of CCL5/RANTES. *J Immunol* 2014 **193** 2661-2668.
700. Li Y, Luo H, Liu T, Zacksenhaus E & Ben-David Y. The ets transcription factor Fli-1 in development, cancer and disease. *Oncogene* 2015 **34** 2022-2031.
701. Cai F, Hong Y, Xu J, Wu Q, Reis C, Yan W, Wang W & Zhang J. A Novel Mutation of Aryl Hydrocarbon Receptor Interacting Protein Gene Associated with Familial Isolated Pituitary Adenoma Mediates Tumor Invasion and Growth Hormone Hypersecretion. *World Neurosurg* 2019 **123** e45-e59.
702. Fukuda T, Tanaka T, Hamaguchi Y, Kawanami T, Nomiyama T & Yanase T. Augmented Growth Hormone Secretion and Stat3 Phosphorylation in an Aryl Hydrocarbon Receptor Interacting Protein (AIP)-Disrupted Somatotroph Cell Line. *PLoS One* 2016 **11** e0164131.
703. Zhou Q, Lavorgna A, Bowman M, Hiscott J & Harhaj EW. Aryl Hydrocarbon Receptor Interacting Protein Targets IRF7 to Suppress Antiviral Signaling and the Induction of Type I Interferon. *J Biol Chem* 2015 **290** 14729-14739.
704. Daly A, Rostomyan L, Betea D, Bonneville JF, Villa C, Pellegata NS, Waser B, Reubi JC, Waeber Stephan C, Christ E & Beckers A. AIP-mutated acromegaly resistant to first-generation somatostatin analogs: long-term control with pasireotide LAR in two patients. *Endocr Connect* 2019.
705. Cazabat L, Bouligand J, Salenave S, Bernier M, Gaillard S, Parker F, Young J, Guiochon-Mantel A & Chanson P. Germline AIP mutations in apparently sporadic pituitary adenomas: prevalence in a prospective single-center cohort of 443 patients. *J Clin Endocrinol Metab* 2012 **97** E663-670.
706. Preda V, Korbonits M, Cudlip S, Karavitaki N & Grossman AB. Low rate of germline AIP mutations in patients with apparently sporadic pituitary adenomas before the age of 40: a single-centre adult cohort. *Eur J Endocrinol* 2014 **171** 659-666.
707. Daly AF, Vanbellinghen JF, Khoo SK, Jaffrain-Rea ML, Naves LA, Guitelman MA, Murat A, Emy P, Gimenez-Roqueplo AP, Tamburrano G, Raverot G, Barlier A, de Herder WW, Penfornis A, Ciccarelli E, Estour B, Lecomte P, Gatta B, Chabre O, Sabate MI, Bertagna X, Garcia BN, Stalldecker G, Colao A, Ferolla P, Wemeau JL, Caron P, Sadoul JL, Oneto A, Archambeaud F, Calender A, Sinilnikova O, Montanana CF, Cavagnini F, Hana V, Solano A, Delettieres D, Luccio-Camelo DC, Basso A, Rohmer V, Brue T, Bours V, Teh BT & Beckers A. Aryl hydrocarbon receptor-interacting protein gene mutations in familial isolated pituitary adenomas: analysis in 73 families. *J. Clin. Endocrinol. Metab* 2007 **92** 1891-1896.
708. Williams F, Hunter S, Bradley L, Chahal HS, Storr HL, Akker SA, Kumar AV, Orme SM, Evanson J, Abid N, Morrison PJ, Korbonits M & Atkinson AB. Clinical experience in the screening and management of a large kindred with familial isolated pituitary adenoma due to an aryl hydrocarbon receptor interacting protein (AIP) mutation. *J Clin Endocrinol Metab* 2014 **99** 1122-1131.
709. Wang K, Li M & Hakonarson H. ANNOVAR: functional annotation of genetic variants from high-throughput sequencing data. *Nucleic Acids Res* 2010 **38** e164.
710. McLaren W, Gil L, Hunt SE, Riat HS, Ritchie GR, Thormann A, Flicek P & Cunningham F. The Ensembl Variant Effect Predictor. *Genome Biol* 2016 **17** 122.
711. Ellard S, Lango Allen H, De Franco E, Flanagan SE, Hysenaj G, Colclough K, Houghton JA, Shepherd M, Hattersley AT, Weedon MN & Caswell R. Improved genetic testing for monogenic diabetes using targeted next-generation sequencing. *Diabetologia* 2013 **56** 1958-1963.
712. Richards S, Aziz N, Bale S, Bick D, Das S, Gastier-Foster J, Grody WW, Hegde M, Lyon E, Spector E, Voelkerding K, Rehm HL & Committee ALQA. Standards and guidelines for the interpretation of sequence variants: a joint consensus recommendation of the American

College of Medical Genetics and Genomics and the Association for Molecular Pathology. *Genet Med* 2015 **17** 405-424.

713. Mothojakan NB, Ferrau F, Dang MN, Barlier A, Chanson P, Occhi G, Daly A, Schofl C, Dal J, Gadelha MR, Ludman M, Kapur S, Iacovazzo D & Korbonits M. Polymorphism or mutation? – The role of the R304Q missense AIP mutation in the predisposition to pituitary adenoma. *In Endocrine Abstracts. Bioscientifica, Brighton, UK* 2016 P167.
714. Georgitsi M, Raitila A, Karhu A, Tuppurainen K, Makinen MJ, Vierimaa O, Paschke R, Saeger W, van der Luijt RB, Sane T, Robledo M, De Menis E, Weil RJ, Wasik A, Zielinski G, Lucewicz O, Lubinski J, Launonen V, Vahteristo P & Aaltonen LA. Molecular diagnosis of pituitary adenoma predisposition caused by aryl hydrocarbon receptor-interacting protein gene mutations. *Proc Natl Acad Sci U S A* 2007 **104** 4101-4105.
715. Raitila A, Georgitsi M, Karhu A, Tuppurainen K, Makinen MJ, Birkenkamp-Demtroder K, Salmenkivi K, Orntoft TF, Arola J, Launonen V, Vahteristo P & Aaltonen LA. No evidence of somatic aryl hydrocarbon receptor interacting protein mutations in sporadic endocrine neoplasia. *Endocr Relat Cancer* 2007 **14** 901-906.
716. Jones MK, Evans PJ, Jones IR & Thomas JP. Familial acromegaly. *Clin Endocrinol (Oxf)* 1984 **20** 355-358.
717. Georgitsi M, De Menis E, Cannavo S, Makinen MJ, Tuppurainen K, Pauletto P, Curto L, Weil RJ, Paschke R, Zielinski G, Wasik A, Lubinski J, Vahteristo P, Karhu A & Aaltonen LA. Aryl hydrocarbon receptor interacting protein (AIP) gene mutation analysis in children and adolescents with sporadic pituitary adenomas. *Clin Endocrinol (Oxf)* 2008 **69** 621-627.
718. Guaraldi F, Corazzini V, Gallia GL, Grottoli S, Stals K, Dalantaeva N, Frohman LA, Korbonits M & Salvatori R. Genetic analysis in a patient presenting with meningioma and familial isolated pituitary adenoma (FIPA) reveals selective involvement of the R81X mutation of the AIP gene in the pathogenesis of the pituitary tumor. *Pituitary* 2012 **15, Suppl.** 61-67.
719. Luccio-Camelo DC, Une KN, Ferreira RE, Khoo SK, Nickolov R, Bronstein MD, Vaisman M, Teh BT, Frohman LA, Mendonca BB & Gadelha MR. A meiotic recombination in a new isolated familial somatotropinoma kindred. *Eur J Endocrinol* 2004 **150** 643-648.
720. Toledo RA, Lourenco DM, Jr., Liberman B, Cunha-Neto MB, Cavalcanti MG, Moyses CB, Toledo SP & Dahia PL. Germline mutation in the aryl hydrocarbon receptor interacting protein gene in familial somatotropinoma. *J Clin Endocrinol Metab* 2007 **92** 1934-1937.
721. Stratakis CA, Tichomirowa MA, Boikos S, Azevedo MF, Lodish M, Martari M, Verma S, Daly AF, Raygada M, Keil MF, Papademetriou J, Drori-Herishanu L, Horvath A, Tsang KM, Nesterova M, Franklin S, Vanbellinghen JF, Bours V, Salvatori R & Beckers A. The role of germline AIP, MEN1, PRKAR1A, CDKN1B and CDKN2C mutations in causing pituitary adenomas in a large cohort of children, adolescents, and patients with genetic syndromes. *Clin Genet* 2010 **78** 457-463.
722. Cazabat L, Libe R, Perlemoine K, Rene-Corail F, Burnichon N, Gimenez-Roqueplo AP, Dupasquier-Fediaevsky L, Bertagna X, Clauser E, Chanson P, Bertherat J & Raffin-Sanson ML. Germline inactivating mutations of the aryl hydrocarbon receptor-interacting protein gene in a large cohort of sporadic acromegaly: mutations are found in a subset of young patients with macroadenomas. *Eur J Endocrinol* 2007 **157** 1-8.
723. Martucci F, Trivellin G & Korbonits M. Familial isolated pituitary adenomas: an emerging clinical entity. *J Endocrinol Invest* 2012 **35** 1003-1014.
724. Garcia WR, Cortes HT & Romero AF. Pituitary gigantism: a case series from Hospital de San Jose (Bogota, Colombia). *Arch Endocrinol Metab* 2019 **63** 385-393.
725. Jorge BH, Agarwal SK, Lando VS, Salvatori R, Barbero RR, Abelin N, Levine MA, Marx SJ & Toledo SP. Study of the multiple endocrine neoplasia type 1, growth hormone-releasing hormone receptor, Gs alpha, and Gi2 alpha genes in isolated familial acromegaly. *J Clin Endocrinol Metab* 2001 **86** 542-544.

726. Jennings JE, Georgitsi M, Holdaway I, Daly A, Tichomirowa M, Beckers A, Aaltonen L, Karhu A & Cameron F. Aggressive pituitary adenomas occurring in young patients in a large Polynesian kindred with a germline R271W mutation in the AIP gene. *Eur. J Endocrinol* 2009 **161** 799-804.
727. Karaca Z, Taheri S, Tanriverdi F, Unluhizarci K & Kelestimur F. Prevalence of AIP mutations in a series of Turkish acromegalic patients: are synonymous AIP mutations relevant? *Pituitary* 2015 **18** 831-837.
728. Ramirez-Renteria C, Hernandez-Ramirez LC, Portocarrero-Ortiz L, Vargas G, Melgar V, Espinosa E, Espinosa-de-Los-Monteros AL, Sosa E, Gonzalez B, Zuniga S, Unterlander M, Burger J, Stals K, Bussell AM, Ellard S, Dang M, Iacovazzo D, Kapur S, Gabrovska P, Radian S, Roncaroli F, Korbonits M & Mercado M. AIP mutations in young patients with acromegaly and the Tampico Giant: the Mexican experience. *Endocrine* 2016 **53** 402-411.
729. Occhi G, Trivellin G, Ceccato F, De Lazzari P, Giorgi G, Dematte S, Grimaldi F, Castello R, Davi MV, Arnaldi G, Salviati L, Opocher G, Mantero F & Scaroni C. Prevalence of AIP mutations in a large series of sporadic Italian acromegalic patients and evaluation of CDKN1B status in acromegalic patients with multiple endocrine neoplasia. *Eur J Endocrinol* 2010 **163** 369-376.
730. Ioannidis NM, Rothstein JH, Pejaver V, Middha S, McDonnell SK, Baheti S, Musolf A, Li Q, Holzinger E, Karyadi D, Cannon-Albright LA, Teerlink CC, Stanford JL, Isaacs WB, Xu J, Cooney KA, Lange EM, Schleutker J, Carpten JD, Powell IJ, Cussenot O, Cancel-Tassin G, Giles GG, MacInnis RJ, Maier C, Hsieh CL, Wiklund F, Catalona WJ, Foulkes WD, Mandal D, Eeles RA, Kote-Jarai Z, Bustamante CD, Schaid DJ, Hastie T, Ostrander EA, Bailey-Wilson JE, Radivojac P, Thibodeau SN, Whittemore AS & Sieh W. REVEL: An Ensemble Method for Predicting the Pathogenicity of Rare Missense Variants. *Am J Hum Genet* 2016 **99** 877-885.
731. van der Velde KJ, de Boer EN, van Diemen CC, Sikkema-Raddatz B, Abbott KM, Knopperts A, Franke L, Sijmons RH, de Koning TJ, Wijmenga C, Sinke RJ & Swertz MA. GAVIN: Gene-Aware Variant INterpretation for medical sequencing. *Genome Biol* 2017 **18** 6.
732. Oriola J, Lucas T, Halperin I, Mora M, Perales MJ, Alvarez-Escola C, Paz de MN, Diaz Soto G, Salinas I, Julian MT, Olaizola I, Bernabeu I, Marazuela M & Puig-Domingo M. Germline mutations of AIP gene in somatotropinomas resistant to somatostatin analogues. *Eur J Endocrinol* 2013 **168** 9-13.
733. Daly A, Cano DA, Venegas E, Petrossians P, Dios E, Castermans E, Flores-Martinez A, Bours V, Beckers A & Soto A. AIP and MEN1 mutations and AIP immunohistochemistry in pituitary adenomas in a tertiary referral center. *Endocr Connect* 2019.
734. Salenave S, Ancelle D, Bahougne T, Raverot G, Kamenicky P, Bouligand J, Guiochon-Mantel A, Linglart A, Souchon PF, Nicolino M, Young J, Borson-Chazot F, Delemer B & Chanson P. Macroprolactinomas in children and adolescents: factors associated with the response to treatment in 77 patients. *J Clin Endocrinol Metab* 2015 **100** 1177-1186.
735. Mangupli R, Rostomyan L, Castermans E, Caberg JH, Camperos P, Krivoy J, Cuauro E, Bours V, Daly AF & Beckers A. Combined treatment with octreotide LAR and pegvisomant in patients with pituitary gigantism: clinical evaluation and genetic screening. *Pituitary* 2016 **19** 507-514.
736. Joshi K, Daly AF, Beckers A & Zacharin M. Resistant Paediatric Somatotropinomas due to AIP Mutations: Role of Pegvisomant. *Horm Res Paediatr* 2018 **90** 196-202.
737. Beckers A, Petrossians P, Hanson J & Daly AF. The causes and consequences of pituitary gigantism. *Nat Rev Endocrinol* 2018 **14** 705-720.
738. Rostomyan L, Potorac I, Beckers P, Daly AF & Beckers A. AIP mutations and gigantism. *Ann Endocrinol (Paris)* 2017 **78** 123-130.

739. Lenders JW, Duh QY, Eisenhofer G, Gimenez-Roqueplo AP, Grebe SK, Murad MH, Naruse M, Pacak K, Young WF, Jr. & Endocrine S. Pheochromocytoma and paraganglioma: an endocrine society clinical practice guideline. *J Clin Endocrinol Metab* 2014 **99** 1915-1942.
740. Muth A, Crona J, Gimm O, Elmgren A, Filipsson K, Stenmark Askmalm M, Sandstedt J, Tengvar M & Tham E. Genetic testing and surveillance guidelines in hereditary pheochromocytoma and paraganglioma. *J Intern Med* 2019 **285** 187-204.
741. Wells SA, Jr., Asa SL, Dralle H, Elisei R, Evans DB, Gagel RF, Lee N, Machens A, Moley JF, Pacini F, Raue F, Frank-Raue K, Robinson B, Rosenthal MS, Santoro M, Schlumberger M, Shah M, Waguespack SG & American Thyroid Association Guidelines Task Force on Medullary Thyroid C. Revised American Thyroid Association guidelines for the management of medullary thyroid carcinoma. *Thyroid* 2015 **25** 567-610.
742. Greenman Y & Stern N. Optimal management of non-functioning pituitary adenomas. *Endocrine* 2015 **50** 51-55.
743. Nieman LK, Biller BM, Findling JW, Murad MH, Newell-Price J, Savage MO, Tabarin A & Endocrine S. Treatment of Cushing's Syndrome: An Endocrine Society Clinical Practice Guideline. *J Clin Endocrinol Metab* 2015 **100** 2807-2831.
744. Blair J, Korbonits M, Ronaldson A, Dang M & Spoudeas H. National UK guidelines for managing pituitary adenomas in children and young people under 19 years developed according to the AGREE II framework. *In International Symposium on Pediatric Neuro-Oncology. Denver.* 2018 **CRAN-40**.
745. Goudet P, Dalac A, Le Bras M, Cardot-Bauters C, Niccoli P, Levy-Bohbot N, du Boullay H, Bertagna X, Ruszniewski P, Borson-Chazot F, Verges B, Sadoul JL, Menegaux F, Tabarin A, Kuhn JM, d'Anella P, Chabre O, Christin-Maitre S, Cadiot G, Binquet C & Delemer B. MEN1 disease occurring before 21 years old: a 160-patient cohort study from the Groupe d'etude des Tumeurs Endocrines. *J Clin Endocrinol Metab* 2015 **100** 1568-1577.
746. Giusti F, Cianferotti L, Boaretto F, Cetani F, Cioppi F, Colao A, Davi MV, Faggiano A, Fanciulli G, Ferolla P, Ferone D, Fossi C, Giudici F, Gronchi G, Loli P, Mantero F, Marcocci C, Marini F, Masi L, Opocher G, Beck-Peccoz P, Persani L, Scillitani A, Sciortino G, Spada A, Tomassetti P, Tonelli F & Brandi ML. Multiple endocrine neoplasia syndrome type 1: institution, management, and data analysis of a nationwide multicenter patient database. *Endocrine* 2017 **58** 349-359.
747. Burgess JR, Shepherd JJ, Parameswaran V, Hoffman L & Greenaway TM. Spectrum of pituitary disease in multiple endocrine neoplasia type 1 (MEN 1): clinical, biochemical, and radiological features of pituitary disease in a large MEN 1 kindred. *J Clin Endocrinol Metab* 1996 **81** 2642-2646.
748. Nunes VS, Souza GL, Perone D, Conde SJ & Nogueira CR. Frequency of multiple endocrine neoplasia type 1 in a group of patients with pituitary adenoma: genetic study and familial screening. *Pituitary* 2014 **17** 30-37.
749. Fassnacht M, Arlt W, Bancos I, Dralle H, Newell-Price J, Sahdev A, Tabarin A, Terzolo M, Tsagarakis S & Dekkers OM. Management of adrenal incidentalomas: European Society of Endocrinology Clinical Practice Guideline in collaboration with the European Network for the Study of Adrenal Tumors. *Eur J Endocrinol* 2016 **175** G1-G34.
750. Oberg K, Jelic S & Group EGW. Neuroendocrine bronchial and thymic tumors: ESMO clinical recommendation for diagnosis, treatment and follow-up. *Ann Oncol* 2008 **19 Suppl 2** ii102-103.
751. Oberg K, Knigge U, Kwekkeboom D, Perren A & Group EGW. Neuroendocrine gastro-entero-pancreatic tumors: ESMO Clinical Practice Guidelines for diagnosis, treatment and follow-up. *Ann Oncol* 2012 **23 Suppl 7** vii124-130.
752. Wilhelm SM, Wang TS, Ruan DT, Lee JA, Asa SL, Duh QY, Doherty GM, Herrera MF, Pasieka JL, Perrier ND, Silverberg SJ, Solorzano CC, Sturgeon C, Tublin ME, Udelsman R & Carty SE.

The American Association of Endocrine Surgeons Guidelines for Definitive Management of Primary Hyperparathyroidism. *JAMA Surg* 2016 **151** 959-968.

753. Vannucci L, Marini F, Giusti F, Ciuffi S, Tonelli F & Brandi ML. MEN1 in children and adolescents: Data from patients of a regional referral center for hereditary endocrine tumors. *Endocrine* 2018 **59** 438-448.

754. Sakurai A, Suzuki S, Kosugi S, Okamoto T, Uchino S, Miya A, Imai T, Kaji H, Komoto I, Miura D, Yamada M, Uruno T, Horiuchi K, Miyauchi A, Imamura M, Japan MENCo, Fukushima T, Hanazaki K, Hirakawa S, Igarashi T, Iwatani T, Kammori M, Katabami T, Katai M, Kikumori T, Kiribayashi K, Koizumi S, Midorikawa S, Miyabe R, Munekage T, Ozawa A, Shimizu K, Sugitani I, Takeyama H & Yamazaki M. Multiple endocrine neoplasia type 1 in Japan: establishment and analysis of a multicentre database. *Clin Endocrinol (Oxf)* 2012 **76** 533-539.

755. Goudet P, Bonithon-Kopp C, Murat A, Ruszniewski P, Niccoli P, Menegaux F, Chabrier G, Borson-Chazot F, Tabarin A, Bouchard P, Cadiot G, Beckers A, Guilhem I, Chabre O, Caron P, Du Boullay H, Verges B & Cardot-Bauters C. Gender-related differences in MEN1 lesion occurrence and diagnosis: a cohort study of 734 cases from the Groupe d'etude des Tumeurs Endocrines. *Eur J Endocrinol* 2011 **165** 97-105.

Appendix 1: Supplemental tables with genes with altered expression in sporadic pituitary adenomas, and the corresponding literature references

Oncogene	Normal function	Altered function in PAs / PA types	References
AKT1	Regulation of metabolism, differentiation, growth, proliferation and angiogenesis	Increased expression Various PA types, mainly NFPAs	Musat *et al* 2005[1]
AKT2	Regulation of metabolism, differentiation, growth, proliferation and angiogenesis	Increased expression Various PA types	Musat *et al* 2005[1]
BAG1	Inhibits chaperone activity of HSP70/HSC70 and the pro-apoptotic function of PPP1R15A	Increased expression Various PA types	Morris *et al* 2005[2]
BMI1	Repress the transcription of many genes	Increased expression; genetic amplification in PAs Various PA types	Sanchez-Beato *et al* 2006[3] Palumbo *et al* 2013[4] Westerman *et al* 2012[5]
CCNA1 (cyclin A1)	Regulation of G1-S and G2-M phases of the cell cycle	Increased expression Various PA types	Turner *et al* 2000[6] Nakabayashi *et al* 2001[7]
CCNB1 (cyclin B1)	Regulation of G2-M transition of the cell cycle	Increased expression Various PA types	Turner *et al* 2000[6] Wierinckx *et al* 2007[8]
CCNB2 (cyclin B2)	Regulation of G2-M transition of the cell cycle	Increased expression Various PA types	De Martino *et al* 2009[9]
CCND1 (cyclin D1)	Progression through G1-S phase of the cell cycle	Increased expression Somatotrophinomas and NFPAs	Hibberts *et al* 1999[10] Jordan *et al* 2000[11] Turner *et al* 2000[6] Simpson *et al* 2001[12]
CCNE1 (cyclin E1)	Progression through the G1-S phase of the cell cycle	Increased expression Mainly corticotrophinomas	Jordan *et al* 2000[11] Turner *et al* 2000[6]
COPS5	Involved in different cellular and developmental processes	Increased expression Pituitary carcinomas	Korbonits *et al* 2002[13]
CREB	Transcriptional activator of CREs, regulating differentiation and proliferation	Constitutive activation by phosphorylation in somatotrophinomas	Bertherat *et al* 1995[14]
DNMT3	Mediator of epigenetic control by histone modifications of gene expression	Increased expression Various PA types	Zhu *et al* 2008[15]
EGFR	Transmembrane glycoprotein needed for cell proliferation, survival and differentiation	Increased expression NFPAs, mainly aggressive PAs	Chaidarun *et al* 1994[16]
ERα	Mediates the actions of estrogens	Increased expression Prolactinomas	Delgrange *et al* 2015[17]
EZH2	Regulation of the cell cycle	Increased expression Various PA types	Schult *et al* 2015[18]
FGF2	Regulation of cell survival, proliferation, differentiation, migration and angiogenesis	Increased expression Various PA types	McCabe *et al* 2003[19]
FGF4	Membrane-anchored receptor for FGF	Increased expression of a N-terminally truncated cytoplasmic form by alternative transcription Various PA types	Jackson *et al* 2006[20]

FGFR1/ FGFR2 FGFR4	Involved in cell proliferation	Increased expression Various PA types	McCabe *et al* 2003[19] Zhu *et al* 2007[21] Ezzat *et al* 2002[22]
FOLR1	Binds to folate, reduces folic acid derivatives and mediates delivery of 5-methyltetra-hydrofolate to the interior of cells	Increased expression in NFPAs, Decreased expression in PRL- and GH-secreting PAs	Evans *et al* 2001[23]
GHRH	Stimulates GH secretion	Increased expression Somatotrophinomas	Thapar *et al* 1997[24]
GLI1	Involved in the Hedgehog signalling; its activation induce stem cell proliferation and pituitary hormone release	Increased expression. ACTH-, GH- and PRL-secreting PAs	Lampichler *et al* 2015[25]
GNAI2	Inhibition of adenylate cyclase and calcium influx	Gain-of-function somatic mutations Various PAs types	Williamson *et al* 1994[26] Williamson *et al* 1995[27]
GNAS1	Stimulatory G protein α-subunit that activates adenylate cyclase	Gain-of-function somatic mutations; loss of imprinting Cause 40% of sporadic GH-secreting PAs	Vallar *et al* 1987[28] Landis *et al* 1989[29] Tordjman *et al* 1993[30] Williamson *et al* 1994[26]
HMGA1/ HMGA2	Regulation of growth and development	Amplification and overexpression Various PAs types	De Martino *et al* 2009[9] Finelli *et al* 2002[31]
HRAS	Regulation of cell division in response to growth factors stimulation	Gain-of-function somatic mutations Invasive prolactinomas/NFPAs and pituitary carcinomas	Karga *et al* 1992[32] Cai *et al* 1994[33] Pei *et al* 1994[34]
hTERT	Plays a role in cellular senescence, causing progressive shortening of telomeres	Increased activating methylation of the promoter	Kochling *et al* 2016[35]
IKZF1	Important function in the hematopoietic and immune systems	Dominant-negative truncated isoform	Ezzat *et al* 2003[36]
LAPTM4B	Involved in the lysosome homeostasis, acidification and function	Increased expression NFPAs and corticotrophinomas	Morris *et al* 2005[2]
LGALS3 (Galectin-3)	Mediation of cell migration, adhesion, cell-to-cell interaction and apoptosis inhibition	Increased expression Various PA types, mainly aggressive PAs	Riss *et al* 2003[37]
MAGEA3	May play a role in embryonal development and tumour transformation or progression	Increased expression by promoter hypomethylation and histone acetylation in association with FGFR2-downregulation Various PA types	Zhu *et al* 2008[38]
MERTK	Receptor-TK involved in signal transduction from extracellular matrix into the cytoplasm	Increased expression in corticotrophinomas Decreased expression in prolactinomas	Evans *et al* 2001[23]
MST4	Involved in cellular responses to hypoxic environments	Increased expression NFPA	Xiong *et al* 2015[39]
MYO5A	Involved in tumour cell migration, invasion and metastasis	Increased expression NFPAs, mainly aggressive PAs	Galland *et al* 2010[40]
OCD1	Catalyzes the decarboxylation of ornithine to form putrescine	Increased expression in somatotrophinomas, and decreased in corticotrophinomas	Evans *et al* 2001[23]
PIK3CA	Regulation of proliferation, cell survival, migration and cell trafficking	Gain-of-function somatic mutations and amplification Various PA types	Lin *et al* 2009[41]

PITX2	Involved in the Wnt/Dvl/β-catenin pathway	Increased expression NFPA	Acunzo *et al* 2011[42]
POU1F1 (PIT1)	Transcription factor involved in the differentiation of the anterior pituitary	Increased expression Various PA types	Palmieri *et al* 2012[43]
PRKCA (PKCα)	Kinase that participates in growth factor and hormone signalling and cell proliferation	Overexpression, gain-of-function somatic mutations NFPAs	Alvaro *et al* 1993[44]
PTTG1	Cell cycle regulation and cell senescence	Increased expression Corticotrophinomas and NFPAs	Zhang *et al* 1999[45] McCabe *et al* 2003[19] Morris *et al* 2005[2]
PTTG1IP	Facilitates nuclear translocation of PTTG1 and potentiates transcriptional activation of FGF2 by PTTG1	Increased expression NFPAs	McCabe *et al* 2003[19]
RSUME	RSUME increase the levels of HIF-1α, which is the most important transcription factor of cellular adaptive processes to hypoxic conditions	Increased expression Various PA types	Shan *et al* 2012[46]
SHH	Hedgehog signalling activation induce the stem cell proliferation and hormone release in the pituitary	Increased expression ACTH-, GH- and PRL-secreting PAs	Vila *et al* 2005[47]
STAT3	Participates in cellular responses to cytokines and growth factors	Decreased expression GH-secreting PAs	Zhou *et al* 2015[48]
TGFα	Competes with EGF for binding to EGFR producing a mitogenic response	Increased expression Prolactinomas	Ezzat *et al* 1995[49]

Genes with increased expression involved in pathogenesis of sporadic pituitary adenomas
CREs, cAMP response elements; EGF, epidermal growth factor; EGFR, epidermal growth factor receptor; EMT, epithelial-mesenchymal transition; FGF, fibroblast growth factor; GH, growth hormone; LOH, loss of heterozygosity; NFPAs, non-functioning pituitary adenomas; PAs, pituitary adenomas; PRL, prolactin; TK, tyrosine kinase. Adapted from Marques & Korbonits (2017)[50].

Tumour suppressor gene	Normal function	Altered function in PAs / PAs types	References
AIP	Co-chaperone protein	Decreased expression Somatotrophinomas	Kasuki *et al* 2011[51] Kasuki *et al* 2012[52]
BMP4	Regulation of differentiation and proliferation of pituitary cells	Downregulated due to histone modification Prolactinomas	Paez-Pereda *et al* 2003[53]
CABLES1	Regulation of proliferation and/or cell differentiation	Decreased expression Corticotrophinomas	Roussel-Gervais *et al* 2016[54]
CDH1	Encodes E-cadherin involved in cell adhesion and inhibits EMT	Decreased expression by promoter methylation Various PA types	Qian *et al* 2007[55]
CDH13	Encodes H-cadherin involved in cell adhesion and inhibits EMT	Decreased expression by promoter methylation Various PA types	Qian *et al* 2007[55]
CDKN1A (p21)	Regulation of the cell cycle progression at G1	Decreased expression in NFPAs; increased expression in GH-secreting PAs	Neto *et al* 2005[56]
CDKN1B (p27)	Blocks cell cycle at G0-G1 phase	Reduced expression Various PA types, mainly corticotrophinomas and carcinomas	Qian *et al* 1996[57] Lloyd *et al* 1997[58] Jin *et al* 1997[59] Bamberger *et al* 1999[60]
CDKN2A (p16)	Induces cell cycle arrest in G1-G2 phases	Reduced expression Various PA types, mainly NFPAs	Woloschak *et al* 1996[61] Jaffrain-Rea *et al* 1999[62] Korbonits *et al* 2002[13]
CDKN2B (p15)	Induces cell cycle arrest at G1 phase	Reduced expression Various PA types	Ogino *et al* 2005[63] Yoshino *et al* 2007[64]
CDKN2C (p18)	Induces cell cycle arrest at G1 phase	Reduced expression Various PA types	Morris *et al* 2005[2] Hossain *et al* 2009[65]
DAPK	Positive mediator of programmed cell death	Decreased expression either by promoter methylation or by homozygous deletion of promoter CpG island Various PA types, mainly aggressive PAs	Simpson *et al* 2002[66] Bello *et al* 2006[67]
DKC1	Modification of rRNA and regulation of telomerase activity	Loss-of-function somatic mutation NFPAs	Bellodi *et al* 2010[68]
DRD2	Dopamine G protein-coupled receptor	Decreased expression Prolactinomas	Caccavelli *et al* 1994[69]
FOLR1	Binds to folate, reduces folic acid derivatives and mediates delivery of 5-methyltetrahydrofolate to the cell interior	Increased expression in NFPA, Decreased expression in PRL- and GH-secreting PAs	Evans *et al* 2001[23]
GADD45-β	Regulation of growth and apoptosis	Decreased expression NFPAs	Michaelis *et al* 2011[70]
GADD45-γ	Regulation of growth and apoptosis	Decreased expression by promoter methylation NFPAs, PRL- and GH-secreting PAs	Zhang *et al* 2002[71] Bahar *et al* 2004[72]
GH-R	Transmembrane receptor that mediates GH action	Loss-of-function somatic mutation Somatotrophinomas	Asa *et al* 2007[73]
HDAC2	Enzyme that deacetylates of lysine residues on core histones	Loss-of-function Corticotrophinomas	Bilodeau *et al* 2006[74]
MEG3	Induces apoptosis and inhibits tumoural cell proliferation	Decreased expression by promoter methylation NFPAs	Zhang *et al* 2002[71] Zhang *et al* 2003[75] Zhao *et al* 2005[76]

MEN1	Transcriptional regulator involved in the cell proliferation control	Somatic mutations or deletions or decreased expression Various PA types	Zhuang *et al* 1997[77] Tanaka *et al* 1998[78] Wenbin *et al* 1999[79]
MERTK	Receptor-TK involved in signal transduction from extracellular matrix into the cytoplasm	Expression increased in corticotrophinomas and decreased in prolactinomas	Evans *et al* 2001[23]
MGMT	Involved in DNA repair and cell cycle regulation	Decreased expression by promoter methylation Various PA types	Lau *et al* 2010[80]
NM23	Downregulate cyclin B and prevent the cell cycle progression	Decreased expression due to allelic loss Various PA types, mainly aggressive PAs	Takino *et al* 1995[81]
NR3C1	Nuclear receptor for glucocorticoids	Loss-of-function somatic mutations, LOH Corticotrophinomas	Karl *et al* 1996[82] Huizenga *et al* 1998[83]
OCD1	Catalyzes the decarboxylation of ornithine to form putrescine	Expression increased in somatotrophinomas and decreased in corticotrophinomas	Evans *et al* 2001[23]
PLAGL1 (ZAC1)	Zinc finger transcription factor that plays a role in pituitary development, differentiation and tumourigenesis	Decreased expression NFPAs	Pagotto *et al* 2000[84] Noh *et al* 2009[85]
RASSF1/ RASSF3	Ras association domain family member-1/3, acting as p53 activator	Decreased expression by promoter methylation Various PA types	Qian *et al* 2005[86]
RB1 (pRB)	Key regulator of cell division	Decreased expression Aggressive PAs	Simpson *et al* 2000[87] Ogino *et al* 2005[63] Yoshino *et al* 2006[64]
RHBDD3 (PTAG)	Pro-apoptotic mediator	Decreased expression Various PA types	Bahar *et al* 2004[72]
RPRM	Downstream effector of p53-induced cell cycle arrest at G2/M	Decreased expression Various PA types	Xu *et al* 2012[88]
SMARCA4 (BRG1)	Regulation of gene transcription by altering the chromatin structure	Decreased expression, altered subcellular localization Corticotrophinomas	Bilodeau *et al* 2006[74]
SOCS1	Inhibitor of JAK/STAT pathway	Decreased expression by promoter methylation. Various PA types	Buslei *et al* 2006[89]
SSTR2	G protein-coupled receptor for somatostatin	Decreased expression Somatotrophinomas	Corbetta *et al* 2001[90]
THRB (TRß)	Nuclear receptor that mediates gene regulation by thyroid hormones	Loss-of-function somatic mutations or aberrant splicing Thyrotrophinomas	Ando *et al* 2001[91]
TP53	Regulation of cell cycle, acting negatively in the cell division	Loss-of-function somatic mutations Various PA types, mainly aggressive PAs	Tanizaki *et al* 2007[92] Kawashima *et al* 2009[93] Pinto *et al* 2011[94]
WEE1	Regulation of cell cycle progression	Decreased expression NFPAs and GH-secreting PAs	Butz *et al* 2010[95]
WIF1	Binds Wnt proteins and inhibits their activities	Decreased expression by promoter methylation Various PA types, mainly NFPAs	Elston *et al* 2008[96]

Genes with decreased expression involved in pathogenesis of sporadic pituitary adenomas
CREs, cAMP response elements; EGF, epidermal growth factor; EGFR, epidermal growth factor receptor; EMT, epithelial-mesenchymal transition; FGF, fibroblast growth factor; GH, growth hormone; LOH, loss of heterozygosity; NFPAs, non-functioning pituitary adenomas; PAs, pituitary adenomas; PRL, prolactin; TK, tyrosine kinase. Adapted from Marques & Korbonits (2017)[50].

Reference list corresponding to the supplemental tables in the Appendix 1

1. Musat M, Korbonits M, Kola B, Borboli N, Hanson MR, Nanzer AM, Grigson J, Jordan S, Morris DG, Gueorguiev M, Coculescu M, Basu S & Grossman AB. Enhanced protein kinase B/Akt signalling in pituitary tumours. *Endocr Relat Cancer* 2005 **12** 423-433.
2. Morris DG, Musat M, Czirjak S, Hanzely Z, Lillington DM, Korbonits M & Grossman AB. Differential gene expression in pituitary adenomas by oligonucleotide array analysis. *Eur J Endocrinol* 2005 **153** 143-151.
3. Sanchez-Beato M, Sanchez E, Gonzalez-Carrero J, Morente M, Diez A, Sanchez-Verde L, Martin MC, Cigudosa JC, Vidal M & Piris MA. Variability in the expression of polycomb proteins in different normal and tumoral tissues. A pilot study using tissue microarrays. *Mod Pathol* 2006 **19** 684-694.
4. Palumbo T, Faucz FR, Azevedo M, Xekouki P, Iliopoulos D & Stratakis CA. Functional screen analysis reveals miR-26b and miR-128 as central regulators of pituitary somatomammotrophic tumor growth through activation of the PTEN-AKT pathway. *Oncogene* 2013 **32** 1651-1659.
5. Westerman BA, Blom M, Tanger E, van der Valk M, Song JY, van Santen M, Gadiot J, Cornelissen-Steijger P, Zevenhoven J, Prosser HM, Uren A, Aronica E & van Lohuizen M. GFAP-Cre-mediated transgenic activation of Bmi1 results in pituitary tumors. *PLoS One* 2012 **7** e35943.
6. Turner HE, Nagy Z, Sullivan N, Esiri MM & Wass JA. Expression analysis of cyclins in pituitary adenomas and the normal pituitary gland. *Clin Endocrinol (Oxf)* 2000 **53** 337-344.
7. Nakabayashi H, Sunada I & Hara M. Immunohistochemical analyses of cell cycle-related proteins, apoptosis, and proliferation in pituitary adenomas. *J Histochem Cytochem* 2001 **49** 1193-1194.
8. Wierinckx A, Auger C, Devauchelle P, Reynaud A, Chevallier P, Jan M, Perrin G, Fevre-Montange M, Rey C, Figarella-Branger D, Raverot G, Belin MF, Lachuer J & Trouillas J. A diagnostic marker set for invasion, proliferation, and aggressiveness of prolactin pituitary tumors. *Endocr Relat Cancer* 2007 **14** 887-900.
9. De Martino I, Visone R, Wierinckx A, Palmieri D, Ferraro A, Cappabianca P, Chiappetta G, Forzati F, Lombardi G, Colao A, Trouillas J, Fedele M & Fusco A. HMGA proteins up-regulate CCNB2 gene in mouse and human pituitary adenomas. *Cancer Res* 2009 **69** 1844-1850.
10. Hibberts NA, Simpson DJ, Bicknell JE, Broome JC, Hoban PR, Clayton RN & Farrell WE. Analysis of cyclin D1 (CCND1) allelic imbalance and overexpression in sporadic human pituitary tumors. *Clin Cancer Res* 1999 **5** 2133-2139.
11. Jordan S, Lidhar K, Korbonits M, Lowe DG & Grossman AB. Cyclin D and cyclin E expression in normal and adenomatous pituitary. *Eur J Endocrinol* 2000 **143** R1-6.
12. Simpson DJ, Frost SJ, Bicknell JE, Broome JC, McNicol AM, Clayton RN & Farrell WE. Aberrant expression of G(1)/S regulators is a frequent event in sporadic pituitary adenomas. *Carcinogenesis* 2001 **22** 1149-1154.
13. Korbonits M, Chahal HS, Kaltsas G, Jordan S, Urmanova Y, Khalimova Z, Harris PE, Farrell WE, Claret FX & Grossman AB. Expression of phosphorylated p27(Kip1) protein and Jun activation domain-binding protein 1 in human pituitary tumors. *J Clin Endocrinol Metab* 2002 **87** 2635-2643.
14. Bertherat J, Chanson P & Montminy M. The cyclic adenosine 3',5'-monophosphate-responsive factor CREB is constitutively activated in human somatotroph adenomas. *Mol Endocrinol* 1995 **9** 777-783.
15. Zhu X, Mao X, Hurren R, Schimmer AD, Ezzat S & Asa SL. Deoxyribonucleic acid methyltransferase 3B promotes epigenetic silencing through histone 3 chromatin modifications in pituitary cells. *J Clin Endocrinol Metab* 2008 **93** 3610-3617.

16. Chaidarun SS, Eggo MC, Sheppard MC & Stewart PM. Expression of epidermal growth factor (EGF), its receptor, and related oncoprotein (erbB-2) in human pituitary tumors and response to EGF in vitro. *Endocrinology* 1994 **135** 2012-2021.
17. Delgrange E, Vasiljevic A, Wierinckx A, Francois P, Jouanneau E, Raverot G & Trouillas J. Expression of estrogen receptor alpha is associated with prolactin pituitary tumor prognosis and supports the sex-related difference in tumor growth. *Eur J Endocrinol* 2015 **172** 791-801.
18. Schult D, Holsken A, Siegel S, Buchfelder M, Fahlbusch R, Kreitschmann-Andermahr I & Buslei R. EZH2 is highly expressed in pituitary adenomas and associated with proliferation. *Sci Rep* 2015 **5** 16965.
19. McCabe CJ, Khaira JS, Boelaert K, Heaney AP, Tannahill LA, Hussain S, Mitchell R, Olliff J, Sheppard MC, Franklyn JA & Gittoes NJ. Expression of pituitary tumour transforming gene (PTTG) and fibroblast growth factor-2 (FGF-2) in human pituitary adenomas: relationships to clinical tumour behaviour. *Clin Endocrinol (Oxf)* 2003 **58** 141-150.
20. Jackson TA, Koterwas DM & Bradford AP. Differential regulation of cell growth and gene expression by FGF-2 and FGF-4 in pituitary lactotroph GH4 cells. *Mol Cell Endocrinol* 2006 **247** 183-191.
21. Zhu X, Lee K, Asa SL & Ezzat S. Epigenetic silencing through DNA and histone methylation of fibroblast growth factor receptor 2 in neoplastic pituitary cells. *Am J Pathol* 2007 **170** 1618-1628.
22. Ezzat S, Zheng L, Zhu XF, Wu GE & Asa SL. Targeted expression of a human pituitary tumor-derived isoform of FGF receptor-4 recapitulates pituitary tumorigenesis. *J Clin Invest* 2002 **109** 69-78.
23. Evans CO, Young AN, Brown MR, Brat DJ, Parks JS, Neish AS & Oyesiku NM. Novel patterns of gene expression in pituitary adenomas identified by complementary deoxyribonucleic acid microarrays and quantitative reverse transcription-polymerase chain reaction. *J Clin Endocrinol Metab* 2001 **86** 3097-3107.
24. Thapar K, Kovacs K, Stefaneanu L, Scheithauer B, Killinger DW, Lioyd RV, Smyth HS, Barr A, Thorner MO, Gaylinn B & Laws ER, Jr. Overexpression of the growth-hormone-releasing hormone gene in acromegaly-associated pituitary tumors. An event associated with neoplastic progression and aggressive behavior. *Am J Pathol* 1997 **151** 769-784.
25. Lampichler K, Ferrer P, Vila G, Lutz MI, Wolf F, Knosp E, Wagner L, Luger A & Baumgartner-Parzer S. The role of proto-oncogene GLI1 in pituitary adenoma formation and cell survival regulation. *Endocr Relat Cancer* 2015 **22** 793-803.
26. Williamson EA, Daniels M, Foster S, Kelly WF, Kendall-Taylor P & Harris PE. Gs alpha and Gi2 alpha mutations in clinically non-functioning pituitary tumours. *Clin Endocrinol (Oxf)* 1994 **41** 815-820.
27. Williamson EA, Ince PG, Harrison D, Kendall-Taylor P & Harris PE. G-protein mutations in human pituitary adrenocorticotrophic hormone-secreting adenomas. *Eur J Clin Invest* 1995 **25** 128-131.
28. Vallar L, Spada A & Giannattasio G. Altered Gs and adenylate cyclase activity in human GH-secreting pituitary adenomas. *Nature* 1987 **330** 566-568.
29. Landis CA, Masters SB, Spada A, Pace AM, Bourne HR & Vallar L. GTPase inhibiting mutations activate the alpha chain of Gs and stimulate adenylyl cyclase in human pituitary tumours. *Nature* 1989 **340** 692-696.
30. Tordjman K, Stern N, Ouaknine G, Yossiphov Y, Razon N, Nordenskjold M & Friedman E. Activating mutations of the Gs alpha-gene in nonfunctioning pituitary tumors. *J Clin Endocrinol Metab* 1993 **77** 765-769.
31. Finelli P, Pierantoni GM, Giardino D, Losa M, Rodeschini O, Fedele M, Valtorta E, Mortini P, Croce CM, Larizza L & Fusco A. The High Mobility Group A2 gene is amplified and overexpressed in human prolactinomas. *Cancer Res* 2002 **62** 2398-2405.

32. Karga HJ, Alexander JM, Hedley-Whyte ET, Klibanski A & Jameson JL. Ras mutations in human pituitary tumors. *J Clin Endocrinol Metab* 1992 **74** 914-919.
33. Cai WY, Alexander JM, Hedley-Whyte ET, Scheithauer BW, Jameson JL, Zervas NT & Klibanski A. ras mutations in human prolactinomas and pituitary carcinomas. *J Clin Endocrinol Metab* 1994 **78** 89-93.
34. Pei L, Melmed S, Scheithauer B, Kovacs K & Prager D. H-ras mutations in human pituitary carcinoma metastases. *J Clin Endocrinol Metab* 1994 **78** 842-846.
35. Kochling M, Ewelt C, Furtjes G, Peetz-Dienhart S, Koos B, Hasselblatt M, Paulus W, Stummer W & Brokinkel B. hTERT promoter methylation in pituitary adenomas. *Brain Tumor Pathol* 2016 **33** 27-34.
36. Ezzat S, Yu S & Asa SL. Ikaros isoforms in human pituitary tumors: distinct localization, histone acetylation, and activation of the 5' fibroblast growth factor receptor-4 promoter. *Am J Pathol* 2003 **163** 1177-1184.
37. Riss D, Jin L, Qian X, Bayliss J, Scheithauer BW, Young WF, Jr., Vidal S, Kovacs K, Raz A & Lloyd RV. Differential expression of galectin-3 in pituitary tumors. *Cancer Res* 2003 **63** 2251-2255.
38. Zhu X, Asa SL & Ezzat S. Fibroblast growth factor 2 and estrogen control the balance of histone 3 modifications targeting MAGE-A3 in pituitary neoplasia. *Clin Cancer Res* 2008 **14** 1984-1996.
39. Xiong W, Knox AJ, Xu M, Kiseljak-Vassiliades K, Colgan SP, Brodsky KS, Kleinschmidt-Demasters BK, Lillehei KO & Wierman ME. Mammalian Ste20-like kinase 4 promotes pituitary cell proliferation and survival under hypoxia. *Mol Endocrinol* 2015 **29** 460-472.
40. Galland F, Lacroix L, Saulnier P, Dessen P, Meduri G, Bernier M, Gaillard S, Guibourdenche J, Fournier T, Evain-Brion D, Bidart JM & Chanson P. Differential gene expression profiles of invasive and non-invasive non-functioning pituitary adenomas based on microarray analysis. *Endocr Relat Cancer* 2010 **17** 361-371.
41. Lin Y, Jiang X, Shen Y, Li M, Ma H, Xing M & Lu Y. Frequent mutations and amplifications of the PIK3CA gene in pituitary tumors. *Endocr Relat Cancer* 2009 **16** 301-310.
42. Acunzo J, Roche C, Defilles C, Thirion S, Quentien MH, Figarella-Branger D, Graillon T, Dufour H, Brue T, Pellegrini I, Enjalbert A & Barlier A. Inactivation of PITX2 transcription factor induced apoptosis of gonadotroph tumoral cells. *Endocrinology* 2011 **152** 3884-3892.
43. Palmieri D, Valentino T, De Martino I, Esposito F, Cappabianca P, Wierinckx A, Vitiello M, Lombardi G, Colao A, Trouillas J, Pierantoni GM, Fusco A & Fedele M. PIT1 upregulation by HMGA proteins has a role in pituitary tumorigenesis. *Endocr Relat Cancer* 2012 **19** 123-135.
44. Alvaro V, Levy L, Dubray C, Roche A, Peillon F, Querat B & Joubert D. Invasive human pituitary tumors express a point-mutated alpha-protein kinase-C. *J Clin Endocrinol Metab* 1993 **77** 1125-1129.
45. Zhang X, Horwitz GA, Heaney AP, Nakashima M, Prezant TR, Bronstein MD & Melmed S. Pituitary tumor transforming gene (PTTG) expression in pituitary adenomas. *J Clin Endocrinol Metab* 1999 **84** 761-767.
46. Shan B, Gerez J, Haedo M, Fuertes M, Theodoropoulou M, Buchfelder M, Losa M, Stalla GK, Arzt E & Renner U. RSUME is implicated in HIF-1-induced VEGF-A production in pituitary tumour cells. *Endocr Relat Cancer* 2012 **19** 13-27.
47. Vila G, Theodoropoulou M, Stalla J, Tonn JC, Losa M, Renner U, Stalla GK & Paez-Pereda M. Expression and function of sonic hedgehog pathway components in pituitary adenomas: evidence for a direct role in hormone secretion and cell proliferation. *J Clin Endocrinol Metab* 2005 **90** 6687-6694.

48. Zhou C, Jiao Y, Wang R, Ren SG, Wawrowsky K & Melmed S. STAT3 upregulation in pituitary somatotroph adenomas induces growth hormone hypersecretion. *J Clin Invest* 2015 **125** 1692-1702.
49. Ezzat S, Walpola IA, Ramyar L, Smyth HS & Asa SL. Membrane-anchored expression of transforming growth factor-alpha in human pituitary adenoma cells. *J Clin Endocrinol Metab* 1995 **80** 534-539.
50. Marques P & Korbonits M. Genetic Aspects of Pituitary Adenomas. *Endocrinol Metab Clin North Am* 2017 **46** 335-374.
51. Kasuki Jomori de Pinho L, Vieira Neto L, Armondi Wildemberg LE, Gasparetto EL, Marcondes J, de Almeida Nunes B, Takiya CM & Gadelha MR. Low aryl hydrocarbon receptor-interacting protein expression is a better marker of invasiveness in somatotropinomas than Ki-67 and p53. *Neuroendocrinology* 2011 **94** 39-48.
52. Kasuki L, Vieira Neto L, Wildemberg LE, Colli LM, de Castro M, Takiya CM & Gadelha MR. AIP expression in sporadic somatotropinomas is a predictor of the response to octreotide LAR therapy independent of SSTR2 expression. *Endocr Relat Cancer* 2012 **19** L25-29.
53. Paez-Pereda M, Giacomini D, Refojo D, Nagashima AC, Hopfner U, Grubler Y, Chervin A, Goldberg V, Goya R, Hentges ST, Low MJ, Holsboer F, Stalla GK & Arzt E. Involvement of bone morphogenetic protein 4 (BMP-4) in pituitary prolactinoma pathogenesis through a Smad/estrogen receptor crosstalk. *Proc Natl Acad Sci U S A* 2003 **100** 1034-1039.
54. Roussel-Gervais A, Couture C, Langlais D, Takayasu S, Balsalobre A, Rueda BR, Zukerberg LR, Figarella-Branger D, Brue T & Drouin J. The Cables1 Gene in Glucocorticoid Regulation of Pituitary Corticotrope Growth and Cushing Disease. *J Clin Endocrinol Metab* 2016 **101** 513-522.
55. Qian ZR, Sano T, Yoshimoto K, Asa SL, Yamada S, Mizusawa N & Kudo E. Tumor-specific downregulation and methylation of the CDH13 (H-cadherin) and CDH1 (E-cadherin) genes correlate with aggressiveness of human pituitary adenomas. *Mod Pathol* 2007 **20** 1269-1277.
56. Neto AG, McCutcheon IE, Vang R, Spencer ML, Zhang W & Fuller GN. Elevated expression of p21 (WAF1/Cip1) in hormonally active pituitary adenomas. *Ann Diagn Pathol* 2005 **9** 6-10.
57. Qian X, Jin L, Grande JP & Lloyd RV. Transforming growth factor-beta and p27 expression in pituitary cells. *Endocrinology* 1996 **137** 3051-3060.
58. Lloyd RV, Jin L, Qian X & Kulig E. Aberrant p27kip1 expression in endocrine and other tumors. *Am J Pathol* 1997 **150** 401-407.
59. Jin L, Qian X, Kulig E, Sanno N, Scheithauer BW, Kovacs K, Young WF, Jr. & Lloyd RV. Transforming growth factor-beta, transforming growth factor-beta receptor II, and p27Kip1 expression in nontumorous and neoplastic human pituitaries. *Am J Pathol* 1997 **151** 509-519.
60. Bamberger CM, Fehn M, Bamberger AM, Ludecke DK, Beil FU, Saeger W & Schulte HM. Reduced expression levels of the cell-cycle inhibitor p27Kip1 in human pituitary adenomas. *Eur J Endocrinol* 1999 **140** 250-255.
61. Woloschak M, Yu A, Xiao J & Post KD. Frequent loss of the P16INK4a gene product in human pituitary tumors. *Cancer Res* 1996 **56** 2493-2496.
62. Jaffrain-Rea ML, Ferretti E, Toniato E, Cannita K, Santoro A, Di Stefano D, Ricevuto E, Maroder M, Tamburrano G, Cantore G, Gulino A & Martinotti S. p16 (INK4a, MTS-1) gene polymorphism and methylation status in human pituitary tumours. *Clin Endocrinol (Oxf)* 1999 **51** 317-325.
63. Ogino A, Yoshino A, Katayama Y, Watanabe T, Ota T, Komine C, Yokoyama T & Fukushima T. The p15(INK4b)/p16(INK4a)/RB1 pathway is frequently deregulated in human pituitary adenomas. *J Neuropathol Exp Neurol* 2005 **64** 398-403.

64. Yoshino A, Katayama Y, Ogino A, Watanabe T, Yachi K, Ohta T, Komine C, Yokoyama T & Fukushima T. Promoter hypermethylation profile of cell cycle regulator genes in pituitary adenomas. *J Neurooncol* 2007 **83** 153-162.
65. Hossain MG, Iwata T, Mizusawa N, Qian ZR, Shima SW, Okutsu T, Yamada S, Sano T & Yoshimoto K. Expression of p18(INK4C) is down-regulated in human pituitary adenomas. *Endocr Pathol* 2009 **20** 114-121.
66. Simpson DJ, Clayton RN & Farrell WE. Preferential loss of Death Associated Protein kinase expression in invasive pituitary tumours is associated with either CpG island methylation or homozygous deletion. *Oncogene* 2002 **21** 1217-1224.
67. Bello MJ, De Campos JM, Isla A, Casartelli C & Rey JA. Promoter CpG methylation of multiple genes in pituitary adenomas: frequent involvement of caspase-8. *Oncol Rep* 2006 **15** 443-448.
68. Bellodi C, Krasnykh O, Haynes N, Theodoropoulou M, Peng G, Montanaro L & Ruggero D. Loss of function of the tumor suppressor DKC1 perturbs p27 translation control and contributes to pituitary tumorigenesis. *Cancer Res* 2010 **70** 6026-6035.
69. Caccavelli L, Feron F, Morange I, Rouer E, Benarous R, Dewailly D, Jaquet P, Kordon C & Enjalbert A. Decreased expression of the two D2 dopamine receptor isoforms in bromocriptine-resistant prolactinomas. *Neuroendocrinology* 1994 **60** 314-322.
70. Michaelis KA, Knox AJ, Xu M, Kiseljak-Vassiliades K, Edwards MG, Geraci M, Kleinschmidt-DeMasters BK, Lillehei KO & Wierman ME. Identification of growth arrest and DNA-damage-inducible gene beta (GADD45beta) as a novel tumor suppressor in pituitary gonadotrope tumors. *Endocrinology* 2011 **152** 3603-3613.
71. Zhang X, Sun H, Danila DC, Johnson SR, Zhou Y, Swearingen B & Klibanski A. Loss of expression of GADD45 gamma, a growth inhibitory gene, in human pituitary adenomas: implications for tumorigenesis. *J Clin Endocrinol Metab* 2002 **87** 1262-1267.
72. Bahar A, Bicknell JE, Simpson DJ, Clayton RN & Farrell WE. Loss of expression of the growth inhibitory gene GADD45gamma, in human pituitary adenomas, is associated with CpG island methylation. *Oncogene* 2004 **23** 936-944.
73. Asa SL, Digiovanni R, Jiang J, Ward ML, Loesch K, Yamada S, Sano T, Yoshimoto K, Frank SJ & Ezzat S. A growth hormone receptor mutation impairs growth hormone autofeedback signaling in pituitary tumors. *Cancer Res* 2007 **67** 7505-7511.
74. Bilodeau S, Vallette-Kasic S, Gauthier Y, Figarella-Branger D, Brue T, Berthelet F, Lacroix A, Batista D, Stratakis C, Hanson J, Meij B & Drouin J. Role of Brg1 and HDAC2 in GR trans-repression of the pituitary POMC gene and misexpression in Cushing disease. *Genes Dev* 2006 **20** 2871-2886.
75. Zhang X, Zhou Y, Mehta KR, Danila DC, Scolavino S, Johnson SR & Klibanski A. A pituitary-derived MEG3 isoform functions as a growth suppressor in tumor cells. *J Clin Endocrinol Metab* 2003 **88** 5119-5126.
76. Zhao J, Dahle D, Zhou Y, Zhang X & Klibanski A. Hypermethylation of the promoter region is associated with the loss of MEG3 gene expression in human pituitary tumors. *J Clin Endocrinol Metab* 2005 **90** 2179-2186.
77. Zhuang Z, Ezzat SZ, Vortmeyer AO, Weil R, Oldfield EH, Park WS, Pack S, Huang S, Agarwal SK, Guru SC, Manickam P, Debelenko LV, Kester MB, Olufemi SE, Heppner C, Crabtree JS, Burns AL, Spiegel AM, Marx SJ, Chandrasekharappa SC, Collins FS, Emmert-Buck MR, Liotta LA, Asa SL & Lubensky IA. Mutations of the MEN1 tumor suppressor gene in pituitary tumors. *Cancer Res* 1997 **57** 5446-5451.
78. Tanaka C, Yoshimoto K, Yamada S, Nishioka H, Ii S, Moritani M, Yamaoka T & Itakura M. Absence of germ-line mutations of the multiple endocrine neoplasia type 1 (MEN1) gene in familial pituitary adenoma in contrast to MEN1 in Japanese. *J Clin Endocrinol Metab* 1998 **83** 960-965.

79. Wenbin C, Asai A, Teramoto A, Sanno N & Kirino T. Mutations of the MEN1 tumor suppressor gene in sporadic pituitary tumors. *Cancer Lett* 1999 **142** 43-47.
80. Lau Q, Scheithauer B, Kovacs K, Horvath E, Syro LV & Lloyd R. MGMT immunoexpression in aggressive pituitary adenoma and carcinoma. *Pituitary* 2010 **13** 367-379.
81. Takino H, Herman V, Weiss M & Melmed S. Purine-binding factor (nm23) gene expression in pituitary tumors: marker of adenoma invasiveness. *J Clin Endocrinol Metab* 1995 **80** 1733-1738.
82. Karl M, Von Wichert G, Kempter E, Katz DA, Reincke M, Monig H, Ali IU, Stratakis CA, Oldfield EH, Chrousos GP & Schulte HM. Nelson's syndrome associated with a somatic frame shift mutation in the glucocorticoid receptor gene. *J Clin Endocrinol Metab* 1996 **81** 124-129.
83. Huizenga NA, de Lange P, Koper JW, Clayton RN, Farrell WE, van der Lely AJ, Brinkmann AO, de Jong FH & Lamberts SW. Human adrenocorticotropin-secreting pituitary adenomas show frequent loss of heterozygosity at the glucocorticoid receptor gene locus. *J Clin Endocrinol Metab* 1998 **83** 917-921.
84. Pagotto U, Arzberger T, Theodoropoulou M, Grubler Y, Pantaloni C, Saeger W, Losa M, Journot L, Stalla GK & Spengler D. The expression of the antiproliferative gene ZAC is lost or highly reduced in nonfunctioning pituitary adenomas. *Cancer Res* 2000 **60** 6794-6799.
85. Noh TW, Jeong HJ, Lee MK, Kim TS, Kim SH & Lee EJ. Predicting recurrence of nonfunctioning pituitary adenomas. *J Clin Endocrinol Metab* 2009 **94** 4406-4413.
86. Qian ZR, Sano T, Yoshimoto K, Yamada S, Ishizuka A, Mizusawa N, Horiguchi H, Hirokawa M & Asa SL. Inactivation of RASSF1A tumor suppressor gene by aberrant promoter hypermethylation in human pituitary adenomas. *Lab Invest* 2005 **85** 464-473.
87. Simpson DJ, Hibberts NA, McNicol AM, Clayton RN & Farrell WE. Loss of pRb expression in pituitary adenomas is associated with methylation of the RB1 CpG island. *Cancer Res* 2000 **60** 1211-1216.
88. Xu M, Knox AJ, Michaelis KA, Kiseljak-Vassiliades K, Kleinschmidt-DeMasters BK, Lillehei KO & Wierman ME. Reprimo (RPRM) is a novel tumor suppressor in pituitary tumors and regulates survival, proliferation, and tumorigenicity. *Endocrinology* 2012 **153** 2963-2973.
89. Buslei R, Kreutzer J, Hofmann B, Schmidt V, Siebzehnrubl F, Hahnen E, Eyupoglu IY, Fahlbusch R & Blumcke I. Abundant hypermethylation of SOCS-1 in clinically silent pituitary adenomas. *Acta Neuropathol* 2006 **111** 264-271.
90. Corbetta S, Ballare E, Mantovani G, Lania A, Losa M, Di Blasio AM & Spada A. Somatostatin receptor subtype 2 and 5 in human GH-secreting pituitary adenomas: analysis of gene sequence and mRNA expression. *Eur J Clin Invest* 2001 **31** 208-214.
91. Ando S, Sarlis NJ, Oldfield EH & Yen PM. Somatic mutation of TRbeta can cause a defect in negative regulation of TSH in a TSH-secreting pituitary tumor. *J Clin Endocrinol Metab* 2001 **86** 5572-5576.
92. Tanizaki Y, Jin L, Scheithauer BW, Kovacs K, Roncaroli F & Lloyd RV. P53 gene mutations in pituitary carcinomas. *Endocr Pathol* 2007 **18** 217-222.
93. Kawashima ST, Usui T, Sano T, Iogawa H, Hagiwara H, Tamanaha T, Tagami T, Naruse M, Hojo M, Takahashi JA & Shimatsu A. P53 gene mutation in an atypical corticotroph adenoma with Cushing's disease. *Clin Endocrinol (Oxf)* 2009 **70** 656-657.
94. Pinto EM, Siqueira SA, Cukier P, Fragoso MC, Lin CJ & de Mendonca BB. Possible role of a radiation-induced p53 mutation in a Nelson's syndrome patient with a fatal outcome. *Pituitary* 2011 **14** 400-404.
95. Butz H, Liko I, Czirjak S, Igaz P, Khan MM, Zivkovic V, Balint K, Korbonits M, Racz K & Patocs A. Down-regulation of Wee1 kinase by a specific subset of microRNA in human sporadic pituitary adenomas. *J Clin Endocrinol Metab* 2010 **95** E181-191.

96. Elston MS, Gill AJ, Conaglen JV, Clarkson A, Shaw JM, Law AJ, Cook RJ, Little NS, Clifton-Bligh RJ, Robinson BG & McDonald KL. Wnt pathway inhibitors are strongly down-regulated in pituitary tumors. *Endocrinology* 2008 **149** 1235-1242.

Appendix 2: Supplemental table with primary antibodies and respective dilutions used for immunohistochemical (IHC) and immunofluorescence (IF) studies

Primary Antibodies	Company	Cat. no.	Species	Dilution IHC	Dilution IF
Actin	Molecular Probes	R37110	Mouse		2 drops/mL (1:500)
α-SMA	Sigma-Aldrich	A5228	Mouse		1:500
CD4	Abcam	Ab133616	Rabbit	1:100	
CD8	DAKO	M7103	Mouse	1:100	
CD20	DAKO	M0755	Mouse	1:300	
CD31	DAKO	M0823	Mouse	1:100	
CD68	DAKO	IR613	Mouse	1:2	
CD163	Abcam	Ab74604	Mouse	Neat	
E-cadherin	BD Biosciences	610181	Mouse	1:50	1:50
FOXP3	Abcam	Ab20034 [236A/E7]	Mouse	1:50	
HLA-DR	Abcam	Ab20181 [TAL1B5]	Mouse	1:100	
MMP-9	Abcam	Ab38898	Rabbit	1:50	
MMP-14	Abcam	Ab3644	Rabbit	1:30	
NCAM	Roche	760-4596	Rabbit	Neat	
Neutrophil elastase	Abcam	Ab68672	Rabbit	1:100	
Vimentin	Abcam	Ab16700	Rabbit		1:1000
Vimentin	DAKO	M7020	Mouse	1:1000	
ZEB1	Santa Cruz Biotechnology	H-102: sc-25388	Rabbit	1:50	1:50

Appendix 3: Supplemental table with primers used in RT-qPCR experiments

Gene	Forward sequence 5'-3'	Reverse sequence 5'-3'	Amplicon length (bp)	Species
Adam10	GCTGGGAGGTCAGTATGGAAAT	TCGTGTGAGACTGCTCGTTT	120	r
Adam17	GCAAACAGTCATGGAGGGGT	CCAGGTCAGCCTCCTTTGTAA	133	r
Arg1	ACATTGGCTTGCGAGACGTA	ATCACCTTGCCAATCCCCAG	109	m
αSMA	CCGGGACTAAGACGGGAATC	TTGTCACACACCAAGGCAGT	80	h
CCL2	TCAAACTGAAGCTCGCACTCT	GGCATTGATTGCATCTGGC	121	h
Ccl2	GTGCTGACCCCAATAAGGAA	TGAGGTGGTTGTGGAAAAGA	185	r
Ccl2	CACTCACCTGCTGCTACTCA	GCTTGGTGACAAAAACTACAGC	117	m
Ccl4	GCAACACCATGAAGCTCTGC	AGAGCCCATTGGTGCTGAGA	92	m
Ccl5	CCAATCTTGCAGTCGTGTTTGT	AGAGCAAGCAATGACAGGGA	159	m
Ccr5	GTATGTCAGCACCCTGCCAA	GAGCAGGAAGAGCAGGTCAG	200	m,r
Cd206	TGCCCTGAACAGCAACTTGA	GTTAGTGTACCGCACCCTCC	70	m,r
Cdh1	ACATCCTGGGCAGAGTGAAA	CCGTTTGACTGTGATGACGC	113	r
Cx3cl1	CCATCATCCTGGAGACGAGA	TGTCACATTGTCCACACGCT	149	r
Cx3cr1	CCATCTGCTCAGGACCTCAC	CACCAGACCGAACGTGAAGA	165	m
Cx3cr1	GGCATGAAGAGGGACCTGAG	CCCCAGCGAAAGCGTAGATA	97	r
Cxcl10	GAAATCATCCCTGCGAGCCT	AGGAGCCCTTTTAGACCTTTTT	150	m
Cxcl10	TGCAAGTCTATCCTGTCCGC	TCTTTGGCTCACCGCTTTCA	121	r
FAP	GGCACGGTATTCAAAAGTCCG	TACCCAAGTCTTCATTTTTCCAGA	172	h
GAPDH	TGCACCACCAACTGCTTAG	GGATGCAGGGATGATGTTC	176	h,m,r
Il1a	GTCAACTCATTGGCGCTTGA	GCTTGCATCATAGAAGGATTTCTGA	155	m,r
Il1b	GCAATGGTCGGGACATAGTT	AGACCTGACTTGGCAGAGGA	158	r
IL6	ACCCCCAATAAATATAGGACTGGA	CGAAGGCGCTTGTGGAGAA	129	h
IL8	AGTTTTTGAAGAGGGCTGAGAAT	TTGCTTGAAGTTTCACTGGCATC	89	h
Il18	CGCAGTAATACGGAGCATAAATGAC	GGTAGACATCCTTCCATCCTTCAC	193	r
Inos	GCAGTCTTTTCCTATGGGG	TGGAACTCTGGGCTGTCAGA	81	m
Mmp9	CTTGAAGTCTCAGAAGGTGGATC	CGCCAGAAGTATTTGTCATGG	145	r
SST1	CACATTTCTCATGGGCTTCCT	ACAAACACCATCACCACCATC	165	h
SST2	GGCATGTTTGACTTTGTGGTG	GTCTCATTCAGCCGGGATTT	185	h
SST3	TGCCTTCTTTGGGCTCTACTT	ATCCTCCTCCTCAGTCTTCTCC	190	h
SST4	TGTGCTACCTGCTCATCGTG	GCTGGTCACGAAGAGGTTCA	176	h
SST5	CTGGTGTTTGCGGGATGTT	GAAGCTCTGGCGGAAGTTGT	183	h
Tnfa	CCCACGTCGTAGCAAACCA	ACAAGGTACAACCCATCGGC	133	m
Vegf	GTAACGATGAAGCCCTGGAGT	TGTTCTGTCTTTCTTTGGTCTGC	156	m
Vegf	ATCATGCGGATCAAACCTCACC	GGTCTGCATTCACATCTGCTATGC	80	r
Zeb1	TGGGATGTACGCATGTGACC	GGGGCCTCTTACCTGTATGC	92	r

ADAM, A Disintegrin And Metalloproteinase domain; ARG1, arginase 1; αSMA, α-smooth muscle actin; bp, base pairs; CDH1, Cadherin 1 (E-cadherin); FAP, fibroblast activation protein; GAPDH, glyceraldehyde-3-phosphate dehydrogenase; h, human; IL, interleukin; iNOS, inducible nitric oxide synthase; m, mouse; MMP, matrix metalloproteinase; r, rat; SST, somatostatin receptor; TNF α, tumour necrosis factor-α; VEGF, vascular endothelial growth factor; ZEB1, Zinc Finger E-Box Binding Homeobox 1.

Appendix 4: Supplemental table with correlation between clinico-pathological and biochemical features and infiltrating immune cells among NFPAs and somatotrophinomas

NFPAs n = 16	% of infiltrating immune cells				
	Macrophages	**CD8+ T cells**	**CD4+ T cells**	**FOXP3+ T cells**	**Neutrophils**
Gender *[Mean±SEM]*					
Male (n=12)	4.1 ± 0.6	1.5 ± 0.3	1.0 ± 0.2	0.3 ± 0.1	1.1 ± 0.3
Female (n=4)	6.0 ± 0.7	2.1 ± 0.3	1.4 ± 0.2	0.7 ± 0.3	0.5 ± 0.3
	p=0.118	*p*=0.268	*p*=0.221	*p*=0.174	*p*=0.284
Age at diagnosis (yrs) *[Pearson correlation r (p value)]*	0.247 (*p*=0.357)	-0.169 (*p*=0.531)	-0.378 (*p*=0.149)	-0.480 (*p*=0.060)	-0.075 (*p*=0.782)
Headache at diagnosis *[Mean±SEM]*					
Yes (n=5)	4.2 ± 0.9	1.4 ± 0.2	1.0 ± 0.1	0.4 ± 0.2	0.7 ± 0.3
No (n=11)	4.7 ± 0.7	1.7 ± 0.3	1.1 ± 0.2	0.4 ± 0.1	1.0 ± 0.3
	p=0.652	*p*=0.586	*p*=0.466	*p*=0.933	*p*=0.584
Visual impairment *[Mean±SEM]*					
Yes (n=12)	4.2 ± 0.7	1.5 ± 0.3	1.1 ± 0.2	0.3 ± 0.1	0.9 ± 0.3
No (n=4)	5.7 ± 0.9	2.0 ± 0.3	1.1 ± 0.2	0.6 ± 0.3	1.0 ± 0.3
	p=0.231	*p*=0.362	*p*=0.845	*p*=0.169	*p*=0.916
Hormonal data at diagnosis *[Pearson correlation r (p value)]*					
Serum GH	-0.067 (*p*=0.837)	0.009 (*p*=0.979)	0.081 (*p*=0.803)	0.308 (*p*=0.330)	0.046 (*p*=0.888)
Serum IGF-1	-0.102 (*p*=0.729)	-0.310 (*p*=0.281)	-0.062 (*p*=0.832)	0.151 (*p*=0.606)	-0.154 (*p*=0.600)
IGF-1 index	-0.186 (*p*=0.523)	-0.499 (*p*=0.069)	-0.464 (*p*=0.095)	0.064 (*p*=0.827)	-0.582 (***p*=0.029**)
Serum PRL	0.286 (*p*=0.321)	0.142 (*p*=0.628)	0.244 (*p*=0.401)	0.440 (p=0.115)	-0.187 (*p*=0.522)
PRL index	-0.047 (*p*=0.873)	-0.084 (*p*=0.774)	0.028 (*p*=0.924)	0.279 (*p*=0.334)	-0.270 (*p*=0.351)
Serum TSH	0.264 (*p*=0.363)	-0.123 (*p*=0.674)	-0.191 (*p*=0.514)	0.383 (*p*=0.177)	-0.232 (*p*=0.425)
Serum FT4	-0.190 (*p*=0.515)	-0.114 (*p*=0.698)	-0.075 (*p*=0.800)	-0.091 (*p*=0.757)	-0.160 (*p*=0.585)
Basal plasma cortisol	-0.149 (*p*=0.628)	0.016 (*p*=0.960)	-0.011 (*p*=0.972)	0.535 (*p*=0.060)	0.096 (*p*=0.749)
Serum LH	0.065 (*p*=0.826)	0.294 (*p*=0.308)	0.119 (*p*=0.685)	0.180 (*p*=0.539)	-0.061 (*p*=0.835)
Serum FSH	-0.023 (*p*=0.937)	-0.327 (*p*=0.299)	-0.018 (*p*=0.950)	0.027 (*p*=0.928)	-0.326 (*p*=0.256)
Hypopituitarism at diagnosis *[Mean±SEM]*					
Yes (n=9)	4.8 ± 0.8	1.5 ± 0.2	1.1 ± 0.2	0.4 ± 0.1	0.8 ± 0.2
No (n=7)	4.2 ± 0.7	1.7 ± 0.5	1.1 ± 0.2	0.4 ± 0.1	1.1 ± 0.4
	p=0.619	*p*=0.635	*p*=0.987	*p*=0.992	*p*=0.460
N pit deficiencies at diagnosis *[Pearson correlation r (p value)]*	0.097 (*p*=0.722)	-0.138 (*p*=0.609)	-0.156 (*p*=0.564)	-0.092 (*p*=0.735)	-0.318 (*p*=0.230)
Cavernous sinus invasion *[Mean±SEM]*					
Yes (n=6)	4.5 ± 1.0	1.3 ± 0.3	0.9 ± 0.1	0.3 ± 0.1	0.7 ± 0.1
No (n=10)	4.6 ± 0.7	1.8 ± 0.4	1.2 ± 0.2	0.4 ± 0.1	1.1 ± 0.3
	p=0.999	*p*=0.402	*p*=0.187	*p*=0.745	*p*=0.326
Ki-67 *[Mean±SEM]*					
< 3% (n=12)	4.3 ± 0.6	1.6 ± 0.3	1.0 ± 0.2	0.3 ± 0.1	1.0 ± 0.2
≥ 3% (n=4)	5.3 ± 1.4	1.6 ± 0.5	1.3 ± 0.3	0.7 ± 0.3	0.7 ± 0.3
	p=0.459	*p*=0.969	*p*=0.483	*p*=0.163	*p*=0.554

Hypopituitarism last follow-up *[Mean±SEM]* Yes (n=10) No (n=6)	 4.8 ± 0.8 4.2 ± 0.7 *p*=0.619	 1.7 ± 0.2 1.5 ± 0.5 *p*=0.763	 1.1 ± 0.2 1.0 ± 0.2 *p*=0.579	 0.4 ± 0.1 0.4 ± 0.1 *p*=0.911	 0.8 ± 0.2 1.2 ± 0.4 *p*=0.395
N pit deficiencies at last follow-up *[Pearson correlation r (p value)]*	0.035 (*p*=0.897)	-0.146 (*p*=0.589)	-0.051 (*p*=0.851)	-0.214 (*p*=0.426)	-0.370 (*p*=0.158)
Microvessel density *[Pearson correlation r (p value)]*	0.339 (*p*=0.199)	0.169 (*p*=0.483)	0.342 (*p*=0.195)	-0.138 (*p*=0.611)	-0.142 (*p*=0.601)
Microvessel area *[Pearson correlation r (p value)]*	0.159 (*p*=0.557)	0.222 (*p*=0.409)	0.330 (*p*=0.211)	-0.109 (*p*=0.689)	-0.274 (*p*=0.305)

Correlation between clinico-pathological and biochemical features and infiltrating immune cells among NFPAs

FSH, follicle-stimulating hormone; FT4, free thyroxine; F-up, follow-up; GH, growth hormone; IGF-1, insulin-like growth factor-1; LH, luteinising hormone; NFPA, non-functioning pituitary adenoma; pit, pituitary; PRL, prolactin; TSH, thyroid-stimulating hormone; SEM, standard error of the mean; yrs, years.

NFPAs n = 16	Cell ratios		
	Ratio M2:M1	**Ratio CD8:CD4**	**Ratio CD8:FOXP3**
Gender *[Mean±SEM]* Male (n=12) Female (n=4)	 2.1 ± 0.2 2.8 ± 0.4 *p*=0.173	 1.8 ± 0.4 1.5 ± 0.2 *p*=0.624	 6.5 ± 1.1 3.3 ± 1.0 *p*=0.154
Age at diagnosis (yrs) *[Pearson correlation r (p value)]*	-0.064 (*p*=0.814)	0.424 (*p*=0.102)	0.447 (*p*=0.109)
Headache at diagnosis *[Mean±SEM]* Yes (n=5) No (n=11)	 2.2 ± 0.3 2.3 ± 0.3 *p*=0.679	 1.5 ± 0.2 1.8 ± 0.4 *p*=0.586	 7.9 ± 2.7 4.7 ± 0.5 *p*=0.315
Visual impairment *[Mean±SEM]* Yes (n=12) No (n=4)	 2.3 ± 0.3 2.4 ± 0.2 *p*=0.797	 1.7 ± 0.4 1.8 ± 0.1 *p*=0.870	 5.5 ± 0.9 6.2 ± 3.0 *p*=0.765
Hormonal data at diagnosis *[Pearson correlation r (p value)]* Serum GH Serum IGF-1 IGF-1 index Serum PRL PRL index Serum TSH Serum FT4 Basal plasma cortisol Serum LH Serum FSH	 -0.347 (*p*=0.269) -0.630 (***p*=0.016**) -0.461 (*p*=0.097) 0.114 (*p*=0.699) 0.083 (*p*=0.779) -0.080 (*p*=0.786) -0.137 (*p*=0.641) -0.385 (*p*=0.194) 0.059 (*p*=0.841) 0.164 (*p*=0.575)	 -0.219 (*p*=0.494) -0.604 (***p*=0.022**) -0.262 (*p*=0.366) -0.004 (*p*=0.989) -0.025 (*p*=0.932) 0.115 (*p*=0.695) -0.262 (*p*=0.366) -0.395 (*p*=0.182) -0.098 (*p*=0.740) -0.114 (*p*=0.697)	 0.186 (*p*=0.563) -0.179 (*p*=0.540) -0.187 (*p*=0.522) -0.195 (*p*=0.503) -0.146 (*p*=0.619) -0.314 (*p*=0.275) 0.116 (*p*=0.692) -0.169 (*p*=0.581) -0.155 (*p*=0.596) -0.148 (*p*=0.613)
Hypopituitarism at diagnosis *[Mean±SEM]* Yes (n=9) No (n=7)	 2.3 ± 0.2 2.3 ± 0.2 *p*=0.867	 1.9 ± 0.5 1.5 ± 0.2 *p*=0.505	 5.5 ± 1.1 5.9 ± 1.7 *p*=0.826
N pit deficiencies at diagnosis *[Pearson correlation r (p value)]*	0.260 (*p*=0.330)	0.458 (*p*=0.074)	-0.188 (*p*=0.467)
Cavernous sinus invasion *[Mean±SEM]* Yes (n=6) No (n=10)	 2.1 ± 0.4 2.4 ± 0.2 *p*=0.490	 1.5 ± 0.3 1.9 ± 0.5 *p*=0.616	 3.9 ± 0.7 6.8 ± 1.4 *p*=0.154
Ki-67 *[Mean±SEM]* < 3% (n=12) ≥ 3% (n=4)	 2.2 ± 0.2 2.5 ± 0.5 *p*=0.615	 1.9 ± 0.4 1.2 ± 0.2 *p*=0.318	 6.8 ± 1.1 2.4 ± 0.7 ***p*=0.037**
Hypopituitarism last follow-up *[Mean±SEM]* Yes (n=10) No (n=6)	 2.5 ± 0.3 2.0 ± 0.2 *p*=0.194	 1.9 ± 0.5 1.4 ± 0.2 *p*=0.484	 5.8 ± 1.0 5.5 ± 2.0 *p*=0.908
N pit deficiencies at last follow-up *[Pearson correlation r (p value)]*	0.232 (*p*=0.386)	0.123 (*p*=0.649)	0.021 (*p*=0.939)
Microvessel density *[Pearson correlation r (p value)]*	0.408 (*p*=0.117)	-0.165 (*p*=0.563)	0.203 (*p*=0.451)
Microvessel area *[Pearson correlation r (p value)]*	0.676 (***p*=0.004**)	-0.059 (*p*=0.828)	0.203 (*p*=0.941)

Correlation between clinico-pathological and biochemical features and immune cell ratios among NFPAs

FSH, follicle-stimulating hormone; FT4, free thyroxine; F-up, follow-up; GH, growth hormone; IGF-1, insulin-like growth factor-1; LH, luteinising hormone; NFPA, non-functioning pituitary adenoma; pit, pituitary; PRL, prolactin; TSH, thyroid-stimulating hormone; SEM, standard error of the mean; yrs, years.

Somatotrophinomas n = 8	% of infiltrating immune cells				
	Macrophages	**CD8+ T cells**	**CD4+ T cells**	**FOXP3+ T cells**	**Neutrophils**
Gender *[Mean±SEM]* Male (n=4) Female (n=4)	 4.7 ± 0.7 4.6 ± 1.3 *p*=0.920	 2.4 ± 0.4 1.7 ± 0.3 *p*=0.249	 0.7 ± 0.1 1.2 ± 0.4 *p*=0.305	 0.5 ± 0.1 0.5 ± 0.2 *p*=0.984	 0.2 ± 0.1 0.1 ± 0.0 *p*=0.439
Age at diagnosis (yrs) *[Pearson correlation r (p value)]*	-0.422 (*p*=0.298)	-0.184 (*p*=0.662)	-0.362 (*p*=0.379)	-0.746 (***p*=0.034**)	-0.174 (*p*=0.681)
Headache at diagnosis *[Mean±SEM]* Yes (n=3) No (n=5)	 3.7 ± 0.9 5.2 ± 1.0 *p*=0.325	 1.9 ± 0.6 2.2 ± 0.3 *p*=0.728	 1.1 ± 0.5 0.9 ± 0.2 *p*=0.722	 0.5 ± 0.3 0.5 ± 0.1 *p*=0.976	 0.1 ± 0.0 0.2 ± 0.1 *p*=0.609
Visual impairment *[Mean±SEM]* Yes (n=1) No (n=7)	 6.3 4.4 ± 0.8 *p*=0.433	 3.4 1.9 ± 0.3 *p*=0.079	 0.5 1.0 ± 0.2 *p*=0.469	 0.8 0.5 ± 0.1 *p*=0.451	 0.0 0.2 ± 0.1 *p*=0.465
Hormonal data at diagnosis *[Pearson correlation r (p value)]* GH nadir on OGTT Serum GH Serum IGF-1 IGF-1 index Serum PRL PRL index Serum TSH Serum FT4 Basal plasma cortisol Serum LH Serum FSH	 -0.458 (*p*=0.542) -0.185 (*p*=0.692) -0.220 (*p*=0.635) -0.464 (*p*=0.246) 0.729 (*p*=0.162) 0.765 (*p*=0.132) -0.044 (*p*=0.925) -0.032 (*p*=0.945) 0.260 (*p*=0.574) 0.210 (*p*=0.651) -0.177 (*p*=0.704)	 0.537 (*p*=0.463) 0.521 (*p*=0.230) 0.550 (*p*=0.201) 0.527 (*p*=0.179) -0.256 (*p*=0.677) -0.193 (*p*=0.756) -0.320 (*p*=0.484) 0.271 (*p*=0.556) 0.517 (*p*=0.235) 0.037 (*p*=0.938) 0.045 (*p*=0.923)	 0.440 (*p*=0.560) 0.105 (*p*=0.823) 0.118 (*p*=0.801) -0.003 (*p*=0.995) 0.319 (*p*=0.601) 0.287 (*p*=0.640) -0.081 (*p*=0.862) 0.059 (*p*=0.900) 0.014 (*p*=0.976) -0.353 (*p*=0.438) -0.243 (*p*=0.599)	 0.527 (*p*=0.473) 0.462 (*p*=0.296) 0.425 (*p*=0.342) 0.115 (*p*=0.786) 0.300 (*p*=0.624) 0.326 (*p*=0.593) -0.141 (*p*=0.763) -0.097 (*p*=0.836) 0.307 (*p*=0.503) -0.469 (*p*=0.289) -0.483 (*p*=0.272)	 0.187 (*p*=0.813) -0.008 (*p*=0.987) -0.024 (*p*=0.959) -0.349 (*p*=0.397) 0.360 (*p*=0.552) 0.299 (*p*=0.625) 0.368 (*p*=0.417) -0.372 (*p*=0.411) -0.067 (*p*=0.887) -0.574 (*p*=0.187) -0.380 (*p*=0.401)
Hypopituitarism at diagnosis *[Mean±SEM]* Yes (n=2) No (n=6)	 5.9 ± 0.4 4.3 ± 0.9 *p*=0.347	 3.1 ± 0.3 1.7 ± 0.2 ***p*=0.020**	 0.6 ± 0.0 1.1 ± 0.3 *p*=0.308	 0.6 ± 0.1 0.5 ± 0.1 *p*=0.600	 0.0 ± 0.0 0.2 ± 0.1 *p*=0.394
N pit deficiencies at diagnosis *[Pearson correlation r (p value)]*	0.085 (*p*=0.957)	0.711 (*p*=0.073)	0.157 (*p*=0.737)	0.580 (*p*=0.172)	-0.024 (*p*=0.959)
Cavernous sinus invasion *[Mean±SEM]* Yes (n=4) No (n=4)	 4.6 ± 1.3 4.7 ± 0.7 *p*=0.920	 1.7 ± 0.3 2.4 ± 0.4 *p*=0.249	 1.2 ± 0.4 0.7 ± 0.1 *p*=0.305	 0.5 ± 0.2 0.5 ± 0.1 *p*=0.984	 0.1 ± 0.0 0.2 ± 0.1 *p*=0.439
Ki-67 *[Mean±SEM]* < 3% (n=7) ≥ 3% (n=1)	 4.1 ± 0.5 8.4 ***p*=0.031**	 2.1 ± 0.3 1.8 *p*=0.737	 0.9 ± 0.2 1.5 *p*=0.342	 0.5 ± 0.1 0.8 *p*=0.322	 0.1 ± 0.1 0.1 *p*=0.959
Pre-operative SSAs *[Mean±SEM]* Yes (n=6) No (n=2)	 4.1 ± 0.6 6.4 ± 2.0 *p*=0.171	 2.1 ± 0.4 2.0 ± 0.2 *p*=0.852	 0.9 ± 0.3 1.1 ± 0.4 *p*=0.708	 0.5 ± 0.1 0.5 ± 0.3 *p*=0.974	 0.2 ± 0.1 0.1 ± 0.1 *p*=0.553
Hypopituitarism last follow-up *[Mean±SEM]* Yes (n=4) No (n=4)	 5.9 ± 0.4 4.3 ± 0.9 *p*=0.347	 2.4 ± 0.4 1.7 ± 0.3 *p*=0.232	 1.0 ± 0.4 0.9 ± 0.2 *p*=0.825	 0.7 ± 0.1 0.4 ± 0.2 *p*=0.238	 0.2 ± 0.1 0.1 ± 0.0 *p*=0.396

N pit deficiencies at last follow-up *[Pearson correlation r (p value)]*	0.002 (*p*=0.996)	0.171 (*p*=0.686)	0.004 (*p*=0.992)	0.266 (*p*=0.525)	0.700 (*p*=0.053)
Microvessel density *[Pearson correlation r (p value)]*	-0.002 (*p*=0.996)	0.517 (*p*=0.189)	-0.257 (*p*=0.539)	-0.132 (*p*=0.755)	-0.368 (*p*=0.369)
Microvessel area *[Pearson correlation r (p value)]*	0.433 (*p*=0.285)	0.598 (*p*=0.118)	-0.264 (*p*=0.527)	0.059 (*p*=0.890)	-0.583 (*p*=0.130)

Correlation between clinico-pathological and biochemical features and infiltrating immune cells among somatotrophinomas

FSH, follicle-stimulating hormone; FT4, free thyroxine; F-up, follow-up; GH, growth hormone; IGF-1, insulin-like growth factor-1; LH, luteinising hormone; OGTT oral glucose tolerance test; pit, pituitary; PRL, prolactin; TSH, thyroid-stimulating hormone; SEM, standard error of the mean; SSAs, somatostatin analogues; yrs, years.

Somatotrophinomas n = 8		Cell ratios		
		Ratio M2:M1	**Ratio CD8:CD4**	**Ratio CD8:FOXP3**
Gender *[Mean±SEM]*				
Male (n=4)		1.8 ± 0.1	3.4 ± 1.0	4.5 ± 0.7
Female (n=4)		2.1 ± 0.5	1.8 ± 0.5	6.6 ± 2.5
		p=0.653	*p*=0.222	*p*=0.481
Age at diagnosis (yrs) *[Pearson correlation r (p value)]*		0.856 (***p*=0.007**)	0.047 (*p*=0.913)	0.677 (*p*=0.065)
Headache at diagnosis *[Mean±SEM]*				
Yes (n=3)		1.7 ± 0.2	2.4 ± 1.0	6.6 ± 2.8
No (n=5)		2.1 ± 0.4	2.8 ± 0.8	4.9 ± 1.3
		p=0.482	*p*=0.777	*p*=0.544
Visual impairment *[Mean±SEM]*				
Yes (n=1)		1.7	5.75	3.8
No (n=7)		2.0 ± 0.3	2.2 ± 0.5	5.8 ± 1.5
		p=0.739	***p*=0.036**	*p*=0.642
Hormonal data at diagnosis *[Pearson correlation r (p value)]*				
GH nadir on OGTT		-0.073 (*p*=0.927)	0.191 (*p*=0.809)	-0.407 (*p*=0.593)
Serum GH		-0.381 (*p*=0.398)	0.347 (*p*=0.446)	-0.396 (*p*=0.379)
Serum IGF-1		-0.232 (*p*=0.616)	0.351 (*p*=0.440)	-0.376 (*p*=0.406)
IGF-1 index		0.054 (*p*=0.899)	0.394 (*p*=0.334)	0.024 (*p*=0.955)
Serum PRL		-0.413 (*p*=0.489)	-0.427 (*p*=0.474)	-0.360 (*p*=0.552)
PRL index		-0.405 (*p*=0.498)	-0.357 (*p*=0.556)	-0.385 (*p*=0.522)
Serum TSH		-0.370 (*p*=0.414)	-0.326 (*p*=0.476)	0.012 (*p*=0.980)
Serum FT4		0.883 (***p*=0.008**)	0.221 (*p*=0.634)	0.104 (*p*=0.825)
Basal plasma cortisol		0.060 (*p*=0.898)	0.410 (*p*=0.361)	-0.299 (*p*=0.515)
Serum LH		0.939 (***p*=0.002**)	0.255 (*p*=0.581)	0.400 (*p*=0.373)
Serum FSH		0.915 (***p*=0.004**)	0.156 (*p*=0.739)	0.397 (*p*=0.378)
Hypopituitarism at diagnosis *[Mean±SEM]*	Yes (n=2)	1.9 ± 0.1	5.0 ± 0.7	4.7 ± 0.9
	No (n=6)	2.0 ± 0.3	1.8 ± 0.4	5.8 ± 1.7
		p=0.835	***p*=0.005**	*p*=0.726
N pit deficiencies at diagnosis *[Pearson correlation r (p value)]*		-0.293 (*p*=0.524)	0.490 (*p*=0.264)	-0.511 (*p*=0.242)
Cavernous sinus invasion *[Mean±SEM]*	Yes (n=4)	2.1 ± 0.5	1.9 ± 0.6	6.6 ± 2.5
	No (n=4)	1.8 ± 0.1	3.4 ± 1.0	4.5 ± 0.7
		p=0.653	*p*=0.222	*p*=0.481
Ki-67 *[Mean±SEM]*	< 3% (n=7)	2.0 ± 0.3	2.8 ± 0.7	6.0 ± 1.3
	≥ 3% (n=1)	1.6	1.2	2.3
		p=0.597	*p*=0.402	*p*=0.372
Pre-operative SSAs *[Mean±SEM]*	Yes (n=6)	1.8 ± 0.1	2.7 ± 0.8	5.4 ± 1.4
	No (n=2)	2.6 ± 1.1	2.3 ± 1.1	6.0 ± 3.6
		p=0.555	*p*=0.781	*p*=0.866
Hypopituitarism last follow-up *[Mean±SEM]*	Yes (n=4)	1.8 ± 0.1	3.1 ± 1.1	3.7 ± 0.7
	No (n=4)	2.2 ± 0.5	2.1 ± 0.5	7.4± 2.1
		p=0.457	*p*=0.442	*p*=0.065
N pit deficiencies at last follow-up *[Pearson correlation r (p value)]*		-0.271 (*p*=0.516)	0.101 (*p*=0.811)	-0.542 (*p*=0.165)
Microvessel density *[Pearson correlation r (p value)]*		0.801 (***p*=0.017**)	0.621 (*p*=0.100)	0.209 (*p*=0.620)
Microvessel area *[Pearson correlation r (p value)]*		0.606 (*p*=0.111)	0.718 (***p*=0.045**)	0.122 (*p*=0.773)

Correlation between clinico-pathological and biochemical features and immune cell ratios among somatotrophinomas

FSH, follicle-stimulating hormone; FT4, free thyroxine; F-up, follow-up; GH, growth hormone; IGF-1, insulin-like growth factor-1; LH, luteinising hormone; OGTT oral glucose tolerance test; pit, pituitary; PRL, prolactin; TSH, thyroid-stimulating hormone; SEM, standard error of the mean; SSAs, somatostatin analogues; yrs, years.

Appendix 5: Supplemental tables with cytokine array data from cell lines

Results from Millipore MILLIPLEX rat 27-plex assay in supernatants from GH3-*Aip*-KD and GH3-NT cells collected at both 24h, 48h and 72h, measuring simultaneously 27 different cytokines/ chemokines. Data are shown as concentration (pg/mL), mean±SEM, and ratio between GH3-*Aip*-KD and GH3-NT cell supernatants is also shown in the table (Mann Whitney U test). n=3.

Cytokine	Collection time	Supernatants GH3-NT cells Mean concentration (pg/mL)	SEM	Supernatants GH3-*Aip*-KD cells Mean concentration (pg/mL)	SEM	*p* value	Ratio KD:NT
CX3CL1	24h	301.80	6.76	382.66	25.74	**0.024**	**1.27**
	48h	657.77	18.85	798.69	20.87	**0.001**	**1.22**
	72h	995.36	41.46	1124.17	42.90	0.056	1.13
IL-10	24h	6.61	1.07	11.64	5.68	0.404	1.9
	48h	7.87	0.96	12.08	2.92	0.220	1.71
	72h	8.77	1.24	16.46	10.13	0.468	1.63
IL-13	24h	6.30	1.06	6.85	1.18	0.736	1.05
	48h	9.73	0.87	9.69	1.51	0.981	1.02
	72h	9.32	0.60	13.95	2.52	0.103	1.49
IL-4	24h	6.72	0.90	7.12	0.77	0.746	1.15
	48h	10.83	1.19	10.49	0.96	0.826	0.97
	72h	13.72	0.66	15.28	2.74	0.529	1.1
IL-6	24h	168.97	31.48	248.28	45.41	0.182	1.43
	48h	286.23	44.84	258.57	75.74	0.760	0.92
	72h	289.55	31.39	516.13	258.97	0.405	1.71
IL-12	24h	31.73	4.06	28.35	4.90	0.607	0.88
	48h	32.09	3.97	32.75	3.17	0.899	1.04
	72h	32.42	3.67	47.33	12.92	0.293	1.61
IL-5	24h	11.77	1.09	11.17	0.84	0.671	0.96
	48h	9.56	2.07	11.04	1.38	0.565	1.33
	72h	9.14	1.31	13.02	3.89	0.367	1.53
IL-2	24h	20.57	2.33	21.10	1.49	0.853	1.08
	48h	22.08	0.63	21.37	1.50	0.677	0.95
	72h	21.72	1.40	29.64	7.20	0.306	1.42
IL-1β	24h	6.59	1.01	6.43	1.54	0.931	1.08
	48h	5.82	1.37	5.99	1.85	0.942	0.96
	72h	6.21	1.17	12.30	6.92	0.406	1.71
IL-1α	24h	17.14	1.10	17.74	1.51	0.754	1.05
	48h	20.57	0.78	19.96	1.04	0.651	0.97
	72h	21.87	1.20	28.45	4.51	0.189	1.28
IL-17A	24h	3.19	0.53	3.74	0.87	0.603	1.34
	48h	3.61	0.70	3.53	0.86	0.944	0.98
	72h	4.19	0.60	5.43	1.63	0.491	1.27
IL-18	24h	3.96	1.93	6.11	1.81	0.436	2.8
	48h	6.76	1.80	4.91	1.71	0.475	0.67
	72h	5.00	0.86	20.96	13.89	0.303	5
CXCL10	24h	6.65	0.55	7.85	0.85	0.264	1.17
	48h	25.06	1.69	31.21	2.41	0.063	1.24
	72h	44.32	2.30	54.67	1.40	**0.003**	1.25

IFN-y	24h	584.94	43.69	584.54	67.09	0.996	1
	48h	597.24	26.62	570.17	52.23	0.654	0.95
	72h	836.46	19.29	774.35	37.44	0.171	0.92
CCL3	24h	0.92	0.31	1.18	0.26	0.525	1.04
	48h	2.36	0.74	1.79	0.17	0.356	0.91
	72h	1.79	0.17	1.83	0.57	0.939	1.04
CXCL2	24h	29.67	2.33	26.94	2.81	0.470	0.92
	48h	31.39	2.8516	28.88	2.34	0.511	0.92
	72h	41.59	1.9985	41.06	5.4	0.928	0.98
CCL2	24h	81.61	25.47	141.52	18.86	0.088	1.99
	48h	127.39	19.16	139.80	20.92	0.671	1.19
	72h	117.41	16.34	149.78	57.18	0.598	1.26
CCL5	24h	0.45	0.03	0.37	0.02	0.068	0.85
	48h	0.57	0.01	0.52	0.03	0.173	0.91
	72h	0.47	0.02	0.48	0.05	0.901	1.01
G-CSF	24h	47.52	5.98	23.93	18.76	0.258	0.8
	48h	30.85	13.10	33.70	14.62	0.888	0.66
	72h	27.74	9.71	29.40	18.42	0.938	0.99
GM-CSF	24h	11.58	1.97	10.23	1.36	0.585	0.95
	48h	10.36	0.86	13.56	1.77	0.135	1.29
	72h	10.07	0.44	20.41	10.62	0.375	2.03
CCL11	24h	2.27	0.35	2.49	0.26	0.627	1.12
	48h	2.62	0.22	2.71	0.26	0.727	1.03
	72h	2.15	0.48	3.30	0.59	0.162	1.57
LIX	24h	25.73	0.67	26.31	2.26	0.811	1.02
	48h	35.42	0.85	36.09	1.19	0.656	1.02
	72h	41.78	1.24	43.45	1.76	0.457	1.04
CXCL1	24h	16.17	4.64	27.23	5.63	0.161	2.44
	48h	29.92	2.31	26.75	6.14	0.640	0.89
	72h	28.26	8.83	24.91	6.67	0.768	2.14
VEGF	24h	2534.20	97.52	2508.51	130.42	0.878	0.99
	48h	7248.94	213.86	6700.94	140.38	0.058	0.92
	72h	12440.23	526.15	10961.23	283.89	**0.033**	0.88
EGF	24h	0.19	0.01	0.19	0.03	0.883	1.03
	48h	0.21	0.02	0.18	0.02	0.278	0.9
	72h	0.19	0.01	0.26	0.09	0.451	1.35
TNF-α	24h	0.24	0.22	0.06	0.05	0.453	1.78
	48h	0.03	0.03	0.05	0.05	0.770	1.56
	72h	0.01	0.01	0.61	0.61	0.373	45.5
Leptin	24h	80.20	9.73	108.03	20.90	0.255	1.4
	48h	126.89	13.78	108.59	24.54	0.530	0.86
	72h	133.15	11.80	129.75	39.00	0.935	0.71

Results from the Millipore MILLIPLEX rat 27-plex assay in supernatants from GH3-*Aip*-KD and GH3-NT cells treated with PMA (5nM)-activated RAW 264.7 macrophage-CM (+Raw-CM) and in medium (untreated) for 24h, highlighting secretome changes induced by macrophage-derived factors. Data regarding the cytokines with measurable concentrations are shown as concentration (pg/mL), mean±SEM, and as ratio between untreated vs macrophage-CM treated GH3-*Aip*-KD and GH3-NT cell supernatants, mean±SEM are also shown. CCL5, G-CSF, IL-17A and TNF-α were not detectable in GH3 supernatants, whereas CCL11, GM-CSF, IL-1α, Leptin, EGF, IL-12 and LIX had very low readings (below the first standard curve point of the assay), and thus not represented. n=3. <0.05, **, <0.01, ***, <0.001 (two-way ANOVA with Bonferroni Multiple Comparison test).

Cytokine	**GH3-NT cells UNTREATED** Mean concentration (pg/mL) ± SEM	**GH3-NT cells +Raw-CM** Mean concentration (pg/mL) ± SEM	**GH3-NT cells Ratio Raw-CM : UNTREATED** Mean ± SEM	**GH3-*Aip*-KD cells UNTREATED** Mean concentration (pg/mL) ± SEM	**GH3-*Aip*-KD cells +Raw-CM** Mean concentration (pg/mL) ± SEM	**GH3-*Aip*-KD cells Ratio Raw-CM : UNTREATED** Mean ± SEM
CX3CL1	301.80 ± 6.76	400.33 ± 31.39	1.33 ± 0.10*	382.66 ± 25.74	635.77 ± 40.27	1.66 ± 0.11*
IL-13	6.30 ± 1.06	11.83 ± 2.99	1.88 ± 0.47*	6.85 ± 1.18	11.58 ± 3.63	1.69 ± 0.53
IL-4	6.72 ± 0.90	6.95 ± 1.43	1.03 ± 0.21	7.12 ± 0.77	9.10 ± 2.04	1.28 ± 0.29
IL-6	168.97 ± 31.48	169.42 ± 98.92	1.00 ± 0.59	248.28 ± 45.41	191.68 ± 22.50	0.77 ± 0.09*
IL-5	11.77 ± 1.09	6.72 ± 4.46	0.57 ± 0.38	11.17 ± 0.84	8.95 ± 5.06	0.80 ± 0.45
IL-2	20.57 ± 2.33	15.07 ± 9.19	0.73 ± 0.45	21.10 ± 1.49	30.49 ± 10.38	1.45 ± 0.49
IL-1β	6.59 ± 1.01	17.32 ± 2.22	2.63 ± 0.34*	6.43 ± 1.54	24.09 ± 1.30	3.75 ± 0.20*
IL-18	3.96 ± 1.93	10.68 ± 5.96	2.70 ± 1.50	6.11 ± 1.81	12.80 ± 6.35	2.10 ± 1.04
CXCL10	6.65 ± 0.55	24.26 ± 1.40	3.65 ± 0.21*	7.85 ± 0.85	33.47 ± 0.96	4.26 ± 0.12
CXCL2	29.67 ± 2.33	7.77 ± 7.77	0.26 ± 0.26*	26.94 ± 2.81	32.70 ± 4.69	1.21 ± 0.17
CCL2	81.61 ± 25.47	48.29 ± 25.04	0.59 ± 0.31	141.52 ± 18.86	132.14 ± 67.61	0.93 ± 0.48
CXCL1	16.17 ± 4.64	135.86 ± 12.31	8.40 ± 0.76*	27.23 ± 5.63	138.92 ± 6.25	5.10 ± 0.23*
VEGF	2534.20 ± 97.52	4521.34 ± 548.86	1.78 ± 0.22*	2508.51 ± 130.42	4596.58 ± 368.73	1.83 ± 0.15*

Results from the Millipore MILLIPLEX mouse 32-plex assay in supernatants from RAW 264.7 macrophages treated with GH3-*Aip*-KD and GH3-NT cell-CM and in medium (untreated) for 24h, highlighting secretome changes induced by GH3 cell-derived factors. IFNγ, IL-3, IL-4, IL-5, IL-6, IL-7, IL-12, IL-13, CXCL1 were not detectable in the RAW 264.7 macrophages, whereas CCL11, GM-CSF, IL-2, IL-10, LIF, LIX, MIG had very low readings (below the first standard curve point of the assay), and thus are not represented. Data are shown as concentration (pg/mL), mean±SEM, and as ratio between untreated vs GH3-CM treated, mean±SEM. n=3. <0.05, **, <0.01, ***, <0.001 (Mann Whitney U test).

Cytokine	**RAW macrophages UNTREATED** Mean concentration (pg/mL) ± SEM	**RAW macrophages +GH3-NT-CM** Mean concentration (pg/mL) ± SEM	**Ratio GH3-NT-CM : UNTREATED** Mean ± SEM	**RAW macrophages +GH3-*Aip*-KD-CM** Mean concentration (pg/mL) ± SEM	**Ratio GH3-*Aip*-KD-CM : UNTREATED** Mean ± SEM
CCL3	3224.50 ± 302.26	2782.46 ± 693.47	0.84 ± 0.16	3245.58 ± 82.10	1.03 ± 0.12
CCL4	6310.65 ± 2686.71	3106.84 ± 1379.51	0.49 ± 0.03*	7529.29 ± 2377.61	1.32 ± 0.15*
CCL2	242.87 ± 147.87	237.26 ± 115.92	1.93 ± 1.43	642.45 ± 341.18	2.97 ± 0.72*
CCL5	3.81 ± 1.29	3.02 ± 0.83	0.86 ± 0.25	7.04 ± 2.23	1.87 ± 0.04*
CXCL2	297.28 ± 135.72	332.08 ± 291.76	1.00 ± 0.56	804.11 ± 458.55	2.05 ± 0.94
VEGF	41.24 ± 26.53	39.50 ± 27.53	0.86 ± 0.14	96.38 ± 37.92	3.26 ± 1.14*
TNF-α	14.56 ± 5.93	13.92 ± 9.47	0.97 ± 0.39	39.03 ± 20.85	2.58 ± 0.58*
CXCL10	6.31 ± 1.85	4.09 ± 1.05	0.68 ± 0.13*	15.13 ± 5.66	2.23 ± 0.49*
IL-1α	3.86 ± 1.12	3.00 ± 0.73	0.99 ± 0.37	26.83 ± 12.91	5.96 ± 2.48*
IL-1β	7.54 ± 1.39	3.57 ± 0.43	0.49 ± 0.06*	6.55 ± 1.98	0.83 ± 0.11
IL-2	1.56 ± 0.27	1.57 ± 0.92	1.13 ± 0.63	2.85 ± 0.48	1.85 ± 0.17*
IL-9	3.49 ± 0.14	4.60 ± 2.47	1.30 ± 0.67	14.08 ± 9.92	3.90 ± 2.72
IL-10	2.03 ± 0.59	1.80 ± 0.57	0.93 ± 0.18	2.12 ± 0.29	1.17 ± 0.24
IL-12	4.70 ± 0.59	4.76 ± 4.60	1.33 ± 1.30	4.04 ± 1.81	0.97 ± 0.52
IL-15	16.24 ± 8.82	11.34 ± 5.40	1.11 ± 0.83	13.60 ± 4.03	1.54 ± 0.99
IL-17	2.01 ± 0.31	1.33 ± 0.32	0.64 ± 0.06*	2.50 ± 0.31	1.25 ± 0.08*
G-CSF	2.23 ± 0.85	1.39 ± 0.82	0.58 ± 0.18*	4.06 ± 1.55	1.93 ± 0.28*
GM-CSF	2.04 ± 0.68	2.12 ± 0.46	1.26 ± 0.45	2.12 ± 0.49	1.15 ± 0.30
M-CSF	1.32 ± 0.95	0.86 ± 0.44	4.07 ± 3.89	1.50 ± 0.23	6.22 ± 4.96

Appendix 6: Supplemental tables with pre-operative haematological parameters and serum inflammation-based scores (NLR, LMR and PLR) and pituitary function and PA-derived cytokine secretome

Pituitary hormone levels in NFPAs (n=16)		White cell count	Neutrophil count	Lymphocyte count	Monocyte count	Eosinophil count	Basophil count	Platelet count	NLR	LMR	PLR
GH (mcg/L)	Pearson correlation *r*	-0.428	-0.190	-0.576	-0.445	-0.188	0.055	-0.316	0.157	-0.041	0.278
	p value	0.166	0.553	0.050	0.147	0.558	0.865	0.318	0.627	0.898	0.381
	N	12	12	12	12	12	12	12	12	12	12
IGF-1 (nmol/L)	Pearson correlation *r*	-0.341	-0.227	-0.323	-0.603	-0.269	0.000	-0.065	0.189	-0.198	0.233
	p value	0.233	0.436	0.259	**.023**	0.352	0.999	0.826	0.517	0.497	0.423
	N	14	14	14	14	14	14	14	14	14	14
IGF-1 index	Pearson correlation *r*	-0.420	-0.240	-0.449	-0.276	-0.026	0.408	0.034	0.176	-0.364	0.170
	p value	0.135	0.408	0.107	0.340	0.929	0.148	0.908	0.546	0.200	0.562
	N	14	14	14	14	14	14	14	14	14	14
PRL (mU/L)	Pearson correlation *r*	-0.188	-0.184	-0.159	-0.199	0.004	0.388	-0.216	-0.084	-0.120	-0.028
	p value	0.520	0.528	0.588	0.495	0.990	0.170	0.458	0.775	0.683	0.925
	N	14	14	14	14	14	14	14	14	14	14
PRL-index	Pearson correlation *r*	-0.378	-0.262	-0.377	-0.038	-0.312	0.324	-0.167	0.078	-0.380	0.104
	p value	0.182	0.365	0.184	0.896	0.278	0.258	0.569	0.792	0.181	0.724
	N	14	14	14	14	14	14	14	14	14	14
TSH (µU/mL)	Pearson correlation *r*	-0.294	-0.058	-0.365	-0.193	-0.320	0.417	0.295	0.186	-0.318	0.300
	p value	0.307	0.844	0.199	0.510	0.264	0.138	0.307	0.524	0.268	0.297
	N	14	14	14	14	14	14	14	14	14	14
FT4 (pmol/L)	Pearson correlation *r*	-0.122	0.039	-0.184	0.075	-0.261	-0.374	-0.242	0.349	-0.197	0.125
	p value	0.678	0.895	0.530	0.800	0.368	0.187	0.404	0.221	0.501	0.670
	N	14	14	14	14	14	14	14	14	14	14

Basal Cortisol (nmol/L)	Pearson correlation *r*	-0.229	-0.095	-0.223	-0.451	-0.120	0.103	-0.099	0.063	0.202	0.071
	p value	0.452	0.758	0.464	0.122	0.696	0.737	0.749	0.837	0.507	0.818
	N	13	13	13	13	13	13	13	13	13	13
LH (U/L)	Pearson correlation *r*	0.214	0.259	0.155	0.116	-0.015	-0.078	0.024	0.107	0.132	-0.005
	p value	0.463	0.372	0.596	0.693	0.960	0.790	0.934	0.715	0.652	0.987
	N	14	14	14	14	14	14	14	14	14	14
FSH (U/L)	Pearson correlation *r*	-0.169	-0.028	-0.222	0.196	-0.223	0.053	-0.016	0.198	-0.254	0.140
	p value	0.562	0.925	0.445	0.503	0.443	0.858	0.957	0.497	0.381	0.633
	N	14	14	14	14	14	14	14	14	14	14
Testosterone (nmol/L)	Pearson correlation *r*	-0.056	0.113	-0.128	-0.084	-0.076	-0.368	0.270	0.218	-0.116	0.090
	p value	0.863	0.727	0.693	0.796	0.815	0.239	0.397	0.496	0.719	0.781
	N	12	12	12	12	12	12	12	12	12	12

Pre-operative haematological parameters and serum inflammation-based scores (NLR, LMR and PLR) and pituitary function in NFPAs

p values were determined by the Pearson correlation coefficient *r*. FSH, follicle-stimulating hormone; FT4, free thyroxine; GH, growth hormone; IGF-1, insulin-like growth factor-1; LH, luteinising hormone; LMR, lymphocyte-to-monocyte ratio; NFPA, non-functioning pituitary adenoma; NLR, neutrophil-to-lymphocyte ratio; PLR, platelet-to-lymphocyte ratio; PRL, prolactin; TSH, thyroid-stimulating hormone.

Pituitary hormone levels in somatotrophinomas (n=8)		White cell count	Neutrophil count	Lymphocyte count	Monocyte count	Eosinophil count	Basophil count	Platelet count	NLR	LMR	PLR
GH (mcg/L)	Pearson correlation *r*	0.008	-0.220	0.306	-0.044	0.043	0.299	-0.127	-0.421	0.153	-0.441
	p value	0.986	0.635	0.505	0.926	0.926	0.515	0.787	0.347	0.744	0.322
	N	7	7	7	7	7	7	7	7	7	7
GH nadir on OGTT (mcg/L)	Pearson correlation *r*	0.861	0.886	0.853	0.513	0.281	0.643	0.498	-0.336	0.314	-0.559
	p value	0.139	0.114	0.147	0.487	0.719	0.357	0.502	0.664	0.686	0.441
	N	4	4	4	4	4	4	4	4	4	4
IGF-1 (nmol/L)	Pearson correlation *r*	0.096	-0.109	0.309	0.095	0.061	0.271	-0.173	-0.298	0.076	-0.478
	p value	0.838	0.817	0.499	0.839	0.897	0.557	0.711	0.516	0.871	0.278
	N	7	7	7	7	7	7	7	7	7	7
IGF-1 index	Pearson correlation *r*	-0.027	-0.206	0.279	0.047	0.308	-0.061	-0.050	-0.249	0.237	-0.294
	p value	0.950	0.624	0.503	0.911	0.458	0.886	0.907	0.551	0.572	0.479
	N	8	8	8	8	8	8	8	8	8	8
PRL (mU/L)	Pearson correlation *r*	-0.414	-0.500	-0.389	-0.037	0.225	-0.068	-0.307	-0.537	-0.492	0.067
	p value	0.489	0.391	0.517	0.953	0.716	0.913	0.616	0.350	0.400	0.915
	N	5	5	5	5	5	5	5	5	5	5
PRL-index	Pearson correlation *r*	-0.434	-0.526	-0.410	0.016	0.199	-0.110	-0.375	-0.568	-0.565	0.030
	p value	0.465	0.363	0.492	0.980	0.748	0.860	0.534	0.318	0.321	0.962
	N	5	5	5	5	5	5	5	5	5	5
TSH (µU/mL)	Pearson correlation *r*	-0.513	-0.705	-0.064	-0.523	0.333	0.181	-0.566	-0.498	0.362	-0.174
	p value	0.239	0.077	0.892	0.229	0.466	0.697	0.185	0.255	0.425	0.709
	N	7	7	7	7	7	7	7	7	7	7
FT4 (pmol/L)	Pearson correlation *r*	0.525	0.790	-0.118	0.927	-0.235	-0.352	0.035	0.865	-0.672	0.030
	p value	0.226	**0.035**	0.801	**0.003**	0.612	0.439	0.941	**0.012**	0.098	0.949
	N	7	7	7	7	7	7	7	7	7	7

Basal Cortisol (nmol/L)	Pearson correlation *r*	0.571	0.501	0.465	0.177	0.214	0.137	0.396	-0.055	0.029	-0.283
	p value	0.180	0.252	0.294	0.704	0.644	0.770	0.379	0.906	0.952	0.539
	N	7	7	7	7	7	7	7	7	7	7
LH (U/L)	Pearson correlation *r*	0.095	0.471	-0.539	0.779	-0.372	-0.735	-0.374	0.907	-0.820	0.247
	p value	0.839	0.286	0.212	**0.039**	0.411	**0.060**	0.409	**.005**	**0.024**	0.594
	N	7	7	7	7	7	7	7	7	7	7
FSH (U/L)	Pearson correlation *r*	0.257	0.518	-0.279	0.732	-0.194	-0.470	-0.370	0.808	-0.554	0.051
	p value	0.579	0.234	0.545	0.061	0.677	0.287	0.413	**0.028**	0.197	0.914
	N	7	7	7	7	7	7	7	7	7	7
Testosterone (nmol/L)	Pearson correlation *r*	-0.005	-0.327	0.365	-0.181	0.646	0.344	-0.623	-0.469	0.350	-0.658
	p value	0.992	0.526	0.477	0.732	0.166	0.504	0.186	0.348	0.496	0.156
	N	6	6	6	6	6	6	6	6	6	6

Pre-operative haematological parameters and serum inflammation-based scores (NLR, LMR and PLR) and pituitary function in somatotrophinomas

p values were determined by the Pearson correlation coefficient *r*. FSH, follicle-stimulating hormone; FT4, free thyroxine; GH, growth hormone; IGF-1, insulin-like growth factor-1; LH, luteinising hormone; LMR, lymphocyte-to-monocyte ratio; NFPA, non-functioning pituitary adenoma; NLR, neutrophil-to-lymphocyte ratio; OGTT, oral glucose tolerance test; PLR, platelet-to-lymphocyte ratio; PRL, prolactin; TSH, thyroid-stimulating hormone.

Cytokine secretome in the overall cohort of PAs (n=24)		Red cell count	White cell count	Neutrophil count	Lymphocyte count	Monocyte count	Eosinophil count	Basophil count	Platelet count	NLR	LMR	PLR
IL-8	Pearson correlation *r*	-0.078	0.064	0.217	-0.052	-0.015	0.093	-0.110	0.182	0.270	-0.018	0.110
	p value	0.719	0.765	0.309	0.810	0.944	0.667	0.610	0.394	0.202	0.934	0.610
	N	24	24	24	24	24	24	24	24	24	24	24
CCL2	Pearson correlation *r*	-0.018	-0.050	0.085	-0.117	-0.097	-0.149	-0.130	0.176	0.228	-0.076	0.183
	p value	0.933	0.815	0.692	0.585	0.653	0.487	0.545	0.411	0.284	0.723	0.393
	N	24	24	24	24	24	24	24	24	24	24	24
CCL3	Pearson correlation *r*	-0.155	-0.031	-0.052	-0.009	-0.224	0.228	0.107	0.112	-0.066	0.094	-0.021
	p value	0.469	0.885	0.808	0.967	0.292	0.284	0.617	0.601	0.761	0.663	0.922
	N	24	24	24	24	24	24	24	24	24	24	24
CCL4	Pearson correlation *r*	-0.087	0.047	0.181	-0.053	-0.039	0.083	-0.062	0.204	0.227	-0.012	0.111
	p value	0.685	0.829	0.396	0.806	0.856	0.699	0.774	0.338	0.285	0.954	0.606
	N	24	24	24	24	24	24	24	24	24	24	24
CXCL10	Pearson correlation *r*	0.072	-0.145	-0.100	-0.122	-0.160	-0.327	-0.163	0.018	0.071	-0.088	0.142
	p value	0.737	0.499	0.640	0.572	0.456	0.119	0.447	0.933	0.742	0.682	0.509
	N	24	24	24	24	24	24	24	24	24	24	24
CCL22	Pearson correlation *r*	0.185	-0.072	0.151	-0.197	-0.099	-0.095	-0.096	0.331	0.375	-0.165	0.377
	p value	0.387	0.736	0.480	0.356	0.645	0.657	0.657	0.114	0.071	0.442	0.069
	N	24	24	24	24	24	24	24	24	24	24	24
CXCL1	Pearson correlation *r*	-0.095	-0.027	0.077	-0.089	-0.155	0.146	0.028	0.223	0.153	-0.007	0.131
	p value	0.659	0.899	0.721	0.678	0.470	0.497	0.898	0.295	0.475	0.973	0.541
	N	24	24	24	24	24	24	24	24	24	24	24
CX3CL1	Pearson correlation *r*	0.073	-0.129	-0.067	-0.120	-0.194	-0.287	-0.212	-0.005	0.110	-0.074	0.144
	p value	0.736	0.547	0.757	0.575	0.363	0.173	0.320	0.983	0.609	0.730	0.501
	N	24	24	24	24	24	24	24	24	24	24	24
FGF-2	Pearson correlation *r*	0.064	-0.316	-0.133	-0.363	-0.237	-0.043	0.077	0.322	0.281	-0.264	0.550
	p value	0.767	0.133	0.534	0.081	0.264	0.841	0.720	0.125	0.184	0.213	**0.005**
	N	24	24	24	24	24	24	24	24	24	24	24

IL-6	Pearson correlation *r*	0.000	0.114	0.352	-0.072	0.145	-0.013	-0.196	0.194	0.428	-0.096	0.166
	p value	0.999	0.595	0.091	0.738	0.500	0.951	0.358	0.363	**0.037**	0.656	0.438
	N	24	24	24	24	24	24	24	24	24	24	24
PDGF-AA	Pearson correlation *r*	0.054	0.107	0.321	-0.046	0.024	-0.177	-0.235	0.122	0.416	-0.055	0.149
	p value	0.803	0.618	0.126	0.830	0.913	0.408	0.269	0.569	**0.043**	0.798	0.486
	N	24	24	24	24	24	24	24	24	24	24	24
VEGF-A	Pearson correlation *r*	-0.015	0.069	0.226	-0.044	-0.020	-0.071	0.011	0.480	0.256	-0.053	0.248
	p value	0.946	0.748	0.289	0.840	0.926	0.741	0.958	**0.018**	0.228	0.807	0.243
	N	24	24	24	24	24	24	24	24	24	24	24

Pre-operative haematological parameters and serum inflammation-based scores (NLR, LMR and PLR) and PA-derived cytokine secretome

p values were determined by the Pearson correlation coefficient *r*. FGF, fibroblast growth factor; IL, interleukin; LMR, lymphocyte-to-monocyte ratio; NLR, neutrophil-to-lymphocyte ratio; PDGF, platelet-derived growth factor; PLR, platelet-to-lymphocyte ratio; VEGF, vascular endothelial growth factor.

Cytokine secretome among NFPAs (n=16)		Red cell count	White cell count	Neutrophil count	Lymphocyte count	Monocyte count	Eosinophil count	Basophil count	Platelet count	NLR	LMR	PLR
IL-8	Pearson correlation *r*	-0.134	0.046	0.246	-0.080	0.052	0.245	-0.054	0.291	0.311	-0.048	0.203
	p value	0.621	0.867	0.359	0.768	0.848	0.360	0.842	0.275	0.241	0.861	0.451
	N	16	16	16	16	16	16	16	16	16	16	16
CCL2	Pearson correlation *r*	-0.078	-0.097	0.061	-0.165	-0.053	-0.037	-0.063	0.288	0.257	-0.127	0.329
	p value	0.775	0.720	0.823	0.541	0.847	0.892	0.818	0.279	0.337	0.640	0.213
	N	16	16	16	16	16	16	16	16	16	16	16
CCL3	Pearson correlation *r*	-0.229	-0.064	-0.112	-0.034	-0.303	0.413	0.229	0.190	-0.120	0.071	0.010
	p value	0.393	0.815	0.679	0.900	0.255	0.112	0.393	0.482	0.658	0.794	0.972
	N	16	16	16	16	16	16	16	16	16	16	16
CCL4	Pearson correlation *r*	-0.155	0.020	0.191	-0.085	0.023	0.241	0.011	0.317	0.253	-0.047	0.206
	p value	0.567	0.941	0.478	0.754	0.933	0.369	0.967	0.232	0.345	0.862	0.444
	N	16	16	16	16	16	16	16	16	16	16	16
CXCL10	Pearson correlation *r*	0.050	-0.186	-0.165	-0.151	-0.192	-0.324	-0.149	0.051	0.063	-0.120	0.236
	p value	0.855	0.491	0.542	0.578	0.476	0.221	0.583	0.850	0.818	0.657	0.378
	N	16	16	16	16	16	16	16	16	16	16	16
CCL22	Pearson correlation *r*	0.293	-0.008	0.396	-0.223	0.187	-0.235	-0.172	0.376	0.670	-0.244	0.500
	p value	0.271	0.977	0.129	0.407	0.487	0.382	0.525	0.151	**0.005**	0.362	**0.048**
	N	16	16	16	16	16	16	16	16	16	16	16
CXCL1	Pearson correlation *r*	-0.135	-0.038	0.104	-0.117	-0.118	0.278	0.111	0.318	0.198	-0.045	0.210
	p value	0.617	0.887	0.702	0.666	0.662	0.298	0.682	0.231	0.462	0.868	0.435
	N	16	16	16	16	16	16	16	16	16	16	16
CX3CL1	Pearson correlation *r*	0.060	-0.150	-0.083	-0.145	-0.199	-0.301	-0.233	0.025	0.145	-0.111	0.232
	p value	0.825	0.579	0.759	0.591	0.460	0.258	0.386	0.926	0.592	0.683	0.387
	N	16	16	16	16	16	16	16	16	16	16	16
FGF-2	Pearson correlation *r*	0.287	-0.241	0.153	-0.395	-0.231	-0.437	0.007	0.346	0.693	-0.324	0.712
	p value	0.281	0.369	0.572	0.130	0.390	0.091	0.979	0.190	**0.003**	0.220	**0.002**
	N	16	16	16	16	16	16	16	16	16	16	16

IL-6	Pearson correlation *r*	-0.034	0.104	0.421	-0.094	0.295	0.071	-0.199	0.284	0.509	-0.123	0.266
	p value	0.901	0.700	0.105	0.729	0.268	0.794	0.460	0.287	**0.044**	0.650	0.319
	N	16	16	16	16	16	16	16	16	16	16	16
PDGF-AA	Pearson correlation *r*	0.035	0.109	0.439	-0.086	0.155	-0.098	-0.192	0.316	0.560	-0.101	0.358
	p value	0.896	0.688	0.089	0.750	0.567	0.718	0.476	0.233	**0.024**	0.711	0.173
	N	16	16	16	16	16	16	16	16	16	16	16
VEGF-A	Pearson correlation *r*	0.160	0.123	0.493	-0.090	0.076	-0.190	-0.062	0.501	0.595	-0.094	0.479
	p value	0.554	0.651	0.053	0.739	0.780	0.481	0.820	**0.048**	**0.015**	0.728	0.061
	N	16	16	16	16	16	16	16	16	16	16	16

Pre-operative haematological parameters and serum inflammation-based scores (NLR, LMR and PLR) and cytokine secretome among NFPAs

p values were determined by the Pearson correlation coefficient *r*. FGF, fibroblast growth factor; IL, interleukin; LMR, lymphocyte-to-monocyte ratio; NLR, neutrophil-to-lymphocyte ratio; PDGF, platelet-derived growth factor; PLR, platelet-to-lymphocyte ratio; VEGF, vascular endothelial growth factor.

Cytokine secretome among somatotrophinomas (n=8)		Red cell count	White cell count	Neutrophil count	Lymphocyte count	Monocyte count	Eosinophil count	Basophil count	Platelet count	NLR	LMR	PLR
IL-8	Pearson correlation *r*	-0.492	-0.466	-0.494	-0.287	-0.010	0.085	-0.232	-0.219	-0.358	-0.379	-0.073
	p value	0.216	0.245	0.213	0.491	0.981	0.841	0.581	0.603	0.384	0.355	0.864
	N	8	8	8	8	8	8	8	8	8	8	8
CCL2	Pearson correlation *r*	-0.477	-0.284	-0.424	0.067	-0.213	0.321	0.121	0.429	-0.491	0.070	0.018
	p value	0.232	0.495	0.295	0.875	0.613	0.438	0.775	0.289	0.217	0.869	0.967
	N	8	8	8	8	8	8	8	8	8	8	8
CCL3	Pearson correlation *r*	-0.453	-0.392	-0.524	-0.007	-0.202	0.146	0.034	-0.103	-0.521	0.079	-0.167
	p value	0.259	0.337	0.183	0.987	0.632	0.729	0.937	0.808	0.185	0.852	0.693
	N	8	8	8	8	8	8	8	8	8	8	8
CCL4	Pearson correlation *r*	-0.286	-0.316	-0.442	0.030	-0.348	0.464	0.169	0.373	-0.464	0.202	0.088
	p value	0.492	0.446	0.273	0.943	0.399	0.247	0.689	0.363	0.246	0.631	0.836
	N	8	8	8	8	8	8	8	8	8	8	8
CXCL10	Pearson correlation *r*	-0.268	-0.227	-0.382	0.155	-0.390	0.483	0.265	0.540	-0.479	0.348	0.097
	p value	0.522	0.589	0.351	0.714	0.339	0.225	0.526	0.167	0.230	0.398	0.819
	N	8	8	8	8	8	8	8	8	8	8	8
CCL22	Pearson correlation *r*	-0.299	-0.496	-0.652	0.035	-0.723	0.479	0.143	0.273	-0.634	0.644	0.183
	p value	0.472	0.211	0.080	0.935	**0.043**	0.230	0.735	0.513	0.091	0.085	0.664
	N	8	8	8	8	8	8	8	8	8	8	8
CXCL1	Pearson correlation *r*	-0.431	-0.606	-0.754	-0.051	-0.733	0.420	0.074	0.241	-0.694	0.563	0.206
	p value	0.287	0.111	**0.031**	0.905	**0.039**	0.300	0.861	0.566	0.056	0.146	0.625
	N	8	8	8	8	8	8	8	8	8	8	8
CX3CL1	Pearson correlation *r*	-0.176	-0.491	-0.627	0.002	-0.700	0.417	0.201	-0.008	-0.639	0.565	0.051
	p value	0.677	0.217	0.096	0.997	0.053	0.304	0.633	0.985	0.088	0.144	0.905
	N	8	8	8	8	8	8	8	8	8	8	8
FGF-2	Pearson correlation *r*	-0.312	-0.552	-0.601	-0.239	-0.509	0.386	-0.076	0.213	-0.414	0.222	0.317
	p value	0.451	0.156	0.115	0.568	0.198	0.345	0.859	0.613	0.308	0.597	0.445
	N	8	8	8	8	8	8	8	8	8	8	8
IL-6	Pearson correlation *r*	-0.303	-0.394	-0.531	0.035	-0.543	0.472	0.187	0.426	-0.545	0.416	0.180
	p value	0.466	0.334	0.175	0.935	0.165	0.238	0.658	0.293	0.163	0.305	0.670
	N	8	8	8	8	8	8	8	8	8	8	8

PDGF-AA	Pearson correlation *r*	-0.288	-0.320	-0.442	-0.014	-0.042	0.208	-0.135	-0.571	-0.430	-0.053	-0.403
	p value	0.489	0.439	0.273	0.975	0.922	0.621	0.749	0.139	0.287	0.901	0.323
	N	8	8	8	8	8	8	8	8	8	8	8
VEGF-A	Pearson correlation *r*	-0.494	-0.130	-0.308	0.247	-0.135	0.223	0.164	0.461	-0.473	0.180	-0.098
	p value	0.213	0.760	0.457	0.555	0.750	0.596	0.697	0.250	0.236	0.669	0.818
	N	8	8	8	8	8	8	8	8	8	8	8

Pre-operative haematological parameters and serum inflammation-based scores (NLR, LMR and PLR) and cytokine secretome among somatotrophinomas

p values were determined by the Pearson correlation coefficient *r*. FGF, fibroblast growth factor; IL, interleukin; LMR, lymphocyte-to-monocyte ratio; NLR, neutrophil-to-lymphocyte ratio; PDGF, platelet-derived growth factor; PLR, platelet-to-lymphocyte ratio; VEGF, vascular endothelial growth factor.

Appendix 7: Supplemental table with cytokine bead array data from TAFs untreated (baseline) and after pasireotide treatment, as well as from normal untreated skin fibroblasts

Basal and pasireotide-treated cytokine secretome from tumour-associated fibroblasts isolated from PAs, as well as from normal skin fibroblasts (untreated) from 2 healthy individuals. PA-derived TAF supernatants were collected following 24h on serum-free medium conditions with pasireotide (10^{-7}M) or without (untreated). Results are shown for all detectable cytokines, chemokines and growth factors as concentration (pg/mL), mean±SEM. IL-1α, IL-2, IL-3, IL-5, IL-7, IL-9, IL-10, IL-13, IL-1ra, CCL4, TNF-α and TGF-α were undetectable in the TAF supernatants (i.e. below the lowest standard curve point and serum-free medium), and thus not represented in the table. Comparative analysis regarding the TAF secretome from pasireotide treated *vs* untreated TAFs (n=16) with respective *p* values (Mann-Whitney U test) are shown in the table.

Cytokine/ Chemokine/ Growth factor	UNTREATED TAFs Mean concentration (pg/mL) ± SEM (n=16)	TAFs TREATED WITH PASIREOTIDE Mean concentration (pg/mL) ± SEM (n=16)	*p* value	UNTREATED SKIN FIBROBLASTS Mean concentration (pg/mL) ± SEM (n=2)
CCL2	4786.86 ± 642.17	3105.43 ± 434.95	**0.038**	2756.56 ± 1585.22
CCL11	836.27 ± 328.16	529.82 ± 173.32	0.415	0
VEGF-A	174.29 ± 80.60	134.11 ± 69.96	0.709	96.09 ± 29.12
CCL22	62.54 ± 21.50	59.15 ± 14.64	0.897	14.87 ± 1.14
IL-6	54.76 ± 6.50	11.83 ± 2.77	**<0.001**	68.42 ± 7.82
FGF-2	42.93 ± 5.82	38.62 ± 4.32	0.557	28.40 ± 0.00
IL-8	42.20 ± 11.11	30.21 ± 9.38	0.416	1.89 ± 0.27
CXCL1	28.20 ± 6.56	28.13 ± 4.32	0.993	28.44 ± 28.44
CX3CL1	26.86 ± 8.34	24.04 ± 5.21	0.776	9.41 ± 1.55
CCL7	13.83 ± 5.97	10.47 ± 3.29	0.626	26.18 ± 15.71
PDGF-AA	11.64 ± 3.71	5.37 ± 1.38	0.130	0.20 ± 0.00
IFNα2	8.82 ± 2.40	6.76 ± 1.35	0.460	1.22 ± 1.04
IL-4	6.44 ± 4.16	5.61 ± 2.76	0.869	0
IL-12p40	5.12 ± 2.32	4.08 ± 1.42	0.706	0.15 ± 0.15
Flt3L	3.86 ± 0.69	3.76 ± 0.44	0.906	2.69 ± 0.00
GM-CSF	3.50 ± 0.85	3.07 ± 0.66	0.695	1.10 ± 0.06
CCL5	3.40 ± 0.62	2.67 ± 1.89	0.360	0.60 ± 0.60
IL-18	3.00 ± 1.20	2.77 ± 0.96	0.880	0
PDGF-BB	2.99 ± 1.11	2.22 ± 0.73	0.565	0
CXCL10	2.67 ± 1.02	2.59 ± 1.02	0.954	0
IL-15	2.57 ± 0.42	2.37 ± 0.28	0.693	2.04 ± 0.06
CCL3	2.49 ± 0.71	2.44 ± 0.62	0.956	0.28 ± 0.28
EGF	2.18 ± 0.68	1.70 ± 0.49	0.570	2.18 ± 0.40

G-CSF	2.05 ± 0.73	1.70 ± 0.53	0.701	1.10 ± 0.06
IFNγ	1.87 ± 0.59	1.52 ± 0.39	0.627	1.56 ± 0.69
IL-12p70	1.32 ± 0.65	1.18 ± 0.35	0.852	0
sCD40L	0.95 ± 0.52	0.45 ± 0.12	0.369	0.27 ± 0.05
IL-1β	0.93 ± 0.18	0.67 ± 0.14	0.253	0.36 ± 0.08
TNF-β	0.92 ± 0.41	0.81 ± 0.25	0.831	0.52 ± 0.05
IL-17A	0.78 ± 0.36	0.34 ± 0.14	0.880	0.62 ± 0.24

Appendix 8: Supplemental table with correlation between TAF-derived cytokine secretome and pituitary hormone levels among NFPAs and somatotrophinomas

NFPA-derived TAFs (n= 11)		CCL2	CCL11	VEGF-A	CCL22	IL-6	FGF-2	IL-8	CXCL1	CX3CL1	CCL7	PDGF-AA	IFNα2
GH (mcg/L)	Pearson correlation *r*	-0.138	0.077	-0.427	-0.266	-0.437	-0.141	-0.205	-0.146	-0.203	-0.280	0.434	-0.193
	p value	0.744	0.856	0.292	0.524	0.279	0.740	0.627	0.730	0.629	0.501	0.283	0.647
	N	8	8	8	8	8	8	8	8	8	8	8	8
IGF-1 (nmol/L)	Pearson correlation *r*	-0.276	0.073	-0.086	-0.101	-0.156	-0.289	-0.107	-0.239	-0.068	-0.047	0.658	0.005
	p value	0.440	0.840	0.813	0.782	0.667	0.418	0.769	0.506	0.853	0.898	**0.039**	0.989
	N	10	10	10	10	10	10	10	10	10	10	10	10
IGF-1 index	Pearson correlation *r*	0.156	0.218	0.275	-0.087	0.173	-0.275	-0.100	-0.126	-0.124	-0.006	0.572	-0.031
	p value	0.666	0.545	0.442	0.812	0.633	0.441	0.784	0.730	0.733	0.988	0.084	0.931
	N	10	10	10	10	10	10	10	10	10	10	10	10
PRL (mU/L)	Pearson correlation *r*	0.587	-0.360	-0.283	-0.223	-0.036	-0.172	-0.543	-0.229	-0.378	-0.248	-0.149	-0.391
	p value	0.074	0.306	0.428	0.536	0.922	0.635	0.105	0.525	0.282	0.490	0.682	0.265
	N	10	10	10	10	10	10	10	10	10	10	10	10
PRL index	Pearson correlation *r*	0.340	-0.212	-0.039	-0.043	0.269	-0.136	-0.445	-0.060	-0.215	-0.024	-0.147	-0.209
	p value	0.336	0.557	0.916	0.906	0.452	0.709	0.198	0.869	0.551	0.947	0.685	0.562
	N	10	10	10	10	10	10	10	10	10	10	10	10
TSH (µU/mL)	Pearson correlation *r*	-0.095	0.196	0.601	0.289	0.523	0.114	0.294	0.330	0.191	0.466	-0.014	0.257
	p value	0.794	0.586	0.066	0.418	0.121	0.753	0.410	0.351	0.598	0.175	0.969	0.473
	N	10	10	10	10	10	10	10	10	10	10	10	10
FT4 (pmol/L)	Pearson correlation *r*	-0.095	0.497	-0.134	0.092	-0.747	0.089	0.284	-0.025	0.296	0.085	0.662	0.285
	p value	0.794	0.144	0.712	0.801	**0.013**	0.808	0.426	0.946	0.406	0.814	**0.037**	0.425
	N	10	10	10	10	10	10	10	10	10	10	10	10
Basal Cortisol (nmol/L)	Pearson correlation *r*	-0.359	0.220	-0.072	-0.205	0.067	-0.425	-0.244	-0.356	-0.378	-0.223	0.643	-0.006
	p value	0.383	0.601	0.865	0.627	0.874	0.294	0.560	0.387	0.357	0.595	0.085	0.989
	N	8	8	8	8	8	8	8	8	8	8	8	8

LH (U/L)	Pearson correlation *r*	-0.271	0.144	0.209	-0.096	-0.094	-0.114	0.332	-0.138	-0.039	-0.030	0.598	0.088
	p value	0.450	0.691	0.562	0.791	0.796	0.753	0.349	0.705	0.915	0.934	0.068	0.808
	N	10	10	10	10	10	10	10	10	10	10	10	10
FSH (U/L)	Pearson correlation *r*	0.089	0.216	0.574	-0.145	0.054	-0.424	0.265	-0.183	-0.042	-0.008	0.677	0.068
	p value	0.806	0.549	0.083	0.690	0.882	0.222	0.459	0.613	0.908	0.982	**0.032**	0.852
	N	10	10	10	10	10	10	10	10	10	10	10	10
Testosterone (nmol/L)	Pearson correlation *r*	-0.066	0.335	0.338	0.600	-0.097	0.287	0.130	0.303	0.554	0.507	-0.109	0.573
	p value	0.876	0.417	0.413	0.116	0.820	0.490	0.758	0.466	0.154	0.199	0.797	0.138
	N	8	8	8	8	8	8	8	8	8	8	8	8

Correlations between TAF-derived cytokines and pituitary hormone levels among NFPAs

FSH, follicle-stimulating hormone; FT4, free thyroxine; GH, growth hormone; IGF-1, insulin-like growth factor-1; LH, luteinising hormone; NFPA, non-functioning pituitary adenoma; PRL, prolactin; TSH, thyroid-stimulating hormone.

Somatotrophinoma-derived TAFs (n = 5)		**CCL2**	**CCL11**	**VEGF-A**	**CCL22**	**IL-6**	**FGF-2**	**IL-8**	**CXCL1**	**CX3CL1**	**CCL7**	**PDGF-AA**	**IFNα2**
GH (mcg/L)	Pearson correlation *r*	-0.203	-0.617	-0.552	-0.449	-0.674	-0.640	-0.751	-0.600	-0.865	-0.568	0.862	-0.939
	p value	0.743	0.268	0.334	0.449	0.212	0.245	0.144	0.284	0.058	0.317	0.060	**0.018**
	N	5	5	5	5	5	5	5	5	5	5	5	5
IGF-1 (nmol/L)	Pearson correlation *r*	-0.382	-0.805	-0.755	-0.184	-0.854	-0.600	-0.766	-0.637	-0.800	-0.656	0.808	-0.837
	p value	0.526	0.100	0.140	0.767	0.066	0.285	0.131	0.248	0.104	0.230	0.098	0.077
	N	5	5	5	5	5	5	5	5	5	5	5	5
IGF-1 index	Pearson correlation *r*	-0.522	-0.748	-0.750	0.018	-0.825	-0.654	-0.572	-0.442	-0.793	-0.535	0.771	-0.708
	p value	0.367	0.146	0.144	0.977	0.085	0.231	0.313	0.456	0.110	0.353	0.127	0.181
	N	5	5	5	5	5	5	5	5	5	5	5	5
PRL (mU/L)	Pearson correlation *r*	0.846	-0.179	-0.326	0.186	-0.155	-0.986	-0.785	-0.851	0.223	-0.831	0.730	-0.159
	p value	0.359	0.886	0.789	0.881	0.901	0.107	0.425	0.352	0.857	0.376	0.479	0.898
	N	3	3	3	3	3	3	3	3	3	3	3	3

PRL index	Pearson correlation *r*	0.846	-0.177	-0.324	0.188	-0.154	-0.986	-0.784	-0.850	0.225	-0.830	0.728	-0.157
	p value	0.358	0.887	0.790	0.880	0.902	0.108	0.426	0.353	0.856	0.377	0.481	0.899
	N	3	3	3	3	3	3	3	3	3	3	3	3
TSH (µU/ml)	Pearson correlation *r*	0.208	-0.079	-0.189	-0.175	-0.180	-0.886	-0.403	-0.326	-0.554	-0.369	0.742	-0.475
	p value	0.737	0.900	0.761	0.778	0.772	**0.045**	0.501	0.592	0.332	0.541	0.151	0.419
	N	5	5	5	5	5	5	5	5	5	5	5	5
FT4 (pmol/L)	Pearson correlation *r*	-0.557	-0.564	-0.553	0.873	-0.479	0.521	0.052	-0.060	0.490	-0.176	-0.495	0.524
	p value	0.330	0.322	0.334	0.053	0.415	0.368	0.934	0.923	0.402	0.777	0.396	0.365
	N	5	5	5	5	5	5	5	5	5	5	5	5
Basal Cortisol (nmol/L)	Pearson correlation *r*	-0.314	0.480	0.611	-0.326	0.498	0.765	0.758	0.807	0.124	0.858	-0.572	0.165
	p value	0.606	0.414	0.274	0.592	0.393	0.131	0.138	0.099	0.843	0.063	0.313	0.791
	N	5	5	5	5	5	5	5	5	5	5	5	5
LH (U/L)	Pearson correlation *r*	-0.256	-0.189	-0.266	0.968	-0.119	0.446	0.276	0.116	0.718	-0.020	-0.618	0.813
	p value	0.677	0.761	0.666	**0.007**	0.848	0.452	0.653	0.853	0.172	0.975	0.267	0.095
	N	5	5	5	5	5	5	5	5	5	5	5	5
FSH (U/L)	Pearson correlation *r*	-0.402	-0.509	-0.594	0.969	-0.469	0.126	-0.026	-0.140	0.398	-0.306	-0.263	0.509
	p value	0.502	0.381	0.291	**0.006**	0.425	0.840	0.966	0.822	0.507	0.616	0.669	0.381
	N	5	5	5	5	5	5	5	5	5	5	5	5
Testosterone (nmol/L)	Pearson correlation *r*	-0.314	-0.257	-0.313	-0.093	-0.369	-0.676	-0.208	-0.077	-0.711	-0.175	0.661	-0.540
	p value	0.606	0.676	0.608	0.881	0.541	0.210	0.738	0.902	0.178	0.779	0.225	0.347
	N	5	5	5	5	5	5	5	5	5	5	5	5

Correlations between TAF-derived cytokines and pituitary hormone levels among somatotrophinomas

FSH, follicle-stimulating hormone; FT4, free thyroxine; GH, growth hormone; IGF-1, insulin-like growth factor-1; LH, luteinising hormone; PRL, prolactin; TSH, thyroid-stimulating hormone.

Appendix 9: Supplemental tables with correlations between hormonal, cytokine and infiltrating immune cell data and TME-related oncogenic mechanisms in PAs

PAs n= 24	MVD	TMVA	Perimeter	Feret's diameter	Area per vessel	Roundness
Hormonal data *[Pearson correlation r (p)]*						
Serum IGF-1	0.192 (*p*=0.404)	-0.269 (*p*=0.238)	-0.550 (***p*=0.010**)	-0.548 (***p*=0.010**)	-0.409 (*p*=0.066)	0.246 (*p*=0.282)
IGF-1 index	0.208 (*p*=0.353)	-0.288 (*p*=0.194)	-0.605 (***p*=0.003**)	-0.601 (***p*=0.003**)	-0.436 (***p*=0.043**)	0.287 (*p*=0.196)
Serum PRL	-0.054 (*p*=0.825)	-0.023 (*p*=0.925)	-0.112 (*p*=0.647)	-0.110 (*p*=0.653)	-0.014 (*p*=0.955)	0.084 (*p*=0.734)
PRL index	-0.072 (*p*=0.768)	-0.018 (*p*=0.942)	-0.047 (*p*=0.849)	-0.051 (*p*=0.835)	0.024 (*p*=0.924)	-0.012 (*p*=0.960)
Serum TSH	-0.316 (*p*=0.163)	-0.088 (*p*=0.704)	0.280 (*p*=0.219)	0.252 (*p*=0.270)	0.144 (*p*=0.533)	-0.295 (*p*=0.194)
Serum FT4	0.207 (*p*=0.367)	-0.034 (*p*=0.885)	-0.392 (*p*=0.079)	-0.369 (*p*=0.100)	-0.324 (*p*=0.152)	0.114 (*p*=0.623)
Basal plasma cortisol	-0.223 (*p*=0.345)	-0.285 (*p*=0.223)	-0.009 (*p*=0.970)	0.014 (*p*=0.952)	-0.121 (*p*=0.610)	-0.357 (*p*=0.122)
Serum LH	0.025 (*p*=0.913)	0.217 (*p*=0.344)	0.044 (*p*=0.851)	0.037 (*p*=0.873)	0.037 (*p*=0.872)	0.096 (*p*=0.680)
Serum FSH	0.084 (*p*=0.719)	0.392 (*p*=0.078)	0.149 (*p*=0.519)	0.138 (*p*=0.551)	0.202 (*p*=0.380)	0.049 (*p*=0.834)
Serum testosterone	-0.386 (*p*=0.114)	-0.442 (*p*=0.067)	0.071 (*p*=0.780)	0.084 (*p*=0.741)	-0.011 (*p*=0.965)	-0.113 (*p*=0.656)
PA-derived cytokine data *[Pearson correlation r (p)]*						
IL-8	-0.088 (*p*=0.683)	-0.128 (*p*=0.552)	-0.004 (*p*=0.984)	-0.007 (*p*=0.973)	-0.045 (*p*=0.835)	-0.026 (*p*=0.904)
CCL2	-0.251 (*p*=0.238)	-0.079 (*p*=0.715)	0.307 (*p*=0.145)	0.301 (*p*=0.153)	0.331 (*p*=0.114)	-0.016 (*p*=0.941)
CCL3	-0.057 (*p*=0.792)	-0.093 (*p*=0.666)	-0.046 (*p*=0.830)	-0.040 (*p*=0.851)	-0.010 (*p*=0.964)	0.109 (*p*=0.612)
CCL4	-0.127 (*p*=0.553)	-0.112 (*p*=0.601)	0.088 (*p*=0.682)	0.088 (p=0.684)	0.084 (*p*=0.696)	-0.044 (*p*=0.840)
CXCL10	-0.266 (*p*=0.210)	-0.041 (*p*=0.848)	0.368 (*p*=0.077)	0.356 (*p*=0.087)	0.407 (***p*=0.049**)	0.087 (*p*=0.685)
CCL22	-0.242 (*p*=0.255)	-0.276 (*p*=0.191)	-0.021 (*p*=0.924)	-0.020 (*p*=0.925)	-0.097 (*p*=0.652)	-0.094 (*p*=0.661)
CXCL1	-0.116 (*p*=0.590)	-0.154 (*p*=0.473)	-0.041 (*p*=0.850)	-0.037 (*p*=0.863)	-0.038 (*p*=0.860)	0.037 (*p*=0.863)
CX3CL1	-0.251 (*p*=0.236)	-0.110 (*p*=0.608)	0.221 (*p*=0.299)	0.206 (*p*=0.333)	0.204 (*p*=0.339)	0.132 (*p*=0.537)
FGF-2	-0.146 (*p*=0.498)	-0.338 (*p*=0.106)	-0.407 (***p*=0.048**)	-0.391 (*p*=0.059)	-0.321 (*p*=0.126)	0.265 (*p*=0.210)
IL-6	-0.073 (*p*=0.736)	-0.113 (*p*=0.599)	0.013 (*p*=0.953)	0.005 (*p*=0.981)	-0.069 (*p*=0.747)	-0.135 (*p*=0.530)
PDGF-AA	-0.194 (*p*=0.365)	-0.122 (*p*=0.571)	0.194 (*p*=0.363)	0.193 (*p*=0.366)	0.138 (*p*=0.520)	-0.065 (*p*=0.762)
VEGF-A	-0.151 (*p*=0.482)	-0.218 (*p*=0.307)	0.036 (*p*=0.866)	0.045 (*p*=0.836)	-0.034 (*p*=0.875)	-0.110 (*p*=0.610)
TAF cytokine data n=16 *[Pearson correlation r (p)]*						
CCL2	0.440 (*p*=0.088)	0.672 (***p*=0.004**)	0.075 (*p*=0.783)	0.043 (*p*=0.874)	0.033 (*p*=0.904)	-0.052 (*p*=0.848)
CCL11	-0.193 (*p*=0.474)	-0.347 (*p*=0.189)	-0.223 (*p*=0.406)	-0.222 (*p*=0.409)	-0.234 (*p*=0.383)	-0.051 (*p*=0.852)
VEGF-A	-0.173 (*p*=0.521)	-0.255 (*p*=0.340)	-0.117 (*p*=0.666)	-0.120 (*p*=0.658)	-0.113 (*p*=0.676)	-0.078 (*p*=0.774)
CCL22	-0.029 (*p*=0.915)	-0.051 (*p*=0.852)	0.062 (*p*=0.820)	0.034 (*p*=0.900)	-0.038 (*p*=0.888)	-0.063 (*p*=0.817)
IL-6	-0.466 (*p*=0.069)	-0.318 (*p*=0.231)	0.387 (*p*=0.139)	0.368 (*p*=0.161)	0.459 (*p*=0.074)	-0.360 (*p*=0.170)
FGF-2	0.177 (*p*=0.511)	-0.016 (*p*=0.954)	-0.242 (*p*=0.366)	-0.263 (*p*=0.324)	-0.326 (*p*=0.218)	0.151 (*p*=0.577)
IL-8	-0.079 (*p*=0.772)	-0.270 (*p*=0.311)	-0.245 (*p*=0.361)	-0.217 (*p*=0.420)	-0.228 (*p*=0.395)	-0.001 (*p*=0.997)
CXCL1	-0.100 (*p*=0.713)	-0.181 (*p*=0.503)	-0.110 (*p*=0.685)	-0.115 (*p*=0.673)	-0.112 (*p*=0.679)	0.035 (*p*=0.899)
CX3CL1	-0.089 (*p*=0.744)	-0.161 (*p*=0.552)	-0.038 (*p*=0.888)	-0.049 (*p*=0.856)	-0.136 (*p*=0.617)	-0.043 (*p*=0.876)
CCL7	-0.076 (*p*=0.779)	-0.199 (*p*=0.460)	-0.155 (*p*=0.568)	-0.150 (*p*=0.580)	-0.173 (*p*=0.522)	-0.045 (*p*=0.869)
PDGF-AA	-0.267 (*p*=0.317)	-0.482 (*p*=0.058)	-0.352 (*p*=0.182)	-0.324 (*p*=0.220)	-0.295 (*p*=0.268)	0.115 (*p*=0.671)
IFNα2	-0.095 (*p*=0.726)	-0.143 (*p*=0.598)	0.037 (*p*=0.891)	0.022 (*p*=0.937)	-0.065 (*p*=0.811)	-0.073 (*p*=0.787)
PA-infiltrating macrophage *[Mean±SEM]*						
< 6% (n=17)	33.16 ± 5.18	6.88 ± 0.91	106.66 ± 8.33	43.36 ± 3.45	0.26 ± 0.05	0.47 ± 0.01
≥ 6% (n=7)	46.43 ± 8.34	9.18 ± 1.90	99.59 ± 3.76	40.24 ± 1.35	0.20 ± 0.02	0.47 ± 0.01
	p=0.184	*p*=0.228	*p*=0.448	*p*=0.408	*p*=0.495	*p*=0.711

PA-infiltrating CD8+ T cells *[Mean±SEM]* < 1% (n=6) ≥ 1% (n=18)	 30.89 ± 6.23 39.07 ± 5.61 *p*=0.441	 6.65 ± 0.90 7.85 ± 1.10 *p*=0.557	 111.42 ± 10.89 102.32 ± 7.18 *p*=0.522	 45.90 ± 4.71 41.30 ± 2.91 *p*=0.432	 0.24 ± 0.04 0.24 ± 0.05 *p*=0.967	 0.44 ± 0.02 0.48 ± 0.01 *p*=0.064
PA-infiltrating CD4+ T cells *[Mean±SEM]* < 1% (n=15) ≥ 1% (n=9)	 32.00 ± 4.40 45.41 ± 9.14 *p*=0.152	 6.18 ± 0.61 9.83 ± 1.86 ***p*=0.035**	 106.28 ± 8.95 101.78 ± 6.22 *p*=0.724	 43.30 ± 3.74 41.03 ± 2.34 *p*=0.665	 0.24 ± 0.05 0.23 ± 0.03 *p*=0.878	 0.45 ± 0.01 0.49 ± 0.01 *p*=0.051
PA-infiltrating B cells *[Mean±SEM]* < 0.5% (n=8) ≥ 0.5% (n=16)	 30.21 ± 6.06 40.44 ± 5.94 *p*=0.292	 6.64 ± 0.85 8.00 ± 1.21 *p*=0.467	 118.62 ± 13.62 97.59 ± 5.39 *p*=0.098	 48.49 ± 5.76 39.43 ± 2.10 *p*=0.174	 0.30 ± 0.09 0.21 ± 0.02 *p*=0.386	 0.43 ± 0.02 0.48 ± 0.01 ***p*=0.015**
PA-infiltrating neutrophils *[Mean±SEM]* < 0.5% (n=13) ≥ 0.5% (n=11)	 39.74 ± 5.96 33.82 ± 6.97 *p*=0.522	 7.84 ± 1.40 7.20 ± 0.92 *p*=0.720	 97.81 ± 5.22 112.62 ± 11.35 *p*=0.225	 39.84 ± 2.05 45.53 ± 4.77 *p*=0.259	 0.20 ± 0.02 0.28 ± 0.07 *p*=0.257	 0.47 ± 0.01 0.47 ± 0.02 *p*=0.927
PA-infiltrating FOXP3+ T cells *[Mean±SEM]* < 0.3% (n=12) ≥ 0.3% (n=12)	 47.42 ± 7.53 26.64 ± 2.79 ***p*=0.021**	 8.70 ± 1.31 6.39 ± 1.04 *p*=0.182	 98.34 ± 4.28 110.86 ± 11.13 *p*=0.312	 39.83 ± 1.72 45.07 ± 4.60 *p*=0.304	 0.19 ± 0.01 0.29 ± 0.07 *p*=0.198	 0.47 ± 0.01 0.46 ± 0.02 *p*=0.659
Immune cell ratios *[Pearson correlation r (p)]* M2:M1 CD8:CD4 CD8:FOXP3 CD68:FOXP3	 0.491 (***p*=0.015**) 0.084 (*p*=0.697) 0.203 (*p*=0.341) 0.111 (*p*=0.606)	 0.666 (***p*<0.001**) 0.016 (*p*=0.942) 0.043 (*p*=0.841) 0.030 (*p*=0.890)	 0.241 (*p*=0.257) -0.073 (*p*=0.734) -0.229 (*p*=0.281) -0.115 (*p*=0.592)	 0.224 (*p*=0.292) -0.063 (*p*=0.769) -0.240 (*p*=0.259) -0.118 (*p*=0.582)	 0.353 (*p*=0.091) -0.038 (*p*=0.861) -0.228 (*p*=0.284) -0.179 (*p*=0.402)	 0.119 (*p*=0.580) -0.045 (*p*=0.833) 0.186 (*p*=0.385) -0.015 (*p*=0.946)

Correlation between hormonal, cytokine and infiltrating immune cell data and PA angiogenesis in the whole cohort of PAs (n=24)

Microvessel density (MVD) is expressed in vessels/HPF; total microvessel area (TMVA) is expressed in % of the high power field; perimeter and Feret's diameter are expressed in µm; area per vessel is expressed in % of the high power field; vessel roundness correspond to a value comprised between 0 and 1 (1=perfect circle). FSH, follicle-stimulating hormone; FT4, free thyroxine; IGF-1, insulin-like growth factor-1; LH, luteinising hormone; MVD, microvessel density; NFPA, non-functioning pituitary adenoma; PRL, prolactin; TMVA, total microvessel area; TSH, thyroid-stimulating hormone.

PAs n= 24	MMP-9	MMP-14	E-cadherin	ZEB1	NCAM
Hormonal data *[Pearson correlation r (p)]*					
Serum IGF-1	0.678 (***p*=0.001**)	-0.127 (*p*=0.582)	-0.127 (*p*=0.582)	-0.170 (*p*=0.461)	0.056 (*p*=0.811)
IGF-1 index	0.733 (***p*<0.001**)	-0.145 (*p*=0.521)	-0.010 (*p*=0.964)	-0.133 (*p*=0.554)	0.154 (*p*=0.493)
Serum PRL	-0.166 (*p*=0.498)	-0.162 (*p*=0.507)	0.062 (*p*=0.801)	-0.085 (*p*=0.729)	-0.354 (*p*=0.137)
PRL index	-0.108 (p=0.659)	-0.151 (*p*=0.537)	0.066 (*p*=0.789)	-0.087 (*p*=0.724)	-0.354 (*p*=0.137)
Serum TSH	-0.320 (*p*=0.157)	0.147 (*p*=0.526)	-0.155 (*p*=0.502)	-0.088 (*p*=0.706)	-0.229 (*p*=0.318)
Serum FT4	0.375 (*p*=0.094)	-0.277 (*p*=0.225)	0.149 (*p*=0.520)	-0.104 (*p*=0.654)	0.115 (*p*=0.618)
Basal plasma cortisol	0.306 (*p*=0.190)	0.340 (*p*=0.142)	-0.098 (*p*=0.681)	-0.045 (*p*=0.849)	-0.042 (*p*=0.861)
Serum LH	0.109 (*p*=0.637)	-0.213 (*p*=0.353)	0.040 (*p*=0.862)	0.131 (*p*=0.573)	0.518 (***p*=0.016**)
Serum FSH	0.115 (*p*=0.618)	-0.331 (*p*=0.143)	0.075 (*p*=0.748)	-0.075 (*p*=0.747)	0.487 (***p*=0.025**)
Serum testosterone	-0.236 (*p*=0.345)	0.379 (*p*=0.121)	0.251 (*p*=0.314)	0.010 (*p*=0.970)	-0.243 (*p*=0.331)
PA-derived cytokine data *[Pearson correlation r (p)]*					
IL-8	-0.350 (*p*=0.093)	0.303 (*p*=0.150)	0.003 (*p*=0.987)	-0.214 (*p*=0.315)	-0.273 (*p*=0.197)
CCL2	-0.450 (***p*=0.027**)	0.138 (*p*=0.522)	0.032 (*p*=0.881)	-0.320 (*p*=0.128)	-0.378 (*p*=0.069)
CCL3	-0.312 (*p*=0.138)	0.134 (*p*=0.531)	-0.086 (*p*=0.690)	-0.181 (*p*=0.398)	-0.080 (*p*=0.709)
CCL4	-0.376 (p=0.070)	0.278 (*p*=0.188)	-0.002 (*p*=0.994)	-0.235 (*p*=0.270)	-0.267 (*p*=0.208)
CXCL10	-0.309 (*p*=0.141)	-0.151 (*p*=0.481)	0.102 (*p*=0.634)	-0.216 (*p*=0.311)	-0.324 (*p*=0.123)
CCL22	-0.131 (*p*=0.541)	0.371 (*p*=0.074)	-0.138 (*p*=0.520)	-0.356 (*p*=0.088)	-0.368 (*p*=0.077)
CXCL1	-0.325 (*p*=0.121)	0.248 (*p*=0.243)	-0.104 (*p*=0.629)	-0.300 (*p*=0.154)	-0.219 (*p*=0.304)
CX3CL1	-0.286 (*p*=0.176)	-0.088 (*p*=0.684)	0.073 (*p*=0.734)	-0.223 (*p*=0.295)	-0.363 (*p*=0.081)
FGF-2	0.140 (*p*=0.513)	-0.105 (*p*=0.626)	-0.165 (*p*=0.442)	-0.543 (***p*=0.006**)	-0.341 (*p*=0.103)
IL-6	-0.248 (*p*=0.243)	0.350 (*p*=0.094)	0.053 (*p*=0.805)	-0.167 (*p*=0.435)	-0.297 (*p*=0.158)
PDGF-AA	-0.289 (*p*=0.171)	0.199 (*p*=0.352)	-0.080 (*p*=0.709)	-0.288 (*p*=0.172)	-0.347 (*p*=0.097)
VEGF-A	-0.086 (*p*=0.690)	0.227 (*p*=0.286)	-0.476 (***p*=0.019**)	-0.366 (*p*=0.078)	-0.269 (*p*=0.203)
TAF cytokine data n=16 *[Pearson correlation r (p)]*					
CCL2	-0.133 (*p*=0.623)	-0.315 (*p*=0.235)	-0.217 (*p*=0.419)	-0.039 (*p*=0.887)	0.059 (*p*=0.829)
CCL11	0.442 (*p*=0.086)	-0.268 (*p*=0.316)	0.174 (*p*=0.519)	-0.401 (*p*=0.124)	-0.085 (*p*=0.755)
VEGF-A	0.461 (*p*=0.072)	-0.338 (*p*=0.200)	0.188 (*p*=0.486)	-0.318 (*p*=0.230)	-0.043 (*p*=0.875)
CCL22	-0.389 (*p*=0.137)	0.284 (*p*=0.286)	0.331 (*p*=0.211)	0.071 (*p*=0.793)	-0.394 (*p*=0.131)
IL-6	0.274 (*p*=0.305)	-0.169 (*p*=0.531)	0.278 (*p*=0.298)	-0.056 (*p*=0.838)	0.139 (*p*=0.606)
FGF-2	-0.230 (*p*=0.391)	0.220 (*p*=0.412)	0.337 (*p*=0.201)	0.061 (*p*=0.821)	-0.631 (***p*=0.009**)
IL-8	0.288 (*p*=0.279)	-0.337 (*p*=0.202)	0.372 (*p*=0.156)	-0.228 (*p*=0.396)	0.011 (*p*=0.967)
CXCL1	0.077 (*p*=0.778)	-0.079 (*p*=0.770)	0.497 (*p*=0.050)	-0.246 (*p*=0.359)	-0.388 (*p*=0.138)
CX3CL1	-0.322 (*p*=0.224)	0.145 (*p*=0.593)	0.173 (*p*=0.523)	-0.221 (*p*=0.410)	-0.493 (*p*=0.052)
CCL7	0.276 (*p*=0.302)	-0.187 (*p*=0.489)	0.426 (*p*=0.100)	-0.248 (*p*=0.354)	-0.223 (*p*=0.406)
PDGF-AA	0.449 (*p*=0.081)	0.170 (*p*=0.529)	-0.564 (***p*=0.023**)	-0.409 (*p*=0.116)	0.301 (*p*=0.257)
IFNα2	-0.307 (*p*=0.826)	0.169 (*p*=0.531)	0.175 (*p*=0.516)	-0.129 (*p*=0.633)	-0.447 (*p*=0.083)
PA-infiltrating macrophage *[Mean±SEM]*					
< 6% (n=17)	2.82 ± 0.55	1.29 ± 0.45	4.71 ± 0.25	1.24 ± 0.44	5.12 ± 0.17
≥ 6% (n=7)	0.71 ± 0.71	1.14 ± 0.60	4.43 ± 0.37	0.57 ± 0.37	4.57 ± 0.20
	***p*=0.042**	*p*=0.852	*p*=0.554	*p*=0.376	*p*=0.077
PA-infiltrating CD8+ T cells *[Mean±SEM]*					
< 1% (n=6)	1.50 ± 0.96	1.33 ± 0.88	4.67 ± 0.33	1.00 ± 0.68	5.00 ± 0.26
≥ 1% (n=18)	2.44 ± 0.56	1.22 ± 0.39	4.61 ± 0.26	1.06 ± 0.39	4.94 ± 0.17
	p=0.404	*p*=0.896	*p*=0.910	*p*=0.944	*p*=0.869
PA-infiltrating CD4+ T cells *[Mean±SEM]*					
< 1% (n=15)	2.47 ± 0.64	1.20 ± 0.48	4.73 ± 0.30	1.07 ± 0.42	5.13 ± 0.17
≥ 1% (n=9)	1.78 ± 0.72	1.33 ± 0.55	4.44 ± 0.24	1.00 ± 0.58	4.67 ± 0.24
	p=0.497	*p*=0.861	*p*=0.511	*p*=0.925	*p*=0.110

PA-infiltrating B cells *[Mean±SEM]*					
< 0.5% (n=8)	2.00 ± 0.98	1.13 ± 0.74	4.88 ± 0.35	0.75 ± 0.53	4.88 ± 0.23
≥ 0.5% (n=16)	2.31 ± 0.55	1.31 ± 0.41	4.50 ± 0.26	1.19 ± 0.43	5.00 ± 0.18
	p=0.765	*p*=0.811	*p*=0.405	*p*=0.547	*p*=0.685
PA-infiltrating neutrophils *[Mean±SEM]*					
< 0.5% (n=13)	2.69 ± 0.65	0.46 ± 0.31	4.46 ± 0.35	0.62 ± 0.35	5.08 ± 0.18
≥ 0.5% (n=11)	1.64 ± 0.69	2.18 ± 0.59	4.82 ± 0.18	1.55 ± 0.58	4.82 ± 0.23
	p=0.280	***p*=0.020**	*p*=0.379	*p*=0.187	*p*=0.372
PA-infiltrating FOXP3+ T cells *[Mean±SEM]*					
< 0.3% (n=12)	1.92 ± 0.69	0.75 ± 0.41	4.58 ± 0.26	0.83 ± 0.39	4.75 ± 0.18
≥ 0.3% (n=12)	2.50 ± 0.68	1.75 ± 0.57	4.67 ± 0.33	1.25 ± 0.55	5.17 ± 0.21
	p=0.553	*p*=0.167	*p*=0.846	*p*=0.543	*p*=0.143
Immune cell ratios *[Pearson correlation r (p)]*					
M2:M1	-0.146 (*p*=0.497)	-0.268 (*p*=0.206)	0.220 (*p*=0.301)	0.265 (*p*=0.212)	0.027 (*p*=0.901)
CD8:CD4	0.240 (*p*=0.260)	-0.276 (*p*=0.191)	-0.050 (*p*=0.816)	-0.127 (*p*=0.554)	0.095 (*p*=0.659)
CD8:FOXP3	0.127 (*p*=0.555)	0.052 (*p*=0.809)	0.195 (*p*=0.362)	-0.113 (*p*=0.598)	-0.219 (*p*=0.303)
CD68:FOXP3	-0.315 (*p*=0.134)	0.002 (*p*=0.994)	0.142 (*p*=0.508)	-0.157 (*p*=0.463)	-0.211 (*p*=0.322)

Correlation between hormonal, cytokine and infiltrating immune cell data and MMP-9, MMP-14, E-cadherin, ZEB1 and NCAM immunoreactivities in the whole cohort of PAs (n=24)

FSH, follicle-stimulating hormone; FT4, free thyroxine; IGF-1, insulin-like growth factor-1; LH, luteinising hormone; NFPA, non-functioning pituitary adenoma; MMP, matrix metalloproteinase; NCAM, neural cell adhesion molecule; PRL, prolactin; TSH, thyroid-stimulating hormone.

NFPAs n = 16	MVD	TMVA	Perimeter	Feret's diameter	Area per vessel	Roundness
Hormonal data *[Pearson correlation r (p)]*						
Serum IGF-1	-0.228 (*p*=0.433)	-0.401 (*p*=0.156)	-0.247 (*p*=0.395)	-0.214 (*p*=0.462)	-0.337 (*p*=0.238)	-0.205 (*p*=0.482)
IGF-1 index	-0.033 (*p*=0.912)	-0.153 (*p*=0.601)	-0.227 (*p*=0.434)	-0.205 (*p*=0.482)	-0.202 (*p*=0.488)	-0.275 (*p*=0.342)
Serum PRL	0.542 (***p*=0.045**)	0.359 (*p*=0.208)	-0.219 (*p*=0.452)	-0.262 (*p*=0.366)	-0.235 (*p*=0.418)	0.023 (*p*=0.938)
PRL index	0.221 (*p*=0.449)	0.230 (*p*=0.430)	0.104 (*p*=0.724)	0.051 (p=0.861)	-0.010 (*p*=0.973)	-0.324 (*p*=0.259)
Serum TSH	-0.220 (*p*=0.450)	-0.274 (*p*=0.344)	-0.013 (*p*=0.965)	-0.049 (*p*=0.867)	-0.099 (*p*=0.735)	-0.334 (*p*=0.242)
Serum FT4	-0.039 (*p*=0.895)	0.043 (*p*=0.885)	-0.132 (*p*=0.653)	-0.106 (*p*=0.717)	-0.162 (*p*=0.581)	-0.029 (*p*=0.922)
Basal plasma cortisol	-0.353 (*p*=0.237)	-0.403 (*p*=0.172)	-0.037 (*p*=0.904)	-0.017 (*p*=0.956)	-0.140 (*p*=0.648)	-0.350 (*p*=0.241)
Serum LH	-0.095 (*p*=0.746)	0.137 (*p*=0.640)	-0.007 (*p*=0.981)	-0.021 (*p*=0.944)	-0.006 (*p*=0.983)	0.142 (*p*=0.629)
Serum FSH	-0.036 (*p*=0.902)	0.359 (*p*=0.208)	0.178 (*p*=0.542)	0.157 (*p*=0.592)	0.209 (*p*=0.474)	0.034 (*p*=0.909)
Serum testosterone	-0.541 (*p*=0.069)	-0.605 (***p*=0.037**)	0.180 (*p*=0.576)	0.197 (*p*=0.539)	-0.058 (*p*=0.859)	-0.486 (*p*=0.109)
PA-derived cytokine data *[Pearson correlation r (p)]*						
IL-8	-0.104 (*p*=0.702)	-0.264 (*p*=0.323)	-0.174 (*p*=0.518)	-0.178 (*p*=0.510)	-0.158 (*p*=0.560)	0.049 (*p*=0.858)
CCL2	-0.297 (*p*=0.264)	-0.244 (*p*=0.362)	0.170 (*p*=0.530)	0.161 (*p*=0.550)	0.241 (*p*=0.368)	0.089 (*p*=0.743)
CCL3	-0.067 (*p*=0.805)	-0.211 (*p*=0.434)	-0.210 (*p*=0.435)	-0.203 (*p*=0.452)	-0.107 (*p*=0.693)	0.198 (*p*=0.462)
CCL4	-0.147 (*p*=0.587)	-0.250 (*p*=0.351)	-0.066 (*p*=0.809)	-0.067 (p=0.806)	-0.017 (*p*=0.949)	0.031 (*p*=0.911)
CXCL10	-0.301 (*p*=0.257)	-0.136 (*p*=0.616)	0.322 (*p*=0.224)	0.307 (*p*=0.247)	0.367 (*p*=0.162)	0.165 (*p*=0.542)
CCL22	-0.171 (*p*=0.528)	-0.271 (*p*=0.309)	-0.043 (*p*=0.875)	-0.044 (*p*=0.871)	-0.147 (*p*=0.587)	-0.139 (*p*=0.609)
CXCL1	-0.112 (*p*=0.680)	-0.263 (*p*=0.324)	-0.198 (*p*=0.463)	-0.193 (*p*=0.473)	-0.139 (*p*=0.607)	0.107 (*p*=0.693)
CX3CL1	-0.263 (*p*=0.325)	-0.190 (*p*=0.480)	0.159 (*p*=0.557)	0.141 (*p*=0.604)	0.149 (*p*=0.582)	0.195 (*p*=0.469)
FGF-2	-0.020 (*p*=0.941)	-0.236 (*p*=0.379)	-0.421 (*p*=0.104)	-0.407 (*p*=0.118)	-0.367 (*p*=0.162)	0.279 (*p*=0.295)
IL-6	-0.083 (*p*=0.760)	-0.208 (*p*=0.440)	-0.099 (*p*=0.714)	-0.109 (*p*=0.689)	-0.150 (*p*=0.580)	-0.102 (*p*=0.706)
PDGF-AA	-0.255 (*p*=0.341)	-0.319 (*p*=0.228)	0.035 (*p*=0.899)	0.035 (*p*=0.898)	0.025 (*p*=0.928)	-0.001 (*p*=0.996)
VEGF-A	-0.219 (*p*=0.416)	-0.341 (*p*=0.196)	-0.012 (*p*=0.964)	-0.001 (*p*=0.997)	-0.059 (*p*=0.828)	-0.054 (*p*=0.841)
TAF cytokine data n=11 *[Pearson correlation r (p)]*						
CCL2	0.572 (*p*=0.066)	0.828 (***p*=0.002**)	0.038 (*p*=0.913)	0.011 (*p*=0.975)	0.020 (*p*=0.954)	-0.002 (*p*=0.996)
CCL11	-0.200 (*p*=0.556)	-0.364 (*p*=0.270)	-0.221 (*p*=0.515)	-0.202 (*p*=0.552)	-0.253 (*p*=0.453)	-0.088 (*p*=0.798)
VEGF-A	-0.229 (*p*=0.497)	-0.148 (*p*=0.665)	0.243 (*p*=0.471)	0.222 (*p*=0.511)	0.296 (*p*=0.377)	-0.165 (*p*=0.627)
CCL22	-0.155 (*p*=0.649)	-0.243 (*p*=0.472)	-0.042 (*p*=0.903)	-0.079 (*p*=0.817)	-0.133 (*p*=0.698)	-0.031 (*p*=0.928)
IL-6	-0.516 (*p*=0.104)	-0.280 (*p*=0.404)	0.651 (***p*=0.030**)	0.618 (***p*=0.043**)	0.674 (***p*=0.023**)	-0.417 (*p*=0.202)
FGF-2	0.159 (*p*=0.641)	-0.146 (*p*=0.668)	-0.477 (*p*=0.138)	-0.499 (*p*=0.118)	-0.462 (*p*=0.153)	0.295 (*p*=0.378)
IL-8	-0.340 (*p*=0.306)	-0.546 (*p*=0.083)	-0.259 (*p*=0.442)	-0.226 (*p*=0.504)	-0.266 (*p*=0.429)	0.027 (*p*=0.937)
CXCL1	-0.174 (*p*=0.608)	-0.286 (*p*=0.393)	-0.147 (*p*=0.666)	-0.181 (*p*=0.595)	-0.134 (*p*=0.694)	0.127 (*p*=0.709)
CX3CL1	-0.129 (*p*=0.706)	-0.274 (*p*=0.415)	-0.164 (*p*=0.630)	-0.173 (*p*=0.611)	-0.216 (*p*=0.525)	0.029 (*p*=0.933)
CCL7	-0.116 (*p*=0.735)	-0.288 (*p*=0.391)	-0.187 (*p*=0.583)	-0.216 (*p*=0.524)	-0.226 (*p*=0.503)	0.013 (*p*=0.971)
PDGF-AA	-0.234 (*p*=0.489)	-0.343 (*p*=0.302)	-0.101 (*p*=0.768)	-0.040 (*p*=0.907)	-0.185 (*p*=0.587)	-0.273 (*p*=0.417)
IFNα2	-0.155 (*p*=0.649)	-0.314 (*p*=0.347)	-0.136 (*p*=0.691)	-0.151 (*p*=0.658)	-0.182 (*p*=0.592)	0.023 (*p*=0.946)
PA-infiltrating macrophage *[Mean±SEM]*						
< 6% (n=11)	31.15 ± 7.13	7.97 ± 1.21	121.76 ± 9.99	49.62 ± 4.14	0.32 ± 0.07	0.45 ± 0.02
≥ 6% (n=5)	50.20 ± 10.07	9.86 ± 2.61	98.86 ± 5.37	39.88 ± 1.86	0.19 ± 0.01	0.47 ± 0.01
	p=0.152	*p*=0.461	*p*=0.162	*p*=0.149	*p*=0.215	*p*=0.464
PA-infiltrating CD8+ T cells *[Mean±SEM]*						
< 1% (n=5)	32.73 ± 7.29	7.22 ± 0.86	114.01 ± 12.95	47.37 ± 5.48	0.25 ± 0.04	0.43 ± 0.03
≥ 1% (n=11)	39.09 ± 8.34	9.17 ± 1.60	114.87 ± 9.54	46.21 ± 3.90	0.29 ± 0.07	0.47 ± 0.01
	p=0.644	*p*=0.444	*p*=0.960	*p*=0.868	*p*=0.678	*p*=0.189
PA-infiltrating CD4+ T cells *[Mean±SEM]*						
< 1% (n=9)	26.56 ± 4.64	6.47 ± 0.68	122.25 ± 11.75	50.13 ± 4.87	0.31 ± 0.08	0.43 ± 0.02
≥ 1% (n=7)	50.67 ± 10.93	11.24 ± 2.11	104.77 ± 7.26	42.00 ± 2.73	0.24 ± 0.04	0.50 ± 0.01
	***p*=0.044**	***p*=0.032**	*p*=0.259	*p*=0.200	*p*=0.477	***p*=0.004**

PA-infiltrating B cells *[Mean±SEM]* < 0.5% (n=5) ≥ 0.5% (n=11)	 26.47 ± 8.04 41.94 ± 7.83 *p*=0.251	 6.98 ± 1.03 9.28 ± 1.57 *p*=0.367	 132.77 ± 19.53 106.34 ± 5.51 *p*=0.254	 54.70 ± 8.18 42.88 ± 2.04 *p*=0.226	 0.38 ± 0.14 0.24 ± 0.03 *p*=0.381	 0.38 ± 0.14 0.24 ± 0.03 ***p*=0.048**
PA-infiltrating neutrophils *[Mean±SEM]* < 0.5% (n=6) ≥ 0.5% (n=10)	 41.95 ± 10.49 34.20 ± 7.70 *p*=0.556	 10.16 ± 2.64 7.60 ± 0.92 *p*=0.394	 110.95 ± 5.71 116.79 ± 11.67 *p*=0.718	 45.25 ± 2.08 47.37 ± 4.87 *p*=0.751	 0.25 ± 0.04 0.30 ± 0.07 *p*=0.602	 0.45 ± 0.01 0.46 ± 0.02 *p*=0.767
PA-infiltrating FOXP3+ T cells *[Mean±SEM]* < 0.3% (n=9) ≥ 0.3% (n=7)	 46.70 ± 9.24 24.76 ± 4.40 *p*=0.071	 9.09 ± 1.67 7.88 ± 1.56 *p*=0.617	 100.74 ± 5.06 132.42 ± 13.42 ***p*=0.029**	 40.95 ± 2.05 53.80 ± 5.61 ***p*=0.033**	 0.21 ± 0.02 0.38 ± 0.10 *p*=0.137	 0.47 ± 0.01 0.44 ± 0.03 *p*=0.195
Immune cell ratios *[Pearson correlation r (p)]* M2:M1 CD8:CD4 CD8:FOXP3 CD68:FOXP3	 0.408 (*p*=0.117) -0.156 (*p*=0.563) 0.203 (*p*=0.451) 0.154 (*p*=0.570)	 0.676 (***p*=0.004**) -0.059 (*p*=0.828) 0.020 (*p*=0.941) -0.064 (*p*=0.814)	 0.277 (*p*=0.299) 0.059 (*p*=0.827) -0.352 (*p*=0.182) -0.357 (*p*=0.175)	 0.239 (*p*=0.373) 0.073 (*p*=0.789) -0.360 (*p*=0.171) -0.351 (*p*=0.182)	 0.408 (*p*=0.117) 0.122 (*p*=0.651) -0.284 (*p*=0.287) -0.328 (*p*=0.215)	 0.222 (*p*=0.408) -0.057 (*p*=0.833) 0.324 (*p*=0.221) 0.118 (*p*=0.662)

Correlation between hormonal, cytokine and infiltrating immune cell data and PA angiogenesis data among NFPAs (n=16)

Microvessel density (MVD) is expressed in vessels/HPF; total microvessel area (TMVA) is expressed in % of the high power field; perimeter and Feret's diameter are expressed in µm; area per vessel is expressed in % of the high power field; vessel roundness correspond to a value comprised between 0 and 1 (1=perfect circle). FSH, follicle-stimulating hormone; FT4, free thyroxine; IGF-1, insulin-like growth factor-1; LH, luteinising hormone; MVD, microvessel density; NFPA, non-functioning pituitary adenoma; PRL, prolactin; TMVA, total microvessel area; TSH, thyroid-stimulating hormone.

NFPAs n = 16	MMP-9	MMP-14	E-cadherin	ZEB1	NCAM
Hormonal data *[Pearson correlation r (p)]*					
Serum IGF-1	0.144 (*p*=0.623)	0.091 (*p*=0.757)	-0.126 (*p*=0.668)	-0.139 (*p*=0.637)	-0.138 (*p*=0.637)
IGF-1 index	0.217 (*p*=0.457)	-0.030 (*p*=0.918)	-0.263 (*p*=0.364)	-0.336 (*p*=0.241)	0.002 (*p*=0.993)
Serum PRL	0.155 (*p*=0.598)	0.147 (*p*=0.616)	-0.186 (*p*=0.525)	0.141 (*p*=0.630)	-0.179 (*p*=0.541)
PRL index	0.305 (p=0.289)	0.190 (*p*=0.516)	0.009 (*p*=0.975)	0.113 (*p*=0.701)	-0.170 (*p*=0.562)
Serum TSH	0.167 (*p*=0.569)	-0.028 (*p*=0.924)	-0.227 (*p*=0.435)	-0.150 (*p*=0.609)	-0.201 (*p*=0.491)
Serum FT4	0.091 (*p*=0.756)	-0.221 (*p*=0.447)	0.085 (*p*=0.774)	-0.262 (*p*=0.366)	-0.025 (*p*=0.931)
Basal plasma cortisol	0.421 (*p*=0.152)	-0.597 (***p*=0.031**)	-0.269 (*p*=0.375)	0.030 (*p*=0.923)	-0.053 (*p*=0.862)
Serum LH	0.377 (*p*=0.184)	-0.219 (*p*=0.453)	-0.135 (*p*=0.645)	-0.030 (*p*=0.920)	0.532 (*p*=0.050)
Serum FSH	0.350 (*p*=0.220)	-0.443 (*p*=0.113)	-0.056 (*p*=0.849)	-0.295 (*p*=0.306)	0.460 (*p*=0.098)
Serum testosterone	-0.423 (*p*=0.170)	0.303 (*p*=0.338)	0.495 (*p*=0.102)	0.158 (*p*=0.623)	-0.219 (*p*=0.493)
PA-derived cytokine data *[Pearson correlation r (p)]*					
IL-8	-0.287 (*p*=0.281)	0.298 (*p*=0.262)	0.050 (*p*=0.854)	-0.287 (*p*=0.282)	-0.270 (*p*=0.312)
CCL2	-0.366 (*p*=0.163)	0.076 (*p*=0.781)	0.118 (*p*=0.664)	-0.433 (*p*=0.094)	-0.387 (*p*=0.138)
CCL3	-0.250 (*p*=0.350)	0.098 (*p*=0.718)	-0.090 (*p*=0.739)	-0.247 (*p*=0.356)	-0.045 (*p*=0.868)
CCL4	-0.313 (p=0.238)	0.260 (*p*=0.331)	0.038 (*p*=0.888)	-0.318 (*p*=0.230)	-0.263 (*p*=0.324)
CXCL10	-0.262 (*p*=0.326)	-0.234 (*p*=0.383)	0.183 (*p*=0.497)	-0.282 (*p*=0.291)	-0.340 (*p*=0.197)
CCL22	-0.092 (*p*=0.734)	0.329 (*p*=0.213)	-0.062 (*p*=0.819)	-0.307 (*p*=0.247)	-0.314 (*p*=0.237)
CXCL1	-0.264 (*p*=0.323)	0.214 (*p*=0.425)	-0.080 (*p*=0.769)	-0.359 (*p*=0.172)	-0.184 (*p*=0.494)
CX3CL1	-0.243 (*p*=0.365)	-0.168 (*p*=0.533)	0.153 (*p*=0.572)	-0.264 (*p*=0.323)	-0.372 (*p*=0.156)
FGF-2	0.147 (*p*=0.587)	-0.080 (*p*=0.769)	-0.310 (*p*=0.243)	-0.612 (***p*=0.012**)	-0.317 (*p*=0.232)
IL-6	-0.203 (*p*=0.452)	0.361 (*p*=0.169)	0.101 (*p*=0.710)	-0.222 (*p*=0.408)	-0.319 (*p*=0.228)
PDGF-AA	-0.144 (*p*=0.595)	0.142 (*p*=0.600)	0.002 (*p*=0.995)	-0.364 (*p*=0.166)	-0.346 (*p*=0.190)
VEGF-A	-0.064 (*p*=0.813)	0.152 (*p*=0.575)	-0.228 (*p*=0.395)	-0.321 (*p*=0.225)	-0.232 (*p*=0.387)
TAF cytokine data n=11 *[Pearson correlation r (p)]*					
CCL2	-0.210 (*p*=0.536)	-0.310 (*p*=0.353)	-0.205 (*p*=0.546)	0.006 (*p*=0.987)	0.103 (*p*=0.763)
CCL11	-0.086 (*p*=0.801)	0.148 (*p*=0.664)	-0.191 (*p*=0.574)	-0.573 (*p*=0.066)	-0.298 (*p*=0.374)
VEGF-A	-0.040 (*p*=0.906)	-0.236 (*p*=0.484)	-0.161 (*p*=0.635)	-0.502 (*p*=0.115)	-0.202 (*p*=0.551)
CCL22	-0.333 (*p*=0.317)	0.353 (*p*=0.286)	0.370 (*p*=0.263)	-0.142 (*p*=0.677)	-0.537 (*p*=0.088)
IL-6	0.072 (*p*=0.833)	0.028 (*p*=0.935)	0.244 (*p*=0.469)	0.072 (*p*=0.834)	0.171 (*p*=0.615)
FGF-2	-0.145 (*p*=0.671)	0.289 (*p*=0.388)	0.431 (*p*=0.186)	-0.025 (*p*=0.941)	-0.716 (***p*=0.013**)
IL-8	-0.211 (*p*=0.533)	-0.101 (*p*=0.767)	-0.284 (*p*=0.398)	-0.573 (*p*=0.065)	-0.260 (*p*=0.440)
CXCL1	-0.221 (*p*=0.513)	0.177 (*p*=0.602)	0.298 (*p*=0.374)	-0.364 (*p*=0.271)	-0.661 (***p*=0.027**)
CX3CL1	-0.323 (*p*=0.332)	0.202 (*p*=0.552)	0.214 (*p*=0.527)	-0.355 (*p*=0.284)	-0.560 (*p*=0.073)
CCL7	-0.140 (*p*=0.680)	0.153 (*p*=0.654)	0.217 (*p*=0.522)	-0.344 (*p*=0.300)	-0.609 (***p*=0.047**)
PDGF-AA	0.380 (*p*=0.249)	-0.002 (*p*=0.996)	-0.806 (***p*=0.003**)	-0.274 (*p*=0.415)	0.599 (*p*=0.051)
IFNα2	-0.225 (*p*=0.506)	0.244 (*p*=0.469)	0.186 (*p*=0.585)	-0.298 (*p*=0.374)	-0.517 (*p*=0.104)
PA-infiltrating macrophage *[Mean±SEM]*					
< 6% (n=11)	1.73 ± 0.62	1.45 ± 0.62	4.55 ± 0.28	1.27 ± 0.57	5.00 ± 0.23
≥ 6% (n=5)	0	1.60 ± 0.75	4.60 ± 0.40	0.80 ± 0.49	4.60 ± 0.25
	***p*=0.019**	*p*=0.893	*p*=0.914	*p*=0.616	*p*=0.319
PA-infiltrating CD8+ T cells *[Mean±SEM]*					
< 1% (n=5)	0.80 ± 0.80	1.60 ± 1.03	4.80 ± 0.37	1.20 ± 0.80	5.00 ± 0.32
≥ 1% (n=11)	1.36 ± 0.59	1.45 ± 0.55	4.45 ± 0.28	1.09 ± 0.51	4.82 ± 0.23
	p=0.594	*p*=0.893	*p*=0.492	*p*=0.908	*p*=0.655
PA-infiltrating CD4+ T cells *[Mean±SEM]*					
< 1% (n=9)	0.78 ± 0.52	1.67 ± 0.71	4.56 ± 0.38	1.00 ± 0.53	5.00 ± 0.24
≥ 1% (n=7)	1.71 ± 0.84	1.29 ± 0.64	4.57 ± 0.20	1.29 ± 0.71	4.71 ± 0.29
	p=0.337	*p*=0.705	*p*=0.973	*p*=0.747	*p*=0.449

PA-infiltrating B cells *[Mean±SEM]*					
< 0.5% (n=5)	0	1.80 ± 1.11	5.20 ± 0.20	1.20 ± 0.80	4.80 ± 0.37
≥ 0.5% (n=11)	1.73 ± 0.62	1.36 ± 0.51	4.27 ± 0.27	1.09 ± 0.51	4.91 ± 0.21
	***p*=0.019**	*p*=0.685	***p*=0.016**	*p*=0.908	*p*=0.789
PA-infiltrating neutrophils *[Mean±SEM]*					
< 0.5% (n=6)	1.00 ± 0.63	0	4.33 ± 0.56	0.67 ± 0.42	5.17 ± 0.31
≥ 0.5% (n=10)	1.30 ± 0.67	2.40 ± 0.60	4.70 ± 0.15	1.40 ± 0.62	4.70 ± 0.21
	p=0.768	***p*=0.003**	*p*=0.550	*p*=0.344	*p*=0.220
PA-infiltrating FOXP3+ T cells *[Mean±SEM]*					
< 0.3% (n=9)	1.00 ± 0.67	1.00 ± 0.53	4.67 ± 0.24	0.67 ± 0.33	4.56 ± 0.18
≥ 0.3% (n=7)	1.43 ± 0.69	2.14 ± 0.83	4.43 ± 0.43	1.71 ± 0.84	5.29 ± 0.29
	p=0.665	*p*=0.245	*p*=0.614	*p*=0.279	***p*=0.039**
Immune cell ratios *[Pearson correlation r (p)]*					
M2:M1	-0.070 (*p*=0.796)	-0.347 (*p*=0.188)	0.084 (*p*=0.756)	0.038 (*p*=0.890)	-0.142 (*p*=0.600)
CD8:CD4	-0.168 (*p*=0.534)	-0.176 (*p*=0.514)	-0.099 (*p*=0.715)	-0.171 (*p*=0.527)	-0.007 (*p*=0.979)
CD8:FOXP3	0.111 (*p*=0.683)	0.149 (*p*=0.583)	0.231 (*p*=0.389)	-0.254 (*p*=0.343)	-0.419 (*p*=0.106)
CD68:FOXP3	-0.303 (*p*=0.253)	0.014 (*p*=0.958)	0.241 (*p*=0.369)	-0.256 (*p*=0.338)	-0.245 (*p*=0.361)

Correlation between hormonal, cytokine and infiltrating immune cell data and MMP-9, MMP-14, E-cadherin, ZEB1 and NCAM immunoreactivities among NFPAs (n=16)

FSH, follicle-stimulating hormone; FT4, free thyroxine; IGF-1, insulin-like growth factor-1; LH, luteinising hormone; NFPA, non-functioning pituitary adenoma; MMP, matrix metalloproteinase; NCAM, neural cell adhesion molecule; PRL, prolactin; TSH, thyroid-stimulating hormone.

Somatotrophinomas n = 8	MVD	TMVA	Perimeter	Feret's diameter	Area per vessel	Roundness
Hormonal data *[Pearson correlation r (p)]*						
Serum GH	0.209 (*p*=0.654)	0.166 (*p*=0.723)	-0.069 (*p*=0.883)	-0.142 (*p*=0.761)	-0.365 (*p*=0.421)	0.130 (*p*=0.781)
Serum IGF-1	0.333 (*p*=0.465)	0.237 (*p*=0.610)	-0.210 (*p*=0.652)	-0.275 (*p*=0.550)	-0.449 (*p*=0.313)	0.242 (*p*=0.602)
IGF-1 index	0.407 (*p*=0.317)	0.196 (*p*=0.641)	-0.414 (*p*=0.308)	-0.405 (*p*=0.320)	-0.554 (*p*=0.154)	0.263 (*p*=0.529)
Serum PRL	-0.497 (*p*=0.394)	0.054 (*p*=0.931)	0.627 (*p*=0.258)	0.755 (*p*=0.140)	0.958 (***p*=0.010**)	0.483 (*p*=0.409)
PRL index	-0.420 (*p*=0.481)	0.144 (*p*=0.817)	0.663 (*p*=0.222)	0.785 (*p*=0.116)	0.959 (***p*=0.010**)	0.479 (*p*=0.414)
Serum TSH	-0.513 (*p*=0.239)	-0.442 (*p*=0.321)	-0.153 (*p*=0.744)	-0.198 (*p*=0.671)	0.226 (*p*=0.626)	0.676 (*p*=0.095)
Serum FT4	0.875 (***p*=0.010**)	0.672 (*p*=0.098)	-0.404 (*p*=0.369)	-0.353 (*p*=0.437)	-0.370 (*p*=0.414)	0.043 (*p*=0.927)
Basal plasma cortisol	0.030 (*p*=0.949)	0.050 (*p*=0.914)	0.192 (*p*=0.679)	0.267 (*p*=0.563)	-0.066 (*p*=0.888)	-0.506 (*p*=0.246)
Serum LH	0.701 (*p*=0.079)	0.676 (*p*=0.098)	-0.175 (*p*=0.708)	-0.130 (*p*=0.782)	0.000 (*p*=0.999)	0.059 (*p*=0.900)
Serum FSH	0.734 (*p*=0.060)	0.498 (*p*=0.255)	-0.596 (*p*=0.158)	-0.579 (*p*=0.173)	-0.389 (*p*=0.388)	0.442 (*p*=0.320)
Serum testosterone	-0.235 (*p*=0.655)	-0.296 (*p*=0.569)	-0.594 (*p*=0.214)	-0.644 (*p*=0.167)	-0.410 (*p*=0.419)	0.897 (***p*=0.015**)
PA-derived cytokine data *[Pearson correlation r (p)]*						
IL-8	0.008 (*p*=0.985)	0.469 (*p*=0.241)	0.679 (*p*=0.064)	0.686 (*p*=0.060)	0.725 (***p*=0.042**)	-0.326 (*p*=0.430)
CCL2	-0.222 (*p*=0.598)	0.078 (*p*=0.855)	0.481 (*p*=0.227)	0.519 (*p*=0.188)	0.559 (*p*=0.150)	-0.347 (*p*=0.400)
CCL3	0.051 (*p*=0.905)	0.210 (*p*=0.618)	0.192 (*p*=0.649)	0.155 (*p*=0.714)	0.131 (*p*=0.758)	0.032 (*p*=0.939)
CCL4	-0.484 (*p*=0.224)	-0.204 (*p*=0.628)	0.330 (*p*=0.425)	0.389 (p=0.341)	0.670 (*p*=0.069)	-0.117 (*p*=0.782)
CXCL10	-0.494 (*p*=0.214)	-0.306 (*p*=0.462)	0.225 (*p*=0.593)	0.283 (*p*=0.498)	0.507 (*p*=0.200)	-0.114 (*p*=0.787)
CCL22	-0.609 (*p*=0.109)	-0.507 (*p*=0.199)	0.024 (*p*=0.954)	0.039 (*p*=0.926)	0.300 (*p*=0.471)	0.162 (*p*=0.701)
CXCL1	-0.571 (*p*=0.139)	-0.387 (*p*=0.344)	0.185 (*p*=0.661)	0.189 (*p*=0.655)	0.403 (*p*=0.322)	0.052 (*p*=0.902)
CX3CL1	-0.640 (*p*=0.087)	-0.510 (*p*=0.197)	0.006 (*p*=0.988)	-0.005 (*p*=0.991)	0.328 (*p*=0.427)	0.323 (*p*=0.434)
FGF-2	-0.588 (*p*=0.125)	-0.269 (*p*=0.519)	0.372 (*p*=0.364)	0.424 (*p*=0.295)	0.769 (***p*=0.026**)	-0.100 (*p*=0.813)
IL-6	-0.596 (*p*=0.119)	-0.377 (*p*=0.357)	0.243 (*p*=0.562)	0.287 (*p*=0.490)	0.564 (*p*=0.145)	-0.053 (*p*=0.901)
PDGF-AA	0.188 (*p*=0.656)	0.322 (*p*=0.437)	0.036 (*p*=0.932)	0.008 (*p*=0.985)	0.015 (*p*=0.973)	0.247 (*p*=0.556)
VEGF-A	0.051 (*p*=0.904)	0.151 (*p*=0.720)	0.252 (*p*=0.548)	0.257 (*p*=0.539)	0.066 (*p*=0.877)	-0.299 (*p*=0.472)
TAF cytokine data n=5 *[Pearson correlation r (p)]*						
CCL2	-0.493 (*p*=0.399)	-0.334 (*p*=0.582)	0.752 (*p*=0.142)	0.636 (*p*=0.249)	0.817 (*p*=0.092)	-0.457 (*p*=0.439)
CCL11	-0.459 (*p*=0.437)	-0.233 (*p*=0.706)	0.759 (*p*=0.137)	0.772 (*p*=0.127)	0.883 (***p*=0.047**)	-0.553 (*p*=0.334)
VEGF-A	-0.474 (*p*=0.420)	-0.258 (*p*=0.676)	0.769 (*p*=0.129)	0.800 (*p*=0.104)	0.836 (*p*=0.077)	-0.610 (*p*=0.275)
CCL22	0.937 (***p*=0.019**)	0.916 (***p*=0.029**)	-0.368 (*p*=0.542)	-0.338 (*p*=0.578)	-0.280 (*p*=0.648)	0.171 (*p*=0.784)
IL-6	-0.375 (*p*=0.534)	-0.138 (*p*=0.825)	0.812 (*p*=0.095)	0.830 (*p*=0.082)	0.912 (***p*=0.031**)	-0.640 (*p*=0.244)
FGF-2	0.532 (*p*=0.356)	0.651 (*p*=0.235)	0.342 (*p*=0.573)	0.482 (*p*=0.411)	0.215 (*p*=0.728)	-0.640 (*p*=0.245)
IL-8	0.142 (*p*=0.819)	0.298 (*p*=0.626)	0.299 (*p*=0.625)	0.417 (*p*=0.485)	0.393 (*p*=0.513)	-0.363 (*p*=0.548)
CXCL1	0.011 (*p*=0.986)	0.138 (*p*=0.825)	0.215 (*p*=0.728)	0.336 (*p*=0.581)	0.301 (*p*=0.623)	-0.264 (*p*=0.668)
CX3CL1	0.585 (*p*=0.300)	0.764 (*p*=0.132)	0.519 (*p*=0.370)	0.555 (*p*=0.331)	0.542 (*p*=0.346)	-0.633 (*p*=0.251)
CCL7	-0.116 (*p*=0.852)	0.031 (*p*=0.960)	0.367 (*p*=0.544)	0.479 (*p*=0.414)	0.417 (*p*=0.485)	-0.394 (*p*=0.512)
PDGF-AA	-0.566 (*p*=0.320)	-0.733 (*p*=0.159)	-0.430 (*p*=0.470)	-0.539 (*p*=0.348)	-0.410 (*p*=0.493)	0.638 (*p*=0.246)
IFNα2	0.643 (*p*=0.242)	0.813 (*p*=0.095)	0.366 (*p*=0.545)	0.420 (*p*=0.481)	0.456 (*p*=0.440)	-0.477 (*p*=0.416)
PA-infiltrating macrophage *[Mean±SEM]*						
< 6% (n=6)	36.84 ± 7.27	4.87 ± 0.95	78.98 ± 5.14	31.90 ± 2.06	0.13 ± 0.01	0.49 ± 0.02
≥ 6% (n=2)	37.00 ± 18.00	7.49 ± 1.90	101.41 ± 1.93	41.12 ± 1.59	0.23 ± 0.06	0.47 ± 0.01
	p=0.992	*p*=0.229	***p*=0.007**	***p*=0.019**	***p*=0.031**	*p*=0.441
PA-infiltrating CD8+ T cells *[Mean±SEM]*						
< 1% (n=1)	21.67	3.83	98.48	38.51	0.18	0.45
≥ 1% (n=7)	39.05 ± 6.85	5.77 ± 0.99	82.60 ± 5.64	33.58 ± 2.39	0.16 ± 0.02	0.49 ± 0.02
	p=0.404	*p*=0.517	*p*=0.358	*p*=0.493	*p*=0.778	*p*=0.358
PA-infiltrating CD4+ T cells *[Mean±SEM]*						
< 1% (n=6)	40.17 ± 7.84	5.73 ± 1.19	82.34 ± 6.18	33.06 ± 2.43	0.14 ± 0.01	0.49 ± 0.02
≥ 1% (n=2)	27.00 ± 8.00	4.91 ± 0.68	91.34 ± 12.00	37.63 ± 5.08	0.21 ± 0.09	0.47 ± 0.00
	p=0.408	*p*=0.723	*p*=0.502	*p*=0.400	*p*=0.210	*p*=0.330

PA-infiltrating B cells *[Mean±SEM]* < 0.5% (n=3) ≥ 0.5% (n=5)	 36.45 ± 9.81 37.13 ± 9.10 *p*=0.963	 6.08 ± 1.69 5.19 ± 1.14 *p*=0.666	 95.03 ± 3.96 78.32 ± 6.85 *p*=0.132	 38.13 ± 0.94 31.84 ± 3.01 *p*=0.173	 0.17 ± 0.01 0.15 ± 0.04 *p*=0.793	 0.46 ± 0.00 0.50 ± 0.02 *p*=0.060
PA-infiltrating neutrophils *[Mean±SEM]* < 0.5% (n=7) ≥ 0.5% (n=1)	 37.86 ± 7.20 30.00 *p*=0.713	 5.85 ± 0.96 3.23 *p*=0.372	 86.54 ± 5.65 70.89 *p*=0.365	 35.21 ± 2.20 27.16 *p*=0.244	 0.17 ± 0.02 0.11 *p*=0.405	 0.48 ± 0.01 0.53 *p*=0.191
PA-infiltrating FOXP3+ T cells *[Mean±SEM]* < 0.3% (n=3) ≥ 0.3% (n=5)	 49.56 ± 14.78 29.27 ± 2.74 *p*=0.302	 7.56 ± 1.86 4.30 ± 0.45 *p*=0.218	 91.13 ± 7.85 80.66 ± 7.00 *p*=0.376	 36.45 ± 2.59 32.85 ± 3.13 *p*=0.462	 0.16 ± 0.01 0.16 ± 0.03 *p*=0.983	 0.46 ± 0.01 0.50 ± 0.02 *p*=0.164
Immune cell ratios *[Pearson correlation r (p)]* M2:M1 CD8:CD4 CD8:FOXP3 CD68:FOXP3	 0.801 (***p*=0.017**) 0.621 (*p*=0.100) 0.209 (*p*=0.620) -0.097 (*p*=0.818)	 0.606 (*p*=0.111) 0.718 (***p*=0.045**) 0.122 (*p*=0.773) -0.052 (*p*=0.903)	 -0.320 (*p*=0.439) 0.223 (*p*=0.595) 0.038 (*p*=0.929) 0.307 (*p*=0.460)	 -0.259 (*p*=0.536) 0.237 (*p*=0.571) 0.007 (*p*=0.986) 0.237 (*p*=0.573)	 -0.260 (*p*=0.534) -0.090 (*p*=0.832) -0.139 (*p*=0.742) 0.116 (*p*=0.785)	 0.023 (*p*=0.957) -0.315 (*p*=0.447) -0.232 (*p*=0.580) -0.355 (*p*=0.389)

Correlation between hormonal, cytokine and infiltrating immune cell data and PA angiogenesis data among somatotrophinomas (n=8)

Microvessel density (MVD) is expressed in vessels/HPF; total microvessel area (TMVA) is expressed in % of the high power field; perimeter and Feret's diameter are expressed in µm; area per vessel is expressed in % of the high power field; vessel roundness correspond to a value comprised between 0 and 1 (1=perfect circle). FSH, follicle-stimulating hormone; FT4, free thyroxine; IGF-1, insulin-like growth factor-1; LH, luteinising hormone; MVD, microvessel density; NFPA, non-functioning pituitary adenoma; PRL, prolactin; TMVA, total microvessel area; TSH, thyroid-stimulating hormone.

Somatotrophinomas n = 8	MMP-9	MMP-14	E-cadherin	ZEB1	NCAM
Hormonal data *[Pearson correlation r (p)]*					
Serum GH	0.328 (*p*=0.472)	0.420 (*p*=0.348)	-0.801 (***p*=0.031**)	-0.361 (*p*=0.426)	0.027 (*p*=0.954)
Serum IGF-1	0.325 (*p*=0.478)	0.473 (*p*=0.284)	-0.719 (*p*=0.069)	-0.213 (*p*=0.646)	0.147 (*p*=0.753)
IGF-1 index	0.491 (*p*=0.216)	0.644 (*p*=0.085)	-0.450 (*p*=0.263)	-0.216 (*p*=0.607)	0.137 (*p*=0.746)
Serum PRL	-0.963 (***p*=0.009**)	-0.268 (*p*=0.663)	0.234 (*p*=0.705)	-	-0.989 (***p*=0.001**)
PRL index	-0.951 (***p*=0.013**)	-0.295 (*p*=0.630)	0.192 (*p*=0.757)	-	-0.978 (***p*=0.004**)
Serum TSH	-0.202 (*p*=0.665)	0.285 (*p*=0.536)	0.034 (*p*=0.943)	-0.379 (*p*=0.402)	-0.442 (*p*=0.320)
Serum FT4	-0.014 (*p*=0.976)	-0.047 (*p*=0.920)	0.300 (*p*=0.513)	0.910 (***p*=0.004**)	0.741 (*p*=0.057)
Basal plasma cortisol	0.304 (*p*=0.508)	-0.232 (*p*=0.617)	0.144 (*p*=0.759)	-0.171 (*p*=0.714)	-0.016 (*p*=0.973)
Serum LH	-0.159 (*p*=0.734)	-0.459 (*p*=0.301)	0.649 (*p*=0.114)	0.933 (***p*=0.002**)	0.576 (*p*=0.176)
Serum FSH	0.060 (*p*=0.898)	-0.008 (*p*=0.986)	0.527 (*p*=0.224)	0.903 (***p*=0.005**)	0.746 (*p*=0.054)
Serum testosterone	0.267 (*p*=0.609)	0.526 (*p*=0.284)	0.120 (*p*=0.820)	-0.299 (*p*=0.565)	-0.299 (*p*=0.565)
PA-derived cytokine data *[Pearson correlation r (p)]*					
IL-8	-0.597 (*p*=0.118)	-0.252 (*p*=0.547)	-0.436 (*p*=0.280)	-0.360 (*p*=0.381)	-0.616 (*p*=0.104)
CCL2	-0.689 (*p*=0.059)	0.271 (*p*=0.517)	-0.655 (*p*=0.078)	-0.493 (*p*=0.214)	-0.692 (*p*=0.057)
CCL3	-0.193 (*p*=0.646)	0.404 (*p*=0.320)	-0.817 (***p*=0.013**)	-0.448 (*p*=0.265)	-0.373 (*p*=0.363)
CCL4	-0.864 (**p=0.006**)	0.315 (*p*=0.447)	-0.315 (*p*=0.448)	-0.438 (*p*=0.278)	-0.769 (***p*=0.026**)
CXCL10	-0.747 (***p*=0.033**)	0.467 (*p*=0.243)	-0.389 (*p*=0.340)	-0.456 (*p*=0.256)	-0.697 (*p*=0.055)
CCL22	-0.402 (*p*=0.324)	0.617 (*p*=0.103)	-0.373 (*p*=0.363)	-0.592 (*p*=0.122)	-0.636 (*p*=0.090)
CXCL1	-0.456 (*p*=0.256)	0.546 (*p*=0.162)	-0.520 (*p*=0.186)	-0.662 (*p*=0.074)	-0.717 (***p*=0.045**)
CX3CL1	-0.414 (*p*=0.308)	0.524 (*p*=0.182)	-0.304 (*p*=0.465)	-0.541 (*p*=0.167)	-0.607 (*p*=0.110)
FGF-2	-0.809 (***p*=0.015**)	0.129 (*p*=0.761)	-0.074 (*p*=0.862)	-0.427 (*p*=0.291)	-0.786 (***p*=0.021**)
IL-6	-0.738 (***p*=0.037**)	0.447 (*p*=0.267)	-0.356 (*p*=0.387)	-0.520 (*p*=0.186)	-0.757 (***p*=0.030**)
PDGF-AA	0.115 (*p*=0.787)	0.185 (*p*=0.660)	-0.409 (*p*=0.314)	-0.344 (*p*=0.405)	-0.210 (*p*=0.617)
VEGF-A	-0.184 (*p*=0.663)	0.473 (*p*=0.237)	-0.886 (***p*=0.003**)	-0.475 (*p*=0.234)	-0.370 (*p*=0.367)
TAF cytokine data n=5 *[Pearson correlation r (p)]*					
CCL2	0.135 (*p*=0.829)	-0.390 (*p*=0.517)	-0.368 (*p*=0.543)	-0.274 (*p*=0.655)	-0.274 (*p*=0.655)
CCL11	0.827 (*p*=0.084)	-0.695 (*p*=0.192)	0.275 (*p*=0.654)	-0.360 (*p*=0.552)	-0.360 (*p*=0.552)
VEGF-A	0.822 (*p*=0.088)	-0.642 (*p*=0.243)	0.218 (*p*=0.724)	-0.414 (*p*=0.489)	-0.414 (*p*=0.489)
CCL22	-0.503 (*p*=0.388)	-0.314 (*p*=0.607)	0.565 (*p*=0.321)	0.978 (***p*=0.004**)	0.978 (***p*=0.004**)
IL-6	0.758 (*p*=0.137)	-0.764 (*p*=0.132)	0.279 (*p*=0.650)	-0.272 (*p*=0.658)	-0.272 (*p*=0.658)
FGF-2	0.096 (*p*=0.878)	-0.635 (*p*=0.250)	0.478 (*p*=0.416)	0.453 (*p*=0.444)	0.453 (*p*=0.444)
IL-8	0.694 (*p*=0.194)	-0.681 (*p*=0.205)	0.751 (*p*=0.144)	0.107 (*p*=0.864)	0.107 (*p*=0.864)
CXCL1	0.770 (*p*=0.128)	-0.522 (*p*=0.367)	0.689 (*p*=0.199)	-0.059 (*p*=0.926)	-0.059 (*p*=0.926)
CX3CL1	-0.109 (*p*=0.861)	-0.901 (***p*=0.037**)	0.448 (*p*=0.449)	0.705 (*p*=0.184)	0.705 (*p*=0.184)
CCL7	0.800 (*p*=0.104)	-0.536 (*p*=0.351)	0.556 (*p*=0.330)	-0.178 (*p*=0.775)	-0.178 (*p*=0.775)
PDGF-AA	-0.148 (*p*=0.812)	0.851 (*p*=0.068)	-0.619 (*p*=0.266)	-0.573 (*p*=0.312)	-0.573 (*p*=0.312)
IFNα2	0.023 (*p*=0.971)	-0.911 (***p*=0.031**)	0.669 (*p*=0.217)	0.745 (*p*=0.149)	0.745 (*p*=0.149)
PA-infiltrating macrophage *[Mean±SEM]*					
< 6% (n=6)	4.83 ± 0.31	1.00 ± 0.63	5.00 ± 0.516	1.17 ± 0.75	5.33 ± 0.21
≥ 6% (n=2)	2.50 ± 2.50	0	4.00 ± 1.00	0	4.50 ± 0.50
	p=0.521	*p*=0.175	*p*=0.379	*p*=0.180	*p*=0.114
PA-infiltrating CD8+ T cells *[Mean±SEM]*					
< 1% (n=1)	5.00	0	4.00	0	5.00
≥ 1% (n=7)	4.14 ± 0.74	0.86 ± 0.55	4.86 ± 0.51	1.00 ± 0.66	5.14 ± 0.26
	p=0.695	*p*=0.604	*p*=0.573	*p*=0.609	*p*=0.853
PA-infiltrating CD4+ T cells *[Mean±SEM]*					
< 1% (n=6)	5.00 ± 0.26	0.50 ± 0.50	5.00 ± 0.52	1.17 ± 0.75	5.33 ± 0.21
≥ 1% (n=2)	2.00 ± 2.00	1.50 ± 1.50	4.00 ± 1.00	0	4.50 ± 0.50
	p=0.371	*p*=0.420	*p*=0.379	*p*=0.426	*p*=0.114

PA-infiltrating B cells *[Mean±SEM]* < 0.5% (n=3) ≥ 0.5% (n=5)	 5.33 ± 0.33 3.60 ± 0.93 *p*=0.218	 0 1.20 ± 0.74 *p*=0.178	 4.33 ± 0.88 5.00 ± 0.55 *p*=0.519	 0 1.40 ± 0.87 *p*=0.274	 5.00 ± 0.00 5.20 ± 0.37 *p*=0.621
PA-infiltrating neutrophils *[Mean±SEM]* < 0.5% (n=7) ≥ 0.5% (n=1)	 4.14 ± 0.74 5.00 *p*=0.695	 0.86 ± 0.55 0 *p*=0.604	 4.57 ± 0.48 6.00 *p*=0.334	 0.57 ± 0.57 3.00 *p*=0.184	 5.00 ± 0.22 6.00 *p*=0.156
PA-infiltrating FOXP3+ T cells *[Mean±SEM]* < 0.3% (n=3) ≥ 0.3% (n=5)	 4.67 ± 0.33 4.00 ± 1.05 *p*=0.655	 0 1.20 ± 0.74 *p*=0.178	 4.33 ± 0.88 5.00 ± 0.55 *p*=0.519	 1.33 ± 1.33 0.60 ± 0.60 *p*=0.582	 5.33 ± 0.33 5.00 ± 0.32 *p*=0.519
Immune cell ratios *[Pearson correlation r (p)]* M2:M1 CD8:CD4 CD8:FOXP3 CD68:FOXP3	 0.078 (*p*=0.853) 0.445 (*p*=0.269) 0.336 (*p*=0.416) 0.127 (*p*=0.764)	 -0.250 (*p*=0.550) -0.375 (*p*=0.359) -0.262 (*p*=0.531) -0.408 (*p*=0.994)	 0.518 (*p*=0.188) -0.061 (*p*=0.885) 0.154 (*p*=0.715) 0.037 (*p*=0.930)	 0.773 (***p*=0.024**) -0.019 (*p*=0.965) 0.209 (*p*=0.620) 0.089 (*p*=0.833)	 0.603 (*p*=0.113) 0.139 (*p*=0.742) 0.296 (*p*=0.476) 0.110 (*p*=0.796)

Correlation between hormonal, cytokine and infiltrating immune cell data and MMP-9, MMP-14, E-cadherin, ZEB1 and NCAM immunoreactivities among somatotrophinomas (n=8)

FSH, follicle-stimulating hormone; FT4, free thyroxine; IGF-1, insulin-like growth factor-1; LH, luteinising hormone; NFPA, non-functioning pituitary adenoma; MMP, matrix metalloproteinase; NCAM, neural cell adhesion molecule; PRL, prolactin; TSH, thyroid-stimulating hormone.

Appendix 10: Supplemental tables summarising the pro-tumoural and anti-tumoural effects of CX3CL1 in different cancers

Pro-tumoural role of CX3CL1-CX3CR1 in different cancer types	
Cancer type (and study)	**Main study findings**
B lymphoma Andreasson 2008 *Cancer Lett*	Andreasson study: CX3CR1, normally not expressed in B cells, was found expressed in several lymphoma subtypes.
Breast cancer Tsang 2003 *Breast Cancer Res Treat* Andre 2006 *Ann Oncol* Jamieson-Gladney 2011 *Breast Cancer Res*	Tsang study: High CX3CL1 expression was detected in 33% of invasive breast cancers, and CX3CL1 expression was correlated with tumour-infiltrating lymphocytes content, as well as with adverse features including lymph node metastasis, high Ki-67 and poorer survival. Andre study: CX3CR1 expression was associated with breast cancer metastasis to the brain, but not with survival or disease-free survival. Jamieson-Gladney study: Functional interactions between CX3CL1 produced by endothelial and stromal cells of the bone marrow and CX3CR1 on breast cancer cells were determinant for skeletal dissemination. Breast cancer cells expressing CX3CR1 displayed a higher propensity to spread to skeleton. CX3CL1-null transgenic mice indicates that the ablation of CX3CL1 impairs skeletal dissemination of circulating breast cancer cells.
Chronic lymphocytic leukaemia Ferretti 2011 *Leukemia*	Ferretti study: CX3CL1-CX3CR1 contributes to interactions between chronic lymphocytic leukaemia cells and the tumour microenvironment by increasing CXCL12-mediated attraction of leukaemic cells. CX3CL1 induced phosphorylation of PI3K, Erk1/2, p38, Akt and Src, pathways involved in the leukaemic cells chemotaxis.
Colon cancer Zheng 2013 *Mol Cancer*	Zheng study: CX3CR1 is expressed in human colon carcinomas in a grade- and stage-dependent manner, and CX3CR1 upregulation in tumour-associated macrophages was correlated with poor prognosis. Furthermore, liver metastasis of colon cancer was inhibited when the tumour microenvironment was lacking CX3CR1, highlightening its role in the macrophage survival in the tumour microenvironment and in metastisation.
Endometriosis Wang 2014 *Int J Clin Exp Pathol* Hou 2016 *Am J Reprod Immunol*	Wang study: CX3CL1induced M2-macrophage polarisation, and also promoted cell invasiveness by activating p38 MAPK and integrin β1 signalling pathways. Hou study: High CX3CL1 levels in the ectopic milieu promoted proliferation and invasion of endometrial stromal cells by activating AKT and p38 signalling pathways. CX3CL1 concentration was higher in the peritoneal fluid from patients with endometriosis and was correlated with endometriosis severity.
Gastric cancer Lv 2014 *World J Gastroenterol* Wei 2015 *Oncol Rep*	Lv study: Expression of CX3CL1 and CX3CR1 in gastric cancer tissues were higher than those in adjacent normal tissue. Moreover, CX3CL1 and CX3CR1 expression were higher in gastric tumours with perineural invasion. Wei study: Gastric cancer tissues expressed higher CX3CR1 levels than non-neoplastic gastric tissues. Overexpression of CX3CR1 promotes metastasis, proliferation and survival. Tumour microenvironment may play a role in the increased CX3CR1 expression in gastric cancer cells.
Glioblastoma Erreni 2010 *Eur J Cancer*	Erreni study: CX3CL1 is highly expressed in the most severe forms of gliomas suggesting its involvement in the malignant glioblastomas behaviour: 31 out of 36 human glioblastomas expressed CX3CL1 and CX3CR1, and uppermost CX3CL1 levels were found in grades III-IV tumours and inversely correlated with patients' survival.
Kidney cancer Yao 2004 *Urol Oncol*	Yao study: CX3CR1 expression is associated with migration and metastisation of clear cell renal cell carcinoma. ERK1/2 and PI3K/Akt were activated upon CX3CL1 stimulation only in CX3CR1-tumour cells. Immunohistochemistry data revealed an association between CX3CR1 expression, metastisation and poor prognosis.
Lung cancer Zhou 2016 *Med Sci Monit*	Zhou study: CX3CL1expression in lung cancer was higher than in normal lung tissue, and increased in the cases with higher pathological stages. CX3CL1 expression was also higher in the lung cancer cases with more metastatic lymph nodes.

Melanoma Ren 2007 *Biochm Biophys Res Commun*	Ren study: CX3CL1 was expressed in both mouse and human melanomas, and knockdown of *CX3CL1* gene inhibited melanoma cells growth which was also correlated to decreased angiogenesis in the tumour.
Multiple myeloma Wada 2015 *Oncol Rep*	Wada study: CX3CL1 mediates progression of myeloma via CX3CR1. CX3CL1 induced Akt and ERK1/2 phosphorylation in CX3CR1-positive myeloma cell lines, but not in CX3CR1-negative cells. CX3CL1 induced cell adhesion to VCAM-1 and fibronectin in a myeloma cell line, and lead to an increased osteoclast differentiation.
Osteosarcoma Liu 2016 *Oncotarget*	Liu study: CX3CL1 expression is higher in osteosarcoma cell lines than in normal osteoblasts. CX3CL1 promotes cell migration and metastisation by upregulating ICAM-1 expression via CX3CR1/PI3K/Akt/NF-kB. Knockdown of CX3CL1 inhibited cell migration and lung metastasis. Clinical correlation between CX3CL1 and ICAM-1 expression as well as tumour stage in human osteosarcoma tissues was noted.
Ovarian cancer Gaudin 2011 *PloS One*	Gaudin study: CX3CL1 expression was correlated with Ki-67 and with GILZ (glucocorticoid-induced leucine zipper), previously identified as an activator of cell proliferation in malignant epithelial ovarian cancer. In a mouse subcutaneous xenograft model, overexpression of GILZ was associated with higher expression of CX3CL1 and faster tumoural growth.
Kim 2012 *Mol Cancer Res*	Kim study: CX3CR1 is expressed in primary and metastatic ovarian carcinoma. Ovarian carcinoma cells migrated towards CX3CL1 in a CX3CR1-dependent manner. Silencing of CX3CR1 reduced migration by 70%. Also CX3CL1 induced cellular proliferation in epithelial ovarian cancer cells.
Gurler Main 2017 *Oncogene*	Gurler Main study: CX3CL1-CX3CR1 axis is relevant for advanced and relapsed peritoneal metastasis in epithelial ovarian carcinoma. CX3CR1 played a role in the initiation of peritoneal adhesion important for relapsed peritoneal metastasis, and the CX3CR1 downregulation reduced the metastatic burden at peritoneal sites. High expression of CX3CR1 correlates with shorter survival, specifically in post-menopausal patients with advanced ovarian cancer.
Pancreatic cancer Marchesi 2008 *Cancer Res*	Marchesi study: Most of pancreatic cancer specimens expressed CX3CR1. Higher CX3CR1 staining score was associated with more prominent perineural invasion and with earlier recurrence. *In vivo* experiments with transplanted pancreatic cancer showed that CX3CR1-transfected tumour cells infiltrated peripheral nerves. Thus, CX3CR1 may be involved in pancreatic cancer neurotropism and is a risk factor for local relapse in operated patients.
Celesti 2013 *Br J Cancer*	Celesti study: Tumour differentiation, rather than inflammatory signalling, modulates CX3CR1 expression in pancreatic cancer. CX3CR1 was upregulated in tumour spheroids, and *in vivo* only in well-differentiated tumours, suggesting its early involvement in pancreatic cancer progression.
Prostate cancer Shulby 2004 *Cancer Res*	Shulby study: CX3CR1 is expressed by human prostate cancer cells, whereas bone marrow endothelial cells and differentiated osteoblasts express CX3CL1. Adhesion of prostate cancer cells to bone marrow endothelial cells is reduced by a neutralising CX3CL1 antibody. CX3CL1 activates PI3K/Akt pathway in prostate cancer cells.
Jamieson 2008 *Cancer Res*	Jamieson study: CX3CR1 is minimally detectable in normal prostate cells, but it is overexpressed upon malignant transformation. Androgens increased CX3CL1 cleavage from the cell membrane and its action was reversed by nilutamide (androgen receptor antagonist) as well as by a matrix metalloproteinase inhibitor.
Xiao 2012 *Int J Oncol*	Xiao study: HIF-1 and NF-kB are essential for hypoxia-regulated CX3CR1 expression, which was associated with increased migratory and invasive potential of prostate cancer cells.
Tang 2015 *Mol Med Rep*	Tang (2015) study: Hypoxia upregulates CX3CL1, which enhanced the prostate cancer cells proliferation. Inhibition of fractalkine activity inhibited hypoxia-induced cell proliferation. Under normoxemia, cell proliferation increased with exogenous recombinant CX3CL1, and this elevation was alleviated by an anti- CX3CL1 treatment.
Tang 2016 *Oncol Rep*	Tang (2016) study: CX3CL1 increased migration and invasiveness of prostate cancer cells DU145 and PC-3 cells, and lead to EMT, via Slug overexpression.

Pro-tumoural role of CX3CL1-CX3CR1 system in different cancers

Anti-tumoural role of CX3CL1-CX3CR1 in different cancer types	
Cancer type (and study)	**Main study findings**
Breast cancer Park 2005 *I Surg Oncol*	Park study: CD8+T cells, intra-tumoural dendritic cells and NK cells were increased in breast cancer cases with high CX3CL1 expression. Patients with high CX3CL1 expression had a more favorable disease-free progression and survival.
Colorectal cancer Ohta 2005 *Int J Oncol*	Ohta study: CX3CL1 expression was correlated with tumour-infiltrating lymphocytes density. Colorectal cancer cases with stronger CX3CL1 expression had better prognosis than those with weak expression, which is likely due to the tumour cell cytotoxicity mediated by CX3CR1-positive NK cells and cytotoxic T cells.
Vitale 2007 *Gut*	Vitale study: Anti-tumoural effects of fractalkine were investigated in its different molecular forms. Native CX3CL1 exhibits the strongest anti-tumoural effect. CX3CL1 expression by tumour cells reduced their metastatic potential, and both molecular forms contributed to its anti-tumoural potential.
Erreni 2016 *J Immunol*	Erreni study: Tumoural expression of CX3CL1-CX3CR1 acts as a retention factor, increasing homotypic cell adhesion and limiting tumour spreading to metastatic sites. Lack or low levels of CX3CL1-CX3CR1 by tumour cells identifies patients at increased risk for metastasis. Co-expression of CX3CL1-CX3CR1 is associated with longer disease-specific survival.
Marelli 2017 *Cancer Res*	Marelli study: CX3CR1 in gut macrophages is essential in resolving inflammation, where it helps to protect against colitis-associated cancer by regulating hemoxygenase-1 expression (anti-oxidant and anti-inflammatory enzyme).
Gastric cancer Hyakudomi 2008 *Ann Surg Oncol*	Hyakudomi study: CX3CL1 expression by tumour cells enhanced the recruitment of CD8+ T and NK cells and induced both innate and adaptive immunity, thereby leading to a more favourable disease-free survival in gastric cancer.
Glioma Sciume 2010 *Neuro Oncol*	Sciume study: Both CX3CL1 and CX3CR1 are expressed by human glioma cells. Endogenously expressed CX3CL1 negatively regulated cell invasion likely by promoting tumour cell aggregation, and TGF-β1 inhibition of CX3CL1 contributed to glioma cell invasiveness.
Hepatocellular carcinoma Matsubara 2007 *J Surg Oncol*	Matsubara study: Tumours with high expression of CX3CL1 and CX3CR1 have fewer intra- and extra-hepatic recurrences, different histological grades and a better prognosis in terms of disease-free and overall survival.
Neuroblastoma Zeng 2005 *Cancer Lett*	Zeng (2005) study: CX3CL1 expression lead to a reduction in primary tumour growth and in spontaneous liver metastasis in a syngenic A/J mice.
Zeng 2007 *Cancer Res*	Zeng (2007) study: Immune mechanisms by which treatment targeted IL-2 of neuroblastoma with a CX3CL1-rich tumour microenvironment induced effective anti-tumoural response. Only CX3CL1- and IL-2-enriched neuroblastoma tumour microenvironment resulted in T-cell activation and release of pro-inflammatory cytokines.
Pancreatic cancer Celesti 2013 *Br J Cancer*	Celesti study: Although CX3CR1 contributed to perineural invasion in pancreas cancer, CX3CR1 expression is a feature of more differentiated (G1-G2) tumour cells, and was associated with better overall survival in radically resected patients.

Anti-tumoural role of CX3CL1-CX3CR1 system in different cancers

Appendix 11: Abstracts presented in scientific meetings

Abstracts presented in scientific meetings containing the data presented in this thesis:

Marques P, *et al*. "Adenomas hipofisários associados a mutações dos genes *AIP* e *MEN1*: diferenças fenotípicas significativas em doentes com formas distintas de adenomas hipofisários familiares" *[Pituitary adenomas associated with AIP and MEN1 gene mutations: significant phenotypic differences in patients with distinct forms of familial pituitary adenomas]*. *Portuguese Congress of Endocrinology, 71st Annual Meeting of Portuguese Society of Endocrinology, Coimbra, Portugal, 23-26 January 2020* – Oral presentation.

Marques P, *et al*. "O papel do microambiente tumoral na angiogénese em adenomas hipofisários" *[The role of the tumour microenvironment in the angiogenesis of pituitary adenomas]*. *Portuguese Congress of Endocrinology, 71st Annual Meeting of Portuguese Society of Endocrinology, Coimbra, Portugal, 23-26 January 2020* – Poster presentation.

Marques P, *et al*. Pituitary tumour-derived chemokines modulate immune cell infiltrates in the tumour microenvironment leading to aggressive phenotype. *European Congress of Endocrinology, Lyon, France, 18-21 May 2019* – Oral presentation.

Marques P, *et al*. Cytokine network in pituitary adenomas and its role in the tumor microenvironment: focus on macrophages. *ENDO2019: The Endocrine Society´s 101st Annual Meeting, New Orleans, USA, 23-26 March 2019* – Poster presentation.

Marques P, *et al*. Pasireotide treatment inhibits cytokine release from pituitary adenoma-associated fibroblasts – is this mechanism playing a key role in its effect? *ENDO2019: The Endocrine Society´s 101st Annual Meeting, New Orleans, USA, 23-26 March 2019* – Poster presentation

Marques P, *et al*. *AIP* mutation-positive patients with somatotropinomas end-up taller and requiring more often radiotherapy compared to *AIP* mutation-negative patients: Data from 784 familial and young-onset cases. *ENDO2019: The Endocrine Society´s 101st Annual Meeting, New Orleans, USA, 23-26 March 2019* – Poster presentation.

Marques P, *et al*. Pasireotide treatment inhibits cytokine release from pituitary adenoma-associated fibroblasts – is this mechanism playing a key role in its effect? Research-in-Progress Seminar Series, William Harvey Research Institute, London, UK, 8 March 2019 – Oral presentation.

Marques P, *et al*. "Papel das citocinas no comportamento biológico e na determinação do microambiente tumoral em adenomas hipofisários, com particular foco nos macrófagos" *[Role of cytokines in the biological behaviour and determination of tumour microenvironment in pituitary adenomas, with particular focus on macrophages]. Portuguese Congress of Endocrinology, 70th Annual Meeting of Portuguese Society of Endocrinology, Braga, Portugal, 24-27 January 2019* – Oral presentation.

Marques P, *et al*. "Fibroblastos associados a tumores hipofisários: papel no comportamento tumoral e promissor alvo de terapêutica farmacológica dirigida com pasireótido?" *[Pituitary tumour-associated fibroblasts: role in the tumoural behaviour and promising target for pharmacological treatment with pasireotide?]. Portuguese Congress of Endocrinology, 70th Annual Meeting of Portuguese Society of Endocrinology, Braga, Portugal, 24-27 January 2019* – Oral presentation.

Marques P, *et al*. "Doentes com somatotropinomas associados a mutação do gene *AIP* apresentam estatura final mais elevada e requerem mais frequentemente radioterapia" *[Patients with somatotropinomas associated with AIP mutations have higher final stature and require more often radiotherapy]. Portuguese Congress of Endocrinology, 70th Annual Meeting of Portuguese Society of Endocrinology, Braga, Portugal, 24-27 January 2019* – Oral presentation.

Marques P, *et al*. Significant phenotypic difference between clinically presenting *vs* prospectively diagnosed pituitary adenoma in *AIP* mutation-positive kindreds. *ENDO2018: The Endocrine Society´s 100th Annual Meeting, Chicago, USA, 17-20 March 2018* – Poster presentation.

Marques P, *et al*. "Adenomas hipofisários associados a mutação do gene *AIP:* fenótipo clínico e benefícios do estudo genético" *[Pituitary adenomas associated with mutations in the AIP gene: clinical phenotype and benefits of genetic study]. Portuguese Congress of Endocrinology, 69th Annual Meeting of Portuguese Society of Endocrinology, Vilamoura, Portuga), 1-4 February 2018* – Oral presentation.

Abstracts presented in scientific meetings in other fields during the period of PhD studies:

Marques P, *et al*. "Paquidermoperiostose: um diagnóstico diferencial de acromegalia – a propósito de 4 casos clínicos" *[Pachydermoperiostosis: a differential diagnosis of acromegalia – 4 clinical cases]*. *Portuguese Congress of Endocrinology, 71st Annual Meeting of Portuguese Society of Endocrinology, Coimbra, Portugal, 23-26 January 2020* – Poster presentation.

Marques P, *et al*. "Síndrome de Marfan como confundidor diagnóstico de gigantismo hipofisário em família com adenomas hipofisários familiares associados a mutação do gene *AIP*" *[Marfan syndrome as diagnostic confounder of pituitary gigantism in a family with pituitary adenomas associated with an AIP gene mutation]*. *Portuguese Congress of Endocrinology, 70th Annual Meeting of Portuguese Society of Endocrinology, Braga, Portugal, 24-27 January 2019* – Oral presentation.

Marques P, *et al*. "Pseudoacromegalia e síndrome de Cantú: nova mutação no gene *ABCC9* em família com adenomas hipofisários familiares" *[Pseudoacromegaly and Cantú syndrome: new mutation in the ABCC9 gene in a family with familial pituitary adenomas]*. *Portuguese Congress of Endocrinology, 69th Annual Meeting of Portuguese Society of Endocrinology, Vilamoura, Portugal, 1-4 February 2018* – Oral presentation.

Marques P, *et al*. Gigantism due to two different causes in the same family – *AIP* mutation-positive acromegaly and Marfan syndrome. *Society for Endocrinology BES 2018, Glasgow, UK, 19-21 November 2018* – Poster presentation.

Marques P, *et al*. Novel *ABCC9* mutation with Cantú syndrome-associated phenotype of hypertrichosis with acromegaloid facial features (HAFF) with coexisting familial pituitary adenoma. *Society for Endocrinology BES 2017, Harrogate, UK. 6-8 November 2017* – Poster presentation.

Marques P, *et al*. Long-term follow-up of a family with a large *AIP* gene deletion: variable phenotypes and challenges in the management. *European Congress of Endocrinology, Lisbon, Portugal, 20-23 May 2017* – Poster presentation.